

Dissertation zur Erlangung des Doktorgrades  
der Fakultät für Chemie und Pharmazie  
der Ludwig-Maximilians-Universität München

# **Kinetics and Mechanism of Electrophilic Fluorinations of Enamines and Carbanions**

Daria Timofeeva

aus

Moskau, Russland

2018

## **Erklärung**

Diese Dissertation wurde im Sinne von § 7 der Promotionsordnung vom 28. November 2011 von Herrn Prof. Dr. Herbert Mayr betreut.

## **Eidesstattliche Versicherung**

Diese Dissertation wurde eigenständig und ohne unerlaubte Hilfe erarbeitet.

München, den

.....  
(Daria Timofeeva)

Dissertation eingereicht am .....

1. Gutachter: Professor Dr. Herbert Mayr

2. Gutachter: Professor Dr. Manfred Heuschmann

Mündliche Prüfung am .....

*For Artem*

*“Fluorine leaves nobody indifferent; it inflames emotions, be that affections or aversions. As a substituent it is rarely boring, always good for a surprise, but often completely unpredictable”*– Manfred Schlosser, 1998.



## Acknowledgements

I want to express my great thanks to many people that have always accompanied and supported me during the last four years, and made this thesis possible.

First, I would specially like to thank my supervisor and Doktorvater, *Professor Dr. Herbert Mayr*, for giving me an opportunity to work and study in Munich. I greatly appreciate his constant support, motivational and fruitful discussions, and I would like to thank him for keeping his door always opened for me. My PhD has been an amazing experience and I thank Prof. Mayr wholeheartedly, not only for his tremendous academic support at all stages of my PhD studies, but also for giving me and the group so many opportunities to see the most wonderful places in the Alps.

Furthermore, I would like to thank *Professor Dr. Manfred Heuschmann* for reviewing my thesis and also the board of examiners for their participation in my defense examination.

Furthermore, I would like to thank *Dr. Armin Ofial* for taking the time to carefully reviewing all my work, excellent advices for improvement of manuscripts as well as the critical and valuable suggestions.

Thanks to former and current AK Mayr/Ofial members: *Elija Wiedemann, Dr. Francisco Corral, Dr. Johannes Ammer, Katharina Böck, Dr. Quan Chen, Prof. Dr. Shinjiro Kobayashi, Dr. Zhen Li, Feng An, Patrick Jüstel, Le Li*. I really appreciate the knowledge they shared, the fun we had, and specially, the friendly atmosphere. I am really grateful to *Robert Mayer* for bringing extra energy and motivation in the group, for his scientific support and for the great ideas and discussions.

Special thanks to *Dr. Ángel Puente* for his help and support in the beginning of my PhD; to *Dr. Guillaume Berionni, Elsa Follet, Ieva Teikmane* for all the time spent together in the lab and beyond (for best coffee breaks, for cooking together on the weekends, for our movie nights and hiking). I am grateful for all your kind support and I was missing you a lot during the last year.

Many thanks to *Frau Hildegard Lipfert* for her kind help in assisting me to fill in the official forms when I first arrived in Munich and for her help over the past four years. I thank *Nathalie Hampel* for solving all organizational problems in the lab and especially for synthesizing reference electrophiles.

I am profoundly grateful to my “Pheromone” family for providing me with fantastic lab training, for encouraging me to embark on the doctorate. I will always cherish the memory of time we work together.

I would like to extend thanks to all my friends: the ones in Moscow, especially *Valusha, Roma, Sasha, Ksusha, Annet, Lili and Pasha* (aka zjat’), who always welcomed me back as well as visited us here in Munich and were the reason for which I always look forward to visit home; to *Misha* and *Masha* in Prague for their warmth and hospitality; to our Munich family, who truly made me feel at home despite the 2,000 km distance, for exciting trips and wonderful events. I would especially like to thank *Varechka* “meow” *Morozova* and her husband *Ilya Makarov* for their friendship, constant support, and for making this stay in Munich a lot more entertaining.

A very special word of thanks goes to my *parents*, my *sister Ksusha* and *grandparents* for their unconditional love and almost unbelievable support. Thank you for always believing in me!

My deepest thank go to the love of my life: *Artem*, thank you so much for providing me an endless source of support, your understanding, your assistance, your encouragement and for always showing how proud you are of me. I could not have done this without you here.

## Publications

### Which Factors Control the Nucleophilic Reactivities of Enamines?

D. S. Timofeeva, R. J. Mayer, P. Mayer, A. R. Ofial, H. Mayr *Chem. Eur. J.* **2018**, *24*, 5901–5910

### Kinetics of Electrophilic Fluorinations of Enamines and Carbanions: Comparison of the Fluorinating Power of N–F Reagents

D. S. Timofeeva, A. R. Ofial, H. Mayr *J. Am. Chem. Soc.* **2018**, *140*, 11474–11486

### Nucleophilic Reactivities of Schiff Base Derivatives of Amino Acids

D. S. Timofeeva, A. R. Ofial, H. Mayr *Tetrahedron* **2018**, *accepted*

## Contributions to Conferences

Parts of this work were presented at the following scientific meetings:

**09/2017**     *GDCh-Wissenschaftsforum Chemie 2017*, Berlin (Germany).

poster presentation: **Nucleophilic Reactivity and Lewis Basicity of Deoxybenzoin-Derived Enamines**

**10/2017**     *SFB749-Meeting*, Kloster Irsee (Germany).

poster presentation: **Nucleophilic Reactivity and Lewis Basicity of Deoxybenzoin-Derived Enamines**

**07/2018**     *22nd International Symposium on Fluorine Chemistry*, Oxford (England).

poster presentation: **Electrophilic Reactivity of N-F Fluorinating Reagents**

# Table of Contents

<b>Chapter 0: Summary</b>	<b>1</b>
0.1. General	1
0.2. Which Factors Control the Nucleophilic Reactivities of Enamines?	1
0.3. Kinetics of Electrophilic Fluorinations of Enamines and Carbanions: Comparison of the Fluorinating Power of N–F Reagents	5
0.4. Nucleophilic Reactivities of Schiff Base Derivatives of Amino Acids	7
<b>Chapter 1: Introduction</b>	<b>9</b>
<b>Chapter 2: Which Factors Control the Nucleophilic Reactivities of Enamines?</b>	<b>19</b>
2.1. Introduction	19
2.2. Results and Discussions	22
2.3. Conclusion	37
2.4. Supplementary Section	39
2.5. Experimental Section	46
2.6. References	121
<b>Chapter 3: Kinetics of Electrophilic Fluorinations of Enamines and Carbanions: Comparison of the Fluorinating Power of N–F Reagents</b>	<b>126</b>
3.1. Introduction	126
3.2. Results and Discussions	130
3.3. Conclusion	146
3.4. Experimental Section	152
3.6. References	189
<b>Chapter 4: Nucleophilic Reactivities of Schiff Base Derivatives of Amino Acids</b>	<b>196</b>
4.1. Introduction	196
4.2. Results and Discussions	198
4.3. Conclusion	205
4.4. Experimental Section	207
4.5. References	222

## Chapter 0

### Summary

#### 0.1. General

Rates of many electrophile-nucleophile combinations were shown to follow the linear free energy relationship (1), where nucleophilic reactivity is expressed by the solvent-dependent parameters  $N$  (nucleophilicity) and  $s_N$  (sensitivity), and electrophiles are characterized by the solvent-independent parameter  $E$  (electrophilicity).

$$\lg k_2 (20\text{ }^\circ\text{C}) = s_N (N + E) \quad (1)$$

Furthermore, it was recently demonstrated that the equilibrium constants for the reactions of benzydrylium ions with phosphines, pyridines, and other Lewis bases can be calculated as the sum of a Lewis acidity parameter  $LA$  and a Lewis basicity parameter  $LB$ , as expressed by Equation (2).

$$\lg K (20\text{ }^\circ\text{C}) = LA + LB \quad (2)$$

The purpose of this thesis is to investigate the kinetics and mechanism of electrophilic fluorinations with N–F reagents and to examine the applicability of eq 1 for these reactions. Since enamines derived from deoxybenzoin are colored ( $\lambda_{\text{max}} = 315 - 465\text{ nm}$ ), they can be used as reference nucleophiles for the characterization of the reactivity of a large number of synthetically important colorless electrophiles. Therefore, the reactions of this new family of nucleophiles with reference electrophiles/Lewis acids were studied in order to quantify their reactivity and Lewis basicity by using eqs 1 and 2, respectively. The electrophilicity parameters of the fluorinating N–F reagents, determined from the kinetics of the reactions with deoxybenzoin-derived enamines, are able to rationalize known fluorination reactions and are, therefore, recommended as guide for designing new electrophilic fluorinations.

#### 0.2. Which Factors Control the Nucleophilic Reactivities of Enamines?

Changes in rate constants, equivalent to changes in Gibbs energies of activation ( $\Delta G^\ddagger$ ), are commonly called kinetic effects and differentiated from thermodynamic effects ( $\Delta_r G^\circ$ ). Often, little attention is paid to the fact that structural effects on  $\Delta G^\ddagger$  are composed from a thermodynamic ( $\Delta_r G^\circ$ ) and a truly kinetic (intrinsic) component ( $\Delta G_0^\ddagger$ ), as expressed by the Marcus equation (3).

$$\Delta G^\ddagger = \Delta_r G_0^\ddagger + \frac{1}{2} \Delta_r G^\circ + \frac{(\Delta_r G^\circ)^2}{16\Delta_r G_0^\ddagger} \quad (3)$$

Second-order rate constants ( $k_2$ ) of the reactions of deoxybenzoin-derived enamines and aminostyrenes with benzhydrylium ions (reference electrophiles) were determined photometrically in acetonitrile solution at 20 °C under pseudo-first-order conditions. The measured rate constants ( $\lg k_2$ ) were found to correlate linearly with the electrophilicities  $E$  of the reference benzhydrylium ions (Figure 1), as required by equation (1), allowing the determination of the nucleophile-specific parameters  $N$  and  $s_N$  for the deoxybenzoin-derived enamines.

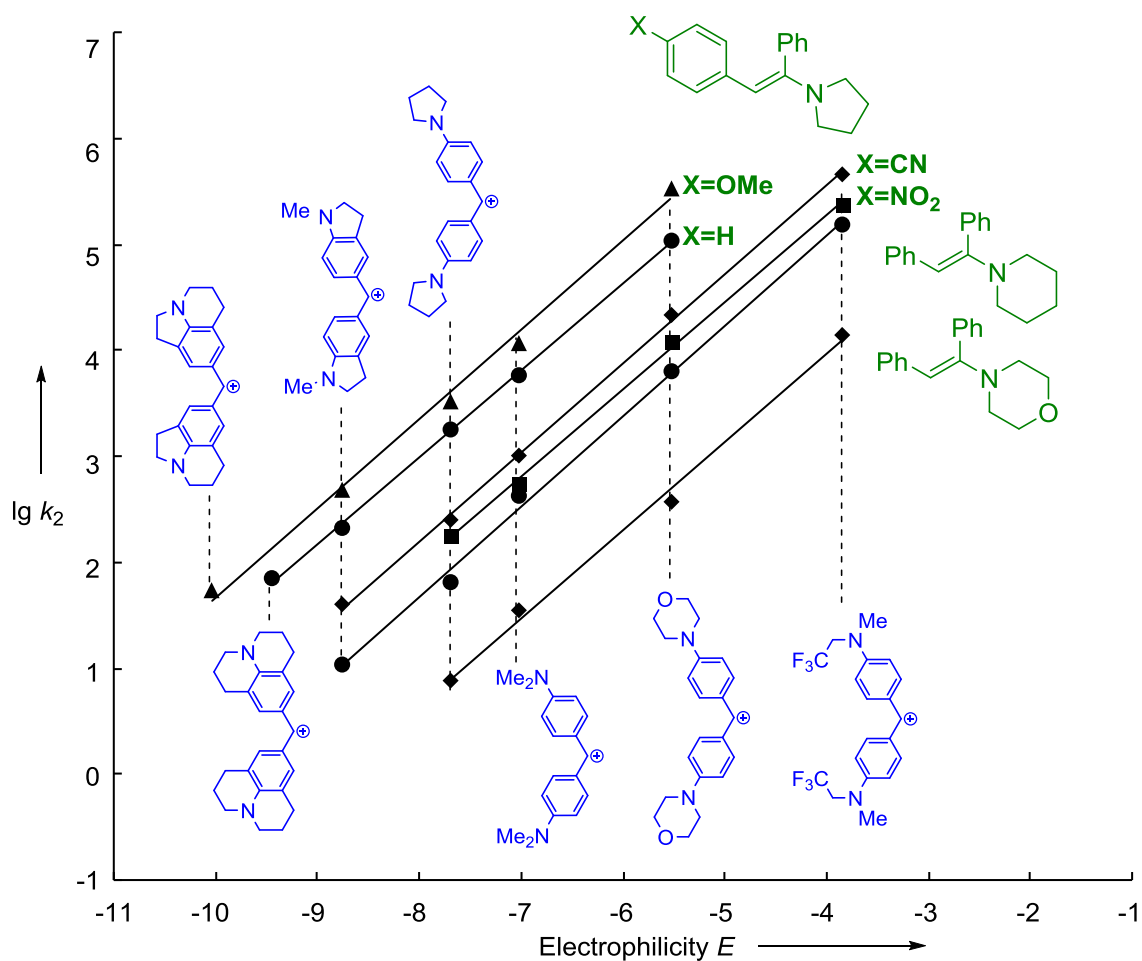


**Figure 1.** Plots of the rate constants ( $\lg k_2$ ) for the reactions of representative enamines with benzhydrylium ions versus their electrophilicities  $E$  (MeCN, 20 °C).

As the reactions of enamines with weakly Lewis-acidic benzhydrylium ions do not go to completion, the corresponding equilibrium constants could be studied through UV-vis spectrophotometric titration in acetonitrile solution at 20 °C. The Lewis basicities  $LB$  of the enamines were calculated from the measured equilibrium constants and the Lewis acidities  $LA$  of benzhydrylium ions using equation (2).

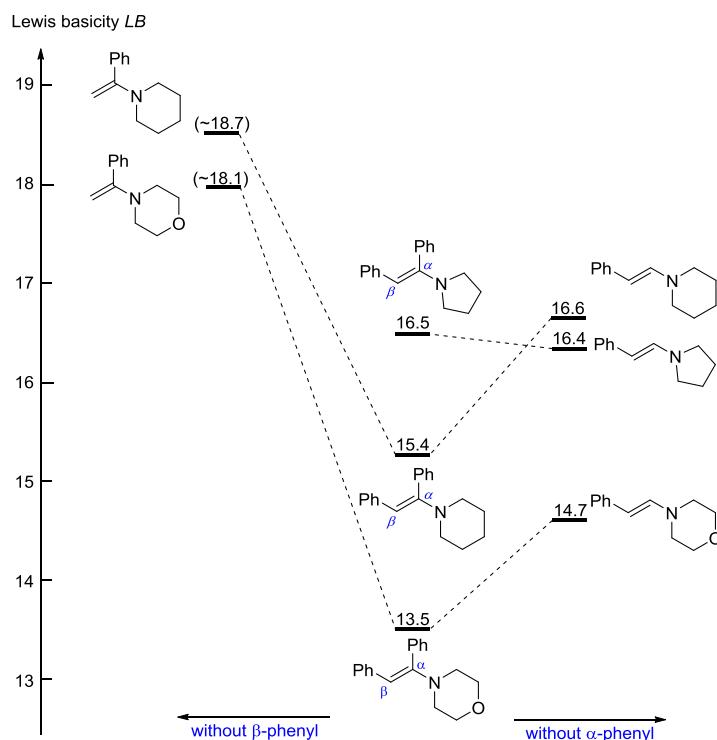


**Figure 2.** Comparison of the Lewis basicities  $LB$  of deoxybenzoin-derived enamines with those of aminostyrenes.

For several reactions of enamines with benzhydrylium ions rate and equilibrium constants could be determined, which allows to calculate the Marcus intrinsic barriers ( $\Delta G_0^\ddagger$ ) by using equation (3).

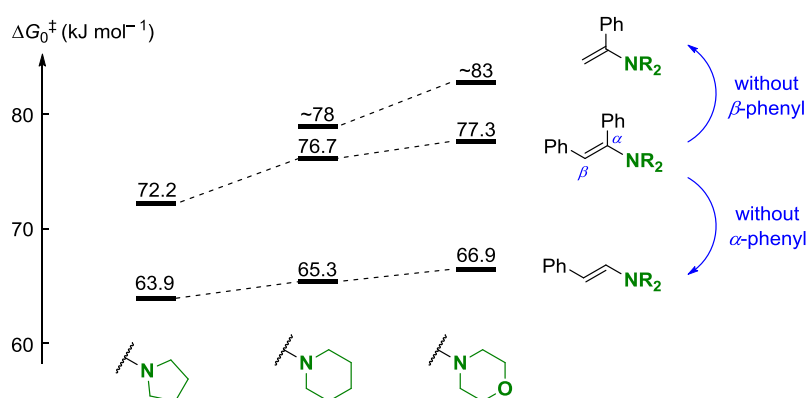


**Figure 3.** Comparison of the intrinsic barriers  $\Delta G_0^\ddagger$  for the reactions of enamines towards benzhydrylium ion **E5**.

The nucleophilicity ordering morpholino < piperidino < pyrrolidino in the series of deoxybenzoin-derived enamines and  $\beta$ -aminostyrenes (Figure 4) is predominantly controlled by thermodynamics (Figure 2) though slightly enhanced by intrinsics (Figure 3).

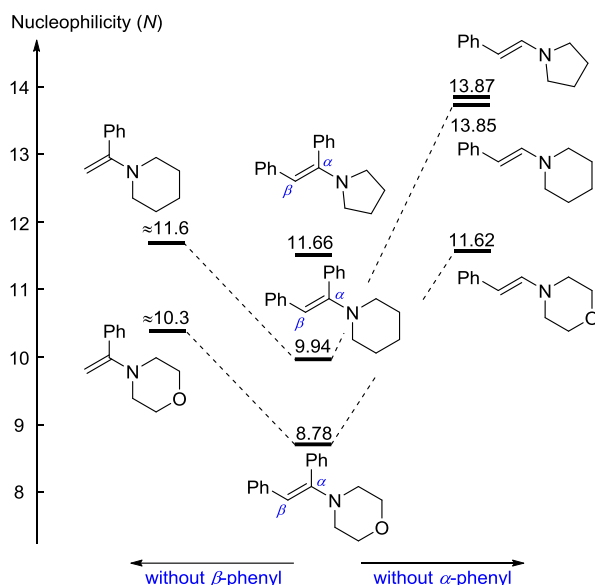


**Figure 4.** Comparison of the nucleophilicities  $N$  of deoxybenzoin-derived enamines with those of aminostyrenes.

Removal of the  $\alpha$ -phenyl group of deoxybenzoin-derived enamines leads to a more significant increase of nucleophilicity (Figure 4), compared to Lewis basicity (Figure 2), because the thermodynamic effect is enhanced by the simultaneous decrease of the intrinsic barrier (Figure 3). At the same time, the strong increase of the Lewis basicity by removal of the  $\beta$ -phenyl group is counterbalanced by larger intrinsic barrier for the reactions with benzhydrylium ions.

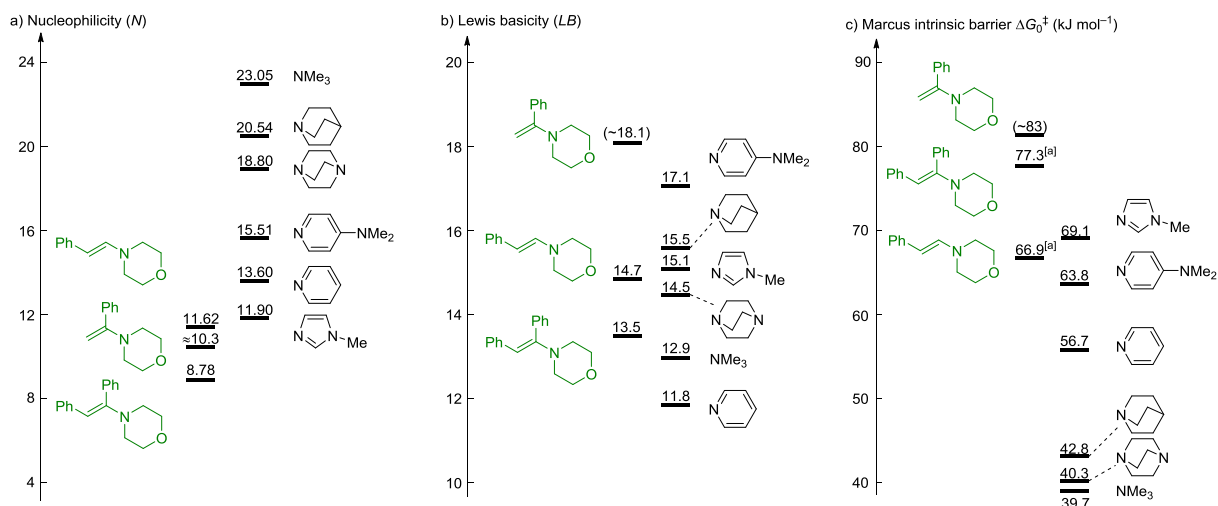


**Figure 5.** Comparison of the a) nucleophilicities, b) Lewis basicities, and c) and intrinsic barriers for the reactions of **E5** with enamines, *tert.* amines, pyridines, and imidazoles.

Figure 5 shows that the enamines are weaker nucleophiles than *tert.* amines, pyridines, and imidazoles, although the Lewis basicities of these enamines are comparable to those of the strong nitrogen bases depicted. The enamines react with higher intrinsic barriers, which reduces their nucleophilicity.

### 0.3. Kinetics of Electrophilic Fluorinations of Enamines and Carbanions: Comparison of the Fluorinating Power of N–F Reagents

Kinetics of the reactions of enamines and carbanions with commonly used fluorinating reagents, *N*-fluorobenzenesulfonimide (NFSI), *N*-fluoropyridinium salts, Selectfluor, and an *N*-fluorinated cinchona alkaloid, have been investigated in acetonitrile. The rate constants for their reactions with deoxybenzoin-derived enamines follow the linear free energy relationship (1), which allows the empirical electrophilicity parameters  $E$  for these fluorinating agents to be derived from the measured rate constants and the  $N$  and  $s_N$  parameters for the nucleophiles determined in Chapter 2. As shown in Figure 6, Selectfluor and the 2,6-dichloro-1-fluoropyridinium ion are the most reactive N–F reagents of this series, followed by NFSI and *N*-fluorinated pyridinium ions. Since the parent *N*-fluoropyridinium ion may also be attacked at C-2 of the pyridinium ion, the *N*-fluoro-substituted collidinium ion can be considered as the reagent of choice, when a mild fluorinating reagent is needed.

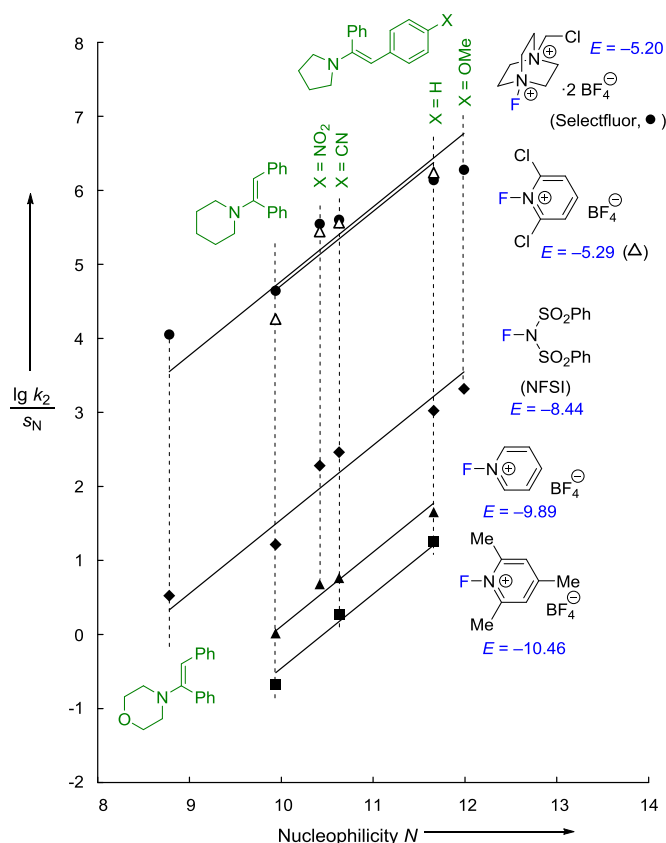


**Figure 6.** Correlations of  $(\lg k_2)/s_N$  for the reactions of fluorinating N–F reagents with the deoxybenzoin-derived enamines against their nucleophilicity parameters  $N$  (MeCN, 20 °C). For all correlations, a slope of 1.0 was enforced, as required by eq 1.

Limitations of equation 1 are illustrated in Figure 7, which depicts that the reactions of NFSI with the deoxybenzoin-derived enamines and the carbanions follow separate



correlations. Application of electrophilicity parameters  $E$ , derived from reactions of NFSI with deoxybenzoin-derived enamines, for calculating the rate constants of reactions of NFSI with carbanions as well as with  $\beta$ -aminostyrenes yields second-order rate constants  $k_2$ , which are 2.5 to 4 orders of magnitude larger than measured.

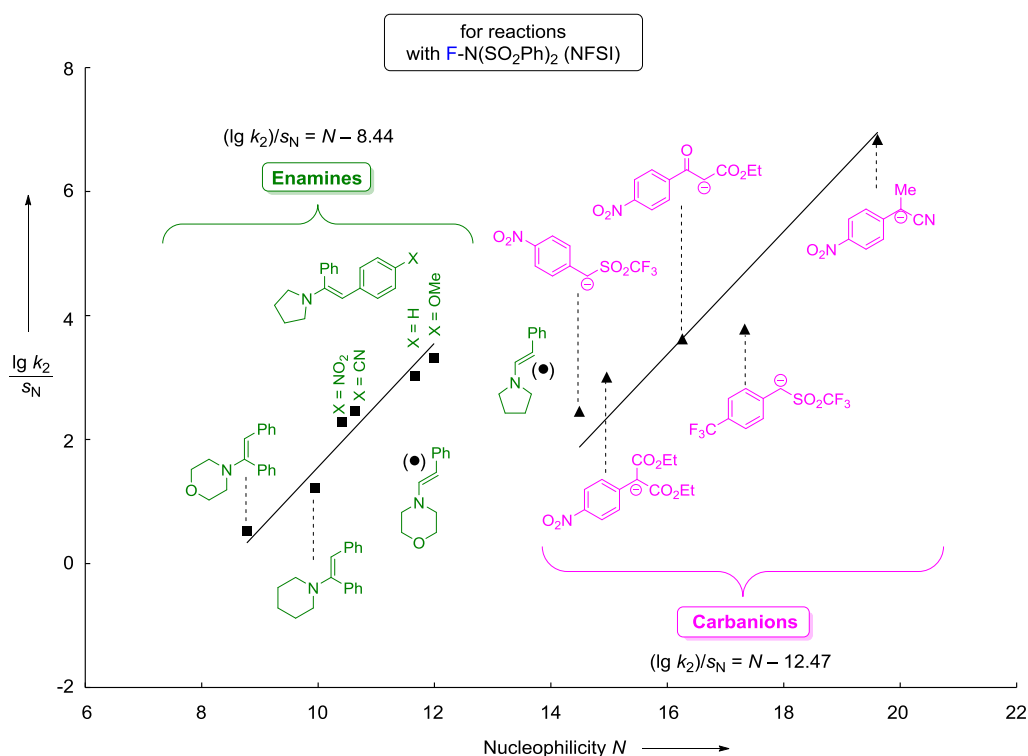
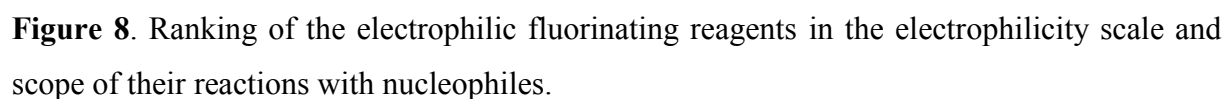


**Figure 7.** Correlations of  $(\lg k_2)/s_N$  versus the nucleophilicity of the enamines (determined in MeCN) and carbanions (determined in DMSO) for their reactions with NFSI in MeCN at 20 °C. Both correlation lines are fixed to a slope of 1.0, as required by eq 1.

The reactions of the enamines derived from cyclic ketones with all fluorinating agents proceed with activation energies  $\Delta G^\ddagger$ , which are smaller than the calculated Gibbs energies of electron transfer  $\Delta G^\circ_{\text{ET}}$ . It can be concluded that the electrophilic fluorinations with N–F reagents studied in this work proceed by an  $S_N2$  type mechanism, in which the rate determining step includes cleavage of the N–F bond.

Though the deviations of the measured rate constants from those calculated by the linear free energy relationship (1) are larger than for reactions of  $C_{\text{sp}2}$ -centered electrophiles with nucleophiles, it is shown that the electrophilicity parameters  $E$  determined in this work are able to rationalize known fluorination reactions and are, therefore, recommended as guide for designing new electrophilic fluorinations. Combination of the electrophilicity descriptors  $E$  determined in this investigation with the tabulated reactivity parameters  $N$  and  $s_N$  for carbon nucleophiles can, therefore, be used for the design of further fluorinations. The fluorinating



Treatment of  $\alpha$ -imino esters derived from glycine esters and benzophenone or benzaldehydes with potassium *tert*.butoxide in DMSO give persistent solutions of 2-aza-allyl anions at 20 °C. The kinetics of their reactions with quinone methides and benzyldiene malonates (reference electrophiles) have been followed photometrically under pseudo-first order conditions. The reactions followed second-order rate laws. Since addition of 18-crown-6 ether did not affect the reaction rates, the measured rate constants correspond to the reactions of the non-paired carbanions. Plots of the second-order rate constants against the electrophilicity parameters  $E$  of the electrophiles are linear (Figure 9), as required by eq 1, which allowed the determination of the nucleophile-specific parameters  $N$  and  $s_N$ .

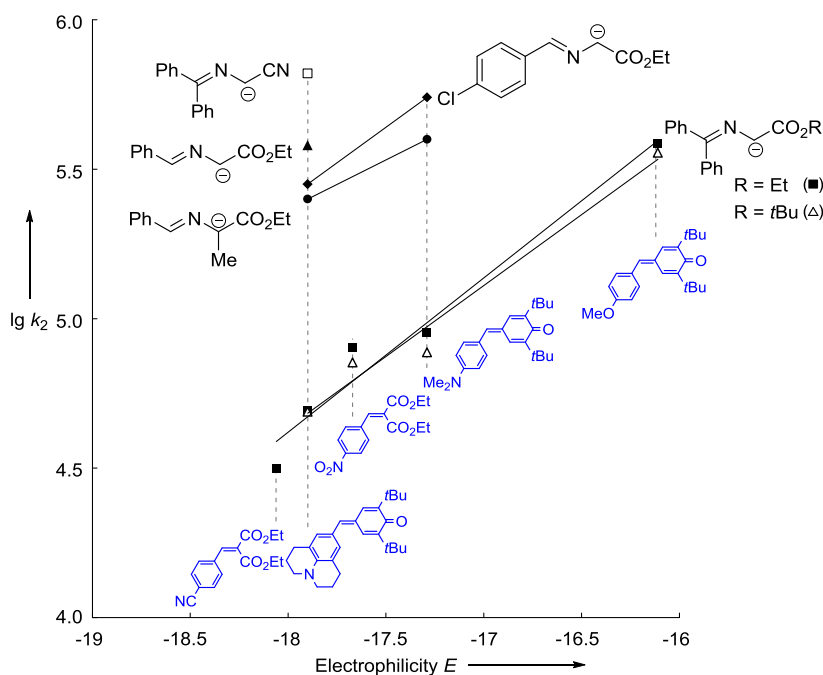


**Figure. 9.** Correlations of  $\lg k_2$  for the reactions of the 2-aza-allyl anions with reference electrophiles at 20 °C in DMSO with their electrophilicity parameters  $E$ .

The  $\text{Ph}_2\text{C}=\text{N}-$  and  $\text{PhCH}=\text{N}-$  groups act as very weak electron acceptors with the consequence that  $\text{Ph}_2\text{C}=\text{N}-\text{CH}^--\text{CO}_2\text{R}$  and  $\text{PhCH}=\text{N}-\text{CH}^--\text{CO}_2\text{R}$  have a similar nucleophilicity as  $\text{Ph}-\text{CH}^--\text{CO}_2\text{Et}$ , the anion of ethyl phenylacetate (Figure 10). Even though the relative reactivities of the carbanions in Figure 10 will somewhat vary with the nature of the electrophile because of the different magnitude of  $s_{\text{N}}$ , one can see that replacement of the imino group by cyano, alkoxy carbonyl, acyl, phosphoryl, and sulfonyl groups leads to a significant reduction of nucleophilicity.

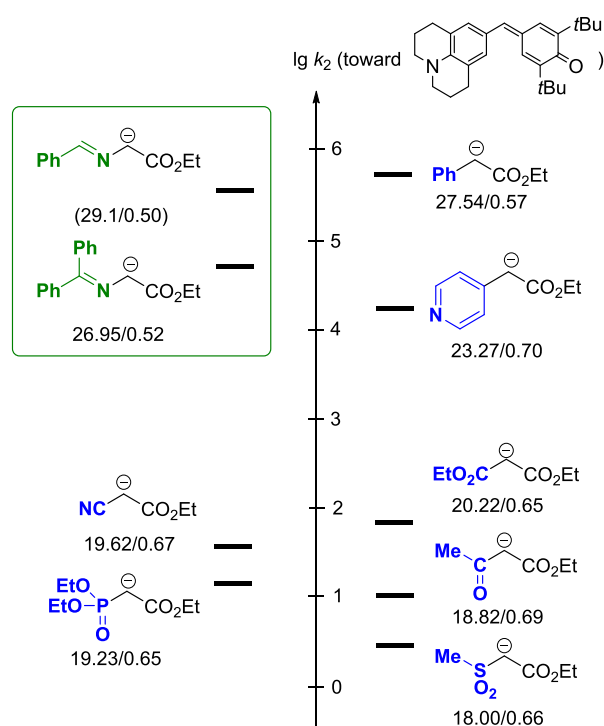


**Figure. 10.** Comparison of second-order rate constants ( $\lg k_2$ ) for the reactions of the depicted quinone methide with the carbanions derived from  $\alpha$ -imino esters and related carbanions.

## Chapter 1

### Introduction

The terms "electrophile" and "nucleophile" were introduced by Ingold in the beginning of 1930s, defining electron-deficient and electron-rich species, respectively.<sup>1</sup> From then on, several efforts have been made by physical organic chemists to find general concepts for numerical quantifying of these terms and to construct empirical scales of electrophilicity and nucleophilicity.

The first attempt to describe the nucleophilic reactivity based on kinetic parameters have been proposed by Swain and Scott in 1963.<sup>2</sup> The investigated rate constants  $k$  of  $S_N2$  reactions were found to follow a linear free-energy relationship (eq 1), where  $k_0$  is the rate constant for the reaction of an electrophile with water, parameter  $n$  characterizes the nucleophilicity of a certain reagent and the parameter  $s$  reflects the sensitivity of the electrophile to the variation in the nucleophile. The  $S_N2$  reactions of methyl bromide ( $s = 1$ ) with various nucleophiles in water ( $n = 0$ ) were chosen as reference system.

$$\lg(k/k_0) = s n \quad (1)$$

A further important contribution to the quantitative description of polar organic reactivity was reported by Ritchie in 1972.<sup>3</sup> He found that the rates of the reactions of various  $n$ -nucleophiles with carbocations and diazonium ions can be described by equation (2), where nucleophiles are characterized by the electrophile-independent parameter  $N_+$ , and the reactivities of the electrophiles are quantified by the rates  $k_0$  of their reactions with water.

$$\lg(k/k_0) = N_+ \quad (2)$$

The resulting nucleophilicity scale covered a broad range of reactivity, which allows to predict the rate constant of the reaction by using only one parameter for the nucleophile and one parameter for the electrophile. However, it turned out that Ritchie's "constant selectivity relationship" has a rather limited applicability and that better correlations are obtained when different classes of electrophiles are treated separately.<sup>4</sup>

In 1994 Mayr and Patz used the rates of the reactions of carbocations, cationic metal- $\pi$ -complexes, and diazonium ions with  $n$ -,  $\pi$ -, and  $\sigma$ -nucleophiles for the development of a new linear free energy relationship (3), where nucleophiles are described by a nucleophilicity

parameter  $N$  and a nucleophile-specific sensitivity parameter  $s_N$ , and electrophiles are described by an electrophilicity parameter  $E$ .<sup>5</sup>

$$\lg k_2 (20\text{ }^\circ\text{C}) = s_N (N + E) \quad (3)$$

By using diarylcarbenium ions and structurally related quinone methides as reference electrophiles, having widely variable reactivities, free-energy relationship (eq 3) was employed to create a comprehensive nucleophilicity scale covering more than 30 orders of magnitude.<sup>6</sup> Furthermore, kinetic investigations of the reactions of both neutral (enamines, silyl enol ethers) and anionic  $C$ -nucleophiles (stabilized carbanions, pyridinium and sulfur ylides) of known nucleophilicity with various  $C$ - and  $N$ -electrophiles (Michael acceptors,<sup>7</sup> iminium ions,<sup>8</sup> quinones<sup>9</sup> and aldehydes/ketones<sup>10</sup>, azodicarboxylates<sup>11</sup>) allowed to determine their  $E$  parameters according to equation (3) and thereby enabling the scales to be extended. An important application for organic reactivity parameters was shown in the field of organocatalysis: the reactivities of key intermediates in these reaction cycles were characterized to give useful insights in the complex reaction mechanisms.<sup>12</sup>

Halogenation reactions used to be among the most significant processes in organic chemistry. The products of these halogenations have long been valued as useful synthetic intermediates. Historically, the most commonly used halogenating reagents for this purpose have been the elemental halogens.

The kinetics of the reactions of polychloroquinone-derived chlorinating reagents<sup>13</sup> with various nucleophiles have already been studied to include these compounds in the comprehensive electrophilicity scale. It has been found that the relative reactivities of enamines and other electron-rich  $\pi$ -systems towards several  $\text{Cl}^+$  equivalents follow the same reactivity order as towards carbenium ions, which were used for the determination of the nucleophilicity parameters of these  $\pi$ -nucleophiles. Even though the obtained correlations were of low quality, the calculated and experimental rate constants agreed within a factor of 12–22, which was considered to be acceptable for a three-parameter equation, covering reactivity range of 40 orders of magnitude.

Fluorine has many unique properties such as small atomic radius, extremely low polarizability, the highest electronegativity and the  $\text{C-F}$  bond is much stronger ( $484\text{ kJ mol}^{-1}$ ) than  $\text{C-H}$  bond ( $411\text{ kJ mol}^{-1}$ ). Unlike other halogens, fluorine can replace any hydrogen atom of an organic molecule since the fluorine atom has the smallest van der Waals radius ( $1.35\text{ \AA}$ )

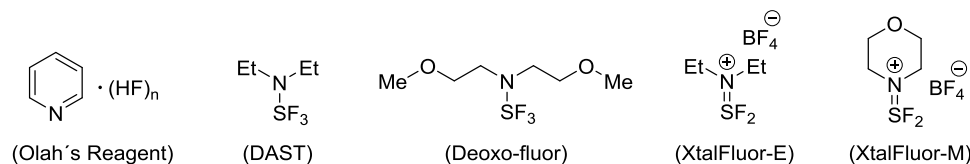
close to that of hydrogen (1.20 Å). Replacement of hydrogen by fluorine can significantly change physical, chemical, and biochemical properties organic molecules.<sup>14</sup>

The synthesis of fluorinated molecules has received considerable attention and still continues to be an active area of research. The importance of fluorinated compounds in pharmaceutical,<sup>15</sup> agrochemical,<sup>16</sup> and material chemistry<sup>17</sup> has led to the development of numerous methods for fluorination. The fluorinating reagents may be divided into two major groups:

- 1) *Nucleophilic sources of fluorine* ( $F^-$ ) and
- 2) *Electrophilic sources of fluorine* ( $F^+$ ).

Radical fluorination represents a complementary approach but has limited applications due to the paucity of selective radical fluorinating agents.<sup>18</sup>

Methods for C–F bond formation through nucleophilic fluorination require fluoride sources that include activated alkali metal fluorides, HF-containing reagents such as Olah's reagent (HF-pyridine), quaternary ammonium fluorides ( $Bu_4N-F$ , TBAF), and various sulfur-based fluorinating reagents as  $SF_4$ , diethylaminosulfur trifluoride (DAST), Deoxo-Fluor and XtalFluor, which are successfully employed for deoxyfluorination (Scheme 1).<sup>19</sup>

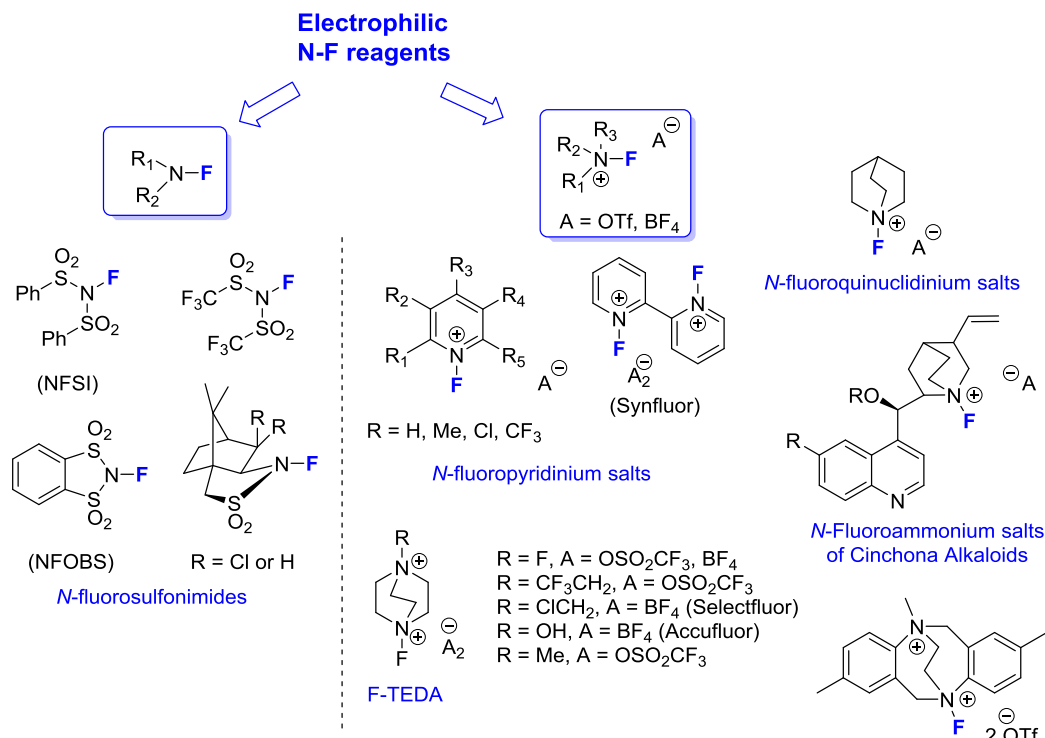


**Scheme 1.** Examples of achiral nucleophilic fluorinating agents.

Classically, the source of electrophilic fluorine ( $F^+$ ) has been fluorine gas ( $F_2$ ), which is highly toxic and has strong oxidizing properties. Perchloryl fluoride ( $FClO_3$ ), xenon difluoride ( $XeF_2$ ), trifluoromethyl hypofluorite ( $CF_3OF$ ), and various acyl- and perfluoroacyl hypofluorites ( $RCOOF$ ) were among the first used sources of positive fluorine.<sup>20</sup>

Remarkable progress in fluorine chemistry has been made with the development of a variety of electrophilic fluorinating reagents containing N–F bonds (Scheme 2). Two classes of N–F reagents are known: neutral N–F reagents ( $R_2NF$ ) and quaternary ammonium N–F reagents ( $R_3NF^+A^-$ , where  $A^-$  is weakly Lewis-basic anion).<sup>21</sup> The main N–F reagents are *N*-fluoro amines or amides, *N*-fluoropyridinium salts and *N*-fluoro derivatives of 1,4-diazoniabicyclo[2.2.2]octane (triethylendiamine; TEDA), among which 1-chloromethyl-4-fluoro-1,4- diazoniabicyclo [2.2.2]octane bis(tetrafluoroborate), known under the trade name

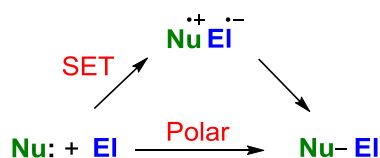
of Selectfluor<sup>TM</sup> (F-TEDA-BF<sub>4</sub>), is the most representative and widely used reagent in this series.



**Scheme 2.** Electrophilic fluorinating reagents of N-F type.

Many attempts have been made to derive the relative reactivities of N-F reagents by determination of their peak reduction potentials,<sup>22</sup> competition experiments,<sup>23</sup> and quantum chemical calculations.<sup>24</sup>

In view of the great synthetic potential of N-F fluorinating reagents, it was an object of the present research to examine the applicability of the linear free-energy relationship (3) for describing the rates of electrophilic fluorination reactions, i.e., whether N-F reagents can be characterized by electrophilicity parameters  $E$  and, thus, provide a quantitative basis for the rational planning of (enantioselective) synthetic strategies.



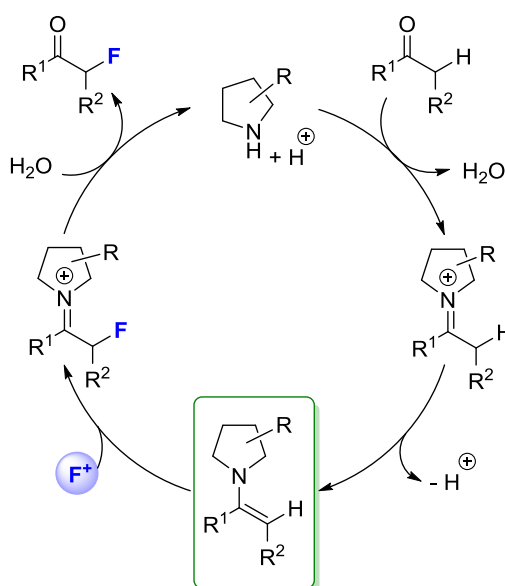
**Scheme 3.** Electron transfer vs polar reaction.

Since the introduction of the N-F reagents, the mechanism of electrophilic fluorination has been a subject of debate. Two possible pathways have been considered for the electrophilic fluorinations: polar (S<sub>N</sub>2 type) mechanism and single electron transfer SET (Scheme 3).

Differding et al. have investigated this question by radical clock experiments and kinetic studies. The experiments excluded radical pathways and indicated the operation of an  $S_N2$  mechanism, at least for the investigated reagent/substrate combinations.<sup>25</sup>

Since UV-vis spectroscopy is an efficient method to determine reaction rates, there was a need to design novel colored nucleophiles of suitable reactivity. As N-F reagents had already been reported to be highly reactive, the previously characterized colored carbanions were expected not to be suitable for characterizing all common fluorinating reagents.

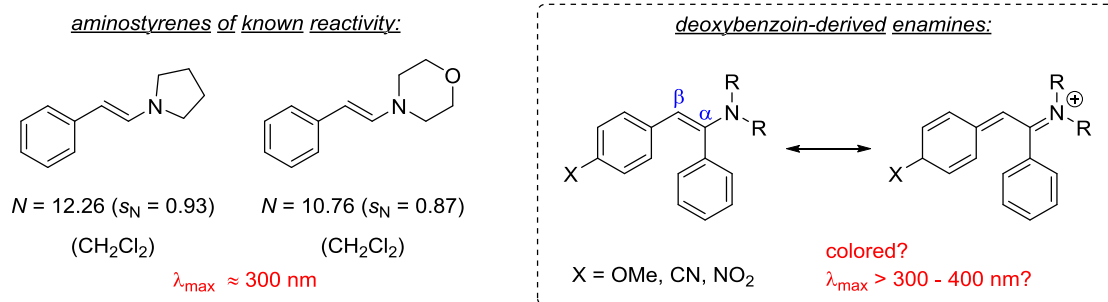
Significant advances in the synthesis of enantiopure organofluorine compounds have been made during the past decades, employing asymmetric catalysis.<sup>26</sup> As depicted in Scheme 4, enamines have been suggested to be key intermediates in organocatalytic fluorinations of carbonyl compounds. Due to this fact, I decided to employ this type of compounds as reference nucleophiles for the kinetic investigations.



**Scheme 4.** Organocatalytic fluorination of carbonyl compounds.

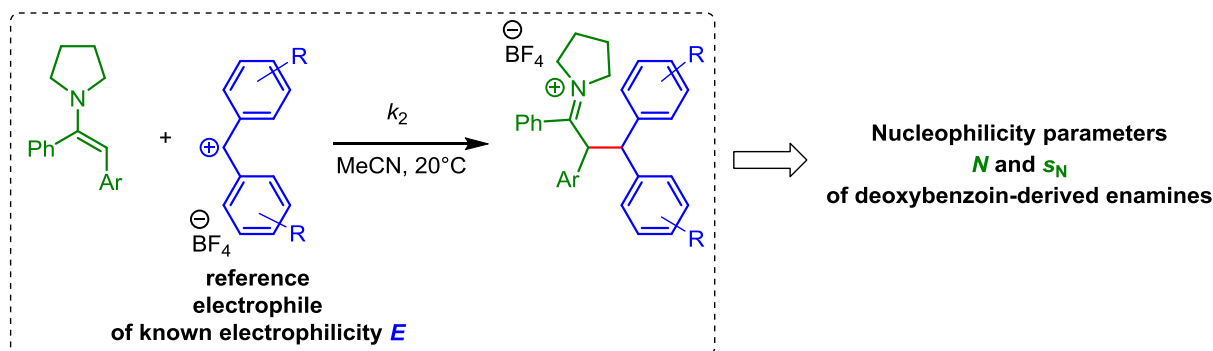
Previously characterized aminostyrenes have been used as a basis for the design of a new family of colored enamines. For this purpose, an additional aryl group was introduced at the  $\alpha$ -position and electron-withdrawing/electron-donating substituents in the  $\beta$ -phenyl ring were added to modify nucleophilicity (Scheme 5).





**Scheme 5.** Enamines employed as reference nucleophiles in this work.

By measuring the rate constants of the reactions of deoxybenzoin-derived enamines with benzhydrylium ions as reference electrophiles, one can determine the reactivity ( $N$  and  $s_N$ ) of these compounds by using eq 3 and employ them as reference nucleophiles.

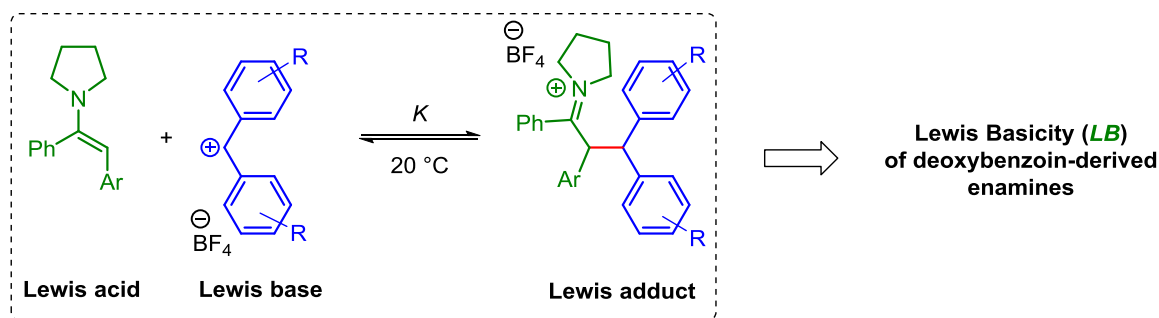


**Scheme 6.** Kinetics investigations of the reactions of deoxybenzoin-derived enamines with benzhydrylium ions as reference electrophiles.

It has been recently demonstrated that the equilibrium constants  $\lg K$  for reactions of benzhydrylium ions  $\text{Ar}_2\text{CH}^+$  with various pyridines, tertiary amines, phosphines and related Lewis bases can be calculated as the sum of a Lewis acidity parameter  $LA$  and a Lewis basicity parameter  $LB$ , as expressed by equation (4).<sup>27</sup>

$$\lg K (20^\circ\text{C}) = LA + LB \quad (4)$$

Although  $\pi_{\text{CC}}$  nucleophiles are the largest group of compounds in the nucleophilicity scale based on equation (4),<sup>6</sup> only few equilibrium constants for the reactions with benzhydrylium ions with enamines have previously been measured. However, this is the first systematic study, where the Lewis basicity of the  $\pi_{\text{CC}}$  bonds towards carbon-centered Lewis acids (for example, carbenium ions) has been quantitatively determined.

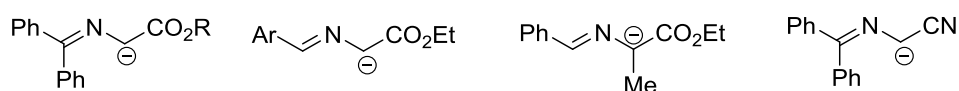


**Scheme 7.** Benzhydrylium ions as reference Lewis acids for the determination of Lewis basicities (*LB*) of the enamines.

The availability of rate and equilibrium constants allows one to calculate the corresponding Marcus intrinsic barriers  $\Delta G_0^\ddagger$  by equation (5)<sup>28</sup> and compare them with those of reactions with other types of nucleophiles.

$$\Delta G^\ddagger = \Delta_r G_0^\ddagger + \frac{1}{2} \Delta_r G^\circ + \frac{(\Delta_r G^\circ)^2}{16 \Delta_r G_0^\ddagger} \quad (5)$$

In addition, the benzhydrylium methodology should be employed for the characterization of the nucleophilic reactivities of  $\alpha$ -imino esters, which became frequently used substrates for the synthesis racemic and optically active unnatural  $\alpha$ -amino acids.<sup>29</sup> The kinetic investigations of the reactions of the potassium salts of different glycine- and alanine-derived imino esters and imino acetonitrile (Scheme 8) with quinone methides and benzylidene malonates as reference electrophiles will then allow to determine the nucleophilicity parameters *N* and *s<sub>N</sub>* of the Schiff base derivatives according to eq 3 and to compare them with the reactivity parameters of various previously published carbanions.



**Scheme 8.** Schiff base derivatives of amino acids investigated in this work.

As all parts of this thesis have already been published or submitted for publication, individual introductions will be given at the beginning of each chapter. In order to identify my contribution to the multiauthor publication described in Chapter 2: quantum chemical calculations were performed by Robert J. Mayer and the X-ray intensity data were measured by Peter Mayer.

## References

- (1) Ingold, C. K. *Chem. Rev.* **1934**, *15*, 225–274.
- (2) Swain, C. G.; Scott, C. B. *J. Am. Chem. Soc.* **1953**, *75*, 141–147.
- (3) Ritchie, C. D. *Acc. Chem. Res.* **1972**, *5*, 348–354.
- (4) Ritchie, C. *Can. J. Chem.* **1986**, *64*, 2239–2250.
- (5) Mayr, H.; Patz, M. *Angew. Chem.* **1994**, *106*, 990–1010; *Angew. Chem. Int. Ed.* **1994**, *33*, 938–957.
- (6) (a) Mayr, H.; Bug, T.; Gotta, M. F.; Hering, N.; Irrgang, B.; Janker, B.; Kempf, B.; Loos, R.; Ofial, A. R.; Remennikov, G.; Schimmel, H. *J. Am. Chem. Soc.* **2001**, *123*, 9500–9512. (b) For a comprehensive database of nucleophilicity parameters  $N$  and  $s_N$  as well as electrophilicity parameters  $E$ , see: <http://www.cup.lmu.de/oc/mayr/DBintro.html>.
- (7) (a) Lucius, R.; Loos, R.; Mayr, H. *Angew. Chem. Int. Ed.* **2002**, *41*, 91–95. (b) Lemek, T.; Mayr, H. *J. Org. Chem.* **2003**, *68*, 6880–6886. (c) Kaumanns, O.; Lucius, R.; Mayr, H. *Chem. Eur. J.* **2008**, *14*, 9675–9682. (d) Asahara, H.; Mayr, H. *Chem. Asian J.* **2012**, *7*, 1401–1407. (e) Allgäuer, D. S.; Jangra, H.; Asahara, H.; Li, Z.; Chen, Q.; Zipse, H.; Ofial, A. R.; Mayr, H. *J. Am. Chem. Soc.* **2017**, *139*, 13318–13329.
- (8) (a) Lakhdar, S.; Ammer, J.; Mayr, H. *Angew. Chem. Int. Ed.* **2011**, *50*, 9953–9956. (b) Appel, R.; Chelli, S.; Tokuyasu, T.; Troshin, K.; Mayr, H. *J. Am. Chem. Soc.* **2013**, *135*, 6579–6587. (c) An, F.; Shyeni, P.; Ammer, J.; Ofial, A. R.; Mayer, P.; Lakhdar, S.; Mayr, H. *Asian J. Org. Chem.* **2014**, *3*, 550–555.
- (9) (a) Guo, X.; Mayr, H. *J. Am. Chem. Soc.* **2013**, *135*, 12377–12387. (b) Guo, X.; Mayr, H. *J. Am. Chem. Soc.* **2014**, *136*, 11499–11512.
- (10) (a) Appel, R.; Mayr, H. *J. Am. Chem. Soc.* **2011**, *133*, 8240–8251. (b) Li, Z.; Jangra, H.; Chen, Q.; Mayer, P.; Ofial, A. R.; Zipse, H.; Mayr, H. *J. Am. Chem. Soc.* **2018**, *140*, 5500–5515.
- (11) Kanzian, T.; Mayr, H. *Chem. Eur. J.* **2010**, *16*, 11670–11677.
- (12) (a) Lakhdar, S.; Tokuyasu, T.; Mayr, H. *Angew. Chem.* **2008**, *120*, 8851–8854; *Angew. Chem. Int. Ed.* **2008**, *47*, 8723–8726. (b) Baidya, M.; Remennikov, G. Y.; Mayer, P.; Mayr, H. *Chem. Eur. J.* **2010**, *16*, 1365–1371. (c) Lakhdar, S.; Ofial, A. R.; Mayr, H. *J. Phys. Org.*

*Chem.* **2010**, 23, 886–892. (d) Kanzian, T.; Lakhdar, S.; Mayr, H. *Angew. Chem.* **2010**, 122, 9717–9720; *Angew. Chem. Int. Ed.* **2010**, 49, 9526–9529.

(13) Duan, X.-H.; Mayr, H. *Org. Lett.* **2010**, 12, 2238–2241.

(14) (a) Chambers, R. D. *Fluorine in Organic Chemistry*; Blackwell: Oxford, UK, 2004. (b) Kirsch, P. *Modern Fluoroorganic Chemistry* 2nd ed.; Wiley-VCH: Weinheim, 2013.

(15) (a) Cartwright, D. Recent Developments in Fluorine-Containing Agrochemicals. In *Organofluorine Chemistry. Principles and Commercial Applications*; Banks, R. E., Smart, B. E., Taflow, J. C., Eds.; Plenum Press: New York, 1994; pp 237–262. (b) Lang, R. W. Fluorinated Agrochemicals. In *Chemistry of Organic Fluorine Compounds II*; Hudlicky, M. Pavlath, A. E., Eds; ACS Monograph 187; American Chemical Society: Washington, DC, 1995; p 1143. (c) Jeschke, P. *ChemBioChem* **2004**, 5, 570–589. (d) Maienfisch, P.; Hall, R. G. *Chimia* **2004**, 58, 93–99. (e) Fujiwara, T.; O'Hagan, D. *J. Fluorine Chem.* **2014**, 167, 16–29.

(16) (a) Elliot, A. J. Fluorinated Pharmaceuticals. In *Chemistry of Organic Fluorine Compounds II*; Hudlicky, M.; Pavlath, A. E., Eds. ACS Monograph 187; American Chemical Society, Washington, DC, 1995. (b) Böhm, H. J.; Banner, D.; Bendels, S.; Kansy, M.; Kuhn, B.; Müller, K.; Obst-Sander, U.; Stahl, M. *ChemBioChem* **2004**, 5, 637–643. (c) Müller, K.; Faeh, C.; Diederich, F. *Science* **2007**, 317, 1881–1886. (d) Bégué, J. P.; Bonnet-Delpon D. *Bioorganic and Medicinal Chemistry of Fluorine*, Wiley: New York, 2008. (e) Tressaud, A.; G. Haufe, *Fluorine and Health – Molecular Imaging, Biomedical Materials and Pharmaceuticals*; Elsevier: Amsterdam, 2008. (f) Kirk, K. L. *Org. Process Res. Dev.* **2008**, 12, 305–321. (g) Purser, S.; Moore, P. R.; Swallow, S., Gouverneur V. *Chem. Soc. Rev.* **2008**, 37, 320–330. (h) Yerien, D. E.; Bonesi, S.; Postigo, A. *Org. Biomol. Chem.* **2016**, 14, 8398–8427.

(17) (a) Hung M. H.; Farnham, W. B.; Feiring, A. E.; Rozen, S. Functional fluoromonomers and fluoropolymers. In: *Fluoropolymers*. Hougham G., Cassidy P. E., Johns K., Davidson T. (Eds), Plenum Publishing Co, New York, 1999. (b) Wei, H. C.; Lagow, R. J. *Chem Commun.* **2000**, 21, 2139–2141. (c) Hird, M. *Chem. Soc. Rev.* **2007**, 36, 2070–2095. (d) Kirsch, P.; Binder, W.; Hahn, A.; Jährling, K.; Lenges, M.; Lietzau, L.; Maillard, D.; Meyer, V.; Poetsch, E.; Ruhl, A.; Unger G.; Fröhlich, R. *Eur. J. Org. Chem.* **2008**, 3479–3487.

(18) Chatalova-Sazepin, C.; Hemelaere, R.; Paquin, J.-F.; Sammis, G. M. *Synthesis* **2015**, 47, 2554–2569.

- (19) (a) Ni, C.; Hu, M.; Hu, J. *Chem. Rev.* **2015**, *115*, 765–825. (b) Wu, J. *Tetrahedron Lett.* **20014**, *55*, 4289–4294.
- (20) (a) Hutchinson J., Sandford G. Elemental Fluorine in Organic Chemistry. In *Organofluorine Chemistry (Topics in Current Chemistry Vol. 193)*; Chambers, R. D., Ed.; Springer: Berlin, Heidelberg, 1997; pp 1–43. (b) For a review about reagents containing the O–F group, see: Rozen, S. *Chem. Rev.* **1996**, *96*, 1717–1736.
- (21) For reviews see: (a) Lal, G. S.; Pez, G. P.; Syvret, R. G. *Chem. Rev.* **1996**, *96*, 1737–1756. (b) Taylor, S. D.; Kotoris, C. C.; Hum, G. *Tetrahedron* **1999**, *55*, 12431–12477. (c) Baudoux, J.; Cahard, D. Electrophilic Fluorination With N–F Reagents. In *Organic Reactions*; Denmark, S. E., Ed.; Wiley: Hoboken, 2007; Chapter 2, pp 347–672.
- (22) (a) Gilicinski, A. G.; Pez, G. P.; Syvret, R. G.; Lal, G. S. *J. Fluorine Chem.* **1992**, *59*, 157–162. (b) Oliver, E. W.; Evans, D. H. *J. Electroanal. Chem.* **1999**, *474*, 1–8.
- (23) Toullec, P. Y.; Devillers, I.; Frantz, R.; Togni, A. *Helv. Chim. Acta* **2004**, *87*, 2706–2711.
- (24) Xue, X.-S.; Wang, Y.; Li, M. Cheng, J.-P. *J. Org. Chem.* **2016**, *81*, 4280–4289.
- (25) (a) Differding, E.; Rüegg, G. M. *Tetrahedron Lett.* **1991**, *32*, 3815–3818. (b) Differding, E.; Wehrli, M. *Tetrahedron Lett.* **1991**, *32*, 3819–3822.
- (26) (a) Brunet, V. A.; O'Hagan, D. *Angew. Chem., Int. Ed.* **2008**, *47*, 1179–1182. (b) Cao, L. L.; Gao, B. L.; Ma, S. T.; Liu, Z. P. *Curr. Org. Chem.* **2010**, *14*, 808–916. (c) Dinér, P.; Kjærsgaard, A.; Lie, M. A.; Jørgensen, K. A. *Chem. Eur. J.* **2008**, *14*, 122–127.
- (27) Mayr, H.; Ammer, J.; Baidya, M.; Maji, B.; Nigst, T. A.; Ofial, A. R.; Singer, T. *J. Am. Chem. Soc.* **2015**, *137*, 2580–2599
- (28) (a) Marcus, R. A. *J. Chem. Phys.* **1956**, *24*, 966–978. (b) Marcus, R. A. *J. Phys. Chem.* **1968**, *72*, 891–899.
- (29) Williams, R. M. *Synthesis of Optically Active  $\alpha$ -Amino Acids*; Pergamon Press: Oxford, 1989.

## Chapter 2

## Which Factors Control the Nucleophilic Reactivities of Enamines?

Daria S. Timofeeva, Robert J. Mayer, Peter Mayer, Armin R. Ofial, and Herbert Mayr

*Chem. Eur. J.* **2018**, *24*, 5901–5910

## 2.1. Introduction

How reaction thermodynamics affects the rates of chemical reactions is a question that has intrigued chemists for almost a century. In historical order, Brønsted correlations,<sup>1</sup> Hammett equation,<sup>2</sup> Bell-Evans-Polanyi relationships,<sup>3</sup> Leffler's equation,<sup>4</sup> and Hammond's postulate<sup>5</sup> are the best known empirical correlations between rates and equilibria of chemical reactions. After developing a theory for the rates of electron transfer reactions<sup>6a</sup> Marcus reported that atom transfer reactions can be treated by the same formalism<sup>6b</sup> and introduced the concept of the “intrinsic barrier”.

According to the Marcus equation (Eq. 1), the intrinsic barrier  $\Delta_r G_0^\ddagger$  equals the Gibbs activation energy of a reaction with a Gibbs energy of reaction  $\Delta_r G^\circ = 0$ .<sup>6</sup> Zhu recently modified the Marcus approach and derived an equation which reproduces electron and group transfer reactions with high precision.<sup>7</sup>

$$\Delta G^\ddagger = \Delta_r G_0^\ddagger + \frac{1}{2} \Delta_r G^\circ + \frac{(\Delta_r G^\circ)^2}{16\Delta_r G_0^\ddagger} \quad (1)$$

Leffler's empirical relationship,<sup>4</sup> which is commonly written as Equation (2), can be integrated to give Equation (3), in which the integration constant  $C$  also represents an intrinsic barrier.

$$\delta \Delta G^\ddagger = \alpha \delta \Delta_r G^\circ \quad (2)$$

$$\Delta G^\ddagger = \alpha \Delta_r G^\circ + C \quad (3)$$

The Bell-Evans-Polanyi relationship<sup>3</sup> correlates the Arrhenius activation energy with the reaction enthalpy  $\Delta_r H^0$  and thus closely resembles Equation (3).

Numerous investigations into the relationships between rate and equilibrium constants have been reported,<sup>8</sup> and Bernasconi introduced the “Principle of Nonperfect Synchronization” to explain deviations from linear correlations between  $\Delta G^\ddagger$  and  $\Delta_r G^\circ$  by

transition-state imbalances, i.e., nonconcerted changes of reactant- and product-stabilizing factors.<sup>9</sup>

By using *para*- and *meta*-substituted benzhydrylium ions as reference electrophiles and as reference Lewis acids with variable reactivities but constant steric surroundings of the reaction center, we have investigated correlations between rate and equilibrium constants for reactions of widely different rates ranging from very slow (hours) to the diffusion limit (nanoseconds). We found that the reactions of these benzhydrylium ions with several hundreds of n,  $\sigma$  and  $\pi$  nucleophiles follow the linear free energy relationship given by Equation (4), in which  $s_N$  and  $N$  are solvent-dependent nucleophile-specific parameters and  $E$  is a solvent-independent electrophile-specific parameter.<sup>10</sup>

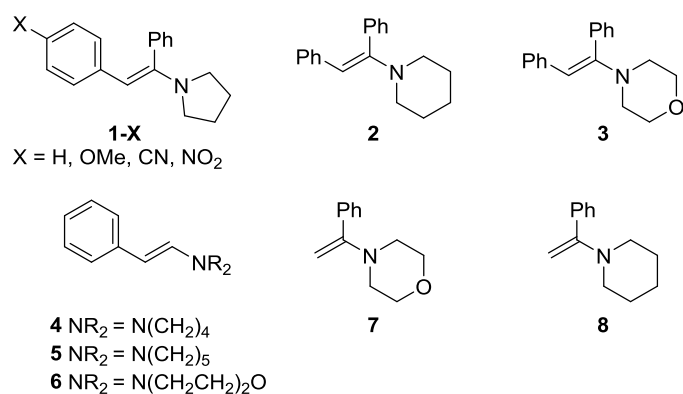
$$\lg k_2(20\text{ }^\circ\text{C}) = s_N(N + E) \quad (4)$$

Furthermore, we recently demonstrated that the equilibrium constants for the reactions of benzhydrylium ions with phosphines, pyridines, and other Lewis bases can be calculated as the sum of a Lewis acidity parameter  $LA$  and a Lewis basicity parameter  $LB$ , as expressed by Equation (5).<sup>11</sup> We now report the first determination of the Lewis basicities of a  $\pi_{CC}$  bond towards carbon-centered Lewis acids.

$$\lg K(20\text{ }^\circ\text{C}) = LA + LB \quad (5)$$

In previous work, rate and equilibrium constants were determined for reactions of benzhydrylium ions with various pyridines, tertiary amines, and phosphines and their Marcus intrinsic barriers calculated.<sup>12</sup> Although  $\pi_{CC}$  nucleophiles are the largest group of compounds in our comprehensive nucleophilicity scale based on Equation (4),<sup>13</sup> we have not measured equilibrium constants for their reactions with benzhydrylium ions so far to derive their Lewis basicities [as defined in Eq. (5)] in this way. As a consequence, a comparison of the corresponding intrinsic barriers or reorganization energies of reactions with n and  $\pi_{CC}$  nucleophiles has not been possible to date.

We now report on the measurement of the rate and equilibrium constants for the reactions of enamines<sup>14</sup> with the benzhydrylium ions **E1–E7** listed in Table 1 to derive the nucleophilic reactivities and Lewis basicities of the enamines **1–8** (Scheme 1) as well as the intrinsic barriers for these reactions. As the deoxybenzoin-derived enamines **1–3** are colored compounds ( $\lambda_{\text{max}} = 296\text{--}465\text{ nm}$ ), which will be used as references for the characterization of the electrophilicities and Lewis acidities of colorless electron-deficient species in future work, their synthesis and properties will be explicitly described in this report.

**Scheme 1.** Enamines **1–8** studied in this work.**Table 1.** Structures, absorption maxima, electrophilicities *E*, and Lewis acidities *LA* of the reference benzhydrylium ions **E** in acetonitrile solution.<sup>[a]</sup>

Electrophile		$\lambda_{\max}^{[b]}$ [nm]	<i>E</i> <sup>[b]</sup>	<i>LA</i> <sup>[c]</sup>
	<b>E1</b>	586	-3.85	-6.33
	<b>E2</b>	611	-5.53	-7.52
	<b>E3</b>	605	-7.02	-9.82
	<b>E4</b>	611	-7.69	-10.83
	<b>E5</b>	619	-8.22	-11.27
	<b>E6</b>	616	-8.76	-11.46
	<b>E7</b>	635	-9.45	-12.61
	<b>E8</b>	631	-10.04	-12.76

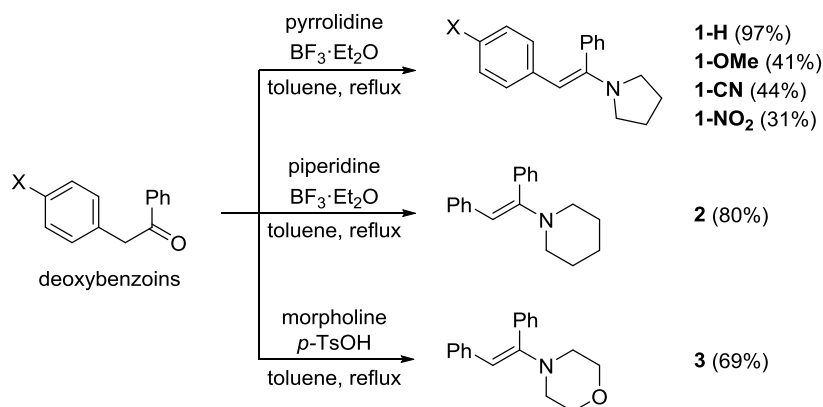
[a] With BF<sub>4</sub><sup>-</sup> as the counter ion. [b] From ref.<sup>10b</sup> [c] From ref.<sup>11</sup>



## 2.2. Results and Discussion

### 2.2.1. Synthesis of Deoxybenzoin-Derived Enamines

Enamines **1–3** were obtained by heating the corresponding deoxybenzoins and secondary amines at reflux in the presence of either 10 mol% of boron trifluoride etherate or 1 mol% of *p*-toluenesulfonic acid in dry toluene under N<sub>2</sub> using a Dean–Stark apparatus to remove the generated water (Scheme 2).<sup>15</sup> After evaporation of the solvent, enamines **1-H** and **2** were purified by distillation and all the others by recrystallization from acetonitrile.



**Scheme 2.** Synthesis of deoxybenzoin-derived enamines **1–3** (yields of the isolated enamines are given in parentheses).

Single crystals suitable for X-ray diffraction were grown by crystallization of **1-OMe**, **1-CN**, **1-NO<sub>2</sub>**, and **3** from acetonitrile solutions at −25 °C.<sup>16</sup> As shown in Figure 1 and Table 2, enamines synthesized by this method have (*E*)-configured double bonds.

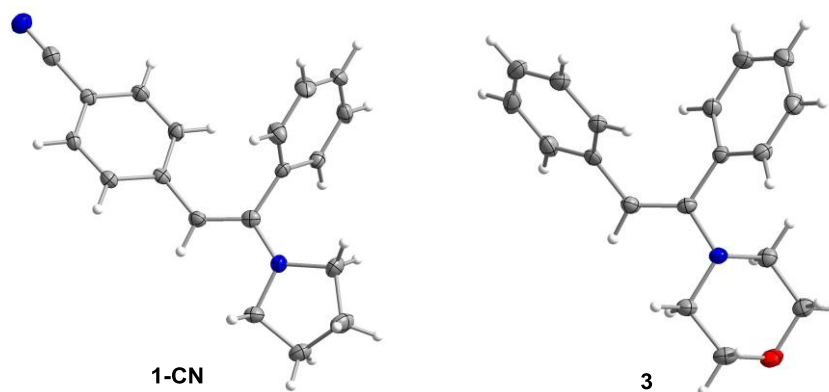
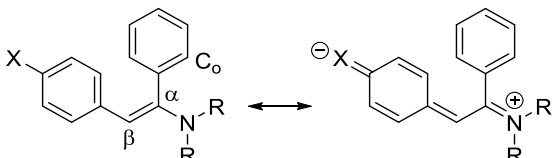


**Figure 1.** Crystal structures of the enamines **1-CN** (left) and **3** (right). Thermal ellipsoids are drawn at a 50% probability level.<sup>16</sup>

The shortened C<sub>α</sub>-N and C<sub>β</sub>-C<sub>Ar</sub> bonds and the elongated C<sub>α</sub>=C<sub>β</sub> double bonds of the acceptor-substituted enamines **1-NO<sub>2</sub>** and **1-CN** reveal an increasing contribution from the zwitterionic resonance structure. Although the β-aryl ring is almost coplanar with the olefinic

double bond (dihedral angles  $\approx 170^\circ$ ), the  $\alpha$ -phenyl group is highly twisted (dihedral angles  $\approx 115\text{--}130^\circ$ ). According to the data Table 2, the structural features of the morpholino-derived enamine **3** resemble those of the *p*-methoxy-substituted pyrrolidine derivative **1-OMe** most closely.

**Table 2.** Selected interatomic distances and dihedral angles in the solid-state structures of **1-X** and **3**.



Enamine	$C_\alpha\text{--}C_\beta$ (Å)	$C_\alpha\text{--}N$ (Å)	$C_\beta\text{--}C_{Ar}$ (Å)	$Ar\text{--}C\text{--}C\text{--}N$ ( $^\circ$ )	$Ar\text{--}C\text{--}C\text{--}Ph$ ( $^\circ$ )	$N\text{--}C_\alpha\text{--}C\text{--}C_0$ ( $^\circ$ )
<b>1-OMe</b>	1.348	1.392	1.471	−167.8	9.2	−117.2
<b>1-NO<sub>2</sub></b>	1.371	1.361	1.446	168.3	−12.6	116.6
<b>1-CN</b>	1.361	1.361	1.460	−171.4	9.2	−115.5
<b>3-cA</b> <sup>[a]</sup>	1.345	1.413	1.475	167.1	−10.5	134.2
<b>3-cB</b> <sup>[a]</sup>	1.348	1.412	1.473	168.5	−9.3	133.9

[a] Two independent molecules in the asymmetric unit of **3**.

The  $^1H$ ,  $^1H$ -NOESY spectra of the enamines reveal the proximity of the  $C_\beta$ -H and the  $N\text{--}CH_2$  protons, thereby confirming that the *E* configurations observed in the crystals also dominate in  $CD_3CN$  solution. Although the  $^1H$  and  $^{13}C$  NMR chemical shifts of the enamines **1-X** show little correlation with the electronic effect of X (Hammett  $\sigma$ ), the UV-Vis maxima of these enamines experience a strong bathochromic shift as the electron-acceptor strength of X increases (Table 3).

**Table 3.** Spectral data for enamines **1–3** (in  $CD_3CN$ )

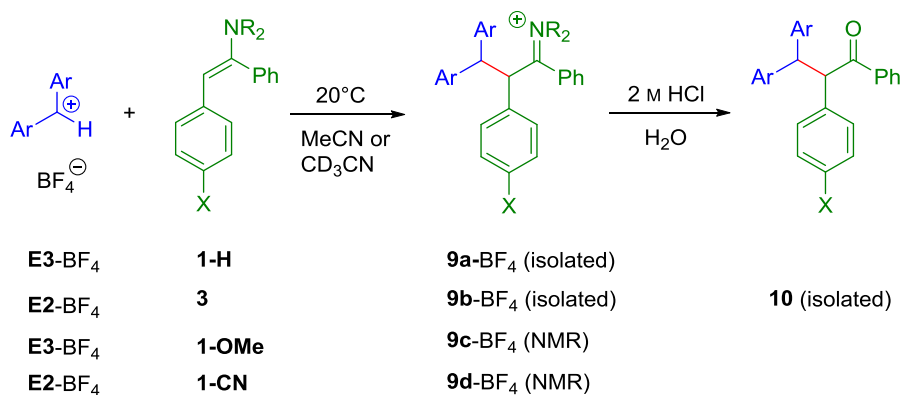
Enamine	$\lambda_{max}$ [nm]	$\delta(H_\beta)$ [ppm]	$\delta(C_\alpha)$ [ppm]	$\delta(C_\beta)$ [ppm]
<b>1-OMe</b>	298	5.32	156.8	99.8
<b>1-H</b>	317	5.34	149.5	99.8
<b>1-CN</b>	375	5.30	152.8	97.5
<b>1-NO<sub>2</sub></b>	465	5.31 <sup>[a]</sup>	152.7 <sup>[a]</sup>	97.3 <sup>[a]</sup>
<b>2</b>	316	5.62	153.0	105.7
<b>3</b>	306	5.67	152.3	106.3

[a] In  $CDCl_3$ .

### 2.2.2. Products of the Reactions of the Enamines with Benzhydrylium Ions

In analogy with the behavior of previously investigated enamines,<sup>10b,17</sup> the reactions of deoxybenzoin-derived enamines **1–3** with benzhydrylium ions led to the formation of iminium ions **9**, which were either isolated or hydrolyzed to the corresponding ketones **10**.

The combination of the enamines **1-H** and **3** with the benzhydrylium tetrafluoroborates **E3-BF<sub>4</sub>** and **E2-BF<sub>4</sub>** in acetonitrile at 20 °C and evaporation of the solvent resulted in quantitative formation of iminium salts **9a-BF<sub>4</sub>** and **9b-BF<sub>4</sub>**, respectively. The iminium salt **9b-BF<sub>4</sub>** was hydrolyzed with dilute hydrochloric acid to give the corresponding ketone **10** in a yield of 30% (with respect to **3**, Scheme 3).



**Scheme 3.** Reactions of enamines **1-X** and **3** with Benzhydrylium tetrafluoroborates **E**.

Monitoring the reactions of the enamines **1-OMe** and **1-CN** (1.05 equiv.) with **E3-BF<sub>4</sub>** and **E2-BF<sub>4</sub>** in CD<sub>3</sub>CN by <sup>1</sup>H and <sup>13</sup>C NMR spectroscopy showed the quantitative formation of the iminium tetrafluoroborates **9c-BF<sub>4</sub>** and **9d-BF<sub>4</sub>** (Scheme 3). These iminium salts decomposed during attempts to recrystallize them from a mixture of dichloromethane and n-pentane or acetone.

### 2.2.3. Kinetic Investigations

The second-order rate constants *k*<sub>2</sub> of the reactions of the enamines **1–8** with benzhydrylium ions **E** were determined photometrically in acetonitrile solution at 20 °C under pseudo-first-order conditions using a high excess (≥ 10 equiv.) of the enamines. The disappearance of the colored benzhydrylium ions was monitored by time-resolved UV-Vis spectroscopy at their maximum wavelengths λ<sub>max</sub> (Table 1). The resulting monoexponential decays of the absorbances of **E1–E7** are illustrated for the reaction of enamine **1-H** with benzhydrylium ion **E3** in Figure 2.

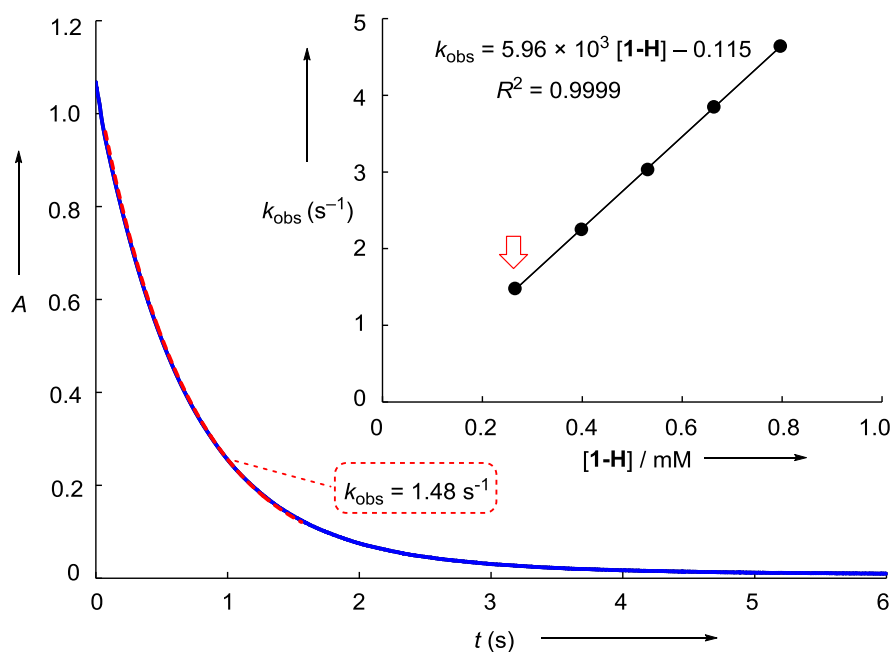


**Figure 2.** Exponential decay of the absorbance of **E3** ( $c_0 = 7.24 \times 10^{-6}$  M) at 605 nm during its reaction with enamine **1-H** ( $c_0 = 2.65 \times 10^{-4}$  M,  $k_{\text{obs}} = 1.48 \text{ s}^{-1}$ ). Inset: Correlation of the rate constants  $k_{\text{obs}}$  with  $[1\text{-H}]$  in MeCN at 20 °C. The labeled data point refers to the depicted absorption versus time trace.

The first-order rate constants  $k_{\text{obs}}$  were derived by least-squares fitting of the exponential function  $A_t = A_0 \exp(-k_{\text{obs}} t) + C$  to the time-dependent absorbances of the benzhydrylium ions **E1–E7**. Plots of  $k_{\text{obs}}$  against the concentrations of the nucleophiles were linear, as exemplified in Figure 2 (inset). The intercepts of these plots for the reactions which proceeded quantitatively were negligible, whereas positive intercepts were found for the reactions that led to equilibria, and in ideal cases, correspond to the rate constants of the backward reactions. The slopes of these plots gave the second-order rate constants  $k_2$ , which are presented in Table 4.

**Table 4.** Second-order rate constants  $k_2$  for the reactions of enamines **1–8** with benzhydrylium ions **E1–E7** in MeCN at 20 °C.

Enamine	$N (s_N)$	$\text{Ar}_2\text{CH}^+$	$k_2 (\text{M}^{-1} \text{s}^{-1})$
<b>1-H</b>	11.66 (0.82)	<b>E2</b>	$1.10 \times 10^5$
		<b>E3</b>	$5.96 \times 10^3$
		<b>E4</b>	$1.79 \times 10^3$
		<b>E5</b>	$2.13 \times 10^2$
		<b>E6</b>	$7.11 \times 10^1$
<b>1-OMe</b>	11.99 (0.84)	<b>E2</b>	$3.46 \times 10^5$
		<b>E3</b>	$1.20 \times 10^4$
		<b>E4</b>	$3.32 \times 10^3$
		<b>E5</b>	$4.87 \times 10^2$
		<b>E7</b>	$5.36 \times 10^1$
<b>1-CN</b>	10.63 (0.84)	<b>E1</b>	$4.68 \times 10^5$
		<b>E2</b>	$2.20 \times 10^4$
		<b>E3</b>	$1.03 \times 10^3$
		<b>E4</b>	$2.59 \times 10^2$
		<b>E5</b>	$3.97 \times 10^1$
<b>1-NO<sub>2</sub></b>	10.42 (0.82)	<b>E1</b>	$2.39 \times 10^5$
		<b>E2</b>	$1.23 \times 10^4$
		<b>E3</b>	$5.69 \times 10^2$
		<b>E4</b>	$1.80 \times 10^2$
<b>2</b>	9.94 (0.86)	<b>E1</b>	$1.54 \times 10^5$
		<b>E2</b>	$6.50 \times 10^3$
		<b>E3</b>	$4.03 \times 10^2$
		<b>E4</b>	$6.42 \times 10^1$
		<b>E5</b>	$1.08 \times 10^1$
<b>3</b>	8.78 (0.83)	<b>E1</b>	$1.41 \times 10^4$
		<b>E2</b>	$3.76 \times 10^2$
		<b>E3</b>	$3.51 \times 10^1$
		<b>E4</b>	7.73
<b>4<sup>[a]</sup></b>	13.87 (0.76)	<b>E3</b>	$1.68 \times 10^5$
		<b>E4</b>	$4.31 \times 10^4$
		<b>E5</b>	$6.08 \times 10^3$
		<b>E6</b>	$2.55 \times 10^3$
<b>5</b>	13.84 (0.73)	<b>E3</b>	$9.32 \times 10^4$
		<b>E4</b>	$3.02 \times 10^4$
		<b>E5</b>	$3.86 \times 10^3$
		<b>E6</b>	$1.80 \times 10^3$
<b>6</b>	11.66 (0.83)	<b>E2</b>	$1.26 \times 10^5$
		<b>E3</b>	$7.39 \times 10^3$
		<b>E4</b>	$2.00 \times 10^3$
<b>7</b>	$\approx 10.3^{[b]}$	<b>E6</b>	4.70
<b>8</b>	$\approx 11.6^{[b]}$	<b>E6</b>	$5.68 \times 10^1$

[a] Rate constants in ref <sup>18</sup> for the reactions of **4** with **E3** and **E4** were 20% smaller, and the rate constant for **4** + **E5** was 50 % smaller. The reason of these discrepancies is not known. [b] For an estimated  $s_N = 0.80$ .

Plots of the rate constants ( $\lg k_2$ ) for the reactions of the enamines with the reference benzhydrylium ions **E** versus their electrophilicities  $E$  (from Table 1) are linear (Figure 3), as required by Equation (4). The slopes of these correlations equal the nucleophile-specific parameters  $s_N$ , and the negative intercepts on the abscissa ( $\lg k_2 = 0$ ) correspond to the nucleophilicity parameters  $N$  which are listed in Table 4.

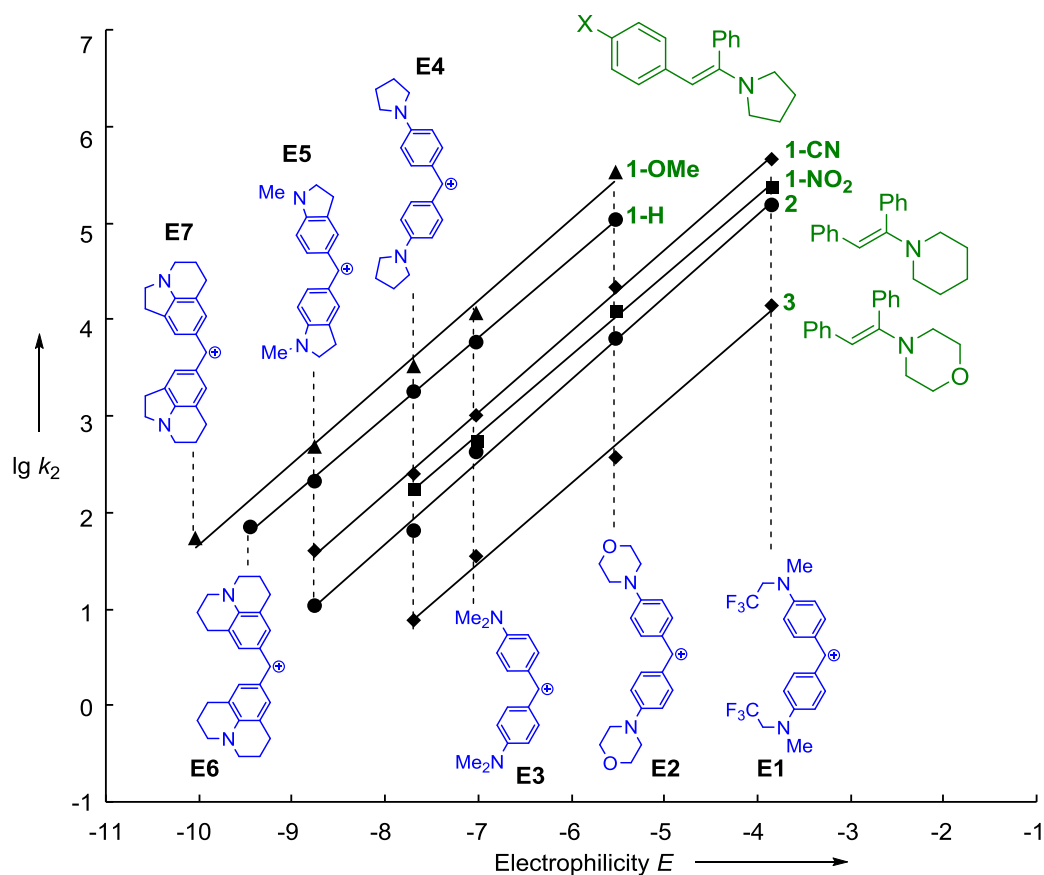


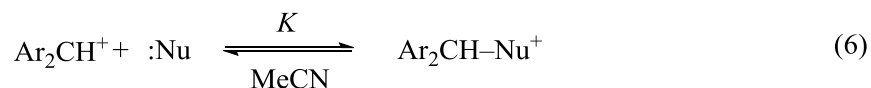
**Figure 3.** Plots of the rate constants ( $\lg k_2$ ) for the reactions of representative enamines with benzhydrylium ions **E** versus their electrophilicities  $E$  (MeCN, 20 °C).

The almost identical values of the slopes ( $0.82 \leq s_N \leq 0.86$ ) for the deoxybenzoin-derived enamines **1–3** listed in Table 4, reflected by the parallel correlation lines in Figure 3, imply that the relative reactivities of these enamines depend only little on the nature of the electrophiles. As the  $\beta$ -aminostyrenes **4** and **5** have somewhat smaller slopes, the relative reactivities **4/1-H** and **5/2** decrease slightly with increasing reactivity of the electrophilic reaction partner. The nucleophilicity parameters  $N$  of **6** and **7** have previously been reported to be 1–2 units higher in dichloromethane.<sup>17</sup>

### 2.2.4. Equilibrium Constants

As the reactions of enamines with weakly Lewis-acidic benzhydrylium ions do not go to completion, the corresponding equilibrium constants could be studied through UV-Vis spectrophotometric titration in acetonitrile solution at 20 °C. In these titrations, the enamines were added portionwise to solutions of the benzhydrylium tetrafluoroborates, and the absorbances of the benzhydrylium ions **E** were measured after each addition, as illustrated in Figure 4.

Because of the proportionality between the absorbances and the concentrations of the benzhydrylium ions in dilute solutions (Beer-Lambert law), the equilibrium constants  $K$  for the reactions in Equation (6) can be derived from the initial absorbances ( $A_0$ ) of the benzhydrylium ions and their absorbances at equilibrium ( $A_{eq}$ ) according to Equation (7).



$$K = \frac{[\text{Ar}_2\text{CH-Nu}^+]_{eq}}{[\text{Ar}_2\text{CH}^+]_{eq} [\text{Nu}]_{eq}} = \frac{A_0 - A_{eq}}{A_{eq} [\text{Nu}]_{eq}} \quad (7)$$

$$[\text{Nu}]_{eq} = [\text{Nu}]_0 - [(A_0 - A_{eq})/ed] \quad (8)$$

The plots of  $(A_0 - A_{eq})/A_{eq}$  versus the concentrations of the enamines at equilibrium [Eq. (8)] are linear (Figure 4, inset) and their slopes give the equilibrium constants  $K$ , which are summarized in Table 5. The Lewis basicities  $LB$  of the enamines were calculated from the equilibrium constants for their reactions with benzhydrylium ions in acetonitrile using Equation (5). As the  $LB$  values derived from equilibrium constants for the reactions of a certain enamine with different benzhydrylium ions differ only insignificantly (Table 5), we can conclude that Equation (5) is applicable.

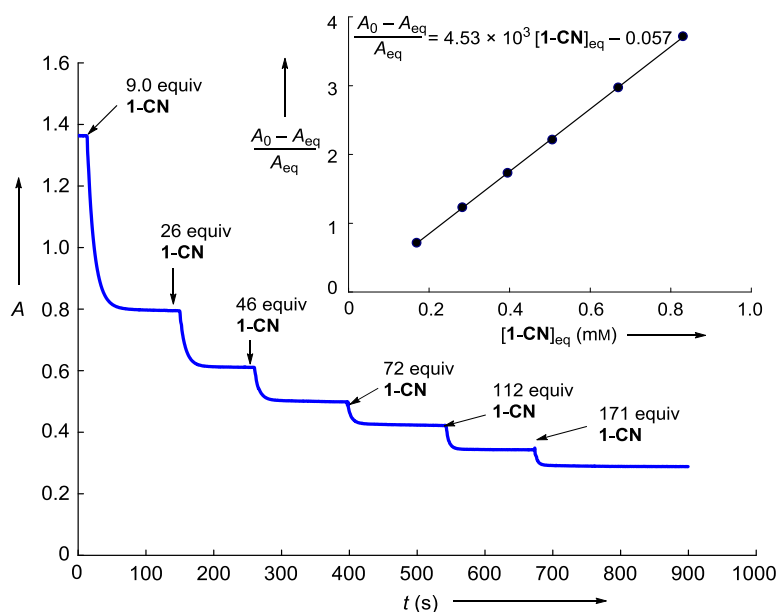


**Figure 4.** Determination of the equilibrium constant for the reaction of enamine **1-CN** with the benzhydrylium ion **E4** ( $c_0 = 1.96 \times 10^{-5}$  M) at 611 nm (MeCN, 20°C).

**Table 5.** Equilibrium constants  $K$  for the reactions of benzhydrylium ions **E** with enamines and the resulting Lewis basicity parameters  $LB$ s in MeCN at 20 °C.

Enamine	Ar <sub>2</sub> CH <sup>+</sup>	$K$ (M <sup>-1</sup> )	$LB$	$\overline{LB}$
<b>1-H</b>	<b>E5</b>	$1.11 \times 10^5$	16.50	16.50
	<b>E6</b>	$6.45 \times 10^3$	16.42	
	<b>E7</b>	$6.55 \times 10^3$	16.58	
<b>1-OMe</b>	<b>E5</b>	$3.45 \times 10^5$	17.00	16.87
	<b>E6</b>	$1.36 \times 10^4$	16.74	
	<b>E7</b>	$1.31 \times 10^4$	16.88	
<b>1-CN</b>	<b>E4</b>	$4.82 \times 10^3$	14.51	14.51
	<b>E5</b>	$1.12 \times 10^3$	14.51	
<b>1-NO<sub>2</sub></b>	<b>E3</b>	$1.93 \times 10^4$	14.10	14.07
	<b>E4</b>	$1.62 \times 10^3$	14.04	
<b>2</b>	<b>E4</b>	$2.76 \times 10^4$	15.26	15.36
	<b>E5</b>	$9.64 \times 10^3$	15.44	
<b>3</b>	<b>E3</b>	$6.00 \times 10^3$	13.60	13.49
	<b>E4</b>	$3.59 \times 10^2$	13.39	
<b>4</b>	<b>E5</b>	$1.15 \times 10^5$	16.52	16.43
	<b>E6</b>	$5.09 \times 10^3$	16.32	
	<b>E7</b>	$4.81 \times 10^3$	16.44	
<b>5</b>	<b>E5</b>	$1.47 \times 10^5$	16.63	16.60
	<b>E6</b>	$8.16 \times 10^3$	16.52	
	<b>E7</b>	$8.03 \times 10^3$	16.66	
<b>6</b>	<b>E3</b>	$7.77 \times 10^4$	14.71	14.65
	<b>E4</b>	$5.78 \times 10^3$	14.59	
<b>7</b>	<b>E6</b>	$3.1 \times 10^{5[a]}$	≈18.1	
<b>8</b>	<b>E6</b>	$1.1 \times 10^{6[a]}$	≈18.7	

[a] Approximate values, because the determination of such large equilibrium constants is less reliable. Weaker Lewis acids, such as **E7**, cannot be used either, because they react so slowly.



### 2.2.5. Quantum Chemical Calculations

Previous investigations have shown that experimental Lewis basicities *LB*s for various classes of nucleophiles correlate well with their corresponding quantum chemically calculated gas phase methyl cation affinities (MCAs).<sup>19</sup> Therefore, the MCAs of the enamines **1–8** were calculated as Gibbs energies  $\Delta G_{298}$  of methyl cation detachment reactions, as depicted in Table 6, by applying the B3LYP/6-311++G(3df,2pd)//B3LYP/6-31G(d,p) level of theory in gas phase with the Gaussian software package.<sup>20–22</sup>

As depicted in Figure S4 in Experimental Section, the plot of gas phase MCAs against the Lewis basicities shows separate linear correlations for the deoxybenzoin-derived enamines **1–3** and  $\beta$ -aminostyrenes **4–6**. However, when solvent effects were included by performing single-point calculations with the SMD solvation model for acetonitrile<sup>23</sup> on the gas phase optimized structures (Table 6), all enamines **1–8** followed the same correlation (see Figure S5 in the Experimental Section).

Analogously, benzhydryl cation affinities (BHCAs) were calculated as Gibbs energies of the dissociation reactions of the benzhydrylium ion adducts (Table 6). Figure 5 illustrated that the calculated BHCA values of enamines **1–8** in acetonitrile solution correlate linearly with their experimental Lewis basicities *LB* (from Table 5).

**Table 6.** Calculated Methyl Cation Affinities (MCA) and Benzhydryl Cation Affinities (BCA) of enamines **1–8** in gas-phase and in solution (SMD = acetonitrile) at the B3LYP/6-311++G(3df,2pd)//B3LYP/6-31G(d,p) level (in kJ mol<sup>-1</sup>).

$  \begin{array}{c}  \text{R}' \\    \\  \text{R}''-\text{C}=\text{N}^+\text{R}_2 \\    \\  \text{CH}_3  \end{array}  \xrightarrow[\text{= MCA}]{\Delta G_{298}}  \begin{array}{c}  \text{R}' \\    \\  \text{R}''-\text{C}=\text{NR}_2  \end{array}  + \text{CH}_3^+  $				
$  \begin{array}{c}  \text{R}' \\    \\  \text{R}''-\text{C}=\text{N}^+\text{R}_2 \\    \\  \text{Ph}-\text{C}^+-\text{Ph}  \end{array}  \xrightarrow[\text{= BHCA}]{\Delta G_{298}}  \begin{array}{c}  \text{R}' \\    \\  \text{R}''-\text{C}=\text{NR}_2  \end{array}  + \text{Ph}-\text{C}^+-\text{Ph}  $				
Enamine	MCA (gas phase)	MCA (SMD = MeCN)	BHCA (gas phase)	BHCA (SMD = MeCN)
<b>1-H</b>	528.5	360.5	72.6	42.9
<b>2</b>	518.8	351.7	63.8	36.7
<b>3</b>	501.5	342.5	49.1	29.0
<b>4</b>	501.2	350.6	63.9	51.9
<b>5</b>	505.7	354.7	68.9	56.8
<b>6</b>	485.9	344.8	50.3	46.3
<b>7</b>	515.2	370.2	85.5	75.5
<b>8</b>	541.4	386.1	101.9	85.4

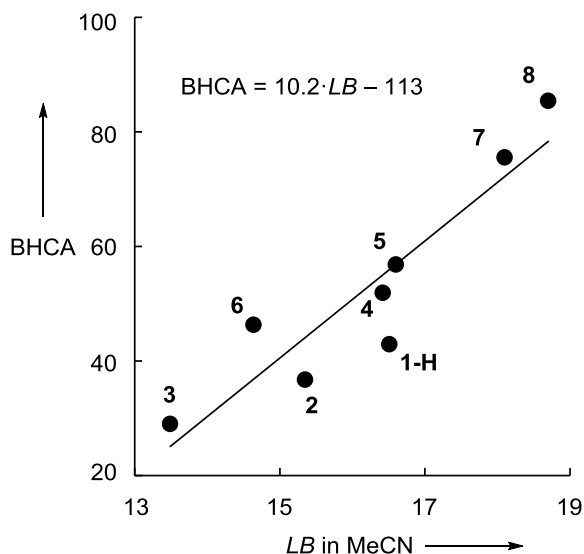


**Figure 5.** Correlation of the benzhydryl cation affinities (BHCA, in  $\text{kJ mol}^{-1}$ ) of enamines **1–8** calculated at the B3LYP/6-311++G(3df,2pd)//B3LYP/6-31G(d,p) level of theory in solution (SMD = acetonitrile) with their Lewis basicities (LB) in acetonitrile ( $R^2 = 0.8456$ ).

### 2.2.6. Discussion

Let us first turn to the question of whether the rate constants determined by our kinetic experiments reflect the direct attack of the benzhydrylium ions at the  $\beta$ -carbon atom or whether we are measuring the rate of attack at the enamine nitrogen to give vinylammonium ions, which rearrange to the NMR-observed iminium ions in a subsequent step. In previous work<sup>24</sup> we have shown that neither *N*-methylpiperidine nor *N*-methylpyrrolidine give adducts with **E4** and less Lewis-basic benzhydrylium ions. Because the replacement of the *N*-methyl group in these two tertiary amines by a vinyl group to give an enamine would reduce the Lewis basicity of the nitrogen, one can conclude that the vinylammonium ions generated by attack of weakly Lewis-basic benzhydrylium ions ( $LA < -9$ ) certainly cannot accumulate during these reactions.

This conclusion was confirmed by another argument. In the preceding section we showed that most of the investigated reactions of benzhydrylium ions with enamines **1–8**, which give iminium ions, are only weakly exergonic. As the *C*-methylation of vinyl amine was calculated to be  $61 \text{ kJ mol}^{-1}$  more exergonic than *N*-methylation,<sup>25</sup> all reactions yielding vinylammonium ions from **E1–E7** and the enamines **1–8** must be highly endergonic. The two arguments do not exclude that attack at the nitrogen is also occurring during the kinetically investigated reactions. The concentrations of the reversibly formed vinylammonium ions would be so low,

however, that their formation would not affect the kinetics, and there is no doubt that the measured rate constants refer to electrophilic attack at the carbon center of the enamines.

Tables 4 and 5 show that nucleophilicities and Lewis basicities of the pyrrolidino-substituted enamines **1-X** increase with increasing electron-donating ability of the *para* substituent X. Replacement of hydrogen by the electron-donating methoxy group increases the nucleophilic reactivity toward various benzhydrylium ions by a factor of two to three, whereas the electron-accepting nitro group reduces the reactivity by a factor of 10 ( $\pm 1$ ). The Hammett plots for the rate and equilibrium constants for the reactions of enamines **1-X** with **E4** versus  $\sigma_p^-$ <sup>26</sup> give the reaction constants of  $\rho = -0.83$  and  $\rho = -1.89$ , respectively, which indicates that the equilibrium constants are more affected by variation of the substituents than the rate constants (Figure 6). The corresponding Hammett plots versus  $\sigma_p$  (see Figure S2 in the Experimental Section) give slightly greater reaction constants of  $\rho = -1.22$  (for  $\lg k_2$ ) and  $\rho = -2.76$  (for  $\lg K$ ), but the correlation of the equilibrium constants versus  $\sigma_p$  is of somewhat lower quality. Because of the paucity of data, a Yukawa-Tsuno analysis was not attempted.

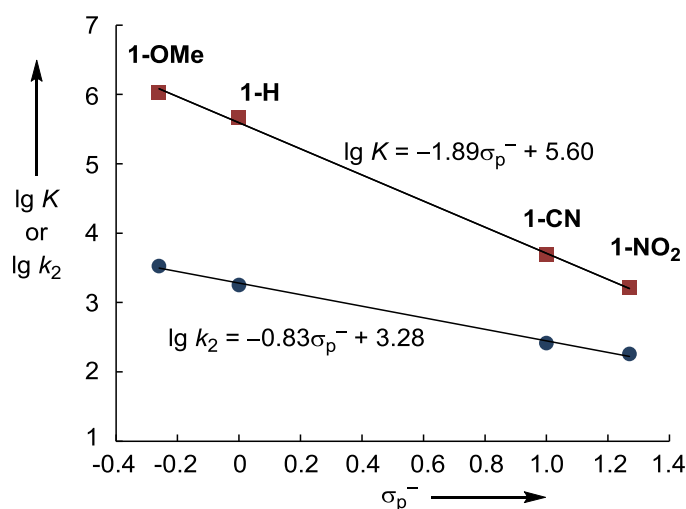


**Figure 6.** Correlation of the rate ( $\lg k_2$ ) and equilibrium constants ( $\lg K$ ) of the reactions of **1-X** with the benzhydrylium ion **E4** with Hammett  $\sigma_p^-$  values for the substituents X (MeCN, 20 °C).<sup>26</sup>

The Leffler-Hammond coefficient  $\alpha = \Delta(\lg k_2)/\Delta(\lg K) = 0.44$  for the reactions of **1-X** with **E4** (Figure 7), which equals the ratio of the two Hammett plots in Figure 6, shows that 44% of the effects that the substituents exert on the equilibrium constants are reflected by the differences of the activation energies.

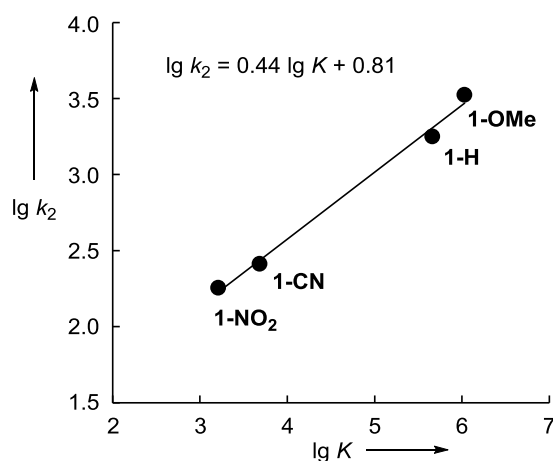


**Figure 7.** Correlation of the rate constants ( $\lg k_2$ , from Table 4) for the reactions of **1-X** with **E4** with the corresponding equilibrium constants ( $\lg K$ , from Table 5).

As illustrated by Figure 8a, the  $\beta$ -piperidino- and  $\beta$ -morpholinostyrenes **5** and **6** are more Lewis-basic than the corresponding deoxybenzoin-derived enamines **2** and **3**, respectively, in line with the calculated benzhydryl cation affinities (BHCA, Figure 8b). Clearly, the steric strain introduced by the extra  $\alpha$ -phenyl group in the products obtained from **2** and **3** cannot be compensated by the electron-releasing effect of the  $\alpha$ -phenyl group, which is almost perpendicular to the  $\pi$  system of the resulting iminium ion according to our calculations. The fact that the Lewis basicities as well as the BHCA of the morpholino derivatives **3** and **6** are 8 to 11 kJ mol<sup>-1</sup> smaller than those of the corresponding piperidino derivatives **2** and **5**, respectively, can be explained by the inductive electron-withdrawing effect of oxygen in the morpholino compounds.

The piperidino and pyrrolidino groups have different effects in the deoxybenzoin and in the  $\beta$ -aminostyrene series, however; whereas piperidinostyrene **5** has almost the same Lewis basicity  $LB$  and even a slightly higher calculated BHCA than the corresponding pyrrolidinostyrene **4**, experiments and calculations agree that this ordering is reversed in the deoxybenzoin series, in which the pyrrolidino enamine **1-H** is a stronger Lewis base than the piperidino enamine **2** ( $\Delta LB = 1.2$  corresponding to 6.8 kJ mol<sup>-1</sup> =  $1.2 \times 2.30RT$ ), close to the difference in the calculated BHCA (6.2 kJ mol<sup>-1</sup>). The same trends are seen in a natural bond orbital (NBO) analysis<sup>27</sup> (see Figures S17 and S18 in the Experimental Section): From the charge density at the iminium carbon one can deduce that the piperidino ring is a better electron donor than the pyrrolidino moiety in the iminium ions obtained from **4** and **5**, whereas the relative electron-donating abilities of the two heterocycles is opposite in the iminium ions formed from **1-H** and **2**, that is, in this pair pyrrolidine is a better electron donor

than piperidine. The reduced electron donating ability of the piperidino group in the iminium ion derived from **2** may be due to steric effects: Although the dihedral angle  $\text{H}_2\text{C-N=C-C}_{\text{Ar}}$  is smaller than  $2^\circ$  in two iminium ions derived from **4** and **5** as well as in the pyrrolidino species from **1-H**, the angle is  $6^\circ$  in the iminium ion derived from **2**.

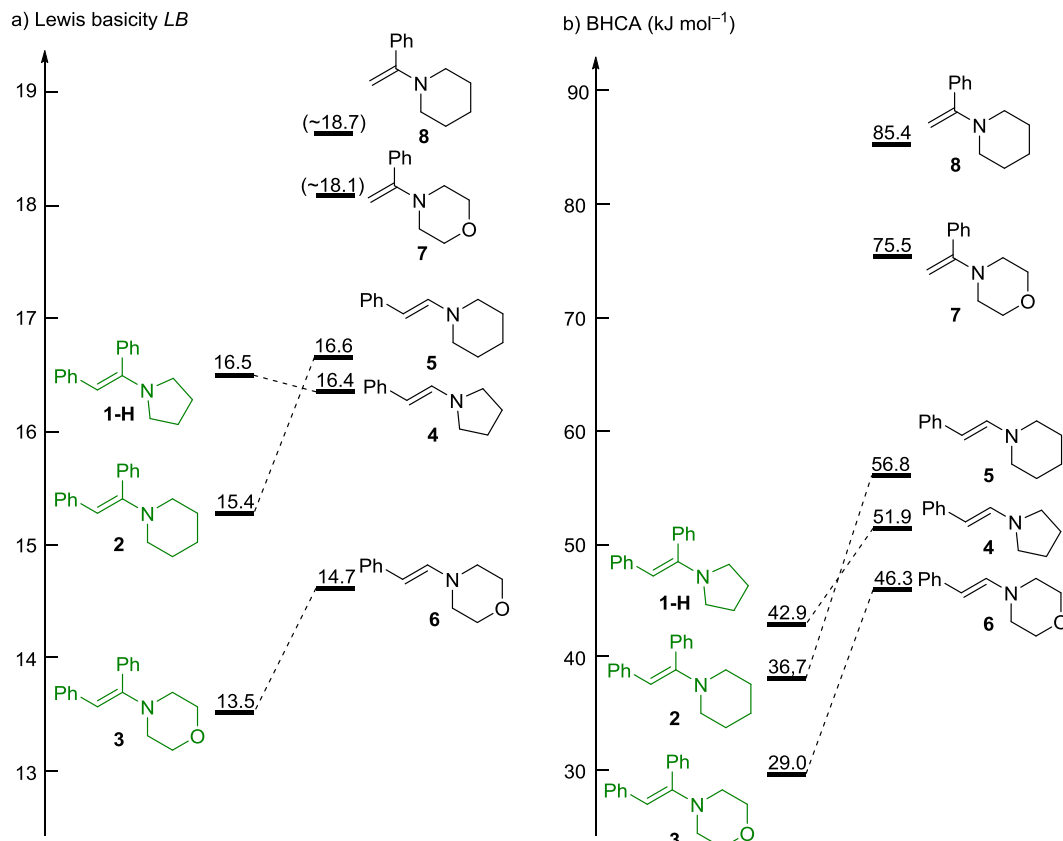


**Figure 8.** Comparison of the a) Lewis basicities and b) calculated BHCA (SMD = acetonitrile) of deoxybenzoin-derived enamines **1**–**3** with those of aminostyrenes **4**–**8**.

Removal of the  $\beta$ -phenyl group from **2** and **3** to give the corresponding  $\alpha$ -aminostyrenes **8** and **7**, respectively, leads to an increase of the Lewis basicity by 3 to 5 orders of magnitude, due to reduction of steric strain in the products, which is also reflected by the computationally determined BHCA (Figure 8). However, the *LB* values of **7** and **8** are only approximations, because benzhydrylium ions that react with reasonable rates give products almost quantitatively, whereas benzhydrylium ions, which form equilibrium mixtures with comparable concentrations of reactants and products, react so slowly that measurements of the equilibrium constants are problematic.

The availability of rate and equilibrium constants for several reactions of enamines with benzhydrylium ions now allows one to calculate the Marcus intrinsic barriers  $\Delta G_0^\ddagger$  by

Equation (1) and compare them with those of reactions with other types of nucleophiles (Table 7).

**Table 7.** Calculation of the intrinsic barriers  $\Delta G_0^\ddagger$  for the reactions of the enamines **1–8** with benzhydrylium ions in MeCN at 20 °C (all Gibbs energies in kJ mol<sup>−1</sup>)

Nu	E	$K$ (M <sup>−1</sup> )	$k_2$ (M <sup>−1</sup> s <sup>−1</sup> )	$\Delta_r G^0$	$\Delta G^\ddagger$	$\Delta G_0^\ddagger$
<b>1-H</b>	<b>E5</b>	$1.11 \times 10^5$	$2.13 \times 10^2$	−28.3	58.7	72.2
	<b>E6</b>	$6.45 \times 10^3$	$7.11 \times 10^1$	−21.4	61.4	71.7
<b>1-OMe</b>	<b>E5</b>	$3.45 \times 10^5$	$4.87 \times 10^2$	−31.1	56.7	71.4
	<b>E7</b>	$1.31 \times 10^4$	$5.36 \times 10^1$	−23.1	62.1	73.2
<b>1-CN</b>	<b>E4</b>	$4.82 \times 10^3$	$2.59 \times 10^2$	−20.7	58.2	68.2
	<b>E5</b>	$1.12 \times 10^3$	$3.97 \times 10^1$	−17.1	62.8	71.1
<b>1-NO<sub>2</sub></b>	<b>E3</b>	$1.93 \times 10^4$	$5.69 \times 10^2$	−24.1	56.3	67.8
	<b>E4</b>	$1.62 \times 10^3$	$1.80 \times 10^2$	−18.0	59.1	67.8
<b>2</b>	<b>E4</b>	$2.76 \times 10^4$	$6.42 \times 10^1$	−24.9	61.6	73.5
	<b>E5</b>	$9.64 \times 10^3$	$1.08 \times 10^1$	−22.4	66.0	76.7
<b>3</b>	<b>E3</b>	$6.00 \times 10^3$	$3.51 \times 10^1$	−21.2	63.1	73.3
	<b>E4</b>	$3.59 \times 10^2$	7.73	−14.3	66.8	73.8
<b>4</b>	<b>E5</b>	$1.15 \times 10^5$	$6.08 \times 10^3$	−28.4	50.5	63.9
	<b>E6</b>	$5.09 \times 10^3$	$2.55 \times 10^3$	−20.8	52.6	62.6
<b>5</b>	<b>E5</b>	$1.47 \times 10^5$	$3.86 \times 10^3$	−29.0	51.6	65.3
	<b>E6</b>	$8.16 \times 10^3$	$1.80 \times 10^3$	−22.0	53.5	64.0
<b>6</b>	<b>E3</b>	$7.77 \times 10^4$	$7.39 \times 10^3$	−27.4	50.0	63.0
	<b>E4</b>	$5.78 \times 10^3$	$2.00 \times 10^3$	−21.1	53.2	63.3
<b>7</b>	<b>E6</b>	$3.1 \times 10^5$	4.70	−31	68.0	≈ 83
<b>8</b>	<b>E6</b>	$1.1 \times 10^6$	$5.68 \times 10^1$	−34	61.9	≈ 78

When the intrinsic barrier  $\Delta G_0^\ddagger$  for the reaction of a certain enamine with different benzhydrylium ions was considered, one generally observes a slight increase of  $\Delta G_0^\ddagger$  in the order **E3** ≈ **E4** < **E6** ≈ **E5** < **E7**. Because the same ordering was previously observed for the reactions of these benzhydrylium ions with pyridines, imidazoles, and tertiary amines, these differences reflect variations in the reorganization energies ( $\lambda = 4\Delta G_0^\ddagger$ ) of the different benzhydrylium ions.<sup>12</sup> As a consequence, only intrinsic barriers for reactions with the same electrophile can be compared when examining the relationship between enamine structure and intrinsic barrier.

Figure 9 illustrates that the intrinsic barriers for the deoxybenzoin-derived enamines **1–3** as well as for the  $\beta$ -aminostyrenes **4–6** generally increase in the order pyrrolidine < piperidine ≈ morpholine. One can furthermore see that the intrinsic barriers  $\Delta G_0^\ddagger$  for the  $\beta$ -aminostyrenes **4–6** are 8–12 kJ mol<sup>−1</sup> smaller (Figure 9), while those for the  $\alpha$ -aminostyrenes **7** and **8** are 5–

10 kJ mol<sup>-1</sup> larger (Table 7) than those for the corresponding deoxybenzoin-derived enamines **1–3**.

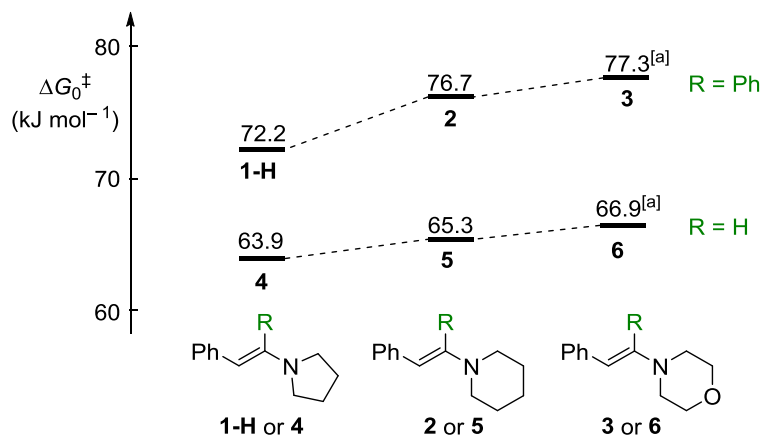


**Figure 9.** Comparison of the intrinsic barriers  $\Delta G_0^\ddagger$  for the reactions of enamines **1–6** towards benzhydrylium ion **E5**. [a] Rate and equilibrium constants,  $k_2$  and  $K$ , were calculated according to Equations (4) and (5) based on the  $N$  ( $s_N$ ) and  $LB$  values from Tables 4 and 5 and then applied in equation (1) to derive  $\Delta G_0^\ddagger$ .

On this basis, a profound analysis of the nucleophilic reactivities of the enamines **1–8** becomes possible. The nucleophilicity ordering morpholino < piperidino < pyrrolidino in the series **3** < **2** < **1-H** and **6** < **4**  $\approx$  **5** (Figure 10) is predominantly controlled by thermodynamics (Figure 8) though slightly enhanced by intrinsics (Figure 9).

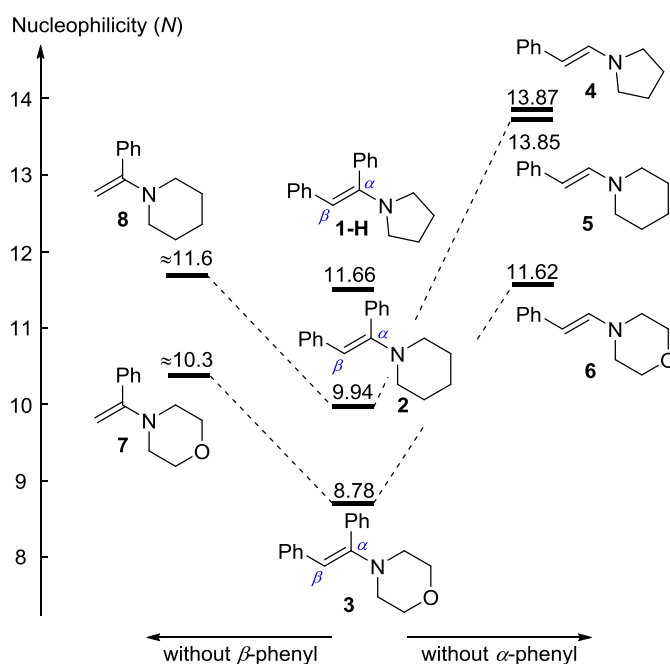


**Figure 10.** Comparison of the nucleophilicities  $N$  of deoxybenzoin-derived enamines **1–3** with those of aminostyrenes **4–8**.

Removal of the  $\alpha$ -phenyl group (**2**→**5**, **3**→**6**) leads to a significant increase of nucleophilicity (by 3 lg  $k$  units, Figure 10), much more than the increase in Lewis basicity (by 1.2 lg  $K$  units, Figure 8a), because the thermodynamic effect is enhanced by the simultaneous decrease of the intrinsic barrier (Figure 9). Because **1-H** and **4** have equal Lewis basicities (Figure 8a), the higher nucleophilicity of the latter (Figure 10) is an entirely intrinsic effect (Figure 9). The dependence of the relative activation of the enamine double bond by pyrrolidino and piperidino groups on the substitution of the double bond has previously been observed for cyclopentanone- and cyclohexanone-derived enamines.<sup>17a</sup> As shown in the Figure 11, pyrrolidinocyclohexene is 33 times more nucleophilic towards **E6** than the corresponding piperidino compound, whereas this difference is reduced to a factor of 7 in the sterically less demanding cyclopentene series.

Removal of the  $\beta$ -phenyl group from the deoxybenzoin-derived enamines **2** and **3** to give **8** and **7**, respectively, increases the nucleophilic reactivity by less than two logarithmic units (Figure 10). Thus, the high increase of Lewis basicity from **2** and **3** to **8** and **7** (Figure 8a), respectively, is largely counterbalanced by the much larger intrinsic barrier for the reactions of **7** and **8** with benzhdrylium ions.

### 2.3. Conclusion

Although changes in  $\Delta G^0$  can unambiguously be assigned to the difference in the thermodynamic stabilities of reactants and products, changes in  $\Delta G^\ddagger$ , that is, kinetic effects, can have a dual origin. As expressed by the Marcus equation, changes in activation Gibbs energies can either be due to changes in the thermodynamic driving force  $\Delta G^0$  or to a truly kinetic, so-called intrinsic effect, that is, a change in  $\Delta G_0^\ddagger$ . We have reported here one of the very few reaction series for which this analysis is possible, because rate and equilibrium constants could be measured.

For the reactions of a series of enamines with benzhdrylium ions, we have shown that the unambiguous interpretation of the origin of structural effects on reaction rates requires a separation of the thermodynamic and intrinsic contributions. This is even more important when the reactivity of structurally diverse nucleophiles is compared.

Figure 12a shows, for example, that the depicted enamines are weaker nucleophiles than the tertiary amines, pyridines, and imidazoles shown in this graph, although the Lewis basicities of these enamines are comparable to those of the strongest nitrogen bases depicted (Figure 12b). Figure 12c shows the reason of this change. The enamines react with higher



intrinsic barriers, which reduce their nucleophilicity. Because the intrinsic barriers are related to Marcus' reorganization energies  $\lambda$  by the relationship  $\Delta G_0^\ddagger = \lambda/4$ ,<sup>6</sup> their ordering can be rationalized. The tertiary amines react with the lowest intrinsic barriers, because their alkylation requires no reorganization of  $\pi$  electrons. Pyridine has a higher intrinsic barrier, which is further increased by a strong mesomeric electron donor, such as the 4-dimethylamino group in 4-dimethylaminopyridine, which enhances the geometrical changes during alkylation of the pyridine nitrogen. Electrophilic attack at the enamines as well as at *N*-methylimidazole is accompanied by changes of bond orders and associated reorganization of solvent molecules resulting in high intrinsic barriers.

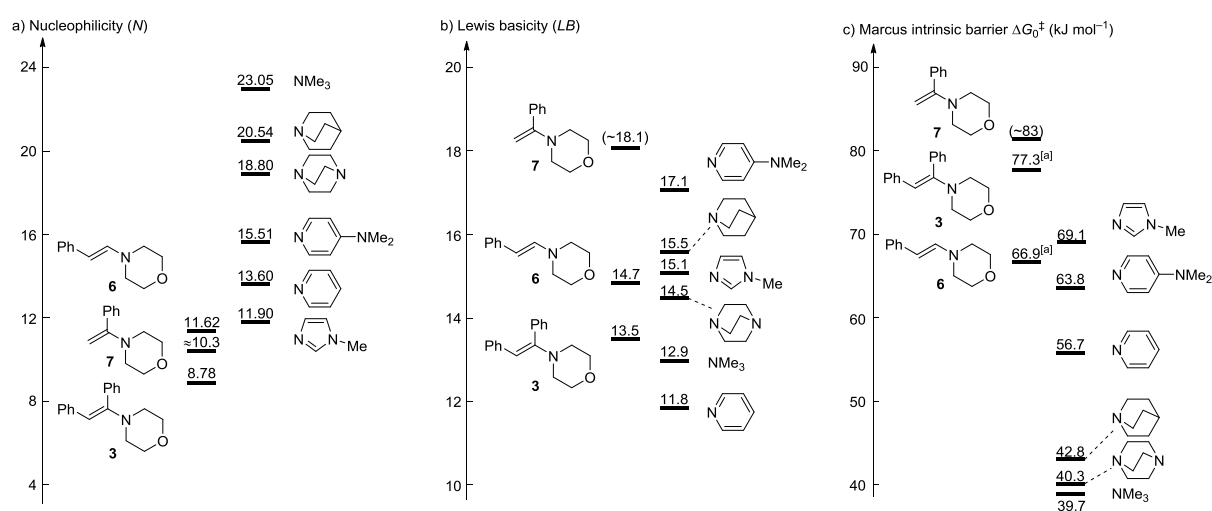


**Figure 12.** Comparison of the a) nucleophilicities, b) Lewis basicities, and c) and intrinsic barriers for the reactions with **E5** with the corresponding descriptors for *tert.* amines,<sup>11,12a,28</sup> pyridines,<sup>11,12a,19g</sup> and imidazoles.<sup>11,12b</sup> [a] Intrinsic barriers were extrapolated according to footnote [a] of Figure 9.

In view of these data, one can expect that electrophilic attack at the enamine nitrogen should also have a low intrinsic barrier. Although the Lewis basicity of the enamine nitrogen is much lower than that of the enamine  $\pi_{CC}$  bond, one cannot exclude that the enamines are initially attacked at nitrogen to give vinyl ammonium ions. From the monoexponential decays observed in the kinetic investigations one can derive, however, that attack at the nitrogen (if it occurs) is so highly reversible that it does not affect the kinetic investigations. Attack at the nitrogen atom in enamines has been observed, however, in reactions with alkyl and allyl halides, when the vinylammonium ions are formed by irreversible processes.<sup>25</sup>

## 2.4. Supplementary Section.

### 2.4.1. Analysis by Leffler's Correlation.

As described in the introduction, the constant  $C$  in eq 3 corresponds to the intrinsic barrier of a reaction series. It has previously been reported that electrophilicities ( $\Delta G^\ddagger$ ) are linearly correlated with Lewis acidities ( $\Delta_r G^\circ$ ) in a wide reactivity range (e.g. 13 LA units).<sup>29</sup> However, deviations are observed in narrow reactivity ranges, for example for electrophiles **E4–E5**, which have similar Lewis acidities but different electrophilicities.

Leffler's intrinsic barriers  $C = \Delta G_0^\ddagger(\text{Leffler})$  were derived in the following way. Figure 13 shows the plots of the rate constants ( $\lg k_2$ ) for the reactions of a certain enamine with a series of benzhydrylium ions **E** versus the corresponding equilibrium constants ( $\lg K$ ). The slopes of these correlations correspond to the Leffler-Hammond coefficient  $\alpha = \Delta(\lg k_2)/\Delta(\lg K)$  and the intercepts ( $\lg K=0$ ) correspond to the rate constants of the reaction without a thermodynamic driving force ( $\Delta_r G^\circ = 0$ ) (Table 8). As shown in Table 8, the intrinsic barriers based on Leffler's relationship are generally 2–7 kJ mol<sup>-1</sup> higher than the Marcus intrinsic barriers.

**Table 8.** Second-order rate constants  $k_2$  for reactions without thermodynamic driving force ( $\Delta_r G^\circ = 0$ ) and comparison of the corresponding intrinsic barriers based on Leffler's relationship with those derived from the Marcus equation.

Enamine	$\lg k_2$ ( $\Delta G^\circ=0$ )	$k_2$ ( $\Delta_r G^\circ = 0$ ), M <sup>-1</sup> s <sup>-1</sup>	$\Delta G_0^\ddagger(\text{Leffler})$ , kJ mol <sup>-1</sup>	$\Delta G_0^\ddagger(\text{Marcus})$ , kJ mol <sup>-1</sup>
<b>1-H</b>	-0.59	$2.57 \times 10^{-1}$	75.1	<b>E5</b> 72.2
				<b>E6</b> 71.7
<b>1-OMe</b>	-1.20	$6.31 \times 10^{-2}$	78.5	<b>E5</b> 71.4
				<b>E7</b> 73.2
<b>1-CN</b>	-0.47	$3.39 \times 10^{-1}$	74.4	<b>E4</b> 68.2
				<b>E5</b> 71.1
<b>1-NO2</b>	-0.04	$9.12 \times 10^{-1}$	72.0	<b>E3</b> 67.8
				<b>E4</b> 67.8
<b>2</b>	-1.69	$2.04 \times 10^{-2}$	81.2	<b>E4</b> 73.5
				<b>E5</b> 76.7
<b>3</b>	-0.94	$1.15 \times 10^{-1}$	77.0	<b>E3</b> 73.3
				<b>E4</b> 73.8
<b>4</b>	0.85	7.08	67.0	<b>E5</b> 63.9
				<b>E6</b> 62.6
<b>5</b>	0.68	4.79	67.9	<b>E5</b> 65.3
				<b>E6</b> 64.0
<b>6</b>	1.27	$1.86 \times 10^1$	64.6	<b>E3</b> 63.0
				<b>E4</b> 63.3

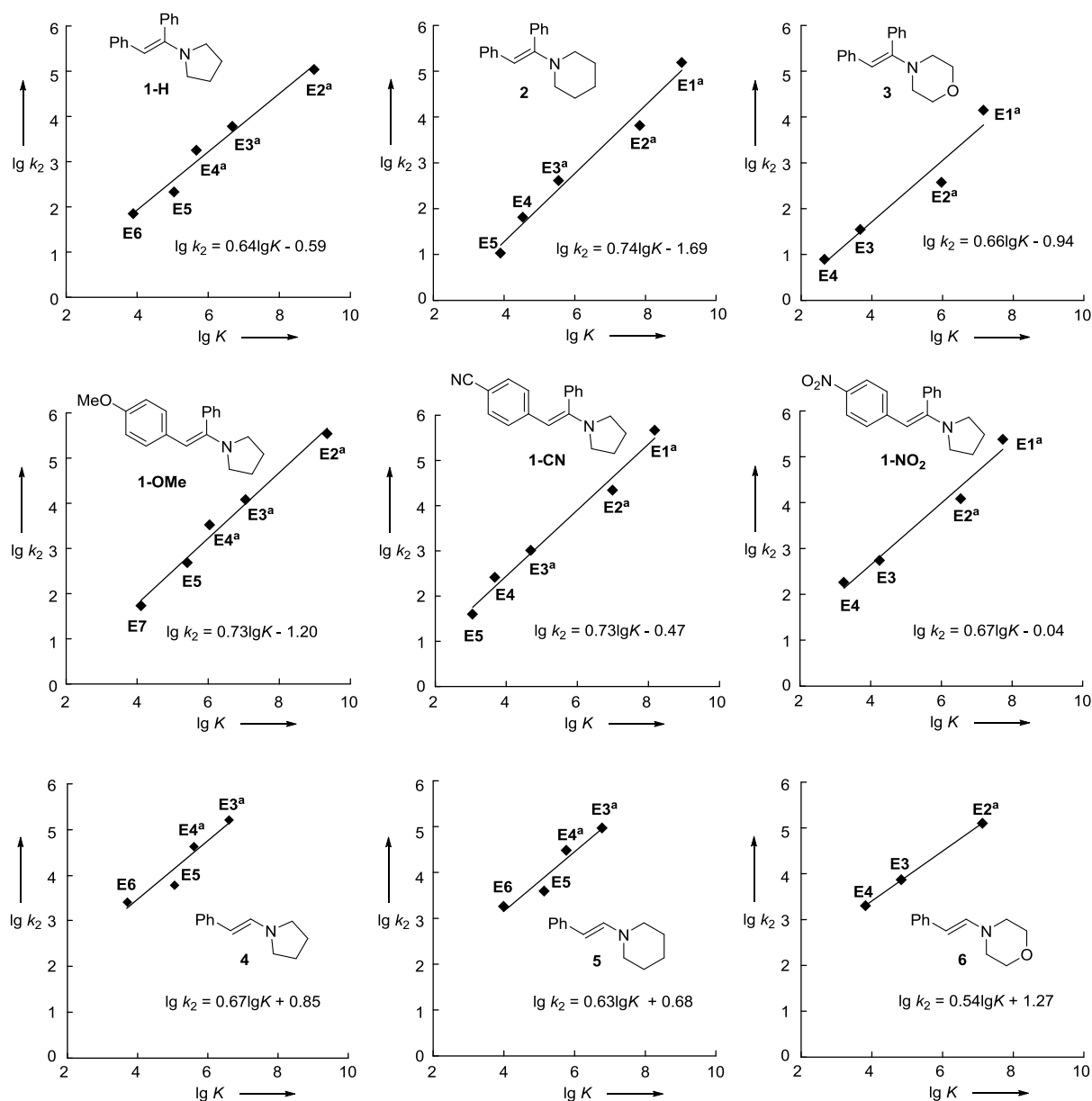


**Figure 13.** Correlation of the rate constants ( $\lg k_2$ , from Table 4) for the reactions of enamines **1**–**6** with benzhydrylium ions **E** with the corresponding equilibrium constants ( $\lg K$ ).  
[a] Calculated using eq 5.

## 2.4.2. Determination of the Nucleofugality of the Enamines.

Nucleofugality and electrofugality are kinetic terms describing leaving group abilities. They are related to the kinetic terms nucleophilicity and electrophilicity and the thermodynamic terms Lewis basicity and Lewis acidity, respectively. A linear free energy relationship (eq 9) analogous to eq 4 was developed by the groups of Mayr and Kronja.<sup>30</sup> In this approach, the rates of bond heterolyses are correlated with two solvent-dependent nucleofuge-specific parameters  $s_f$  and  $N_f$  and one solvent-independent electrofuge-specific parameter  $E_f$ .

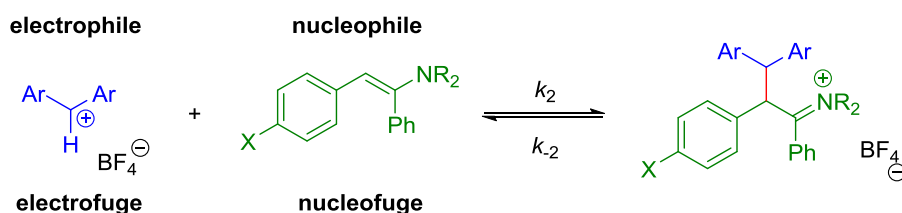
$$\lg k(25\text{ }^\circ\text{C}) = s_f(N_f + E_f) \quad (9)$$

By using benzhydrylium ions of variable stabilization as reference electrofuges, it was possible to compare nucleofugalities of anions and neutral leaving groups in different solvents over a wide range of nucleofugality.<sup>31</sup>

Electrofuge <sup>[a]</sup>		$E_f$ <sup>[b]</sup>
	<b>E3</b>	4.84
	<b>E4</b>	5.35
	<b>E5</b>	4.83
	<b>E6</b>	5.61
	<b>E7</b>	5.05

[a] With  $\text{BF}_4^-$  as the counter ion. [b] From ref. 31

**Table 9.** Electrofugality ( $E_f$ ) of the reference benzhydrylium ions **E**.



**Scheme 4.** Reactions of enamines with benzhydrylium ions.

The availability of second-order rate constants  $k_2$  as well as the corresponding equilibrium constants  $K$  for several reactions of enamines with benzhydrylium ions (Scheme 4) now allows one to calculate the heterolysis rate constant  $k_{-2}$  by using eq 10 (Table 10).

$$k_{-2} = k_2 / K \quad (10)$$

Plots of these rate constants ( $\lg k_{-2}$ ) for the heterolytic cleavage of the iminium ions formed from **1-8** and benzhydrylium ions **E** versus the electrofugalities of the benzhydrylium ions **E** (from Table 9) are linear (Figure 14), as required by eq 9. The nucleofugality parameters  $N_f$

are then obtained as the negative intercepts on the abscissa ( $E_f$  axis) and the  $s_f$  parameters correspond to the slopes of these correlations.

**Table 10.** Determination of the rate constants  $k_2$  for the heterolysis of the iminium ions formed from **1–8** and benzhydrylium ions **E** in MeCN (20 °C).

Enamine	$N_f(s_f)$	Electrophile	$K (M^{-1})$	$k_2 (M^{-1} s^{-1})$	$k_2 (s^{-1})$
<b>1-H</b>	-7.63 (0.97)	<b>E5</b>	$1.11 \times 10^5$	$2.13 \times 10^2$	$1.92 \times 10^{-3}$
		<b>E6</b>	$6.45 \times 10^3$	$7.11 \times 10^1$	$1.10 \times 10^{-2}$
		<b>E7</b>	$6.55 \times 10^3$	$2.14 \times 10^1$	$3.27 \times 10^{-3}$
<b>1-OMe</b>	-7.55 (1.01)	<b>E5</b>	$3.45 \times 10^5$	$4.87 \times 10^2$	$1.41 \times 10^{-3}$
		<b>E6</b>	$1.36 \times 10^4$	$1.36 \times 10^2$	$1.00 \times 10^{-2}$
		<b>E7</b>	$1.31 \times 10^4$	$5.36 \times 10^1$	$4.09 \times 10^{-3}$
<b>1-CN</b>	-9.00 <sup>[a]</sup> (0.35)	<b>E4</b>	$4.82 \times 10^3$	$2.59 \times 10^2$	$5.37 \times 10^{-2}$
		<b>E5</b>	$1.12 \times 10^3$	$3.97 \times 10^1$	$3.54 \times 10^{-2}$
<b>1-NO2</b>	-6.19 (1.13)	<b>E3</b>	$1.93 \times 10^4$	$5.69 \times 10^2$	$2.95 \times 10^{-2}$
		<b>E4</b>	$1.62 \times 10^3$	$1.80 \times 10^2$	$1.11 \times 10^{-1}$
<b>2</b>	-9.67 <sup>[a]</sup> (0.61)	<b>E4</b>	$2.76 \times 10^4$	$6.42 \times 10^1$	$2.33 \times 10^{-3}$
		<b>E5</b>	$9.64 \times 10^3$	$1.08 \times 10^1$	$1.12 \times 10^{-3}$
<b>3</b>	-6.85 (1.11)	<b>E3</b>	$6.00 \times 10^3$	$3.51 \times 10^1$	$5.85 \times 10^{-3}$
		<b>E4</b>	$3.59 \times 10^2$	7.73	$2.15 \times 10^{-2}$
<b>4</b>	-5.83 (1.17)	<b>E5</b>	$1.15 \times 10^5$	$6.08 \times 10^3$	$5.29 \times 10^{-2}$
		<b>E6</b>	$5.09 \times 10^3$	$2.55 \times 10^3$	$5.01 \times 10^{-1}$
		<b>E7</b>	$4.81 \times 10^3$	$8.14 \times 10^2$	$1.69 \times 10^{-1}$
<b>5</b>	-6.17 (1.12)	<b>E5</b>	$1.47 \times 10^5$	$3.86 \times 10^3$	$2.63 \times 10^{-2}$
		<b>E6</b>	$8.16 \times 10^3$	$1.80 \times 10^3$	$2.21 \times 10^{-1}$
		<b>E7</b>	$8.03 \times 10^3$	$5.94 \times 10^2$	$7.40 \times 10^{-2}$
<b>6</b>	-5.77 (1.10)	<b>E3</b>	$7.77 \times 10^4$	$7.39 \times 10^3$	$9.51 \times 10^{-2}$
		<b>E4</b>	$5.78 \times 10^3$	$2.00 \times 10^3$	$3.46 \times 10^{-1}$
<b>7</b>	ca. -10.4	<b>E6</b>	$3.1 \times 10^5$	4.70	$1.52 \times 10^{-5}$
<b>8</b>	ca. -9.9-	<b>E6</b>	$1.1 \times 10^6$	$5.68 \times 10^1$	$5.16 \times 10^{-5}$

[a] Nucleofugality parameters  $N_f$  are considered to be unreliable, because of the significantly smaller slopes

As the 2-point correlation for the compounds **1-CN** and **2** have significantly smaller slopes, the corresponding nucleofugality parameters  $N_f$  are considered to be unreliable and not used in the comparison. Table 10 shows that nucleofugalities for the deoxybenzoin-derived enamines **2** < **1-H** < **3** as well as for the  $\beta$ -aminostyrenes **5** < **4** < **6** generally increase in the order piperidine < pyrrolidine < morpholine. Removal of the  $\beta$ -phenyl group from the deoxybenzoin-derived enamines **3** to give **7** leads to a significant increase of nucleofugality (by 3 lg  $k$  units), while the removal of the  $\alpha$ -phenyl group (**3**→**6**) decreases the nucleofugality by less than two logarithmic units.

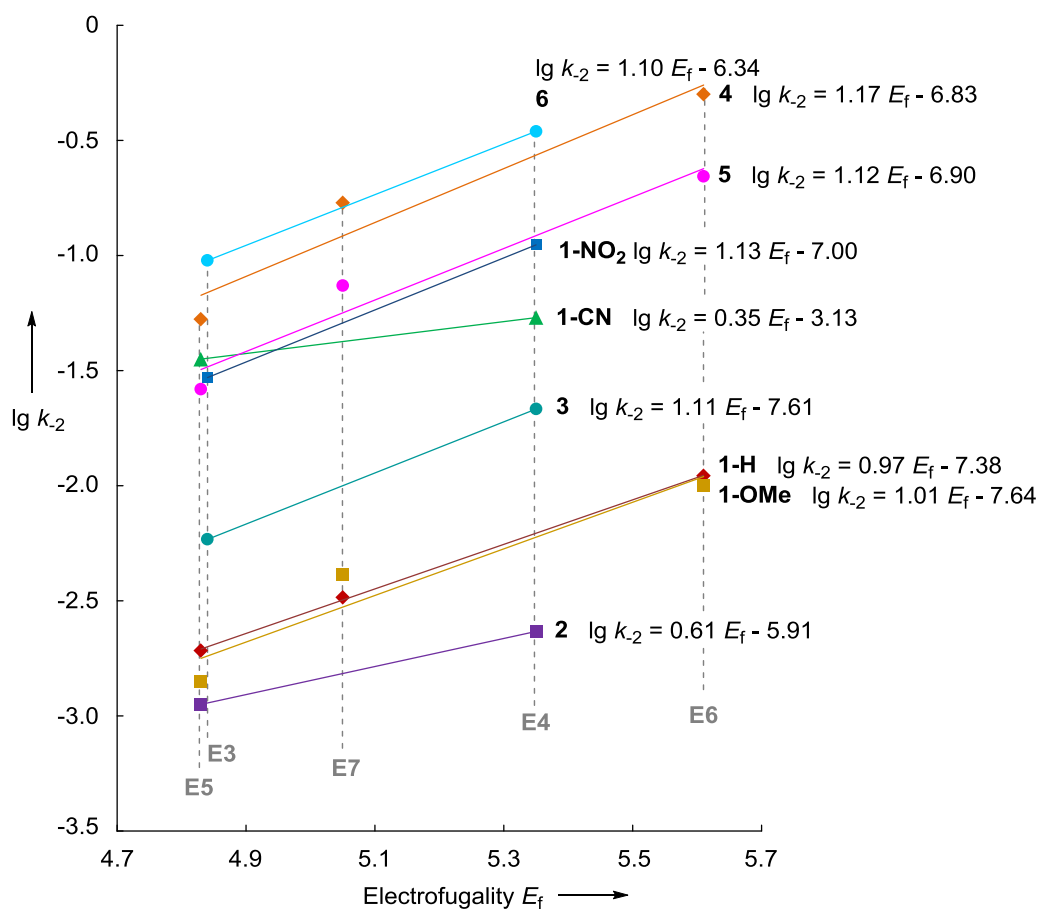


**Figure 14.** Plots of the rate constants  $k_2$  (at 20 °C) of the heterolysis of iminium ions formed from **1-8** and benzhydrylium ions **E** against the electrofugality parameters  $E_f$  of the benzhydrylium ions **E**.

Figure 15 compares the leaving group abilities (nucleofugalities) of enamines with those of tertiary amines, pyridines. One can see that the depicted enamines are weaker nucleofuges than the tertiary amines, pyridines, and imidazoles shown in this graph. This observation is in line with earlier conclusions for nucleophilic reactivities (Figure 12a), since a change of the intrinsic barrier affects forward and backward reactions in the same sense.

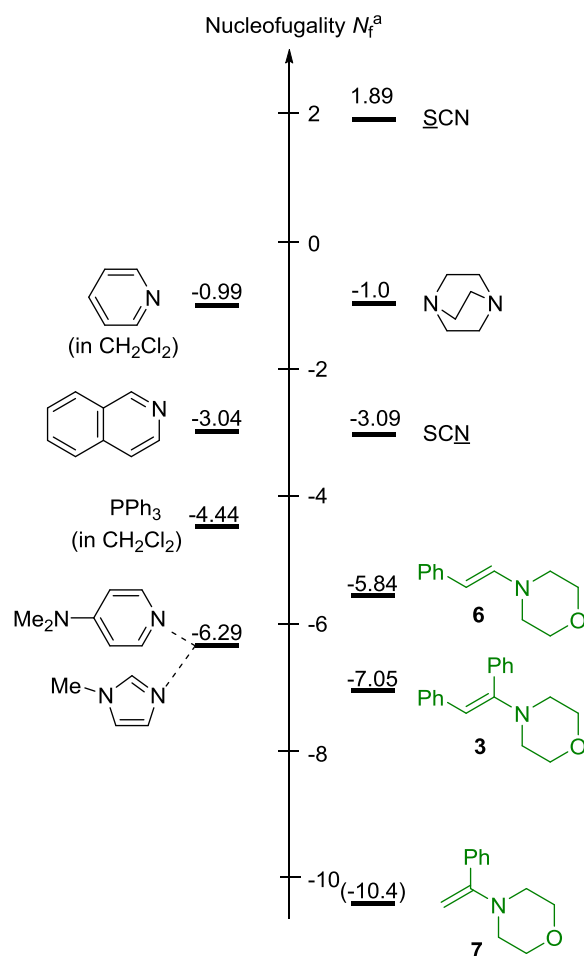


**Figure 15.** Comparison of the nucleofugality parameters  $N_f$  of various nucleofuges (Determined at 20 °C in acetonitrile unless noted otherwise).

## 2.5. Experimental Section.

### 2.5.1. General

#### Materials

All solvents were of p.a. quality and were dried by standard procedures prior to use. Commercially available MeCN (Acros Organics, H<sub>2</sub>O content < 50 ppm) was used without further purification. Unless otherwise specified, materials were obtained from commercial sources and used without further purification. The reference electrophiles used in this work were synthesized according to literature procedures.<sup>10b</sup> Enamines **4-6** were synthesized from phenylacetaldehyde according to a reported method.<sup>32</sup> Acetophenone derived enamines **7** and **8** were synthesized according to a reported method.<sup>33</sup> Deoxybenzoin-derived enamines **1-3** were synthesized from the corresponding ketones and amines as described in Section 2.5.2. Deoxybenzoin was purchased Sigma Aldrich, all other methoxy-, cyano-, nitro-substituted deoxybenzoins were prepared following the literature.<sup>34</sup> All reactions were performed in carefully dried Schlenk glassware under N<sub>2</sub> atmosphere.

#### Analytics

<sup>1</sup>H-NMR (400 MHz) and <sup>13</sup>C-NMR (100 MHz) were recorded on Varian or Bruker NMR spectrometers. The chemical shifts are given in ppm and refer to the solvent residual signal as internal standard ( $\delta_{\text{H}}$  (CDCl<sub>3</sub>) = 7.26,  $\delta_{\text{C}}$  (CDCl<sub>3</sub>) = 77.16 ppm;  $\delta_{\text{H}}$  (CD<sub>3</sub>CN) = 1.94,  $\delta_{\text{C}}$  (CD<sub>3</sub>CN) = 1.32, 118.26 ppm).<sup>35</sup> The following abbreviations were used for signal multiplicities: s = singlet, d = doublet, t = triplet, q = quartet, bs = broad signal. Signal assignments are based on additional 2D-NMR experiments (COSY, HSQC, and HMBC). High-resolution mass spectra (HRMS) were obtained by using a Thermo Finnigan LTQ FT (ESI) or a Thermo Finnigan MAT 95 instrument (EI). Melting points were determined on a Büchi B-540 and are not corrected. UV-vis spectra of enamines were recorded by using a J&M TIDAS diode array spectrometer controlled by Labcontrol spectacle software and connected to a Helma 661.502-QX quartz suprasil immersion probe (5 mm light path) via fiber optic cables and standard SMA connectors.

The X-ray intensity data were measured on a Bruker D8 Venture TXS system equipped with a multilayer mirror optics monochromator and a Mo K $\alpha$  rotating-anode X-ray tube ( $\lambda$  = 0.71073 Å) at a temperature of 100 K (**1-OMe**, **1-NO<sub>2</sub>**, **3**) or 123 K (**1-CN**). The frames were integrated with the Bruker SAINT software package using a narrow-frame algorithm.<sup>36</sup> Data



were corrected for absorption effects using the Multi-Scan method (SADABS).<sup>37</sup> The structures were solved and refined using the Bruker SHELXTL Software Package.<sup>38</sup>

### Kinetics

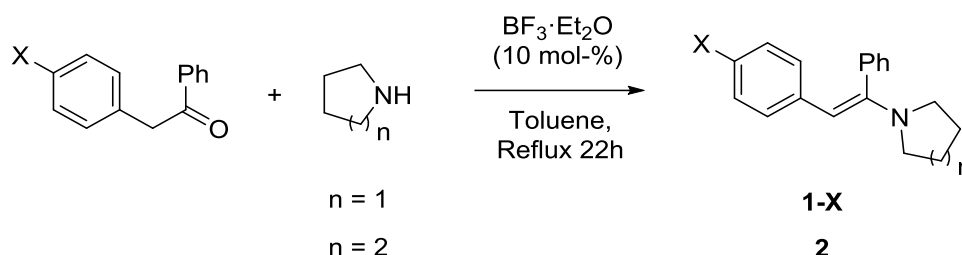
The rates of all investigated reactions between enamines and benzhydrylium ions were determined photometrically. The kinetics of fast reactions were monitored using stopped-flow techniques (Applied Photophysics SX.18MV-R). Slow reactions ( $\tau_{1/2} > 100$  s) were determined by using a J&M TIDAS diode array spectrometer controlled by Labcontrol spectacle software and connected to a Helma 661.502-QX quartz suprasil immersion probe (5 mm light path) via fiber optic cables and standard SMA connectors. All kinetic measurements were carried out in MeCN (Acros Organics, H<sub>2</sub>O content < 50 ppm) under exclusion of moisture (N<sub>2</sub> atmosphere). The temperature of all solutions was kept constant at  $20.0 \pm 0.1$  °C by using a circulating bath thermostat. In all runs the concentration of the enamine was at least 8 times higher than the concentration of the benzhydrylium ion **E**, resulting in pseudo-first-order kinetics with an exponential decay of the concentration of the reference electrophile. First-order rate constants  $k_{\text{obs}}$  [s<sup>-1</sup>] were obtained by least-squares fitting of the absorbances to a single-exponential  $A_t = A_0 \exp(-k_{\text{obs}}t) + C$  (average from 3 to 10 kinetic runs for each nucleophile concentration). The second-order rate constants  $k_2$  were obtained from the slopes of the linear plots of  $k_{\text{obs}}$  against the concentration of the excess components (typically 3 to 6 different concentrations were used for this evaluation).

### Photometric Determination of Equilibrium Constants

The equilibrium constants  $K$  for the reactions of enamines **1–8** (Lewis bases) with benzhydrylium ions **E** (Lewis acids) were determined photometrically by monitoring the decays of the Lewis acids at  $\lambda_{\text{max}}$ . The measurements were carried out using a J&M TIDAS diode array spectrophotometer, which was controlled by Labcontrol Spectacle software and connected to a Hellma 661.502-QX quartz Suprasil immersion probe (light path  $d = 5$  mm) via fiber optic cables and standard SMA connectors. When a small volume of a stock solution of the Lewis base (in MeCN) was added to a solution of the stable benzhydrylium tetrafluoroborate **E** (in MeCN) the absorbance gradually decreased from a constant  $A_0$ . After a few seconds, when the equilibrium was reached, the absorbances became constant ( $A_{\text{eq}}$ ) and another portion of the stock solution was added. This procedure (titration experiment) was repeated several times for each benzhydrylium salt solution and the averaged  $K$  values are calculated and reported with their standard deviation (Table S107).

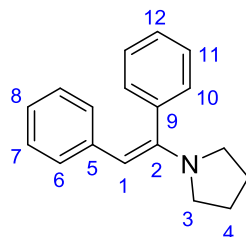
## 2.5.2. Synthesis of Enamines 1-3

General procedure for pyrrolidine and piperidine derived enamines 1-X and 2 (GP1)<sup>15a</sup>



A mixture of the ketone (1 equiv.), pyrrolidine (4 equiv.), and boron trifluoride etherate (10 mol-%) in anhydrous toluene (100 mL) was refluxed for 20 h under nitrogen in a two-necked flask fitted with a Dean-Stark water separator. The mixture was concentrated in vacuum and the residue was purified either by distillation (**1-H** and **2**) or recrystallization from MeCN at -25 °C (**1-OMe**, **1-CN**, **1-NO<sub>2</sub>**).

**(E)-1-(1,2-Diphenylvinyl)pyrrolidine (1-H)** was prepared according to GP1 from deoxybenzoin (3.0 g, 15 mmol), pyrrolidine (5.0 mL, 60 mmol), and boron trifluoride etherate (0.19 mL, 1.5 mmol) to give a yellow oil (3.70 g, 97%) after distillation. The <sup>1</sup>H and <sup>13</sup>C NMR spectra are in agreement with those described in ref 15a.



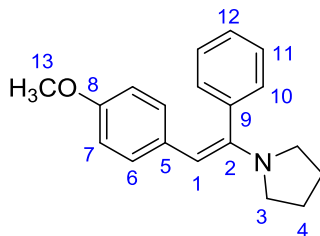
**b.p.** 132-135 °C ( $2 \times 10^{-2}$  mbar);

**<sup>1</sup>H NMR** (400 MHz, CD<sub>3</sub>CN):  $\delta$  = 7.39–7.37 (m, 3H, H-11 and H-12), 7.26–7.23 (m, 2H, H-10), 6.92–6.89 (m, 2H, H-7), 6.80–6.76 (m, 1H, H-8), 6.64–6.62 (m, 2H, H-6), 5.34 (s, 1H, H-1), 3.05–3.01 (m, 4H, H-3), 1.88–1.85 (m, 4H, H-4);

**<sup>13</sup>C {<sup>1</sup>H} NMR** (101 MHz, CD<sub>3</sub>CN):  $\delta$  = 149.5 (C-2), 141.0 (C-9), 139.5 (C-5), 130.5 (C-6), 129.7 (C-7), 128.9 (C-8), 128.6 (C-11), 128.2 (C-10), 123.5 (C-12), 99.8 (C-1), 49.4 (C-3), 25.7 (C-4);

**HRMS** (EI):  $m/z$  calculated for C<sub>18</sub>H<sub>18</sub>N<sup>+</sup> [M-H]<sup>+</sup>: 248.1434; found: 248.1429.

**(E)-1-(2-(4-Methoxyphenyl)-1-phenylvinyl)pyrrolidine (1-OMe)** was prepared according to GP1 from the *p*-methoxy-substituted deoxybenzoin (507 mg, 2.24 mmol), pyrrolidine (0.74 mL, 8.9 mmol), and boron trifluoride etherate (30  $\mu$ L, 0.24 mmol) to give pale pink needles (256 mg, 41%) after recrystallization from acetonitrile solution at -25 °C.



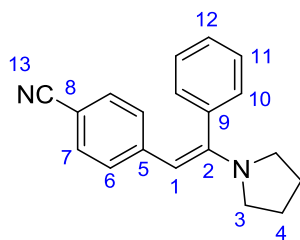
**m.p.** 92–94 °C

**$^1\text{H}$  NMR** (400 MHz,  $\text{CD}_3\text{CN}$ ):  $\delta$  = 7.38–7.35 (m, 3H, H-11 and H-12), 7.25–7.22 (m, 2H, H-10), 6.59–6.55 (m, 2H, H-7), 6.53–6.49 (m, 2H, H-6), 5.32 (s, 1H, H-1), 3.64 (s, 3H, H-13), 3.01–2.97 (m, 4H, H-3), 1.88–1.84 (m, 4H, 4H, H-4).

**$^{13}\text{C}\{^1\text{H}\}$  NMR** (101 MHz,  $\text{CD}_3\text{CN}$ ):  $\delta$  = 156.8 (C-8), 148.3 (C-2), 139.6 (C-9), 133.3 (C-5), 130.6 (C-11), 129.5 (C-10), 129.3 (C-6), 128.7 (C-12), 114.1 (C-7), 99.8 (C-1), 55.6 (C-13), 49.4 (C-3), 25.5 (C-4).

**HRMS** (EI):  $m/z$  calculated for  $\text{C}_{19}\text{H}_{21}\text{NO}^{+}$   $[M]^{+}$ : 279.1618; found: 279.1615.

**(E)-4-(2-Phenyl-2-(pyrrolidin-1-yl)vinyl)benzonitrile (1-CN)** was prepared according to GP1 from the *p*-cyano-substituted deoxybenzoin (333 mg, 1.51 mmol), pyrrolidine (0.50 mL, 6.0 mmol), and boron trifluoride etherate (20  $\mu$ L, 0.16 mmol) to give a yellow powder (184 mg, 44%) after recrystallization from acetonitrile solution at -25 °C.



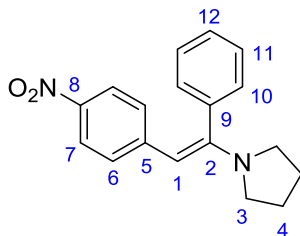
**m.p.** 135–137 °C

**$^1\text{H}$  NMR** (400 MHz,  $\text{CD}_3\text{CN}$ ):  $\delta$  = 7.47–7.44 (m, 3H, H-11 and H-12), 7.28–7.25 (m, 2H, H-10), 7.16–7.14 (m, 2H, H-7), 6.59–6.57 (m, 2H, H-6), 5.30 (s, 1H, H-1), 3.13–3.10 (m, 4H, H-3), 1.90–1.87 (m, 4H, 4H, H-4).

**$^{13}\text{C}\{^1\text{H}\}$  NMR** (101 MHz,  $\text{CD}_3\text{CN}$ ):  $\delta$  = 152.8 (C-2), 146.7 (C-5), 138.7 (C-9), 132.3 (C-7), 130.2 (C-11), 129.9 (C-10), 129.6 (C-12), 127.1 (C-6), 120.8 (C-13), 104.3 (C-8), 97.5 (C-1), 49.5 (C-3), 25.9 (C-4).

**HRMS** (EI):  $m/z$  calculated for  $\text{C}_{19}\text{H}_{17}\text{N}_2^{+}$   $[M-H]^{+}$ : 273.1386; found: 273.1383.

**(E)-1-(2-(4-Nitrophenyl)-1-phenylvinyl)pyrrolidine (1-NO<sub>2</sub>)** was prepared according to GP1 from the *p*-nitro-substituted deoxybenzoin (650 mg, 2.69 mmol), pyrrolidine (0.88 mL, 11 mmol), and boron trifluoride etherate (40  $\mu$ L, 0.32 mmol) to give red needles (246 mg, 31%) after recrystallization from acetonitrile solution at -25 °C.



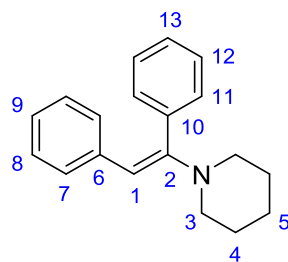
**m.p.** 133–135 °C

**<sup>1</sup>H NMR** (400 MHz, CDCl<sub>3</sub>):  $\delta$  = 7.76–7.74 (m, 2H, H-7), 7.45–7.42 (m, 3H, H-11 and H-12), 7.29–7.26 (m, 2H, H-10), 6.55–6.52 (m, 2H, H-6), 5.31 (s, 1H, H-1), 3.20–3.18 (m, 4H, H-3), 1.94–1.92 (m, 4H, 4H, H-4).

**<sup>13</sup>C {<sup>1</sup>H} NMR** (101 MHz, CDCl<sub>3</sub>):  $\delta$  = 152.7 (C-2), 148.0 (C-5), 141.9 (C-8), 137.4 (C-9), 129.5 (C-11), 129.02 (C-12), 128.97 (C-10), 125.8 (C-6), 123.8 (C-7), 97.3 (C-1), 49.0 (C-3), 25.4 (C-4).

**HRMS** (EI): *m/z* calculated for C<sub>18</sub>H<sub>18</sub>N<sub>2</sub>O<sub>2</sub><sup>++</sup> [M]<sup>++</sup>: 294.1363; found: 294.1366.

**(E)-1-(1,2-Diphenylvinyl)piperidine (2)** was prepared according to GP1 from the deoxybenzoin (1.04 g, 5.30 mmol), piperidine (2.0 mL, 20.2 mmol), and boron trifluoride etherate (60  $\mu$ L, 0.48 mmol) to give a yellow oil (1.12 g, 4.25 mmol, 80%) after distillation. The <sup>1</sup>H and <sup>13</sup>C NMR spectra are in agreement with those described in ref 39.



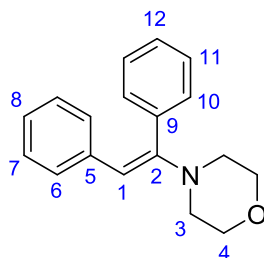
**b.p.** 188–190 °C (9.6  $\times$  10<sup>-1</sup> mbar);

**<sup>1</sup>H NMR** (400 MHz, CD<sub>3</sub>CN):  $\delta$  = 7.32–7.24 (m, 5H, H-11, H-12 and H-13), 6.99–6.94 (m, 2H, H-8), 6.89–6.85 (m, 1H, H-9), 6.75–6.71 (m, 2H, H-7), 5.62 (s, 1H, H-1), 2.87–2.85 (m, 4H, H-3), 1.59–1.56 (m, 6H, H-4 and H-5).

**<sup>13</sup>C {<sup>1</sup>H} NMR** (101 MHz, CD<sub>3</sub>CN):  $\delta$  = 153.0 (C-2), 140.5 (C-6), 139.1 (C-10), 131.2 (C-11), 129.4 (C-12), 129.2 (C-7), 129.0 (C-13), 128.6 (C-8), 124.7 (C-9), 105.7 (C-1), 50.8 (C-3), 26.8 (C-4), 25.3 (C-5).

**HRMS** (EI):  $m/z$  calculated for  $C_{19}H_{20}N^{+}$   $[M-H]^+$ : 262.1590; found: 262.1593.

**(E)-4-(1,2-Diphenylvinyl)morpholine (3)** was prepared according to Munk and Kim.<sup>15b</sup> A mixture of deoxybenzoin (5.04 g, 25.7 mmol), morpholine (3.1 ml, 35 mmol), and *p*-toluenesulfonic acid (0.05 g) in anhydrous toluene (100 mL) was refluxed for 36 h under nitrogen in a two-necked flask fitted with Dean-Stark water separator. The reaction mixture was neutralized with a freshly prepared solution of sodium methoxide in methanol. The toluene solution was washed with water and dried over anhydrous  $MgSO_4$ . After removal of toluene the product crystallized from methanol solution as pale yellow needles (4.72 g, 69 %). The  $^1H$  and  $^{13}C$  NMR spectra are in agreement with those described in refs 15b, 40.



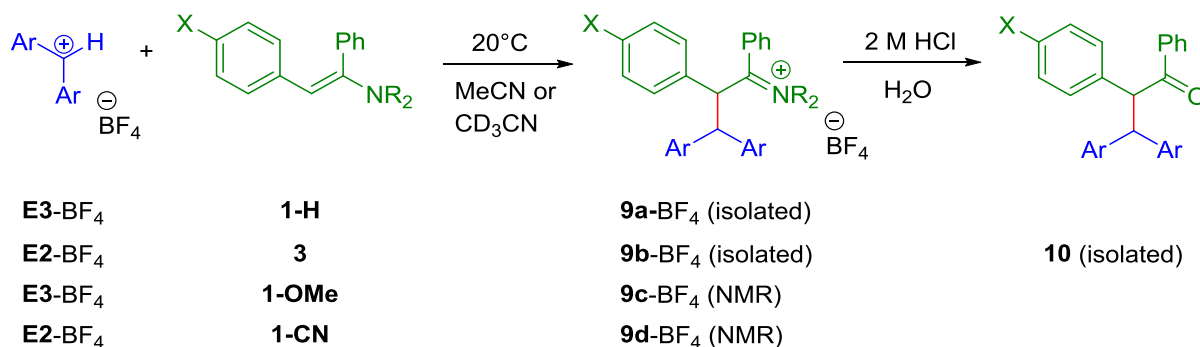
**m.p.** 89–91 °C.

**$^1H$  NMR** (400MHz,  $CD_3CN$ ):  $\delta$  = 7.35–7.26 (m, 5H, H-10, H-11 and H-12), 7.01–6.97 (m, 2H, H-7), 6.93–6.89 (m, 1H, H-8), 6.78–6.75 (m, 2H, H-6), 5.67 (s, 1H, H-1), 3.68–3.65 (m, 4H, H-4), 2.85–2.82 (m, 4H, H-3).

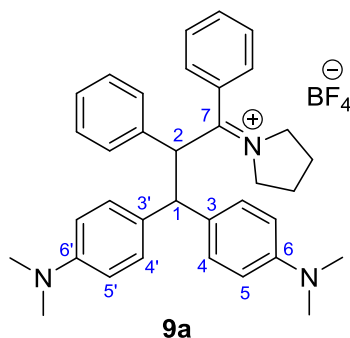
**$^{13}C$  { $^1H$ } NMR** (101 MHz,  $CD_3CN$ ):  $\delta$  = 152.3 (C-2), 139.9 (C-5), 138.1 (C-9), 131.3 (C-10), 129.5 (C-6), 129.3 (C-11), 129.2 (C-12), 128.6 (C-7), 125.1 (C-8), 106.3 (C-1), 67.5 (C-4), 50.3 (C-3).

**HRMS** (EI):  $m/z$  calculated for  $C_{18}H_{18}NO^{+}$   $[M-H]^+$ : 264.1383; found: 264.1379.

## 2.5.3. Reactions of the Enamines 1-X and 3 with Benzhydrylium Ions

Reaction of enamine 1-H with the benzhydrylium ion E3-BF<sub>4</sub>

Enamine **1-H** (40 mg, 0.16 mmol) was dissolved in dry acetonitrile (10 mL) under N<sub>2</sub> in a Schlenk flask. Then a solution of **E3-BF<sub>4</sub>** (52 mg, 0.15 mmol) in acetonitrile (8 mL) was added. The resulting mixture was stirred for 10 min, and then the solvent was removed under reduced pressure to yield quantitatively (88 mg) **9b-BF<sub>4</sub>** as a green solid.

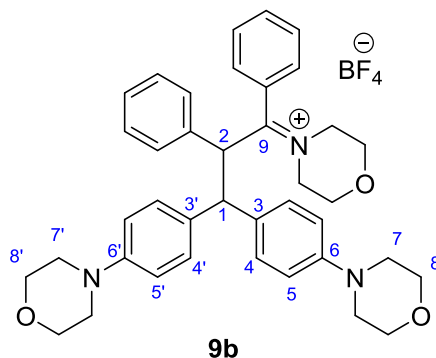


**<sup>1</sup>H NMR** (400 MHz, CDCl<sub>3</sub>): δ = 7.50–7.35 (m, 4H, Ph), 7.29–7.27 (m, 2H, H-4 or H-4'), 7.19–7.15 (m, 3H, Ph), 7.12–7.10 (m, 2H, Ph), 6.98–6.94 (m, 2H, H-4 or H-4'), 6.76 (bs, 2H, Ph), 6.75–6.71 (m, 2 H, H-5 or H-5', superimposed with the broad signal at 6.76 ppm), 6.45–6.41 (m, 2 H, H-5 or H-5'), 5.52 (d, <sup>3</sup>J<sub>H-1, H-2</sub> = 12.2 Hz, 1H, H-1), 4.70–4.62 (m, 1H, ½ <sup>+</sup>NCH<sub>2</sub>), 4.37 (d, <sup>3</sup>J<sub>H-2, H-1</sub> = 12.2 Hz, 1H, H-2), 4.20–4.13 (m, 1H, ½ <sup>+</sup>NCH<sub>2</sub>), 3.54–3.48 (m, 1H, ½ <sup>+</sup>NCH<sub>2</sub>), 3.42–3.35 (m, 1H, ½ <sup>+</sup>NCH<sub>2</sub>), 2.93 (s, 6H, NMe<sub>2</sub>), 2.76 (s, 6H, NMe<sub>2</sub>), 2.39–2.31 (m, 1H, ½ CH<sub>2</sub>), 2.09–1.98 (m, 2H, CH<sub>2</sub>), 1.85–1.79 (m, 1H, ½ CH<sub>2</sub>).

**<sup>13</sup>C {<sup>1</sup>H} NMR** (101 MHz, CDCl<sub>3</sub>): δ = 186.4 (C=N<sup>+</sup>), 150.1 (C-6 or C-6'), 149.1 (C-6 or C-6'), 133.2 (C, Ph), 132.0 (C, Ph), 131.4 (CH, Ph), 130.7 (CH, Ph), 129.2 (C-3 or C-3'), 129.0 (CH, Ph), 129.0 (CH, Ph), 128.8 (C-4 or C-4'), 128.7 (C-4 or C-4'), 128.2 (C-3 or C-3'), 126.4 (CH, Ph), 113.2 (C-5 or C-5'), 112.8 (C-5 or C-5'), 59.0 (<sup>+</sup>NCH<sub>2</sub>), 57.7 (C-1), 55.8 (<sup>+</sup>NCH<sub>2</sub>), 51.0 (C-2), 40.6 (NMe<sub>2</sub>), 40.5 (NMe<sub>2</sub>), 24.7 (CH<sub>2</sub>), 24.0 (CH<sub>2</sub>).

Reaction of enamine **3** with the benzhydrylium ion **E2**-BF<sub>4</sub>

Enamine **3** (33 mg, 0.12 mmol) was dissolved in dry acetonitrile (10 mL) under N<sub>2</sub> in a Schlenk flask. Then a solution of **E2**-BF<sub>4</sub> (50 mg, 0.12 mmol) in acetonitrile (8 mL) was added. The resulting mixture was stirred for 10 min, and then the solvent was removed under reduced pressure to yield quantitatively (83 mg) **9b**-BF<sub>4</sub> as a turquoise solid.

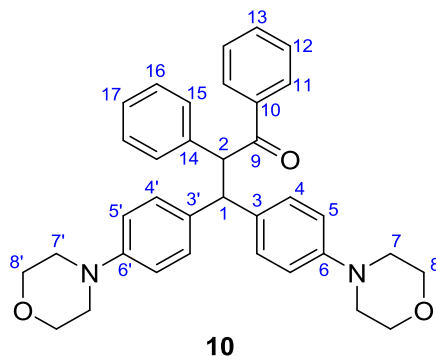


**<sup>1</sup>H NMR** (400MHz, CD<sub>3</sub>CN):  $\delta$  = 7.61–7.58 (m, 2H, Ph), 7.38–7.35 (m, 2H, H-4 or H-4'), 7.31–7.21 (m, 4H, Ph), 7.19–7.16 (m, 2H, H-4 or H-4'), 7.13–7.11 (m, 2H, Ph), 7.04–6.99 (m, 3H, H-5 or H-5' and H-Ph), 6.68–6.66 (m, 2 H, H-5 or H-5'), 6.13–6.11 (m, 1H, Ph), 5.82 (d, <sup>3</sup>J<sub>H-1, H-2</sub> = 12.3 Hz, 1H, H-1), 4.78–4.74 (m, 1H,  $\frac{1}{2}$  CH<sub>2</sub>), 4.56–4.50 (m, 2H, H-2 and  $\frac{1}{2}$  <sup>+</sup>NCH<sub>2</sub>, overlapping with the doublet signal at 4.52 ppm), 4.09–4.00 (m, 1H,  $\frac{1}{2}$  <sup>+</sup>NCH<sub>2</sub>), 3.80–3.77 (m, 4H, H-8 or H-8'), 3.71–3.65 (m, 5H, H-8 or H-8' and  $\frac{1}{2}$  CH<sub>2</sub>), 3.55–3.32 (m, 4H, CH<sub>2</sub>), 3.15–3.13 (m, 4H, H-7 or H-7'), 2.96–2.94 (m, 4H, H-7 or H-7').

**<sup>13</sup>C {<sup>1</sup>H} NMR** (101 MHz, CD<sub>3</sub>CN):  $\delta$  = 189.1 (C=N<sup>+</sup>), 152.1 (C-6 or C-6'), 150.8 (C-6 or C-6'), 134.1 (C-Ph), 133.0 (C-3 and C-3'), 132.6 (CH-Ph), 132.0 (CH-Ph), 130.5 (C-Ph), , 129.89 (CH-Ph), 129.86 (C-4 or C-4'), 129.7 (CH-Ph), 129.6 (CH-Ph and C-4 or C-4'), 129.5 (CH-Ph), 128.7 (CH-Ph), 127.6 (CH-Ph), 117.1 (C-5 or C-5'), 116.1 (C-5 or C-5'), 67.5 (CH<sub>2</sub>), 67.3 (CH<sub>2</sub>), 67.3 (C-8' or C-8), 67.2 (C-8' or C-8), 58.5 (CH<sub>2</sub>), 55.7 (<sup>+</sup>NCH<sub>2</sub>), 54.3 (C-1), 50.9 (C-2), 49.7 (C-7' or C-7), 49.6 (C-7' or C-7).

**HRMS** (ESI):  $m/z$  calculated for C<sub>39</sub>H<sub>44</sub> N<sub>3</sub>O<sub>3</sub> [M]<sup>+</sup>: 602.3377; found: 602.3362.

The crude product **9b**-BF<sub>4</sub> obtained by the procedure above was dissolved in dilute HCl and stirred for 30 min. The solution was then neutralized by treatment with dilute aq. NaOH and extracted with CH<sub>2</sub>Cl<sub>2</sub> (3  $\times$  30 mL). The combined organic layers were dried over MgSO<sub>4</sub>, filtered, and concentrated under vacuum. The recrystallization from EtOH of the crude product gave **10** as a purple solid (19 mg, 30 % referring to **E2**).



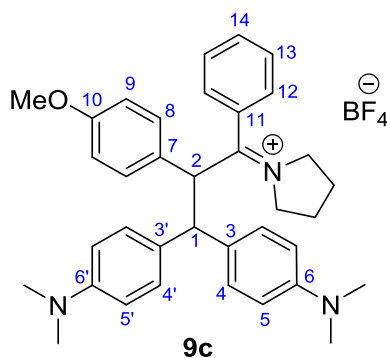
**$^1\text{H}$  NMR** (400 MHz,  $\text{CDCl}_3$ ):  $\delta$  = 7.93–7.91 (m, 2H, H-11), 7.49–7.45 (m, 1H, H-13), 7.39–7.35 (m, 2H, H-12), 7.23–7.21 (m, 4H, H-12 and H-4 or H-4'), 7.15–7.11 (m, 2H, H-16), 7.08–7.05 (m, 2H, H-17), 6.91–6.89 (m, 2H, H-4 or H-4'), 6.77–6.75 (m, 2H, H-5 or H-5'), 6.64–6.62 (m, 2H, H-5 or H-5'), 5.39 (d,  $^3J_{\text{H-1, H-2}} = 11.6$  Hz, 1H, H-1), 4.82 (d,  $^3J_{\text{H-2, H-1}} = 11.6$  Hz, 1H, H-2), 3.81–3.79 (m, 8H, H-8 and H-8'), 3.06–3.01 (m, 8H, H-7 and H-7').

**$^{13}\text{C}$   $\{^1\text{H}\}$  NMR** (101 MHz,  $\text{CDCl}_3$ ):  $\delta$  = 199.1 (C-9), 149.3 (C-6' or C-6), 149.1 (C-6 or C-6'), 137.5 (C-14), 137.4 (C-10), 135.7 (C-3' or C-3), 134.8 (C-3' or C-3), 132.9 (C-13), 129.3 (C-4' or C-4), 129.2 (C-4' or C-4), 128.6 (C-16), 128.65 (C-12), 128.63 (C-11), 128.4 (C-15), 67.01 (C-8' or C-8), 66.96 (C-8' or C-8), 58.5 (C-2), 53.4 (C-1), 49.6 (C-7' or C-7), 49.5 (C-7' or C-7).

**HRMS** (ESI):  $m/z$  calculated for  $\text{C}_{35}\text{H}_{37}\text{N}_2\text{O}_3$   $[\text{M} + \text{H}]^+$ : 533.2799; found: 533.2796.

#### Reaction of enamine **1-OMe** with the benzhydrylium ion **E3-BF<sub>4</sub>**

$^1\text{H}$  and  $^{13}\text{C}$  NMR monitoring of the reaction of the enamine **1-OMe** (9.8 mg, 0.035 mmol) with **E3-BF<sub>4</sub>** (8.9 mg, 0.026 mmol) in  $\text{CD}_3\text{CN}$  showed the quantitative formation of the iminium tetrafluoroborate **9c-BF<sub>4</sub>**.



**$^1\text{H}$  NMR** (400 MHz,  $\text{CDCl}_3$ ):  $\delta$  = 7.61–7.56 (m, 1H, H-14), 7.45–7.41 (m, 2H, H-13), 7.31–7.27 (m, 2H, H-4 or H-4'), 7.11–7.06 (m, 4H, H-4 or H-4' and H-8), 6.80–6.75 (m, 4H, H-5 or H-5' and H-9), 6.62–6.60 (bs, 2H, H-12), 6.49–6.45 (m, 2H, H-5 or H-5'), 5.49 (d,  $^3J_{\text{H-2, H-1}} = 12.4$  Hz, 1H, H-1), 4.57–4.50 (m, 1H,  $\frac{1}{2} \text{ } ^+\text{NCH}_2$ ), 4.35 (d,  $^3J_{\text{H-1, H-2}} = 12.5$  Hz, 1H, H-2),

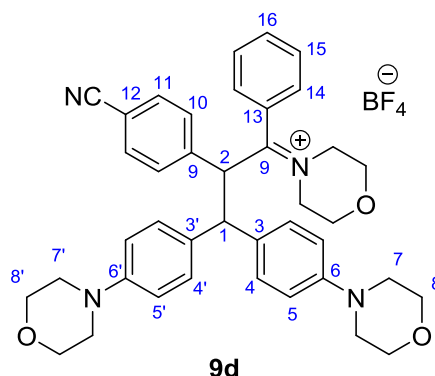


4.38–4.31 (m, 1H,  $\frac{1}{2}$   $^+\text{NCH}_2$ , superimposed with the signal at 4.35 ppm), 3.73 (s, 3H,  $\text{OCH}_3$ ), 3.34–3.29 (m, 2H,  $^+\text{NCH}_2$ ), 2.92 (s, 6H,  $\text{NMe}_2$ ), 2.76 (s, 6H,  $\text{NMe}_2$ ), 2.23–2.17 (m, 1H,  $\frac{1}{2}$   $\text{CH}_2$ ), 2.08–2.01 (m, 1H,  $\frac{1}{2}$   $\text{CH}_2$ ), 1.91–1.76 (m, 2H,  $\text{CH}_2$ ).

$^{13}\text{C}$   $\{^1\text{H}\}$  NMR (101 MHz,  $\text{CD}_3\text{CN}$ )  $\delta$  = 186.8 ( $\text{C}=\text{N}^+$ ), 160.8 (C-10), 151.2 (C-6 or C-6'), 150.2 (C-6 or C-6'), 133.0 (C-8), 132.3 (C-14), 132.2 (C-11), 130.4 (C-3 or C-3'), 130.2 (C-3 or C-3'), 129.6 (C-13), 129.5 (C-4 or C-4'), 129.2 (C-4 or C-4'), 127.5 (C-12), 125.9 (C-7), 114.8 (C-9), 114.0 (C-5 or C-5'), 113.3 (C-5 or C-5'), 59.6 ( $^+\text{NCH}_2$ ), 56.6 ( $^+\text{NCH}_2$ ), 56.6 (C-1), 55.9 ( $\text{OCH}_3$ ), 51.3 (C-2), 40.7 ( $\text{NMe}_2$ ), 40.6 ( $\text{NMe}_2$ ), 25.2 ( $\text{CH}_2$ ), 24.5 ( $\text{CH}_2$ ).

#### Reaction of enamine **1-CN** with the benzhydrylium ion **E2-BF<sub>4</sub>**

$^1\text{H}$  and  $^{13}\text{C}$  NMR monitoring of the reaction of the enamine **1-CN** (10 mg, 0.036 mmol) with **E2-BF<sub>4</sub>** (15 mg, 0.035 mmol) in  $\text{CD}_3\text{CN}$  showed the quantitative formation of the iminium tetrafluoroborate **9d-BF<sub>4</sub>**.

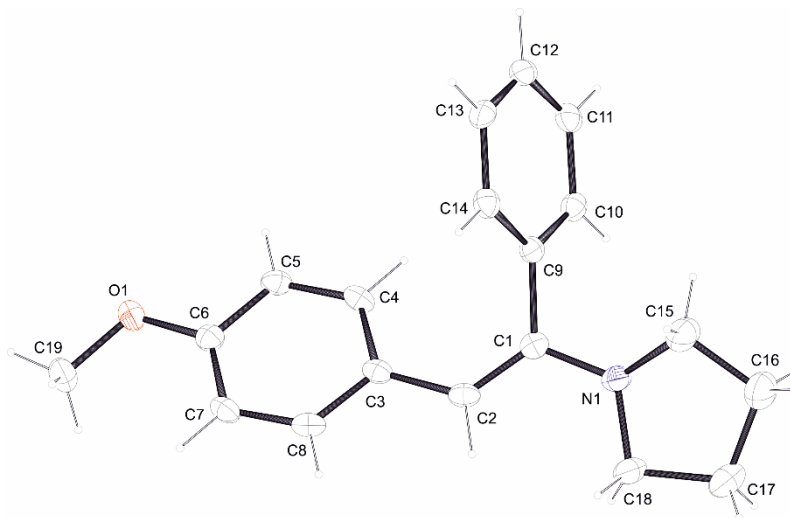


$^1\text{H}$  NMR (400 MHz,  $\text{CDCl}_3$ ): 7.60–7.54 (m, 3H, H-16 and H-11), 7.48–7.44 (m, 2H, H-15), 7.38–7.36 (m, 2H, H-4 or H-4'), 7.32–7.30 (m, 2H, H-10), 7.15–7.12 (m, 2H, H-4 or H-4'), 7.00–6.97 (m, 2H, H-5 or H-5'), 6.72–6.73 (bs, 2H, H-14), 6.67–6.65 (m, 2H, H-5 or H-5'), 5.60 (d,  $^3J_{\text{H-1}, \text{H-2}}$  = 12.3 Hz, 1H, H-1), 4.56 (d,  $^3J_{\text{H-2}, \text{H-1}}$  = 12.3 Hz, 1H, H-2), 4.49–4.42 (m, 1H,  $\frac{1}{2}$   $^+\text{NCH}_2$ ), 4.20–4.13 (m, 1H,  $\frac{1}{2}$   $^+\text{NCH}_2$ ), 3.79–3.77 (m, 4H, H-7 or H-7'), 3.68–3.66 (m, 4H, H-7 or H-7'), 3.43–3.31 (m, 2H,  $^+\text{NCH}_2$ ), 3.14–3.11 (m, 4H, H-8 or H-8'), 2.96–2.94 (m, 4H, H-8 or H-8'), 2.21–2.15 (m, 1H,  $\frac{1}{2}$   $\text{CH}_2$ ), 2.04–1.98 (m, 1H,  $\frac{1}{2}$   $\text{CH}_2$ ), 1.92–1.85 (m, 1H,  $\frac{1}{2}$   $\text{CH}_2$ ), 1.82–1.75 (m, 1H,  $\frac{1}{2}$   $\text{CH}_2$ ).

$^{13}\text{C}$   $\{^1\text{H}\}$  NMR (101 MHz,  $\text{CD}_3\text{CN}$ )  $\delta$  = 185.2 ( $\text{C}=\text{N}^+$ ), 151.9 (C-6 or C-6'), 150.7 (C-6 or C-6'), 139.7 (C-9), 133.1 (C-11), 132.7 (C-10 and C-3 or C-3'), 132.5 (C-16 and C-3 or C-3'), 131.9 (C-13), 129.9 (C-15), 129.8 (C-4 or C-4'), 129.5 (C-4 or C-4'), 127.2 (C-14), 119.0 (CN), 117.0 (C-5 or C-5'), 116.2 (C-5 or C-5'), 113.1 (C-12), 67.3 (C-7 or C-7'), 67.2 (C-7 or C-7'), 60.2 ( $^+\text{NCH}_2$ ), 57.4 (C-1), 57.1 ( $^+\text{NCH}_2$ ), 51.4 (C-2), 49.8 (C-8 or C-8'), 49.6 (C-7 or C-7'), 25.2 ( $\text{CH}_2$ ), 24.5 ( $\text{CH}_2$ ).

#### 2.5.4. Crystallographic Data for the Enamines **1-OMe**, **1-CN**, **1-NO<sub>2</sub>** and **3**.

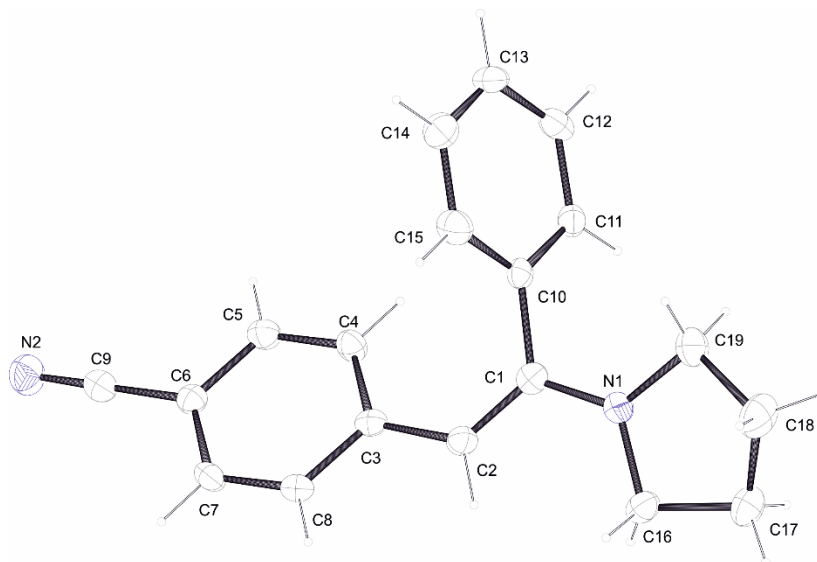
The structure of **1-OMe** was refined as a perfect inversion twin. In **1-NO<sub>2</sub>**, the disorder of a 5-membered ring was described by a split model. The site occupation factors finally refined to 0.52 and 0.48. The structure of **1-CN** was refined as a non-merohedral 2-component twin with (010) as C<sub>2</sub> twin axis. The volume ratio of the two components refined to 0.83/0.17.



Single crystal x-ray structure of **1-OMe**

(thermal ellipsoids are drawn at a 50% probability level at  $T = 100$  K)

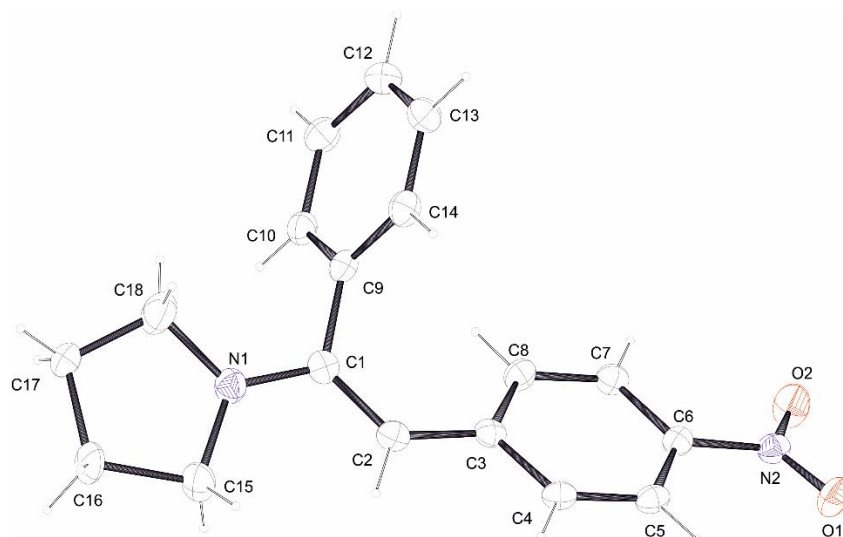
CCDC 1589744 (**1-OMe**) contains the supplementary crystallographic data. These data are provided free of charge by The Cambridge Crystallographic Data Centre.



Single crystal x-ray structure of **1-CN**

(thermal ellipsoids are drawn at a 50% probability level at  $T = 123$  K)

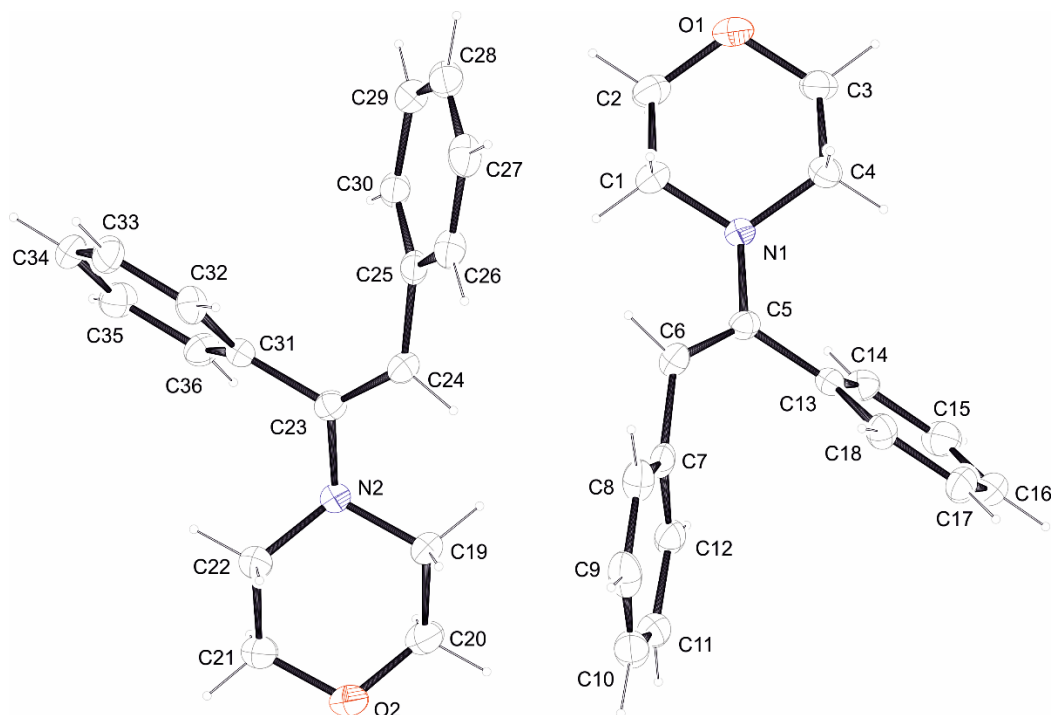
CCDC 1589747 (**1-CN**) contains the supplementary crystallographic data. These data are provided free of charge by The Cambridge Crystallographic Data Centre.



Single crystal x-ray structure of **1-NO<sub>2</sub>**

(thermal ellipsoids are drawn at a 50% probability level at  $T = 100$  K)

CCDC 1589745 (**1-NO<sub>2</sub>**) contains the supplementary crystallographic data. These data are provided free of charge by The Cambridge Crystallographic Data Centre.



Single crystal x-ray structure of **3**

**3** crystallizes with two independent molecules in the asymmetric unit

(thermal ellipsoids are drawn at a 50% probability level at  $T = 100$  K)

CCDC 1589746 (**3**) contains the supplementary crystallographic data. These data are provided free of charge by The Cambridge Crystallographic Data Centre.

	<b>1-OMe</b>	<b>1-CN</b>
net formula	C <sub>19</sub> H <sub>21</sub> NO	C <sub>19</sub> H <sub>18</sub> N <sub>2</sub>
$M_r/\text{g mol}^{-1}$	279.37	274.35
crystal size/mm	0.100 × 0.020 × 0.020	0.100 × 0.030 × 0.030
$T/\text{K}$	100.(2)	123.(2)
radiation	MoK $\alpha$	MoK $\alpha$
diffractometer	'Bruker D8 Venture TXS'	'Bruker D8 Venture TXS'
crystal system	tetragonal	triclinic
space group	'P -4 21 c'	'P -1'
$a/\text{\AA}$	22.5590(10)	5.8921(8)
$b/\text{\AA}$	22.5590(10)	10.7709(13)
$c/\text{\AA}$	5.8766(4)	11.9599(16)
$\alpha/^\circ$	90	96.185(4)
$\beta/^\circ$	90	93.764(4)
$\gamma/^\circ$	90	98.552(4)
$V/\text{\AA}^3$	2990.7(3)	743.63(17)
$Z$	8	2
calc. density/ $\text{g cm}^{-3}$	1.241	1.225
$\mu/\text{mm}^{-1}$	0.076	0.072
absorption correction	Multi-Scan	Multi-Scan
transmission factor range	0.7867–0.9705	0.8553–0.9705
refls. measured	12798	2557
$R_{\text{int}}$	0.0721	0.0658
mean $\sigma(I)/I$	0.0598	0.0551
$\theta$ range	3.256–25.346	3.439–25.025
observed refls.	2205	2162
$x, y$ (weighting scheme)	0.0283, 1.2683	0.0206, 0.8841
hydrogen refinement	constr	constr
Flack parameter	0.5	
refls in refinement	2721	2557
parameters	191	191
restraints	0	0
$R(F_{\text{obs}})$	0.0448	0.0661
$R_w(F^2)$	0.1022	0.1387
$S$	1.070	1.162
shift/error <sub>max</sub>	0.001	0.001
max electron density/ $\text{e \AA}^{-3}$	0.171	0.205
min electron density/ $\text{e \AA}^{-3}$	–0.217	–0.233

	<b>1-NO<sub>2</sub></b>	<b>3</b>
net formula	C <sub>18</sub> H <sub>18</sub> N <sub>2</sub> O <sub>2</sub>	C <sub>18</sub> H <sub>19</sub> NO
$M_r/\text{g mol}^{-1}$	294.34	265.34
crystal size/mm	0.090 × 0.080 × 0.040	0.100 × 0.090 × 0.080
$T/\text{K}$	100.(2)	100.(2)
radiation	MoK $\alpha$	MoK $\alpha$
diffractometer	'Bruker D8 Venture TXS'	'Bruker D8 Venture TXS'
crystal system	monoclinic	triclinic
space group	'P 1 2/c 1'	'P -1'
$a/\text{\AA}$	11.7839(6)	10.1814(6)
$b/\text{\AA}$	5.9331(3)	11.0589(6)
$c/\text{\AA}$	21.5761(11)	14.6310(7)
$\alpha/^\circ$	90	102.316(2)
$\beta/^\circ$	98.121(2)	98.102(2)
$\gamma/^\circ$	90	110.728(2)
$V/\text{\AA}^3$	1493.37(13)	1462.45(14)
$Z$	4	4
calc. density/g cm <sup>-3</sup>	1.309	1.205
$\mu/\text{mm}^{-1}$	0.086	0.074
absorption correction	Multi-Scan	Multi-Scan
transmission factor range	0.8929–0.9705	0.9064–0.9705
refls. measured	16896	18256
$R_{\text{int}}$	0.0424	0.0395
mean $\sigma(I)/I$	0.0324	0.0420
$\theta$ range	3.434–26.372	3.224–26.364
observed refls.	2478	4582
$x, y$ (weighting scheme)	0.0365, 1.0008	0.0299, 0.5305
hydrogen refinement	constr	constr
refls in refinement	3057	5914
parameters	218	361
restraints	0	0
$R(F_{\text{obs}})$	0.0440	0.0416
$R_w(F^2)$	0.1071	0.0988
$S$	1.065	1.063
shift/error <sub>max</sub>	0.001	0.001
max electron density/e $\text{\AA}^{-3}$	0.249	0.219
min electron density/e $\text{\AA}^{-3}$	−0.283	−0.213

### 2.5.5. UV-Vis Spectra of Enamines 1-3

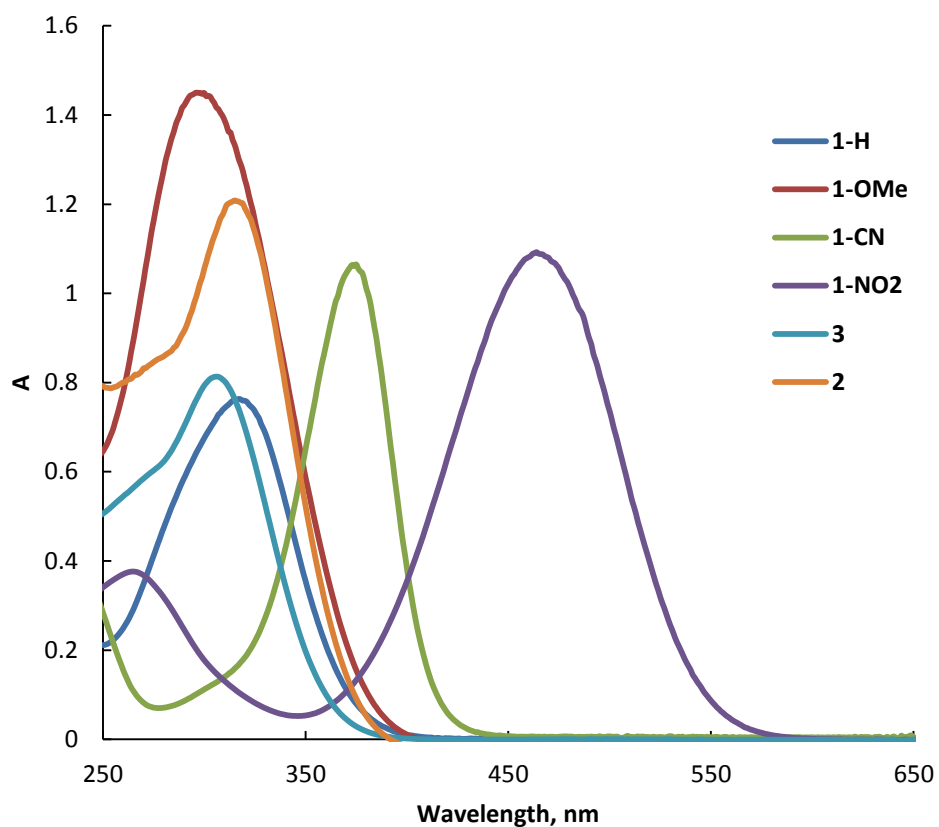


**Figure S1.** UV-Vis-spectra of the enamines **1-X**, **2** and **3** in MeCN (20 °C).

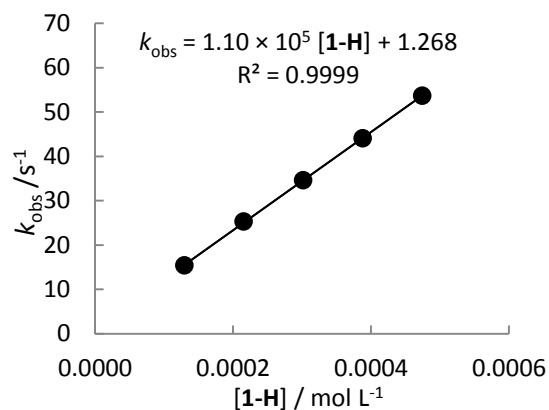
## 2.5.6. Determination of Rate Constants

## 2.5.6.1. Kinetic Investigations of the Reactions of Enamine 1-H

**Table S1.** Kinetics of the reaction of **1-H** with **E2** in MeCN (20 °C, stopped flow,  $\lambda = 611$  nm)

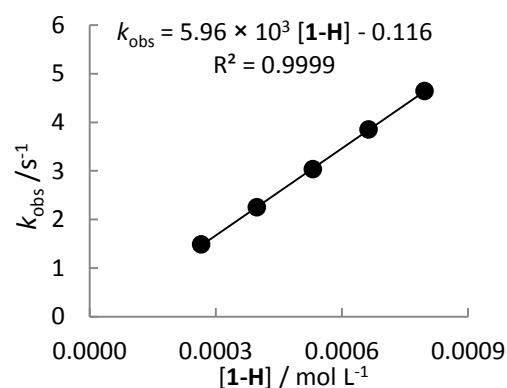
[E2] / mol L <sup>-1</sup>	[1-H] / mol L <sup>-1</sup>	[1-H]/ [E2]	$k_{\text{obs}} / \text{s}^{-1}$
$9.99 \times 10^{-6}$	$1.29 \times 10^{-4}$	12.9	$1.54 \times 10^1$
	$2.16 \times 10^{-4}$	21.6	$2.53 \times 10^1$
	$3.02 \times 10^{-4}$	30.2	$3.46 \times 10^1$
	$3.88 \times 10^{-4}$	38.8	$4.41 \times 10^1$
	$4.74 \times 10^{-4}$	47.5	$5.36 \times 10^1$

$$k_2 = 1.10 \times 10^5 \text{ L mol}^{-1} \text{ s}^{-1}$$

**Table S2.** Kinetics of the reaction of **1-H** with **E3** in MeCN (20 °C, stopped flow,  $\lambda = 605$  nm)

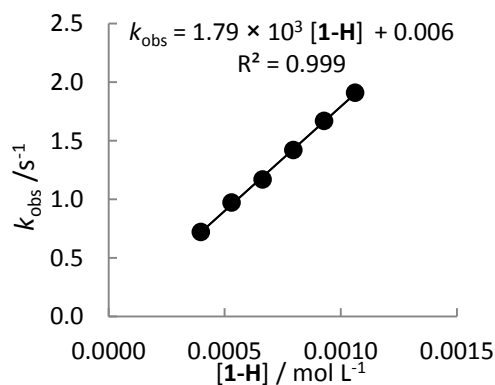
[E3] / mol L <sup>-1</sup>	[1-H] / mol L <sup>-1</sup>	[1-H]/ [E3]	$k_{\text{obs}} / \text{s}^{-1}$
$7.24 \times 10^{-6}$	$2.65 \times 10^{-4}$	36.7	1.48
	$3.98 \times 10^{-4}$	55.0	2.25
	$5.31 \times 10^{-4}$	73.3	3.03
	$6.64 \times 10^{-4}$	91.7	3.85
	$7.96 \times 10^{-4}$	110	4.64

$$k_2 = 5.96 \times 10^3 \text{ L mol}^{-1} \text{ s}^{-1}$$

**Table S3.** Kinetics of the reaction of **1-H** with **E4** in MeCN (20 °C, stopped flow,  $\lambda = 611$  nm)

[E4] / mol L <sup>-1</sup>	[1-H] / mol L <sup>-1</sup>	[1-H]/ [E4]	$k_{\text{obs}} / \text{s}^{-1}$
$9.06 \times 10^{-6}$	$3.98 \times 10^{-4}$	43.9	$7.20 \times 10^{-1}$
	$5.31 \times 10^{-4}$	58.6	$9.73 \times 10^{-1}$
	$6.64 \times 10^{-4}$	73.2	1.17
	$7.96 \times 10^{-4}$	87.9	1.42
	$9.29 \times 10^{-4}$	103	1.67
	$1.06 \times 10^{-3}$	117	1.91

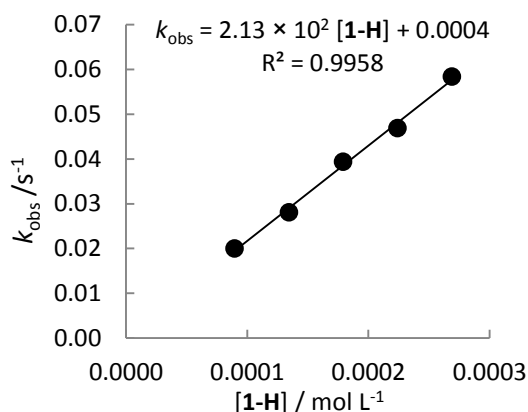
$$k_2 = 1.79 \times 10^3 \text{ L mol}^{-1} \text{ s}^{-1}$$



**Table S4.** Kinetics of the reaction of **1-H** with **E5** in MeCN (20 °C, stopped flow,  $\lambda = 616$  nm)

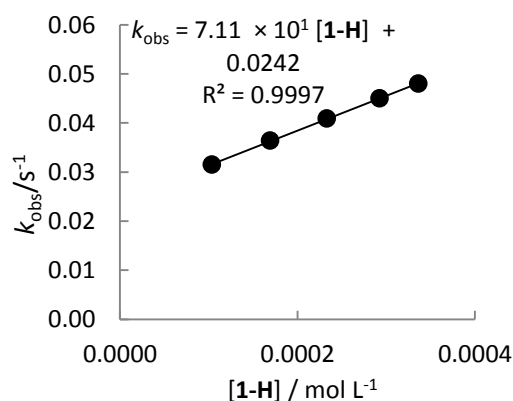
[ <b>E5</b> ] / mol L <sup>-1</sup>	[ <b>1-H</b> ] / mol L <sup>-1</sup>	[ <b>1-H</b> ]/ [ <b>E5</b> ]	$k_{\text{obs}} / \text{s}^{-1}$
$7.77 \times 10^{-6}$	$8.96 \times 10^{-5}$	11.5	$2.00 \times 10^{-2}$
	$1.34 \times 10^{-4}$	17.3	$2.81 \times 10^{-2}$
	$1.79 \times 10^{-4}$	23.1	$3.94 \times 10^{-2}$
	$2.24 \times 10^{-4}$	28.8	$4.69 \times 10^{-2}$
	$2.69 \times 10^{-4}$	34.6	$5.84 \times 10^{-2}$

$$k_2 = 2.13 \times 10^2 \text{ L mol}^{-1} \text{ s}^{-1}$$

**Table S5.** Kinetics of the reaction of **1-H** with **E6** in MeCN (20 °C, diode array UV-Vis spectrometer,  $\lambda = 635$  nm)

[ <b>E6</b> ] / mol L <sup>-1</sup>	[ <b>1-H</b> ] / mol L <sup>-1</sup>	[ <b>1-H</b> ]/ [ <b>E6</b> ]	$k_{\text{obs}} / \text{s}^{-1}$
$1.34 \times 10^{-5}$	$1.04 \times 10^{-4}$	7.8	$3.15 \times 10^{-2}$
$1.30 \times 10^{-5}$	$1.69 \times 10^{-4}$	13.0	$3.64 \times 10^{-2}$
$1.29 \times 10^{-5}$	$2.33 \times 10^{-4}$	18.0	$4.09 \times 10^{-2}$
$1.33 \times 10^{-5}$	$2.93 \times 10^{-4}$	22.1	$4.50 \times 10^{-2}$
$1.29 \times 10^{-5}$	$3.36 \times 10^{-4}$	25.8	$4.81 \times 10^{-2}$

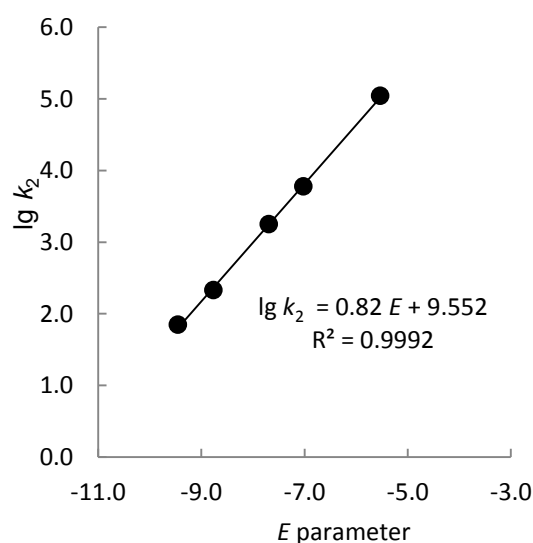
$$k_2 = 7.11 \times 10^1 \text{ L mol}^{-1} \text{ s}^{-1}$$



#### Determination of the Reactivity Parameters $N$ and $s_N$ of the Enamine **1-H** in MeCN

Electrophile	$E$	$k_2 / \text{L mol}^{-1} \text{ s}^{-1}$	$\lg k_2$
<b>E2</b>	- 5.53	$1.10 \times 10^5$	5.04
<b>E3</b>	- 7.02	$5.96 \times 10^3$	3.78
<b>E4</b>	- 7.69	$1.79 \times 10^3$	3.25
<b>E5</b>	- 8.76	$2.13 \times 10^2$	2.33
<b>E6</b>	- 9.45	$7.11 \times 10^1$	1.85

$$N = 11.66, s_N = 0.82$$



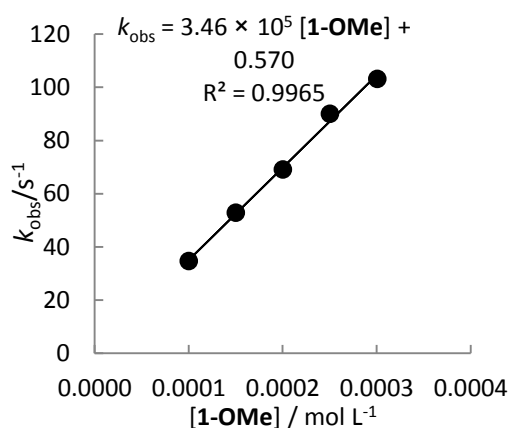


## 2.5.6.2. Kinetic Investigations of the Reactions of Enamine 1-OMe

**Table S6.** Kinetics of the reaction of **1-OMe** with **E2** in MeCN (20 °C, stopped flow,  $\lambda = 611$  nm)

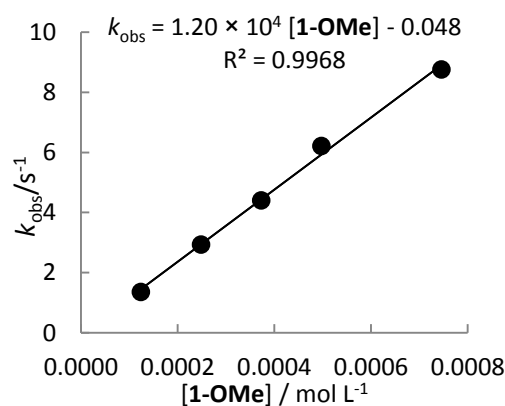
[E2] / mol L <sup>-1</sup>	[1-OMe] / mol L <sup>-1</sup>	[1-OMe]/ [E2]	$k_{\text{obs}} / \text{s}^{-1}$
$9.03 \times 10^{-6}$	$1.00 \times 10^{-4}$	11.1	$3.46 \times 10^1$
	$1.50 \times 10^{-4}$	16.6	$5.28 \times 10^1$
	$2.00 \times 10^{-4}$	22.2	$6.91 \times 10^1$
	$2.51 \times 10^{-4}$	27.7	$9.00 \times 10^1$
	$3.01 \times 10^{-4}$	33.3	$1.03 \times 10^2$

$$k_2 = 3.46 \times 10^5 \text{ L mol}^{-1} \text{ s}^{-1}$$

**Table S7.** Kinetics of the reaction of **1-OMe** with **E3** in MeCN (20 °C, stopped flow,  $\lambda = 605$  nm)

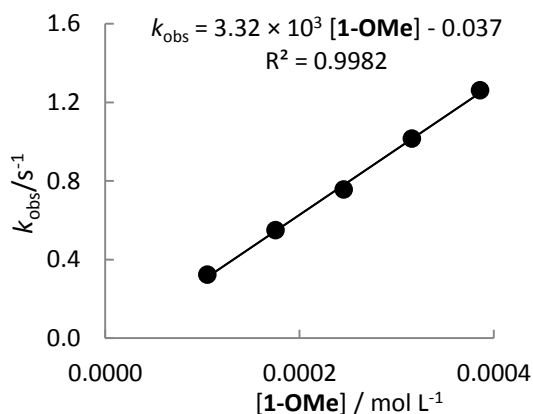
[E3] / mol L <sup>-1</sup>	[1-OMe] / mol L <sup>-1</sup>	[1-OMe]/ [E3]	$k_{\text{obs}} / \text{s}^{-1}$
$1.07 \times 10^{-5}$	$1.24 \times 10^{-4}$	11.6	1.36
	$2.49 \times 10^{-4}$	23.2	2.93
	$3.73 \times 10^{-4}$	34.8	4.40
	$4.98 \times 10^{-4}$	46.4	6.21
	$7.46 \times 10^{-4}$	69.6	8.76

$$k_2 = 1.20 \times 10^4 \text{ L mol}^{-1} \text{ s}^{-1}$$

**Table S8.** Kinetics of the reaction of **1-OMe** with **E4** in MeCN (20 °C, stopped flow,  $\lambda = 611$  nm)

[E4] / mol L <sup>-1</sup>	[1-OMe] / mol L <sup>-1</sup>	[1-OMe]/ [E4]	$k_{\text{obs}} / \text{s}^{-1}$
$6.40 \times 10^{-6}$	$1.05 \times 10^{-4}$	16.4	$3.23 \times 10^{-1}$
	$1.75 \times 10^{-4}$	27.4	$5.48 \times 10^{-1}$
	$2.46 \times 10^{-4}$	38.3	$7.55 \times 10^{-1}$
	$3.16 \times 10^{-4}$	49.3	1.01
	$3.86 \times 10^{-4}$	60.3	1.26

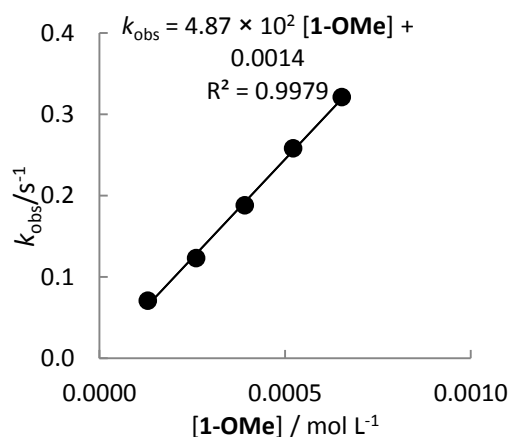
$$k_2 = 3.32 \times 10^3 \text{ L mol}^{-1} \text{ s}^{-1}$$



**Table S9.** Kinetics of the reaction of **1-OMe** with **E5** in MeCN (20 °C, stopped flow,  $\lambda = 616$  nm)

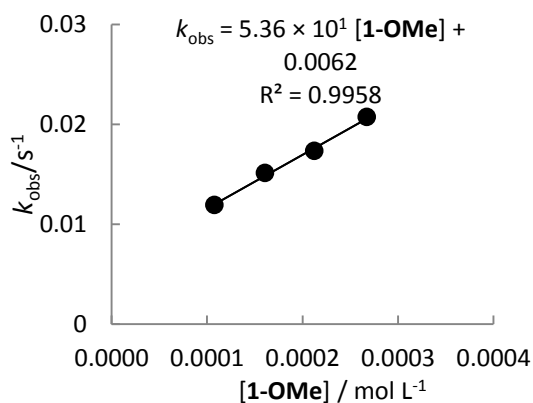
[ <b>3e</b> ] / mol L <sup>-1</sup>	[ <b>1-OMe</b> ] / mol L <sup>-1</sup>	[ <b>1-OMe</b> ]/ [ <b>E5</b> ]	$k_{\text{obs}} / \text{s}^{-1}$
$7.07 \times 10^{-6}$	$1.31 \times 10^{-4}$	18.5	$7.08 \times 10^{-2}$
	$2.61 \times 10^{-4}$	37.0	$1.23 \times 10^{-1}$
	$3.92 \times 10^{-4}$	55.4	$1.88 \times 10^{-1}$
	$5.23 \times 10^{-4}$	73.9	$2.58 \times 10^{-1}$
	$6.53 \times 10^{-4}$	92.4	$3.21 \times 10^{-1}$

$$k_2 = 4.87 \times 10^2 \text{ L mol}^{-1} \text{ s}^{-1}$$

**Table S10.** Kinetics of the reaction of **1-OMe** with **E7** in MeCN (20 °C, diode array UV-Vis spectrometer,  $\lambda = 631$  nm)

[ <b>E7</b> ] / mol L <sup>-1</sup>	[ <b>1-OMe</b> ] / mol L <sup>-1</sup>	[ <b>1-OMe</b> ]/ [ <b>E7</b> ]	$k_{\text{obs}} / \text{s}^{-1}$
$1.05 \times 10^{-6}$	$1.08 \times 10^{-4}$	10.3	$1.20 \times 10^{-2}$
$1.05 \times 10^{-6}$	$1.61 \times 10^{-4}$	15.4	$1.51 \times 10^{-2}$
$1.05 \times 10^{-6}$	$2.12 \times 10^{-4}$	20.3	$1.73 \times 10^{-2}$
$1.05 \times 10^{-6}$	$2.67 \times 10^{-4}$	25.5	$2.07 \times 10^{-2}$

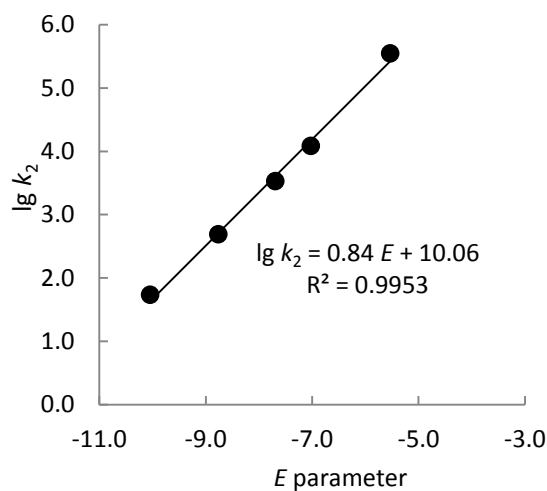
$$k_2 = 5.36 \times 10^1 \text{ L mol}^{-1} \text{ s}^{-1}$$



#### Determination of the Reactivity Parameters $N$ and $s_N$ of the Enamine **1-OMe** in MeCN

Electrophile	$E$	$k_2 / \text{L mol}^{-1} \text{ s}^{-1}$	$\lg k_2$
<b>E2</b>	- 5.53	$3.46 \times 10^5$	5.54
<b>E3</b>	- 7.02	$1.20 \times 10^4$	4.08
<b>E4</b>	- 7.69	$3.32 \times 10^3$	3.52
<b>E5</b>	- 8.76	$4.87 \times 10^2$	2.69
<b>E7</b>	- 10.04	$5.36 \times 10^1$	1.73

$$N = 11.99, s_N = 0.84$$

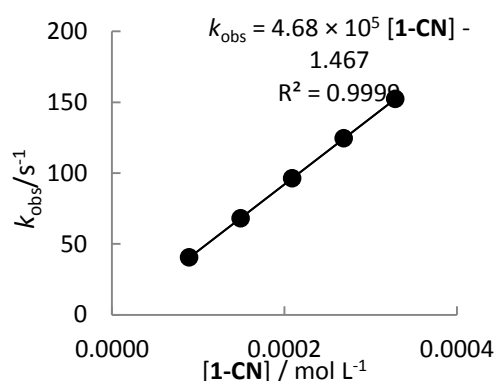


## 2.5.6.3. Kinetic Investigations of the Reactions of Enamine 1-CN

**Table S11.** Kinetics of the reaction of **1-CN** with **E1** in MeCN (20 °C, stopped flow,  $\lambda = 586$  nm)

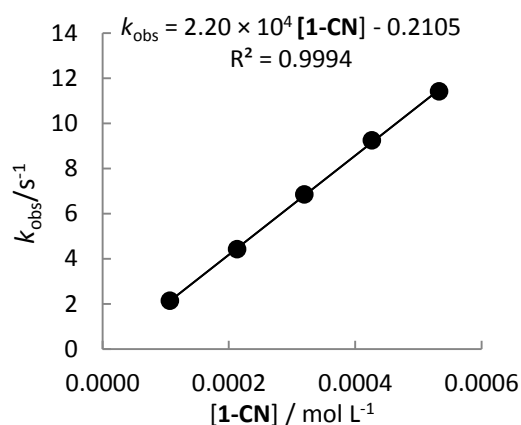
[ <b>3a</b> ] / mol L <sup>-1</sup>	[ <b>1-CN</b> ] / mol L <sup>-1</sup>	[ <b>1-CN</b> ]/ [ <b>E1</b> ]	$k_{\text{obs}} / \text{s}^{-1}$
6.60 $\times 10^{-6}$	$8.97 \times 10^{-5}$	13.6	$4.05 \times 10^1$
	$1.49 \times 10^{-4}$	22.7	$6.80 \times 10^1$
	$2.09 \times 10^{-4}$	31.7	$9.63 \times 10^1$
	$2.69 \times 10^{-4}$	40.8	$1.25 \times 10^2$
	$3.29 \times 10^{-4}$	49.8	$1.52 \times 10^2$

$$k_2 = 4.68 \times 10^5 \text{ L mol}^{-1} \text{ s}^{-1}$$

**Table S12.** Kinetics of the reaction of **1-CN** with **E2** in MeCN (20 °C, stopped flow,  $\lambda = 611$  nm)

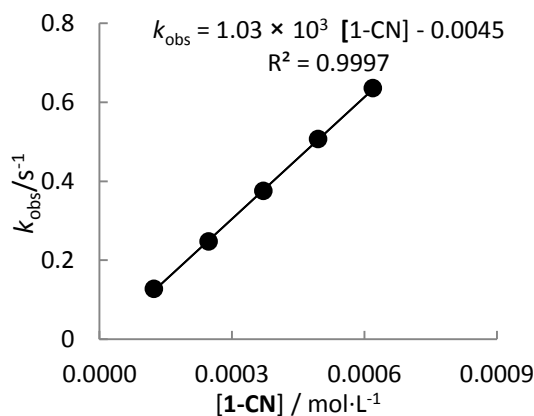
[ <b>E2</b> ] / mol L <sup>-1</sup>	[ <b>1-CN</b> ] / mol L <sup>-1</sup>	[ <b>1-CN</b> ]/ [ <b>E2</b> ]	$k_{\text{obs}} / \text{s}^{-1}$
$1.01 \times 10^{-5}$	$1.07 \times 10^{-4}$	10.6	2.13
	$2.13 \times 10^{-4}$	21.2	4.42
	$3.20 \times 10^{-4}$	31.7	6.85
	$4.26 \times 10^{-4}$	42.3	9.24
	$5.33 \times 10^{-4}$	52.8	$1.14 \times 10^1$

$$k_2 = 2.20 \times 10^4 \text{ L mol}^{-1} \text{ s}^{-1}$$

**Table S13.** Kinetics of the reaction of **1-CN** with **E3** in MeCN (20 °C, stopped flow,  $\lambda = 605$  nm)

[ <b>E3</b> ] / mol L <sup>-1</sup>	[ <b>1-CN</b> ] / mol L <sup>-1</sup>	[ <b>1-CN</b> ]/ [ <b>E3</b> ]	$k_{\text{obs}} / \text{s}^{-1}$
$1.06 \times 10^{-5}$	$1.24 \times 10^{-4}$	11.7	$1.27 \times 10^{-1}$
	$2.48 \times 10^{-4}$	23.4	$2.47 \times 10^{-1}$
	$3.72 \times 10^{-4}$	35.1	$3.75 \times 10^{-1}$
	$4.96 \times 10^{-4}$	46.8	$5.06 \times 10^{-1}$
	$6.20 \times 10^{-4}$	58.5	$6.35 \times 10^{-1}$

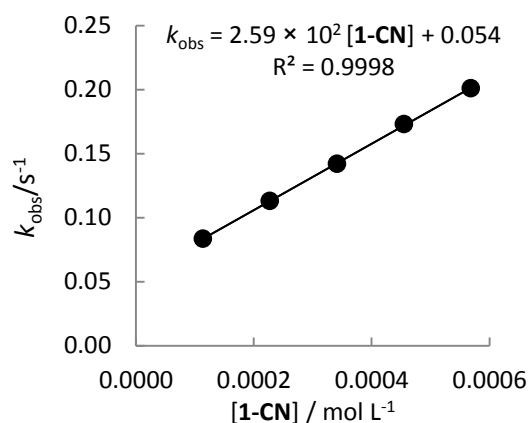
$$k_2 = 1.03 \times 10^3 \text{ L mol}^{-1} \text{ s}^{-1}$$



**Table S14.** Kinetics of the reaction of **1-CN** with **E4** in MeCN (20 °C, stopped flow,  $\lambda = 611$  nm)

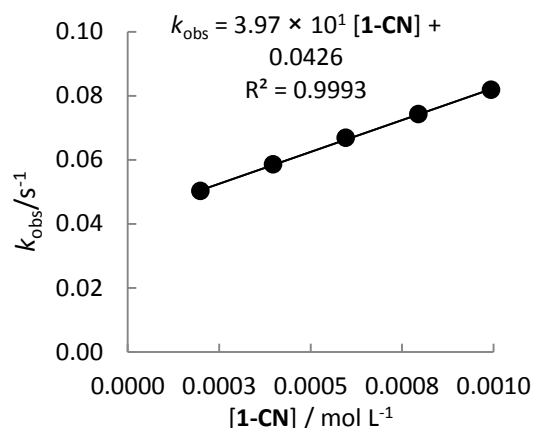
[ <b>E4</b> ] / mol L <sup>-1</sup>	[ <b>1-CN</b> ] / mol L <sup>-1</sup>	[ <b>1-CN</b> ]/ [ <b>E4</b> ]	$k_{\text{obs}} / \text{s}^{-1}$
$1.04 \times 10^{-5}$	$1.14 \times 10^{-4}$	10.9	$8.35 \times 10^{-2}$
	$2.27 \times 10^{-4}$	21.8	$1.13 \times 10^{-1}$
	$3.41 \times 10^{-4}$	32.7	$1.42 \times 10^{-1}$
	$4.55 \times 10^{-4}$	43.6	$1.73 \times 10^{-1}$
	$5.69 \times 10^{-4}$	54.5	$2.01 \times 10^{-1}$

$$k_2 = 2.59 \times 10^2 \text{ L mol}^{-1} \text{ s}^{-1}$$

**Table S15.** Kinetics of the reaction of **1-CN** with **E5** in MeCN (20 °C, stopped flow,  $\lambda = 616$  nm)

[ <b>E5</b> ] / mol L <sup>-1</sup>	[ <b>1-CN</b> ] / mol L <sup>-1</sup>	[ <b>1-CN</b> ]/ [ <b>E5</b> ]	$k_{\text{obs}} / \text{s}^{-1}$
$1.01 \times 10^{-5}$	$1.99 \times 10^{-4}$	19.7	$5.02 \times 10^{-2}$
	$3.97 \times 10^{-4}$	39.3	$5.85 \times 10^{-2}$
	$5.96 \times 10^{-4}$	59.0	$6.68 \times 10^{-2}$
	$7.95 \times 10^{-4}$	78.7	$7.42 \times 10^{-2}$
	$9.93 \times 10^{-4}$	98.3	$8.18 \times 10^{-2}$

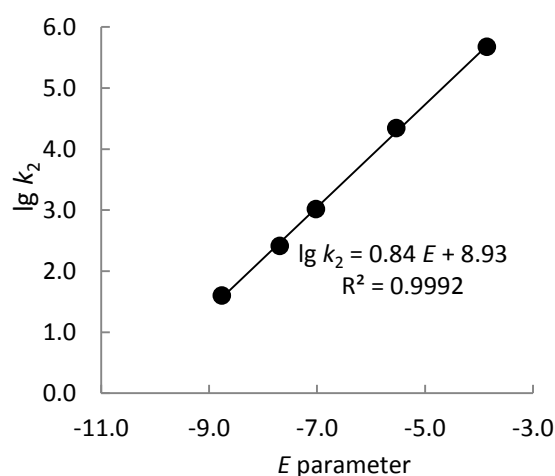
$$k_2 = 3.97 \times 10^1 \text{ L mol}^{-1} \text{ s}^{-1}$$



#### Determination of the Reactivity Parameters $N$ and $s_N$ of the Enamine **1-CN** in MeCN

Electrophile	$E$	$k_2 / \text{L mol}^{-1} \text{ s}^{-1}$	$\lg k_2$
<b>E1</b>	- 3.85	$4.68 \times 10^5$	5.67
<b>E2</b>	- 5.53	$2.20 \times 10^4$	4.34
<b>E3</b>	- 7.02	$1.03 \times 10^3$	3.01
<b>E4</b>	- 7.69	$2.59 \times 10^2$	2.41
<b>E5</b>	- 8.76	$3.97 \times 10^1$	1.60

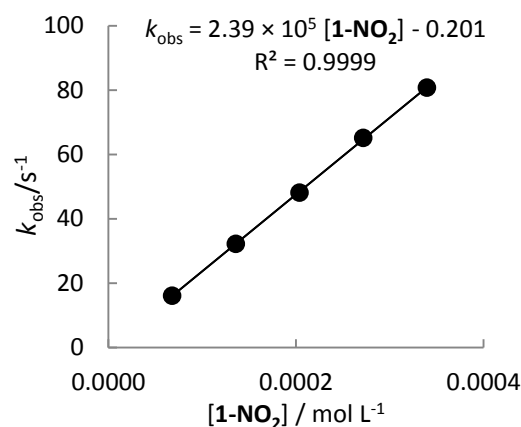
$$N = 10.63, s_N = 0.84$$



2.5.6.4. Kinetic Investigations of the Reactions of Enamine 1-NO<sub>2</sub>**Table S16.** Kinetics of the reaction of 1-NO<sub>2</sub> with E1 in MeCN (20 °C, stopped flow, λ = 586 nm)

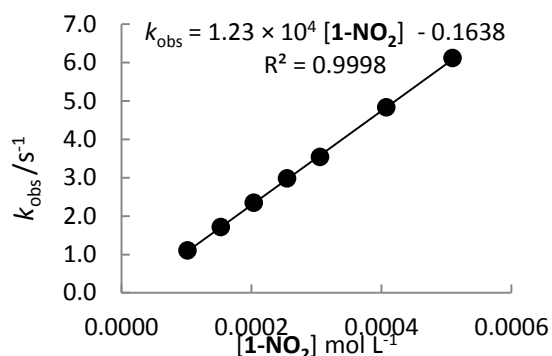
[E1] / mol L <sup>-1</sup>	[1-NO <sub>2</sub> ] / mol L <sup>-1</sup>	[1-NO <sub>2</sub> ]/ [E1]	<i>k</i> <sub>obs</sub> / s <sup>-1</sup>
8.37 × 10 <sup>-6</sup>	6.79 × 10 <sup>-5</sup>	8.1	1.61 × 10 <sup>1</sup>
	1.36 × 10 <sup>-4</sup>	16.2	3.22 × 10 <sup>1</sup>
	2.04 × 10 <sup>-4</sup>	24.3	4.82 × 10 <sup>1</sup>
	2.72 × 10 <sup>-4</sup>	32.5	6.52 × 10 <sup>1</sup>
	3.40 × 10 <sup>-4</sup>	33.7	8.08 × 10 <sup>1</sup>

$$k_2 = 2.39 \times 10^5 \text{ L mol}^{-1} \text{ s}^{-1}$$

**Table S17.** Kinetics of the reaction of 1-NO<sub>2</sub> with E2 in MeCN (20 °C, stopped flow, λ = 611 nm)

[E2] / mol L <sup>-1</sup>	[1- NO <sub>2</sub> ] / mol L <sup>-1</sup>	[1-NO <sub>2</sub> ]/ [E2]	<i>k</i> <sub>obs</sub> / s <sup>-1</sup>
1.04 × 10 <sup>-5</sup>	1.02 × 10 <sup>-4</sup>	9.1	1.10
	1.53 × 10 <sup>-4</sup>	13.7	1.71
	2.04 × 10 <sup>-4</sup>	18.3	2.34
	2.55 × 10 <sup>-4</sup>	22.9	2.98
	3.06 × 10 <sup>-4</sup>	27.4	3.54
	4.08 × 10 <sup>-4</sup>	36.6	4.83
	5.10 × 10 <sup>-4</sup>	45.7	6.11

$$k_2 = 1.23 \times 10^4 \text{ L mol}^{-1} \text{ s}^{-1}$$

**Table S18.** Kinetics of the reaction of 1-NO<sub>2</sub> with E3 in MeCN (20 °C, stopped flow, λ = 605 nm)

[E3] / mol L <sup>-1</sup>	[1- NO <sub>2</sub> ] / mol L <sup>-1</sup>	[1-NO <sub>2</sub> ]/ [E3]	<i>k</i> <sub>obs</sub> / s <sup>-1</sup>
7.38 × 10 <sup>-6</sup>	1.80 × 10 <sup>-4</sup>	24.4	1.12 × 10 <sup>-1</sup>
	3.60 × 10 <sup>-4</sup>	48.8	2.10 × 10 <sup>-1</sup>
	5.40 × 10 <sup>-4</sup>	73.2	3.06 × 10 <sup>-1</sup>
	7.20 × 10 <sup>-4</sup>	97.6	4.09 × 10 <sup>-1</sup>
	9.00 × 10 <sup>-4</sup>	122	5.25 × 10 <sup>-1</sup>

$$k_2 = 5.69 \times 10^2 \text{ L mol}^{-1} \text{ s}^{-1}$$

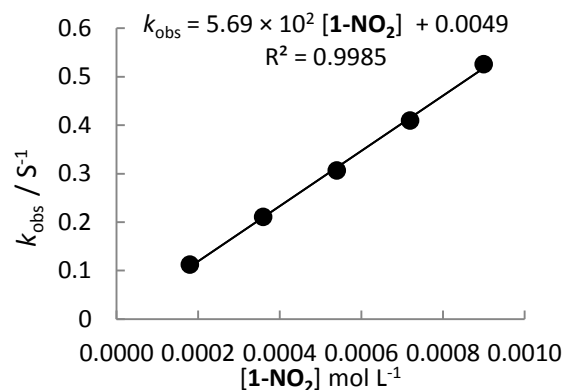
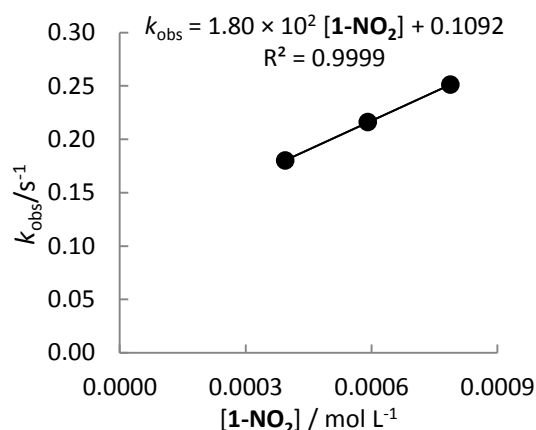


**Table S19.** Kinetics of the reaction of **1-NO<sub>2</sub>** with **E4** in MeCN (20 °C, stopped flow,  $\lambda = 611$  nm)

[ <b>E4</b> ] / mol L <sup>-1</sup>	[ <b>1-NO<sub>2</sub></b> ] / mol L <sup>-1</sup>	[ <b>1-NO<sub>2</sub></b> ] / [ <b>E4</b> ]	$k_{\text{obs}} / \text{s}^{-1}$
$7.41 \times 10^{-6}$	$3.94 \times 10^{-4}$	53.2	$1.80 \times 10^{-1}$
	$5.91 \times 10^{-4}$	79.8	$2.16 \times 10^{-1}$
	$7.88 \times 10^{-4}$	106.4	$2.51 \times 10^{-1}$

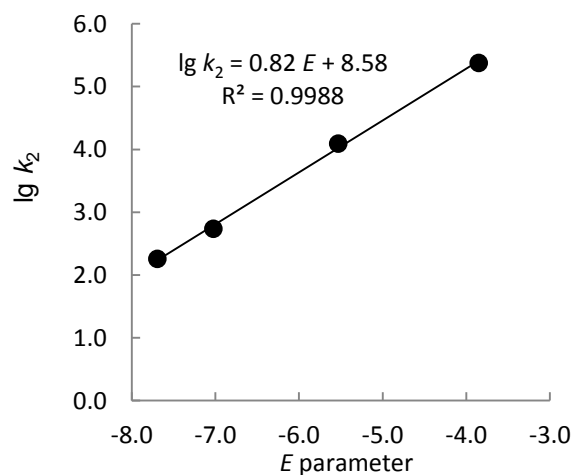
$$k_2 = 1.80 \times 10^2 \text{ L mol}^{-1} \text{ s}^{-1}$$



#### Determination of the Reactivity Parameters $N$ and $s_N$ of the Enamine **1-NO<sub>2</sub>** in MeCN

Electrophile	$E$	$k_2 / \text{L mol}^{-1} \text{ s}^{-1}$	$\lg k_2$
<b>E1</b>	-3.85	$2.39 \times 10^5$	5.24
<b>E2</b>	-5.53	$1.23 \times 10^4$	3.92
<b>E3</b>	-7.02	$5.69 \times 10^2$	2.76
<b>E4</b>	-7.69	$1.80 \times 10^2$	1.97

$$N = 10.42, s_N = 0.82$$

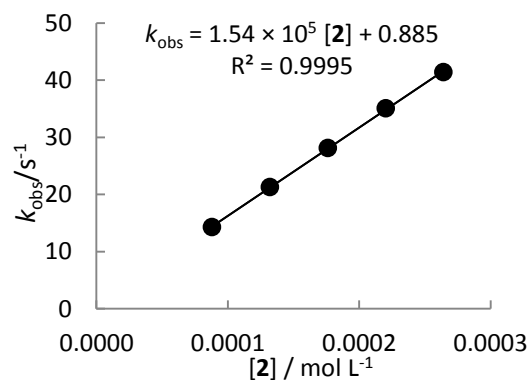


#### 2.5.6.5. Kinetic Investigations of the Reactions of Enamine **2**

**Table S20.** Kinetics of the reaction of **2** with **E1** in MeCN (20 °C, stopped flow,  $\lambda = 586$  nm)

[ <b>E1</b> ] / mol L <sup>-1</sup>	[ <b>2</b> ] / mol L <sup>-1</sup>	[ <b>2</b> ] / [ <b>E1</b> ]	$k_{\text{obs}} / \text{s}^{-1}$
$7.54 \times 10^{-6}$	$8.81 \times 10^{-5}$	11.7	$1.43 \times 10^1$
	$1.32 \times 10^{-4}$	17.5	$2.13 \times 10^1$
	$1.76 \times 10^{-4}$	23.4	$2.81 \times 10^1$
	$2.20 \times 10^{-4}$	29.2	$3.51 \times 10^1$
	$2.64 \times 10^{-4}$	35.1	$4.13 \times 10^1$

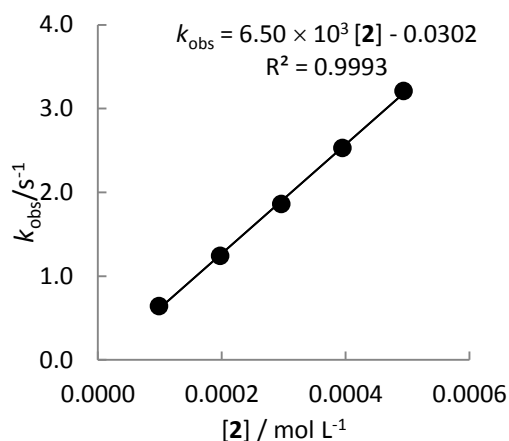
$$k_2 = 1.54 \times 10^5 \text{ L mol}^{-1} \text{ s}^{-1}$$



**Table S21.** Kinetics of the reaction of **2** with **E2** in MeCN (20 °C, stopped flow,  $\lambda = 611$  nm)

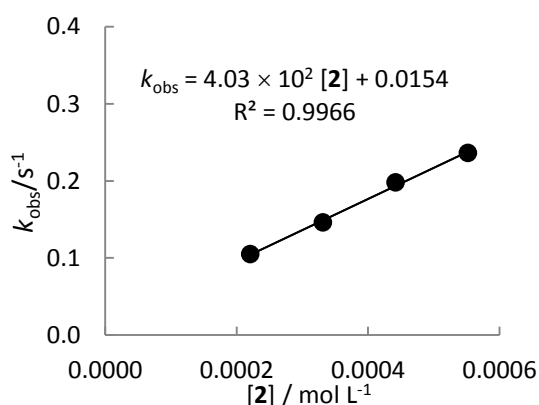
[E2] / mol L <sup>-1</sup>	[2] / mol L <sup>-1</sup>	[2]/ [E2]	$k_{\text{obs}} / \text{s}^{-1}$
$9.51 \times 10^{-6}$	$9.87 \times 10^{-5}$	10.4	$6.40 \times 10^{-1}$
	$1.97 \times 10^{-4}$	20.8	1.24
	$2.96 \times 10^{-4}$	31.1	1.86
	$3.95 \times 10^{-4}$	41.5	2.53
	$4.94 \times 10^{-4}$	51.9	3.21

$$k_2 = 6.50 \times 10^3 \text{ L mol}^{-1} \text{ s}^{-1}$$

**Table S22.** Kinetics of the reaction of **2** with **E3** in MeCN (20 °C, stopped flow,  $\lambda = 605$  nm)

[E3] / mol L <sup>-1</sup>	[2] / mol L <sup>-1</sup>	[2]/ [E3]	$k_{\text{obs}} / \text{s}^{-1}$
$7.51 \times 10^{-6}$	$2.21 \times 10^{-4}$	29.4	$1.05 \times 10^{-1}$
	$3.31 \times 10^{-4}$	44.1	$1.46 \times 10^{-1[a]}$
	$4.42 \times 10^{-4}$	58.8	$1.98 \times 10^{-1[a]}$
	$5.52 \times 10^{-4}$	73.5	$2.36 \times 10^{-1[a]}$

$$k_2 = 4.03 \times 10^2 \text{ L mol}^{-1} \text{ s}^{-1}$$



[a] The decays of absorbances were not strictly monoexponential.

**Table S23.** Kinetics of the reaction of **2** with **E4** in MeCN (20 °C, diode array UV-Vis spectrometer,  $\lambda = 611$  nm)

[E4] / mol L <sup>-1</sup>	[2] / mol L <sup>-1</sup>	[2]/ [E4]	$k_{\text{obs}} / \text{s}^{-1}$
$1.66 \times 10^{-5}$	$1.27 \times 10^{-4}$	7.7	$1.08 \times 10^{-2}$
$1.67 \times 10^{-5}$	$2.12 \times 10^{-4}$	12.7	$1.52 \times 10^{-2}$
$1.61 \times 10^{-5}$	$3.32 \times 10^{-4}$	20.6	$2.32 \times 10^{-2}$
$1.70 \times 10^{-5}$	$4.30 \times 10^{-4}$	25.4	$3.01 \times 10^{-2}$

$$k_2 = 6.42 \times 10^1 \text{ L mol}^{-1} \text{ s}^{-1}$$

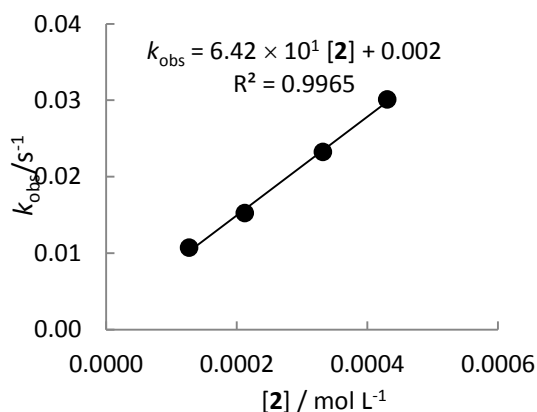
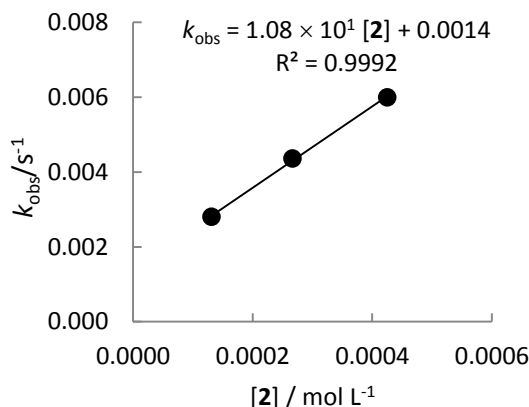


**Table S24.** Kinetics of the reaction of **2** with **E5** in MeCN (20 °C, diode array UV-Vis spectrometer,  $\lambda = 616$  nm)

[E5] / mol L <sup>-1</sup>	[2] / mol L <sup>-1</sup>	[2]/ [E5]	$k_{\text{obs}} / \text{s}^{-1}$
$1.46 \times 10^{-5}$	$1.32 \times 10^{-4}$	9.0	$2.82 \times 10^{-3}$
$1.46 \times 10^{-5}$	$2.67 \times 10^{-4}$	18.3	$4.36 \times 10^{-3}$
$1.45 \times 10^{-5}$	$4.25 \times 10^{-4}$	29.4	$6.00 \times 10^{-3}$

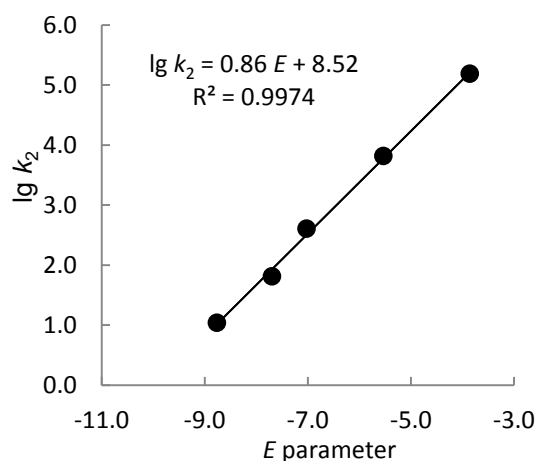
$$k_2 = 1.08 \times 10^1 \text{ L mol}^{-1} \text{ s}^{-1}$$



#### Determination of the Reactivity Parameters $N$ and $s_N$ of the Enamine **2** in MeCN

Electrophile	$E$	$k_2 / \text{L mol}^{-1} \text{ s}^{-1}$	$\lg k_2$
<b>E1</b>	- 3.85	$1.54 \times 10^5$	5.19
<b>E2</b>	- 5.53	$6.50 \times 10^3$	3.81
<b>E3</b>	- 7.02	$4.03 \times 10^2$	2.61
<b>E4</b>	- 7.69	$6.42 \times 10^1$	1.81
<b>E5</b>	- 8.76	$1.08 \times 10^1$	1.03

$$N = 9.94, s_N = 0.86$$

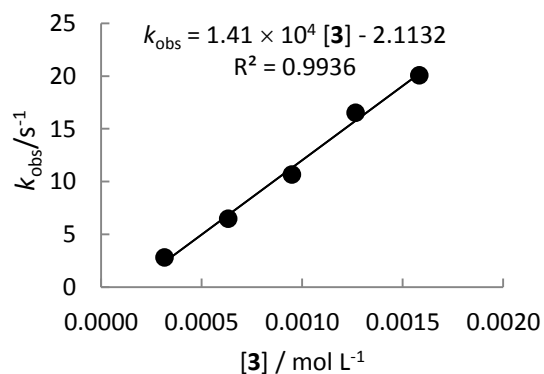


#### 2.5.6.6. Kinetic Investigations of the Reactions of Enamine **3**

**Table S25.** Kinetics of the reaction of **3** with **E1** in MeCN (20 °C, stopped flow,  $\lambda = 586$  nm)

[E1] / mol L <sup>-1</sup>	[3] / mol L <sup>-1</sup>	[3]/ [E1]	$k_{\text{obs}} / \text{s}^{-1}$
$9.05 \times 10^{-6}$	$3.17 \times 10^{-4}$	35.0	2.80
	$6.33 \times 10^{-4}$	70.0	6.47
	$9.50 \times 10^{-4}$	105	10.6
	$1.27 \times 10^{-3}$	140	16.5
	$1.58 \times 10^{-3}$	175	20.1

$$k_2 = 1.41 \times 10^4 \text{ L mol}^{-1} \text{ s}^{-1}$$

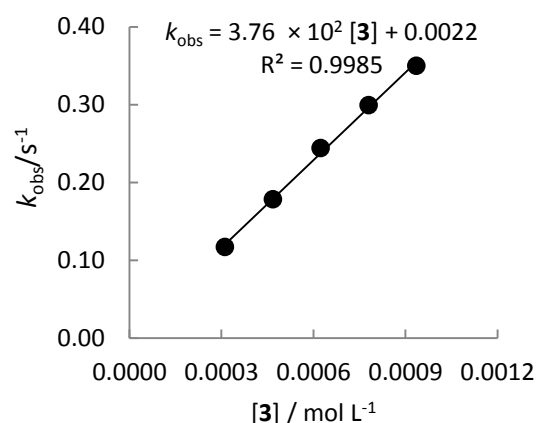




**Table S26.** Kinetics of the reaction of **3** with **E2** in MeCN (20 °C, stopped flow,  $\lambda = 611$  nm)

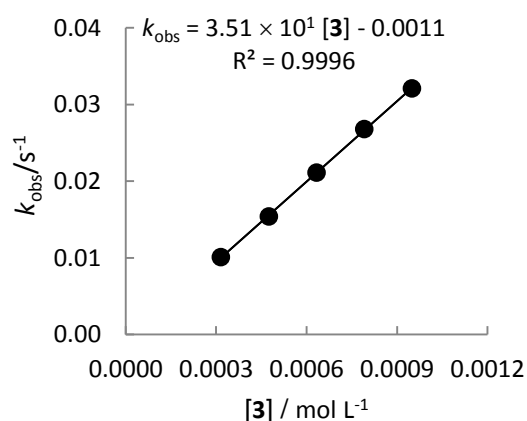
[E2] / mol L <sup>-1</sup>	[3] / mol L <sup>-1</sup>	[3]/ [E2]	$k_{\text{obs}} / \text{s}^{-1}$
$1.34 \times 10^{-5}$	$3.12 \times 10^{-4}$	23.2	$1.17 \times 10^{-1}$
	$4.68 \times 10^{-4}$	34.8	$1.78 \times 10^{-1}$
	$6.24 \times 10^{-4}$	46.4	$2.41 \times 10^{-1}$
	$7.80 \times 10^{-4}$	58.0	$2.99 \times 10^{-1}$
	$9.36 \times 10^{-4}$	69.6	$3.50 \times 10^{-1}$

$$k_2 = 3.76 \times 10^2 \text{ L mol}^{-1} \text{ s}^{-1}$$

**Table S27.** Kinetics of the reaction of **3** with **E3** in MeCN (20 °C, stopped flow,  $\lambda = 605$  nm)

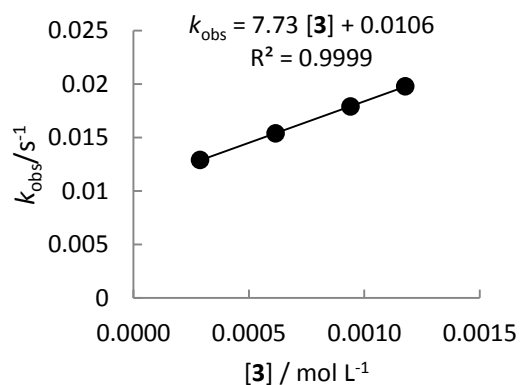
[E3] / mol L <sup>-1</sup>	[3] / mol L <sup>-1</sup>	[3]/ [E3]	$k_{\text{obs}} / \text{s}^{-1}$
$7.45 \times 10^{-6}$	$3.17 \times 10^{-4}$	42.5	$1.01 \times 10^{-2}$
	$4.75 \times 10^{-4}$	63.8	$1.53 \times 10^{-2}$
	$6.33 \times 10^{-4}$	85.0	$2.11 \times 10^{-2}$
	$7.91 \times 10^{-4}$	106.3	$2.68 \times 10^{-2}$
	$9.50 \times 10^{-4}$	127.5	$3.21 \times 10^{-2}$

$$k_2 = 3.51 \times 10^1 \text{ L mol}^{-1} \text{ s}^{-1}$$

**Table S28.** Kinetics of the reaction of **3** with **E4** in MeCN (20 °C, diode array UV-Vis spectrometer,  $\lambda = 611$  nm)

[E4] / mol L <sup>-1</sup>	[3] / mol L <sup>-1</sup>	[3]/ [E4]	$k_{\text{obs}} / \text{s}^{-1}$
$1.47 \times 10^{-5}$	$2.89 \times 10^{-4}$	19.6	$1.29 \times 10^{-2}$
$1.25 \times 10^{-5}$	$6.16 \times 10^{-4}$	49.4	$1.54 \times 10^{-2}$
$1.22 \times 10^{-5}$	$9.41 \times 10^{-4}$	76.9	$1.79 \times 10^{-2}$
$1.20 \times 10^{-5}$	$1.18 \times 10^{-3}$	98.1	$1.98 \times 10^{-2}$

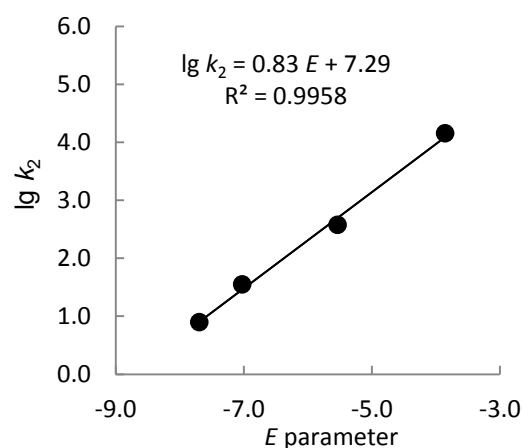
$$k_2 = 7.73 \text{ L mol}^{-1} \text{ s}^{-1}$$



Determination of the Reactivity Parameters  $N$  and  $s_N$  of the Enamine **3** in MeCN

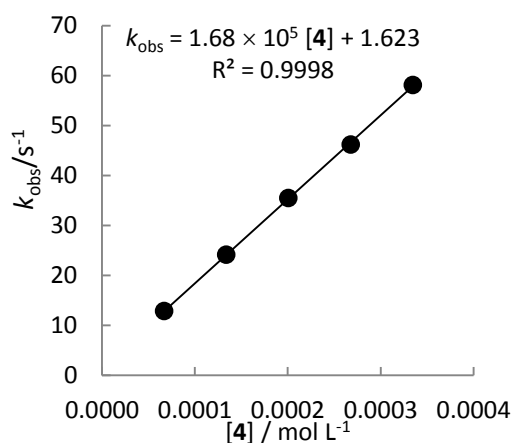
Electrophile	$E$	$k_2 / \text{L mol}^{-1} \text{s}^{-1}$	$\lg k_2$
<b>E1</b>	-3.85	$1.41 \times 10^4$	4.15
<b>E2</b>	-5.53	$3.76 \times 10^2$	2.58
<b>E3</b>	-7.02	$3.51 \times 10^1$	1.54
<b>E4</b>	-7.69	$7.73 \times 10^0$	0.89

$$N = 8.78, s_N = 0.83$$

2.5.6.7. Kinetic Investigations of the Reactions of Enamine **4**Table S29. Kinetics of the reaction of **4** with **E3** in MeCN (20 °C, stopped flow,  $\lambda = 605$  nm)

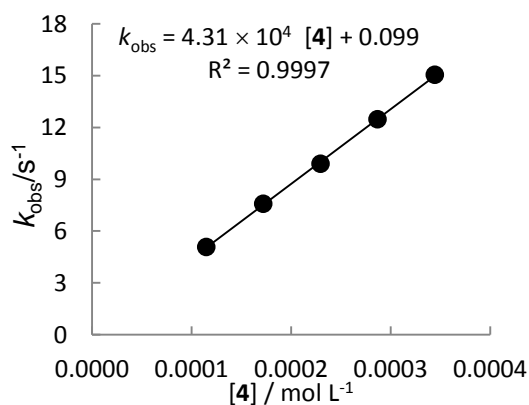
[ <b>E3</b> ] / mol L <sup>-1</sup>	[ <b>4</b> ] / mol L <sup>-1</sup>	[ <b>4</b> ]/ [ <b>E3</b> ]	$k_{\text{obs}} / \text{s}^{-1}$
$8.88 \times 10^{-6}$	$6.69 \times 10^{-5}$	7.5	$1.29 \times 10^1$
	$1.34 \times 10^{-4}$	15.1	$2.41 \times 10^1$
	$2.01 \times 10^{-4}$	22.6	$3.55 \times 10^1$
	$2.68 \times 10^{-4}$	30.2	$4.62 \times 10^1$
	$3.35 \times 10^{-4}$	37.7	$5.81 \times 10^1$

$$k_2 = 1.68 \times 10^5 \text{ L mol}^{-1} \text{s}^{-1}$$

Table S30. Kinetics of the reaction of **4** with **E4** in MeCN (20 °C, stopped flow,  $\lambda = 611$  nm)

[ <b>E4</b> ] / mol L <sup>-1</sup>	[ <b>4</b> ] / mol L <sup>-1</sup>	[ <b>4</b> ]/ [ <b>E4</b> ]	$k_{\text{obs}} / \text{s}^{-1}$
$6.69 \times 10^{-6}$	$1.15 \times 10^{-4}$	17.2	5.07
	$1.72 \times 10^{-4}$	35.7	7.57
	$2.30 \times 10^{-4}$	34.3	9.89
	$2.87 \times 10^{-4}$	42.9	$1.25 \times 10^1$
	$3.45 \times 10^{-4}$	51.5	$1.50 \times 10^1$

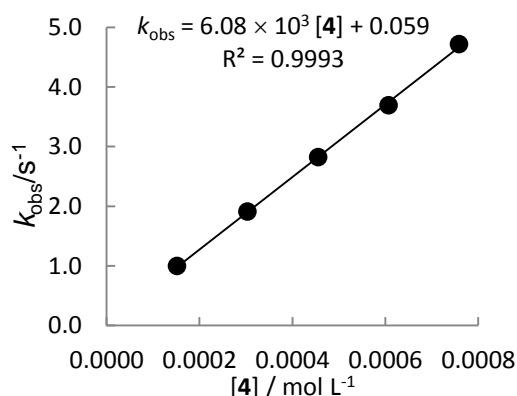
$$k_2 = 4.31 \times 10^4 \text{ L mol}^{-1} \text{s}^{-1}$$



**Table S31.** Kinetics of the reaction of **4** with **E5** in MeCN (20 °C, stopped flow,  $\lambda = 616$  nm)

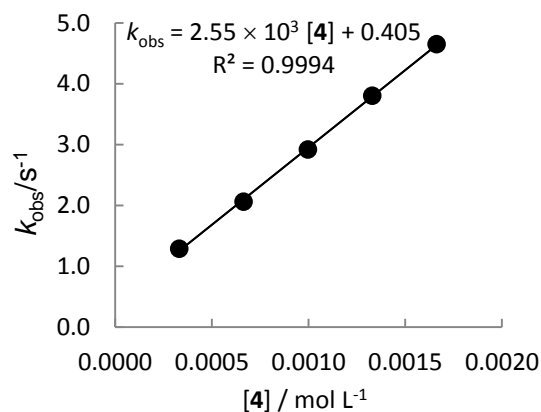
[E5] / mol L <sup>-1</sup>	[4] / mol L <sup>-1</sup>	[4]/ [E5]	$k_{\text{obs}} / \text{s}^{-1}$
$9.71 \times 10^{-6}$	$1.52 \times 10^{-4}$	15.6	$9.98 \times 10^{-1}$
	$3.04 \times 10^{-4}$	31.3	1.91
	$4.55 \times 10^{-4}$	46.9	2.82
	$6.07 \times 10^{-4}$	62.5	3.69
	$7.59 \times 10^{-4}$	78.1	4.72

$$k_2 = 6.08 \times 10^3 \text{ L mol}^{-1} \text{ s}^{-1}$$

**Table S32.** Kinetics of the reaction of **4** with **E6** in MeCN (20 °C, stopped flow,  $\lambda = 635$  nm)

[E6] / mol L <sup>-1</sup>	[4] / mol L <sup>-1</sup>	[4]/ [E6]	$k_{\text{obs}} / \text{s}^{-1}$
$6.95 \times 10^{-6}$	$3.32 \times 10^{-4}$	47.8	1.29
	$6.65 \times 10^{-4}$	95.7	2.06
	$9.97 \times 10^{-4}$	143.5	2.92
	$1.33 \times 10^{-3}$	191.4	3.80
	$1.66 \times 10^{-3}$	239.2	4.65

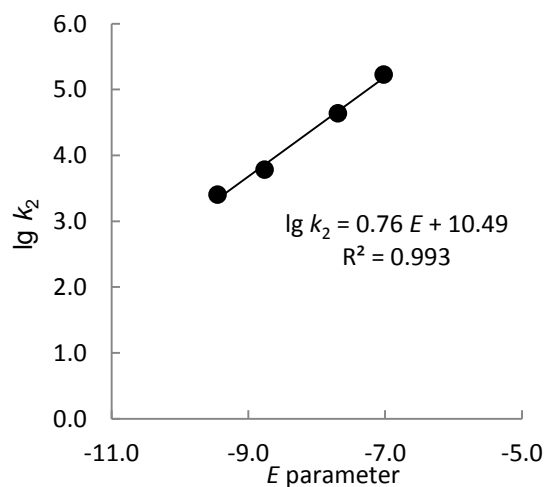
$$k_2 = 2.55 \times 10^3 \text{ L mol}^{-1} \text{ s}^{-1}$$



#### Determination of the Reactivity Parameters $N$ and $s_N$ of the Enamine **4** in MeCN

Electrophile	$E$	$k_2 / \text{L mol}^{-1} \text{ s}^{-1}$	$\lg k_2$
<b>E3</b>	- 7.02	$1.68 \times 10^5$	5.23
<b>E4</b>	- 7.69	$4.31 \times 10^4$	4.63
<b>E5</b>	- 8.76	$6.08 \times 10^3$	3.78
<b>E6</b>	- 9.45	$2.55 \times 10^3$	3.41

$$N = 13.87, s_N = 0.76$$

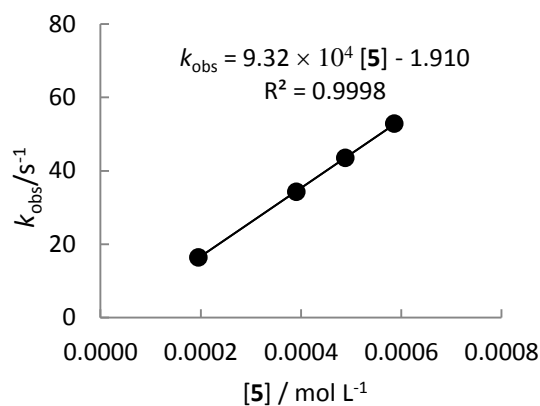


## 2.5.6.8. Kinetic Investigations of the Reactions of Enamine 5

**Table S33.** Kinetics of the reaction of **5** with **E3** in MeCN (20 °C, stopped flow,  $\lambda = 605$  nm)

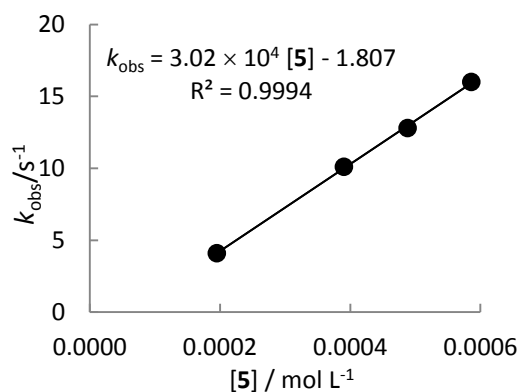
[E3] / mol L <sup>-1</sup>	[5] / mol L <sup>-1</sup>	[5]/ [E3]	$k_{\text{obs}} / \text{s}^{-1}$
$7.99 \times 10^{-6}$	$1.95 \times 10^{-4}$	24.5	$1.64 \times 10^1$
	$3.91 \times 10^{-4}$	48.9	$3.43 \times 10^1$
	$4.89 \times 10^{-4}$	61.1	$4.35 \times 10^1$
	$5.86 \times 10^{-4}$	73.4	$5.29 \times 10^1$

$$k_2 = 9.32 \times 10^4 \text{ L mol}^{-1} \text{ s}^{-1}$$

**Table S34.** Kinetics of the reaction of **5** with **E4** in MeCN (20 °C, stopped flow,  $\lambda = 611$  nm)

[E4] / mol L <sup>-1</sup>	[5] / mol L <sup>-1</sup>	[5]/ [E4]	$k_{\text{obs}} / \text{s}^{-1}$
$1.21 \times 10^{-5}$	$1.95 \times 10^{-4}$	16.2	4.09
	$3.91 \times 10^{-4}$	32.3	$1.01 \times 10^1$
	$4.89 \times 10^{-4}$	40.4	$1.28 \times 10^1$
	$5.86 \times 10^{-4}$	48.5	$1.60 \times 10^1$

$$k_2 = 3.02 \times 10^4 \text{ L mol}^{-1} \text{ s}^{-1}$$

**Table S35.** Kinetics of the reaction of **5** with **E5** in MeCN (20 °C, stopped flow,  $\lambda = 616$  nm)

[E5] / mol L <sup>-1</sup>	[5] / mol L <sup>-1</sup>	[5]/ [E5]	$k_{\text{obs}} / \text{s}^{-1}$
$8.86 \times 10^{-6}$	$5.57 \times 10^{-5}$	6.5	$2.06 \times 10^{-1}$
	$1.15 \times 10^{-4}$	13.0	$3.95 \times 10^{-1}$
	$1.73 \times 10^{-4}$	19.5	$6.60 \times 10^{-1}$
	$2.31 \times 10^{-4}$	26.0	$8.70 \times 10^{-1}$

$$k_2 = 3.86 \times 10^3 \text{ L mol}^{-1} \text{ s}^{-1}$$

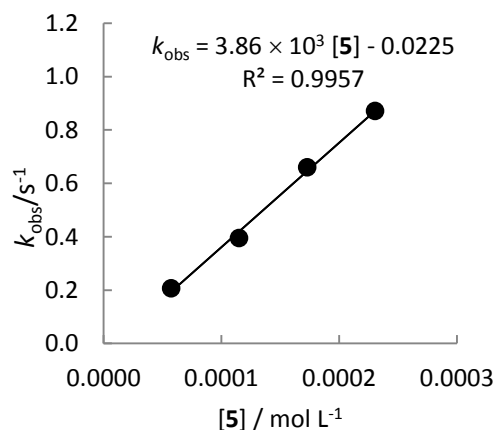
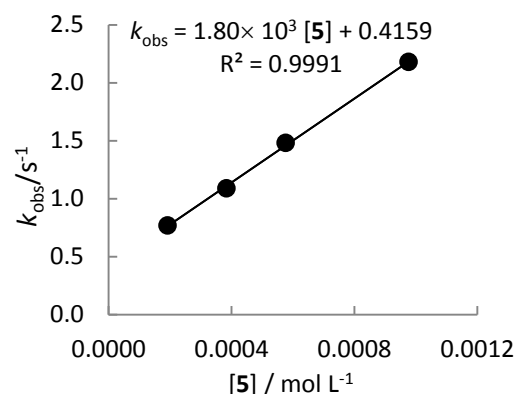


**Table S36.** Kinetics of the reaction of **5** with **E6** in MeCN (20 °C, stopped flow,  $\lambda = 635$  nm)

[E6] / mol L <sup>-1</sup>	[5] / mol L <sup>-1</sup>	[1-H]/ [5]	$k_{\text{obs}}^{[a]} / \text{s}^{-1}$
$7.24 \times 10^{-6}$	$1.92 \times 10^{-4}$	26.6	$7.78 \times 10^{-1}$
$1.12 \times 10^{-5}$	$3.84 \times 10^{-4}$	34.4	1.09
$1.12 \times 10^{-5}$	$5.77 \times 10^{-4}$	51.6	1.48
$7.99 \times 10^{-6}$	$9.77 \times 10^{-4}$	122	2.18

$$k_2 = 1.80 \times 10^3 \text{ L mol}^{-1} \text{ s}^{-1}$$

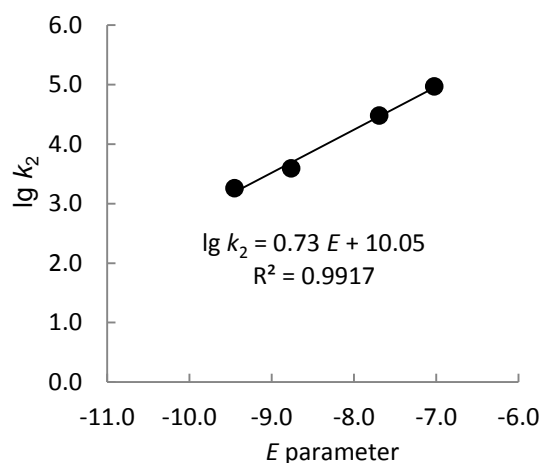


[a] Since the decays of absorbances were not strictly monoexponential, only the first 50% of the decays were evaluated

#### Determination of the Reactivity Parameters $N$ and $s_N$ of the Enamine **5** in MeCN

Electrophile	$E$	$k_2 / \text{L mol}^{-1} \text{ s}^{-1}$	$\lg k_2$
<b>E3</b>	-7.02	$9.32 \times 10^4$	4.97
<b>E4</b>	-7.69	$3.03 \times 10^4$	4.48
<b>E5</b>	-8.76	$3.86 \times 10^3$	3.59
<b>E6</b>	-9.45	$1.80 \times 10^3$	3.26

$$N = 13.84, s_N = 0.73$$

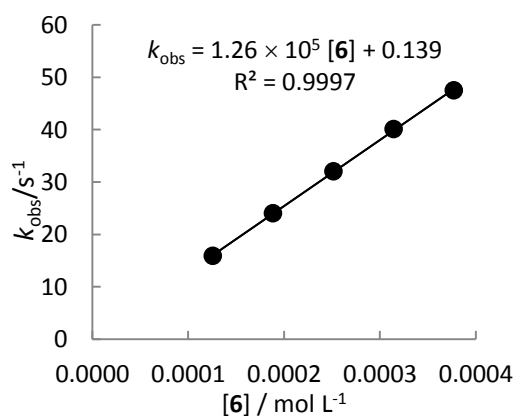


#### 2.5.6.9. Kinetic Investigations of the Reactions of Enamine **6**

**Table S37.** Kinetics of the reaction of **6** with **E2** in MeCN (20 °C, stopped flow,  $\lambda = 611$  nm)

[E2] / mol L <sup>-1</sup>	[6] / mol L <sup>-1</sup>	[6]/ [E2]	$k_{\text{obs}} / \text{s}^{-1}$
$1.24 \times 10^{-5}$	$1.26 \times 10^{-4}$	10.1	$1.59 \times 10^1$
	$1.89 \times 10^{-4}$	15.2	$2.41 \times 10^1$
	$2.52 \times 10^{-4}$	20.3	$3.20 \times 10^1$
	$3.14 \times 10^{-4}$	25.4	$4.01 \times 10^1$
	$3.77 \times 10^{-4}$	30.4	$4.75 \times 10^1$

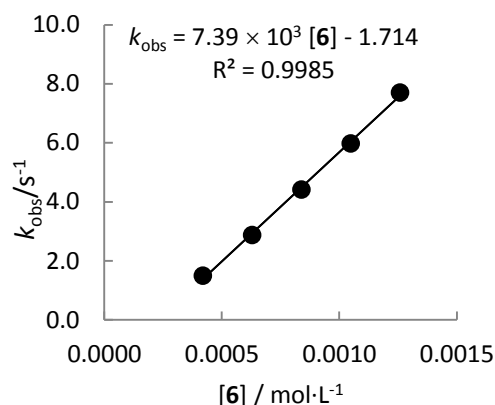
$$k_2 = 1.26 \times 10^5 \text{ L mol}^{-1} \text{ s}^{-1}$$



**Table S38.** Kinetics of the reaction of **6** with **E3** in MeCN (20 °C, stopped flow,  $\lambda = 605$  nm)

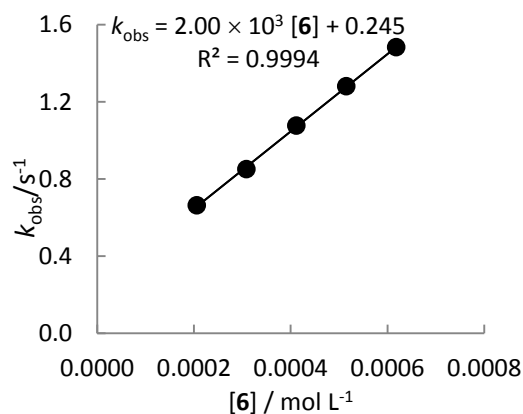
[E3] / mol L <sup>-1</sup>	[6] / mol L <sup>-1</sup>	[6]/ [E3]	$k_{\text{obs}} / \text{s}^{-1}$
$7.46 \times 10^{-6}$	$4.20 \times 10^{-4}$	56.3	1.49
	$6.29 \times 10^{-4}$	84.5	2.87
	$8.39 \times 10^{-4}$	113	4.41
	$1.05 \times 10^{-3}$	141	5.97
	$1.26 \times 10^{-3}$	169	7.70

$$k_2 = 7.39 \times 10^3 \text{ L mol}^{-1} \text{ s}^{-1}$$

**Table S39.** Kinetics of the reaction of **6** with **E4** in MeCN (20 °C, stopped flow,  $\lambda = 611$  nm)

[E4] / mol L <sup>-1</sup>	[6] / mol L <sup>-1</sup>	[6]/ [E4]	$k_{\text{obs}} / \text{s}^{-1}$
$6.19 \times 10^{-6}$	$2.06 \times 10^{-4}$	33.3	$6.63 \times 10^{-1}$
	$3.09 \times 10^{-4}$	50.0	$8.50 \times 10^{-1}$
	$4.12 \times 10^{-4}$	66.6	1.08
	$5.15 \times 10^{-4}$	83.3	1.28
	$6.18 \times 10^{-4}$	99.9	1.48

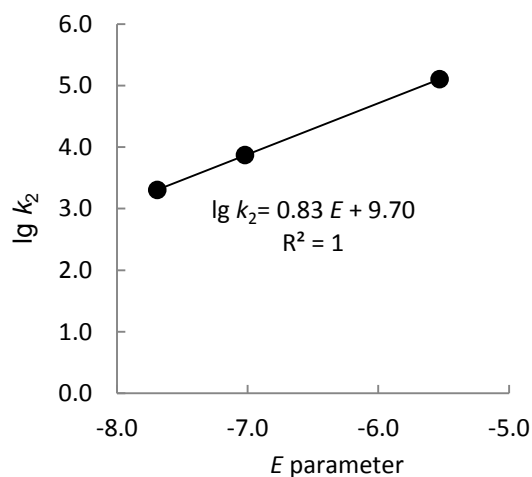
$$k_2 = 2.00 \times 10^3 \text{ L mol}^{-1} \text{ s}^{-1}$$



#### Determination of the Reactivity Parameters $N$ and $s_N$ of the Enamine **6** in MeCN

Electrophile	$E$	$k_2 / \text{L mol}^{-1} \text{ s}^{-1}$	$\lg k_2$
<b>E2</b>	- 5.53	$1.26 \times 10^5$	5.10
<b>E3</b>	- 7.02	$7.39 \times 10^3$	3.87
<b>E4</b>	- 7.69	$2.00 \times 10^3$	3.30

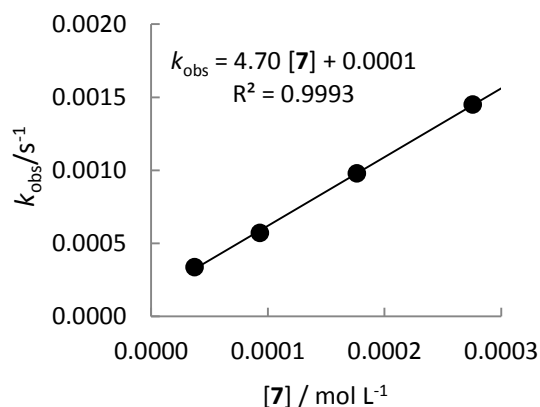
$$N = 11.66, s_N = 0.83$$



2.5.6.10. Kinetic Investigations of the Reactions of Enamines **7** and **8****Table S40.** Kinetics of the reaction of **7** with **E6** in MeCN (20 °C, diode array UV-Vis spectrometer,  $\lambda = 635$  nm)

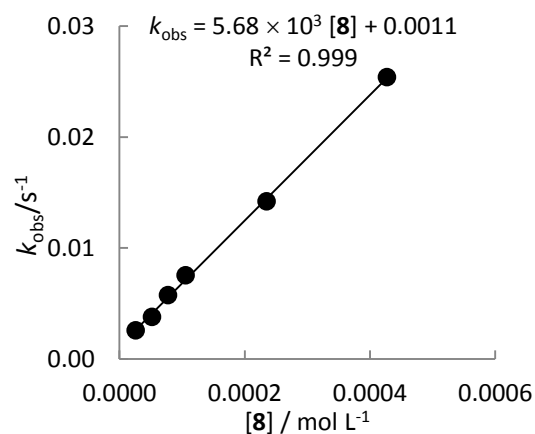
[ <b>E6</b> ] / mol L <sup>-1</sup>	[ <b>7</b> ] / mol L <sup>-1</sup>	[ <b>7</b> ]/ [ <b>E6</b> ]	$k_{\text{obs}} / \text{s}^{-1}$
$1.22 \times 10^{-5}$	$3.72 \times 10^{-5}$	3.1	$3.37 \times 10^{-4}$
$1.14 \times 10^{-5}$	$9.34 \times 10^{-5}$	8.2	$5.70 \times 10^{-4}$
$1.68 \times 10^{-5}$	$1.77 \times 10^{-4}$	10.5	$9.78 \times 10^{-4}$
$1.27 \times 10^{-5}$	$2.76 \times 10^{-4}$	21.6	$1.45 \times 10^{-3}$

$$k_2 = 4.70 \times 10^0 \text{ L mol}^{-1} \text{ s}^{-1}$$

**Table S41.** Kinetics of the reaction of **8** with **E6** in MeCN (20 °C, diode array UV-Vis spectrometer,  $\lambda = 635$  nm)

[ <b>E6</b> ] / mol L <sup>-1</sup>	[ <b>8</b> ] / mol L <sup>-1</sup>	[ <b>8</b> ]/ [ <b>E6</b> ]	$k_{\text{obs}} / \text{s}^{-1}$
$5.30 \times 10^{-6}$	$2.59 \times 10^{-5}$	4.9	$2.56 \times 10^{-3}$
$5.36 \times 10^{-6}$	$5.24 \times 10^{-5}$	9.8	$3.81 \times 10^{-3}$
$5.25 \times 10^{-6}$	$7.78 \times 10^{-5}$	14.8	$5.75 \times 10^{-3}$
$5.44 \times 10^{-6}$	$1.06 \times 10^{-4}$	19.5	$7.55 \times 10^{-3}$
$1.66 \times 10^{-5}$	$2.35 \times 10^{-4}$	14.4	$1.44 \times 10^{-2}$
$1.64 \times 10^{-5}$	$4.27 \times 10^{-4}$	26.2	$2.54 \times 10^{-2}$

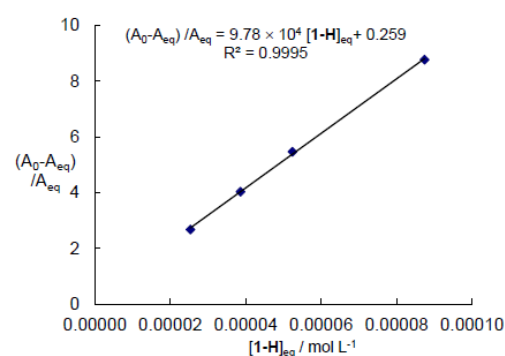
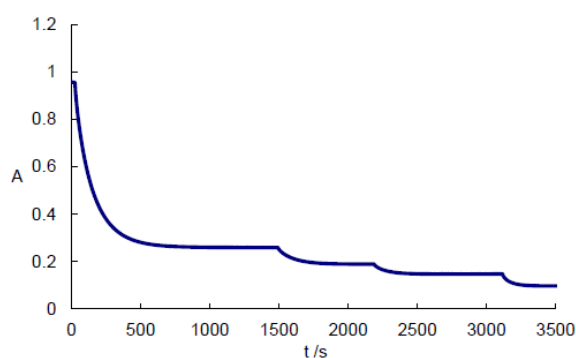
$$k_2 = 5.68 \times 10^1 \text{ L mol}^{-1} \text{ s}^{-1}$$



## 2.5.7. Determination of the Equilibrium Constants.

Table S42. Reaction of **1-H** with **E5** ( $\varepsilon = 1.287 \times 10^5 \text{ L mol}^{-1} \text{ cm}^{-1}$ ,  $\lambda = 616 \text{ nm}$ ) in MeCN at 20 °C.

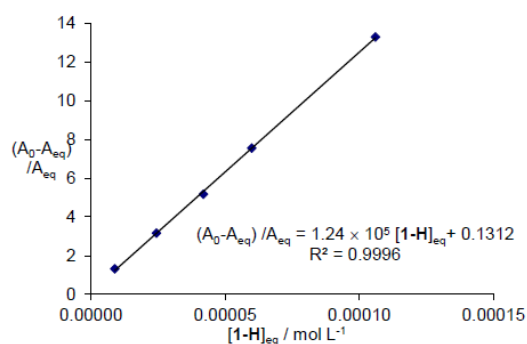
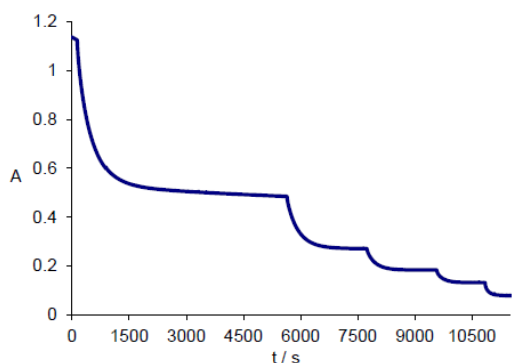
Step	V( <b>1-H</b> ) / mL	V ( <b>1-H</b> ) <sub>total</sub> / mL	V <sub>total</sub> / mL	A <sub>eq</sub>	[ <b>E5</b> ]	A <sub>0</sub> -A <sub>eq</sub>	[ <b>1-H</b> ] <sub>0</sub>	[ <b>1-H</b> ] <sub>0</sub> / [ <b>E5</b> ] <sub>0</sub>	[ <b>1-H</b> ] <sub>eq</sub>	(A <sub>0</sub> -A <sub>eq</sub> )/A <sub>eq</sub>
0			23.03	0.957	$1.49 \times 10^{-5}$					
1	0.05	0.05	23.08	0.260	$4.04 \times 10^{-6}$	0.697	$3.61 \times 10^{-5}$	2.4	$2.53 \times 10^{-5}$	2.681
2	0.02	0.07	23.10	0.190	$2.95 \times 10^{-6}$	0.767	$5.05 \times 10^{-5}$	12.5	$3.86 \times 10^{-5}$	4.037
3	0.02	0.09	23.12	0.148	$2.30 \times 10^{-6}$	0.809	$6.49 \times 10^{-5}$	22.0	$5.24 \times 10^{-5}$	5.466
4	0.05	0.14	23.17	0.098	$1.52 \times 10^{-6}$	0.859	$1.01 \times 10^{-4}$	43.8	$8.74 \times 10^{-5}$	8.765



$$K = 9.78 \times 10^4 \text{ L mol}^{-1}$$

Table S43. Reaction of **1-H** with **E5** ( $\varepsilon = 1.287 \times 10^5 \text{ L mol}^{-1} \text{ cm}^{-1}$ ,  $\lambda = 616 \text{ nm}$ ) in MeCN at 20 °C.

Step	V( <b>1-H</b> ) / mL	V ( <b>1-H</b> ) <sub>total</sub> / mL	V <sub>total</sub> / mL	A <sub>eq</sub>	[ <b>E5</b> ]	A <sub>0</sub> -A <sub>eq</sub>	[ <b>1-H</b> ] <sub>0</sub>	[ <b>1-H</b> ] <sub>0</sub> / [ <b>E5</b> ] <sub>0</sub>	[ <b>1-H</b> ] <sub>eq</sub>	(A <sub>0</sub> -A <sub>eq</sub> )/A <sub>eq</sub>
0			23.55	1.130	$1.76 \times 10^{-5}$					
1	0.02	0.02	23.57	0.487	$7.57 \times 10^{-6}$	0.643	$1.89 \times 10^{-5}$	1.1	$8.92 \times 10^{-6}$	1.320
2	0.02	0.04	23.59	0.271	$4.21 \times 10^{-6}$	0.859	$3.78 \times 10^{-5}$	5.0	$2.45 \times 10^{-5}$	3.170
3	0.02	0.06	23.61	0.183	$2.84 \times 10^{-6}$	0.947	$5.67 \times 10^{-5}$	13.5	$4.19 \times 10^{-5}$	5.175
4	0.02	0.08	23.63	0.132	$2.05 \times 10^{-6}$	0.998	$7.55 \times 10^{-5}$	26.5	$6.00 \times 10^{-5}$	7.561
5	0.05	0.13	23.68	0.079	$1.23 \times 10^{-6}$	1.051	$1.22 \times 10^{-4}$	59.7	$1.06 \times 10^{-4}$	13.304

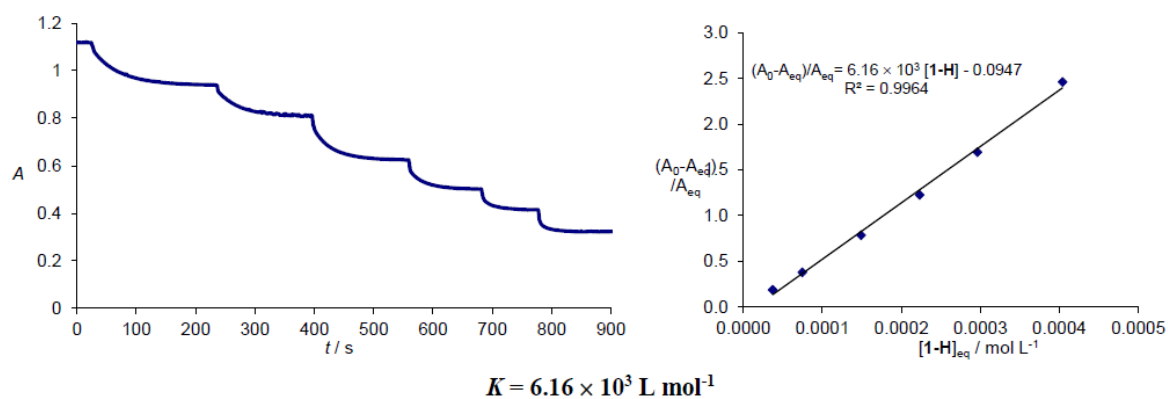


$$K = 1.24 \times 10^5 \text{ L mol}^{-1}$$

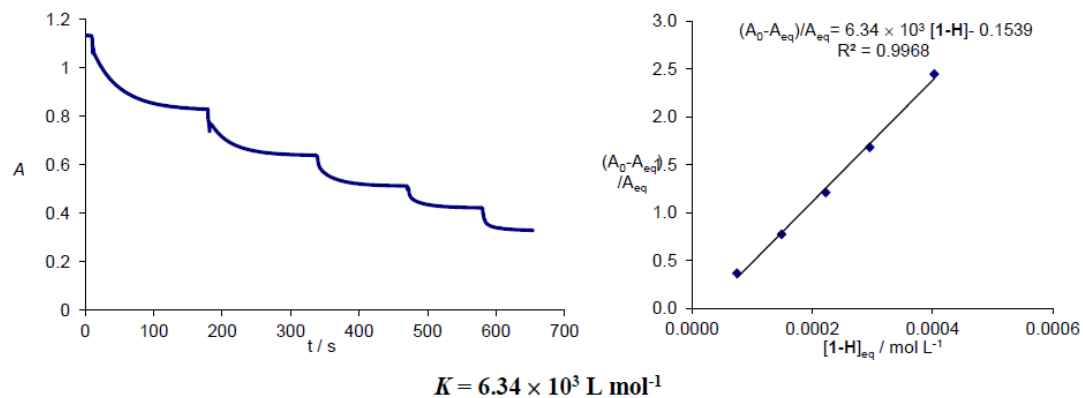


**Table S44.** Reaction of **1-H** with **E6** ( $\varepsilon = 1.727 \times 10^5 \text{ L mol}^{-1} \text{ cm}^{-1}$ ,  $\lambda = 635 \text{ nm}$ ) in MeCN at 20 °C.

Step	V( <b>1-H</b> ) / mL	V ( <b>1-H</b> ) <sub>total</sub> / mL	V <sub>total</sub> / mL	A <sub>eq</sub>	[ <b>E6</b> ]	A <sub>0</sub> -A <sub>eq</sub>	[ <b>1-H</b> ] <sub>0</sub>	[ <b>1-H</b> ] <sub>0</sub> / [ <b>E6</b> ] <sub>0</sub>	[ <b>1-H</b> ] <sub>eq</sub>	(A <sub>0</sub> -A <sub>eq</sub> )/A <sub>eq</sub>
0			22.17	1.118	$1.29 \times 10^{-5}$					
1	0.10	0.10	22.27	0.941	$1.09 \times 10^{-5}$	0.177	$3.93 \times 10^{-5}$	3.0	$3.72 \times 10^{-5}$	0.188
2	0.10	0.20	22.37	0.811	$9.39 \times 10^{-6}$	0.307	$7.82 \times 10^{-5}$	7.2	$7.46 \times 10^{-5}$	0.379
3	0.20	0.40	22.57	0.626	$7.25 \times 10^{-6}$	0.492	$1.55 \times 10^{-4}$	16.5	$1.49 \times 10^{-4}$	0.786
4	0.20	0.60	22.77	0.502	$5.81 \times 10^{-6}$	0.616	$2.30 \times 10^{-4}$	31.8	$2.23 \times 10^{-4}$	1.227
5	0.20	0.80	22.97	0.415	$4.81 \times 10^{-6}$	0.703	$3.04 \times 10^{-4}$	52.4	$2.96 \times 10^{-4}$	1.694
6	0.30	1.10	23.27	0.323	$3.74 \times 10^{-6}$	0.795	$4.13 \times 10^{-4}$	86.0	$4.04 \times 10^{-4}$	2.461

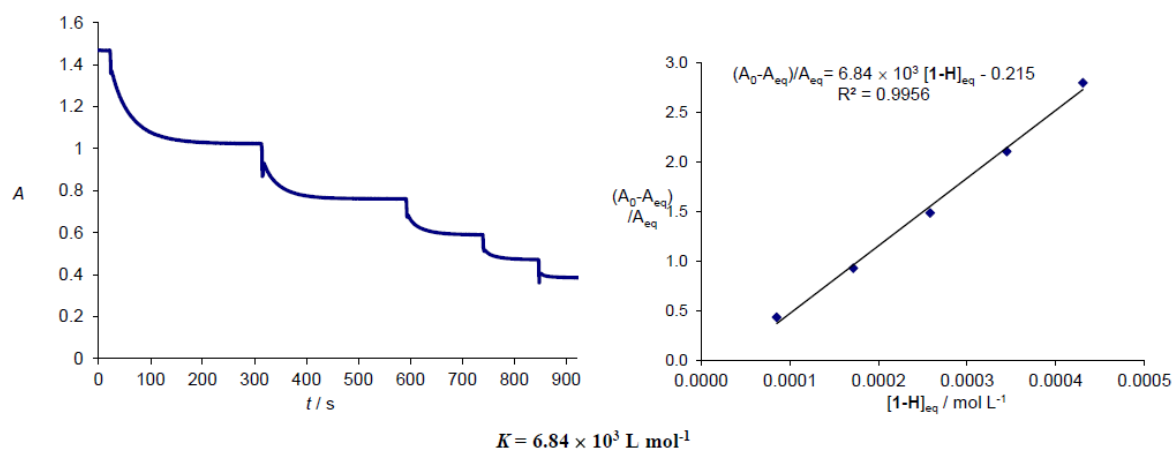
**Table S45.** Reaction of **1-H** with **E6** ( $\varepsilon = 1.727 \times 10^5 \text{ L mol}^{-1} \text{ cm}^{-1}$ ,  $\lambda = 635 \text{ nm}$ ) in MeCN at 20 °C.

Step	V( <b>1-H</b> ) / mL	V ( <b>1-H</b> ) <sub>total</sub> / mL	V <sub>total</sub> / mL	A <sub>eq</sub>	[ <b>E6</b> ]	A <sub>0</sub> -A <sub>eq</sub>	[ <b>1-H</b> ] <sub>0</sub>	[ <b>1-H</b> ] <sub>0</sub> / [ <b>E6</b> ] <sub>0</sub>	[ <b>1-H</b> ] <sub>eq</sub>	(A <sub>0</sub> -A <sub>eq</sub> )/A <sub>eq</sub>
0			22.23	1.135	$1.31 \times 10^{-5}$					
1	0.20	0.20	22.43	0.830	$9.61 \times 10^{-6}$	0.305	$7.79 \times 10^{-5}$	5.9	$7.44 \times 10^{-5}$	0.367
2	0.20	0.40	22.63	0.640	$7.41 \times 10^{-6}$	0.495	$1.54 \times 10^{-4}$	16.1	$1.49 \times 10^{-4}$	0.773
3	0.20	0.60	22.83	0.513	$5.94 \times 10^{-6}$	0.622	$2.30 \times 10^{-4}$	31.0	$2.23 \times 10^{-4}$	1.212
4	0.20	0.80	23.03	0.423	$4.90 \times 10^{-6}$	0.712	$3.04 \times 10^{-4}$	51.1	$2.95 \times 10^{-4}$	1.683
5	0.30	1.10	23.33	0.329	$3.81 \times 10^{-6}$	0.806	$4.12 \times 10^{-4}$	84.1	$4.03 \times 10^{-4}$	2.450



**Table S46.** Reaction of **1-H** with **E6** ( $\varepsilon = 1.727 \times 10^5 \text{ L mol}^{-1} \text{ cm}^{-1}$ ,  $\lambda = 635 \text{ nm}$ ) in MeCN at 20 °C.

Step	V( <b>1-H</b> ) / mL	V ( <b>1-H</b> ) <sub>total</sub> / mL	V <sub>total</sub> / mL	A <sub>eq</sub>	[ <b>E6</b> ]	A <sub>0</sub> -A <sub>eq</sub>	[ <b>1-H</b> ] <sub>0</sub>	[ <b>1-H</b> ] <sub>0</sub> / [ <b>E6</b> ] <sub>0</sub>	[ <b>1-H</b> ] <sub>eq</sub>	(A <sub>0</sub> -A <sub>eq</sub> )/A <sub>eq</sub>
0			21.98	1.467	$1.70 \times 10^{-5}$					
1	0.10	0.10	22.08	1.024	$1.19 \times 10^{-5}$	0.443	$9.03 \times 10^{-5}$	5.3	$8.51 \times 10^{-5}$	0.433
2	0.10	0.20	22.18	0.761	$8.81 \times 10^{-6}$	0.706	$1.80 \times 10^{-4}$	15.2	$1.72 \times 10^{-4}$	0.928
3	0.10	0.30	22.28	0.590	$6.83 \times 10^{-6}$	0.877	$2.68 \times 10^{-4}$	30.4	$2.58 \times 10^{-4}$	1.486
4	0.10	0.40	22.38	0.472	$5.47 \times 10^{-6}$	0.995	$3.56 \times 10^{-4}$	52.1	$3.45 \times 10^{-4}$	2.108
5	0.10	0.50	22.48	0.386	$4.47 \times 10^{-6}$	1.081	$4.43 \times 10^{-4}$	81.1	$4.31 \times 10^{-4}$	2.801

**Table S47.** Reaction of **1-H** with **E7** ( $\varepsilon = 1.318 \times 10^5 \text{ L mol}^{-1} \text{ cm}^{-1}$ ,  $\lambda = 631 \text{ nm}$ ) in MeCN at 20 °C.

Step	V( <b>1-H</b> ) / mL	V ( <b>1-H</b> ) <sub>total</sub> / mL	V <sub>total</sub> / mL	A <sub>eq</sub>	[ <b>E7</b> ]	A <sub>0</sub> -A <sub>eq</sub>	[ <b>1-H</b> ] <sub>0</sub>	[ <b>1-H</b> ] <sub>0</sub> / [ <b>E7</b> ] <sub>0</sub>	[ <b>1-H</b> ] <sub>eq</sub>	(A <sub>0</sub> -A <sub>eq</sub> )/A <sub>eq</sub>
0			22.10	1.058	$1.61 \times 10^{-5}$					
1	0.10	0.10	22.20	0.667	$1.01 \times 10^{-5}$	0.391	$1.31 \times 10^{-4}$	8.2	$1.25 \times 10^{-4}$	0.586
2	0.10	0.20	22.30	0.468	$7.10 \times 10^{-6}$	0.590	$2.61 \times 10^{-4}$	25.8	$2.52 \times 10^{-4}$	1.261
3	0.10	0.30	22.40	0.349	$5.30 \times 10^{-6}$	0.709	$3.90 \times 10^{-4}$	54.9	$3.79 \times 10^{-4}$	2.032
4	0.10	0.40	22.50	0.271	$4.11 \times 10^{-6}$	0.787	$5.18 \times 10^{-4}$	97.7	$5.06 \times 10^{-4}$	2.904
5	0.10	0.50	22.60	0.217	$3.29 \times 10^{-6}$	0.841	$6.44 \times 10^{-4}$	157	$6.31 \times 10^{-4}$	3.876

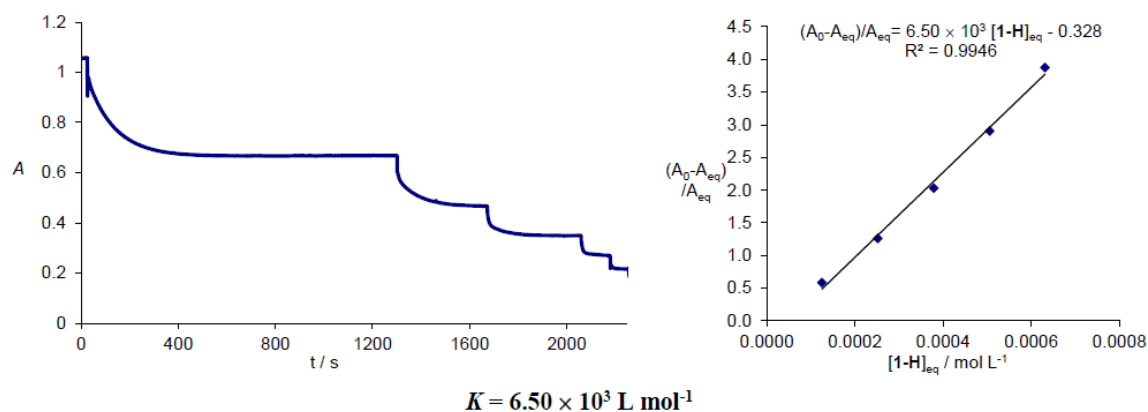
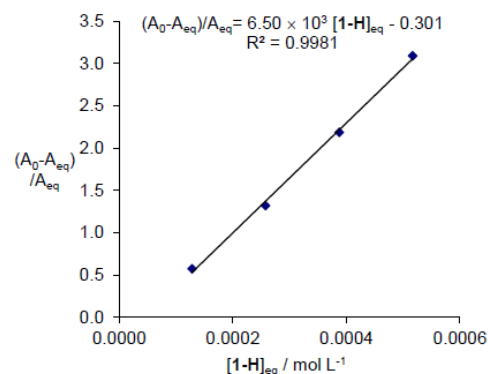
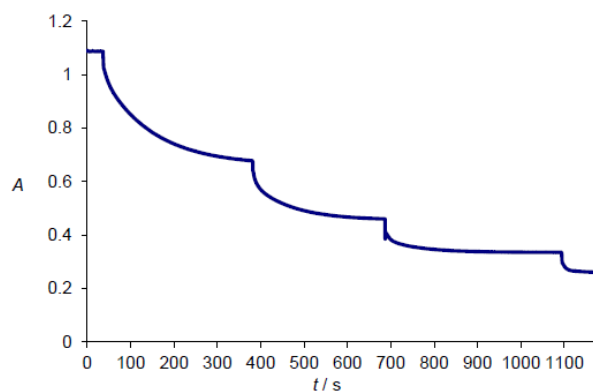


**Table S48.** Reaction of **1-H** with **E7** ( $\varepsilon = 1.318 \times 10^5 \text{ L mol}^{-1} \text{ cm}^{-1}$ ,  $\lambda = 631 \text{ nm}$ ) in MeCN at 20 °C.

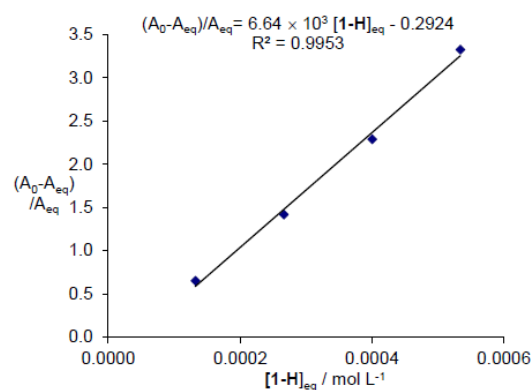
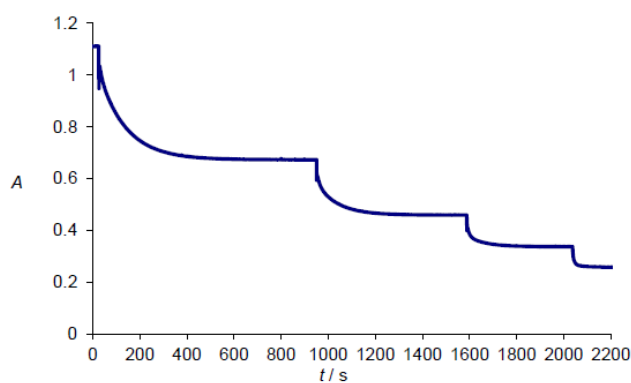
Step	V( <b>1-H</b> ) / mL	V ( <b>1-H</b> ) <sub>total</sub> / mL	V <sub>total</sub> / mL	A <sub>eq</sub>	[ <b>E7</b> ]	A <sub>0</sub> -A <sub>eq</sub>	[ <b>1-H</b> ] <sub>0</sub>	[ <b>1-H</b> ] <sub>0</sub> / [ <b>E7</b> ] <sub>0</sub>	[ <b>1-H</b> ] <sub>eq</sub>	(A <sub>0</sub> -A <sub>eq</sub> )/A <sub>eq</sub>
0			21.62	1.068	$1.62 \times 10^{-5}$					
1	0.10	0.10	21.72	0.678	$1.03 \times 10^{-5}$	0.390	$1.34 \times 10^{-4}$	8.3	$1.28 \times 10^{-4}$	0.575
2	0.10	0.20	21.82	0.460	$6.98 \times 10^{-6}$	0.608	$2.67 \times 10^{-4}$	25.9	$2.58 \times 10^{-4}$	1.322
3	0.10	0.30	21.92	0.335	$5.08 \times 10^{-6}$	0.733	$3.98 \times 10^{-4}$	57.1	$3.87 \times 10^{-4}$	2.188
4	0.10	0.40	22.02	0.261	$3.96 \times 10^{-6}$	0.807	$5.29 \times 10^{-4}$	104	$5.17 \times 10^{-4}$	3.092



$$K = 6.50 \times 10^3 \text{ L mol}^{-1}$$

**Table S49.** Reaction of **1-H** with **E7** ( $\varepsilon = 1.318 \times 10^5 \text{ L mol}^{-1} \text{ cm}^{-1}$ ,  $\lambda = 631 \text{ nm}$ ) in MeCN at 20 °C.

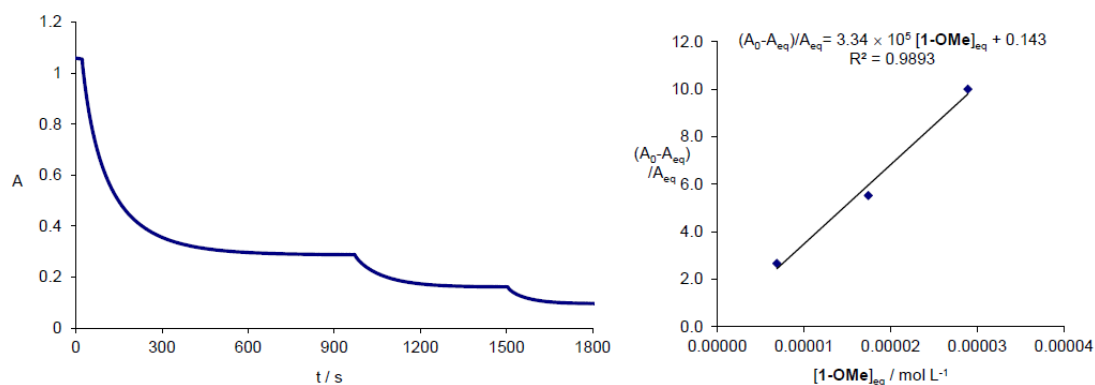
Step	V( <b>1-H</b> ) / mL	V ( <b>1-H</b> ) <sub>total</sub> / mL	V <sub>total</sub> / mL	A <sub>eq</sub>	[ <b>E7</b> ]	A <sub>0</sub> -A <sub>eq</sub>	[ <b>1-H</b> ] <sub>0</sub>	[ <b>1-H</b> ] <sub>0</sub> / [ <b>E7</b> ] <sub>0</sub>	[ <b>1-H</b> ] <sub>eq</sub>	(A <sub>0</sub> -A <sub>eq</sub> )/A <sub>eq</sub>
0			20.89	1.112	$1.69 \times 10^{-5}$					
1	0.10	0.10	20.99	0.674	$1.02 \times 10^{-5}$	0.438	$1.39 \times 10^{-4}$	8.2	$1.32 \times 10^{-4}$	0.650
2	0.10	0.20	21.09	0.460	$6.98 \times 10^{-6}$	0.652	$2.76 \times 10^{-4}$	27.0	$2.66 \times 10^{-4}$	1.417
3	0.10	0.30	21.19	0.338	$5.13 \times 10^{-6}$	0.774	$4.12 \times 10^{-4}$	59.0	$4.00 \times 10^{-4}$	2.290
4	0.10	0.40	21.29	0.257	$3.90 \times 10^{-6}$	0.855	$5.47 \times 10^{-4}$	107	$5.34 \times 10^{-4}$	3.327



$$K = 6.64 \times 10^3 \text{ L mol}^{-1}$$

**Table S50.** Reaction of **1-OMe** with **E5** ( $\varepsilon = 1.287 \times 10^5 \text{ L mol}^{-1} \text{ cm}^{-1}$ ,  $\lambda = 616 \text{ nm}$ ) in MeCN at 20 °C.

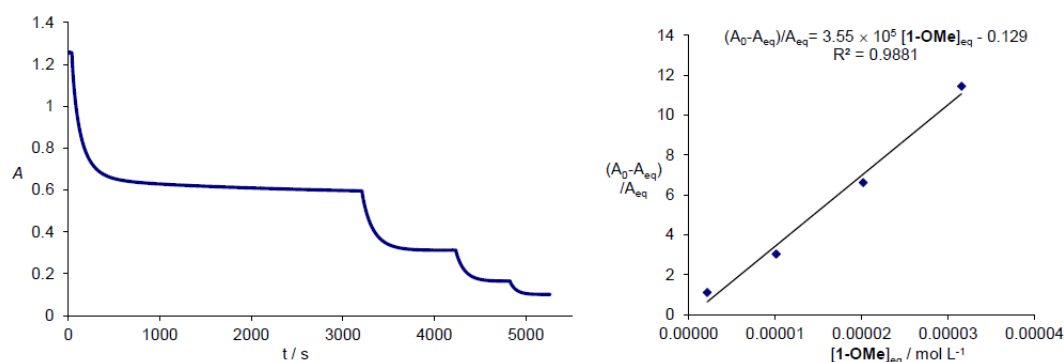
Step	V (1-OMe) / mL	V (1-OMe) total / mL	V total / mL	A <sub>eq</sub>	[E5]	A <sub>0</sub> -A <sub>eq</sub>	[1-OMe] <sub>0</sub>	[1-OMe] <sub>0</sub> / [E5] <sub>0</sub>	[1-OMe] <sub>eq</sub>	(A <sub>0</sub> -A <sub>eq</sub> )/A <sub>eq</sub>
0			22.78	1.057	$1.64 \times 10^{-5}$					
1	0.03	0.03	22.81	0.288	$4.48 \times 10^{-6}$	0.769	$1.88 \times 10^{-5}$	1.1	$6.88 \times 10^{-6}$	2.670
2	0.02	0.05	22.83	0.162	$2.52 \times 10^{-6}$	0.895	$3.14 \times 10^{-5}$	7.0	$1.75 \times 10^{-5}$	5.525
3	0.02	0.07	22.85	0.096	$1.49 \times 10^{-6}$	0.961	$4.39 \times 10^{-5}$	17.4	$2.89 \times 10^{-5}$	10.010



$$K = 3.34 \times 10^5 \text{ L mol}^{-1}$$

**Table S51.** Reaction of **1-OMe** with **E5** ( $\varepsilon = 1.287 \times 10^5 \text{ L mol}^{-1} \text{ cm}^{-1}$ ,  $\lambda = 616 \text{ nm}$ ) in MeCN at 20 °C.

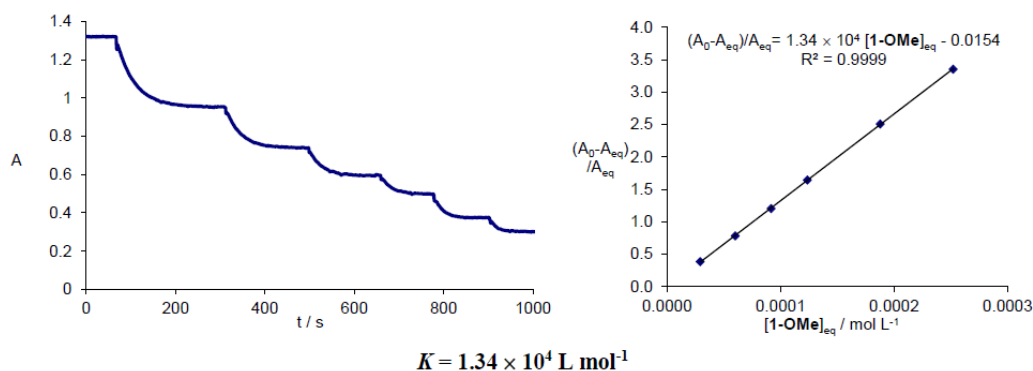
Step	V (1-OMe) / mL	V (1-OMe) total / mL	V total / mL	A <sub>eq</sub>	[E5]	A <sub>0</sub> -A <sub>eq</sub>	[1-OMe] <sub>0</sub>	[1-OMe] <sub>0</sub> / [E5] <sub>0</sub>	[1-OMe] <sub>eq</sub>	(A <sub>0</sub> -A <sub>eq</sub> )/A <sub>eq</sub>
0			23.05	1.257	$1.95 \times 10^{-5}$					
1	0.02	0.02	23.07	0.596	$9.26 \times 10^{-6}$	0.661	$1.24 \times 10^{-5}$	0.6	$2.14 \times 10^{-6}$	1.109
2	0.02	0.04	23.09	0.312	$4.85 \times 10^{-6}$	0.945	$2.48 \times 10^{-5}$	2.7	$1.01 \times 10^{-5}$	3.029
3	0.02	0.06	23.11	0.165	$2.56 \times 10^{-6}$	1.092	$3.72 \times 10^{-5}$	7.7	$2.02 \times 10^{-5}$	6.618
4	0.02	0.08	23.13	0.101	$1.57 \times 10^{-6}$	1.156	$4.95 \times 10^{-5}$	19.3	$3.16 \times 10^{-5}$	11.446



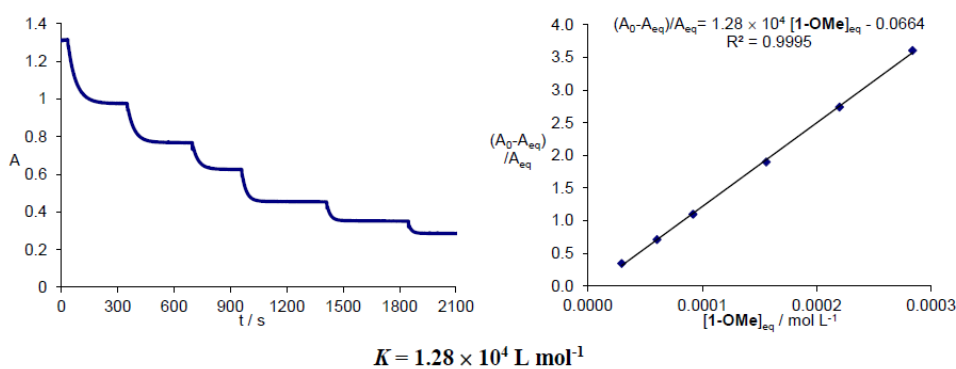
$$K = 3.55 \times 10^5 \text{ L mol}^{-1}$$

**Table S52.** Reaction of **1-OMe** with **E6** ( $\varepsilon = 1.727 \times 10^5 \text{ L mol}^{-1} \text{ cm}^{-1}$ ,  $\lambda = 635 \text{ nm}$ ) in MeCN at 20 °C.

Step	V (1-OMe) / mL	V (1-OMe) total / mL	V <sub>total</sub> / mL	A <sub>eq</sub>	[E6]	A <sub>0</sub> -A <sub>eq</sub>	[1-OMe] <sub>0</sub>	[1-OMe] <sub>0</sub> / [E6] <sub>0</sub>	[1-OMe] <sub>eq</sub>	(A <sub>0</sub> -A <sub>eq</sub> )/A <sub>eq</sub>
0			22.12	1.320	$1.53 \times 10^{-5}$					
1	0.05	0.05	22.17	0.954	$1.10 \times 10^{-5}$	0.366	$3.35 \times 10^{-5}$	2.2	$2.93 \times 10^{-5}$	0.384
2	0.05	0.10	22.22	0.740	$8.57 \times 10^{-6}$	0.580	$6.69 \times 10^{-5}$	6.1	$6.01 \times 10^{-5}$	0.784
3	0.05	0.15	22.27	0.599	$6.94 \times 10^{-6}$	0.721	$1.00 \times 10^{-4}$	11.7	$9.17 \times 10^{-5}$	1.204
4	0.05	0.20	22.32	0.499	$5.78 \times 10^{-6}$	0.821	$1.33 \times 10^{-4}$	19.2	$1.24 \times 10^{-4}$	1.645
5	0.10	0.30	22.42	0.376	$4.35 \times 10^{-6}$	0.944	$1.99 \times 10^{-4}$	34.4	$1.88 \times 10^{-4}$	2.511
6	0.10	0.40	22.52	0.303	$3.51 \times 10^{-6}$	1.017	$2.64 \times 10^{-4}$	60.6	$2.52 \times 10^{-4}$	3.356

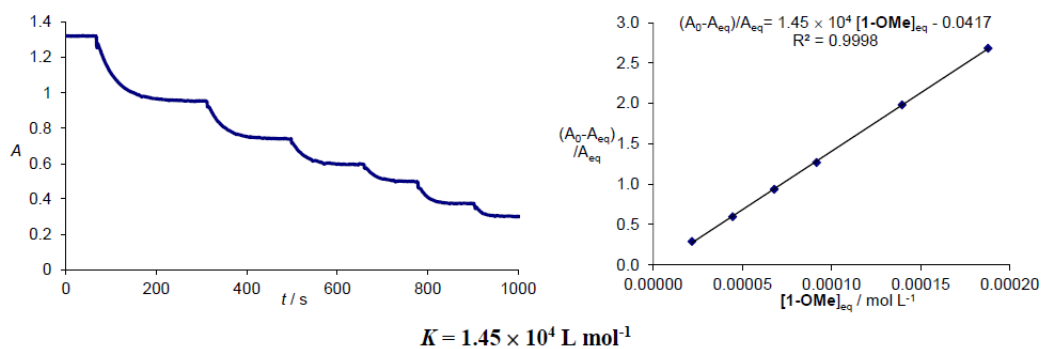
**Table S53.** Reaction of **1-OMe** with **E6** ( $\varepsilon = 1.727 \times 10^5 \text{ L mol}^{-1} \text{ cm}^{-1}$ ,  $\lambda = 635 \text{ nm}$ ) in MeCN at 20 °C.

Step	V (1-OMe) / mL	V (1-OMe) total / mL	V <sub>total</sub> / mL	A <sub>eq</sub>	[E6]	A <sub>0</sub> -A <sub>eq</sub>	[1-OMe] <sub>0</sub>	[1-OMe] <sub>0</sub> / [E6] <sub>0</sub>	[1-OMe] <sub>eq</sub>	(A <sub>0</sub> -A <sub>eq</sub> )/A <sub>eq</sub>
0			22.14	1.313	$1.52 \times 10^{-5}$					
1	0.05	0.05	22.19	0.976	$1.13 \times 10^{-5}$	0.337	$3.35 \times 10^{-5}$	2.2	$2.96 \times 10^{-5}$	0.345
2	0.05	0.10	22.24	0.768	$8.89 \times 10^{-6}$	0.545	$6.68 \times 10^{-5}$	5.9	$6.05 \times 10^{-5}$	0.710
3	0.05	0.15	22.29	0.626	$7.25 \times 10^{-6}$	0.687	$1.00 \times 10^{-4}$	11.2	$9.20 \times 10^{-5}$	1.097
4	0.10	0.25	22.39	0.453	$5.25 \times 10^{-6}$	0.860	$1.66 \times 10^{-4}$	22.9	$1.56 \times 10^{-4}$	1.898
5	0.10	0.35	22.49	0.351	$4.06 \times 10^{-6}$	0.962	$2.31 \times 10^{-4}$	44.1	$2.20 \times 10^{-4}$	2.741
6	0.10	0.45	22.59	0.285	$3.30 \times 10^{-6}$	1.028	$2.96 \times 10^{-4}$	72.8	$2.84 \times 10^{-4}$	3.607



**Table S54.** Reaction of **1-OMe** with **E6** ( $\varepsilon = 1.727 \times 10^5 \text{ L mol}^{-1} \text{ cm}^{-1}$ ,  $\lambda = 635 \text{ nm}$ ) in MeCN at 20 °C.

Step	V (1-OMe) / mL	V (1-OMe) total / mL	V <sub>total</sub> / mL	A <sub>eq</sub>	[E6]	A <sub>0</sub> -A <sub>eq</sub>	[1-OMe] <sub>0</sub>	[1-OMe] <sub>0</sub> / [E6] <sub>0</sub>	[1-OMe] <sub>eq</sub>	(A <sub>0</sub> -A <sub>eq</sub> )/A <sub>eq</sub>
0			22.52	1.422	$1.65 \times 10^{-5}$					
1	0.05	0.05	22.57	1.103	$1.28 \times 10^{-5}$	0.319	$2.54 \times 10^{-5}$	1.5	$2.17 \times 10^{-5}$	0.289
2	0.05	0.10	22.62	0.891	$1.03 \times 10^{-5}$	0.531	$5.06 \times 10^{-5}$	4.0	$4.45 \times 10^{-5}$	0.596
3	0.05	0.15	22.67	0.735	$8.51 \times 10^{-6}$	0.687	$7.58 \times 10^{-5}$	7.3	$6.78 \times 10^{-5}$	0.935
4	0.05	0.20	22.72	0.627	$7.26 \times 10^{-6}$	0.795	$1.01 \times 10^{-4}$	11.8	$9.16 \times 10^{-5}$	1.268
5	0.10	0.30	22.82	0.477	$5.52 \times 10^{-6}$	0.945	$1.51 \times 10^{-4}$	20.7	$1.40 \times 10^{-4}$	1.981
6	0.10	0.40	22.92	0.386	$4.47 \times 10^{-6}$	1.036	$2.00 \times 10^{-4}$	36.2	$1.88 \times 10^{-4}$	2.684

**Table S55.** Reaction of **1-OMe** with **E7** ( $\varepsilon = 1.318 \times 10^5 \text{ L mol}^{-1} \text{ cm}^{-1}$ ,  $\lambda = 631 \text{ nm}$ ) in MeCN at 20 °C.

Step	V (1-OMe) / mL	V (1-OMe) total / mL	V <sub>total</sub> / mL	A <sub>eq</sub>	[E7]	A <sub>0</sub> -A <sub>eq</sub>	[1-OMe] <sub>0</sub>	[1-OMe] <sub>0</sub> / [E7] <sub>0</sub>	[1-OMe] <sub>eq</sub>	(A <sub>0</sub> -A <sub>eq</sub> )/A <sub>eq</sub>
0			23.53	1.455	$2.21 \times 10^{-5}$					
1	0.05	0.05	23.58	1.168	$1.77 \times 10^{-5}$	0.287	$2.43 \times 10^{-5}$	1.1	$1.99 \times 10^{-5}$	0.246
2	0.05	0.10	23.63	0.958	$1.45 \times 10^{-5}$	0.497	$4.85 \times 10^{-5}$	2.7	$4.09 \times 10^{-5}$	0.519
3	0.10	0.20	23.73	0.692	$1.05 \times 10^{-5}$	0.763	$9.65 \times 10^{-5}$	6.6	$8.50 \times 10^{-5}$	1.103
4	0.10	0.30	23.83	0.538	$8.16 \times 10^{-6}$	0.917	$1.44 \times 10^{-4}$	13.7	$1.30 \times 10^{-4}$	1.704
5	0.20	0.50	24.03	0.372	$5.64 \times 10^{-6}$	1.083	$2.38 \times 10^{-4}$	29.2	$2.22 \times 10^{-4}$	2.911
6	0.20	0.70	24.23	0.284	$4.31 \times 10^{-6}$	1.171	$3.31 \times 10^{-4}$	58.6	$3.13 \times 10^{-4}$	4.123

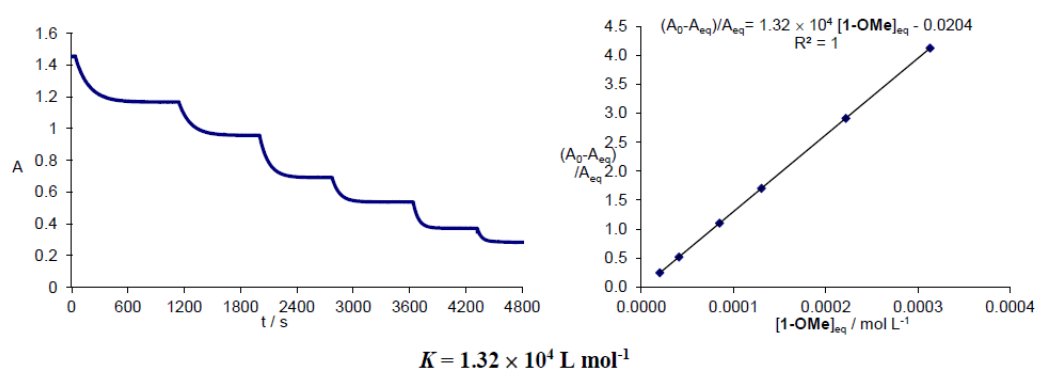
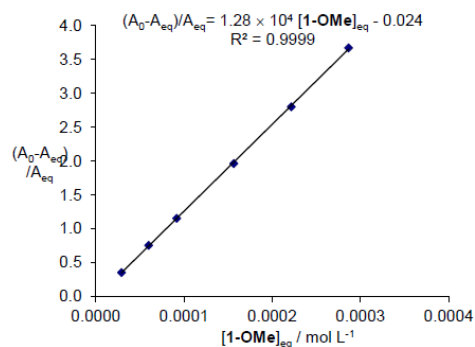
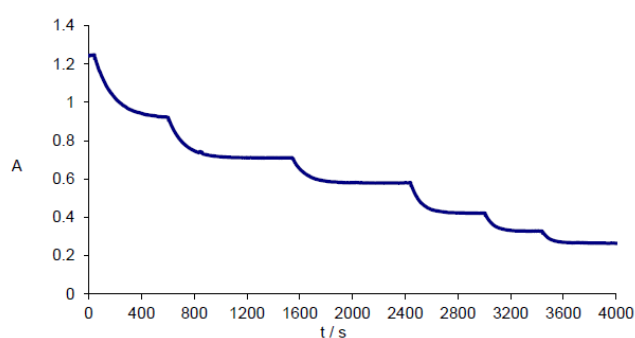


**Table S56.** Reaction of **1-OMe** with **E7** ( $\varepsilon = 1.318 \times 10^5 \text{ L mol}^{-1} \text{ cm}^{-1}$ ,  $\lambda = 631 \text{ nm}$ ) in MeCN at 20 °C.

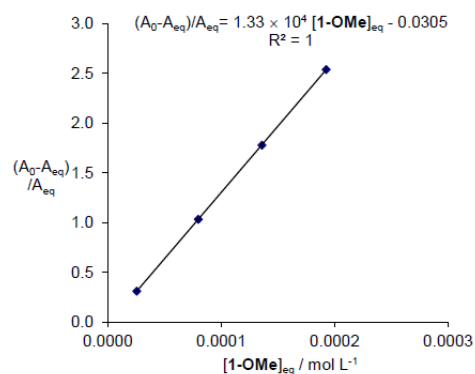
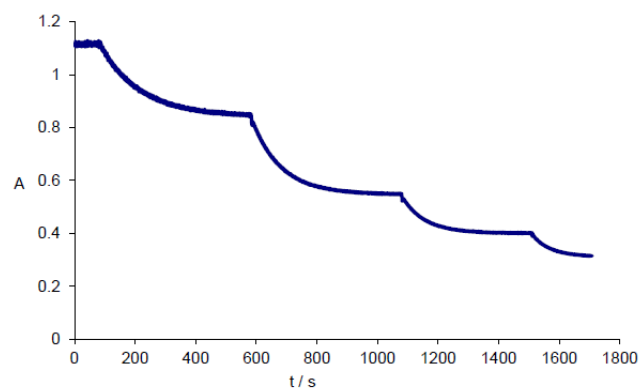
Step	V (1-OMe) / mL	V (1-OMe) total / mL	V <sub>total</sub> / mL	A <sub>eq</sub>	[E7]	A <sub>0</sub> -A <sub>eq</sub>	[1-OMe] <sub>0</sub>	[1-OMe] <sub>0</sub> / [E7] <sub>0</sub>	[1-OMe] <sub>eq</sub>	(A <sub>0</sub> -A <sub>eq</sub> )/A <sub>eq</sub>
0			21.72	1.247	$1.89 \times 10^{-5}$					
1	0.05	0.05	21.77	0.922	$1.40 \times 10^{-5}$	0.325	$3.41 \times 10^{-5}$	1.8	$2.92 \times 10^{-5}$	0.352
2	0.05	0.10	21.82	0.710	$1.08 \times 10^{-5}$	0.537	$6.81 \times 10^{-5}$	4.9	$5.99 \times 10^{-5}$	0.756
3	0.05	0.15	21.87	0.579	$8.79 \times 10^{-6}$	0.668	$1.02 \times 10^{-4}$	9.5	$9.17 \times 10^{-5}$	1.154
4	0.10	0.25	21.97	0.421	$6.39 \times 10^{-6}$	0.826	$1.69 \times 10^{-4}$	19.2	$1.57 \times 10^{-4}$	1.962
5	0.10	0.35	22.07	0.328	$4.98 \times 10^{-6}$	0.919	$2.36 \times 10^{-4}$	36.9	$2.22 \times 10^{-4}$	2.802
6	0.10	0.45	22.17	0.267	$4.05 \times 10^{-6}$	0.980	$3.02 \times 10^{-4}$	60.6	$2.87 \times 10^{-4}$	3.670



$$K = 1.28 \times 10^4 \text{ L mol}^{-1}$$

**Table S57.** Reaction of **1-OMe** with **E7** ( $\varepsilon = 1.318 \times 10^5 \text{ L mol}^{-1} \text{ cm}^{-1}$ ,  $\lambda = 631 \text{ nm}$ ) in MeCN at 20 °C.

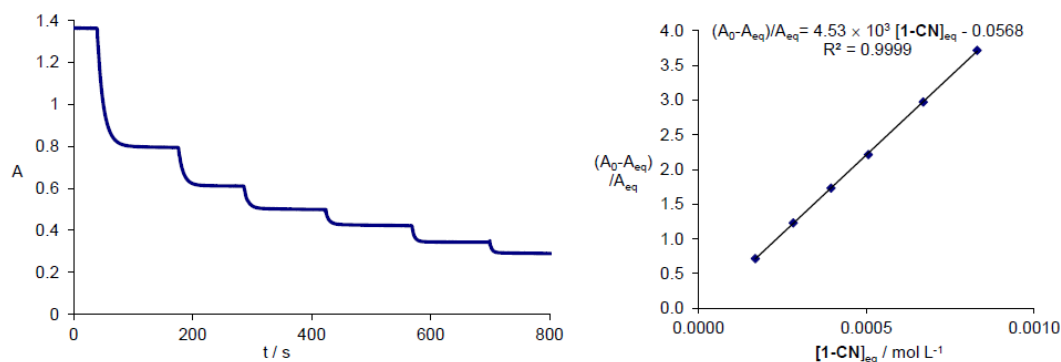
Step	V (1-OMe) / mL	V (1-OMe) total / mL	V <sub>total</sub> / mL	A <sub>eq</sub>	[E7]	A <sub>0</sub> -A <sub>eq</sub>	[1-OMe] <sub>0</sub>	[1-OMe] <sub>0</sub> / [E7] <sub>0</sub>	[1-OMe] <sub>eq</sub>	(A <sub>0</sub> -A <sub>eq</sub> )/A <sub>eq</sub>
0			22.61	1.114	$1.69 \times 10^{-5}$					
1	0.05	0.05	22.66	0.849	$1.29 \times 10^{-5}$	0.265	$2.96 \times 10^{-5}$	1.8	$2.56 \times 10^{-5}$	0.312
2	0.10	0.15	22.76	0.548	$8.32 \times 10^{-6}$	0.566	$8.85 \times 10^{-5}$	6.9	$7.99 \times 10^{-5}$	1.033
3	0.10	0.25	22.86	0.401	$6.08 \times 10^{-6}$	0.713	$1.47 \times 10^{-4}$	17.7	$1.36 \times 10^{-4}$	1.778
4	0.10	0.35	22.96	0.315	$4.78 \times 10^{-6}$	0.799	$2.05 \times 10^{-4}$	33.6	$1.92 \times 10^{-4}$	2.537



$$K = 1.33 \times 10^4 \text{ L mol}^{-1}$$

**Table S58.** Reaction of **1-CN** with **E4** ( $\varepsilon = 1.390 \times 10^5 \text{ L mol}^{-1} \text{ cm}^{-1}$ ,  $\lambda = 611 \text{ nm}$ ) in MeCN at 20 °C.

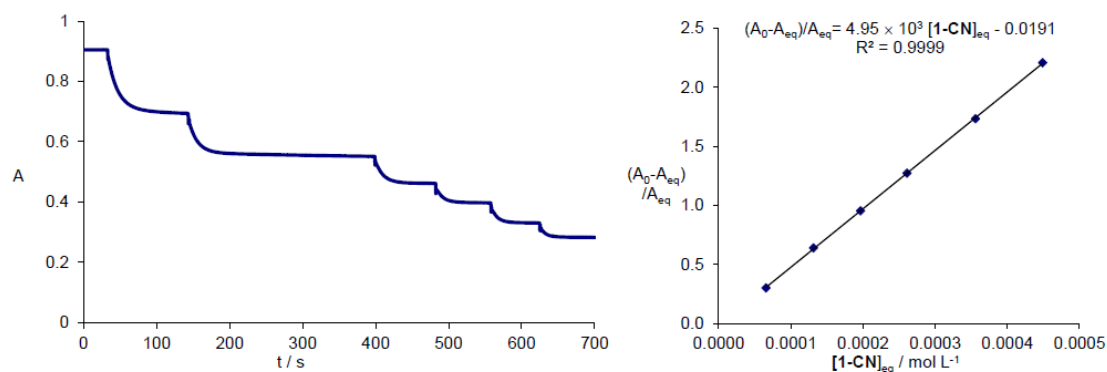
Step	V (1-CN) / mL	V (1-CN) total / mL	V <sub>total</sub> / mL	A <sub>eq</sub>	[E4]	A <sub>0</sub> -A <sub>eq</sub>	[1-CN] <sub>0</sub>	[1-CN] <sub>0</sub> / [E4] <sub>0</sub>	[1-CN] <sub>eq</sub>	(A <sub>0</sub> -A <sub>eq</sub> )/A <sub>eq</sub>
0			24.28	1.363	$1.96 \times 10^{-5}$					
1	0.30	0.30	24.58	0.795	$1.14 \times 10^{-5}$	0.568	$1.77 \times 10^{-4}$	9.0	$1.69 \times 10^{-4}$	0.714
2	0.20	0.50	24.78	0.611	$8.79 \times 10^{-6}$	0.752	$2.93 \times 10^{-4}$	25.6	$2.82 \times 10^{-4}$	1.231
3	0.20	0.70	24.98	0.499	$7.18 \times 10^{-6}$	0.864	$4.07 \times 10^{-4}$	46.3	$3.95 \times 10^{-4}$	1.731
4	0.20	0.90	25.18	0.424	$6.10 \times 10^{-6}$	0.939	$5.19 \times 10^{-4}$	72.4	$5.06 \times 10^{-4}$	2.215
5	0.30	1.20	25.48	0.343	$4.94 \times 10^{-6}$	1.020	$6.84 \times 10^{-4}$	112	$6.70 \times 10^{-4}$	2.974
6	0.30	1.50	25.78	0.289	$4.16 \times 10^{-6}$	1.074	$8.46 \times 10^{-4}$	171	$8.30 \times 10^{-4}$	3.716



$$K = 4.53 \times 10^3 \text{ L mol}^{-1}$$

**Table S59.** Reaction of **1-CN** with **E4** ( $\varepsilon = 1.390 \times 10^5 \text{ L mol}^{-1} \text{ cm}^{-1}$ ,  $\lambda = 611 \text{ nm}$ ) in MeCN at 20 °C.

Step	V (1-CN) / mL	V (1-CN) total / mL	V <sub>total</sub> / mL	A <sub>eq</sub>	[E4]	A <sub>0</sub> -A <sub>eq</sub>	[1-CN] <sub>0</sub>	[1-CN] <sub>0</sub> / [E4] <sub>0</sub>	[1-CN] <sub>eq</sub>	(A <sub>0</sub> -A <sub>eq</sub> )/A <sub>eq</sub>
0			22.68	0.905	$1.30 \times 10^{-5}$					
1	0.20	0.20	22.88	0.695	$1.00 \times 10^{-5}$	0.210	$6.88 \times 10^{-5}$	5.3	$6.58 \times 10^{-5}$	0.302
2	0.20	0.40	23.08	0.552	$7.94 \times 10^{-6}$	0.353	$1.36 \times 10^{-4}$	13.6	$1.31 \times 10^{-4}$	0.639
3	0.20	0.60	23.28	0.463	$6.66 \times 10^{-6}$	0.442	$2.03 \times 10^{-4}$	25.6	$1.97 \times 10^{-4}$	0.955
4	0.20	0.80	23.48	0.398	$5.73 \times 10^{-6}$	0.507	$2.68 \times 10^{-4}$	40.3	$2.61 \times 10^{-4}$	1.274
5	0.30	1.10	23.78	0.331	$4.76 \times 10^{-6}$	0.574	$3.64 \times 10^{-4}$	63.6	$3.56 \times 10^{-4}$	1.734
6	0.30	1.40	24.08	0.282	$4.06 \times 10^{-6}$	0.623	$4.58 \times 10^{-4}$	96.1	$4.49 \times 10^{-4}$	2.209

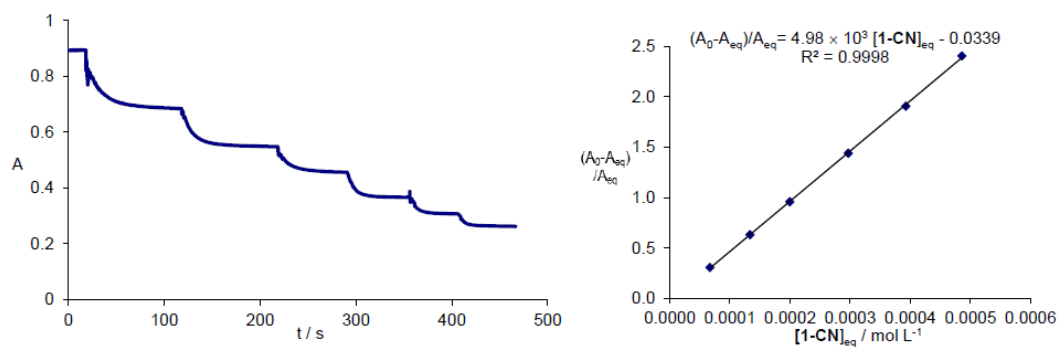


$$K = 4.95 \times 10^3 \text{ L mol}^{-1}$$



**Table S60.** Reaction of 1-CN with E4 ( $\varepsilon = 1.390 \times 10^5 \text{ L mol}^{-1} \text{ cm}^{-1}$ ,  $\lambda = 611 \text{ nm}$ ) in MeCN at 20 °C.

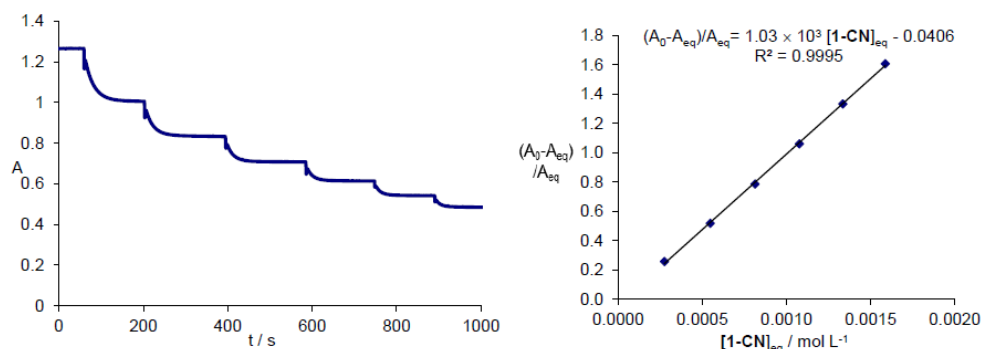
Step	V (1-CN) / mL	V (1-CN) total / mL	V <sub>total</sub> / mL	A <sub>eq</sub>	[E4]	A <sub>0</sub> -A <sub>eq</sub>	[1-CN] <sub>0</sub>	[1-CN] <sub>0</sub> / [E4] <sub>0</sub>	[1-CN] <sub>eq</sub>	(A <sub>0</sub> -A <sub>eq</sub> )/A <sub>eq</sub>
0			22.37	0.895	$1.29 \times 10^{-5}$					
1	0.20	0.20	22.57	0.685	$9.86 \times 10^{-6}$	0.210	$6.98 \times 10^{-5}$	5.4	$6.68 \times 10^{-5}$	0.307
2	0.20	0.40	22.77	0.549	$7.90 \times 10^{-6}$	0.346	$1.38 \times 10^{-4}$	14.0	$1.33 \times 10^{-4}$	0.630
3	0.20	0.60	22.97	0.457	$6.58 \times 10^{-6}$	0.438	$2.06 \times 10^{-4}$	26.0	$1.99 \times 10^{-4}$	0.958
4	0.30	0.90	23.27	0.367	$5.28 \times 10^{-6}$	0.528	$3.05 \times 10^{-4}$	46.3	$2.97 \times 10^{-4}$	1.439
5	0.30	1.20	23.57	0.308	$4.43 \times 10^{-6}$	0.587	$4.01 \times 10^{-4}$	75.9	$3.92 \times 10^{-4}$	1.906
6	0.30	1.50	23.87	0.263	$3.78 \times 10^{-6}$	0.632	$4.95 \times 10^{-4}$	112	$4.86 \times 10^{-4}$	2.403



$$K = 4.98 \times 10^3 \text{ L mol}^{-1}$$

**Table S61.** Reaction of 1-CN with E5 ( $\varepsilon = 1.287 \times 10^5 \text{ L mol}^{-1} \text{ cm}^{-1}$ ,  $\lambda = 616 \text{ nm}$ ) in MeCN at 20 °C.

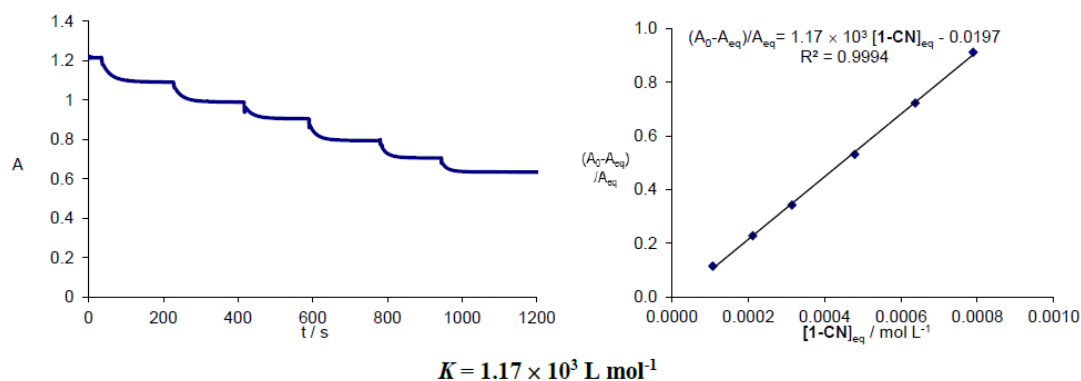
Step	V (1-CN) / mL	V (1-CN) total / mL	V <sub>total</sub> / mL	A <sub>eq</sub>	[E5]	A <sub>0</sub> -A <sub>eq</sub>	[1-CN] <sub>0</sub>	[1-CN] <sub>0</sub> / [E5] <sub>0</sub>	[1-CN] <sub>eq</sub>	(A <sub>0</sub> -A <sub>eq</sub> )/A <sub>eq</sub>
0			20.67	1.265	$1.97 \times 10^{-5}$					
1	0.20	0.20	20.87	1.006	$1.56 \times 10^{-5}$	0.259	$2.79 \times 10^{-4}$	14.2	$2.75 \times 10^{-4}$	0.257
2	0.20	0.40	21.07	0.833	$1.29 \times 10^{-5}$	0.432	$5.54 \times 10^{-4}$	35.4	$5.47 \times 10^{-4}$	0.519
3	0.20	0.60	21.27	0.708	$1.10 \times 10^{-5}$	0.557	$8.23 \times 10^{-4}$	63.5	$8.14 \times 10^{-4}$	0.787
4	0.20	0.80	21.47	0.614	$9.54 \times 10^{-6}$	0.651	$1.09 \times 10^{-3}$	98.8	$1.08 \times 10^{-3}$	1.060
5	0.20	1.00	21.67	0.542	$8.42 \times 10^{-6}$	0.723	$1.35 \times 10^{-3}$	141	$1.33 \times 10^{-3}$	1.334
6	0.20	1.20	21.87	0.485	$7.54 \times 10^{-6}$	0.780	$1.60 \times 10^{-3}$	190	$1.59 \times 10^{-3}$	1.608



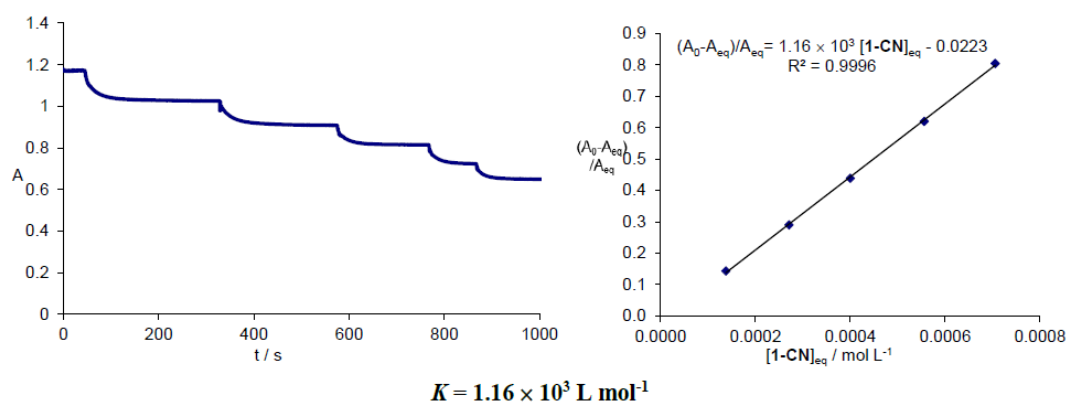
$$K = 1.03 \times 10^3 \text{ L mol}^{-1}$$

**Table S62.** Reaction of **1-CN** with **E5** ( $\varepsilon = 1.287 \times 10^5 \text{ L mol}^{-1} \text{ cm}^{-1}$ ,  $\lambda = 616 \text{ nm}$ ) in MeCN at 20 °C.

Step	V (1-CN) / mL	V (1-CN) total / mL	V <sub>total</sub> / mL	A <sub>eq</sub>	[E5]	A <sub>0</sub> -A <sub>eq</sub>	[1-CN] <sub>0</sub>	[1-CN] <sub>0</sub> / [E5] <sub>0</sub>	[1-CN] <sub>eq</sub>	(A <sub>0</sub> -A <sub>eq</sub> )/A <sub>eq</sub>
0			21.71	1.216	$1.89 \times 10^{-5}$					
1	0.30	0.30	22.01	1.091	$1.70 \times 10^{-5}$	0.125	$1.09 \times 10^{-4}$	5.8	$1.07 \times 10^{-4}$	0.115
2	0.30	0.60	22.31	0.990	$1.54 \times 10^{-5}$	0.226	$2.16 \times 10^{-4}$	12.7	$2.12 \times 10^{-4}$	0.228
3	0.30	0.90	22.61	0.906	$1.41 \times 10^{-5}$	0.310	$3.19 \times 10^{-4}$	20.7	$3.14 \times 10^{-4}$	0.342
4	0.50	1.40	23.11	0.794	$1.23 \times 10^{-5}$	0.422	$4.86 \times 10^{-4}$	34.5	$4.79 \times 10^{-4}$	0.531
5	0.50	1.90	23.61	0.706	$1.10 \times 10^{-5}$	0.510	$6.45 \times 10^{-4}$	52.3	$6.37 \times 10^{-4}$	0.722
6	0.50	2.40	24.11	0.636	$9.88 \times 10^{-6}$	0.580	$7.98 \times 10^{-4}$	72.8	$7.89 \times 10^{-4}$	0.912

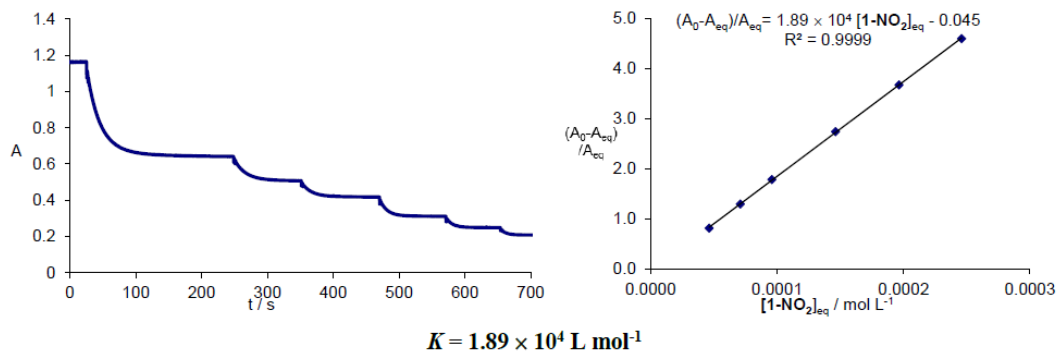
**Table S63.** Reaction of **1-CN** with **E5** ( $\varepsilon = 1.287 \times 10^5 \text{ L mol}^{-1} \text{ cm}^{-1}$ ,  $\lambda = 616 \text{ nm}$ ) in MeCN at 20 °C.

Step	V (1-CN) / mL	V (1-CN) total / mL	V <sub>total</sub> / mL	A <sub>eq</sub>	[E5]	A <sub>0</sub> -A <sub>eq</sub>	[1-CN] <sub>0</sub>	[1-CN] <sub>0</sub> / [E5] <sub>0</sub>	[1-CN] <sub>eq</sub>	(A <sub>0</sub> -A <sub>eq</sub> )/A <sub>eq</sub>
0			22.51	1.173	$1.82 \times 10^{-5}$					
1	0.40	0.40	22.91	1.026	$1.59 \times 10^{-5}$	0.147	$1.40 \times 10^{-4}$	7.7	$1.38 \times 10^{-4}$	0.143
2	0.40	0.80	23.31	0.909	$1.41 \times 10^{-5}$	0.264	$2.75 \times 10^{-4}$	17.3	$2.71 \times 10^{-4}$	0.290
3	0.40	1.20	23.71	0.815	$1.27 \times 10^{-5}$	0.358	$4.06 \times 10^{-4}$	28.7	$4.00 \times 10^{-4}$	0.439
4	0.50	1.70	24.21	0.724	$1.13 \times 10^{-5}$	0.449	$5.63 \times 10^{-4}$	44.5	$5.56 \times 10^{-4}$	0.620
5	0.50	2.20	24.71	0.650	$1.01 \times 10^{-5}$	0.523	$7.14 \times 10^{-4}$	63.5	$7.06 \times 10^{-4}$	0.805



**Table S64.** Reaction of **1-NO<sub>2</sub>** with **E3** ( $\varepsilon = 1.464 \times 10^5 \text{ L mol}^{-1} \text{ cm}^{-1}$ ,  $\lambda = 605 \text{ nm}$ ) in MeCN at 20 °C.

Step	V (1-NO <sub>2</sub> ) / mL	V (1-NO <sub>2</sub> ) <sub>total</sub> / mL	V <sub>total</sub> / mL	A <sub>eq</sub>	[E3]	A <sub>0</sub> -A <sub>eq</sub>	[1-NO <sub>2</sub> ] <sub>0</sub>	[1-NO <sub>2</sub> ] <sub>0</sub> / [E3] <sub>0</sub>	[1-NO <sub>2</sub> ] <sub>eq</sub>	(A <sub>0</sub> -A <sub>eq</sub> )/A <sub>eq</sub>
0			24.18	1.163	$1.59 \times 10^{-5}$					
1	0.20	0.20	24.38	0.641	$8.76 \times 10^{-6}$	0.522	$5.35 \times 10^{-5}$	3.4	$4.64 \times 10^{-5}$	0.814
2	0.10	0.30	24.48	0.507	$6.93 \times 10^{-6}$	0.656	$7.99 \times 10^{-5}$	9.1	$7.10 \times 10^{-5}$	1.294
3	0.10	0.40	24.58	0.418	$5.71 \times 10^{-6}$	0.745	$1.06 \times 10^{-4}$	15.3	$9.60 \times 10^{-5}$	1.782
4	0.20	0.60	24.78	0.311	$4.25 \times 10^{-6}$	0.852	$1.58 \times 10^{-4}$	27.7	$1.46 \times 10^{-4}$	2.740
5	0.20	0.80	24.98	0.249	$3.40 \times 10^{-6}$	0.914	$2.09 \times 10^{-4}$	49.2	$1.96 \times 10^{-4}$	3.671
6	0.20	1.00	25.18	0.208	$2.84 \times 10^{-6}$	0.955	$2.59 \times 10^{-4}$	76.1	$2.46 \times 10^{-4}$	4.591

**Table S65.** Reaction of **1-NO<sub>2</sub>** with **E3** ( $\varepsilon = 1.464 \times 10^5 \text{ L mol}^{-1} \text{ cm}^{-1}$ ,  $\lambda = 605 \text{ nm}$ ) in MeCN at 20 °C.

Step	V (1-NO <sub>2</sub> ) / mL	V (1-NO <sub>2</sub> ) <sub>total</sub> / mL	V <sub>total</sub> / mL	A <sub>eq</sub>	[E3]	A <sub>0</sub> -A <sub>eq</sub>	[1-NO <sub>2</sub> ] <sub>0</sub>	[1-NO <sub>2</sub> ] <sub>0</sub> / [E3] <sub>0</sub>	[1-NO <sub>2</sub> ] <sub>eq</sub>	(A <sub>0</sub> -A <sub>eq</sub> )/A <sub>eq</sub>
0			23.19	1.055	$1.44 \times 10^{-5}$					
1	0.10	0.10	23.29	0.752	$1.03 \times 10^{-5}$	0.303	$2.80 \times 10^{-5}$	1.9	$2.39 \times 10^{-5}$	0.403
2	0.10	0.20	23.39	0.552	$7.54 \times 10^{-6}$	0.503	$5.58 \times 10^{-5}$	5.4	$4.89 \times 10^{-5}$	0.911
3	0.10	0.30	23.49	0.434	$5.93 \times 10^{-6}$	0.621	$8.33 \times 10^{-5}$	11.0	$7.48 \times 10^{-5}$	1.431
4	0.20	0.50	23.69	0.307	$4.19 \times 10^{-6}$	0.748	$1.38 \times 10^{-4}$	23.2	$1.27 \times 10^{-4}$	2.436
5	0.20	0.70	23.89	0.237	$3.24 \times 10^{-6}$	0.818	$1.91 \times 10^{-4}$	45.6	$1.80 \times 10^{-4}$	3.451
6	0.20	0.90	24.09	0.193	$2.64 \times 10^{-6}$	0.862	$2.44 \times 10^{-4}$	75.3	$2.32 \times 10^{-4}$	4.466

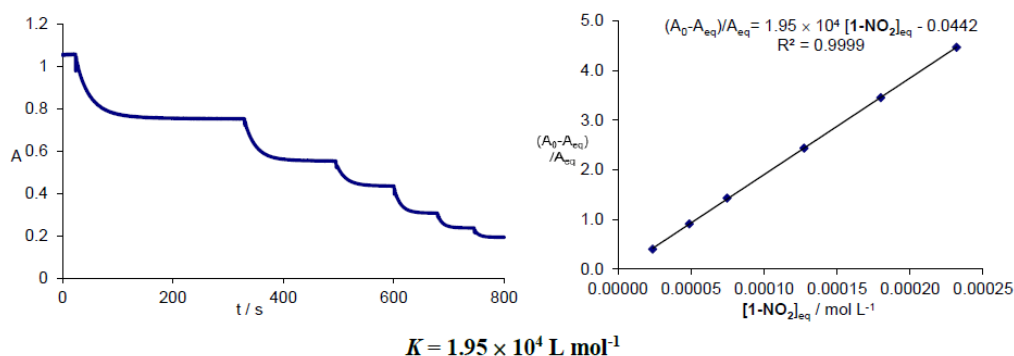
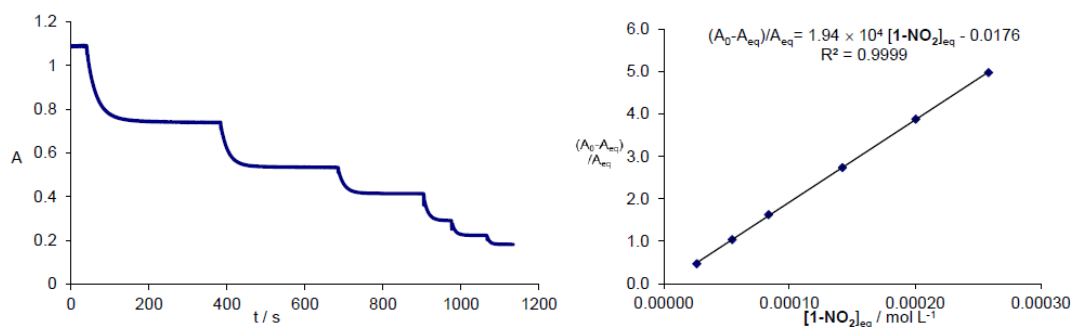


**Table S66.** Reaction of 1-NO<sub>2</sub> with E3 ( $\epsilon = 1.464 \times 10^5 \text{ L mol}^{-1} \text{ cm}^{-1}$ ,  $\lambda = 605 \text{ nm}$ ) in MeCN at 20 °C.

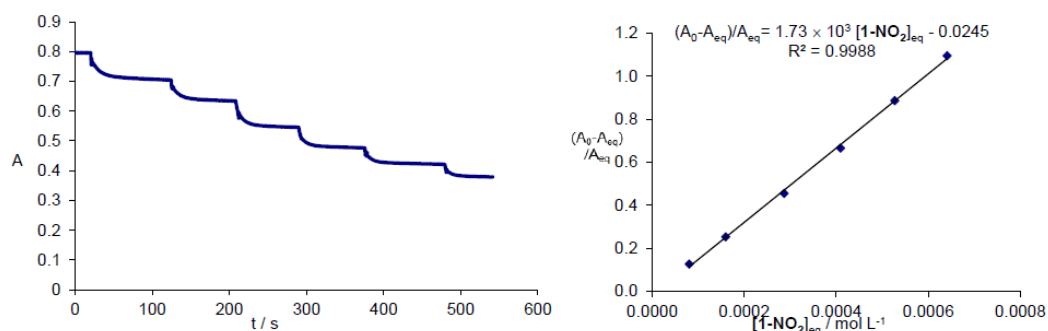
Step	V (1-NO <sub>2</sub> ) / mL	V (1-NO <sub>2</sub> ) <sub>total</sub> / mL	V <sub>total</sub> / mL	A <sub>eq</sub>	[E3]	A <sub>0</sub> -A <sub>eq</sub>	[1-NO <sub>2</sub> ] <sub>0</sub>	[1-NO <sub>2</sub> ] <sub>0</sub> / [E3] <sub>0</sub>	[1-NO <sub>2</sub> ] <sub>eq</sub>	(A <sub>0</sub> -A <sub>eq</sub> )/A <sub>eq</sub>
0			22.60	1.088	$1.49 \times 10^{-5}$					
1	0.10	0.10	22.70	0.740	$1.01 \times 10^{-5}$	0.348	$3.11 \times 10^{-5}$	2.1	$2.64 \times 10^{-5}$	0.470
2	0.10	0.20	22.80	0.534	$7.30 \times 10^{-6}$	0.554	$6.20 \times 10^{-5}$	6.1	$5.44 \times 10^{-5}$	1.037
3	0.10	0.30	22.90	0.414	$5.66 \times 10^{-6}$	0.674	$9.26 \times 10^{-5}$	12.7	$8.34 \times 10^{-5}$	1.628
4	0.20	0.50	23.10	0.291	$3.98 \times 10^{-6}$	0.797	$1.53 \times 10^{-4}$	27.0	$1.42 \times 10^{-4}$	2.739
5	0.20	0.70	23.30	0.223	$3.05 \times 10^{-6}$	0.865	$2.12 \times 10^{-4}$	53.4	$2.01 \times 10^{-4}$	3.879
6	0.20	0.90	23.50	0.182	$2.49 \times 10^{-6}$	0.906	$2.71 \times 10^{-4}$	88.9	$2.58 \times 10^{-4}$	4.978



$$K = 1.94 \times 10^4 \text{ L mol}^{-1}$$

**Table S67.** Reaction of 1-NO<sub>2</sub> with E4 ( $\epsilon = 1.390 \times 10^5 \text{ L mol}^{-1} \text{ cm}^{-1}$ ,  $\lambda = 611 \text{ nm}$ ) in MeCN at 20 °C.

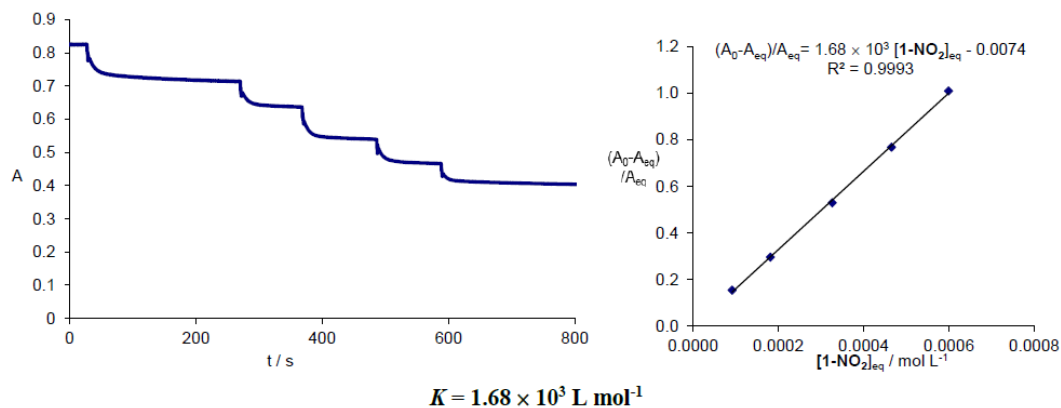
Step	V (1-NO <sub>2</sub> ) / mL	V (1-NO <sub>2</sub> ) <sub>total</sub> / mL	V <sub>total</sub> / mL	A <sub>eq</sub>	[E4]	A <sub>0</sub> -A <sub>eq</sub>	[1-NO <sub>2</sub> ] <sub>0</sub>	[1-NO <sub>2</sub> ] <sub>0</sub> / [E4] <sub>0</sub>	[1-NO <sub>2</sub> ] <sub>eq</sub>	(A <sub>0</sub> -A <sub>eq</sub> )/A <sub>eq</sub>
0			23.62	0.796	$1.15 \times 10^{-5}$					
1	0.30	0.30	23.92	0.706	$1.02 \times 10^{-5}$	0.090	$8.18 \times 10^{-5}$	7.1	$8.05 \times 10^{-5}$	0.127
2	0.30	0.60	24.22	0.635	$9.14 \times 10^{-6}$	0.161	$1.62 \times 10^{-4}$	15.9	$1.59 \times 10^{-4}$	0.254
3	0.50	1.10	24.72	0.547	$7.87 \times 10^{-6}$	0.249	$2.90 \times 10^{-4}$	31.8	$2.87 \times 10^{-4}$	0.455
4	0.50	1.60	25.22	0.478	$6.88 \times 10^{-6}$	0.318	$4.14 \times 10^{-4}$	52.6	$4.09 \times 10^{-4}$	0.665
5	0.50	2.10	25.72	0.422	$6.07 \times 10^{-6}$	0.374	$5.33 \times 10^{-4}$	77.4	$5.27 \times 10^{-4}$	0.886
6	0.50	2.60	26.22	0.380	$5.47 \times 10^{-6}$	0.416	$6.47 \times 10^{-4}$	107	$6.41 \times 10^{-4}$	1.095



$$K = 1.73 \times 10^3 \text{ L mol}^{-1}$$

**Table S68.** Reaction of **1-NO<sub>2</sub>** with **E4** ( $\varepsilon = 1.390 \times 10^5 \text{ L mol}^{-1} \text{ cm}^{-1}$ ,  $\lambda = 611 \text{ nm}$ ) in MeCN at 20 °C.

Step	V (1-NO <sub>2</sub> ) / mL	V (1-NO <sub>2</sub> ) <sub>total</sub> / mL	V <sub>total</sub> / mL	A <sub>eq</sub>	[E4]	A <sub>0</sub> -A <sub>eq</sub>	[1-NO <sub>2</sub> ] <sub>0</sub>	[1-NO <sub>2</sub> ] <sub>0</sub> / [E4] <sub>0</sub>	[1-NO <sub>2</sub> ] <sub>eq</sub>	(A <sub>0</sub> -A <sub>eq</sub> )/A <sub>eq</sub>
0			22.42	0.826	$1.19 \times 10^{-5}$					
1	0.30	0.30	22.72	0.715	$1.03 \times 10^{-5}$	0.111	$9.33 \times 10^{-5}$	7.8	$9.17 \times 10^{-5}$	0.155
2	0.30	0.60	23.02	0.637	$9.17 \times 10^{-6}$	0.189	$1.84 \times 10^{-4}$	17.9	$1.81 \times 10^{-4}$	0.297
3	0.50	1.10	23.52	0.540	$7.77 \times 10^{-6}$	0.286	$3.30 \times 10^{-4}$	36.1	$3.26 \times 10^{-4}$	0.530
4	0.50	1.60	24.02	0.467	$6.72 \times 10^{-6}$	0.359	$4.71 \times 10^{-4}$	60.6	$4.65 \times 10^{-4}$	0.769
5	0.50	2.10	24.52	0.411	$5.91 \times 10^{-6}$	0.415	$6.05 \times 10^{-4}$	90.1	$5.99 \times 10^{-4}$	1.010

**Table S69.** Reaction of **1-NO<sub>2</sub>** with **E4** ( $\varepsilon = 1.390 \times 10^5 \text{ L mol}^{-1} \text{ cm}^{-1}$ ,  $\lambda = 611 \text{ nm}$ ) in MeCN at 20 °C.

Step	V (1-NO <sub>2</sub> ) / mL	V (1-NO <sub>2</sub> ) <sub>total</sub> / mL	V <sub>total</sub> / mL	A <sub>eq</sub>	[E4]	A <sub>0</sub> -A <sub>eq</sub>	[1-NO <sub>2</sub> ] <sub>0</sub>	[1-NO <sub>2</sub> ] <sub>0</sub> / [E4] <sub>0</sub>	[1-NO <sub>2</sub> ] <sub>eq</sub>	(A <sub>0</sub> -A <sub>eq</sub> )/A <sub>eq</sub>
0			22.34	1.030	$1.48 \times 10^{-5}$					
1	0.20	0.20	22.54	0.804	$1.16 \times 10^{-5}$	0.226	$2.20 \times 10^{-4}$	14.8	$2.17 \times 10^{-4}$	0.281
2	0.10	0.30	22.64	0.720	$1.04 \times 10^{-5}$	0.310	$3.29 \times 10^{-4}$	28.4	$3.24 \times 10^{-4}$	0.431
3	0.10	0.40	22.74	0.650	$9.35 \times 10^{-6}$	0.380	$4.36 \times 10^{-4}$	42.1	$4.31 \times 10^{-4}$	0.585
4	0.10	0.50	22.84	0.592	$8.52 \times 10^{-6}$	0.438	$5.43 \times 10^{-4}$	58.0	$5.37 \times 10^{-4}$	0.740
5	0.15	0.65	22.99	0.522	$7.51 \times 10^{-6}$	0.508	$7.01 \times 10^{-4}$	82.3	$6.94 \times 10^{-4}$	0.973
6	0.15	0.80	23.14	0.468	$6.73 \times 10^{-6}$	0.562	$8.57 \times 10^{-4}$	114	$8.49 \times 10^{-4}$	1.201

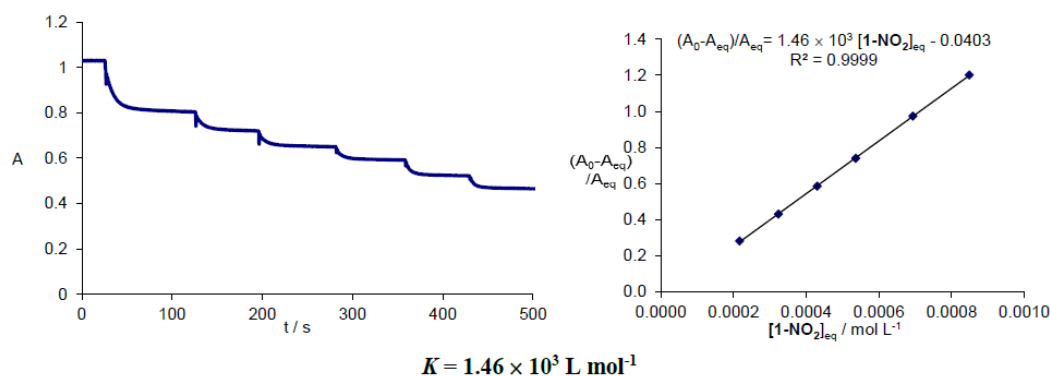
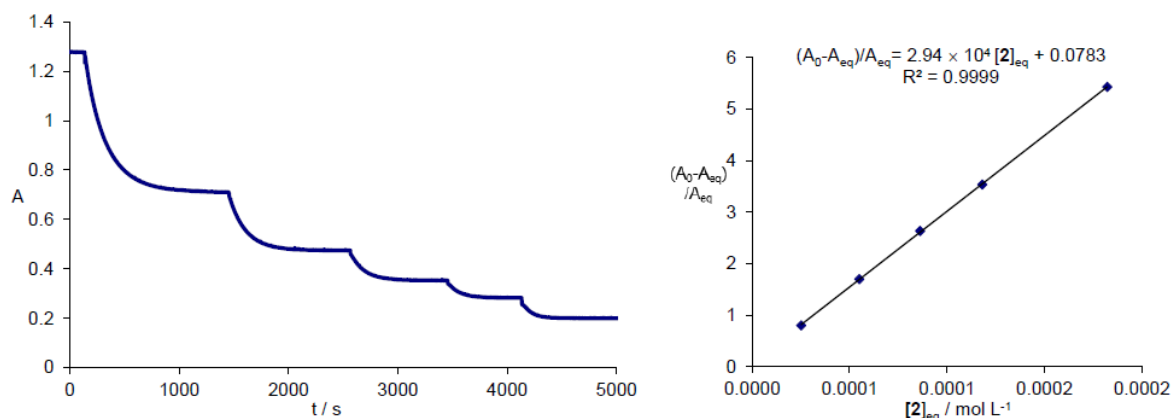


**Table S70.** Reaction of **2** with **E4** ( $\varepsilon = 1.390 \times 10^5 \text{ L mol}^{-1} \text{ cm}^{-1}$ ,  $\lambda = 611 \text{ nm}$ ) in MeCN at 20 °C.

Step	V (2) / mL	V (2) total / mL	V total / mL	A <sub>eq</sub>	[E4]	A <sub>0</sub> -A <sub>eq</sub>	[2] <sub>0</sub>	[2] <sub>0</sub> / [E4] <sub>0</sub>	[2] <sub>eq</sub>	(A <sub>0</sub> -A <sub>eq</sub> )/A <sub>eq</sub>
0			22.73	1.279	$1.84 \times 10^{-5}$					
1	0.05	0.05	22.78	0.710	$1.02 \times 10^{-5}$	0.569	$3.33 \times 10^{-5}$	1.8	$2.51 \times 10^{-5}$	0.801
2	0.05	0.10	22.83	0.474	$6.82 \times 10^{-6}$	0.805	$6.65 \times 10^{-5}$	6.5	$5.49 \times 10^{-5}$	1.698
3	0.05	0.15	22.88	0.352	$5.06 \times 10^{-6}$	0.927	$9.95 \times 10^{-5}$	14.6	$8.62 \times 10^{-5}$	2.634
4	0.05	0.20	22.93	0.282	$4.06 \times 10^{-6}$	0.997	$1.32 \times 10^{-4}$	26.2	$1.18 \times 10^{-4}$	3.535
5	0.10	0.30	23.03	0.199	$2.86 \times 10^{-6}$	1.080	$1.98 \times 10^{-4}$	48.7	$1.82 \times 10^{-4}$	5.427

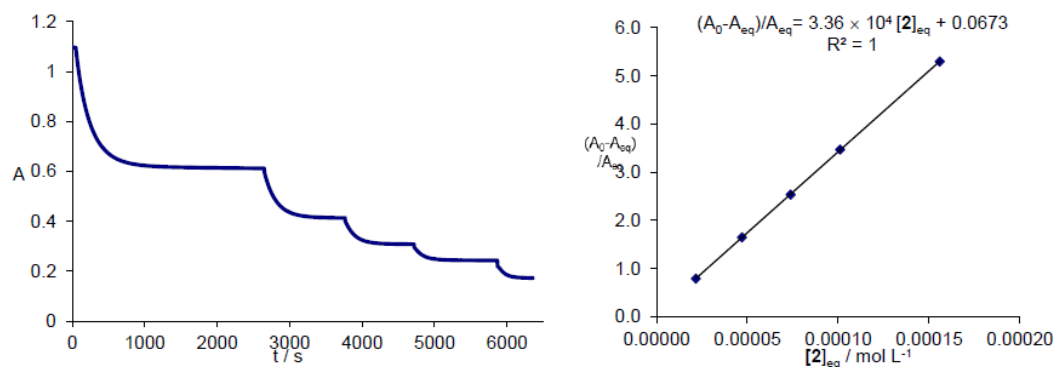


$$K = 2.94 \times 10^4 \text{ L mol}^{-1}$$

S62

**Table S71.** Reaction of **2** with **E4** ( $\varepsilon = 1.390 \times 10^5 \text{ L mol}^{-1} \text{ cm}^{-1}$ ,  $\lambda = 611 \text{ nm}$ ) in MeCN at 20 °C.

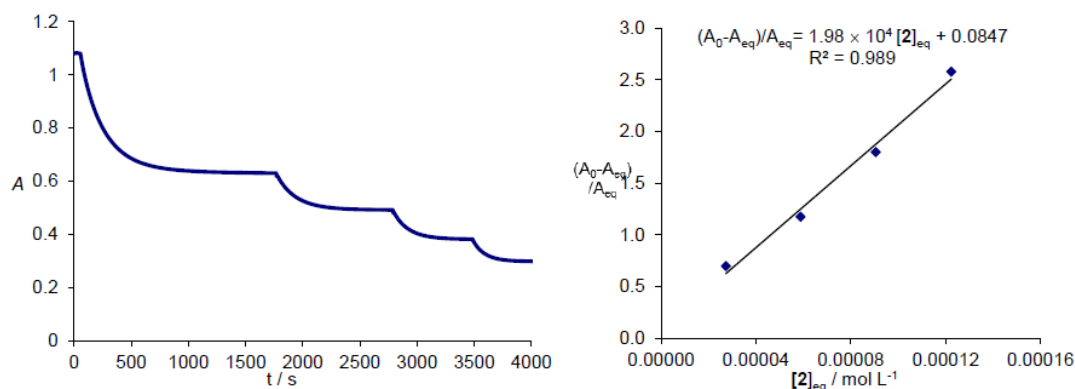
Step	V (2) / mL	V (2) total / mL	V total / mL	A <sub>eq</sub>	[E4]	A <sub>0</sub> -A <sub>eq</sub>	[2] <sub>0</sub>	[2] <sub>0</sub> / [E4] <sub>0</sub>	[2] <sub>eq</sub>	(A <sub>0</sub> -A <sub>eq</sub> )/A <sub>eq</sub>
0			23.80	1.096	$1.58 \times 10^{-5}$					
1	0.05	0.05	23.85	0.612	$8.81 \times 10^{-6}$	0.484	$2.85 \times 10^{-5}$	1.8	$2.15 \times 10^{-5}$	0.791
2	0.05	0.10	23.90	0.414	$5.96 \times 10^{-6}$	0.682	$5.69 \times 10^{-5}$	6.5	$4.70 \times 10^{-5}$	1.647
3	0.05	0.15	23.95	0.310	$4.46 \times 10^{-6}$	0.786	$8.51 \times 10^{-5}$	14.3	$7.38 \times 10^{-5}$	2.535
4	0.05	0.20	24.00	0.245	$3.53 \times 10^{-6}$	0.851	$1.13 \times 10^{-4}$	25.4	$1.01 \times 10^{-4}$	3.473
5	0.10	0.30	24.10	0.174	$2.50 \times 10^{-6}$	0.922	$1.69 \times 10^{-4}$	48.0	$1.56 \times 10^{-4}$	5.299



$$K = 3.36 \times 10^4 \text{ L mol}^{-1}$$

**Table S72.** Reaction of **2** with **E4** ( $\varepsilon = 1.390 \times 10^5 \text{ L mol}^{-1} \text{ cm}^{-1}$ ,  $\lambda = 611 \text{ nm}$ ) in MeCN at 20 °C.

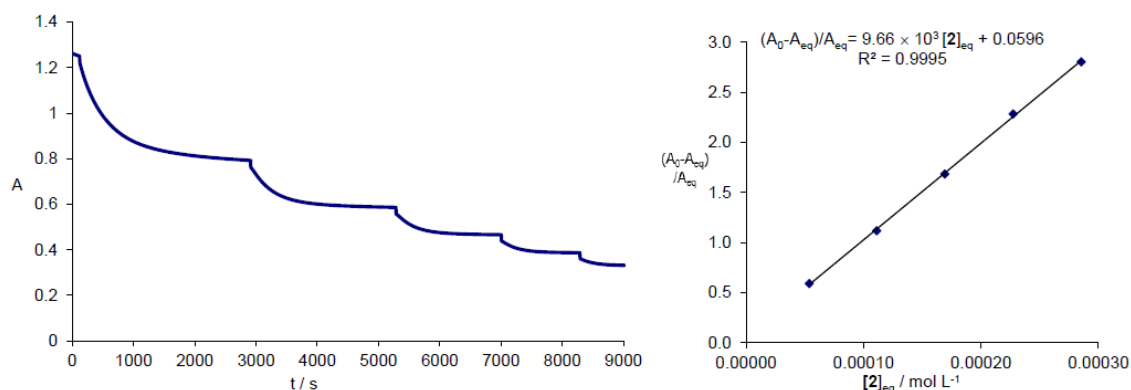
Step	V (2) / mL	V (2) total / mL	V total / mL	A <sub>eq</sub>	[E4]	A <sub>0</sub> -A <sub>eq</sub>	[2] <sub>0</sub>	[2] <sub>0</sub> / [E4] <sub>0</sub>	[2] <sub>eq</sub>	(A <sub>0</sub> -A <sub>eq</sub> )/A <sub>eq</sub>
0			23.01	1.070	$1.54 \times 10^{-5}$					
1	0.02	0.02	23.03	0.630	$9.06 \times 10^{-6}$	0.440	$3.36 \times 10^{-5}$	2.2	$2.73 \times 10^{-5}$	0.698
2	0.02	0.04	23.07	0.492	$7.08 \times 10^{-6}$	0.578	$6.71 \times 10^{-5}$	7.4	$5.88 \times 10^{-5}$	1.175
3	0.02	0.06	23.13	0.382	$5.50 \times 10^{-6}$	0.688	$1.00 \times 10^{-4}$	14.2	$9.06 \times 10^{-5}$	1.801
4	0.02	0.08	23.21	0.299	$4.30 \times 10^{-6}$	0.771	$1.33 \times 10^{-4}$	24.3	$1.22 \times 10^{-4}$	2.579



$$K = 1.98 \times 10^4 \text{ L mol}^{-1}$$

**Table S73.** Reaction of **2** with **E5** ( $\varepsilon = 1.287 \times 10^5 \text{ L mol}^{-1} \text{ cm}^{-1}$ ,  $\lambda = 616 \text{ nm}$ ) in MeCN at 20 °C.

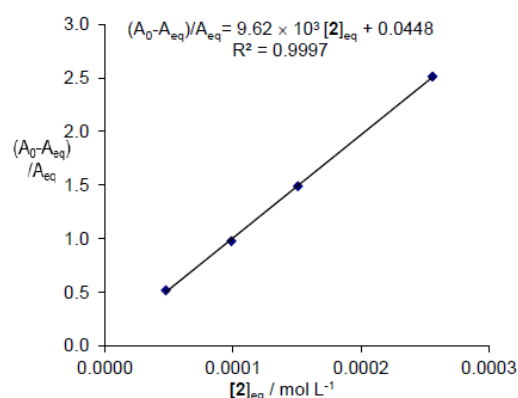
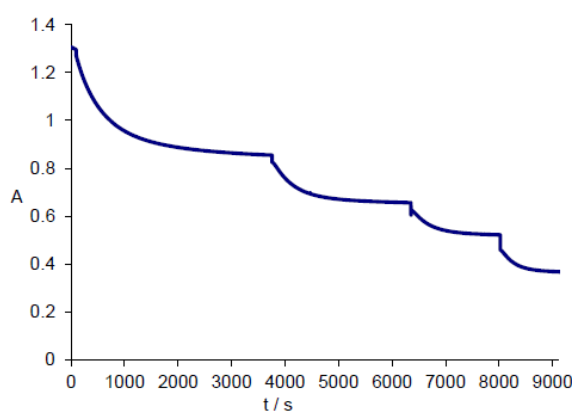
Step	V (2) / mL	V (2) total / mL	V total / mL	A <sub>eq</sub>	[E5]	A <sub>0</sub> -A <sub>eq</sub>	[2] <sub>0</sub>	[2] <sub>0</sub> / [E5] <sub>0</sub>	[2] <sub>eq</sub>	(A <sub>0</sub> -A <sub>eq</sub> )/A <sub>eq</sub>
0			21.95	1.248	$1.94 \times 10^{-5}$					
1	0.1	0.1	22.05	0.785	$1.22 \times 10^{-5}$	0.463	$6.10 \times 10^{-5}$	3.1	$5.38 \times 10^{-5}$	0.590
2	0.1	0.2	22.15	0.589	$9.15 \times 10^{-6}$	0.659	$1.22 \times 10^{-4}$	10.0	$1.11 \times 10^{-4}$	1.119
3	0.1	0.3	22.25	0.465	$7.23 \times 10^{-6}$	0.783	$1.81 \times 10^{-4}$	19.8	$1.69 \times 10^{-4}$	1.684
4	0.1	0.4	22.35	0.380	$5.91 \times 10^{-6}$	0.868	$2.41 \times 10^{-4}$	33.3	$2.27 \times 10^{-4}$	2.284
5	0.1	0.5	22.45	0.328	$5.10 \times 10^{-6}$	0.920	$3.00 \times 10^{-4}$	50.8	$2.85 \times 10^{-4}$	2.805



$$K = 9.66 \times 10^3 \text{ L mol}^{-1}$$

**Table S74.** Reaction of **2** with **E5** ( $\varepsilon = 1.287 \times 10^5 \text{ L mol}^{-1} \text{ cm}^{-1}$ ,  $\lambda = 616 \text{ nm}$ ) in MeCN at 20 °C.

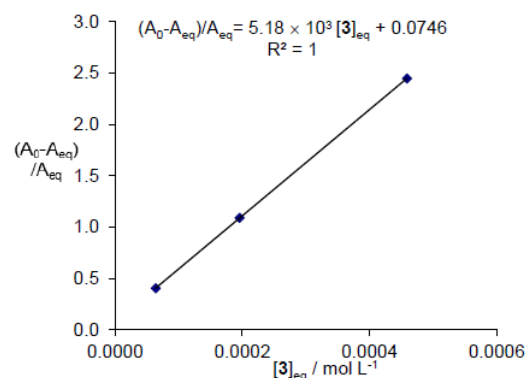
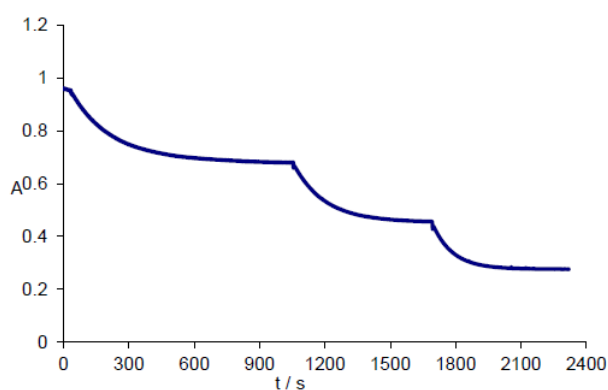
Step	V (2) / mL	V (2) total / mL	V total / mL	A <sub>eq</sub>	[E5]	A <sub>0</sub> -A <sub>eq</sub>	[2] <sub>0</sub>	[2] <sub>0</sub> / [E5] <sub>0</sub>	[2] <sub>eq</sub>	(A <sub>0</sub> -A <sub>eq</sub> )/A <sub>eq</sub>
0			23.07	1.300	$2.02 \times 10^{-5}$					
1	0.05	0.05	23.12	0.856	$1.33 \times 10^{-5}$	0.444	$5.45 \times 10^{-5}$	2.7	$4.76 \times 10^{-5}$	0.519
2	0.05	0.10	23.17	0.657	$1.02 \times 10^{-5}$	0.643	$1.09 \times 10^{-4}$	8.2	$9.88 \times 10^{-5}$	0.979
3	0.05	0.15	23.22	0.522	$8.11 \times 10^{-6}$	0.778	$1.63 \times 10^{-4}$	16.0	$1.51 \times 10^{-4}$	1.490
4	0.10	0.25	23.32	0.370	$5.75 \times 10^{-6}$	0.930	$2.70 \times 10^{-4}$	33.3	$2.56 \times 10^{-4}$	2.514



$$K = 9.62 \times 10^3 \text{ L mol}^{-1}$$

**Table S75.** Reaction of **3** with **E3** ( $\varepsilon = 1.464 \times 10^5 \text{ L mol}^{-1} \text{ cm}^{-1}$ ,  $\lambda = 605 \text{ nm}$ ) in MeCN at 20 °C.

Step	V (3) / mL	V (3) total / mL	V total / mL	A <sub>eq</sub>	[E3]	A <sub>0</sub> -A <sub>eq</sub>	[3] <sub>0</sub>	[3] <sub>0</sub> / [E3] <sub>0</sub>	[3] <sub>eq</sub>	(A <sub>0</sub> -A <sub>eq</sub> )/A <sub>eq</sub>
0			20.96	0.955	$1.30 \times 10^{-5}$					
1	0.05	0.05	21.01	0.680	$9.29 \times 10^{-6}$	0.275	$6.78 \times 10^{-5}$	5.2	$6.40 \times 10^{-5}$	0.404
2	0.10	0.15	21.11	0.457	$6.24 \times 10^{-6}$	0.498	$2.02 \times 10^{-4}$	21.8	$1.96 \times 10^{-4}$	1.090
3	0.20	0.35	21.31	0.277	$3.78 \times 10^{-6}$	0.678	$4.68 \times 10^{-4}$	75.0	$4.59 \times 10^{-4}$	2.448

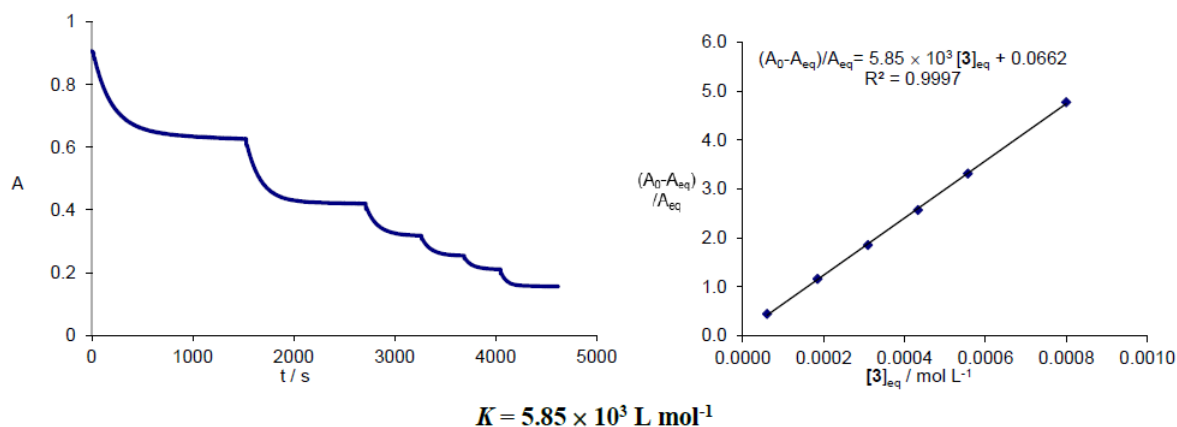


$$K = 5.18 \times 10^3 \text{ L mol}^{-1}$$



**Table S76.** Reaction of **3** with **E3** ( $\epsilon = 1.464 \times 10^5 \text{ L mol}^{-1} \text{ cm}^{-1}$ ,  $\lambda = 605 \text{ nm}$ ) in MeCN at 20 °C.

Step	V ( <b>3</b> ) / mL	V ( <b>3</b> ) <sub>total</sub> / mL	V <sub>total</sub> / mL	A <sub>eq</sub>	[ <b>E3</b> ]	A <sub>0</sub> -A <sub>eq</sub>	[ <b>3</b> ] <sub>0</sub>	[ <b>3</b> ] <sub>0</sub> / [ <b>E3</b> ] <sub>0</sub>	[ <b>3</b> ] <sub>eq</sub>	(A <sub>0</sub> -A <sub>eq</sub> )/A <sub>eq</sub>
0			22.22	0.906	$1.24 \times 10^{-5}$					
1	0.05	0.05	22.27	0.628	$8.58 \times 10^{-6}$	0.278	$6.40 \times 10^{-5}$	5.2	$6.02 \times 10^{-5}$	0.443
2	0.10	0.15	22.37	0.420	$5.74 \times 10^{-6}$	0.486	$1.91 \times 10^{-4}$	22.3	$1.84 \times 10^{-4}$	1.157
3	0.10	0.25	22.47	0.318	$4.34 \times 10^{-6}$	0.588	$3.17 \times 10^{-4}$	55.2	$3.09 \times 10^{-4}$	1.849
4	0.10	0.35	22.57	0.254	$3.47 \times 10^{-6}$	0.652	$4.42 \times 10^{-4}$	102	$4.33 \times 10^{-4}$	2.567
5	0.10	0.45	22.67	0.210	$2.87 \times 10^{-6}$	0.696	$5.66 \times 10^{-4}$	163	$5.56 \times 10^{-4}$	3.314
6	0.20	0.65	22.87	0.157	$2.14 \times 10^{-6}$	0.749	$8.10 \times 10^{-4}$	282	$8.00 \times 10^{-4}$	4.771

**Table S77.** Reaction of **3** with **E3** ( $\epsilon = 1.464 \times 10^5 \text{ L mol}^{-1} \text{ cm}^{-1}$ ,  $\lambda = 605 \text{ nm}$ ) in MeCN at 20 °C.

Step	V ( <b>3</b> ) / mL	V ( <b>3</b> ) <sub>total</sub> / mL	V <sub>total</sub> / mL	A <sub>eq</sub>	[ <b>E3</b> ]	A <sub>0</sub> -A <sub>eq</sub>	[ <b>3</b> ] <sub>0</sub>	[ <b>3</b> ] <sub>0</sub> / [ <b>E3</b> ] <sub>0</sub>	[ <b>3</b> ] <sub>eq</sub>	(A <sub>0</sub> -A <sub>eq</sub> )/A <sub>eq</sub>
0			22.47	0.878	$1.20 \times 10^{-5}$					
1	0.1	0.1	22.57	0.507	$6.93 \times 10^{-6}$	0.371	$6.98 \times 10^{-5}$	5.8	$6.47 \times 10^{-5}$	0.732
2	0.1	0.2	22.67	0.391	$5.34 \times 10^{-6}$	0.487	$1.39 \times 10^{-4}$	20.1	$1.32 \times 10^{-4}$	1.246
3	0.2	0.4	22.87	0.276	$3.77 \times 10^{-6}$	0.602	$2.75 \times 10^{-4}$	51.6	$2.67 \times 10^{-4}$	2.181
4	0.2	0.6	23.07	0.215	$2.94 \times 10^{-6}$	0.663	$4.10 \times 10^{-4}$	109	$4.01 \times 10^{-4}$	3.084

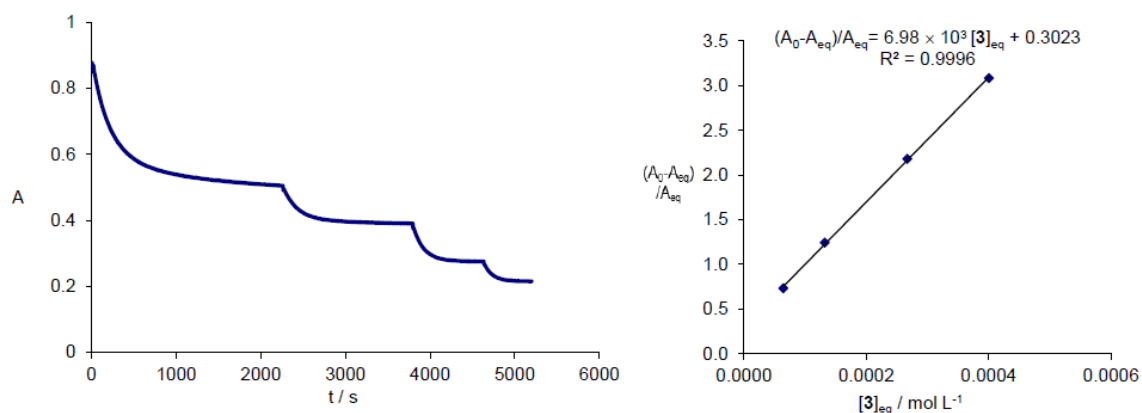
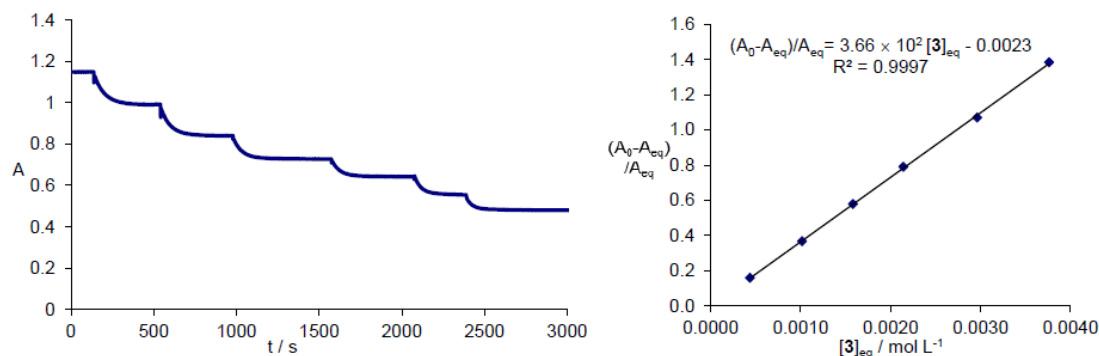


**Table S78.** Reaction of **3** with **E4** ( $\epsilon = 1.390 \times 10^5 \text{ L mol}^{-1} \text{ cm}^{-1}$ ,  $\lambda = 611 \text{ nm}$ ) in MeCN at 20 °C.

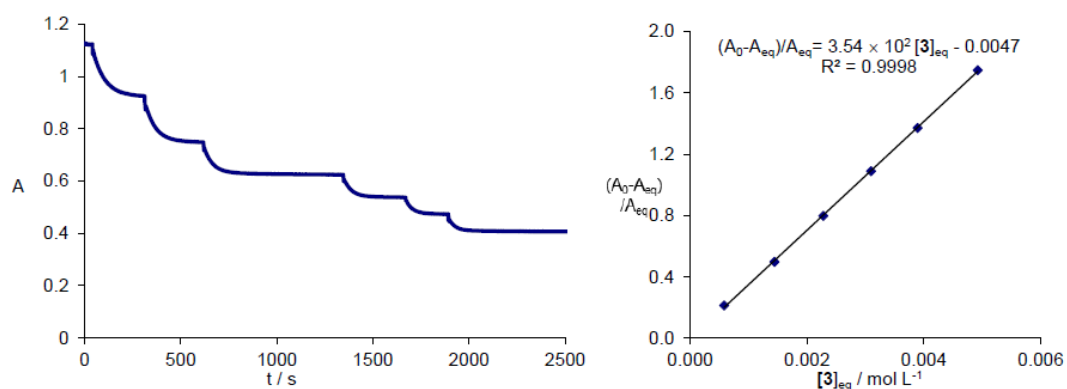
Step	V ( <b>3</b> ) / mL	V ( <b>3</b> ) <sub>total</sub> / mL	V <sub>total</sub> / mL	A <sub>eq</sub>	[ <b>E4</b> ]	A <sub>0</sub> -A <sub>eq</sub>	[ <b>3</b> ] <sub>0</sub>	[ <b>3</b> ] <sub>0</sub> / [ <b>E4</b> ] <sub>0</sub>	[ <b>3</b> ] <sub>eq</sub>	(A <sub>0</sub> -A <sub>eq</sub> )/A <sub>eq</sub>
0			22.45	1.149	$1.65 \times 10^{-5}$					
1	0.15	0.15	22.60	0.990	$1.42 \times 10^{-5}$	0.159	$4.41 \times 10^{-4}$	26.7	$4.39 \times 10^{-4}$	0.161
2	0.20	0.35	22.80	0.840	$1.21 \times 10^{-5}$	0.309	$1.02 \times 10^{-3}$	71.7	$1.02 \times 10^{-3}$	0.368
3	0.20	0.55	23.00	0.728	$1.05 \times 10^{-5}$	0.421	$1.59 \times 10^{-3}$	132	$1.58 \times 10^{-3}$	0.578
4	0.20	0.75	23.20	0.642	$9.24 \times 10^{-6}$	0.507	$2.15 \times 10^{-3}$	205	$2.14 \times 10^{-3}$	0.790
5	0.30	1.05	23.50	0.555	$7.99 \times 10^{-6}$	0.594	$2.97 \times 10^{-3}$	322	$2.96 \times 10^{-3}$	1.070
6	0.30	1.35	23.80	0.482	$6.94 \times 10^{-6}$	0.667	$3.77 \times 10^{-3}$	472	$3.76 \times 10^{-3}$	1.384



$$K = 3.66 \times 10^2 \text{ L mol}^{-1}$$

**Table S79.** Reaction of **3** with **E4** ( $\epsilon = 1.390 \times 10^5 \text{ L mol}^{-1} \text{ cm}^{-1}$ ,  $\lambda = 611 \text{ nm}$ ) in MeCN at 20 °C.

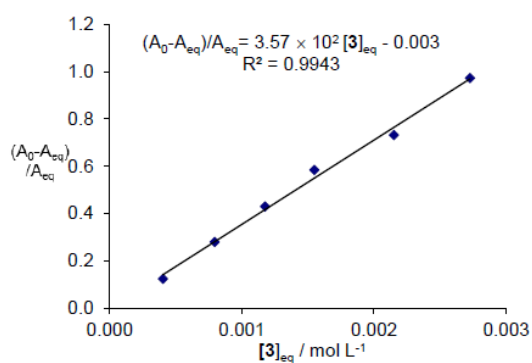
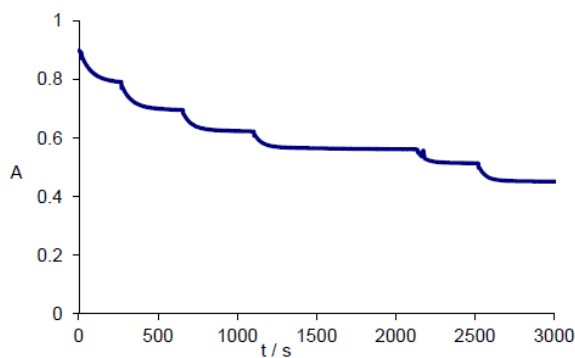
Step	V ( <b>3</b> ) / mL	V ( <b>3</b> ) <sub>total</sub> / mL	V <sub>total</sub> / mL	A <sub>eq</sub>	[ <b>E4</b> ]	A <sub>0</sub> -A <sub>eq</sub>	[ <b>3</b> ] <sub>0</sub>	[ <b>3</b> ] <sub>0</sub> / [ <b>E4</b> ] <sub>0</sub>	[ <b>3</b> ] <sub>eq</sub>	(A <sub>0</sub> -A <sub>eq</sub> )/A <sub>eq</sub>
0			22.46	1.124	$1.62 \times 10^{-5}$					
1	0.20	0.20	22.66	0.926	$1.33 \times 10^{-5}$	0.198	$5.87 \times 10^{-4}$	36.3	$5.84 \times 10^{-4}$	0.214
2	0.30	0.50	22.96	0.750	$1.08 \times 10^{-5}$	0.374	$1.45 \times 10^{-3}$	109	$1.44 \times 10^{-3}$	0.499
3	0.30	0.80	23.26	0.625	$8.99 \times 10^{-6}$	0.499	$2.29 \times 10^{-3}$	212	$2.28 \times 10^{-3}$	0.798
4	0.30	1.10	23.56	0.538	$7.74 \times 10^{-6}$	0.586	$3.11 \times 10^{-3}$	345	$3.10 \times 10^{-3}$	1.089
5	0.30	1.40	23.86	0.474	$6.82 \times 10^{-6}$	0.650	$3.90 \times 10^{-3}$	504	$3.89 \times 10^{-3}$	1.371
6	0.40	1.80	24.26	0.409	$5.88 \times 10^{-6}$	0.715	$4.93 \times 10^{-3}$	724	$4.92 \times 10^{-3}$	1.748



$$K = 3.54 \times 10^2 \text{ L mol}^{-1}$$

**Table S80.** Reaction of **3** with **E4** ( $\varepsilon = 1.390 \times 10^5 \text{ L mol}^{-1} \text{ cm}^{-1}$ ,  $\lambda = 611 \text{ nm}$ ) in MeCN at 20 °C.

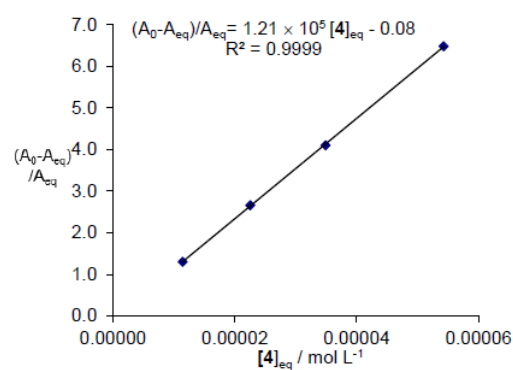
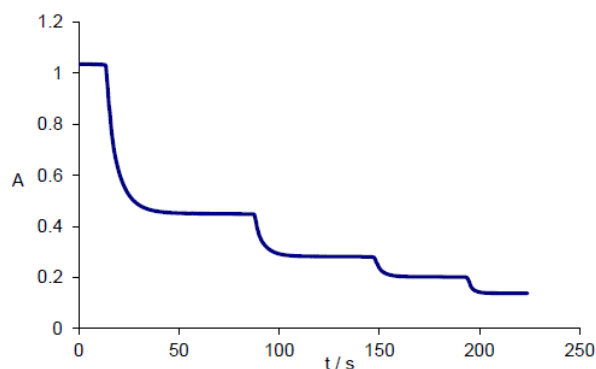
Step	V ( <b>3</b> ) / mL	V ( <b>3</b> ) <sub>total</sub> / mL	V <sub>total</sub> / mL	A <sub>eq</sub>	[ <b>E4</b> ]	A <sub>0</sub> -A <sub>eq</sub>	[ <b>3</b> ] <sub>0</sub>	[ <b>3</b> ] <sub>0</sub> / [ <b>E4</b> ] <sub>0</sub>	[ <b>3</b> ] <sub>eq</sub>	(A <sub>0</sub> -A <sub>eq</sub> )/A <sub>eq</sub>
0			22.37	0.892	$1.28 \times 10^{-5}$					
1	0.30	0.30	22.67	0.794	$1.14 \times 10^{-5}$	0.098	$4.04 \times 10^{-4}$	31.5	$4.03 \times 10^{-4}$	0.123
2	0.30	0.60	22.97	0.697	$1.00 \times 10^{-5}$	0.195	$7.97 \times 10^{-4}$	69.8	$7.95 \times 10^{-4}$	0.280
3	0.30	0.90	23.27	0.624	$8.98 \times 10^{-6}$	0.268	$1.18 \times 10^{-3}$	118	$1.18 \times 10^{-3}$	0.429
4	0.30	1.20	23.57	0.563	$8.10 \times 10^{-6}$	0.329	$1.55 \times 10^{-3}$	173	$1.55 \times 10^{-3}$	0.584
5	0.50	1.70	24.07	0.515	$7.41 \times 10^{-6}$	0.377	$2.16 \times 10^{-3}$	266	$2.15 \times 10^{-3}$	0.732
6	0.50	2.20	24.57	0.452	$6.50 \times 10^{-6}$	0.440	$2.73 \times 10^{-3}$	369	$2.73 \times 10^{-3}$	0.973



$$K = 3.57 \times 10^2 \text{ L mol}^{-1}$$

**Table S81.** Reaction of **4** with **E5** ( $\varepsilon = 1.287 \times 10^5 \text{ L mol}^{-1} \text{ cm}^{-1}$ ,  $\lambda = 616 \text{ nm}$ ) in MeCN at 20 °C.

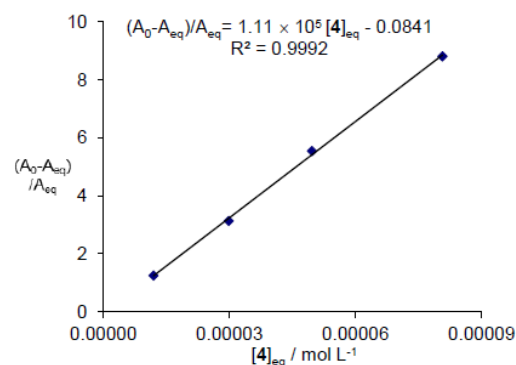
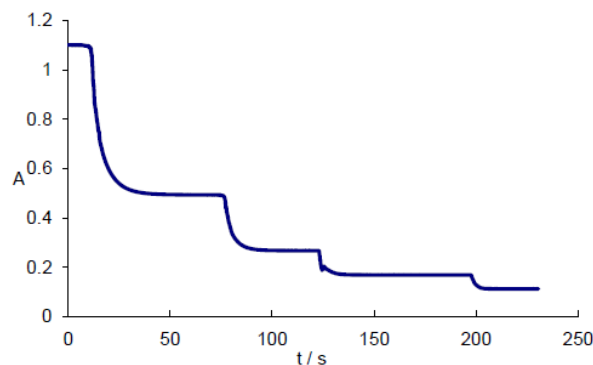
Step	V ( <b>4</b> ) / mL	V ( <b>4</b> ) <sub>total</sub> / mL	V <sub>total</sub> / mL	A <sub>eq</sub>	[ <b>E5</b> ]	A <sub>0</sub> -A <sub>eq</sub>	[ <b>4</b> ] <sub>0</sub>	[ <b>4</b> ] <sub>0</sub> / [ <b>E5</b> ] <sub>0</sub>	[ <b>4</b> ] <sub>eq</sub>	(A <sub>0</sub> -A <sub>eq</sub> )/A <sub>eq</sub>
0			23.12	1.025	$1.59 \times 10^{-5}$					
1	0.03	0.03	23.15	0.445	$6.92 \times 10^{-6}$	0.580	$2.05 \times 10^{-5}$	1.3	$1.15 \times 10^{-5}$	1.303
2	0.02	0.05	23.17	0.280	$4.35 \times 10^{-6}$	0.745	$3.41 \times 10^{-5}$	4.9	$2.25 \times 10^{-5}$	2.661
3	0.02	0.07	23.19	0.201	$3.12 \times 10^{-6}$	0.824	$4.77 \times 10^{-5}$	11.0	$3.49 \times 10^{-5}$	4.100
4	0.03	0.10	23.22	0.137	$2.13 \times 10^{-6}$	0.888	$6.81 \times 10^{-5}$	21.8	$5.43 \times 10^{-5}$	6.482



$$K = 1.21 \times 10^5 \text{ L mol}^{-1}$$

**Table S82.** Reaction of **4** with **E5** ( $\varepsilon = 1.287 \times 10^5 \text{ L mol}^{-1} \text{ cm}^{-1}$ ,  $\lambda = 616 \text{ nm}$ ) in MeCN at 20 °C.

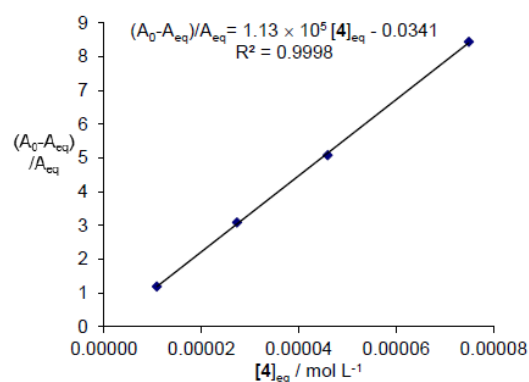
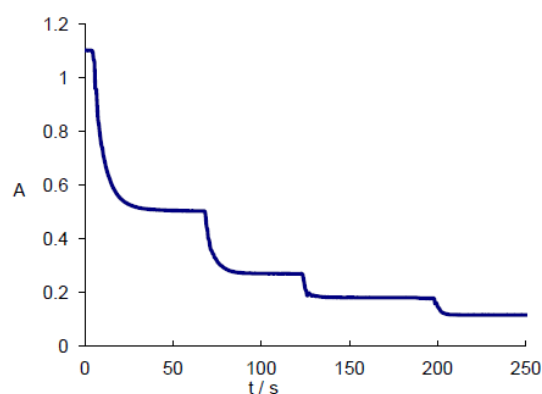
Step	V ( <b>4</b> ) / mL	V ( <b>4</b> ) <sub>total</sub> / mL	V <sub>total</sub> / mL	A <sub>eq</sub>	[ <b>E5</b> ]	A <sub>0</sub> -A <sub>eq</sub>	[ <b>4</b> ] <sub>0</sub>	[ <b>4</b> ] <sub>0</sub> / [ <b>E5</b> ] <sub>0</sub>	[ <b>4</b> ] <sub>eq</sub>	(A <sub>0</sub> -A <sub>eq</sub> )/A <sub>eq</sub>
0			23.38	1.099	$1.71 \times 10^{-5}$					
1	0.02	0.02	23.40	0.489	$7.60 \times 10^{-6}$	0.610	$2.14 \times 10^{-5}$	1.3	$1.19 \times 10^{-5}$	1.247
2	0.02	0.04	23.42	0.266	$4.13 \times 10^{-6}$	0.833	$4.28 \times 10^{-5}$	5.6	$2.98 \times 10^{-5}$	3.132
3	0.02	0.06	23.44	0.168	$2.61 \times 10^{-6}$	0.931	$6.41 \times 10^{-5}$	15.5	$4.97 \times 10^{-5}$	5.542
4	0.03	0.09	23.47	0.112	$1.74 \times 10^{-6}$	0.987	$9.61 \times 10^{-5}$	36.8	$8.07 \times 10^{-5}$	8.813



$$K = 1.11 \times 10^5 \text{ L mol}^{-1}$$

**Table S83.** Reaction of **4** with **E5** ( $\varepsilon = 1.287 \times 10^5 \text{ L mol}^{-1} \text{ cm}^{-1}$ ,  $\lambda = 616 \text{ nm}$ ) in MeCN at 20 °C.

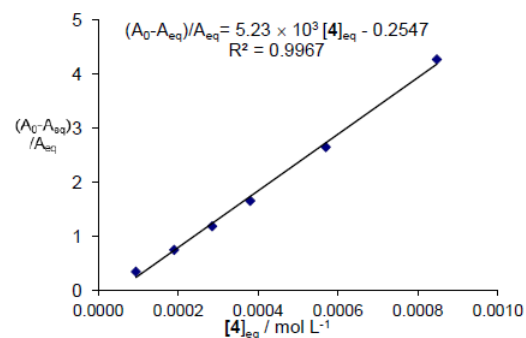
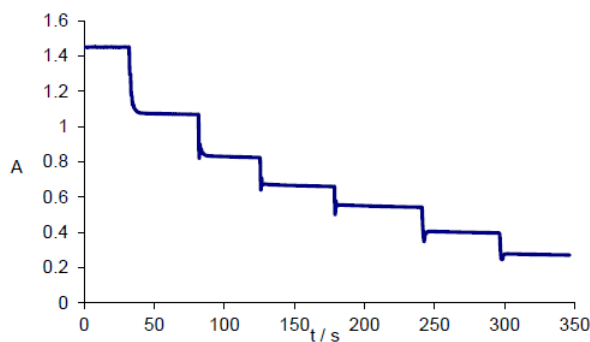
Step	V ( <b>4</b> ) / mL	V ( <b>4</b> ) <sub>total</sub> / mL	V <sub>total</sub> / mL	A <sub>eq</sub>	[ <b>E5</b> ]	A <sub>0</sub> -A <sub>eq</sub>	[ <b>4</b> ] <sub>0</sub>	[ <b>4</b> ] <sub>0</sub> / [ <b>E5</b> ] <sub>0</sub>	[ <b>4</b> ] <sub>eq</sub>	(A <sub>0</sub> -A <sub>eq</sub> )/A <sub>eq</sub>
0			23.31	1.094	$1.70 \times 10^{-5}$					
1	0.02	0.02	23.33	0.500	$7.77 \times 10^{-6}$	0.594	$2.01 \times 10^{-5}$	1.2	$1.09 \times 10^{-5}$	1.188
2	0.02	0.04	23.35	0.268	$4.16 \times 10^{-6}$	0.826	$4.01 \times 10^{-5}$	5.2	$2.73 \times 10^{-5}$	3.082
3	0.02	0.06	23.37	0.180	$2.80 \times 10^{-6}$	0.914	$6.02 \times 10^{-5}$	14.4	$4.59 \times 10^{-5}$	5.078
4	0.03	0.09	23.40	0.116	$1.80 \times 10^{-6}$	0.978	$9.01 \times 10^{-5}$	32.2	$7.49 \times 10^{-5}$	8.431



$$K = 1.13 \times 10^5 \text{ L mol}^{-1}$$

**Table S84.** Reaction of **4** with **E6** ( $\varepsilon = 1.727 \times 10^5 \text{ L mol}^{-1} \text{ cm}^{-1}$ ,  $\lambda = 635 \text{ nm}$ ) in MeCN at 20 °C.

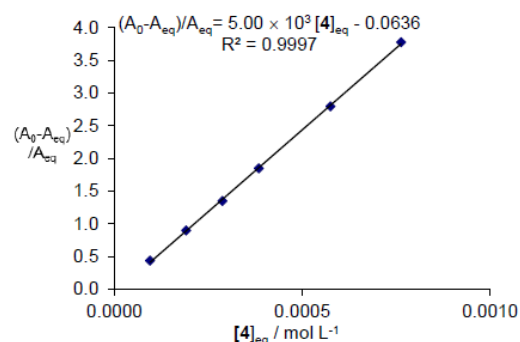
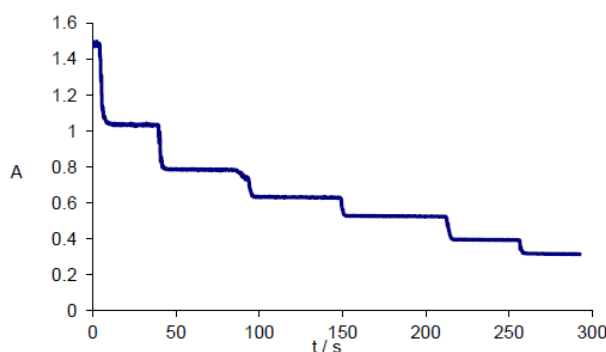
Step	V ( <b>4</b> ) / mL	V ( <b>4</b> ) <sub>total</sub> / mL	V <sub>total</sub> / mL	A <sub>eq</sub>	[ <b>E6</b> ]	A <sub>0</sub> -A <sub>eq</sub>	[ <b>4</b> ] <sub>0</sub>	[ <b>4</b> ] <sub>0</sub> / [ <b>E6</b> ] <sub>0</sub>	[ <b>4</b> ] <sub>eq</sub>	(A <sub>0</sub> -A <sub>eq</sub> )/A <sub>eq</sub>
0			22.02	1.450	$1.68 \times 10^{-5}$					
1	0.10	0.10	22.12	1.073	$1.24 \times 10^{-5}$	0.377	$9.92 \times 10^{-5}$	5.9	$9.48 \times 10^{-5}$	0.351
2	0.10	0.20	22.22	0.829	$9.60 \times 10^{-6}$	0.621	$1.97 \times 10^{-4}$	15.9	$1.90 \times 10^{-4}$	0.749
3	0.10	0.30	22.32	0.663	$7.68 \times 10^{-6}$	0.787	$2.95 \times 10^{-4}$	30.7	$2.86 \times 10^{-4}$	1.187
4	0.10	0.40	22.42	0.545	$6.31 \times 10^{-6}$	0.905	$3.91 \times 10^{-4}$	51.0	$3.81 \times 10^{-4}$	1.661
5	0.20	0.60	22.62	0.397	$4.60 \times 10^{-6}$	1.053	$5.82 \times 10^{-4}$	92.2	$5.70 \times 10^{-4}$	2.652
6	0.30	0.90	22.92	0.275	$3.18 \times 10^{-6}$	1.175	$8.61 \times 10^{-4}$	187	$8.48 \times 10^{-4}$	4.273



$$K = 5.23 \times 10^3 \text{ L mol}^{-1}$$

**Table S85.** Reaction of **4** with **E6** ( $\varepsilon = 1.727 \times 10^5 \text{ L mol}^{-1} \text{ cm}^{-1}$ ,  $\lambda = 635 \text{ nm}$ ) in MeCN at 20 °C.

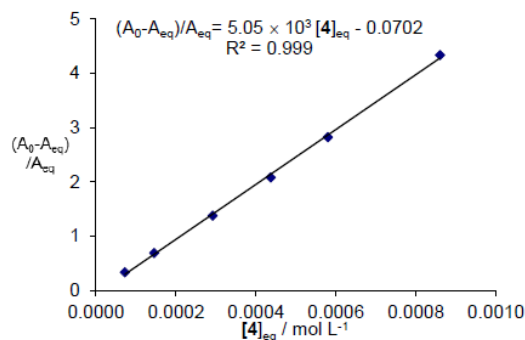
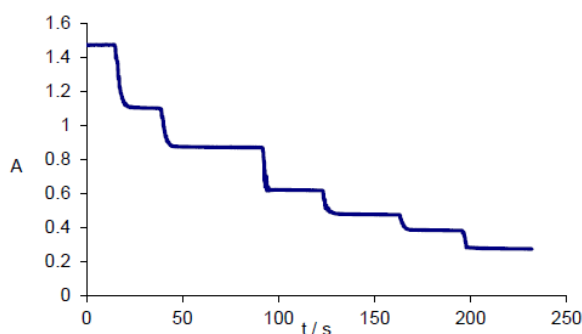
Step	V ( <b>4</b> ) / mL	V ( <b>4</b> ) <sub>total</sub> / mL	V <sub>total</sub> / mL	A <sub>eq</sub>	[ <b>E6</b> ]	A <sub>0</sub> -A <sub>eq</sub>	[ <b>4</b> ] <sub>0</sub>	[ <b>4</b> ] <sub>0</sub> / [ <b>E6</b> ] <sub>0</sub>	[ <b>4</b> ] <sub>eq</sub>	(A <sub>0</sub> -A <sub>eq</sub> )/A <sub>eq</sub>
0			21.78	1.480	$1.71 \times 10^{-5}$					
1	0.1	0.1	21.88	1.030	$1.19 \times 10^{-5}$	0.450	$1.00 \times 10^{-4}$	5.8	$9.50 \times 10^{-5}$	0.437
2	0.1	0.2	21.98	0.780	$9.03 \times 10^{-6}$	0.700	$2.00 \times 10^{-4}$	16.7	$1.91 \times 10^{-4}$	0.897
3	0.1	0.3	22.08	0.630	$7.30 \times 10^{-6}$	0.850	$2.98 \times 10^{-4}$	33.0	$2.88 \times 10^{-4}$	1.349
4	0.1	0.4	22.18	0.520	$6.02 \times 10^{-6}$	0.960	$3.95 \times 10^{-4}$	54.2	$3.84 \times 10^{-4}$	1.846
5	0.2	0.6	22.38	0.390	$4.52 \times 10^{-6}$	1.090	$5.88 \times 10^{-4}$	97.6	$5.75 \times 10^{-4}$	2.795
6	0.2	0.8	22.58	0.310	$3.59 \times 10^{-6}$	1.170	$7.77 \times 10^{-4}$	172	$7.63 \times 10^{-4}$	3.774



$$K = 5.00 \times 10^3 \text{ L mol}^{-1}$$

**Table S86.** Reaction of **4** with **E6** ( $\varepsilon = 1.727 \times 10^5 \text{ L mol}^{-1} \text{ cm}^{-1}$ ,  $\lambda = 635 \text{ nm}$ ) in MeCN at 20 °C.

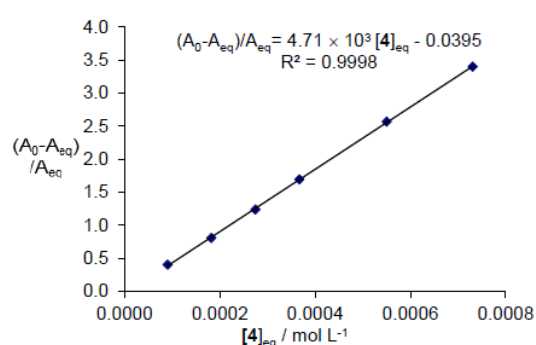
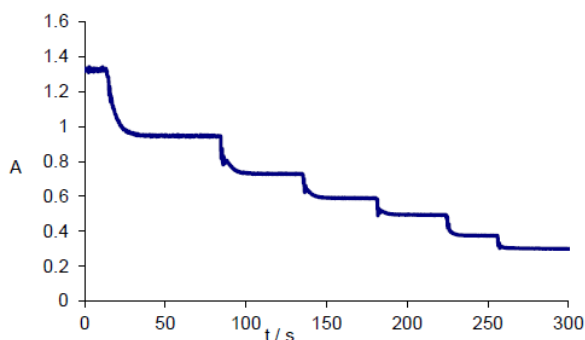
Step	V ( <b>4</b> ) / mL	V ( <b>4</b> ) <sub>total</sub> / mL	V <sub>total</sub> / mL	A <sub>eq</sub>	[ <b>E6</b> ]	A <sub>0</sub> -A <sub>eq</sub>	[ <b>4</b> ] <sub>0</sub>	[ <b>4</b> ] <sub>0</sub> / [ <b>E6</b> ] <sub>0</sub>	[ <b>4</b> ] <sub>eq</sub>	(A <sub>0</sub> -A <sub>eq</sub> )/A <sub>eq</sub>
0			22.42	1.472	$1.70 \times 10^{-5}$					
1	0.1	0.1	22.52	1.102	$1.28 \times 10^{-5}$	0.370	$7.64 \times 10^{-5}$	4.5	$7.21 \times 10^{-5}$	0.336
2	0.1	0.2	22.62	0.871	$1.01 \times 10^{-5}$	0.601	$1.52 \times 10^{-4}$	11.9	$1.45 \times 10^{-4}$	0.690
3	0.2	0.4	22.82	0.620	$7.18 \times 10^{-6}$	0.852	$3.01 \times 10^{-4}$	29.9	$2.92 \times 10^{-4}$	1.374
4	0.2	0.6	23.02	0.478	$5.54 \times 10^{-6}$	0.994	$4.48 \times 10^{-4}$	62.4	$4.37 \times 10^{-4}$	2.079
5	0.2	0.8	23.22	0.385	$4.46 \times 10^{-6}$	1.087	$5.93 \times 10^{-4}$	107	$5.80 \times 10^{-4}$	2.823
6	0.4	1.2	23.62	0.276	$3.20 \times 10^{-6}$	1.196	$8.74 \times 10^{-4}$	196	$8.60 \times 10^{-4}$	4.333



$$K = 5.05 \times 10^3 \text{ L mol}^{-1}$$

**Table S87.** Reaction of **4** with **E7** ( $\varepsilon = 1.318 \times 10^5 \text{ L mol}^{-1} \text{ cm}^{-1}$ ,  $\lambda = 631 \text{ nm}$ ) in MeCN at 20 °C.

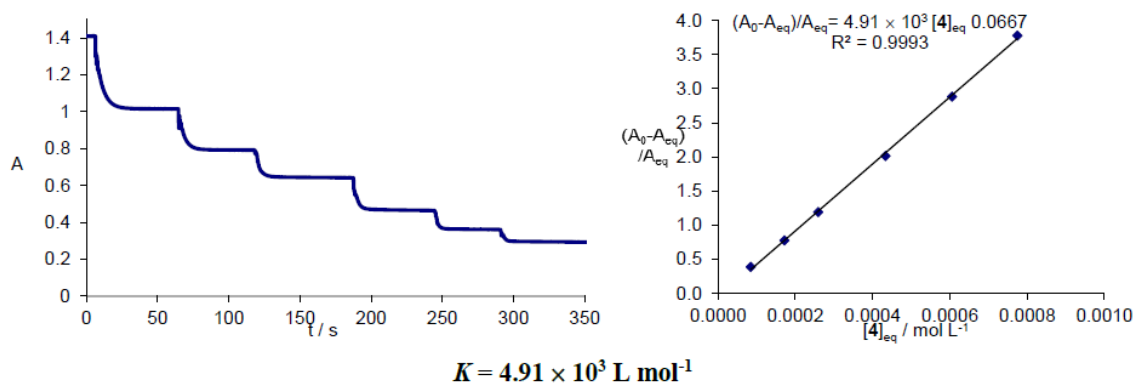
Step	V ( <b>4</b> ) / mL	V ( <b>4</b> ) <sub>total</sub> / mL	V <sub>total</sub> / mL	A <sub>eq</sub>	[ <b>E7</b> ]	A <sub>0</sub> -A <sub>eq</sub>	[ <b>4</b> ] <sub>0</sub>	[ <b>4</b> ] <sub>0</sub> / [ <b>E7</b> ] <sub>0</sub>	[ <b>4</b> ] <sub>eq</sub>	(A <sub>0</sub> -A <sub>eq</sub> )/A <sub>eq</sub>
0			22.70	1.320	$2.00 \times 10^{-5}$					
1	0.1	0.1	22.80	0.940	$1.43 \times 10^{-5}$	0.380	$9.62 \times 10^{-5}$	4.8	$9.04 \times 10^{-5}$	0.404
2	0.1	0.2	22.90	0.730	$1.11 \times 10^{-5}$	0.590	$1.92 \times 10^{-4}$	13.4	$1.83 \times 10^{-4}$	0.808
3	0.1	0.3	23.00	0.590	$8.95 \times 10^{-6}$	0.730	$2.86 \times 10^{-4}$	25.8	$2.75 \times 10^{-4}$	1.237
4	0.1	0.4	23.10	0.490	$7.44 \times 10^{-6}$	0.830	$3.80 \times 10^{-4}$	42.4	$3.67 \times 10^{-4}$	1.694
5	0.2	0.6	23.30	0.370	$5.61 \times 10^{-6}$	0.950	$5.65 \times 10^{-4}$	76.0	$5.50 \times 10^{-4}$	2.568
6	0.2	0.8	23.50	0.300	$4.55 \times 10^{-6}$	1.020	$7.47 \times 10^{-4}$	133	$7.31 \times 10^{-4}$	3.400



$$K = 4.71 \times 10^3 \text{ L mol}^{-1}$$

**Table S88.** Reaction of **4** with **E7** ( $\varepsilon = 1.318 \times 10^5 \text{ L mol}^{-1} \text{ cm}^{-1}$ ,  $\lambda = 631 \text{ nm}$ ) in MeCN at 20 °C.

Step	V ( <b>4</b> ) / mL	V ( <b>4</b> ) <sub>total</sub> / mL	V <sub>total</sub> / mL	A <sub>eq</sub>	[ <b>E7</b> ]	A <sub>0</sub> -A <sub>eq</sub>	[ <b>4</b> ] <sub>0</sub>	[ <b>4</b> ] <sub>0</sub> / [ <b>E7</b> ] <sub>0</sub>	[ <b>4</b> ] <sub>eq</sub>	(A <sub>0</sub> -A <sub>eq</sub> )/A <sub>eq</sub>
0			22.45	1.410	$2.14 \times 10^{-5}$					
1	0.1	0.1	22.55	1.015	$1.54 \times 10^{-5}$	0.395	$9.11 \times 10^{-5}$	4.3	$8.51 \times 10^{-5}$	0.389
2	0.1	0.2	22.65	0.793	$1.20 \times 10^{-5}$	0.617	$1.81 \times 10^{-4}$	11.8	$1.72 \times 10^{-4}$	0.778
3	0.1	0.3	22.75	0.643	$9.76 \times 10^{-6}$	0.767	$2.71 \times 10^{-4}$	22.5	$2.59 \times 10^{-4}$	1.193
4	0.2	0.5	22.95	0.468	$7.10 \times 10^{-6}$	0.942	$4.48 \times 10^{-4}$	45.9	$4.33 \times 10^{-4}$	2.013
5	0.2	0.7	23.15	0.363	$5.51 \times 10^{-6}$	1.047	$6.21 \times 10^{-4}$	87.5	$6.06 \times 10^{-4}$	2.884
6	0.2	0.9	23.35	0.295	$4.48 \times 10^{-6}$	1.115	$7.92 \times 10^{-4}$	144	$7.75 \times 10^{-4}$	3.780

**Table S89.** Reaction of **4** with **E7** ( $\varepsilon = 1.318 \times 10^5 \text{ L mol}^{-1} \text{ cm}^{-1}$ ,  $\lambda = 631 \text{ nm}$ ) in MeCN at 20 °C.

Step	V ( <b>4</b> ) / mL	V ( <b>4</b> ) <sub>total</sub> / mL	V <sub>total</sub> / mL	A <sub>eq</sub>	[ <b>E7</b> ]	A <sub>0</sub> -A <sub>eq</sub>	[ <b>4</b> ] <sub>0</sub>	[ <b>4</b> ] <sub>0</sub> / [ <b>E7</b> ] <sub>0</sub>	[ <b>4</b> ] <sub>eq</sub>	(A <sub>0</sub> -A <sub>eq</sub> )/A <sub>eq</sub>
0			22.60	1.377	$2.09 \times 10^{-5}$					
1	0.1	0.1	22.70	1.041	$1.58 \times 10^{-5}$	0.336	$7.58 \times 10^{-5}$	3.6	$7.07 \times 10^{-5}$	0.323
2	0.1	0.2	22.80	0.834	$1.27 \times 10^{-5}$	0.543	$1.51 \times 10^{-4}$	9.6	$1.43 \times 10^{-4}$	0.651
3	0.2	0.4	23.00	0.597	$9.06 \times 10^{-6}$	0.780	$2.99 \times 10^{-4}$	23.6	$2.87 \times 10^{-4}$	1.307
4	0.2	0.6	23.20	0.460	$6.98 \times 10^{-6}$	0.917	$4.45 \times 10^{-4}$	49.1	$4.31 \times 10^{-4}$	1.993
5	0.2	0.8	23.40	0.375	$5.69 \times 10^{-6}$	1.002	$5.88 \times 10^{-4}$	84.2	$5.73 \times 10^{-4}$	2.672
6	0.4	1.2	23.80	0.271	$4.11 \times 10^{-6}$	1.106	$8.67 \times 10^{-4}$	152	$8.50 \times 10^{-4}$	4.081

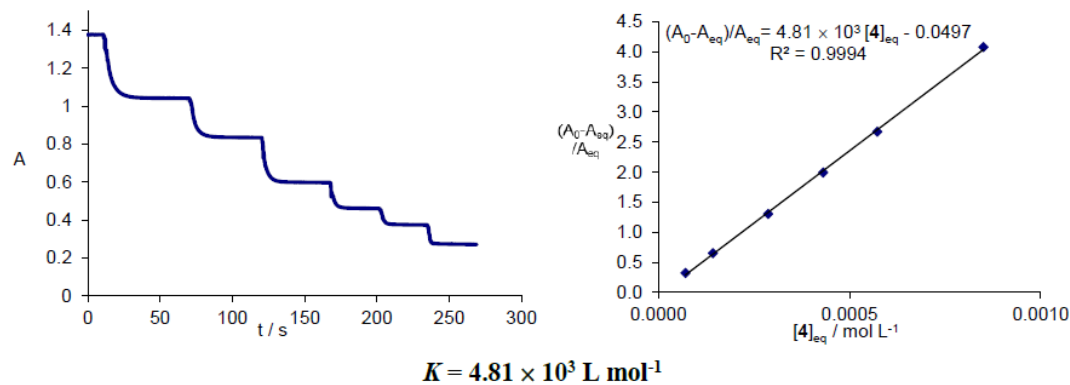
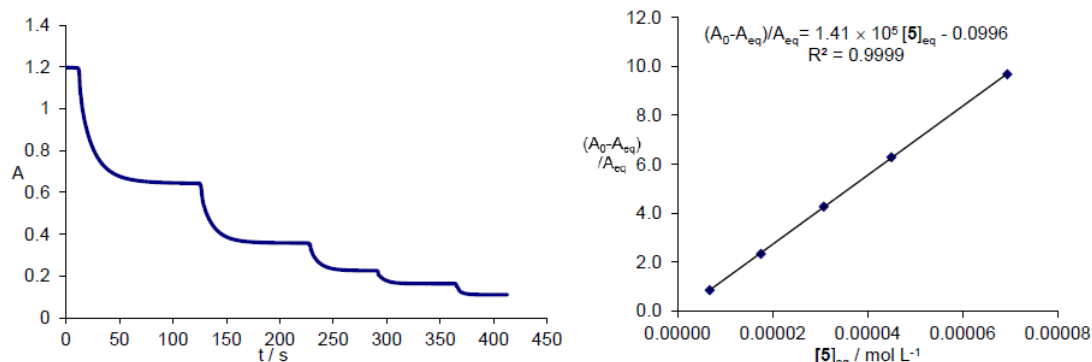


**Table S90.** Reaction of **5** with **E5** ( $\varepsilon = 1.287 \times 10^5 \text{ L mol}^{-1} \text{ cm}^{-1}$ ,  $\lambda = 616 \text{ nm}$ ) in MeCN at 20 °C.

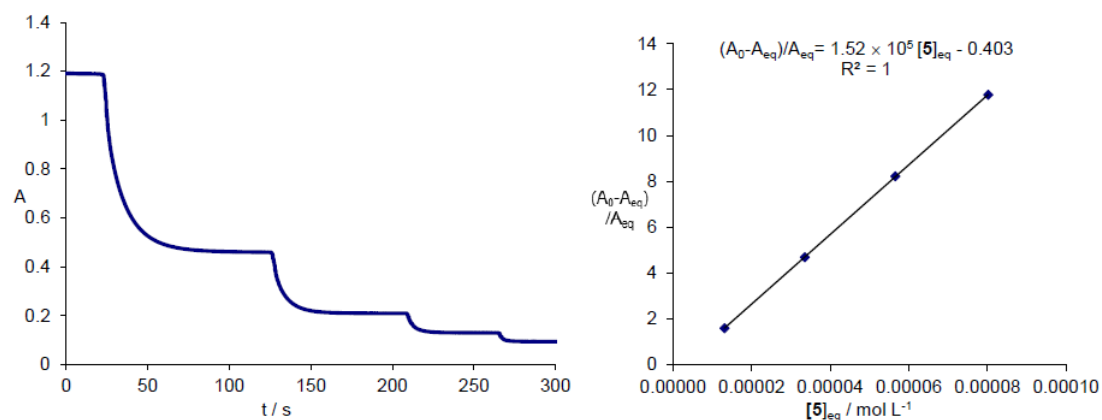
Step	V ( <b>5</b> ) / mL	V ( <b>5</b> ) <sub>total</sub> / mL	V <sub>total</sub> / mL	A <sub>eq</sub>	[ <b>E5</b> ]	A <sub>0</sub> -A <sub>eq</sub>	[ <b>5</b> ] <sub>0</sub>	[ <b>5</b> ] <sub>0</sub> / [ <b>E5</b> ] <sub>0</sub>	[ <b>5</b> ] <sub>eq</sub>	(A <sub>0</sub> -A <sub>eq</sub> )/A <sub>eq</sub>
0			22.56	1.196	$1.86 \times 10^{-5}$					
1	0.03	0.03	22.59	0.644	$1.00 \times 10^{-5}$	0.552	$1.53 \times 10^{-5}$	0.8	$6.74 \times 10^{-6}$	0.857
2	0.03	0.06	22.62	0.358	$5.56 \times 10^{-6}$	0.838	$3.06 \times 10^{-5}$	3.1	$1.76 \times 10^{-5}$	2.341
3	0.03	0.09	22.65	0.227	$3.53 \times 10^{-6}$	0.969	$4.58 \times 10^{-5}$	8.2	$3.08 \times 10^{-5}$	4.269
4	0.03	0.12	22.68	0.164	$2.55 \times 10^{-6}$	1.032	$6.10 \times 10^{-5}$	17.3	$4.50 \times 10^{-5}$	6.293
5	0.05	0.17	22.73	0.112	$1.74 \times 10^{-6}$	1.084	$8.63 \times 10^{-5}$	33.8	$6.94 \times 10^{-5}$	9.679



$$K = 1.41 \times 10^5 \text{ L mol}^{-1}$$

**Table S91.** Reaction of **5** with **E5** ( $\varepsilon = 1.287 \times 10^5 \text{ L mol}^{-1} \text{ cm}^{-1}$ ,  $\lambda = 616 \text{ nm}$ ) in MeCN at 20 °C.

Step	V ( <b>5</b> ) / mL	V ( <b>5</b> ) <sub>total</sub> / mL	V <sub>total</sub> / mL	A <sub>eq</sub>	[ <b>E5</b> ]	A <sub>0</sub> -A <sub>eq</sub>	[ <b>5</b> ] <sub>0</sub>	[ <b>5</b> ] <sub>0</sub> / [ <b>E5</b> ] <sub>0</sub>	[ <b>5</b> ] <sub>eq</sub>	(A <sub>0</sub> -A <sub>eq</sub> )/A <sub>eq</sub>
0			22.33	1.189	$1.85 \times 10^{-5}$					
1	0.04	0.04	22.37	0.459	$7.13 \times 10^{-6}$	0.730	$2.44 \times 10^{-5}$	1.3	$1.31 \times 10^{-5}$	1.590
2	0.04	0.08	22.41	0.209	$3.25 \times 10^{-6}$	0.980	$4.88 \times 10^{-5}$	6.8	$3.36 \times 10^{-5}$	4.689
3	0.04	0.12	22.45	0.129	$2.00 \times 10^{-6}$	1.060	$7.31 \times 10^{-5}$	22.5	$5.66 \times 10^{-5}$	8.217
4	0.04	0.16	22.49	0.093	$1.45 \times 10^{-6}$	1.096	$9.72 \times 10^{-5}$	48.5	$8.02 \times 10^{-5}$	11.785

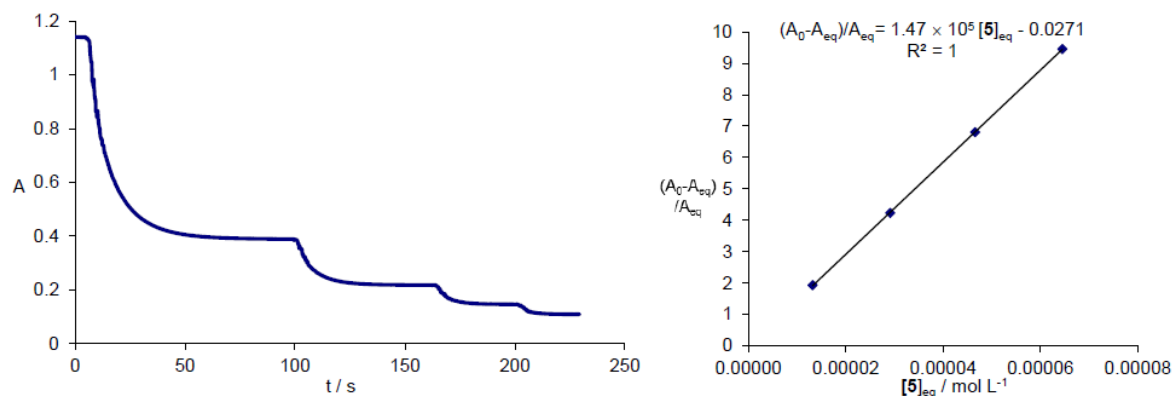


$$K = 1.52 \times 10^5 \text{ L mol}^{-1}$$



**Table S92.** Reaction of **5** with **E5** ( $\varepsilon = 1.287 \times 10^5 \text{ L mol}^{-1} \text{ cm}^{-1}$ ,  $\lambda = 616 \text{ nm}$ ) in MeCN at 20 °C.

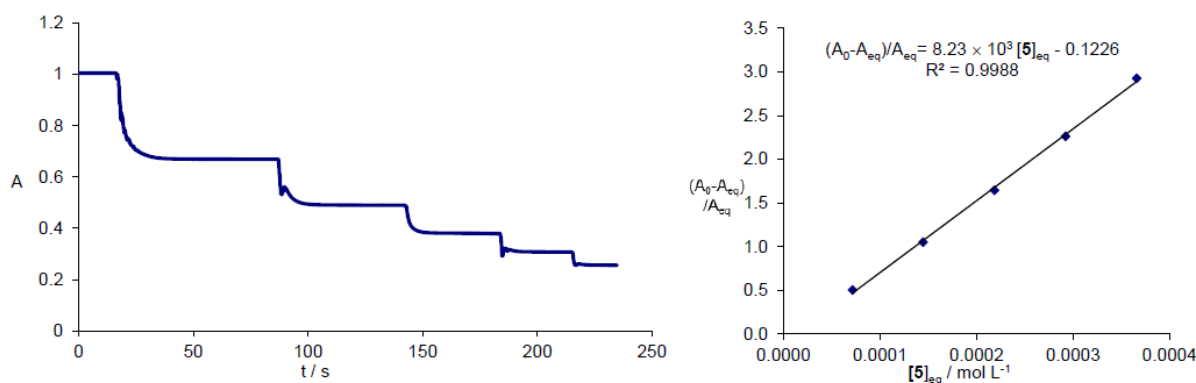
Step	V ( <b>5</b> ) / mL	V ( <b>5</b> ) <sub>total</sub> / mL	V <sub>total</sub> / mL	A <sub>eq</sub>	[ <b>E5</b> ]	A <sub>0</sub> -A <sub>eq</sub>	[ <b>5</b> ] <sub>0</sub>	[ <b>5</b> ] <sub>0</sub> / [ <b>E5</b> ] <sub>0</sub>	[ <b>5</b> ] <sub>eq</sub>	(A <sub>0</sub> -A <sub>eq</sub> )/A <sub>eq</sub>
0			22.98	1.140	$1.77 \times 10^{-5}$					
1	0.04	0.04	23.02	0.389	$6.05 \times 10^{-6}$	0.751	$2.49 \times 10^{-5}$	1.4	$1.32 \times 10^{-5}$	1.931
2	0.03	0.07	23.05	0.218	$3.39 \times 10^{-6}$	0.922	$4.35 \times 10^{-5}$	7.2	$2.91 \times 10^{-5}$	4.229
3	0.03	0.10	23.08	0.146	$2.27 \times 10^{-6}$	0.994	$6.20 \times 10^{-5}$	18.3	$4.66 \times 10^{-5}$	6.808
4	0.03	0.13	23.11	0.109	$1.69 \times 10^{-6}$	1.031	$8.05 \times 10^{-5}$	35.5	$6.45 \times 10^{-5}$	9.459



$$K = 1.47 \times 10^5 \text{ L mol}^{-1}$$

**Table S93.** Reaction of **5** with **E6** ( $\varepsilon = 1.727 \times 10^5 \text{ L mol}^{-1} \text{ cm}^{-1}$ ,  $\lambda = 635 \text{ nm}$ ) in MeCN at 20 °C.

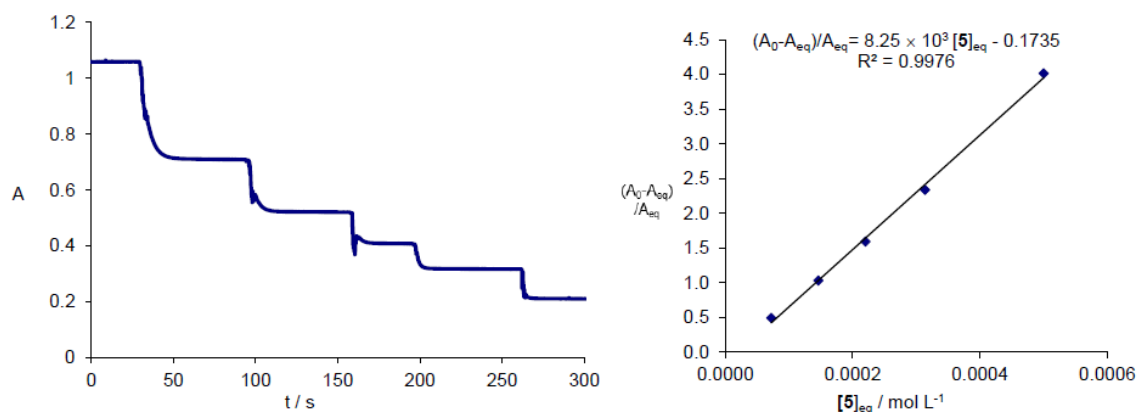
Step	V ( <b>5</b> ) / mL	V ( <b>5</b> ) <sub>total</sub> / mL	V <sub>total</sub> / mL	A <sub>eq</sub>	[ <b>E6</b> ]	A <sub>0</sub> -A <sub>eq</sub>	[ <b>5</b> ] <sub>0</sub>	[ <b>5</b> ] <sub>0</sub> / [ <b>E6</b> ] <sub>0</sub>	[ <b>5</b> ] <sub>eq</sub>	(A <sub>0</sub> -A <sub>eq</sub> )/A <sub>eq</sub>
0			23.82	1.005	$1.16 \times 10^{-5}$					
1	0.05	0.05	23.87	0.669	$7.75 \times 10^{-6}$	0.336	$7.56 \times 10^{-5}$	6.5	$7.17 \times 10^{-5}$	0.502
2	0.05	0.10	23.92	0.490	$5.67 \times 10^{-6}$	0.515	$1.51 \times 10^{-4}$	19.5	$1.45 \times 10^{-4}$	1.051
3	0.05	0.15	23.97	0.380	$4.40 \times 10^{-6}$	0.625	$2.26 \times 10^{-4}$	39.8	$2.19 \times 10^{-4}$	1.645
4	0.05	0.20	24.02	0.308	$3.57 \times 10^{-6}$	0.697	$3.00 \times 10^{-4}$	68.3	$2.92 \times 10^{-4}$	2.263
5	0.05	0.25	24.07	0.256	$2.96 \times 10^{-6}$	0.749	$3.75 \times 10^{-4}$	105	$3.66 \times 10^{-4}$	2.926



$$K = 8.23 \times 10^3 \text{ L mol}^{-1}$$

**Table S94.** Reaction of **5** with **E6** ( $\varepsilon = 1.727 \times 10^5 \text{ L mol}^{-1} \text{ cm}^{-1}$ ,  $\lambda = 635 \text{ nm}$ ) in MeCN at 20 °C.

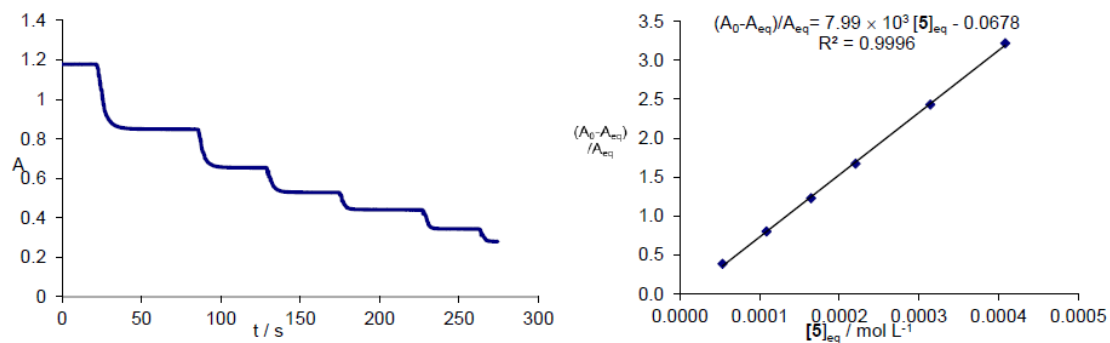
Step	V ( <b>5</b> ) / mL	V ( <b>5</b> ) <sub>total</sub> / mL	V <sub>total</sub> / mL	A <sub>eq</sub>	[ <b>E6</b> ]	A <sub>0</sub> -A <sub>eq</sub>	[ <b>5</b> ] <sub>0</sub>	[ <b>5</b> ] <sub>0</sub> / [ <b>E6</b> ] <sub>0</sub>	[ <b>5</b> ] <sub>eq</sub>	(A <sub>0</sub> -A <sub>eq</sub> )/A <sub>eq</sub>
0			22.51	1.058	$1.23 \times 10^{-5}$					
1	0.04	0.04	22.55	0.709	$8.21 \times 10^{-6}$	0.349	$7.63 \times 10^{-5}$	6.2	$7.23 \times 10^{-5}$	0.492
2	0.04	0.08	22.59	0.521	$6.03 \times 10^{-6}$	0.537	$1.52 \times 10^{-4}$	18.6	$1.46 \times 10^{-4}$	1.031
3	0.04	0.12	22.63	0.408	$4.72 \times 10^{-6}$	0.650	$2.28 \times 10^{-4}$	37.8	$2.21 \times 10^{-4}$	1.593
4	0.05	0.17	22.68	0.317	$3.67 \times 10^{-6}$	0.741	$3.23 \times 10^{-4}$	68.3	$3.14 \times 10^{-4}$	2.338
5	0.10	0.27	22.78	0.211	$2.44 \times 10^{-6}$	0.847	$5.10 \times 10^{-4}$	139	$5.00 \times 10^{-4}$	4.014



$$K = 8.25 \times 10^3 \text{ L mol}^{-1}$$

**Table S95.** Reaction of **5** with **E6** ( $\varepsilon = 1.727 \times 10^5 \text{ L mol}^{-1} \text{ cm}^{-1}$ ,  $\lambda = 635 \text{ nm}$ ) in MeCN at 20 °C.

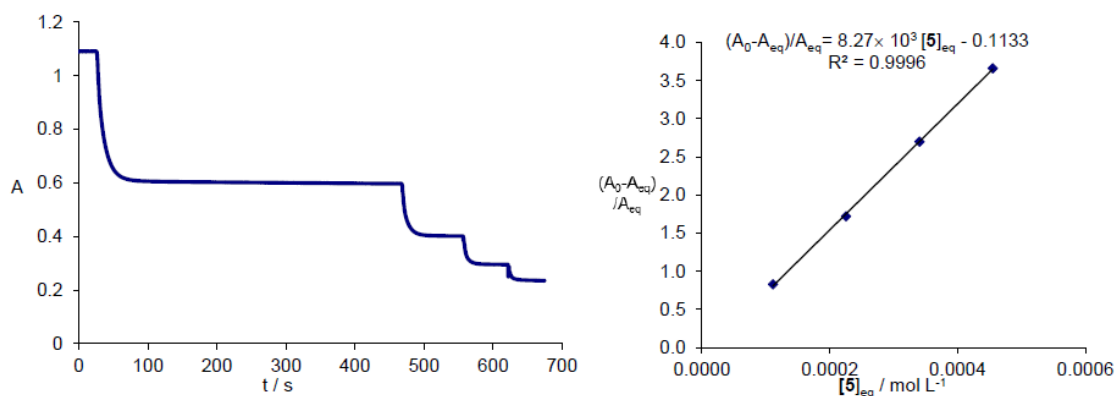
Step	V ( <b>5</b> ) / mL	V ( <b>5</b> ) <sub>total</sub> / mL	V <sub>total</sub> / mL	A <sub>eq</sub>	[ <b>E6</b> ]	A <sub>0</sub> -A <sub>eq</sub>	[ <b>5</b> ] <sub>0</sub>	[ <b>5</b> ] <sub>0</sub> / [ <b>E6</b> ] <sub>0</sub>	[ <b>5</b> ] <sub>eq</sub>	(A <sub>0</sub> -A <sub>eq</sub> )/A <sub>eq</sub>
0			24.24	1.177	$1.36 \times 10^{-5}$					
1	0.03	0.03	24.27	0.848	$9.82 \times 10^{-6}$	0.329	$5.75 \times 10^{-5}$	4.2	$5.37 \times 10^{-5}$	0.388
2	0.03	0.06	24.30	0.653	$7.56 \times 10^{-6}$	0.524	$1.15 \times 10^{-4}$	11.7	$1.09 \times 10^{-4}$	0.802
3	0.03	0.09	24.33	0.528	$6.11 \times 10^{-6}$	0.649	$1.72 \times 10^{-4}$	22.8	$1.65 \times 10^{-4}$	1.229
4	0.03	0.12	24.36	0.440	$5.10 \times 10^{-6}$	0.737	$2.29 \times 10^{-4}$	37.5	$2.21 \times 10^{-4}$	1.675
5	0.05	0.17	24.41	0.343	$3.97 \times 10^{-6}$	0.834	$3.24 \times 10^{-4}$	63.6	$3.15 \times 10^{-4}$	2.431
6	0.05	0.22	24.46	0.279	$3.23 \times 10^{-6}$	0.898	$4.19 \times 10^{-4}$	105	$4.08 \times 10^{-4}$	3.219



$$K = 7.99 \times 10^3 \text{ L mol}^{-1}$$

**Table S96.** Reaction of **5** with **E7** ( $\varepsilon = 1.318 \times 10^5 \text{ L mol}^{-1} \text{ cm}^{-1}$ ,  $\lambda = 631 \text{ nm}$ ) in MeCN at 20 °C.

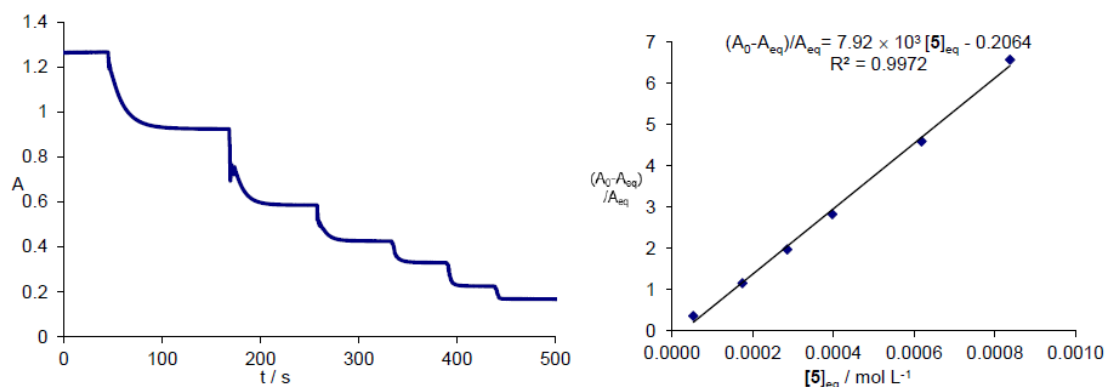
Step	V ( <b>5</b> ) / mL	V ( <b>5</b> ) <sub>total</sub> / mL	V <sub>total</sub> / mL	A <sub>eq</sub>	[ <b>E7</b> ]	A <sub>0</sub> -A <sub>eq</sub>	[ <b>5</b> ] <sub>0</sub>	[ <b>5</b> ] <sub>0</sub> / [ <b>E7</b> ] <sub>0</sub>	[ <b>5</b> ] <sub>eq</sub>	(A <sub>0</sub> -A <sub>eq</sub> )/A <sub>eq</sub>
0			22.41	1.091	$1.66 \times 10^{-5}$					
1	0.10	0.10	22.51	0.597	$9.06 \times 10^{-6}$	0.494	$1.19 \times 10^{-4}$	7.2	$1.11 \times 10^{-4}$	0.827
2	0.10	0.20	22.61	0.401	$6.08 \times 10^{-6}$	0.690	$2.36 \times 10^{-4}$	26.1	$2.26 \times 10^{-4}$	1.721
3	0.10	0.30	22.71	0.295	$4.48 \times 10^{-6}$	0.796	$3.53 \times 10^{-4}$	58.0	$3.41 \times 10^{-4}$	2.698
4	0.10	0.40	22.81	0.234	$3.55 \times 10^{-6}$	0.857	$4.68 \times 10^{-4}$	105	$4.55 \times 10^{-4}$	3.662



$$K = 8.27 \times 10^3 \text{ L mol}^{-1}$$

**Table S97.** Reaction of **5** with **E7** ( $\varepsilon = 1.318 \times 10^5 \text{ L mol}^{-1} \text{ cm}^{-1}$ ,  $\lambda = 631 \text{ nm}$ ) in MeCN at 20 °C.

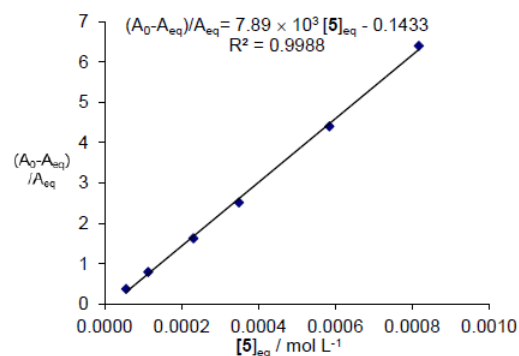
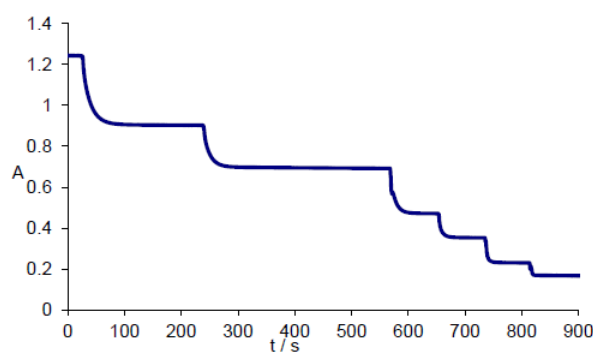
Step	V ( <b>5</b> ) / mL	V ( <b>5</b> ) <sub>total</sub> / mL	V <sub>total</sub> / mL	A <sub>eq</sub>	[ <b>E7</b> ]	A <sub>0</sub> -A <sub>eq</sub>	[ <b>5</b> ] <sub>0</sub>	[ <b>5</b> ] <sub>0</sub> / [ <b>E7</b> ] <sub>0</sub>	[ <b>5</b> ] <sub>eq</sub>	(A <sub>0</sub> -A <sub>eq</sub> )/A <sub>eq</sub>
0			23.66	1.265	$1.92 \times 10^{-5}$					
1	0.05	0.05	23.71	0.925	$1.40 \times 10^{-5}$	0.340	$5.79 \times 10^{-5}$	3.0	$5.27 \times 10^{-5}$	0.368
2	0.11	0.16	23.82	0.586	$8.89 \times 10^{-6}$	0.679	$1.84 \times 10^{-4}$	13.1	$1.74 \times 10^{-4}$	1.159
3	0.10	0.26	23.92	0.425	$6.45 \times 10^{-6}$	0.840	$2.98 \times 10^{-4}$	33.6	$2.86 \times 10^{-4}$	1.976
4	0.10	0.36	24.02	0.330	$5.01 \times 10^{-6}$	0.935	$4.11 \times 10^{-4}$	63.8	$3.97 \times 10^{-4}$	2.833
5	0.20	0.56	24.22	0.226	$3.43 \times 10^{-6}$	1.039	$6.35 \times 10^{-4}$	127	$6.19 \times 10^{-4}$	4.597
6	0.20	0.76	24.42	0.167	$2.53 \times 10^{-6}$	1.098	$8.54 \times 10^{-4}$	249	$8.38 \times 10^{-4}$	6.575



$$K = 7.92 \times 10^3 \text{ L mol}^{-1}$$

**Table S98.** Reaction of **5** with **E7** ( $\varepsilon = 1.318 \times 10^5 \text{ L mol}^{-1} \text{ cm}^{-1}$ ,  $\lambda = 631 \text{ nm}$ ) in MeCN at 20 °C.

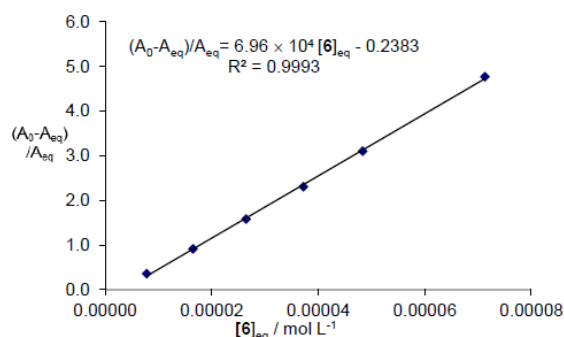
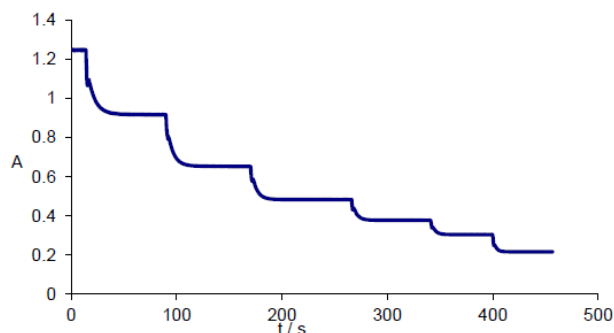
Step	V ( <b>5</b> ) / mL	V ( <b>5</b> ) <sub>total</sub> / mL	V <sub>total</sub> / mL	A <sub>eq</sub>	[ <b>E7</b> ]	A <sub>0</sub> -A <sub>eq</sub>	[ <b>5</b> ] <sub>0</sub>	[ <b>5</b> ] <sub>0</sub> / [ <b>E7</b> ] <sub>0</sub>	[ <b>5</b> ] <sub>eq</sub>	(A <sub>0</sub> -A <sub>eq</sub> )/A <sub>eq</sub>
0			23.96	1.243	$1.89 \times 10^{-5}$					
1	0.05	0.05	24.01	0.903	$1.37 \times 10^{-5}$	0.340	$6.12 \times 10^{-5}$	3.2	$5.60 \times 10^{-5}$	0.377
2	0.05	0.10	24.06	0.692	$1.05 \times 10^{-5}$	0.551	$1.22 \times 10^{-4}$	8.9	$1.14 \times 10^{-4}$	0.796
3	0.10	0.20	24.16	0.472	$7.16 \times 10^{-6}$	0.771	$2.43 \times 10^{-4}$	23.1	$2.31 \times 10^{-4}$	1.633
4	0.10	0.30	24.26	0.353	$5.36 \times 10^{-6}$	0.890	$3.63 \times 10^{-4}$	50.7	$3.50 \times 10^{-4}$	2.521
5	0.20	0.50	24.46	0.230	$3.49 \times 10^{-6}$	1.013	$6.00 \times 10^{-4}$	112	$5.85 \times 10^{-4}$	4.404
6	0.20	0.70	24.66	0.168	$2.55 \times 10^{-6}$	1.075	$8.34 \times 10^{-4}$	239	$8.17 \times 10^{-4}$	6.399



$$K = 7.89 \times 10^3 \text{ L mol}^{-1}$$

**Table S99.** Reaction of **6** with **E3** ( $\varepsilon = 1.464 \times 10^5 \text{ L mol}^{-1} \text{ cm}^{-1}$ ,  $\lambda = 605 \text{ nm}$ ) in MeCN at 20 °C.

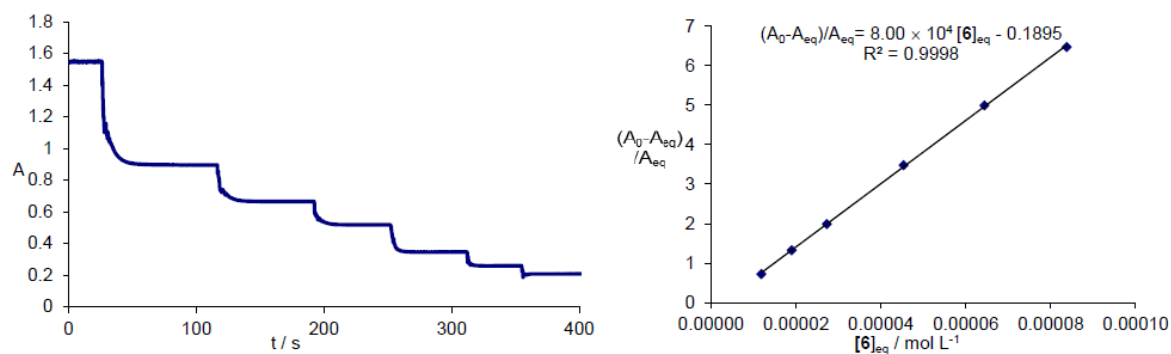
Step	V ( <b>6</b> ) / mL	V ( <b>6</b> ) <sub>total</sub> / mL	V <sub>total</sub> / mL	A <sub>eq</sub>	[ <b>E3</b> ]	A <sub>0</sub> -A <sub>eq</sub>	[ <b>6</b> ] <sub>0</sub>	[ <b>6</b> ] <sub>0</sub> / [ <b>E3</b> ] <sub>0</sub>	[ <b>6</b> ] <sub>eq</sub>	(A <sub>0</sub> -A <sub>eq</sub> )/A <sub>eq</sub>
0			21.75	1.247	$1.70 \times 10^{-5}$					
1	0.05	0.05	21.80	0.916	$1.25 \times 10^{-5}$	0.331	$1.24 \times 10^{-5}$	0.7	$7.84 \times 10^{-6}$	0.361
2	0.05	0.10	21.85	0.652	$8.91 \times 10^{-6}$	0.595	$2.47 \times 10^{-5}$	2.0	$1.65 \times 10^{-5}$	0.913
3	0.05	0.15	21.90	0.483	$6.60 \times 10^{-6}$	0.764	$3.69 \times 10^{-5}$	4.1	$2.65 \times 10^{-5}$	1.582
4	0.05	0.20	21.95	0.377	$5.15 \times 10^{-6}$	0.870	$4.91 \times 10^{-5}$	7.4	$3.72 \times 10^{-5}$	2.308
5	0.05	0.25	22.00	0.304	$4.15 \times 10^{-6}$	0.943	$6.13 \times 10^{-5}$	11.9	$4.84 \times 10^{-5}$	3.102
6	0.10	0.35	22.10	0.216	$2.95 \times 10^{-6}$	1.031	$8.54 \times 10^{-5}$	20.6	$7.13 \times 10^{-5}$	4.773



$$K = 6.96 \times 10^4 \text{ L mol}^{-1}$$

**Table S100.** Reaction of **6** with **E3** ( $\varepsilon = 1.464 \times 10^5 \text{ L mol}^{-1} \text{ cm}^{-1}$ ,  $\lambda = 605 \text{ nm}$ ) in MeCN at 20 °C.

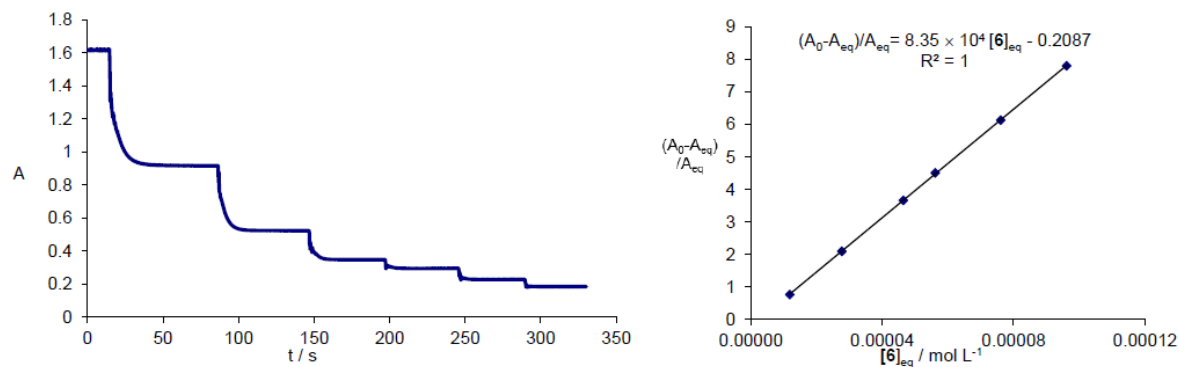
Step	V ( <b>6</b> ) / mL	V ( <b>6</b> ) <sub>total</sub> / mL	V <sub>total</sub> / mL	A <sub>eq</sub>	[ <b>E3</b> ]	A <sub>0</sub> -A <sub>eq</sub>	[ <b>6</b> ] <sub>0</sub>	[ <b>6</b> ] <sub>0</sub> / [ <b>E3</b> ] <sub>0</sub>	[ <b>6</b> ] <sub>eq</sub>	(A <sub>0</sub> -A <sub>eq</sub> )/A <sub>eq</sub>
0			24.88	1.546	$2.11 \times 10^{-5}$					
1	0.10	0.10	24.98	0.895	$1.22 \times 10^{-5}$	0.651	$2.07 \times 10^{-5}$	1.0	$1.18 \times 10^{-5}$	0.727
2	0.05	0.15	25.03	0.664	$9.07 \times 10^{-6}$	0.882	$3.10 \times 10^{-5}$	2.5	$1.90 \times 10^{-5}$	1.328
3	0.05	0.20	25.08	0.517	$7.06 \times 10^{-6}$	1.029	$4.13 \times 10^{-5}$	4.6	$2.72 \times 10^{-5}$	1.990
4	0.10	0.30	25.18	0.345	$4.71 \times 10^{-6}$	1.201	$6.17 \times 10^{-5}$	8.7	$4.53 \times 10^{-5}$	3.481
5	0.10	0.40	25.28	0.258	$3.52 \times 10^{-6}$	1.288	$8.19 \times 10^{-5}$	17.4	$6.44 \times 10^{-5}$	4.992
6	0.10	0.50	25.38	0.207	$2.83 \times 10^{-6}$	1.339	$1.02 \times 10^{-4}$	28.9	$8.37 \times 10^{-5}$	6.469



$$K = 8.00 \times 10^4 \text{ L mol}^{-1}$$

**Table S101.** Reaction of **6** with **E3** ( $\varepsilon = 1.464 \times 10^5 \text{ L mol}^{-1} \text{ cm}^{-1}$ ,  $\lambda = 605 \text{ nm}$ ) in MeCN at 20 °C.

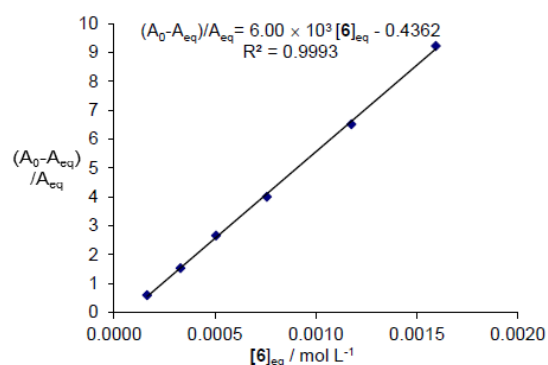
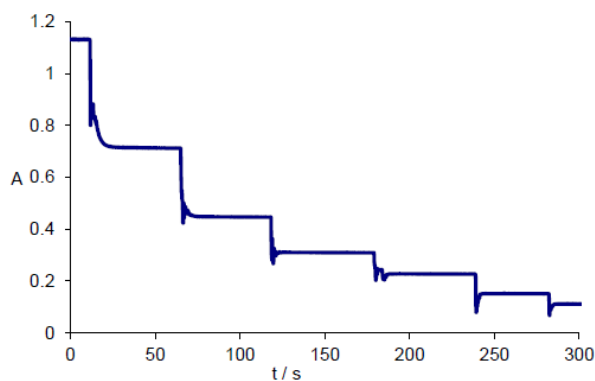
Step	V ( <b>6</b> ) / mL	V ( <b>6</b> ) <sub>total</sub> / mL	V <sub>total</sub> / mL	A <sub>eq</sub>	[ <b>E3</b> ]	A <sub>0</sub> -A <sub>eq</sub>	[ <b>6</b> ] <sub>0</sub>	[ <b>6</b> ] <sub>0</sub> / [ <b>E3</b> ] <sub>0</sub>	[ <b>6</b> ] <sub>eq</sub>	(A <sub>0</sub> -A <sub>eq</sub> )/A <sub>eq</sub>
0			24.05	1.620	$2.21 \times 10^{-5}$					
1	0.10	0.10	24.15	0.916	$1.25 \times 10^{-5}$	0.704	$2.14 \times 10^{-5}$	1.0	$1.18 \times 10^{-5}$	0.769
2	0.10	0.20	24.25	0.523	$7.14 \times 10^{-6}$	1.097	$4.27 \times 10^{-5}$	3.4	$2.77 \times 10^{-5}$	2.098
3	0.10	0.30	24.35	0.347	$4.74 \times 10^{-6}$	1.273	$6.38 \times 10^{-5}$	8.9	$4.64 \times 10^{-5}$	3.669
4	0.05	0.35	24.40	0.294	$4.02 \times 10^{-6}$	1.326	$7.43 \times 10^{-5}$	15.7	$5.62 \times 10^{-5}$	4.510
5	0.10	0.45	24.50	0.227	$3.10 \times 10^{-6}$	1.393	$9.51 \times 10^{-5}$	23.7	$7.61 \times 10^{-5}$	6.137
6	0.10	0.55	24.60	0.184	$2.51 \times 10^{-6}$	1.436	$1.16 \times 10^{-4}$	37.3	$9.62 \times 10^{-5}$	7.804



$$K = 8.35 \times 10^4 \text{ L mol}^{-1}$$

**Table S102.** Reaction of **6** with **E4** ( $\varepsilon = 1.390 \times 10^5 \text{ L mol}^{-1} \text{ cm}^{-1}$ ,  $\lambda = 611 \text{ nm}$ ) in MeCN at 20 °C.

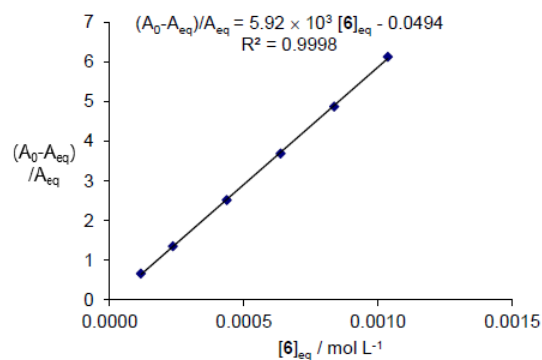
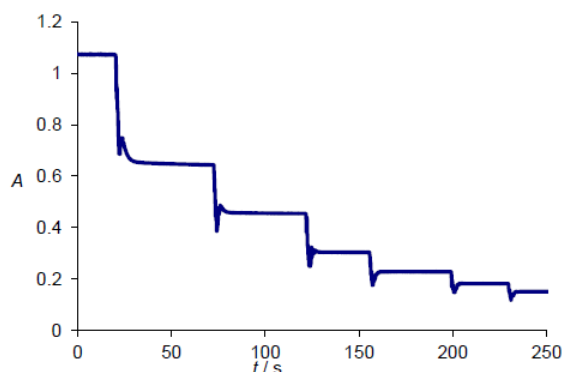
Step	V ( <b>6</b> ) / mL	V ( <b>6</b> ) <sub>total</sub> / mL	V <sub>total</sub> / mL	A <sub>eq</sub>	[ <b>E4</b> ]	A <sub>0</sub> -A <sub>eq</sub>	[ <b>6</b> ] <sub>0</sub>	[ <b>6</b> ] <sub>0</sub> / [ <b>E4</b> ] <sub>0</sub>	[ <b>6</b> ] <sub>eq</sub>	(A <sub>0</sub> -A <sub>eq</sub> )/A <sub>eq</sub>
0			20.57	1.135	$1.63 \times 10^{-5}$					
1	0.02	0.02	20.59	0.713	$1.03 \times 10^{-5}$	0.422	$1.70 \times 10^{-4}$	10.4	$1.64 \times 10^{-4}$	0.592
2	0.02	0.04	20.61	0.448	$6.45 \times 10^{-6}$	0.687	$3.39 \times 10^{-4}$	33.1	$3.30 \times 10^{-4}$	1.533
3	0.02	0.06	20.63	0.310	$4.46 \times 10^{-6}$	0.825	$5.17 \times 10^{-4}$	80.2	$5.05 \times 10^{-4}$	2.661
4	0.03	0.09	20.66	0.227	$3.27 \times 10^{-6}$	0.908	$7.70 \times 10^{-4}$	173	$7.57 \times 10^{-4}$	4.000
5	0.05	0.14	20.71	0.151	$2.17 \times 10^{-6}$	0.984	$1.19 \times 10^{-3}$	365	$1.18 \times 10^{-3}$	6.517
6	0.05	0.19	20.76	0.111	$1.60 \times 10^{-6}$	1.024	$1.61 \times 10^{-3}$	741	$1.59 \times 10^{-3}$	9.225



$$K = 6.00 \times 10^3 \text{ L mol}^{-1}$$

**Table S103.** Reaction of **6** with **E4** ( $\varepsilon = 1.390 \times 10^5 \text{ L mol}^{-1} \text{ cm}^{-1}$ ,  $\lambda = 611 \text{ nm}$ ) in MeCN at 20 °C.

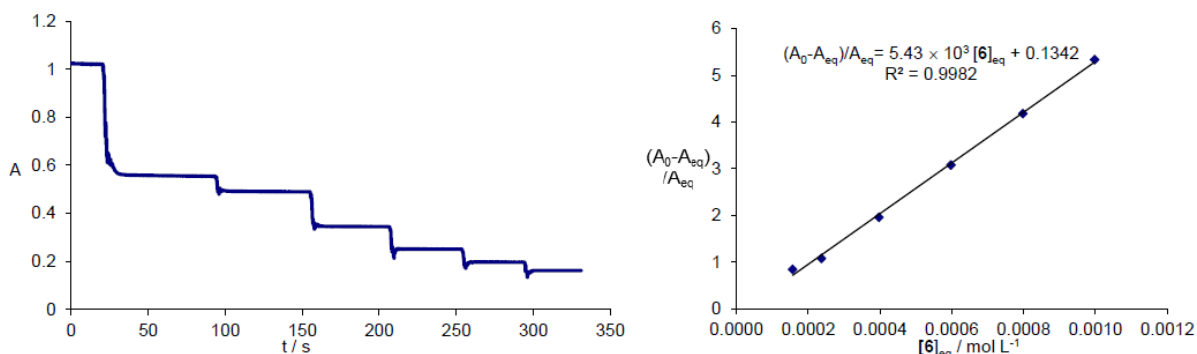
Step	V ( <b>6</b> ) / mL	V ( <b>6</b> ) <sub>total</sub> / mL	V <sub>total</sub> / mL	A <sub>eq</sub>	[ <b>E4</b> ]	A <sub>0</sub> -A <sub>eq</sub>	[ <b>6</b> ] <sub>0</sub>	[ <b>6</b> ] <sub>0</sub> / [ <b>E4</b> ] <sub>0</sub>	[ <b>6</b> ] <sub>eq</sub>	(A <sub>0</sub> -A <sub>eq</sub> )/A <sub>eq</sub>
0			22.90	1.070	$1.54 \times 10^{-5}$					
1	0.03	0.03	22.93	0.644	$9.27 \times 10^{-6}$	0.426	$1.22 \times 10^{-4}$	7.9	$1.16 \times 10^{-4}$	0.661
2	0.03	0.06	22.96	0.455	$6.55 \times 10^{-6}$	0.615	$2.44 \times 10^{-4}$	26.4	$2.36 \times 10^{-4}$	1.352
3	0.05	0.11	23.01	0.304	$4.37 \times 10^{-6}$	0.766	$4.47 \times 10^{-4}$	68.3	$4.36 \times 10^{-4}$	2.520
4	0.05	0.16	23.06	0.228	$3.28 \times 10^{-6}$	0.842	$6.49 \times 10^{-4}$	148	$6.37 \times 10^{-4}$	3.693
5	0.05	0.21	23.11	0.182	$2.62 \times 10^{-6}$	0.888	$8.50 \times 10^{-4}$	259	$8.37 \times 10^{-4}$	4.879
6	0.05	0.26	23.16	0.150	$2.16 \times 10^{-6}$	0.920	$1.05 \times 10^{-3}$	401	$1.04 \times 10^{-3}$	6.133



$$K = 5.92 \times 10^3 \text{ L mol}^{-1}$$

**Table S104.** Reaction of **6** with **E4** ( $\varepsilon = 1.390 \times 10^5 \text{ L mol}^{-1} \text{ cm}^{-1}$ ,  $\lambda = 611 \text{ nm}$ ) in MeCN at 20 °C.

Step	V ( <b>6</b> ) / mL	V ( <b>6</b> ) <sub>total</sub> / mL	V <sub>total</sub> / mL	A <sub>eq</sub>	[ <b>E4</b> ]	A <sub>0</sub> -A <sub>eq</sub>	[ <b>6</b> ] <sub>0</sub>	[ <b>6</b> ] <sub>0</sub> / [ <b>E4</b> ] <sub>0</sub>	[ <b>6</b> ] <sub>eq</sub>	(A <sub>0</sub> -A <sub>eq</sub> )/A <sub>eq</sub>
0			22.90	1.020	$1.47 \times 10^{-5}$					
1	0.04	0.04	22.94	0.554	$7.97 \times 10^{-6}$	0.466	$1.63 \times 10^{-4}$	11.1	$1.56 \times 10^{-4}$	0.841
2	0.02	0.06	22.96	0.490	$7.05 \times 10^{-6}$	0.530	$2.44 \times 10^{-4}$	30.7	$2.37 \times 10^{-4}$	1.082
3	0.04	0.10	23.00	0.345	$4.96 \times 10^{-6}$	0.675	$4.07 \times 10^{-4}$	57.7	$3.97 \times 10^{-4}$	1.957
4	0.05	0.15	23.05	0.250	$3.60 \times 10^{-6}$	0.770	$6.09 \times 10^{-4}$	123	$5.98 \times 10^{-4}$	3.080
5	0.05	0.20	23.10	0.197	$2.83 \times 10^{-6}$	0.823	$8.10 \times 10^{-4}$	225	$7.98 \times 10^{-4}$	4.178
6	0.05	0.25	23.15	0.161	$2.32 \times 10^{-6}$	0.859	$1.01 \times 10^{-3}$	356	$9.98 \times 10^{-4}$	5.335



$$K = 5.43 \times 10^3 \text{ L mol}^{-1}$$

**Table S105.** Reaction of **7** with **E6** ( $\varepsilon = 1.727 \times 10^5 \text{ L mol}^{-1} \text{ cm}^{-1}$ ,  $\lambda = 635 \text{ nm}$ ) in MeCN at 20 °C.

Step	V ( <b>7</b> ) / mL	V ( <b>7</b> ) <sub>total</sub> / mL	V <sub>total</sub> / mL	A <sub>eq</sub>	[ <b>E6</b> ]	A <sub>0</sub> -A <sub>eq</sub>	[ <b>7</b> ] <sub>0</sub>	[ <b>7</b> ] <sub>0</sub> / [ <b>E6</b> ] <sub>0</sub>	[ <b>7</b> ] <sub>eq</sub>	(A <sub>0</sub> -A <sub>eq</sub> )/A <sub>eq</sub>
0			23.60	1.056	$1.22 \times 10^{-5}$					
1	0.03	0.03	23.63	0.306	$3.54 \times 10^{-6}$	0.750	$1.77 \times 10^{-5}$	1.4	$9.02 \times 10^{-6}$	2.451

$$K = 2.72 \times 10^5 \text{ L mol}^{-1}$$

Step	V ( <b>7</b> ) / mL	V ( <b>7</b> ) <sub>total</sub> / mL	V <sub>total</sub> / mL	A <sub>eq</sub>	[ <b>E6</b> ]	A <sub>0</sub> -A <sub>eq</sub>	[ <b>7</b> ] <sub>0</sub>	[ <b>7</b> ] <sub>0</sub> / [ <b>E6</b> ] <sub>0</sub>	[ <b>7</b> ] <sub>eq</sub>	(A <sub>0</sub> -A <sub>eq</sub> )/A <sub>eq</sub>
0			22.52	1.015	$1.18 \times 10^{-5}$					
1	0.02	0.02	22.54	0.215	$2.49 \times 10^{-6}$	0.800	$1.98 \times 10^{-5}$	1.7	$1.05 \times 10^{-5}$	3.721

$$K = 3.54 \times 10^5 \text{ L mol}^{-1}$$

Approximate  $K$  values, because the determination of such high equilibrium constants is less reliable and the endabsorption is not stable.

**Table S106.** Reaction of **8** with **E6** ( $\varepsilon = 1.727 \times 10^5 \text{ L mol}^{-1} \text{ cm}^{-1}$ ,  $\lambda = 635 \text{ nm}$ ) in MeCN at 20 °C.

Step	V ( <b>8</b> ) / mL	V ( <b>8</b> ) <sub>total</sub> / mL	V <sub>total</sub> / mL	A <sub>eq</sub>	[ <b>E6</b> ]	A <sub>0</sub> -A <sub>eq</sub>	[ <b>8</b> ] <sub>0</sub>	[ <b>8</b> ] <sub>0</sub> / [ <b>E6</b> ] <sub>0</sub>	[ <b>8</b> ] <sub>eq</sub>	(A <sub>0</sub> -A <sub>eq</sub> )/A <sub>eq</sub>
0			21.54	0.968	$1.12 \times 10^{-5}$					
1	0.03	0.03	21.57	0.100	$1.16 \times 10^{-6}$	0.868	$1.96 \times 10^{-5}$	1.7	$9.55 \times 10^{-6}$	8.680

$$K = 9.09 \times 10^5 \text{ L mol}^{-1}$$

Step	V ( <b>8</b> ) / mL	V ( <b>8</b> ) <sub>total</sub> / mL	V <sub>total</sub> / mL	A <sub>eq</sub>	[ <b>E6</b> ]	A <sub>0</sub> -A <sub>eq</sub>	[ <b>8</b> ] <sub>0</sub>	[ <b>8</b> ] <sub>0</sub> / [ <b>E6</b> ] <sub>0</sub>	[ <b>8</b> ] <sub>eq</sub>	(A <sub>0</sub> -A <sub>eq</sub> )/A <sub>eq</sub>
0			22.88	1.110	$1.29 \times 10^{-5}$					
1	0.02	0.02	22.90	0.157	$1.82 \times 10^{-6}$	0.953	$1.62 \times 10^{-5}$	1.3	$5.19 \times 10^{-6}$	6.070

$$K = 1.17 \times 10^6 \text{ L mol}^{-1}$$

Step	V ( <b>8</b> ) / mL	V ( <b>8</b> ) <sub>total</sub> / mL	V <sub>total</sub> / mL	A <sub>eq</sub>	[ <b>E6</b> ]	A <sub>0</sub> -A <sub>eq</sub>	[ <b>8</b> ] <sub>0</sub>	[ <b>8</b> ] <sub>0</sub> / [ <b>E6</b> ] <sub>0</sub>	[ <b>8</b> ] <sub>eq</sub>	(A <sub>0</sub> -A <sub>eq</sub> )/A <sub>eq</sub>
0			23.03	1.360	$1.57 \times 10^{-5}$					
1	0.03	0.03	23.06	0.107	$1.24 \times 10^{-6}$	1.253	$2.36 \times 10^{-5}$	1.5	$9.10 \times 10^{-6}$	11.710

$$K = 1.29 \times 10^6 \text{ L mol}^{-1}$$

Approximate  $K$  values, because the determination of such high equilibrium constants is less reliable and the endabsorption is not stable.

**Table S107.** Averaged Equilibrium Constants  $K$  for the reactions of benzhydrylium ions **E** with enamines **1–8**.

Enamine	Electrophile	$K / \text{L mol}^{-1}$	Averaged $K / \text{L mol}^{-1}$
<b>1-H</b>	<b>E5</b>	$9.78 \times 10^4$	$(1.11 \pm 0.19) \times 10^5$
		$1.24 \times 10^5$	
	<b>E6</b>	$6.16 \times 10^3$	$(6.45 \pm 0.35) \times 10^3$
		$6.34 \times 10^3$	
		$6.84 \times 10^3$	
	<b>E7</b>	$6.50 \times 10^3$	$(6.55 \pm 0.08) \times 10^3$
		$6.50 \times 10^3$	
		$6.64 \times 10^3$	
<b>1-OMe</b>	<b>E5</b>	$3.34 \times 10^5$	$(3.45 \pm 0.15) \times 10^5$
		$3.55 \times 10^5$	
	<b>E6</b>	$1.34 \times 10^4$	$(1.36 \pm 0.08) \times 10^4$
		$1.28 \times 10^4$	
		$1.45 \times 10^4$	
	<b>E7</b>	$1.32 \times 10^4$	$(1.31 \pm 0.03) \times 10^4$
		$1.28 \times 10^4$	
		$1.33 \times 10^4$	
<b>1-CN</b>	<b>E4</b>	$4.53 \times 10^3$	$(4.82 \pm 0.25) \times 10^3$
		$4.95 \times 10^3$	
		$4.98 \times 10^3$	
	<b>E5</b>	$1.03 \times 10^3$	$(1.12 \pm 0.08) \times 10^3$
		$1.17 \times 10^3$	
		$1.16 \times 10^3$	
<b>1-NO<sub>2</sub></b>	<b>E3</b>	$1.89 \times 10^4$	$(1.93 \pm 0.03) \times 10^4$
		$1.95 \times 10^4$	
		$1.94 \times 10^4$	
	<b>E4</b>	$1.73 \times 10^3$	$(1.62 \pm 0.14) \times 10^3$
		$1.68 \times 10^3$	
		$1.46 \times 10^3$	
<b>2</b>	<b>E4</b>	$2.94 \times 10^4$	$(2.76 \pm 0.71) \times 10^4$
		$3.36 \times 10^4$	
		$1.98 \times 10^4$	
	<b>E5</b>	$9.66 \times 10^3$	$(9.64 \pm 0.03) \times 10^3$
		$9.62 \times 10^3$	
<b>3</b>	<b>E3</b>	$5.18 \times 10^3$	$(6.00 \pm 0.91) \times 10^3$
		$5.85 \times 10^3$	
		$6.98 \times 10^3$	
	<b>E4</b>	$3.66 \times 10^2$	$(3.59 \pm 0.06) \times 10^2$
		$3.54 \times 10^2$	
		$3.57 \times 10^2$	

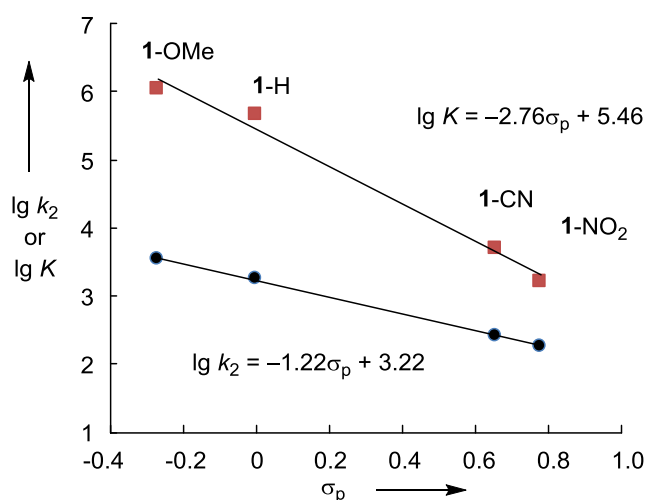


**Table S107.** (continued)

Enamine	Electrophile	$K / \text{L mol}^{-1}$	Averaged $K / \text{L mol}^{-1}$
<b>4</b>	<b>E5</b>	$1.21 \times 10^5$	<b><math>(1.15 \pm 0.05) \times 10^5</math></b>
		$1.11 \times 10^5$	
		$1.13 \times 10^5$	
	<b>E6</b>	$5.23 \times 10^3$	<b><math>(5.09 \pm 0.12) \times 10^3</math></b>
		$5.00 \times 10^3$	
		$5.05 \times 10^3$	
	<b>E7</b>	$4.71 \times 10^3$	<b><math>(4.81 \pm 0.10) \times 10^3</math></b>
		$4.91 \times 10^3$	
		$4.81 \times 10^3$	
<b>5</b>	<b>E5</b>	$1.41 \times 10^5$	<b><math>(1.47 \pm 0.06) \times 10^5</math></b>
		$1.52 \times 10^5$	
		$1.47 \times 10^5$	
	<b>E6</b>	$8.23 \times 10^3$	<b><math>(8.16 \pm 0.14) \times 10^3</math></b>
		$8.25 \times 10^3$	
		$7.99 \times 10^3$	
	<b>E7</b>	$8.27 \times 10^3$	<b><math>(8.03 \pm 0.21) \times 10^3</math></b>
		$7.92 \times 10^3$	
		$7.89 \times 10^3$	
<b>6</b>	<b>E3</b>	$6.96 \times 10^4$	<b><math>(7.77 \pm 0.72) \times 10^4</math></b>
		$8.00 \times 10^4$	
		$8.35 \times 10^4$	
	<b>E4</b>	$6.00 \times 10^3$	<b><math>(5.78 \pm 0.31) \times 10^3</math></b>
		$5.43 \times 10^3$	
		$5.92 \times 10^3$	
<b>7</b>	<b>E6</b>	$2.7 \times 10^5$	<b><math>(3.1 \pm 0.58) \times 10^5</math> [a]</b>
		$3.5 \times 10^5$	
<b>8</b>	<b>E6</b>	$9.1 \times 10^5$	<b><math>(1.1 \pm 0.08) \times 10^6</math> [a]</b>
		$1.2 \times 10^6$	
		$1.3 \times 10^6$	

[a] Approximate values, because the determination of such high equilibrium constants is less reliable. Weaker Lewis acids, as **E7** cannot be used either, because they react so slowly.

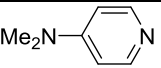
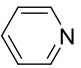
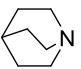
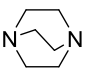
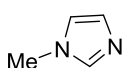
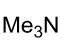
## 2.5.8. Hammett Plot



**Figure S2.** Correlation of the rate and equilibrium constants of the reactions of **1-X** with the benzhydrylium ion **E4** vs Hammett's  $\sigma_p$  values for substituents X (MeCN, 20 °C).<sup>26</sup>

## 2.5.9. Intrinsic Barriers

**Table S108.** The determination of the intrinsic barriers for the reactions of the benzhydrylium ion **E5** with *tert.* amines, pyridines and imidazoles in MeCN (20 °C).

	<i>LB</i> <sup>[a]</sup>	<i>K</i> (L mol <sup>-1</sup> )	<i>N</i> ( <i>s<sub>N</sub></i> )	<i>k<sub>2</sub></i> (L mol <sup>-1</sup> s <sup>-1</sup> )	$\Delta G^\circ$ (kJ mol <sup>-1</sup> )	$\Delta G^\ddagger$ (kJ mol <sup>-1</sup> )	$\Delta G_0^\ddagger$ (kJ mol <sup>-1</sup> )
	17.13	$5.60 \times 10^{5[a]}$	15.51 <sup>[b]</sup> (0.62)	$1.29 \times 10^{4[b]}$	-32.3	48.7	63.8 <sup>[b]</sup>
	11.82	2.78 <sup>[a]</sup>	13.60 <sup>[c]</sup> (0.60)	$8.02 \times 10^{2[d]}$	-2.5	55.5	56.7
	15.48	$1.05 \times 10^{4[e]}$	20.54 <sup>[b]</sup> (0.60)	$1.08 \times 10^{7[b]}$	-22.6	32.3	42.8 <sup>[b]</sup>
	14.49	$1.07 \times 10^{3[e]}$	18.80 <sup>[b]</sup> (0.70)	$1.10 \times 10^{7[b]}$	-17.0	32.2	40.3 <sup>[b]</sup>
	15.14	$5.56 \times 10^{3[f]}$	11.90 <sup>[f]</sup> (0.73)	$1.88 \times 10^{2[f]}$	-21.0	59.0	69.1 <sup>[f]</sup>
	12.92	$2.88 \times 10^{1[e]}$	23.05 <sup>[g]</sup> (0.45)	$2.69 \times 10^{6[d]}$	-8.2	35.7	39.7

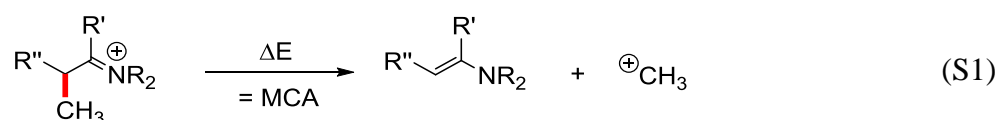
[a] From ref. 11a [b] From ref. 12a [c] From ref. 19g [d] Calcd. from *N* and *s<sub>N</sub>* parameters [e] Calcd. from *LB* parameter [f] From ref. 12b [g] From ref. 28

## 2.5.10. Quantum Chemical Calculations

### Method

Quantum chemical calculations were performed with the Gaussian 09 program package.<sup>21</sup> Generally, geometries of reactants and products were optimized in gas-phase applying the B3LYP/6-31(d,p) method.<sup>20</sup> Thermal corrections at the B3LYP/6-31(d,p) level were subsequently combined with single point energies obtained with the B3LYP/6-311++(3df,2pd) method to give  $\Delta G_{298}$  (abbreviated by B3LYP/6-311++G(3df,2pd) // B3LYP/6-31G(d,p)). The single point calculations were either performed in gas phase or with the SMD continuum solvation model for acetonitrile.<sup>23</sup> Optimization of reactants and products with the solvent model did not show an improvement in the correlation of calculated methyl and benzhydryl cation affinities with the experimental Lewis basicities. For all calculations, conformers were generated using the TINKER package with the MM3 force field.<sup>41</sup> Conformers of the reactants (enamines) were Boltzmann weighted. In case of the methyl and benzhydryl cation adducts, consideration of multiple conformers and Boltzmann weighting caused only a minor change of  $\approx 1$  kJ/mol to the MCA/BHCA values and was therefore neglected. Thus, only the global minimum conformer of the iminium ions was considered for the calculation of the reaction energies.

### Methyl Cation Affinities (MCA)



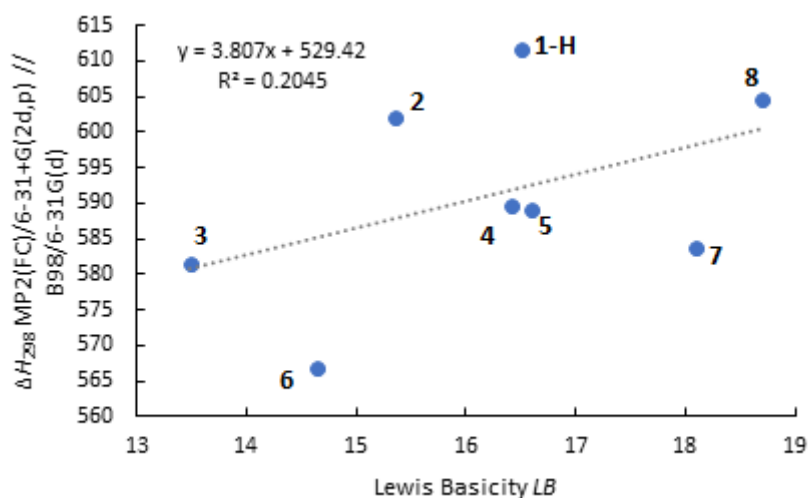
The correlation of gas phase methyl cation affinities (MCAs) of nucleophiles with their Lewis basicities has been shown previously.<sup>19</sup> Following this original procedure, the gas phase methyl cation affinities (MCAs) of the enamines **1–8** were calculated as reaction enthalpies  $\Delta H_{298}$  of methyl cation detachment reactions applying the MP2(FC)/6-31+G(2d,p)//B98/6-31+G(d) method. However, practically no correlation was observed in the plot of MCAs versus Lewis basicity (Figure S3). This could be overcome by applying a DFT based method which allowed the economic use of a large basis set (6-311++(3df,2pd)) for the calculation of single-point energies.<sup>1</sup> The plot depicted in Figure S4 shows that the gas phase MCAs (B3LYP/6-311++G(3df,2pd) // B3LYP/6-31G(d,p)) of enamines **1–3** are elevated in comparison to **4–6**. If solvation is included by a single point calculation, enamines **1–8** are on

<sup>1</sup> This method had shown to be reliable for the calculation of related methyl anion affinities of acceptor-substituted olefins. See ref. 42 for details.

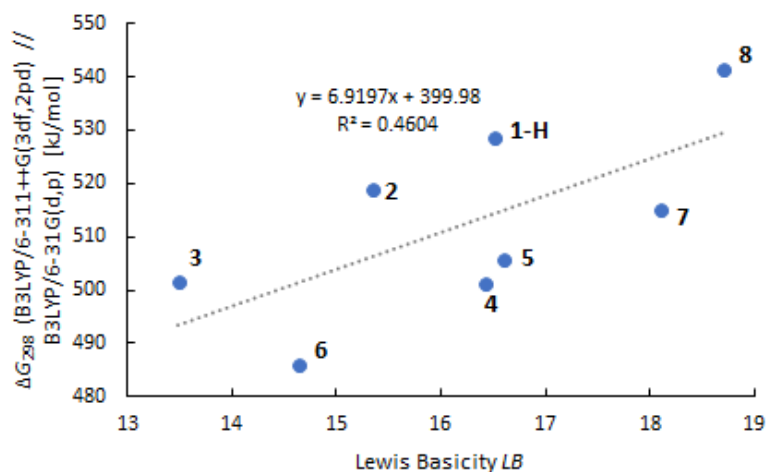
the same correlation line with reduced scattering (Figure S5). The inclusion of the solvent model especially influences enamines **1–3** as shown in Figure S6.

**Table S109:** Lewis basicity *LB* and methyl cation affinities (MCA) for enamines **1–8** with different methods.

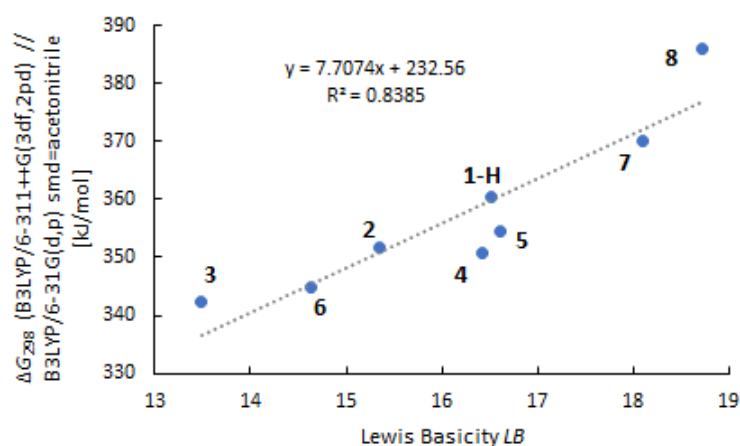
System	Lewis Basicity <i>LB</i>	$\Delta H_{298}$ MP2(FC)/6- 31+G(2d,p)//B98/6- 31+G(d)	$\Delta E_{\text{tot}}$ B3LYP/6- 31G(d,p)	$\Delta G_{298}$ B3LYP/6- 31G(d,p)	$\Delta E_{\text{tot}}$ B3LYP/6- 311++G(3df,2pd)// B3LYP/6- 31G(d,p)	$\Delta G_{298}$ B3LYP/6- 311++G(3df,2pd)// B3LYP/6- 31G(d,p)	$\Delta E_{\text{tot}}$ B3LYP/6- 311++G(3df,2pd)// B3LYP/6- 31G(d,p)	$\Delta G_{298}$ B3LYP/6- 311++G(3df,2pd)// B3LYP/6- 31G(d,p)
							smd=acetonitrile	smd=acetonitrile
<b>1-H</b>	16.50	611.7	625.3	551.9	601.8	528.5	434.0	360.5
<b>2</b>	15.35	602.2	613.1	543.4	588.5	518.8	421.5	351.7
<b>3</b>	13.49	581.5	595.9	527.0	570.5	501.5	411.4	342.5
<b>4</b>	16.43	589.8	596.0	524.6	572.6	501.2	422.0	350.6
<b>5</b>	16.60	589.2	598.1	528.7	575.1	505.7	424.1	354.7
<b>6</b>	14.65	567.0	578.6	509.5	555.0	485.9	413.9	344.8
<b>7</b>	$\approx 18.1$	583.7	611.4	541.3	585.3	515.2	440.2	370.2
<b>8</b>	$\approx 18.7$	604.5	636.0	565.7	611.8	541.4	456.4	386.1



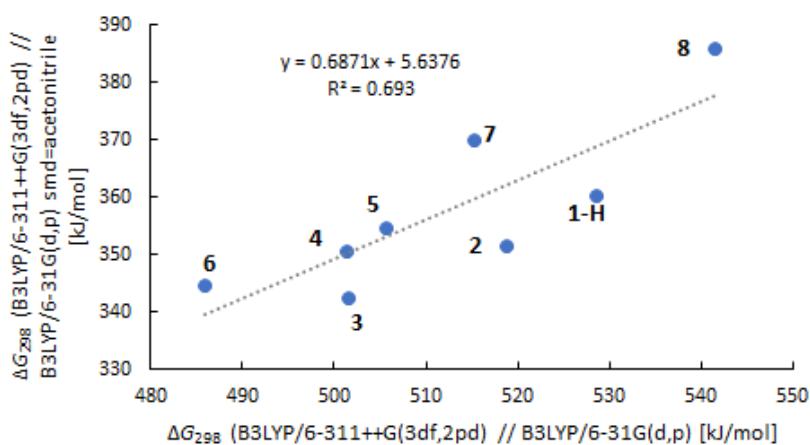
**Figure S3.** Correlation of Lewis Basicity *LB* and MCA calculated as the enthalpy  $\Delta H_{298}$  with the MP2(FC)/6-31+G(2d,p) // B98/6-31G(d) method in gas-phase (only shown for rationalization; numbers and geometries are not further discussed in this work).



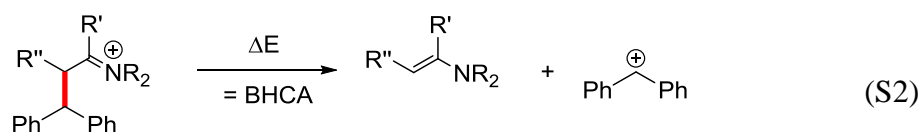
**Figure S4.** Correlation of Lewis Basicity  $LB$  and MCA calculated as Gibbs energy  $\Delta G_{298}$  with the B3LYP/6-311++G(3df,2pd) // B3LYP/6-31G(d,p) method in gas-phase.



**Figure S5.** Correlation of Lewis Basicity  $LB$  and MCA calculated as Gibbs energy  $\Delta G_{298}$  with the B3LYP/6-311++G(3df,2pd) // B3LYP/6-31G(d,p) method in acetonitrile solution.



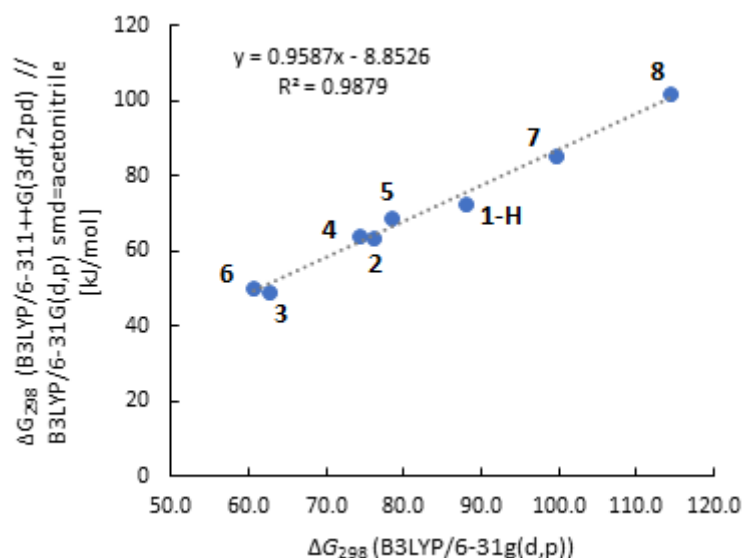
**Figure S6.** Comparison of the MCA obtained as Gibbs energy in gas-phase with the one in acetonitrile solution with the B3LYP/6-311++G(3df,2pd) // B3LYP/6-31G(d,p) method.

Benzhydryl Cation Affinities (BHCA)

Benzhydryl cation affinities were calculated with the B3LYP/6-311++G(3df,2pd) // B3LYP/6-31G(d,p) procedure in gas phase and in solution. In general, the correlations of calculated BHCAs with experimental Lewis basicities (*LB*) of the enamines **1–8** are slightly better than the corresponding correlations with MCAs.

Various methods to calculate the BHCA based on the B3LYP basis were tested, which included calculation of electronic energies, entropies and free energies in gas-phase and in acetonitrile. Use of the larger 6-311++G(3df,2pd) basis set (Figures S10-S12) in comparison to 6-31G(d,p) (Figures S8-S9) slightly improved the quality of the correlations with the Lewis basicities *LB*. As with MCA, inclusion of a solvent model significantly reduced the BHCA of enamines **1–3** (both electronics and Gibbs energies by ca. 16 kJ/mol, Figure S13, S14) in comparison to **4–8**.

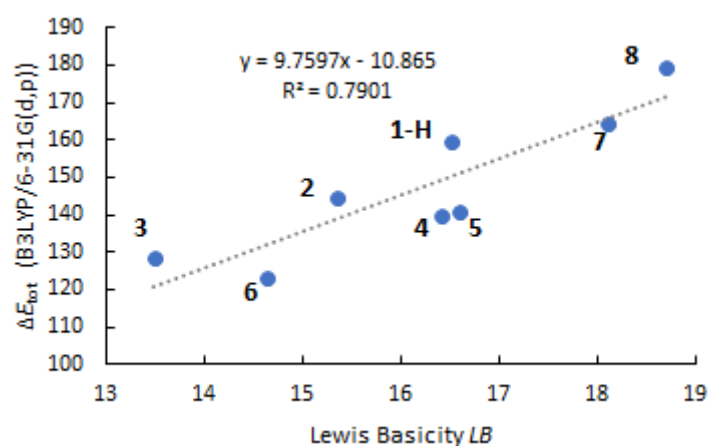
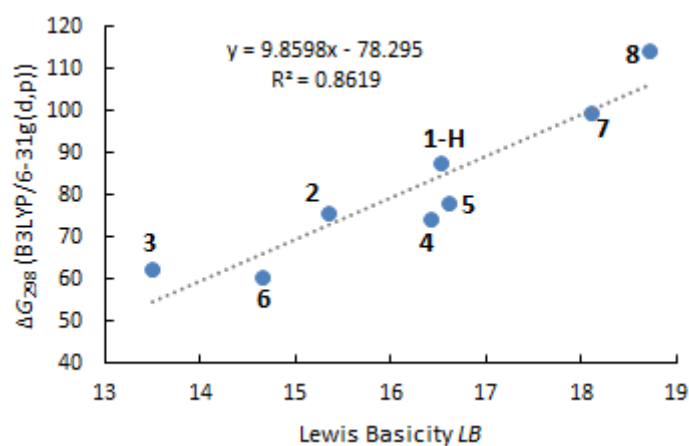
Of all the obtained BHCA, the best correlation with the experimental Lewis Basicities (*LB*) is found with electronic energies  $\Delta E_{\text{tot}}$  calculated with the B3LYP/6-311++G(3df,2pd) // B3LYP/6-31G(d,p) method in acetonitrile solution (Figure S11) while the correlation with Gibbs energies is of lower quality (Figure S12).

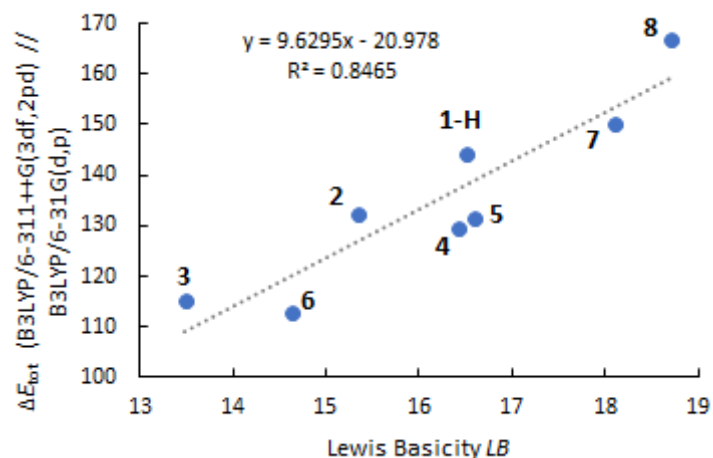


**Figure S7.** Basis set dependence of BHCAs obtained as Gibbs energy of the reaction in equation (S2) in gas-phase.

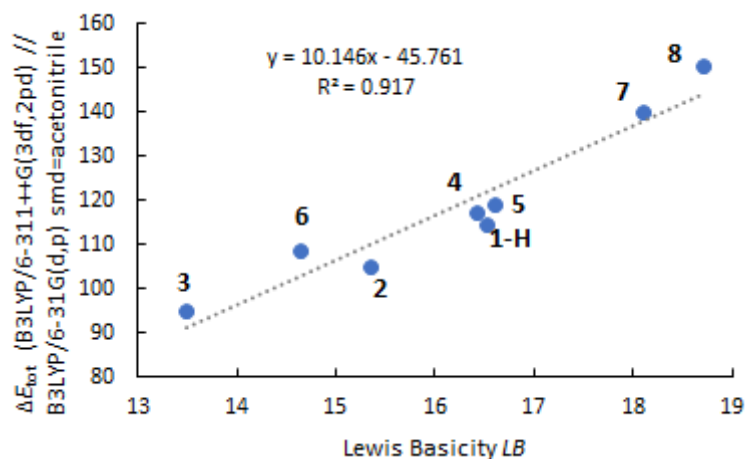
**Table S110:** Lewis basicity  $LB$  and benzhydryl cation affinities (BHCA) for enamines **1-8** with different methods.

System	Lewis Basicity $LB$	$\Delta E_{\text{tot}}$ B3LYP/6- 31G(d,p)	$\Delta G_{298}$ B3LYP/6- 31G(d,p)	$\Delta E_{\text{tot}}$ B3LYP-6- 311++G(3df,2pd)// B3LYP/6- 31G(d,p)	$\Delta G_{298}$ B3LYP-6- 311++G(3df,2pd)// B3LYP/6- 31G(d,p)	$\Delta E_{\text{tot}}$ B3LYP-6- 311++G(3df,2pd)// B3LYP/6- 31G(d,p) smd=acetonitrile	$\Delta G_{298}$ B3LYP-6- 311++G(3df,2pd)// B3LYP/6- 31G(d,p) smd=acetonitrile
<b>1-H</b>	16.50	159.6	87.9	144.2	72.6	114.6	42.9
<b>2</b>	15.35	144.6	76.0	132.3	63.8	105.3	36.7
<b>3</b>	13.49	128.7	62.7	115.1	49.1	95.0	29.0
<b>4</b>	16.43	139.8	74.2	129.5	63.9	117.5	51.9
<b>5</b>	16.60	140.8	78.3	131.4	68.9	119.3	56.8
<b>6</b>	14.65	123.3	60.6	112.9	50.3	108.9	46.3
<b>7</b>	$\approx 18.1$	164.3	99.6	150.1	85.5	140.1	75.5
<b>8</b>	$\approx 18.7$	179.2	114.3	166.8	101.9	150.4	85.4

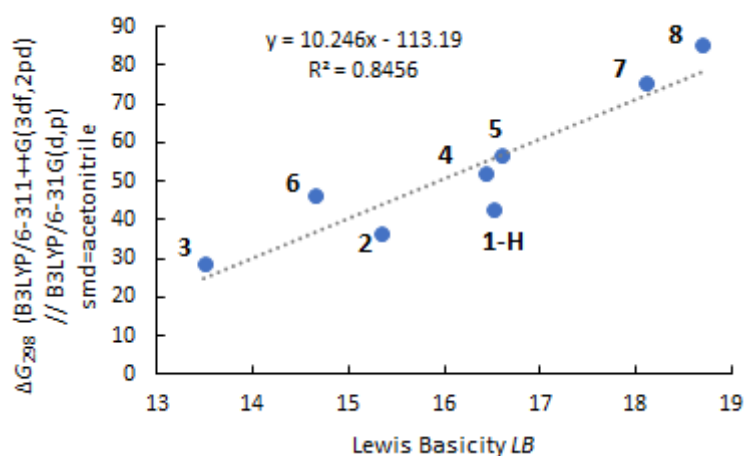
**Figure S8.** Correlation of Lewis Basicity  $LB$  and the electronic energy  $\Delta E_{\text{tot}}$  calculated with the B3LYP/6-31G(d,p) method in gas-phase.**Figure S9.** Correlation of Lewis Basicity  $LB$  and the Gibbs free energy  $\Delta G_{298}$  calculated with the B3LYP/6-31G(d,p) method in gas-phase.



**Figure S10.** Correlation of Lewis Basicity  $LB$  and the electronic energy  $\Delta E_{\text{tot}}$  calculated with the B3LYP/6-311++G(3df,2pd) // B3LYP/6-31G(d,p) method in gas-phase.

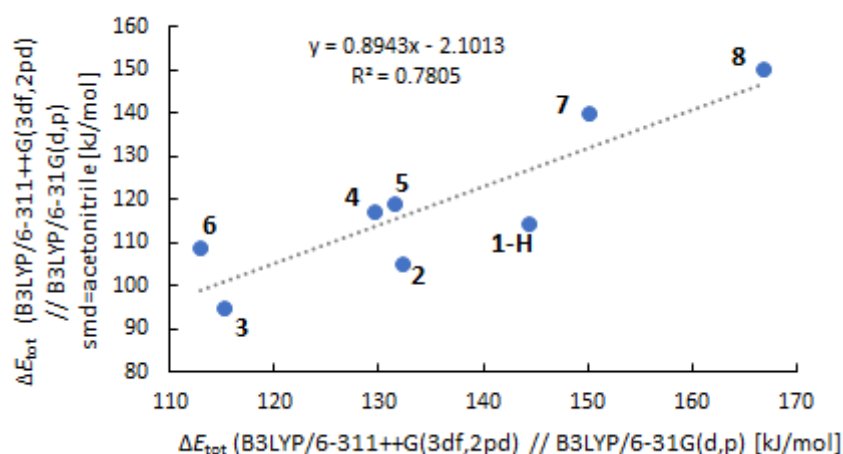


**Figure S11.** Correlation of Lewis Basicity  $LB$  and the electronic energy  $\Delta E_{\text{tot}}$  calculated with the B3LYP/6-311++G(3df,2pd) // B3LYP/6-31G(d,p) method in acetonitrile solution.

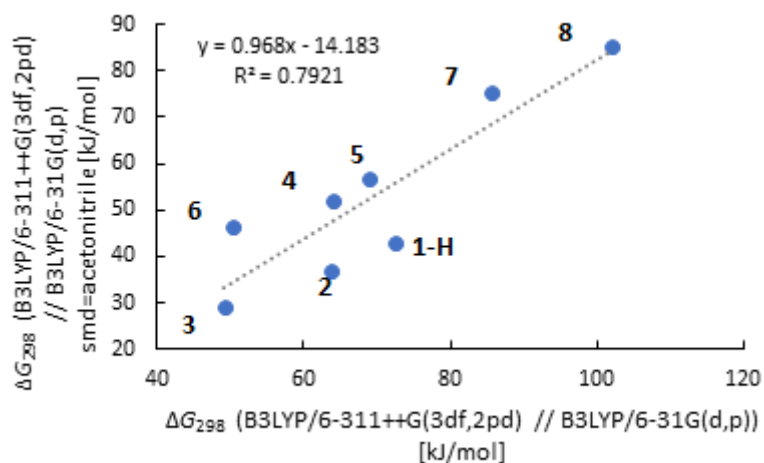


**Figure S12.** Correlation of Lewis Basicity  $LB$  and the Gibbs free energy  $\Delta G_{298}$  calculated with the B3LYP/6-311++G(3df,2pd) // B3LYP/6-31G(d,p) method in acetonitrile solution.



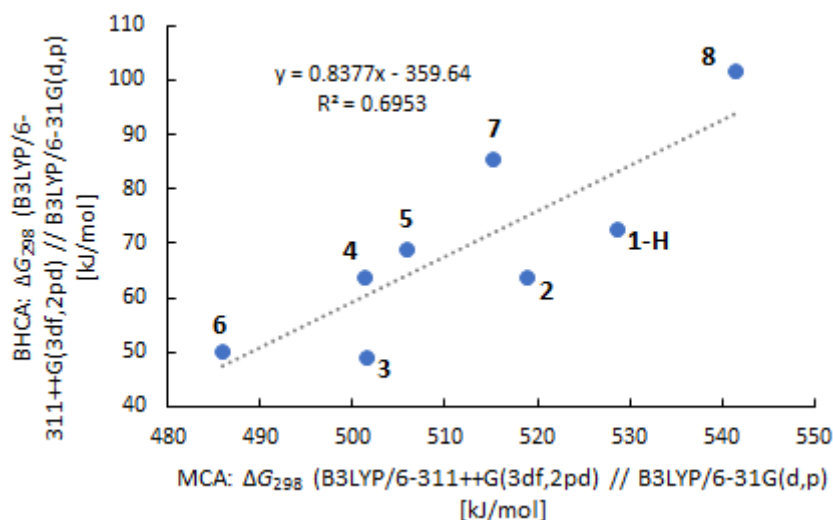


**Figure S13.** Influence of solvation shown as correlation of BHCA obtained as electronic energy  $E_{\text{tot}}$  in gas-phase and in acetonitrile solvation with the B3LYP/6-311++G(3df,2pd) // B3LYP/6-31G(d,p) method.

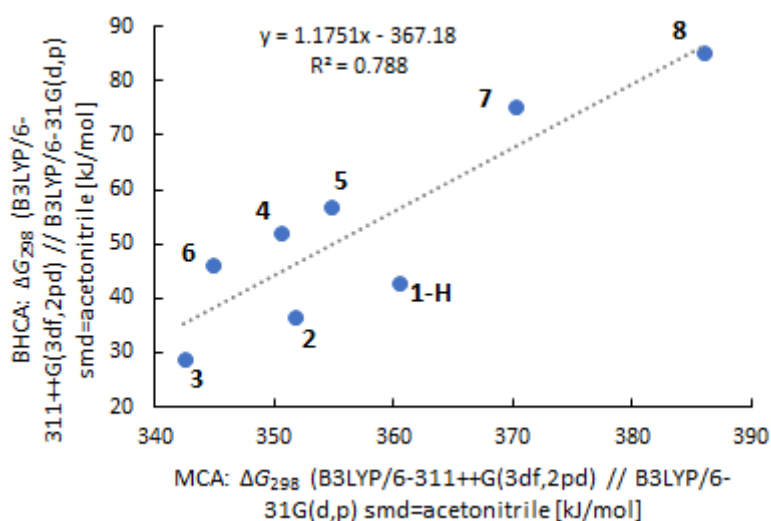


**Figure S14.** Comparison of BHCA obtained as Gibbs free energy in gas-phase and in acetonitrile solvation with the B3LYP/6-311++G(3df,2pd) // B3LYP/6-31G(d,p) method.

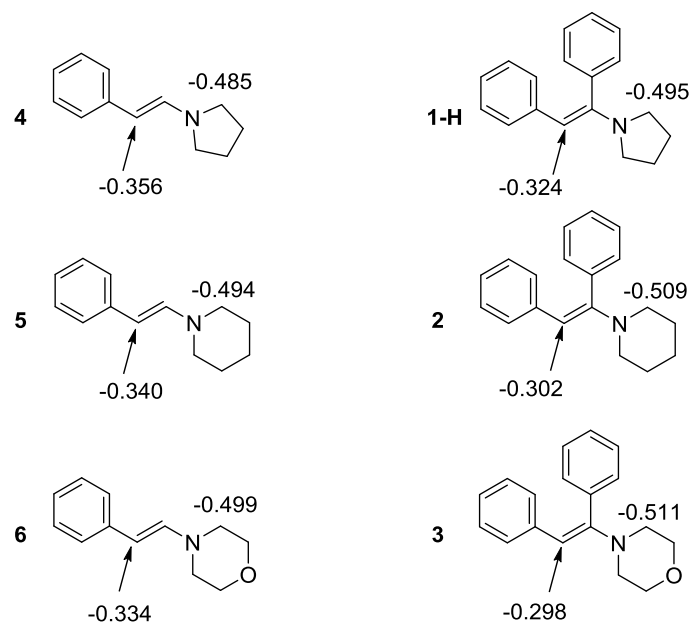
Figure S15 and S16 show the correlation of methyl- and benzhydryl cation affinities for enamines **1–8**.



**Figure S15.** Correlation of gas-phase MCA and gas-phase BHCA calculated as Gibbs free energy  $\Delta G_{298}$  with the B3LYP/6-311++G(3df,2pd) // B3LYP/6-31G(d,p) method.



**Figure S16.** Correlation of MCA and BHCA in acetonitrile solution calculated as Gibbs free energy  $\Delta G_{298}$  with the B3LYP/6-311++G(3df,2pd) // B3LYP/6-31G(d,p) method.

NBO Analysis

**Figure S17.** NBO Analysis of the enamines **1–6** at the B3LYP/6-31+G(d,p) level in gas phase.

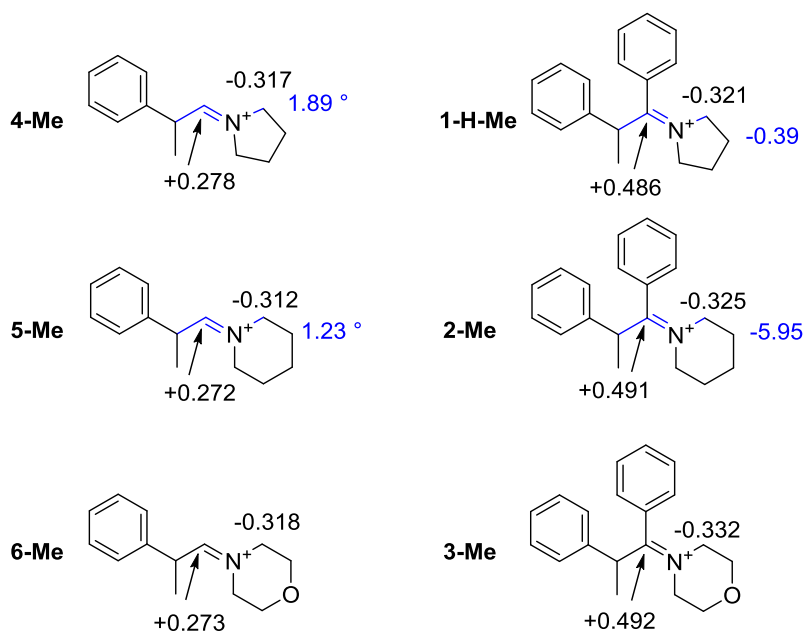


**Figure S18.** NBO Analysis of the methyl cation adducts of **1–6** at the B3LYP/6-31+G(d,p) level in gas phase and  $\text{H}_2\text{C}-\text{N}_q=\text{C}-\text{C}$  dihedral angles (blue).

## 2.6. References

- [1] a) J. N. Brønsted, K. J. Pedersen, *Z. Phys. Chem.* **1924**, *108*, 185–235; b) F. A. Carroll, *Perspectives on Structure and Mechanism in Organic Chemistry*, 2<sup>nd</sup> Ed., Wiley, Hoboken, NJ, 2010, pp. 437–438.
- [2] L. P. Hammett, *Chem. Rev.* **1935**, *17*, 125–136.
- [3] a) R. P. Bell, *Proc. R. Soc. London Ser. A* **1936**, *154*, 414–429; b) M. G. Evans, M. Polanyi, *Trans Faraday Soc.* **1938**, *34*, 1333–1359; c) M. J. S. Dewar, R. C. Dougherty, *The PMO Theory of Organic Chemistry*, Plenum, New York, 1975, pp. 212–220.
- [4] J. E. Leffler, *Science*, **1953**, *117*, 340–341.
- [5] G. S. Hammond, *J. Am. Chem. Soc.* **1955**, *77*, 334–338.
- [6] a) R. A. Marcus, *J. Chem. Phys.* **1956**, *24*, 966–978; b) R. A. Marcus, *J. Phys. Chem.* **1968**, *72*, 891–899; c) W. J. Albery, *Annu. Rev. Phys. Chem.* **1980**, *31*, 227–263; d) J. R. Murdoch, D. E. Magnoli, *J. Am. Chem. Soc.* **1982**, *104*, 3792–3800; e) M. Y. Chen, J. R. Murdoch, *J. Am. Chem. Soc.* **1984**, *106*, 4735–4743.
- [7] a) X.-Q. Zhu, F.-H. Deng, J.-D. Yang, X.-T. Li, Q. Chen, N.-P. Lei, F.-K. Meng, X.-P. Zhao, S.-H. Han, E.-J. Hao, Y.-Y. Mu, *Org. Biomol. Chem.* **2013**, *11*, 6071–6089; b) Y.-H. Fu, G.-B. Shen, Y. Li, L. Yuan, J.-L. Li, L. Li, A.-K. Fu, J.-T. Chen, B.-L. Chen, L. Zhu, X.-Q. Zhu, *ChemistrySelect* **2017**, *2*, 904–925; and refs cited therein.
- [8] a) A. Williams, *Free Energy Relationships in Organic and Bio-organic Chemistry*, Royal Society of Chemistry, Cambridge, **2003**; b) W. P. Jencks, *Chem. Rev.* **1985**, *85*, 511–527; c) F. G. Bordwell, T. A. Cripe, D. L. Hughes In *Nucleophilicity* (Eds.: J. M. Harris, S. P. McManus) American Chemical Society, Washington, DC, **1987**; Chapter 9.
- [9] a) C. F. Bernasconi, *Adv. Phys. Org. Chem.* **2010**, *44*, 223–324; b) C. F. Bernasconi, *Tetrahedron* **1989**, *45*, 4017–4090; c) C. F. Bernasconi, *Acc. Chem. Res.* **1987**, *20*, 301–308.
- [10] a) H. Mayr, M. Patz, *Angew. Chem.* **1994**, *106*, 990–1010; *Angew. Chem. Int. Ed.* **1994**, *33*, 938–957; b) H. Mayr, T. Bug, M. F. Gotta, N. Hering, B. Irrgang, B. Janker, B. Kempf, R. Loos, A. R. Ofial, G. Remennikov, H. Schimmel, *J. Am. Chem. Soc.* **2001**, *123*, 9500–9512; c) H. Mayr, B. Kempf, A. R. Ofial, *Acc. Chem. Res.* **2003**, *36*, 66–77; d) H. Mayr, A. R. Ofial, *Pure Appl. Chem.* **2005**, *77*, 1807–1821; e) H. Mayr, A. R. Ofial,

- SAR QSAR Environ. Res. **2015**, 26, 619–646; f) H. Mayr, *Tetrahedron* **2015**, 71, 5095–5111.
- [11] a) H. Mayr, J. Ammer, M. Baidya, B. Maji, T. A. Nigst, A. R. Ofial, T. Singer, *J. Am. Chem. Soc.* **2015**, 137, 2580–2599; b) H. Mayr, A. R. Ofial, *Acc. Chem. Res.* **2016**, 49, 952–965.
- [12] a) M. Baidya, S. Kobayashi, F. Brotzel, U. Schmidhammer, E. Riedle, H. Mayr, *Angew. Chem.* **2007**, 119, 6288–6292; *Angew. Chem. Int. Ed.* **2007**, 46, 6176–6179; b) M. Baidya, F. Brotzel, H. Mayr, *Org. Biomol. Chem.* **2010**, 8, 1929–1935; c) B. Maji, M. Baidya, J. Ammer, S. Kobayashi, P. Mayer, A. R. Ofial, H. Mayr, *Eur. J. Org. Chem.* **2013**, 3369–3377.
- [13] For a comprehensive listing of nucleophilicity parameters  $N$ ,  $s_N$  and electrophilicity parameters  $E$ , see <http://www.cup.uni-muenchen.de/oc/mayr/DBintro.html>.
- [14] a) P. W. Hickmott, *Tetrahedron* **1982**, 38, 1975–2050; b) G. Pitacco, E. Valentin in *Supplement F: The Chemistry of Amino, Nitroso and Nitro Compounds and their Derivatives* (Ed.: S. Patai), Wiley, Chichester, **1982**, pp. 623–714; c) V. G. Granik, *Russ. Chem. Rev.* **1984**, 53, 383–400; *Usp. Khim.* **1984**, 53, 651–688; d) *Enamines: Synthesis: Structure, and Reactions, Second Edition* (Ed.: A. G. Cook), Marcel Dekker Inc., New York, **1988**. e) P. W. Hickmott in *The chemistry of enamines* (Ed.: Z. Rappoport), Wiley, Chichester, **1994**, pp. 727–871; f) A. Berkessel, H. Gröger, *Asymmetric Organocatalysis – From Biomimetic Concepts to Applications in Asymmetric Synthesis*, Wiley-VCH, Weinheim, **2005**, Chapt. 4.1.1.2, pp 55–68; g) G. Stork, *Tetrahedron* **2011**, 67, 9754–9764; h) B. List, S.-H. Liao, S. Shirakawa, K. Maruoka, L.-Z. Gong, W.-J. Xiao in *Organic Chemistry – Breakthroughs and Perspectives*, First Edition (Eds.: K. Ding, L.-X. Dai), Wiley-VCH, Weinheim, 2012, Chap. 10, pp 367–384. i) D. Seebach, X. Sun, M.-O. Ebert, W. B. Schweizer, N. Purkayastha, A. K. Beck, J. Duschmalé, H. Wennemers, T. Mukaiyama, M. Benohoud, Y. Hayashi, M. Reiher, *Helv. Chim. Acta* **2013**, 96, 799–852; j) Y.-Q. Zou, F. B. Hörmann, T. Bach, *Chem. Soc. Rev.* **2017**, DOI: 10.1039/c7cs00509a; k) A. Castro-Alvarez, H. Carneros, A. M. Costa, J. Vilarrasa, *Synthesis* **2017**, 49, 5285–5306.
- [15] For enamines **1-X** and **2**: a) N. Kato, Y. Hamada, T. Shioiri, *Chem. Pharm. Bull.* **1984**, 32, 2496–2502; for enamine **3**: b) M. E. Munk, Y. K. Kim, *J. Org. Chem.* **1965**, 30, 3705–3710.

- [16] CCDC 1589744 (**1-OMe**), 1589747 (**1-CN**), 1589745 (**1-NO<sub>2</sub>**), and 1589746 (**3**) contain the supplementary crystallographic data for this paper. These data are provided free of charge by The Cambridge Crystallographic Data Centre.
- [17] a) B. Kempf, N. Hampel, A. R. Ofial, H. Mayr, *Chem. Eur. J.* **2003**, *9*, 2209–2218; b) T. Kanzian, S. Lakhdar, H. Mayr, *Angew. Chem.* **2010**, *122*, 9717–9720; *Angew. Chem. Int. Ed.* **2010**, *49*, 9526–9529; c) H. Erdmann, F. An, P. Mayer, A. R. Ofial, S. Lakhdar, H. Mayr, *J. Am. Chem. Soc.* **2014**, *136*, 14263–14269.
- [18] S. Lakhdar, B. Maji, H. Mayr, *Angew. Chem.* **2012**, *124*, 5837–5840; *Angew. Chem. Int. Ed.* **2012**, *51*, 5739–5742.
- [19] a) Y. Wei, T. Singer, H. Mayr, G. N. Sastry, H. Zipse, *J. Comput. Chem.* **2008**, *29*, 291–297; b) Y. Wei, G. N. Sastry, H. Zipse, *J. Am. Chem. Soc.* **2008**, *130*, 3473–3477; c) Y. Wei, G. N. Sastry, H. Zipse, *Org. Lett.* **2008**, *10*, 5413–5417; d) C. Lindner, B. Maryasin, F. Richter, H. Zipse, *J. Phys. Org. Chem.* **2010**, *23*, 1036–1042; e) C. Lindner, R. Tandon, B. Maryasin, E. Larionov, H. Zipse, *Beilstein J. Org. Chem.* **2012**, *8*, 1406–1442; f) A. Levens, F. An, M. Breugst, H. Mayr, D. W. Lupton, *Org. Lett.* **2016**, *18*, 3566–3569; g) E. Follet, H. Zipse, S. Lakhdar, A. R. Ofial, G. Berionni, *Synthesis* **2017**, *49*, 3495–3504.
- [20] a) R. Ditchfield, W. J. Hehre, J. A. Pople, *J. Chem. Phys.* **1971**, *54*, 724–728; b) R. Krishnan, J. S. Binkley, R. Seeger, J. A. Pople, *J. Chem. Phys.* **1980**, *72*, 650–654; c) T. Clark, J. Chandrasekhar, G. W. Spitznagel, P. v. R. Schleyer, *J. Comput. Chem.* **1983**, *4*, 294–301; d) T. H. Dunning Jr., *J. Chem. Phys.* **1989**, *90*, 1007–1023; e) A. D. Becke, *J. Chem. Phys.* **1993**, *98*, 5648–5652.
- [21] *Gaussian 09, Revision A.02*, M. J. Frisch, G. W. Trucks, H. B. Schlegel, G. E. Scuseria, M. A. Robb, J. R. Cheeseman, G. Scalmani, V. Barone, B. Mennucci, G. A. Petersson, H. Nakatsuji, M. Caricato, X. Li, H. P. Hratchian, A. F. Izmaylov, J. Bloino, G. Zheng, J. L. Sonnenberg, M. Hada, M. Ehara, K. Toyota, R. Fukuda, J. Hasegawa, M. Ishida, T. Nakajima, Y. Honda, O. Kitao, H. Nakai, T. Vreven, J. A. Montgomery, Jr., J. E. Peralta, F. Ogliaro, M. Bearpark, J. J. Heyd, E. Brothers, K. N. Kudin, V. N. Staroverov, R. Kobayashi, J. Normand, K. Raghavachari, A. Rendell, J. C. Burant, S. S. Iyengar, J. Tomasi, M. Cossi, N. Rega, J. M. Millam, M. Klene, J. E. Knox, J. B. Cross, V. Bakken, C. Adamo, J. Jaramillo, R. Gomperts, R. E. Stratmann, O. Yazyev, A. J. Austin, R. Cammi, C. Pomelli, J. W. Ochterski, R. L. Martin, K. Morokuma, V. G. Zakrzewski, G.

- A. Voth, P. Salvador, J. J. Dannenberg, S. Dapprich, A. D. Daniels, O. Farkas, J. B. Foresman, J. V. Ortiz, J. Cioslowski, and D. J. Fox, Gaussian, Inc., Wallingford CT, 2009.
- [22] Full details of the computational method are given in the Experimental Section.
- [23] A. V. Marenich, C. J. Cramer, D. G. Truhlar, *J. Phys. Chem. B.* **2009**, *113*, 6378–6396.
- [24] J. Ammer, M. Baidya, S. Kobayashi, H. Mayr, *J. Phys. Org. Chem.* **2010**, *23*, 1029–1035.
- [25] H. Mayr, M. Breugst, A. R. Ofial, *Angew. Chem.* **2011**, *123*, 6598–6634; *Angew. Chem. Int. Ed.* **2011**, *50*, 6470–6505.
- [26] C. Hansch, A. Leo, R. W. Taft, *Chem. Rev.* **1991**, *91*, 165–195.
- [27] A. E. Reed, L. A. Curtiss, F. Weinhold, *Chem. Rev.* **1988**, *88*, 899–926.
- [28] T. A. Nigst, A. Antipova, H. Mayr, *J. Org. Chem.* **2012**, *77*, 8142–8155.
- [29] a) H. Mayr, A. R. Ofial, *Acc. Chem. Res.* **2016**, *49*, 952–965. b) H. Mayr, A. R. Ofial, *Pure Appl. Chem.* **2017**, *89*, 729–744.
- [30] B. Denegri, A. Streiter, S. Juric, A. R. Ofial, O. Kronja, H. Mayr, *Chem. Eur. J.* **2006**, *12*, 1648–1656.
- [31] a) N. Streidl, B. Denegri, O. Kronja, H. Mayr, *Acc. Chem. Res.* **2010**, *43*, 1537–1549. b) S. Jurić, O. Kronja, *J. Phys. Org. Chem.* **2015**, *28*, 314–319 and refs cited there in.
- [32] G. Bélanger, M. Doré, F. Ménard, V. Darsigny, *J. Org. Chem.* **2006**, *71*, 7481–7484.
- [33] R. Carlson, Å. Nilsson, *Acta Chem. Scand., Ser. B.* **1984**, *38*, 49–53.
- [34] a) **MeO**-substituted deoxybenzoin: I. Lantos, P. E. Bender, K. A. Razgaitis, B. M. Sutton, M. J. DiMartino, D. E. Griswold, D. T. Walz, *J. Med. Chem.* **1984**, *27*, 72–75. b) **CN**-substituted deoxybenzoin: E. Anders, T. Gaßner, *Chem. Ber.* **1984**, *117*, 1034–1038. c) **NO<sub>2</sub>**-substituted deoxybenzoin: P. Wan, S. Muralidhara, *J. Am. Chem. Soc.* **1988**, *110*, 4336–4345.
- [35] G. R. Fulmer, A. J. M. Miller, N. H. Sherden, H. E. Gottlieb, A. Nudelman, B. M. Stoltz, J. E. Bercaw, K. I. Goldberg, *Organometallics* **2010**, *29*, 2176–2179.
- [36] Bruker (2012). SAINT. Bruker AXS Inc., Madison, Wisconsin, USA.
- [37] G. M. Sheldrick, (1996). SADABS. University of Göttingen, Germany
- [38] G. M. Sheldrick, *Acta Crystallogr., Sect. C: Struct. Chem.* **2015**, *71*, 3–8.

- [39] C. Brinkmann, A. G. M. Barrett, M. S. Hill, P. A. Procopiou, *J. Am. Chem. Soc.* **2012**, *134*, 2193–2207.
- [40] A. M. Lluch, M. Gibert, F. Sánchez-Baeza, A. Messegue, *Tetrahedron* **1996**, *52*, 3973–3982.
- [41] Tinker Version 8.2, J. W. Ponder, <http://dasher.wustl.edu/tinker>.
- [42] D. S. Allgäuer, H. Jangra, H. Asahara, Z. Li, Q. Chen, H. Zipse, A. R. Ofial, H. Mayr, *J. Am. Chem. Soc.* **2017**, *139*, 13318–13329.



## Chapter 3

# Kinetics of Electrophilic Fluorinations of Enamines and Carbanions: Comparison of the Fluorinating Power of N–F Reagents

Daria S. Timofeeva, Armin R. Ofial, and Herbert Mayr

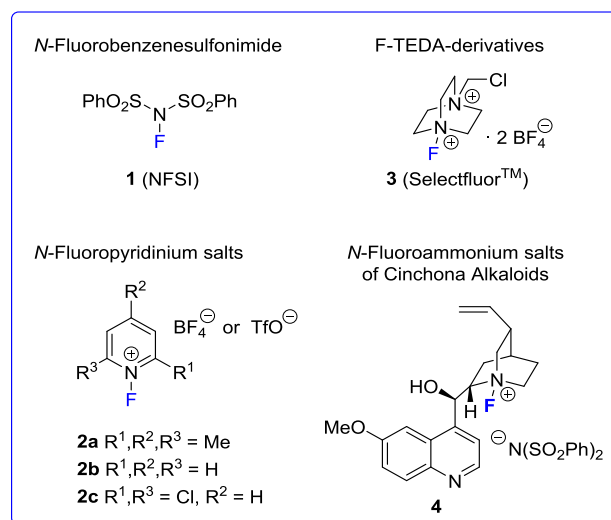
*J. Am. Chem. Soc.* **2018**, *140*, 11474–11486

### 3.1. Introduction

Since fluorine significantly affects the physical, chemical, and biological properties of organic molecules, fluorinated compounds have been gaining increasing importance in many fields such as agrochemistry,<sup>1</sup> medicinal chemistry,<sup>2</sup> and materials science.<sup>3</sup> For that reason, a wide variety of methods to synthesize organofluorine compounds have been developed during the past decades.<sup>4</sup> Initially, molecular fluorine (F<sub>2</sub>),<sup>5</sup> perchloryl fluoride (FClO<sub>3</sub>),<sup>6</sup> xenon difluoride (XeF<sub>2</sub>),<sup>7</sup> trifluoromethyl hypofluorite (CF<sub>3</sub>OF)<sup>8</sup>, various acyl<sup>9</sup> and perfluoroacyl hypofluorites<sup>10</sup> (CH<sub>3</sub>COOF, CF<sub>3</sub>COOF) were the most common reagents available for electrophilic fluorination. Handling these reagents requires special techniques, as they are highly toxic and very reactive, which also hampers their use for asymmetric synthesis.

In order to overcome these disadvantages, new electrophilic fluorination reagents containing N–F bonds were developed.<sup>11</sup> Two types of N–F reagents can be differentiated: neutral (R<sub>2</sub>NF) compounds on one side, and quaternary ammonium (R<sub>3</sub>N<sup>+</sup>F<sup>–</sup> A<sup>–</sup>) and pyridinium salts with weakly basic counterions on the other. The discovery of N–F reagents, such as *N*-fluorobenzenesulfonimide (NFSI, **1**)<sup>12</sup> and analogues,<sup>13</sup> *N*-fluoropyridinium salts (**2**),<sup>14</sup> *N*-fluoroquinuclidinium salts<sup>15</sup> and 1-chloromethyl-4-fluoro-1,4-diazoniabicyclo[2.2.2]octane bis(tetrafluoroborate) (**3**, well known as Selectfluor or F-TEDA-BF<sub>4</sub>),<sup>16</sup> resulted in the rapid progress of electrophilic fluorinations. Compared to O–F and other types of previously used electrophilic fluorinating reagents, N–F reagents are generally more stable, safer and more easily to handle, and they are able to oxidize and fluorinate many substrates under mild conditions.

**Chart 1.** Electrophilic Fluorinating N–F Reagents Studied in This Work.



A significant step in the development of asymmetric fluorinations<sup>17</sup> was the introduction of the *N*-fluoroammonium salts of cinchona alkaloids, which can either be isolated as stable salts or generated in situ from the corresponding cinchona alkaloids and various commercially available fluorinating reagents.<sup>18</sup> Thus the chiral cinchona-derived reagents serve as cheap sources of chirality, which are easier to synthesize than *N*-fluorocamphorsultam and related structures.<sup>19</sup> While preparation of the latter requires several steps and the use of elemental  $\text{F}_2$ , the cinchona alkaloid derived *N*-fluoroammonium salt **4** can be obtained by transfer fluorination of quinine by *N*-fluorobenzenesulfonimide following the procedure by Cahard.<sup>18c</sup> Gouverneur and co-workers<sup>20</sup> have recently developed new classes of chiral N–F reagents with the dicationic DABCO core and derivatives of ethano bridged Tröger's bases.

Several attempts to rank electrophilic fluorination agents with respect to relative reactivities have been reported. Gilicinski et al.<sup>21</sup> found a correlation between the peak potentials of the first one-electron reduction ( $E_p^{\text{red}}$ ) of the N–F reagents and their reactivities in synthetic fluorinations (Figure 1).

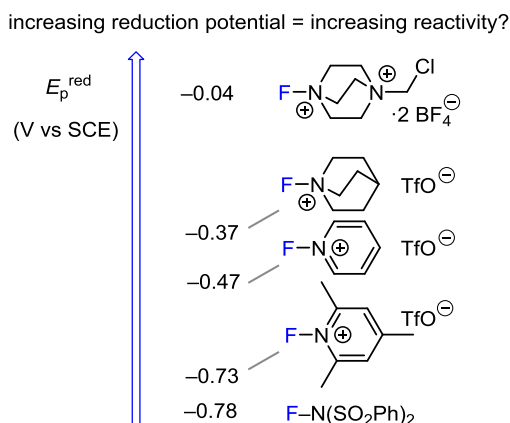


**Figure 1.** Peak reduction potentials  $E_p^{\text{red}}$  (in MeCN) of selected electrophilic fluorinating N-F reagents (from ref 21)

Sudlow and Woolf<sup>22</sup> criticized this work due to uncertainties in the measurements and interpretation of the electrochemical data and suggested a thermodynamic ordering based on the calculated  $F^+$  detachment enthalpies, which correlated with LUMO energies of the *N*-fluoropyridinium ions. Related electrochemical studies for six recently used fluorinating reagents with the tetrafluoroborate counterion have been reported by Evans et al.<sup>23</sup> Umemoto and coworkers discussed the relationship between the variable fluorinating power of *N*-fluoropyridinium salts and their  $^{19}\text{F}$  NMR chemical shifts.<sup>24</sup>

Togni et al. determined the relative fluorinating activity of various fluorinating N-F reagents in Ti(TADDOLato)-catalyzed fluorinations of  $\beta$ -keto esters by competitive halogenations (Figure 2).<sup>25</sup>

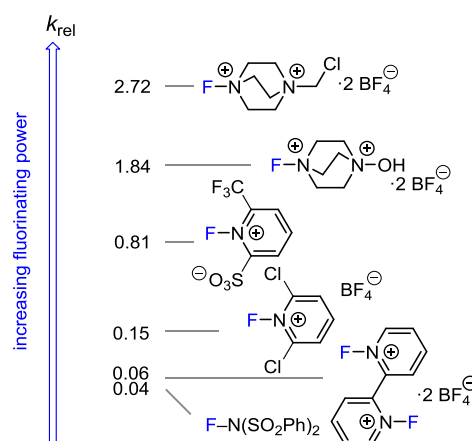
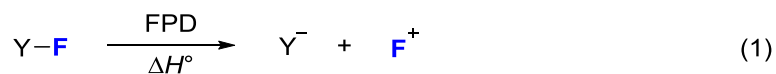


**Figure 2.** Relative fluorination rates derived from competition experiments ( $k_{\text{rel}}$  from ref 25)

Assuming that the fluorinating power of Y-F reagents is related to the  $F^+$  detachment energy (FPD) defined by equation 1, Xue, Cheng, and co-workers calculated  $\Delta H^\circ$  (eq 1) for

130 N–F reagents at the (SMD)M06-2X/6-311++G(2d,p)//M05-2X/6-31+G(d) level of theory in MeCN and CH<sub>2</sub>Cl<sub>2</sub> solution.<sup>26</sup>



In this article we report on the first kinetic investigations of the reactions of the most common commercially available fluorinating reagents **1–4** (Chart 1) with carbon nucleophiles and show how the rate constants for the reactions with the enamines **5** and carbanions **6** (Chart 2) can be combined with the nucleophilicity parameters  $N(s_N)$ <sup>27</sup> to define the synthetic potential of these fluorinating agents.

**Chart 2.** Reference Nucleophiles Used in This Work and Their Nucleophilicity Parameters  $N$  and  $s_N$  in Acetonitrile and DMSO<sup>27</sup>

Enamines			$N(s_N)$ in MeCN	$\lambda_{\text{max}}$ in MeCN
	X = H	<b>5a</b>	11.66 (0.82)	317 nm
	X = OMe	<b>5b</b>	11.99 (0.84)	296 nm
	X = CN	<b>5c</b>	10.63 (0.84)	375 nm
	X = NO <sub>2</sub>	<b>5d</b>	10.42 (0.82)	465 nm
		<b>5e</b>	9.94 (0.86)	316 nm
		<b>5f</b>	8.78 (0.83)	306 nm
		<b>5g</b>	13.87 (0.76)	310 nm
		<b>5h</b>	11.66 (0.83)	300 nm

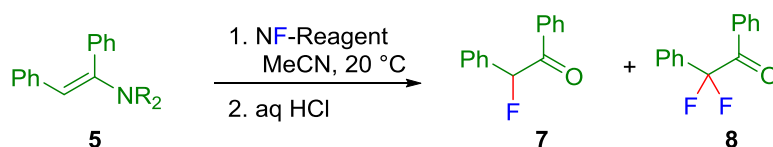
Carbanions			$N(s_N)$ in DMSO	$\lambda_{\text{max}}$ in DMSO
		<b>6a</b>	14.49 (0.86)	476 nm
		<b>6b</b>	14.96 (0.96)	538 nm
		<b>6c</b>	16.26 (0.83)	450 nm
		<b>6d</b>	17.33 (0.74)	305 nm
		<b>6e</b>	19.61 (0.60)	590 nm
		<b>6f</b>	20.00 (0.71)	550 nm

## 3.2. Results and discussion

### 3.2.1. Product Analysis

To establish the course of the reactions, which were investigated kinetically, we have studied the products of some representative fluorination reactions. As shown in Table 1, treatment of the deoxybenzoin-derived enamines **5a** and **5f** with 1.05 equivalents of the fluorinating agents **1–3** in acetonitrile at room temperature and subsequent hydrolysis gave mixtures of the mono- and difluorinated deoxybenzoins **7** and **8**, the ratio of which was determined by integration of the  $^{19}\text{F}$  NMR spectra of the crude reaction mixtures. Due to the formation of the difluorinated deoxybenzoin **8** and other side products, 1.05 equivalents of the fluorinating agents were not sufficient for full conversion of the enamines.

**Table 1.** Reactions of the Enamines **5a** and **5f** with N–F Reagents in Acetonitrile at 20 °C



Entry	Enamine	N-F Reagent <sup>a</sup>	Fluorination products		
			Crude (7/8) <sup>b</sup>	7 (%) <sup>c</sup>	8 (%) <sup>c</sup>
1	<b>5a</b>	NFSI ( <b>1</b> )	77/23	55	
2	<b>5a</b>	<b>2a</b> -BF <sub>4</sub>	77/23	43	
3	<b>5a</b>	<b>2b</b> -BF <sub>4</sub>	74/26 <sup>d</sup>	28	8
4	<b>5f</b>	<b>2c</b> -BF <sub>4</sub>	91/9	78	
5	<b>5f</b>	Selectfluor ( <b>3</b> )	95/5	80	

<sup>a</sup> A slight excess of the N-F reagent (1.05 equiv) was used. <sup>b</sup> Product ratio as determined from the  $^{19}\text{F}$  NMR spectrum of the crude product. <sup>c</sup> Yields refer to the isolated products. <sup>d</sup> In addition, **9** was isolated (11% yield).

As shown in Scheme 1, electrophilic fluorination of the enamines first gives monofluorinated iminium ions, which may be deprotonated by the amine, amide, or pyridine released from the N–F reagents **1–3** during  $\text{F}^+$  transfer. The resulting monofluorinated enamines can be fluorinated by another molecule of fluorinating agent to give the difluorinated iminium salts, and hydrolysis yields a mixture of the ketones **7** and **8**.

**Scheme 1.** Mechanism of the Fluorination of the Enamines

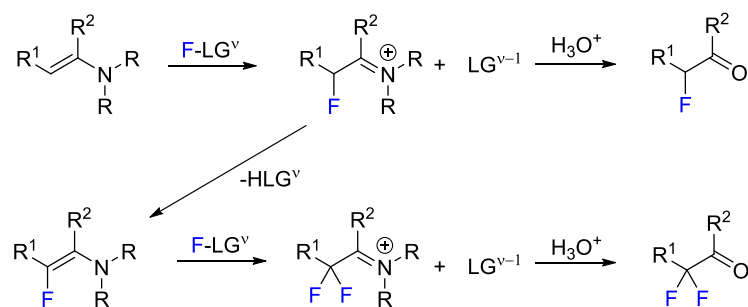
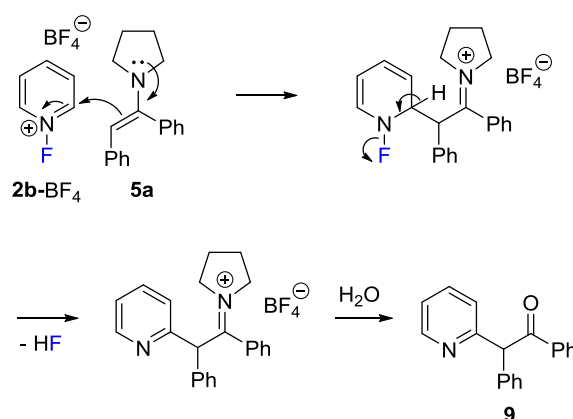


Table 1 shows that the reactions of the enamine **5a** with the less reactive fluorinating reagents **1**, **2a**, and **2b** yielded mono- and difluoro-substituted products in a ratio of 3/1 (entries 1–3 in Table 1), while the reactions of the enamine **5f** with the more reactive fluorinating reagents **2c** and **3** gave the monofluorinated ketone **7** predominantly, accompanied by only a small amount of the difluorinated ketone **8**. This difference can be explained by the fact that 2,6-dichloro-pyridine (from **2c**) and DABCO-derived ammonium ions (from **3**) are weak bases, which do not efficiently convert the monofluorinated iminium ions into the fluorinated enamines. Therefore, in entries 4 and 5 of Table 1 the second fluorination plays a minor role.

Reactions of enamines with electrophilic fluorinating reagents have previously been reported to give mono- and difluorinated ketones after hydrolysis,<sup>28</sup> and the reactions of enamines with two equivalents of Selectfluor (**3**) in the presence of Et<sub>3</sub>N have been described as a synthetic method for the formation of difluorinated carbonyl compounds.<sup>28a</sup> Dilman et al. reported the fluorocyanation of enamines involving the electrophilic fluorination of the C=C bonds with N–F reagents to form fluoroiminium ions, which were trapped by cyanide ions.<sup>29</sup>

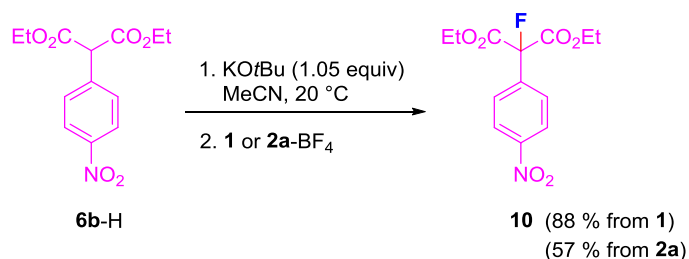
In the reaction of the enamine **5a** with **2b** (Table 1, entry 3), the fluorinated ketones **7** and **8** were accompanied by the 2-substituted pyridine **9**. Formation of **9** can be explained by the mechanism shown in Scheme 2. The unsubstituted *N*-fluoropyridinium ion **2b** is an ambident electrophile, which is not only attacked at the fluorine atom, but also at the 2-position of the pyridinium ring. HF-elimination from the intermediate dihydropyridine and hydrolysis yields ketone **9**. The observation that nucleophilic attack at the chlorinated 2-positions of **2c** does not occur is in line with the observation that C–H positions are more reactive than C–Cl positions in nucleophilic aromatic and vinylic substitutions.<sup>30</sup>

**Scheme 2.** Mechanism of the Reaction of the Pyridinium Salt **2b**-BF<sub>4</sub> with Enamine **5a**



Treatment of the deep-pink solution of the potassium salt of the diethyl malonate **6b**-H with **1** (NFSI, 1.1 equiv) or *N*-fluoro-2,4,6-trimethylpyridinium tetrafluoroborate (**2a**-BF<sub>4</sub>, 1.1 equiv) at 20 °C led to complete fading of the color within a few minutes. After workup of the reaction mixture with 2 M aq HCl, the crude 2-fluorinated diethyl malonate **10** was obtained, purified by column chromatography, and characterized by NMR spectroscopy and mass spectrometry (Scheme 3).

**Scheme 3.** Reactions of the N-F Reagents **1** and **2a**-BF<sub>4</sub> with Nucleophile **6b**-K



Since reactions of the fluorinating reagents **2b**, **2c**, and **3** with carbanions **6a**–**f** were too fast for kinetic measurements, we have not studied the products of these reactions. Reactions of various *C*-nucleophiles with *N*-fluoropyridinium tetrafluoroborate **2b**-BF<sub>4</sub> have previously been reported to give products arising from pyridylation, rather than the fluorinated products.<sup>31</sup> Attack at the 2-position of the *N*-fluoropyridinium ion **2b** is also preferred by sulfur-, oxygen- and nitrogen-centered nucleophiles; reactions with *N*-fluoropyridinium salts were, therefore, recommended as routes to 2-substituted pyridines.<sup>32</sup> Umemoto and co-workers showed that 2,4,6-trimethyl-substituted *N*-fluoropyridinium triflate (**2a**-OTf) afforded only the fluorinated product in the reaction with diethyl phenylmalonate. In contrast, 2- and/or 4-unsubstituted *N*-fluoropyridinium salts reacted with the formation of pyridyl derivatives as by-products.<sup>14e</sup>

### 3.2.2. Kinetic Investigations.

The kinetics of the reactions of the reference nucleophiles (Chart 2) with the fluorinating reagents **1–4** were studied at 20 °C in acetonitrile solution. All reactions were monitored photometrically by following the disappearance of the enamines **5** or the carbanions **6** at or close to their absorption maxima (see Experimental Section). Due to the low stability and poor solubility of the isolated carbanion salts (**6a–f**)-K in acetonitrile, these carbanions were generated in acetonitrile solution prior to each kinetic measurement by treatment of the conjugate CH acids **6-H** with potassium *tert*-butoxide (1.05 equiv). To simplify the kinetics, the fluorinating agents were used in sufficient excess ( $\geq 10$  equiv) to achieve pseudo-first-order conditions (eq 2).

$$-d[\text{Nu}]/dt = k_{\text{obs}}[\text{Nu}], \quad k_{\text{obs}} = k_2[\text{E}]_0 \quad (2)$$

An example for the resulting monoexponential decays of the UV–Vis absorbances of the minor components **5** or **6** is shown in Figure 3 for the reaction of **5a** with **1** (NFSI). The first-order rate constants  $k_{\text{obs}}$  ( $\text{s}^{-1}$ ) were derived by least-squares fitting of the exponential function  $A_t = A_0 \exp(-k_{\text{obs}}t) + C$  to the time-dependent absorbances of the reference nucleophiles.

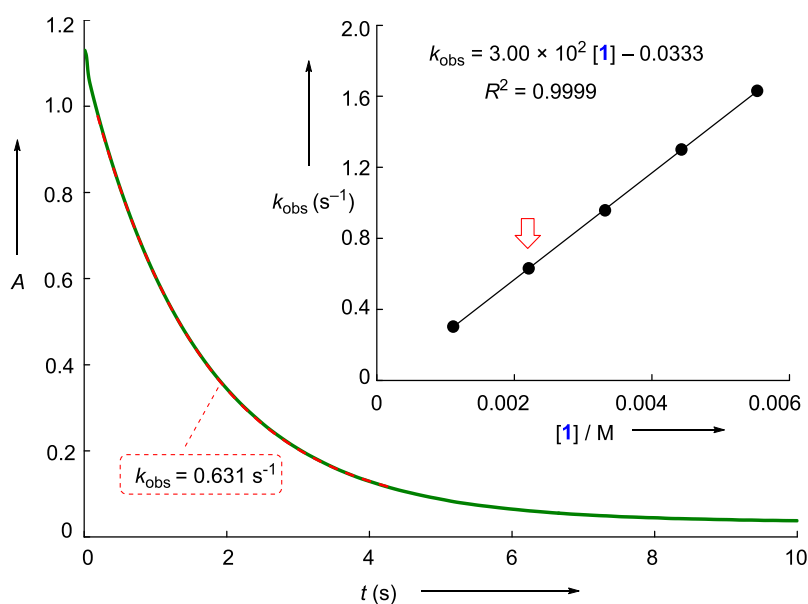


**Figure 3.** Exponential decay of the absorbance of enamine **5a** ( $c_0 = 1.06 \times 10^{-4}$  M) at 315 nm during its reaction with the N-F reagent **1** (NFSI,  $c_0 = 2.21 \times 10^{-3}$  M). Inset: Correlation of the rate constants  $k_{\text{obs}}$  with [**1**] in MeCN at 20 °C. The tagged data point refers to the depicted absorption-time trace.



The correlations of  $k_{\text{obs}}$  with the concentrations of the electrophiles were linear for all reactant combinations, as illustrated by the inset of Figure 3. The slopes of such correlations were used to derive the second-order rate constants  $k_2$  for the reactions of electrophilic fluorinating reagents **1–4** with the reference nucleophiles **5** and **6** in acetonitrile (see Experimental Section for the individual correlations of all investigated reactions). Table 2 summarizes the obtained second-order rate constants for electrophilic fluorinations.

As shown in Table 2, the rate constants of the reactions of *N*-fluoropyridinium salt **2a** with carbanions **6b,c** increased by a factor of 2.3 when tetrafluoroborate ions were replaced by triflate counterions. In contrast, enamine **5a** reacts even 1.3 times faster with **2a**-BF<sub>4</sub> than with **2a**-OTf. Since the influence of the counterions on the rates of the fluorinations is small compared to the substituent effects in the pyridinium ions we will neglect them in the following discussion.

Table 3 compares the influence of 18-crown-6 ether on the second-order rate constants of the reactions of N–F fluorinating reagents with **6b**-K. The rate constants of the reactions with **1** (NFSI) and *N*-fluorocollidinium triflate (**2a**-OTf) with and without added crown ether agree within experimental error, while the fluorination with the tetrafluoroborate salt of **2a** is accelerated by a factor of 1.2 by the 18-crown-6 ether.

**Table 2.** Second-Order Rate Constants  $k_2$  for the Reactions of Fluorinating N–F Reagents **1–4** with Enamines **5a–h** and Carbanions **6a–f** in MeCN at 20 °C

N–F Reagent	Nucleophile	$k_2$ (M <sup>-1</sup> s <sup>-1</sup> )
NFSI ( <b>1</b> )	<b>5a</b>	$3.00 \times 10^2$
	<b>5b</b>	$6.13 \times 10^2$
	<b>5c</b>	$1.17 \times 10^2$
	<b>5d</b>	$7.41 \times 10^1$
	<b>5e</b>	$1.11 \times 10^1$
	<b>5f</b>	2.72
	<b>5g</b>	$2.42 \times 10^2$
	<b>5h</b>	$2.38 \times 10^1$
	<b>6a</b>	$1.29 \times 10^2$
	<b>6b</b>	$7.71 \times 10^2$
	<b>6c</b>	$1.02 \times 10^3$
	<b>6d</b>	$6.28 \times 10^2$
	<b>6e</b>	$1.27 \times 10^4$

**Table 2.** (continued)

N-F Reagent	Nucleophile	$k_2$ ( $\text{M}^{-1} \text{s}^{-1}$ )
<b>2a-BF<sub>4</sub></b>	<b>5a</b>	$1.08 \times 10^1$
	<b>5c</b>	1.68
	<b>5e</b>	$2.62 \times 10^{-1}$
	<b>5g</b>	9.99
	<b>6a</b>	$7.43 \times 10^2$
	<b>6b</b>	$1.34 \times 10^3$
	<b>6c</b>	$4.15 \times 10^3$
	<b>6d</b>	$2.00 \times 10^4$
<b>2a-OTf</b>	<b>6f</b>	$8.18 \times 10^4$
	<b>5a</b>	8.60
	<b>6b</b>	$2.92 \times 10^3$
<b>2b-BF<sub>4</sub></b>	<b>6c</b>	$1.02 \times 10^4$
	<b>5a</b>	$2.26 \times 10^1$
	<b>5c</b>	4.38
<b>2c-BF<sub>4</sub></b>	<b>5d</b>	3.61
	<b>5e</b>	1.03
	<b>5g</b>	$4.53 \times 10^1$
	<b>5a</b>	$1.30 \times 10^5$
	<b>5c</b>	$4.71 \times 10^4$
	<b>5d</b>	$2.91 \times 10^4$
Selectfluor ( <b>3</b> )	<b>5e</b>	$4.61 \times 10^3$
	<b>5g</b>	$2.40 \times 10^5$
	<b>5h</b>	$9.97 \times 10^3$
	<b>5a</b>	$1.08 \times 10^5$
	<b>5b</b>	$1.87 \times 10^5$
	<b>5c</b>	$5.09 \times 10^4$
	<b>5d</b>	$3.53 \times 10^4$
	<b>5e</b>	$9.82 \times 10^3$
NF-QN-N(SO <sub>2</sub> Ph) <sub>2</sub> ( <b>4</b> )	<b>5f</b>	$2.30 \times 10^3$
	<b>5g</b>	$8.14 \times 10^4$
	<b>5h</b>	$7.75 \times 10^3$
	<b>5d</b>	$2.27 \times 10^2$
	<b>6b</b>	$1.57 \times 10^5$

**Table 3.** The Second-Order Rate Constants for the Reactions of Fluorinating N–F Reagents **1** and **2a** with **6b-K** (20 °C, MeCN) With or Without Added 18-Crown-6 Ether

N–F Reagent	$k_2$ (M <sup>-1</sup> s <sup>-1</sup> )		$k_{\text{rel}}^b$
	<b>6b-K</b>	<b>6b-K</b> + 18-c-6 <sup>a</sup>	
<b>1</b>	$7.71 \times 10^2$	$8.35 \times 10^2$	1.1
<b>2a-BF<sub>4</sub></b>	$1.34 \times 10^3$	$1.66 \times 10^3$	1.2
<b>2a-OTf</b>	$2.92 \times 10^3$	$3.04 \times 10^3$	1.0

<sup>a</sup> In the presence of 18-crown-6 ether (1.05 equiv with respect to **6b-K**). <sup>b</sup>  $k_{\text{rel}} = k_2(\text{K}^+/\text{18-c-6})/k_2(\text{K}^+)$ .

### 3.2.3. Correlation Analysis

During the last decades, we have shown that a large variety of reactions of  $\pi$ -electrophiles with  $n$ -,  $\pi$ -, and  $\sigma$ -nucleophiles can be described by equation 3,

$$\log k_2(20\text{ °C}) = s_{\text{N}}(N + E) \quad (3)$$

where  $k_2$  is the second-order rate constant,  $s_{\text{N}}$  and  $N$  are solvent-dependent nucleophile-specific parameters and  $E$  is an electrophile-specific parameter.<sup>33</sup> On the basis of this linear free-energy relationship we have created a comprehensive nucleophilicity scale covering more than 30 orders of magnitude.<sup>27g</sup>

To examine the applicability of equation 3 for the fluorination reactions studied in this work,  $(\log k_2)/s_{\text{N}}$  for the reactions of **1–3** with the deoxybenzoin-derived enamines **5a–f** was plotted against the nucleophilicity parameters  $N$  listed in Chart 2. Since the slopes of these correlations deviated only marginally from 1.0, we abstained from adding an extra electrophile-specific susceptibility parameter  $s_{\text{E}}$ , as suggested for  $\text{S}_{\text{N}}2$  reactions,<sup>34</sup> and enforced a slope of 1 for the correlations shown in Figure 4. The fact that the individual data points are close to the corresponding correlation lines shows that these reactions follow equation 3, and the intercepts (at  $N = 0$ ) correspond to the electrophilicity parameters  $E$  for the fluorinating N–F reagents **1–3**. The  $E$  values given in Figure 4 show that Selectfluor (**3**) and 1-fluoro-2,6-dichloropyridinium ions **2c** are of similar electrophilicity, three powers of ten more reactive than NFSI (**1**), which is followed by the unsubstituted  $N$ -fluoropyridinium ion **2b** and the least reactive collidine-derived fluorinating reagent **2a**, which is two orders of magnitude less reactive than **1**.

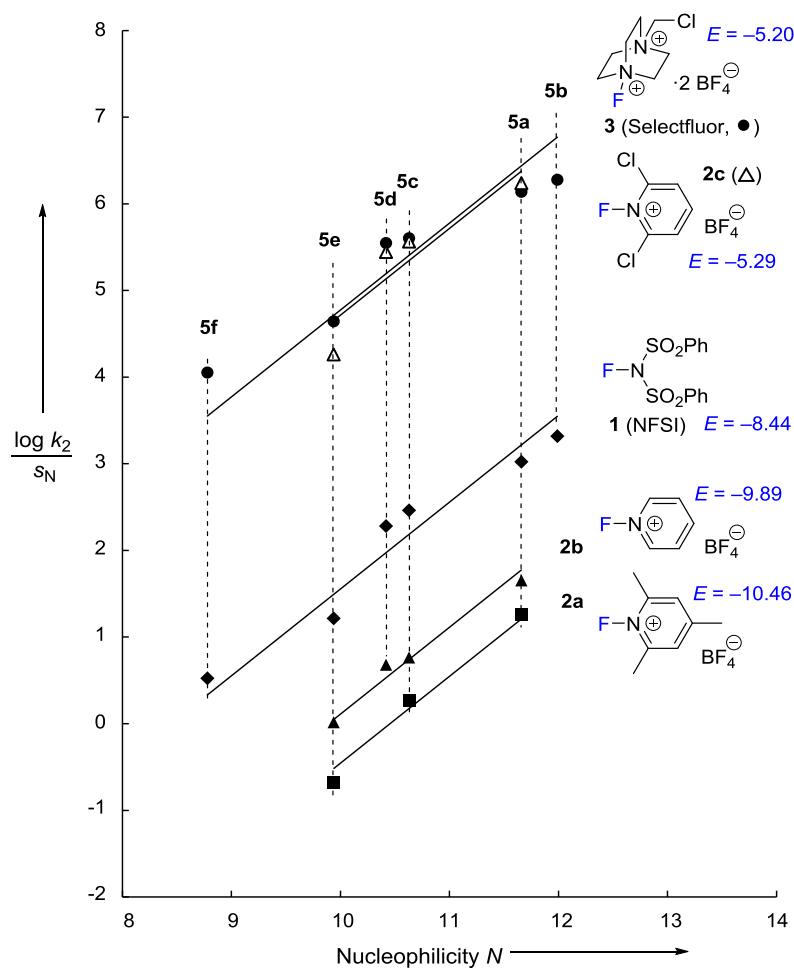


**Figure 4.** Correlations of  $(\log k_2)/s_N$  for the reactions of fluorinating N–F reagents **1–3** with the enamines **5** against the nucleophilicity parameters  $N$  of **5** (MeCN, 20 °C). For all correlations, a slope of 1.0 was enforced, as required by equation 3 (individual correlations for all electrophiles investigated in this work are shown in the Supporting Information).

Figure 5 illustrates that the rate constants of the electrophilic fluorinations of the X-substituted deoxybenzoin-derived enamines with NFSI (**1**) and Selectfluor (**3**) correlate linearly with Hammett substituent constants  $\sigma_p$ .<sup>35</sup> The resulting reaction constants of  $\rho = 0.63$  and 0.80 reach only about half the amount of the corresponding  $\rho$  for the reactions with the 4,4'-(dimethylamino)-substituted benzhydrylium ion,<sup>27a</sup> indicating that the rates of the electrophilic fluorinations are less sensitive to variation of the nucleophile than the rates of the reactions with carbenium ions.

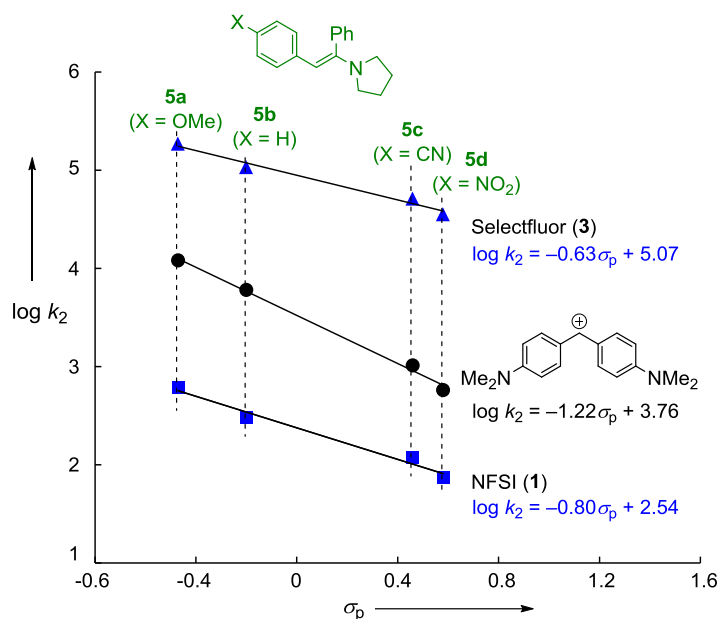


**Figure 5.** Correlations of the second-order rate constants ( $\log k_2$ ) for the reactions of enamines **5a–d** with the 4,4'-(dimethylamino)-substituted benzhydrylium ion (from ref 27a) and the fluorinating reagents **1** and **3** (MeCN, 20 °C) with the Hammett substituent constants  $\sigma_p$  (from ref 35).

When the electrophilicity parameters  $E$  of the fluorinating agents **1–3**, originating from the rate constants of their reactions with the deoxybenzoin-derived enamines **5a–f** (Figure 4), are employed to calculate the second-order rate constants for the fluorinations of the  $\beta$ -aminostyrenes **5g,h**, one obtains values which are 14–55 fold higher than measured (Table 4).

**Table 4.** Experimental and Calculated Second-Order Rate Constants for the Reactions of Fluorinating N–F Reagents **1–3** with  $\beta$ -Aminostyrenes **5g,h** at 20 °C in MeCN

N-F reagent	Nucleophile	$k_2^{\text{exp}}$ (M <sup>-1</sup> s <sup>-1</sup> )	$k_2^{\text{calcd},a}$ (M <sup>-1</sup> s <sup>-1</sup> )	$k_2^{\text{calcd}}/k_2^{\text{exp}}$
<b>1</b>	<b>5g</b>	$2.42 \times 10^2$	$1.34 \times 10^4$	55
<b>2a</b> -BF <sub>4</sub>	<b>5g</b>	9.99	$3.90 \times 10^2$	39
<b>2b</b> -BF <sub>4</sub>	<b>5g</b>	$4.53 \times 10^1$	$1.06 \times 10^3$	23
<b>2c</b> -BF <sub>4</sub>	<b>5g</b>	$2.40 \times 10^5$	$3.32 \times 10^6$	14
<b>3</b>	<b>5g</b>	$8.14 \times 10^4$	$3.88 \times 10^6$	48
<b>1</b>	<b>5h</b>	$2.38 \times 10^1$	$4.71 \times 10^2$	20
<b>2c</b> -BF <sub>4</sub>	<b>5h</b>	$9.97 \times 10^3$	$1.94 \times 10^5$	19
<b>3</b>	<b>5h</b>	$7.75 \times 10^3$	$2.30 \times 10^5$	30

<sup>a</sup> Calculated by using equation 3,  $N$  and  $s_N$  from Chart 2, and  $E$  from Figure 4.

Though these deviations are within the tolerance limit of eq 3, the constantly higher calculated rate constants indicate a common origin: The calibration of the nucleophilicities of the enamines **5a–h** was based on reactions with benzhydrylium ions, which are electrophiles of intermediate steric demand. Since the fluorinating agents are sterically less demanding than benzhydrylium ions, the relative reactivities of the highly substituted enamines **5a–f** and the less substituted enamines **5g,h** will be less affected by steric effects in reactions with the fluorinating agents than in reactions with benzhydrylium ions. As the electrophilicities  $E$  of the fluorinating agents were derived from their reactions with the enamines **5a–f**, one can explain why the rate constants with the sterically less demanding  $\beta$ -aminostyrenes **5g,h** are calculated too high.

Limitations of equation 3 are illustrated in Figure 6, which depicts that the reactions of **1** with the deoxybenzoin-derived enamines **5a–f** and the carbanions **6a–e** follow separate correlations. Application of  $E(1)$ , derived from reactions of **1** with enamines **5a–f**, for calculating the rate constants of reactions of **1** with carbanions **6a–e** yields second-order rate constants  $k_2$ , which are 2.5 to 4 orders of magnitude larger than measured.

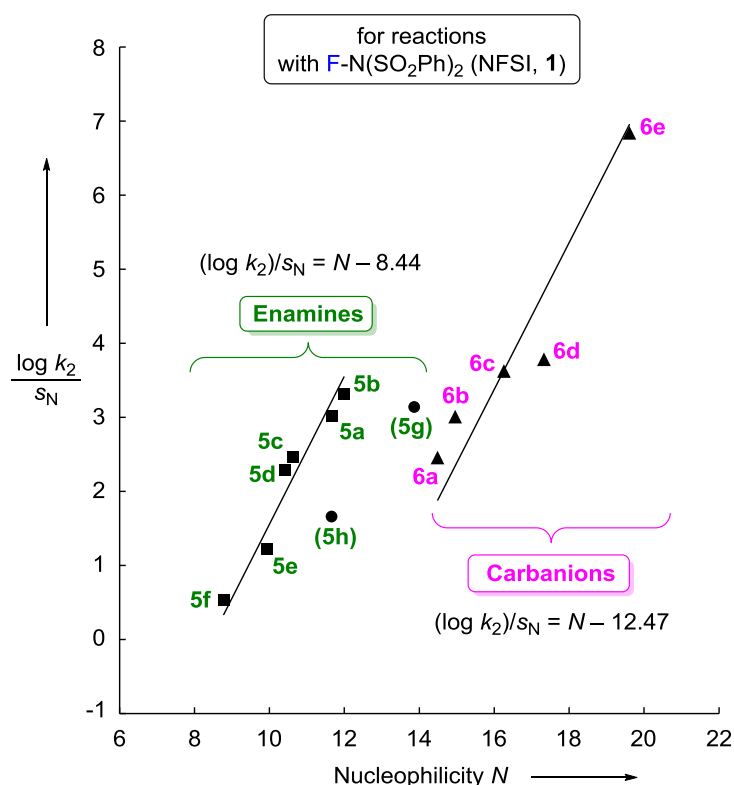
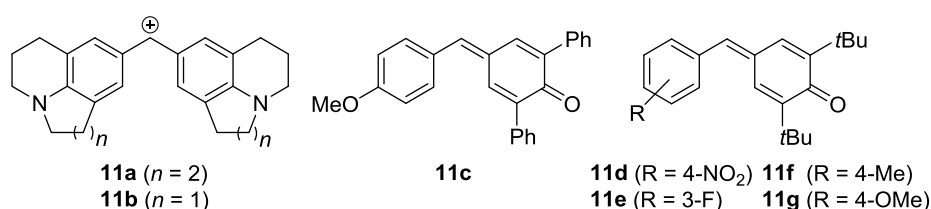


**Figure 6.** Correlations of  $(\log k_2)/s_N$  versus the nucleophilicity of the enamines **5** (determined in MeCN) and carbanions **6** (determined in DMSO) for their reactions with NFSI (**1**) in MeCN at 20 °C. Both correlation lines are fixed to a slope of 1.0, as required by eq 3.

Is this discrepancy due to the fact that the rate constants for the reactions of **1** with **6a–e** in acetonitrile were used in a correlation along with the  $N$  parameters of **6a–e**, which had been derived from the kinetics of reactions in DMSO?

For answering this question, we have investigated the kinetics of the reactions of the carbanions **6a** and **6f** with the reference electrophiles **11** (benzhydrylium ions and quinone methides) in acetonitrile solution and compared the resulting second-order rate constants with those previously reported in DMSO. Table 5 shows that the reactions of **6a** with the benzhydrylium ions **11a** and **11b** are 18- and 12-fold faster in acetonitrile than in DMSO solution. Moreover, the reactions of carbanion **6f** with the quinone methides **11c–g** are only 1.7 to 4 times faster in acetonitrile than in DMSO. These differences are too small to assign the observation of separate correlation lines in Figure 6 to a solvent effect. The nucleophilicity parameter of carbanion **6f** in acetonitrile derived from the rate constants in Table 5 ( $N = 20.43$ ,  $s_N = 0.73$ , Supporting Information) is so close to that in DMSO ( $N = 20.00$ ,  $s_N = 0.71$ , Chart 2), that this agreement of the carbanion reactivities in acetonitrile and DMSO justifies to generally use the  $N$  and  $s_N$  parameters for carbanions in DMSO when correlating rate constants measured in acetonitrile.

**Table 5.** Comparison of the Second-Order Rate Constants for the Reactions of Carbanions **6a,f** with Benzhydrylium Ions and Quinone Methides in Acetonitrile ( $k_2^{\text{AN}}$ ) and DMSO ( $k_2^{\text{DMSO}}$ ) at 20 °C



Entry	Carbanion	Electrophile	$E^a$	$k_2^{\text{AN},b} (\text{M}^{-1} \text{s}^{-1})$	$k_2^{\text{DMSO},c} (\text{M}^{-1} \text{s}^{-1})$	$k_2^{\text{AN}}/k_2^{\text{DMSO}}$
1	<b>6a</b>	<b>11a</b>	−9.45	$3.44 \times 10^5$	$1.89 \times 10^4$	18
2	<b>6a</b>	<b>11b</b>	−10.04	$8.24 \times 10^4$	$6.73 \times 10^3$	12
3	<b>6f</b>	<b>11c</b>	−12.18	$9.10 \times 10^5$	$2.63 \times 10^5$	3.5
4	<b>6f</b>	<b>11d</b>	−14.36	$5.37 \times 10^4$	$1.35 \times 10^4$	4.0
5	<b>6f</b>	<b>11e</b>	−15.03	$6.31 \times 10^3$	$3.68 \times 10^3$	1.7
6	<b>6f</b>	<b>11f</b>	−15.83	$1.99 \times 10^3$	$8.80 \times 10^2$	2.3
7	<b>6f</b>	<b>11g</b>	−16.11	$1.51 \times 10^3$	$4.90 \times 10^2$	3.1

<sup>a</sup> From ref 33b,c,g. <sup>b</sup> For details see Supporting Information. <sup>c</sup> Rate constants were taken from ref 27b (for **6a**) and ref 27f (for **6f**).

Figure 7 shows that the correlation lines for the reactions of the *N*-fluorocollidinium ion **2a** with enamines and carbanions are only slightly separated that one might even consider to construct a single correlation line, that is, derive  $E(\mathbf{2a})$  from all available rate constants (reactions with enamines and carbanions). However, the usage of different sets of reference nucleophiles for the characterization of the different fluorinating agents would reduce the comparability of the corresponding electrophilicity parameters. We decided, therefore, to stay consistently with the enamine-derived electrophilicity parameters  $E$  (as shown in Figure 4) and emphasize that deviations up to four orders of magnitude have to be tolerated when the  $E$  parameters for **1–4** are used to calculate rate constants for the fluorination of carbanions.

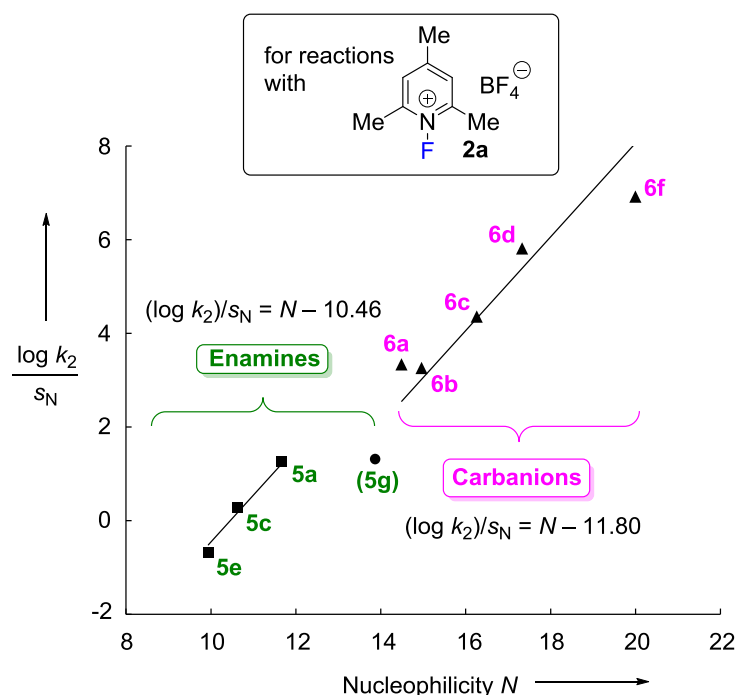


**Figure 7.** Correlations of  $(\log k_2)/s_N$  versus the nucleophilicity of the enamines **5** (determined in MeCN) and carbanions **6** (determined in DMSO) for their reactions with **2a** (MeCN, 20 °C). Both correlation lines are fixed to a slope of 1.0, as required by equation 3.

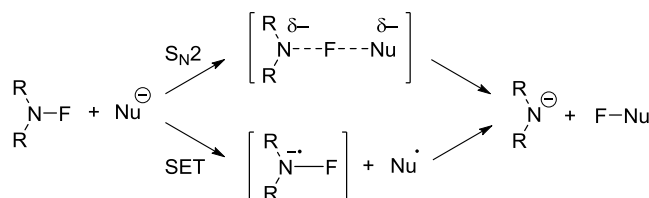
### 3.2.4. Which Factors Control the Fluorinating Power of the Reagents **1–4**?

The question whether electrophilic fluorinations with N–F reagents proceed via  $S_N2$  type mechanisms or via single electron transfer (SET) has previously been discussed (Scheme 4).<sup>21,36</sup> Radical clock experiments<sup>36a</sup> and comparison of observed rate constants with those expected for SET processes<sup>36b</sup> led Differding and Wehrli to the conclusion that electrophilic fluorinations of typical silyl enol ethers, malonate and enolate ions with an *N*-fluorosultam generally proceed by direct nucleophilic attack at fluorine, while electron transfer occurs only



in rare cases. By using a cyclopropyl radical probe, Wong and coworkers excluded an SET mechanism for the reactions of vinyl ethers with Selectfluor (**3**) because products of cyclopropane ring-opening were not observed.<sup>36e</sup>

**Scheme 4.** Possible Mechanistic Pathways of Electrophilic Fluorinations



Our kinetic data confirm these conclusions. Figure 8 shows that the rate constants for the reactions of the enamine **5d** with the cationic reagents **2–3** (Table 1) correlate linearly with the corresponding reduction potentials,<sup>23</sup> while NFSI (**1**) reacts much faster than expected from the depicted correlation for the other fluorinating agents.

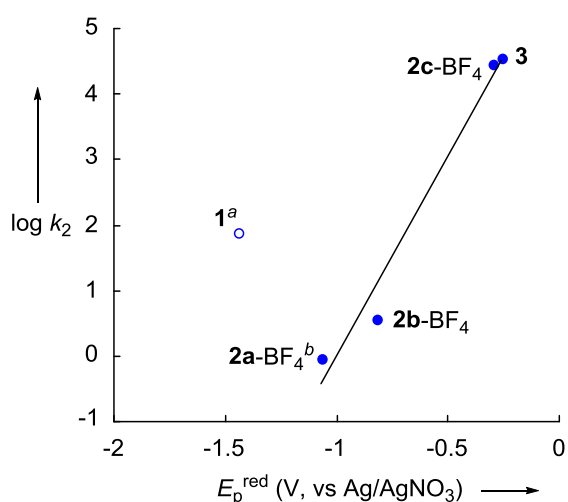


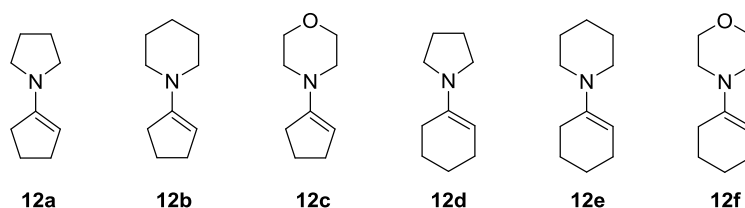
**Figure 8.** Plot of measured rate constants  $\log k_2$  for the reactions of fluorinating N–F reagents **1–3** with the enamine **5d** against the corresponding cathodic peak potentials  $E_p^{\text{red}}$  (taken from ref 23). <sup>a</sup> NFSI (**1**) not included in the correlation. <sup>b</sup> Rate constant ( $\log k_2$ ) calculated by applying  $N$  and  $s_N$  (from Chart 2) and  $E$  (from Figure 4) in eq 3.

Since oxidation potentials for the nucleophiles in Chart 2, which we investigated in this work, are not available, we examined the mechanistic alternatives for the fluorinations of the enamines **12a–f** (Table 6). The reported anodic peak potentials of the enamines **12a–f**<sup>37</sup> and peak reduction potentials of **1–3**<sup>21</sup> (see Figure 1) were used to calculate the Gibbs energy for electron transfer  $\Delta G^\circ_{\text{ET}}$  by eq 4.

$$\Delta G^\circ_{\text{ET}} = F(E^{\text{ox}} - E^{\text{red}}) \quad (4)$$

Equation 3 was then applied to calculate the second-order rate constants at 20 °C for the polar reactions of the fluorinating agents **1–3** with the enamines **12a–f** from the  $E$  values in Figure 4 and the corresponding  $N$  and  $s_N$  parameters<sup>38a</sup> given in Table 6. Conversion of the second-order rate constants for the polar fluorination reactions into the Gibbs energies of activation  $\Delta G^\ddagger_P$  was performed with the Eyring equation.<sup>39a</sup>

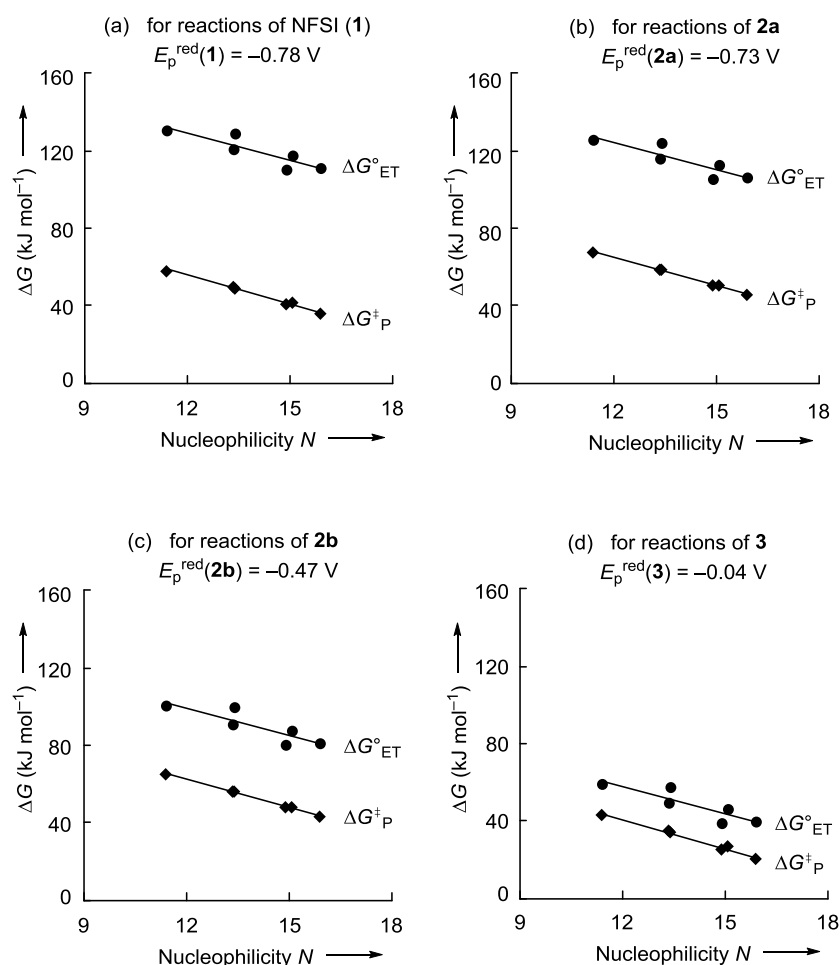
**Table 6.** Calculated Gibbs Energies for Electron Transfer from the Enamines **12a–f** to the N-F Reagents **1–3**,  $\Delta G^\circ_{ET}$  (from eq 4), Compared with Gibbs Energies of Activation for the Polar Fluorine Transfer from the N-F Reagents **1–3** to the Enamines **12**,  $\Delta G^\ddagger_P$  (from eq 3)<sup>a</sup>



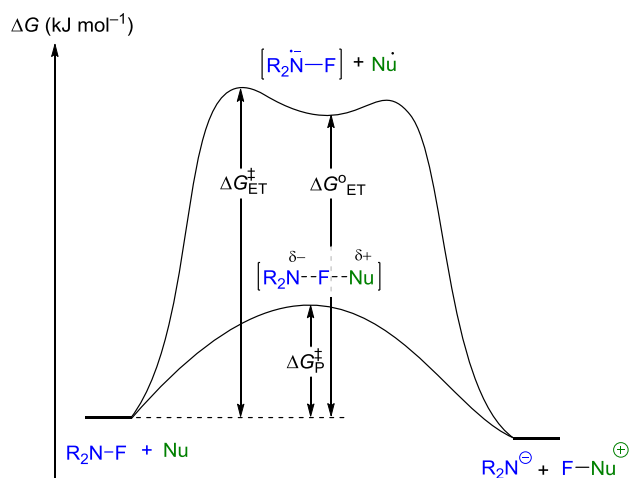
Enamine	$N/s_N^b$	$E_p^{ox,c}$	<b>1</b>		<b>2a</b>		<b>2b</b>		<b>3</b>	
			$\Delta G^\circ_{ET}$	$\Delta G^\ddagger_P$	$\Delta G^\circ_{ET}$	$\Delta G^\ddagger_P$	$\Delta G^\circ_{ET}$	$\Delta G^\ddagger_P$	$\Delta G^\circ_{ET}$	$\Delta G^\ddagger_P$
<b>12a</b>	15.91/0.86	0.37	111	36	106	45	81	43	40	20
<b>12b</b>	15.06/0.82	0.44	118	41	113	51	88	48	46	26
<b>12c</b>	13.41/0.82	0.56	129	49	125	58	99	56	58	34
<b>12d</b>	14.91/0.86	0.36	110	41	105	50	80	48	39	25
<b>12e</b>	13.36/0.81	0.47	121	49	116	59	91	56	49	35
<b>12f</b>	11.40/0.83	0.57	130	58	125	67	100	65	59	43

<sup>a</sup> Gibbs energies are in kJ mol<sup>-1</sup>. <sup>b</sup> In CH<sub>2</sub>Cl<sub>2</sub>, taken from ref 38a;  $N$  and  $s_N$  for neutral  $\pi$ -systems are almost identical in dichloromethane and acetonitrile (as shown in ref 38b). <sup>c</sup> Anodic peak potential  $E_p^{ox}$  (in V vs SCE) in MeCN at 25 °C, taken from ref 37.

Table 6 shows and Figure 9 illustrates that the fluorinations of the enamines **12a–f** with all fluorinating agents proceed with activation energies  $\Delta G^\ddagger_P$ , which are smaller than the Gibbs energies of electron transfer  $\Delta G^\circ_{ET}$ . If one considers that the energy of activation for electron transfer  $\Delta G^\ddagger_{ET}$  must be greater than  $\Delta G^\circ_{ET}$  (Figure 10) we can conclude that none of the reactions considered proceeds via SET.<sup>39b,c</sup>



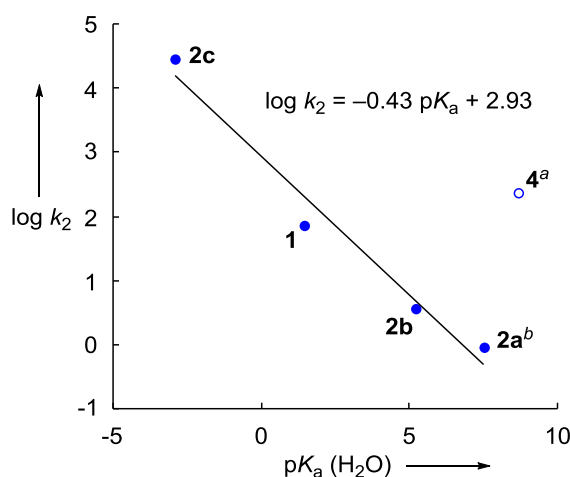
**Figure 9.** Comparison of the calculated Gibbs energies of electron transfer ( $\Delta G^{\circ}_{\text{ET}}$ ) and the Gibbs energies of activation for the polar mechanism ( $\Delta G^{\ddagger}_{\text{P}}$ ) of the reactions of cyclic enamines **12a–f** with (a) NFSI (**1**), (b) the *N*-fluorocollidinium ion (**2a**), (c) the *N*-fluoropyridinium ion (**2b**), and (d) Selectfluor (**3**) (data from Table 6).



**Figure 10.** Gibbs energy profiles for the polar and electron-transfer mechanism of the reactions of cyclic enamines **12a–f** with NFSI (**1**).

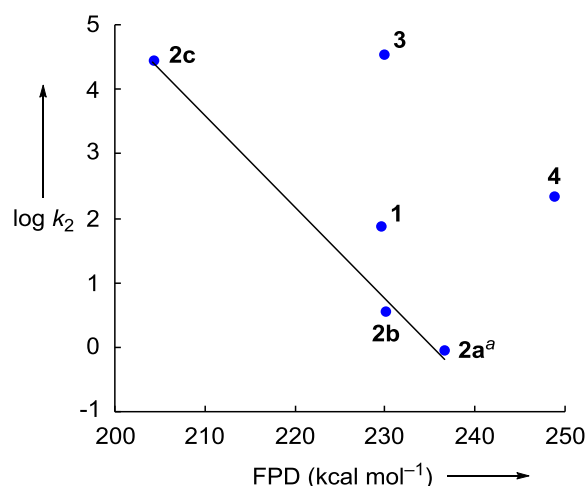
In line with previous analyses<sup>36b</sup> we thus conclude that the electrophilic fluorinations with **1–4** proceed in an S<sub>N</sub>2 type mechanism in which the rate determining step includes cleavage of the N-F bond. Since nucleofugality is often correlated with the basicity of the leaving group, we have also examined the relationships between the fluorinating activities of **1–4** with the pK<sub>a</sub> values of the conjugate acids of the nucleofuges.

Figure 11 shows a fair correlation between the electrophilic reactivities of **1** and **2** with the basicities of the nucleofuges (leaving groups). The positive deviation of **4** from this correlation line reflects the lower intrinsic barrier in reactions of tertiary amines (N<sub>sp3</sub>) compared to pyridines (N<sub>sp2</sub>), which has previously been observed for reactions of electrophiles with amines and pyridines of equal basicity<sup>40</sup> as well as for the corresponding reverse reactions.<sup>40b</sup>



**Figure 11.** Correlation between the rate constants (log  $k_2$ ) for the reactions of fluorinating N-F reagents **1–4** with the enamine **5d** in MeCN against the acidities of the corresponding N-H compounds in water (taken from ref 41). <sup>a</sup> Not used for the correlation. <sup>b</sup> Rate constant (log  $k_2$ ) calculated by applying  $N$  and  $s_N$  (from Chart 2) and  $E$  (from Figure 4) in equation 3.

Enthalpies for the heterolytic cleavage of N-F reagents, so-called Fluorine Plus Detachment (FPD) energies (eq 1), were used by Christe and Dixon in 1992 as a quantitative measure for the oxidizing strengths of “oxidative fluorinators”.<sup>42</sup> As mentioned in the introduction, Xue, Cheng, and coworkers have recently calculated FPDs for 130 fluorinating agents, including those for compounds **1–4**. Figure 12 shows that the electrophilic reactivities of the *N*-fluorinated pyridinium ions **2a–c** correlate linearly with their FPD values. In analogy to the correlation depicted in Figure 11, also Figure 12 indicates that the F-N<sub>sp3</sub> reagents **3** and **4** react significantly faster than N<sub>sp2</sub> reagents of equal FPDs.



**Figure 12.** Correlation between the rate constants ( $\log k_2$ ) for the reactions of fluorinating N-F reagents **1–4** with the enamine **5d** against the corresponding FPD values (eq 1) calculated in MeCN (taken from ref 26). Only the data for **2a–c** were used to calculate the correlation line.  
<sup>a</sup> Rate constant ( $\log k_2$ ) calculated by applying  $N$  and  $s_N$  (from Chart 2) and  $E$  (from Figure 4) in equation 3.

The role of intrinsic barriers (proportional to reorganization energies)<sup>43</sup> is best illustrated by the fact that compounds **2b**, **1**, and **3**, all of which have the same FPD value, differ by 4 orders of magnitude in electrophilicity (Figure 12). Whereas the thermodynamic FPD values thus cannot directly be correlated with rate constants, they can be used for predicting equilibrium constants: Though **4** is a stronger electrophile than **1**, **4** has been synthesized by the reaction of quinine with **1**, in line with the higher  $F^+$  affinity of quinine shown in Figure 12.

### 3.3. Conclusions

The deoxybenzoin-derived enamines **5a–f** have suitable nucleophilicities for determining the electrophilic reactivities of the fluorinating reagents **1–4** by direct rate measurements. As shown in Figure 13, Selectfluor (**3**) and the 2,6-dichloro-1-fluoro-pyridinium ion (**2c**) are by far the most reactive N-F reagents of this series, followed by the *N*-fluorinated quinine **4** and NFSI (**1**). The pyridinium ions **2a** and **2b** are at the lower end of the scale, five orders of magnitude less reactive than Selectfluor (**3**). Since the parent *N*-fluoropyridinium ion **2b** may also be attacked at C-2 of the pyridinium ion, the *N*-fluoro-substituted collidinium ion **2a** can be considered as the reagent of choice, when a mild fluorinating reagent is needed. In agreement with Togni's competition experiments,<sup>25</sup> our direct rate measurements also showed Selectfluor (**3**) to be the most reactive fluorination reagent, but in contrast to Togni's ranking,

which indicated that **3** reacts 18 times faster with carbanions than **2c**, our direct rate measurements reveal comparable fluorinating activities of **2c** and **3**.

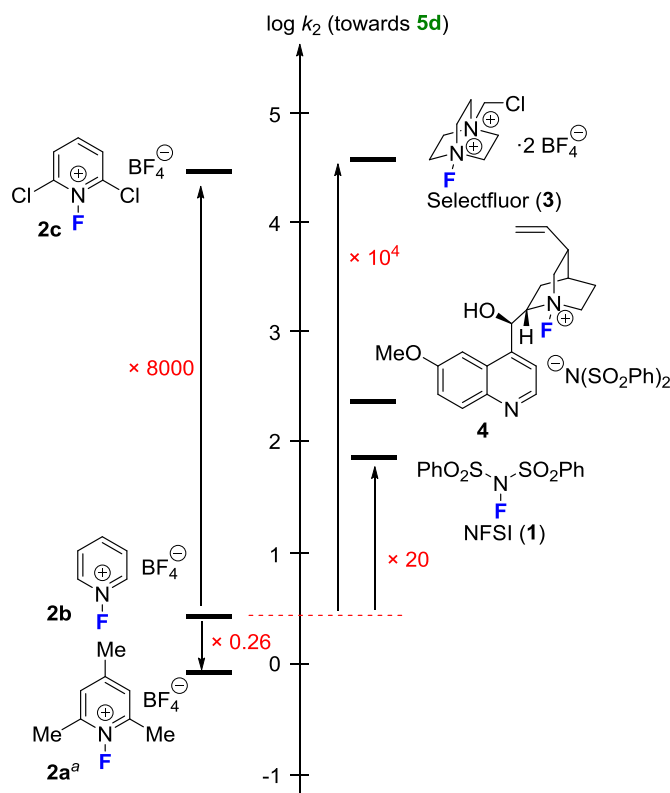


**Figure 13.** Comparison of the rate constants ( $\log k_2$ ) for the reactions of the N-F fluorinating reagents **1–4** with the deoxybenzoin-derived enamine **5d** (MeCN, 20 °C). <sup>a</sup> Rate constant ( $\log k_2$ ) calculated by applying  $N$  and  $s_N$  (from Chart 2) and  $E$  (from Figure 4) in eq 3.

Though the nature of the counterions of the cationic fluorinating agents sometimes affects the isolable yields of the fluorinations, counterions have only a small effect on the rates of the fluorine transfer. Whereas the electrophilic reactivities of the *N*-fluoropyridines **2a–c** correlate with the corresponding  $pK_a$  values and Fluorine Plus Detachment (FPD) energies, reagents **3** and **4** with F–N( $sp^3$ ) functionalities react much faster than expected from the corresponding thermodynamic quantities due to the lower intrinsic barriers of their reactions. Lower intrinsic barriers for the reactions of F–N( $sp^3$ ) reagents also explain, why **4** is a faster fluorinating agent than **1**, though **4** can be synthesized by the reaction of quinine with **1** in acetonitrile.

The rate constants of the reactions of **1–4** with the enamines **5a–f** follow the linear free energy relationship (eq 3) and were used to derive the electrophilicity parameters  $E$  for these fluorinating agents. The previously known qualitative ranking of the strengths of the fluorinating agents **1–4** has thus been quantified. In addition, the  $E$  values of **1–4** can now be combined with the tabulated reactivity parameters  $N$  and  $s_N$  of C-nucleophiles<sup>27g</sup> to derive

absolute rate constants for electrophilic fluorinations by eq 3. In this way the electrophilicity parameters  $E$  provide a quantitative basis for selecting suitable fluorinating agents and conditions for desired synthetic transformations, which will be illustrated by the following examples.

On the right of Figure 14, the electrophilic reactivities of **1–3** are compared with those of C-centered electrophiles. The left column of Figure 14 orders C-nucleophiles with increasing strengths from top to bottom, and arranges them in a way, that  $(E + N) = -3$  for electrophiles and nucleophiles that are located at the same horizontal level. Since the nucleophile-specific susceptibilities  $s_N$  are typically in the range of  $0.7 < s_N < 1.0$ , equation 3 predicts second-order rate constants from  $10^{-3}$  to  $10^{-2} \text{ M}^{-1} \text{ s}^{-1}$  at 20 °C for such electrophile-nucleophile combinations, which corresponds to half-reaction times of approximately one hour for 0.1 M solutions of the reactants. Accordingly, fluorinating reagents can be expected to undergo noncatalyzed reactions at room temperature with those nucleophiles located below them, while reactions with nucleophiles positioned higher in Figure 14 do not occur or require harsher conditions.

According to their electrophilicity parameters none of the N–F reagents in Figure 14 should be able to attack anisole, styrene, or phenylacetylene at ambient temperature. In line with this prediction heating to 70 °C for three hours was needed to fluorinate anisole with Selectfluor (**3**) or *N*-fluoropyridinium salt **2c** with 47% and 56% yield, respectively.<sup>44</sup> The fluorination of benzene, anisole, and other arenes with **3** was achieved at 0–40 °C in dichloromethane in the presence of trifluoromethanesulfonic acid. Protonated trifluoromethanesulfonyl hypofluorite was suggested to be the actual fluorinating reagent in these reactions.<sup>45</sup> The noncatalyzed fluorination of anisole with NFSI (**1**) required harsh conditions (100% conversion after 5h at 150°C with 22 equiv of anisole).<sup>12</sup>

Reactions of 1,3-dimethoxybenzene ( $N = 2.48$ ) with Selectfluor (**3**) and NFSI (**1**) were accomplished by heating to 85 to 90 °C for 1–8 hours under solvent-free conditions to yield 1-fluoro-2,4-dimethoxybenzene (78% from **3**, 73% from **1**) along with some 1,5-difluoro-2,4-dimethoxybenzene (13% from **3**, 15% from **1**).<sup>46</sup>

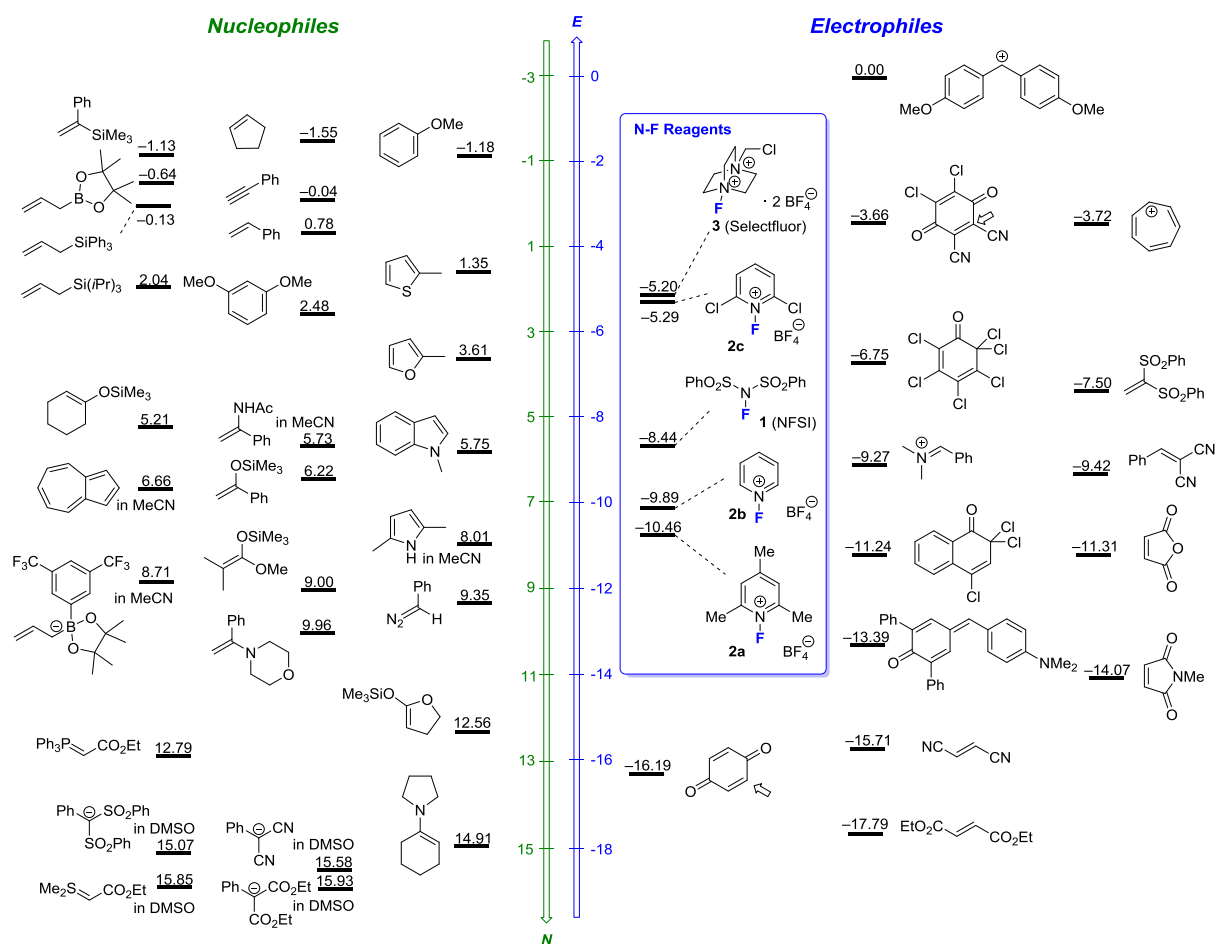


**Figure 14.** Ranking of the electrophilic fluorinating reagents **1–3** in the electrophilicity scale and scope of their reactions with nucleophiles (nucleophilicity parameters  $N$  in  $\text{CH}_2\text{Cl}_2$  if not mentioned otherwise,  $N$  and  $E$  were taken from ref 27g)

Phenylacetylene was reported to be fluorinated by Selectfluor (**3**) in refluxing  $\text{MeCN}/\text{H}_2\text{O}$  mixture within 10 to 20 h to give 2,2-difluoro-1-phenylethanone in 36% yield.<sup>47</sup> The fluorination of styrene with **3** in aqueous acetonitrile yielded 48% of the corresponding fluorohydrin at room temperature (reaction time was not given).<sup>16b</sup>

The strongest N–F reagent in this study, that is, Selectfluor (**3**), was also employed in reactions with allylsilanes, such as allyltriisopropylsilane ( $N = 2.04$ ) and allyltriphenylsilane ( $N = -0.13$ ). At room temperature, fluorohydrins were formed by “ $\text{F}^+$ ” transfer from **3** to the allylsilanes and subsequent trapping of the intermediate  $\beta$ -silyl stabilized carbenium ions by water or alcohols in acetonitrile solutions and isolated in 43–62% yield after 24–36 h reaction time.<sup>48</sup> High yielding Selectfluor-based fluorodesilylations and fluorocyclizations of allylsilanes at room temperature have been developed by Gouverneur and co-workers.<sup>49</sup>



Only 9–16 % of fluorinated product was obtained when azulene ( $N = 6.66$ ) and *N*-fluorocollidinium tetrafluoroborate (**2a**-BF<sub>4</sub>) or *N*-fluoropyridinium tetrafluoroborate (**2b**-BF<sub>4</sub>) were heated under reflux in acetonitrile for 30–60 min.<sup>50a</sup> With Selectfluor (**3**) as fluorinating reagent conversion of azulene was complete within 5 minutes at room temperature, and 34 % of 1-fluoroazulene was isolated.<sup>50b</sup> The low yields were explained by a competing SET process with formation of radical species, which initiated polymerization.

Aggarwal and co-workers<sup>51</sup> reported the fluorination of boronate complexes, similar to that depicted in Figure 14, using Selectfluor (**3**) in the absence of metal catalysts at low temperature within 16 h as a method to prepare the corresponding allyl fluorides. Based on the nucleophilicity of the boronate complexes determined from the reactions with benzhydrylium ions and electrophilicities of N-F reagents obtained in this work, one can conclude that the depicted boronate complex ( $N = 8.71$ ) should be fluorinated with any of the N-F reagents from this study.

In accord with the position of 1-(trimethylsiloxy)cyclohexene ( $N = 5.21$ ) at the same level as NFSI (**1**) in Figure 14, Differding et al. reported the fluorination of this silyl enol ether by **1** at room temperature within 24 h in dichloromethane, which after aqueous work-up, yielded 46% of 2-fluorocyclohexanone.<sup>12</sup> The reaction of 1-(trimethylsiloxy)cyclohexene with *N*-fluoropyridinium tetrafluoroborate (**2b**), for which a half reaction time of around 70 h is expected when applying equation 3, was reported to give only traces of the corresponding fluorinated ketone within 72 h at room temperature in dichloromethane. Yet, refluxing the reaction mixture for 6 h resulted in a yield of 41% of 2-fluorocyclohexanone. The corresponding reaction with **2b**-OTf yielded 87% of fluorinated product within 7 h at room temperature and the same reactions of the cyclohexanone-derived silyl enol ether with **2b**-BF<sub>4</sub> and **2b**-OTf in acetonitrile gave 54% and 83% of 2-fluorocyclohexanone, respectively, within 15 h at room temperature.<sup>14e</sup>

A series of ring-substituted acetophenone-derived silyl enol ethers was efficiently monofluorinated by Selectfluor (**3**) to furnish 2-fluoro-1-aryl-ethanones. In accord with the nucleophilicity of the parent 1-phenyl-1-(trimethylsiloxy)ethane ( $N = 6.22$ ), these fluorinations proceeded smoothly at room temperature in acetonitrile solutions (reaction times not given)<sup>52</sup> and may also be possible with the less reactive NFSI (**1**).

$\alpha$ -Fluoro- $\gamma$ -butyrolactone was obtained in 30–40% yield through the reaction of 4,5-dihydro-2-(trimethylsiloxy)furan ( $N = 12.56$ ) with *N*-fluorocollidinium triflate (**2a**) in the

presence of two equivalents of 2,6-di-*tert*-butylpyridine after 12 hours at room temperature.<sup>14c</sup> Figure 14 suggests that this reaction should be complete within seconds at room temperature.

In line with Figure 14 and the product studies with enamines in Table 1, the reaction of Selectfluor **3** (2 equiv) with  $\alpha$ -morpholinostyrene ( $N = 9.96$ ) gave 74 % of difluorinated acetophenone within 7-8 h at  $-10\text{ }^{\circ}\text{C}$ .<sup>28a</sup> According to Figure 14, this reaction should be complete after much shorter reaction time, and the fluorination of enamines is also possible with less reactive fluorination reagents (see Table 1).

In accord with their positions in Figure 14, the diethyl 2-phenylmalonate anion ( $N = 15.93$ ) and the 2-phenyl malononitrile anion ( $N = 15.58$ ) have been reported to be rapidly fluorinated by NFSI (**1**)<sup>12</sup> and fluorocollidinium salt **2a**<sup>14e</sup> at low to room temperature.

Since published reaction times for synthetic transformations often do not refer to optimized procedures, the comparison of predictions by Figure 14 and reported reaction conditions is not unambiguous. The preceding analysis shows, however, that all reported fluorination reactions with **1–4** are consistent with the pattern described in Figure 14: Combination of the electrophilicity descriptors  $E$  determined in this investigation with the tabulated reactivity parameters  $N$  and  $s_N$  for carbon nucleophiles can, therefore, be used for the design of further fluorinations.

### 3.4. Experimental Section

#### 3.4.1. General

##### Materials

Commercially available MeCN (Acros Organics, H<sub>2</sub>O content < 50 ppm) was used without further purification. The electrophilic N–F fluorinating reagents were purchased as follows: *N*-fluorobenzene-sulphonimide **1** (NFSI) and 1-fluoro-2,4,6-trimethylpyridinium triflate **2a-TfO** from ABCR Germany (97%), 1-fluoro-2,4,6-trimethylpyridinium tetrafluoroborate **2a-BF<sub>4</sub>** and 1-chloromethyl-4-fluoro-1,4-diazoniabicyclo- [2.2.2]octane bis(tetrafluoroborate) **3** (Selectfluor) from TCI (>95%), 1-fluoropyridinium tetrafluoroborate **2b** (≥ 95%) and 2,6-dichloro-1-fluoropyridinium tetrafluoroborate **2c** (97%) from Sigma-Aldrich Germany. The chemicals of less than 97% purity were recrystallized from MeCN; the others were used as received. The chiral N–F fluorinating reagent **4** was obtained as described in Section 2 from quinine (ABCR Germany; anhydrous, 98 %) and NFSI. All N–F reagents were stored under an atmosphere of argon in a glove box. Phenylacetaldehyde-derived enamines **5g** and **5h** were synthesized according to a reported procedure.<sup>53</sup> The deoxybenzoin-derived enamines **5a-f** were synthesized from the corresponding ketones and amines.<sup>27a</sup> Triflones **6a-H** and **6d-H** were synthesized by Hendrickson's procedure and purified by crystallization from pentane.<sup>53</sup> Diethyl 2-(4-nitrophenyl)malonate **6b-H** was synthesized following the procedure described before.<sup>55</sup> Compound **6e-H** were prepared by methylation of the corresponding phenylacetonitriles by using methyl iodide as described in ref.<sup>56</sup> All reactions were performed in carefully dried Schlenk glassware under N<sub>2</sub> atmosphere.

##### Analytics

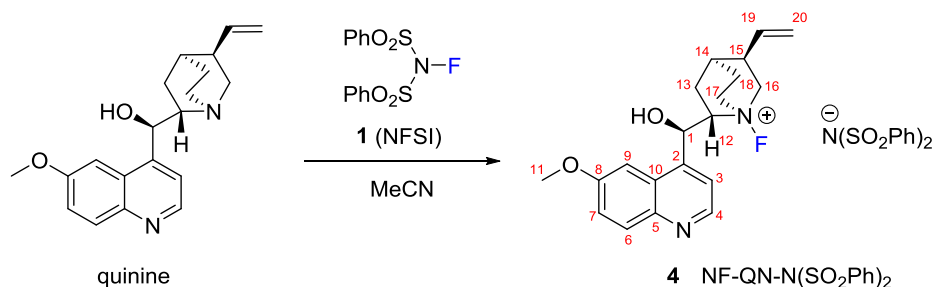
<sup>1</sup>H-NMR (400 MHz), <sup>19</sup>F NMR (376 MHz) and broadband proton-decoupled <sup>13</sup>C-NMR (100 MHz) spectra were recorded on Bruker NMR spectrometers. The chemical shifts are given in ppm and refer to the solvent residual signal as internal standard [ $\delta_{\text{H}}$  (CDCl<sub>3</sub>) = 7.26,  $\delta_{\text{C}}$  (CDCl<sub>3</sub>) = 77.16 ppm].<sup>57</sup> <sup>19</sup>F NMR spectra were recorded without decoupling. The following abbreviations were used for signal multiplicities: s = singlet, d = doublet, t = triplet, q = quartet, bs = broad signal. Signal assignments are based on additional 2D-NMR experiments (COSY, NOESY, HSQC, and HMBC). High-resolution mass spectra (HRMS) were obtained by using a Thermo Finnigan LTQ FT (ESI) or a Thermo Finnigan MAT 95 instrument (EI). Infrared (IR) spectra were either recorded on a Perkin Elmer Spectrum BX-59343 instrument with a Smiths Detection DuraSamplIR II Diamond ATR sensor for detection in the range 4500–600 cm<sup>-1</sup> either as a film for liquids or neat for solids.

### Kinetics

The rates of all investigated reactions between N–F fluorinating reagents and reference nucleophiles were determined photometrically. The kinetics of fast reactions were monitored using stopped-flow techniques (Applied Photophysics SX.20MV-R). Slow reactions ( $\tau_{1/2} > 100$  s) were determined by using a J&M TIDAS diode array spectrometer controlled by TIDASDAQ3 (v3) software and connected to a Hellma 661.502-QX quartz Suprasil immersion probe (light path  $d = 5$  mm) via fiber optic cables and standard SMA connectors. All kinetic measurements were carried out in MeCN (Acros Organics, H<sub>2</sub>O content < 50 ppm) under exclusion of moisture (N<sub>2</sub> atmosphere). The temperature of all solutions was kept constant at  $20.0 \pm 0.1$  °C by using a circulating bath thermostat. In all runs the concentration of the N–F reagents was at least 6 times higher than the concentration of the reference nucleophile, resulting in pseudo-first-order kinetics with an exponential decay of the concentration of the reference nucleophile. First-order rate constants  $k_{\text{obs}}$  [s<sup>-1</sup>] were obtained by least-squares fitting of the absorbances to a single-exponential  $A_t = A_0 \exp(-k_{\text{obs}}t) + C$  (average from 3 to 10 kinetic runs for each nucleophile concentration). The second-order rate constants  $k_2$  were obtained from the slopes of the linear plots of  $k_{\text{obs}}$  against the concentration of the excess components (typically 3 to 6 different concentrations were used for this evaluation).

#### 3.4.2. Synthesis of the N–F Reagent **4** Derived from Cinchona Alkaloid

According to Cahard,<sup>18c</sup> *N*-fluoroammonium salts of cinchona alkaloids can be obtained by transfer fluorination, using commercially available N–F reagents. The reactions with Selectfluor and other F-TEDA derivatives lead to by-products, such as monoquaternary ammonium salts, and thus require double precipitation procedures. While the reaction of cinchona alkaloid with fluorinating reagent **2c** gives the equimolar amount of 2,6-dichloropyridine, the *N*-fluorobenzenesulfonimide **1** forms only the expected chiral [N–F]<sup>+</sup> salt. Based on this report, we have chosen the [N–F]<sup>+</sup> salt **4** as the representative example to study its reactivity in comparison with achiral electrophilic fluorinating reagents. The *N*-fluoroammonium salt **4** was isolated from the reaction of quinine with NFSI (**1**) in MeCN.



A solution of **1** (200 mg, 0.634 mmol) in acetonitrile (5 mL) was added slowly to a solution of quinine (206 mg, 0.635 mmol) in acetonitrile (5 mL). The resulting mixture was stirred for 30 min, then the solvent was removed under reduced pressure, and the resulting white solid was dried in the vacuum to afford NF-QN-N(SO<sub>2</sub>Ph)<sub>2</sub> (406 mg, 100% yield).

mp 130–135 °C dec.

**<sup>1</sup>H NMR** (400 MHz, CDCl<sub>3</sub>): δ = 8.78 (d, *J* = 4.5 Hz, 1 H, 4-H), 8.05 (d, *J* = 9.2 Hz, 1 H, 6-H), 7.76 (d, *J* = 4.5 Hz, 1 H, 3-H), 7.38–7.33 (m, 5 H, 7-H and Ph), 7.16–7.12 (m, 3 H, 9-H and Ph), 6.97–6.93 (m, 4H, Ph), 6.84 (d, *J* = 5.1 Hz, 1 H, 1-H), 6.46 (d, *J* = 5.2 Hz, 1 H, OH), 5.72–5.63 (m, 1 H, 19-H), 5.36–5.28 (m, 1 H, 17-H), 5.21–5.11 (m, 3 H, 16-H and 20-H), 4.80 (bs, 1 H, H-17'), 4.09 (bs, 1 H, 12-H), 3.86 (s, 1 H, 11-H), 3.68 (bs, 2 H, 15-H and 16'-H), 2.82–2.63 (m, 3 H, 13-H and 18-H), 2.16 (bs, 1 H, 14-H), 1.96–1.87 (m, 1 H, 13'-H).

**<sup>13</sup>C {<sup>1</sup>H} NMR** (101 MHz, CDCl<sub>3</sub>): δ = 158.6 (C-8), 147.9 (C-4), 144.4 (C-5), 143.2 (C<sub>q</sub>, Ph), 143.0 (C-2), 135.5 (C-19), 132.2 (C-6), 130.6 (CH, Ph), 127.9 (CH, Ph), 126.4 (CH, Ph), 125.4 (C-10), 122.1 (C-7), 119.7 (C-3), 118.9 (C-20), 100.2 (C-9), 75.5 (d, *J*<sub>C-F</sub> = 8.9 Hz, C-12), 68.4 (d, *J*<sub>C-F</sub> = 9.2 Hz, C-16), 62.3 (C-1), 58.6 (d, *J*<sub>C-F</sub> = 8.9 Hz, C-17), 55.8 (C-11), 42.4 (C-15), 28.0 (C-18), 26.9 (C-14), 23.6 (C-13).

**<sup>19</sup>F NMR** (376 MHz, CDCl<sub>3</sub>): δ = 44.8 (s).

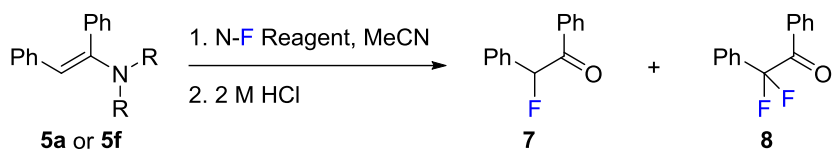
**HRMS** (ESI<sup>+</sup>): *m/z* calcd for [C<sub>20</sub>H<sub>24</sub>FN<sub>2</sub>O<sub>2</sub><sup>+</sup>]: 343.1816; found: 343.1815.

**HRMS** (ESI<sup>-</sup>): *m/z* calcd for [C<sub>12</sub>H<sub>10</sub>O<sub>4</sub>NFS<sup>-</sup>]: 296.0057; found: 296.0057.

### 3.4.3. Reaction Products

#### 3.4.3.1. Fluorination of Enamines

##### General Procedure (GP1):



To a solution of enamine in acetonitrile (5 mL) was added a solution of the N-F reagent (1.05 equiv.) in acetonitrile (5 mL). The reaction mixture was stirred for 1 h at room temperature under nitrogen atmosphere. Then the reaction mixture was stirred with 2 M HCl (20 mL) for 30 min, extracted with CH<sub>2</sub>Cl<sub>2</sub> (3 × 10 mL), the combined organic layers were washed with brine (ca 20 mL) and dried over MgSO<sub>4</sub>. The solvent was removed under reduced pressure and the crude mixture of fluoroketones was analyzed by <sup>19</sup>F NMR spectroscopy. The crude reaction products were purified by column chromatography (silica gel, pentane/ethyl acetate = 10/1) to give mono- and difluorinated deoxybenzoins **7** and **8**.

Reaction of **5a** (72 mg, 0.29 mmol) with **1** (101 mg, 0.32 mmol) by following GP1 gave a 77:23 mixture of mono- and difluorinated ketones, from which **7** (34 mg, 55%) was isolated.

Reaction of **5a** (95 mg, 0.38 mmol) with **2a**-BF<sub>4</sub> (91 mg, 0.40 mmol) by following GP1 gave a 77:23 mixture of mono- and difluorinated ketones, from which **7** (35 mg, 43%) was isolated.

Reaction of **5a** (117 mg, 0.47 mmol) with **2b**-BF<sub>4</sub> (91 mg, 0.49 mmol) by following GP1 gave a product mixture (the ratio of mono- and difluorinated ketones is 74:26), from which **7** (28 mg, 28%), **8** (9 mg, 8%) and by product **9** (14 mg, 11%) were isolated.

Reaction of **5f** (72 mg, 0.27 mmol) with **2c**-BF<sub>4</sub> (74 mg, 0.29 mmol) by following GP1 gave a 91:9 mixture of mono- and difluorinated ketones from which **7** (45 mg, 78%) was isolated.

Reaction of **5f** (105 mg, 0.40 mmol) with **3** (148 mg, 0.42 mmol) by following GP1 gave a 95:5 mixture of mono- and difluorinated ketones from which **7** (69 mg, 80%) was isolated.

**2-Fluoro-1,2-diphenylethan-1-one (7)** was isolated as white solid. The <sup>1</sup>H, <sup>13</sup>C and <sup>19</sup>F NMR spectra are in agreement with those described previously.<sup>58</sup>

mp 59–61 °C.

**$^1\text{H}$  NMR** (400 MHz,  $\text{CDCl}_3$ ):  $\delta$  = 7.96–7.93 (m, 2 H, Ph), 7.57–7.52 (m, 1 H, Ph), 7.51–7.48 (m, 2 H, Ph), 7.44–7.37 (m, 5 H, Ph), 6.52 (d,  $J_{\text{H-F}}$  = 48.6 Hz, CHF).

**$^{13}\text{C}$  { $^1\text{H}$ } NMR** (101 MHz,  $\text{CDCl}_3$ ):  $\delta$  = 194.4 ( $\text{C}_\text{q}$ , d,  $J_{\text{C-F}}$  = 21.4 Hz, C=O), 134.4 ( $\text{C}_\text{q}$ , d,  $J_{\text{C-F}}$  = 19.9 Hz, Ph), 134.2 ( $\text{C}_\text{q}$ , Ph), 133.9 (CH, Ph), 129.8 (CH, d,  $J_{\text{C-F}}$  = 2.6 Hz, Ph), 129.23 (CH, Ph), 129.22 (CH, Ph), 129.21 (CH, Ph), 127.5 (CH, d,  $J_{\text{C-F}}$  = 5.5 Hz, Ph), 94.1 (CH, d,  $J_{\text{C-F}}$  = 185.8 Hz, CHF).

**$^{19}\text{F}$  NMR** (376 MHz,  $\text{CDCl}_3$ ):  $\delta$  = 176.0 (d,  $J_{\text{H-F}}$  = 48.6 Hz).

**HRMS** (EI):  $m/z$  calcd for  $\text{C}_{14}\text{H}_{11}\text{FO}^{+\bullet}$  [ $\text{M}^{+\bullet}$ ]: 214.0788; found: 214.0783.

**IR** (ATR)  $\nu$  ( $\text{cm}^{-1}$ ) = 2961, 1689, 1593, 1577, 1491, 1448, 1357, 1332, 1302, 1261, 1223, 1189, 1176, 1158, 1080, 1054, 1027, 971, 935, 860, 842, 766, 758, 700, 694, 686, 665.

**2,2-Difluoro-1,2-diphenylethan-1-one (8)** was isolated as colorless oil. The  $^1\text{H}$ ,  $^{13}\text{C}$  and  $^{19}\text{F}$  NMR spectra are in agreement with those described previously.<sup>59</sup>

**$^1\text{H}$  NMR** (400 MHz,  $\text{CDCl}_3$ ):  $\delta$  = 8.04–8.02 (m, 2 H, Ph), 7.63–7.57 (m, 3 H, Ph), 7.50–7.42 (m, 5 H, Ph).

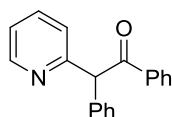
**$^{13}\text{C}$  { $^1\text{H}$ } NMR** (101 MHz,  $\text{CDCl}_3$ ):  $\delta$  = 189.1 ( $\text{C}_\text{q}$ , t,  $J_{\text{C-F}}$  = 31.1 Hz, C=O), 134.3 (CH, Ph), 133.3 ( $\text{C}_\text{q}$ , t,  $J_{\text{C-F}}$  = 25.0 Hz, Ph), 132.3 ( $\text{C}_\text{q}$ , t,  $J_{\text{C-F}}$  = 1.5 Hz, Ph), 131.1 (CH, t,  $J_{\text{C-F}}$  = 1.9 Hz, Ph), 130.4 (CH, t,  $J_{\text{C-F}}$  = 3.0 Hz, Ph), 129.0 (CH, Ph), 128.8 (CH, Ph), 125.8 (CH, t,  $J_{\text{C-F}}$  = 6.0 Hz, Ph), 117.1 (t,  $J_{\text{C-F}}$  = 253.2 Hz,  $\text{CF}_2$ ).

**$^{19}\text{F}$  NMR** (376 MHz,  $\text{CDCl}_3$ ):  $\delta$  = -97.5 (s).

**HRMS** (EI):  $m/z$  calcd for  $\text{C}_{14}\text{H}_{10}\text{F}_2\text{O}^{+\bullet}$  [ $\text{M}^{+\bullet}$ ]: 232.0694; found: 232.0662.

**IR** (ATR)  $\nu$  ( $\text{cm}^{-1}$ ) = 3064, 1699, 1597, 1579, 1449, 1308, 1237, 1162, 1118, 1067, 1007, 894, 857, 758, 711, 693, 683.

**1,2-Diphenyl-2-(pyridin-2-yl)ethan-1-one (9)** was isolated as orange solid. The  $^1\text{H}$  and  $^{13}\text{C}$  are in agreement with those described previously.<sup>60</sup> NMR shows ca 10 % of contaminations by further unidentified by products.

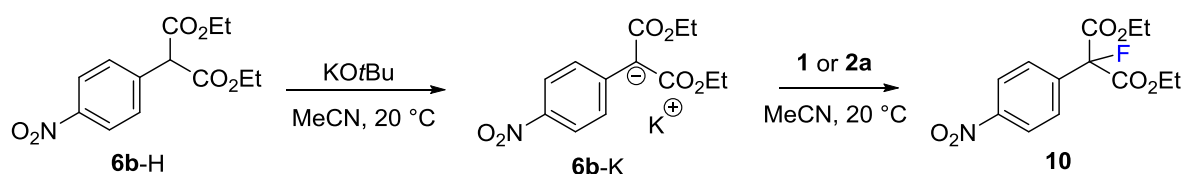


**$^1\text{H}$  NMR** (400 MHz,  $\text{CDCl}_3$ ): 8.56–8.54 (m, 2 H), 8.04–8.02 (m, 2 H), 7.65–7.60 (m, 1 H), 7.42–7.35 (m, 5 H), 7.29–7.27 (m, 2 H), 7.17–7.14 (m, 2 H), 6.29 (s, 1 H).

**$^{13}\text{C}$  { $^1\text{H}$ } NMR** (101 MHz,  $\text{CDCl}_3$ ): 197.6 (C=O), 159.5, 149.5, 137.8, 136.8, 133.2, 129.3, 129.2, 129.1, 128.7, 127.6, 124.0, 122.1, 62.3. One of  $\text{C}_q$  was not detected.

**HRMS** (EI):  $m/z$  calcd for  $\text{C}_{19}\text{H}_{15}\text{NO}^{+}$  [ $\text{M}^{+}$ ]: 273.1148; found: 273.1151.

#### 4.3.3.2. Fluorination of Carbanion **6b** with **1** and **2a**



The salt **6b-K** was generated by addition of a solution of **6b-H** (100 mg, 0.36 mmol) to KOtBu (43 mg, 0.38 mmol 1.05 equiv.) in dry acetonitrile (5 mL). Subsequently, a solution of the N-F reagent (1.1 equiv., **1**: 122 mg, 0.40 mmol or **2a**: 90 mg, 0.40 mmol) in acetonitrile (5 mL) was added. The mixture was stirred for 5 min before 2 M aq HCl (ca 20 mL) was added. The mixture was extracted with  $\text{CH}_2\text{Cl}_2$  ( $3 \times 10$  mL), the combined organic layers were washed with brine (20 mL) and dried over  $\text{MgSO}_4$ . The solvent was removed under reduced pressure and the crude product was purified by column chromatography (silica gel, pentane/ethyl acetate = 10/1) to give the fluoromalonate **10** as a colorless oil (95 mg, 0.32 mmol, 88% yield starting from **1** and 63 mg, 0.21 mmol, 57 % yield starting from **2a**)

**$^1\text{H}$  NMR** (400 MHz,  $\text{CDCl}_3$ ):  $\delta$  = 8.28–8.25 (m, 2 H, Ar), 7.85–7.82 (m, 2 H, Ar), 4.34 (q,  $J$  = 7.1 Hz, 4 H,  $\text{CH}_2$ ), 1.32 (t,  $J$  = 7.1 Hz, 6 H,  $\text{CH}_3$ ).

**$^{13}\text{C}$  { $^1\text{H}$ } NMR** (101 MHz,  $\text{CDCl}_3$ ):  $\delta$  = 164.7 ( $\text{C}_q$ , d,  $J_{\text{C-F}}$  = 25.3 Hz, C=O), 148.7 ( $\text{C}_q$ , Ar), 139.6 ( $\text{C}_q$ , d,  $J_{\text{C-F}}$  = 22.3 Hz, Ar), 127.1 (CH, d,  $J_{\text{C-F}}$  = 9.6 Hz, Ar), 123.5 (CH, d,  $J_{\text{C-F}}$  = 1.9 Hz, Ar), 93.6 ( $\text{C}_q$ , d,  $J_{\text{C-F}}$  = 204.1 Hz, CF), 63.7 ( $\text{CH}_2$ ), 14.0 ( $\text{CH}_3$ ).

**$^{19}\text{F}$  NMR** (376 MHz,  $\text{CDCl}_3$ ):  $\delta$  = 163.2 (s).

**HRMS** (EI):  $m/z$  calcd for  $\text{C}_{13}\text{H}_{15}\text{FNO}_6$  [ $\text{M}+\text{H}$ ] $^+$ : 300.0878; found: 300.0878.

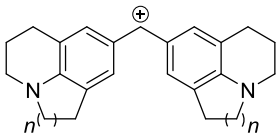
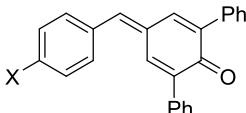
**IR** (ATR)  $\nu$  ( $\text{cm}^{-1}$ ) = 2984, 1752, 1608, 1524, 1495, 1467, 1446, 1368, 1349, 1300, 1269, 1215, 1129, 1092, 1042, 1024, 1013, 856, 816, 778, 736, 693, 664.



### 3.4.4. Determination of $N$ and $s_N$ Parameters for Carbanion **6c** in DMSO

The nucleophilicity parameters  $N$  and  $s_N$  of carbanion **6c** in DMSO were determined by using the same methods as reported in our previous article<sup>61</sup> on related acceptor-substituted phenacyl anions ( $\text{PhCO}-\text{CH}^--\text{Acc}$ ) from the rates of its reactions with benzhydrylium ions and structurally related quinone methides (Table S1). The potassium salt **6c** was generated by treatment of the CH acid **6c-H** with  $\text{KO}^t\text{Bu}$  in ethanol and isolated after washing the precipitated salt with dry diethyl ether.

**Table S1.** Benzhydrylium ions and quinone methides used as reference electrophiles for the determination of the nucleophilicity parameter ( $N$ ,  $s_N$ ) of **6c** in DMSO.

Electrophile			$E^{33b,c}$	$\lambda_{\text{max}}$ in DMSO
	$n = 2$	<b>11a</b>	-9.45	644 nm
	$n = 1$	<b>11b</b>	-10.04	640 nm
	$X = \text{H}$	<b>11h</b>	-11.87	384 nm
	$X = \text{NMe}_2$	<b>11i</b>	-13.39	533 nm

The kinetics of the reactions of the potassium salt (**6c**)-K with the reference electrophiles were monitored by UV/Vis spectroscopy at the absorption maxima of the colored electrophile in DMSO solution at 20 °C (Table S1) by using stopped-flow techniques. All kinetic measurements were carried out in DMSO (Acros Organics,  $\text{H}_2\text{O}$  content < 50 ppm) under exclusion of moisture ( $\text{N}_2$  atmosphere). To simplify the evaluation of the kinetic experiments, the **6c** was used in large excess (> 8 equiv.). Thus, the concentrations of **6c** remained almost constant throughout the reactions, and pseudo-first-order kinetics were obtained in all runs. The pseudo-first-order rate constants  $k_{\text{obs}}$  were obtained as described in part 1 of this Supporting Information. The second-order rate constants  $k_2$  were obtained as the slopes of linear correlations of  $k_{\text{obs}}$  with the concentrations of the carbanion.

Some pseudo-first-order rate constants  $k_{\text{obs}}$  were measured in the presence of 18-crown-6 ether (1.05 equiv. with respect to the potassium ions). As found in the reactions with other carbanions, the  $k_{\text{obs}}$  values for the reactions of the carbanion **6c** with reference electrophiles obtained either with or without added crown ether were on the same linear  $k_{\text{obs}}$  vs. nucleophile concentration plots, indicating that the determined rate constants correspond to the reactivities of the non-paired anions.

**Table S2.** Kinetics of the reaction of **11a** with **6c** in DMSO (20 °C, stopped-flow,  $\lambda = 644$  nm)

[ <b>11a</b> ]/ mol L <sup>-1</sup>	[ <b>6c</b> ]/ mol L <sup>-1</sup>	[18-crown-6]/ mol L <sup>-1</sup>	[ <b>6c</b> ]/[ <b>E</b> ]	$k_{\text{obs}}/\text{s}^{-1}$
$9.18 \times 10^{-6}$	$1.73 \times 10^{-4}$	$1.82 \times 10^{-4}$	18.8	82.5
	$2.62 \times 10^{-4}$		28.5	121
	$3.45 \times 10^{-4}$		37.6	155
	$4.35 \times 10^{-4}$	$4.57 \times 10^{-4}$	47.4	191
	$5.18 \times 10^{-4}$		56.4	225

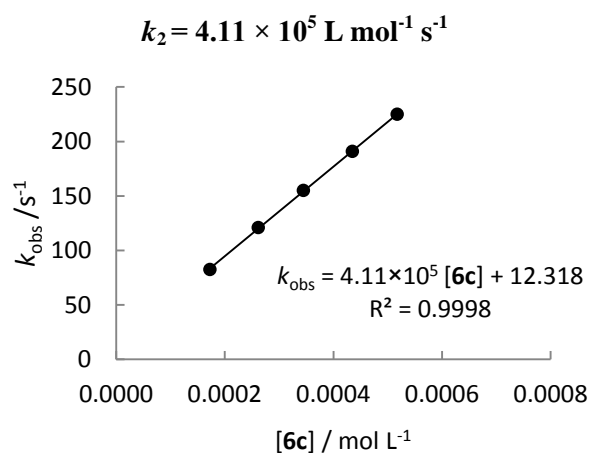


**Table S3.** Kinetics of the reaction of **11b** with **6c** in DMSO (20 °C, stopped-flow,  $\lambda = 640$  nm)

[ <b>11b</b> ]/ mol L <sup>-1</sup>	[ <b>6c</b> ]/ mol L <sup>-1</sup>	[18-crown-6]/ mol L <sup>-1</sup>	[ <b>6c</b> ]/[ <b>11b</b> ]	$k_{\text{obs}}/\text{s}^{-1}$
$1.51 \times 10^{-5}$	$1.73 \times 10^{-4}$	$1.82 \times 10^{-4}$	11.5	31.1
	$2.62 \times 10^{-4}$		17.4	44.6
	$3.45 \times 10^{-4}$		22.8	58.4
	$4.35 \times 10^{-4}$	$4.57 \times 10^{-4}$	28.8	71.3
	$5.18 \times 10^{-4}$		34.3	83.2

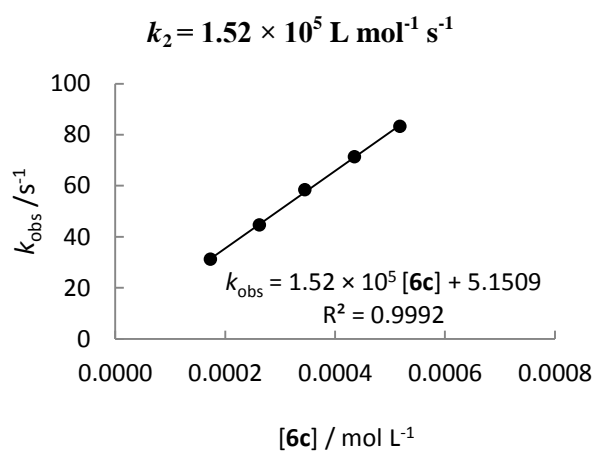


**Table S4.** Kinetics of the reaction of **11h** with **6c** in DMSO (20 °C, stopped-flow,  $\lambda = 384$  nm)

[ <b>11h</b> ]/ mol L <sup>-1</sup>	[ <b>6c</b> ]/ mol L <sup>-1</sup>	[18-crown-6]/ mol L <sup>-1</sup>	[ <b>6c</b> ]/[ <b>11h</b> ]	$k_{\text{obs}}/\text{s}^{-1}$
$2.15 \times 10^{-5}$	$1.73 \times 10^{-4}$	$1.82 \times 10^{-4}$	8.0	$9.05 \times 10^{-1}$
	$2.62 \times 10^{-4}$		12.2	1.32
	$3.45 \times 10^{-4}$		16.0	1.77
	$4.35 \times 10^{-4}$	$4.57 \times 10^{-4}$	20.2	2.26
	$5.18 \times 10^{-4}$		24.1	2.69

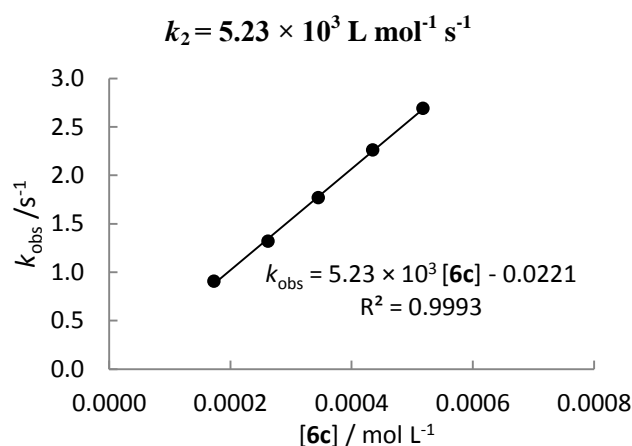
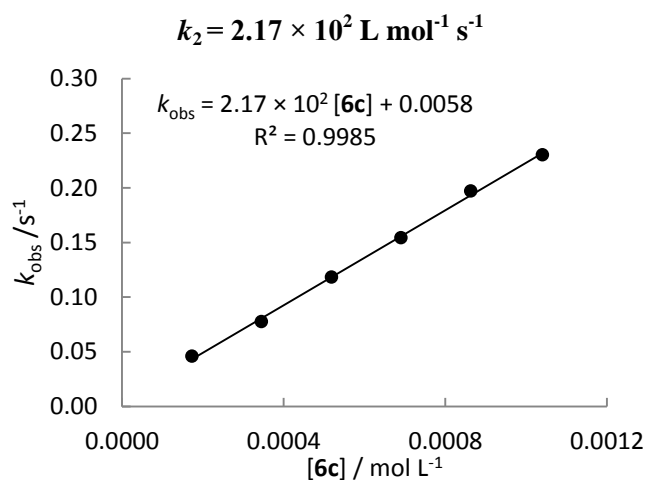


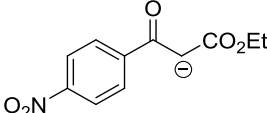
**Table S5.** Kinetics of the reaction of **11i** with **6c** in DMSO (20 °C, stopped-flow,  $\lambda = 533$  nm)

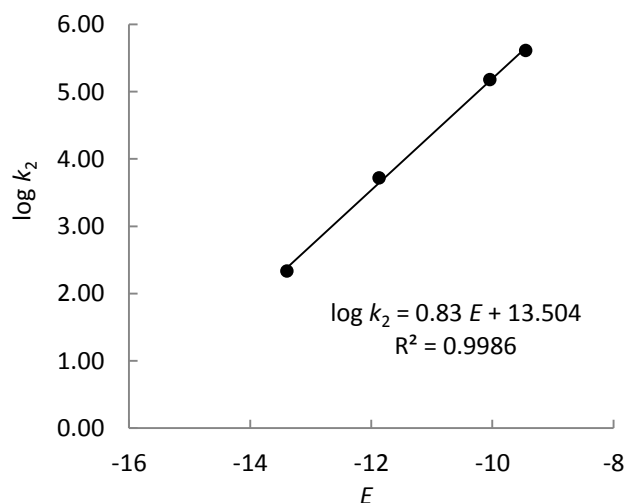
[ <b>11i</b> ]/ mol L <sup>-1</sup>	[ <b>6c</b> ]/ mol L <sup>-1</sup>	[18-crown-6]/ mol L <sup>-1</sup>	[ <b>6c</b> ]/[ <b>11i</b> ]	$k_{\text{obs}}/\text{s}^{-1}$
$1.06 \times 10^{-5}$	$1.73 \times 10^{-4}$	$1.82 \times 10^{-4}$	16.3	$4.58 \times 10^{-2}$
	$3.45 \times 10^{-4}$		32.5	$7.75 \times 10^{-2}$
	$5.18 \times 10^{-4}$		48.9	$1.18 \times 10^{-1}$
	$6.90 \times 10^{-4}$		65.1	$1.54 \times 10^{-1}$
	$8.63 \times 10^{-4}$	$9.06 \times 10^{-4}$	81.4	$1.97 \times 10^{-1}$
	$1.04 \times 10^{-3}$		98.1	$2.30 \times 10^{-1}$



Linear correlation was obtained for  $\log k_2$  of the reactions of the carbanion **6c** with the reference electrophiles and their electrophilicity parameters  $E$ , as depicted below. The slope of this linear correlation corresponds to the  $s_N$  parameter (0.83) and the intercept divided by  $s_N$  corresponds to the  $N$  parameter (16.26) of carbanion **6c**.

**Table S6.** Second-order rate constants  $k_2$  for the reactions of the carbanion **6c** with the reference electrophiles in DMSO at 20 °C.

Nucleophile	Electrophile	$E$	$k_2 / \text{L mol}^{-1} \text{s}^{-1}$
 $N = 16.26$ $s_N = 0.83$	<b>11a</b>	-9.45	$4.11 \times 10^5$
	<b>11b</b>	-10.04	$1.52 \times 10^5$
	<b>11h</b>	-11.87	$5.23 \times 10^3$
	<b>11i</b>	-13.39	$2.17 \times 10^2$



### 3.4.5. Determination of Rate Constants of the Electrophilic Fluorination

#### 3.4.5.1. Kinetic Investigations of the Reactions of NFSI (**1**) with Enamines **5**

**Table S7.** Kinetics of the reaction of **1** with **5a** in MeCN (20 °C, stopped-flow,  $\lambda = 315$  nm)

[ <b>5a</b> ]/ mol L <sup>-1</sup>	[ <b>1</b> ]/ mol L <sup>-1</sup>	[ <b>1</b> ]/[ <b>5a</b> ]	$k_{\text{obs}} / \text{s}^{-1}$
$1.06 \times 10^{-4}$	$1.11 \times 10^{-3}$	10.5	$3.03 \times 10^{-1}$
	$2.21 \times 10^{-3}$	20.8	$6.31 \times 10^{-1}$
	$3.32 \times 10^{-3}$	31.3	$9.57 \times 10^{-1}$
	$4.43 \times 10^{-3}$	41.8	1.30
	$5.53 \times 10^{-3}$	52.2	1.63
$k_2 = 3.00 \times 10^2 \text{ L mol}^{-1} \text{ s}^{-1}$			

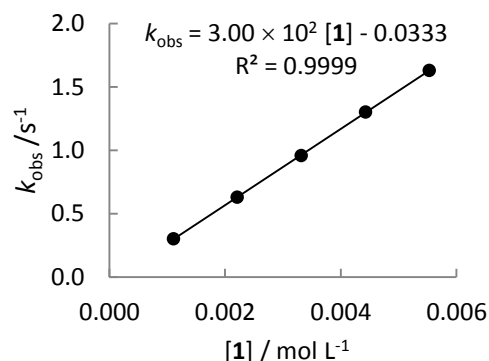


**Table S8.** Kinetics of the reaction of **1** with **5b** in MeCN (20 °C, stopped-flow,  $\lambda = 300$  nm)

[ <b>5b</b> ]/ mol L <sup>-1</sup>	[ <b>1</b> ]/ mol L <sup>-1</sup>	[ <b>1</b> ]/[ <b>5b</b> ]	$k_{\text{obs}} / \text{s}^{-1}$
$1.08 \times 10^{-4}$	$1.17 \times 10^{-3}$	10.8	$6.89 \times 10^{-1}$
	$1.67 \times 10^{-3}$	15.5	1.00
	$2.17 \times 10^{-3}$	20.1	1.34
	$2.84 \times 10^{-3}$	26.3	1.70
	$3.34 \times 10^{-3}$	30.9	2.03
$k_2 = 6.13 \times 10^2 \text{ L mol}^{-1} \text{ s}^{-1}$			

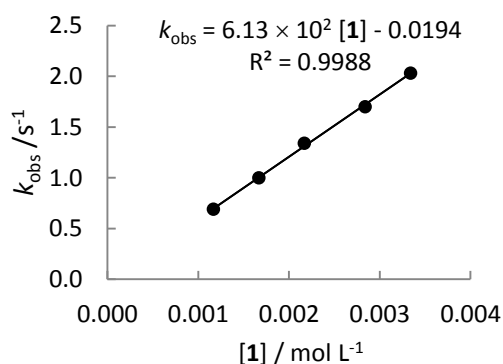


**Table S9.** Kinetics of the reaction of **1** with **5c** in MeCN (20 °C, stopped-flow,  $\lambda = 375$  nm)

[ <b>5c</b> ]/ mol L <sup>-1</sup>	[ <b>1</b> ]/ mol L <sup>-1</sup>	[ <b>1</b> ]/[ <b>5c</b> ]	$k_{\text{obs}} / \text{s}^{-1}$
$3.64 \times 10^{-5}$	$5.64 \times 10^{-4}$	15.5	$6.59 \times 10^{-2}$
	$9.67 \times 10^{-4}$	26.6	$1.12 \times 10^{-1}$
	$1.37 \times 10^{-3}$	37.6	$1.59 \times 10^{-1}$
	$1.77 \times 10^{-3}$	48.6	$2.05 \times 10^{-1}$
	$2.18 \times 10^{-3}$	59.9	$2.56 \times 10^{-1}$
$k_2 = 1.17 \times 10^2 \text{ L mol}^{-1} \text{ s}^{-1}$			

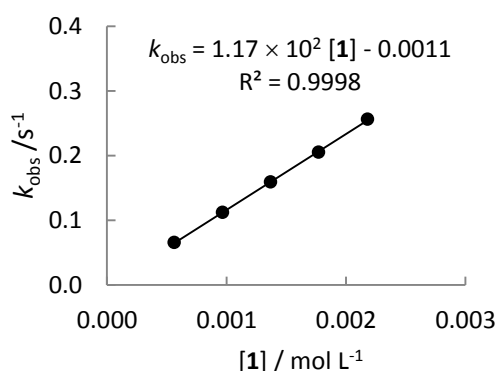


**Table S10.** Kinetics of the reaction of **1** with **5d** in MeCN (20 °C, stopped-flow,  $\lambda = 465$  nm)

[ <b>5d</b> ]/ mol L <sup>-1</sup>	[ <b>1</b> ]/ mol L <sup>-1</sup>	[ <b>1</b> ]/[ <b>5d</b> ]	$k_{\text{obs}} / \text{s}^{-1}$
$3.74 \times 10^{-5}$	$6.70 \times 10^{-4}$	17.9	$6.01 \times 10^{-2}$
	$1.34 \times 10^{-3}$	35.8	$1.12 \times 10^{-1}$
	$2.01 \times 10^{-3}$	53.7	$1.62 \times 10^{-1}$
	$2.68 \times 10^{-3}$	71.7	$2.16 \times 10^{-1}$
	$3.35 \times 10^{-3}$	89.6	$2.62 \times 10^{-1}$
	$4.19 \times 10^{-3}$	112.0	$3.20 \times 10^{-1}$

$$k_2 = 7.41 \times 10^1 \text{ L mol}^{-1} \text{ s}^{-1}$$

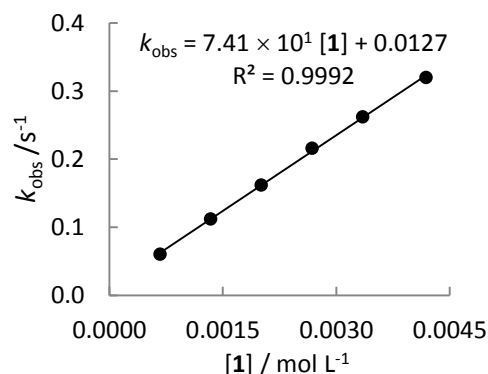


**Table S11.** Kinetics of the reaction of **1** with **5e** in MeCN (20 °C, stopped-flow,  $\lambda = 316$  nm)

[ <b>5e</b> ]/ mol L <sup>-1</sup>	[ <b>1</b> ]/ mol L <sup>-1</sup>	[ <b>1</b> ]/[ <b>5e</b> ]	$k_{\text{obs}} / \text{s}^{-1}$
$7.97 \times 10^{-5}$	$9.12 \times 10^{-4}$	11.4	$1.13 \times 10^{-2}$
	$1.82 \times 10^{-3}$	22.8	$2.16 \times 10^{-2}$
	$2.74 \times 10^{-3}$	34.4	$3.16 \times 10^{-2}$
	$3.65 \times 10^{-3}$	45.8	$4.15 \times 10^{-2}$
	$4.56 \times 10^{-3}$	57.2	$5.18 \times 10^{-2}$

$$k_2 = 1.11 \times 10^1 \text{ L mol}^{-1} \text{ s}^{-1}$$

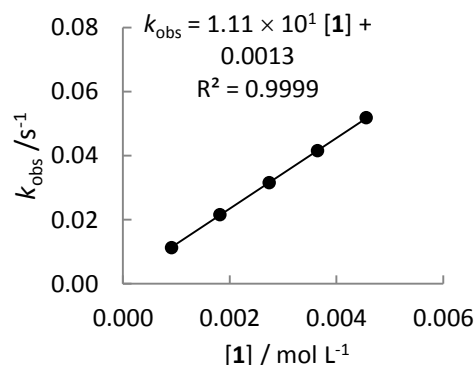


**Table S12.** Kinetics of the reaction of **1** with **5f** in MeCN (20 °C, stopped-flow,  $\lambda = 310$  nm)

[ <b>5f</b> ]/ mol L <sup>-1</sup>	[ <b>1</b> ]/ mol L <sup>-1</sup>	[ <b>1</b> ]/[ <b>5f</b> ]	$k_{\text{obs}} / \text{s}^{-1}$
$1.03 \times 10^{-4}$	$9.80 \times 10^{-4}$	9.5	$3.83 \times 10^{-3}$
	$2.94 \times 10^{-3}$	28.5	$8.70 \times 10^{-3}$
	$4.90 \times 10^{-3}$	47.6	$1.45 \times 10^{-2}$

$$k_2 = 2.72 \text{ L mol}^{-1} \text{ s}^{-1}$$

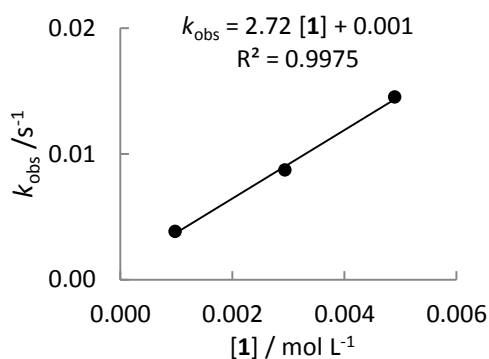


**Table S13.** Kinetics of the reaction of **1** with **5g** in MeCN (20 °C, stopped-flow,  $\lambda = 310$  nm)

[ <b>5g</b> ]/ mol L <sup>-1</sup>	[ <b>1</b> ]/ mol L <sup>-1</sup>	[ <b>1</b> ]/[ <b>5g</b> ]	$k_{\text{obs}} / \text{s}^{-1}$
$1.01 \times 10^{-4}$	$9.31 \times 10^{-4}$	9.2	$2.18 \times 10^{-1}$
	$1.86 \times 10^{-3}$	18.4	$4.36 \times 10^{-1}$
	$2.79 \times 10^{-3}$	27.6	$6.54 \times 10^{-1}$
	$3.72 \times 10^{-3}$	36.8	$8.82 \times 10^{-1}$
	$4.65 \times 10^{-3}$	46.0	1.12

$$k_2 = 2.42 \times 10^2 \text{ L mol}^{-1} \text{ s}^{-1}$$

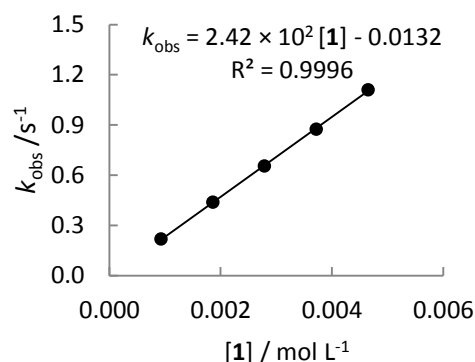


**Table S14.** Kinetics of the reaction of **1** with **5h** in MeCN (20 °C, stopped-flow,  $\lambda = 300$  nm)

[ <b>5h</b> ]/ mol L <sup>-1</sup>	[ <b>1</b> ]/ mol L <sup>-1</sup>	[ <b>1</b> ]/[ <b>5h</b> ]	$k_{\text{obs}} / \text{s}^{-1}$
$6.34 \times 10^{-5}$	$8.48 \times 10^{-4}$	13.4	$2.46 \times 10^{-2}$
	$1.70 \times 10^{-3}$	26.8	$4.36 \times 10^{-2}$
	$2.54 \times 10^{-3}$	40.1	$6.29 \times 10^{-2}$
	$3.39 \times 10^{-3}$	53.5	$8.41 \times 10^{-2}$
	$4.24 \times 10^{-3}$	66.9	$1.05 \times 10^{-1}$

$$k_2 = 2.38 \times 10^1 \text{ L mol}^{-1} \text{ s}^{-1}$$

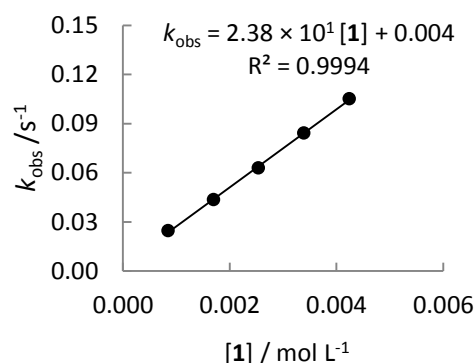


**Table S15.** Determination of the reactivity parameter  $E$  of NFSI (**1**) towards enamines in MeCN

Nucleophile	$N$ (MeCN)	$s_N$ (MeCN)	$k_2 / \text{L mol}^{-1} \text{ s}^{-1}$	$\log k_2$	$\log k_2/s_N$
<b>5a</b>	11.66	0.82	$3.00 \times 10^2$	2.48	3.02
<b>5b</b>	11.99	0.84	$6.13 \times 10^2$	2.79	3.32
<b>5c</b>	10.63	0.84	$1.17 \times 10^2$	2.07	2.46
<b>5d</b>	10.42	0.82	$7.41 \times 10^1$	1.87	2.28
<b>5e</b>	9.94	0.86	$1.11 \times 10^1$	1.05	1.22
<b>5f</b>	8.78	0.83	2.72	0.43	0.52
<b>5g</b> <sup>a</sup>	13.87	0.76	$2.42 \times 10^2$	2.38	3.13
<b>5h</b> <sup>a</sup>	11.66	0.83	$2.38 \times 10^1$	1.38	1.66

<sup>a</sup> Aminostyrenes **5g** and **5h** were not used in the correlation for determination of electrophilicity parameter  $E$ .

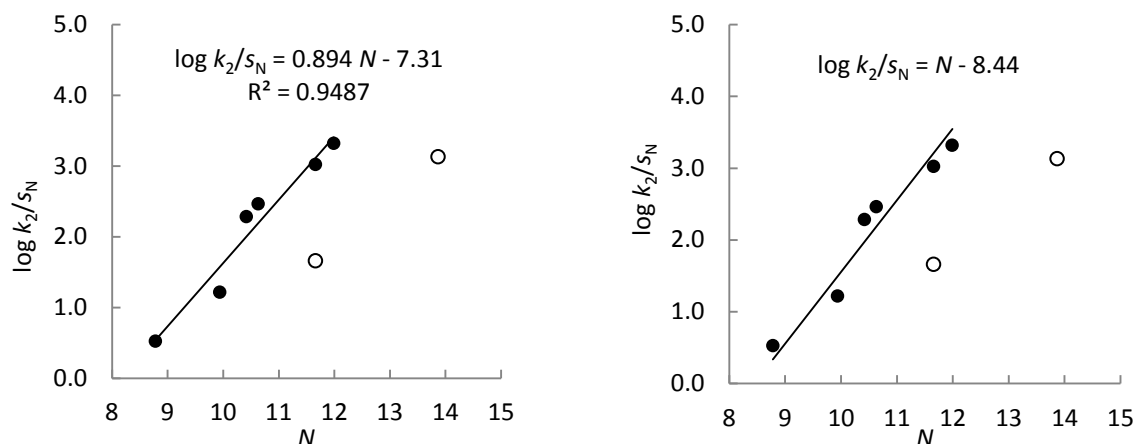


**Figure S1.** Correlations of  $(\log k_2)/s_N$  versus the nucleophilicity of enamines **5a–f** (determined in MeCN) for their reactions with NFSI (**1**) in MeCN at 20 °C: as obtained (left) and with slope enforced to 1.0, as required by eq (3) (right). Open circles:  $\beta$ -aminostyrenes **5g,h**, which were not used for the determination of  $E$  parameter.

### 3.4.5.2. Kinetic Investigations of the Reactions of NFSI (**1**) with Carbanions **6**

**Table S16.** Kinetics of the reaction of **1** with **6a** in MeCN (20 °C, stopped-flow,  $\lambda = 476$  nm)

$[\mathbf{6a}]/\text{mol L}^{-1}$	$[\mathbf{1}]/\text{mol L}^{-1}$	$[\mathbf{1}]/[\mathbf{6a}]$	$k_{\text{obs}}/\text{s}^{-1}$
$4.76 \times 10^{-5}$	$7.67 \times 10^{-4}$	16.1	$1.45 \times 10^{-1}$
	$1.15 \times 10^{-3}$	24.2	$2.00 \times 10^{-1}$
	$1.53 \times 10^{-3}$	32.1	$2.45 \times 10^{-1}$
	$1.92 \times 10^{-3}$	40.3	$2.91 \times 10^{-1}$
	$2.30 \times 10^{-3}$	48.3	$3.41 \times 10^{-1}$
	$2.69 \times 10^{-3}$	56.5	$3.96 \times 10^{-1}$
	$3.07 \times 10^{-3}$	64.5	$4.45 \times 10^{-1}$

$$k_2 = 1.29 \times 10^2 \text{ L mol}^{-1} \text{ s}^{-1}$$

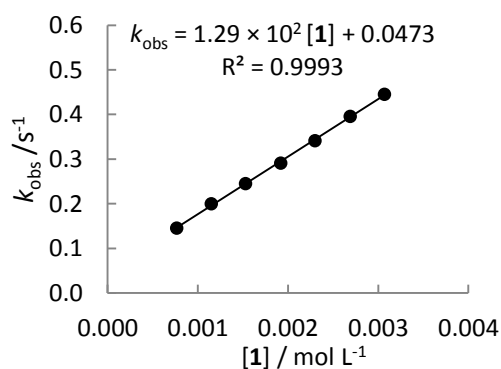




**Table S17.** Kinetics of the reaction of **1** with **6b** in MeCN (20 °C, stopped-flow,  $\lambda = 530$  nm)

[ <b>6b</b> ]/ mol L <sup>-1</sup>	[ <b>1</b> ]/ mol L <sup>-1</sup>	[ <b>1</b> ]/[ <b>6b</b> ]	$k_{\text{obs}} / \text{s}^{-1}$
$5.62 \times 10^{-5}$	$5.53 \times 10^{-4}$	9.8	$4.23 \times 10^{-1}$
	$1.11 \times 10^{-3}$	19.8	$8.48 \times 10^{-1}$
	$1.66 \times 10^{-3}$	29.5	1.28
	$2.21 \times 10^{-3}$	39.3	1.68
	$2.77 \times 10^{-3}$	49.3	2.14

$$k_2 = 7.71 \times 10^2 \text{ L mol}^{-1} \text{ s}^{-1}$$

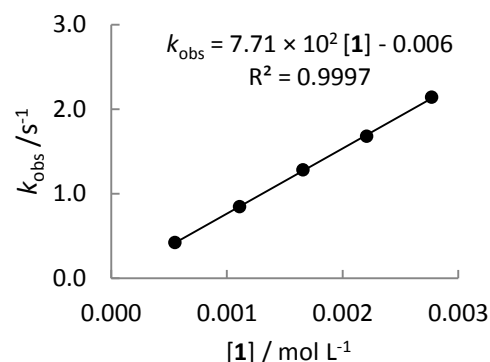


**Table S18.** Kinetics of the reaction of **1** with **6c** in MeCN (20 °C, stopped-flow,  $\lambda = 450$  nm)

[ <b>6c</b> ]/ mol L <sup>-1</sup>	[ <b>1</b> ]/ mol L <sup>-1</sup>	[ <b>1</b> ]/[ <b>6c</b> ]	$k_{\text{obs}} / \text{s}^{-1}$
$2.66 \times 10^{-4}$	$2.32 \times 10^{-3}$	8.7	2.23
	$3.47 \times 10^{-3}$	13.0	3.34
	$4.63 \times 10^{-3}$	17.4	4.37
	$5.79 \times 10^{-3}$	21.8	5.76
	$6.93 \times 10^{-3}$	26.1	6.89

$$k_2 = 1.02 \times 10^3 \text{ L mol}^{-1} \text{ s}^{-1}$$

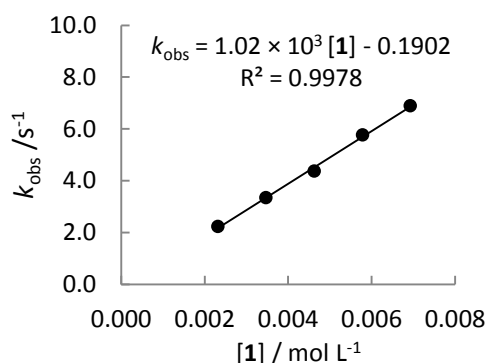


**Table S19.** Kinetics of the reaction of **1** with **6d** in MeCN (20 °C, stopped-flow,  $\lambda = 305$  nm)

[ <b>6d</b> ]/ mol L <sup>-1</sup>	[ <b>1</b> ]/ mol L <sup>-1</sup>	[ <b>1</b> ]/[ <b>6d</b> ]	$k_{\text{obs}} / \text{s}^{-1}$
$5.91 \times 10^{-5}$	$6.11 \times 10^{-4}$	10.3	$6.78 \times 10^{-1}$
	$1.22 \times 10^{-3}$	20.6	1.08
	$1.83 \times 10^{-3}$	31.0	1.45
	$2.44 \times 10^{-3}$	41.3	1.83

$$k_2 = 6.28 \times 10^2 \text{ L mol}^{-1} \text{ s}^{-1}$$

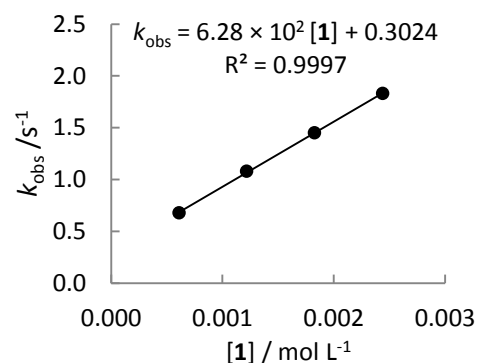


**Table S20.** Kinetics of the reaction of **1** with **6e** in MeCN (20 °C, stopped-flow,  $\lambda = 590$  nm)

[ <b>6e</b> ]/ mol L <sup>-1</sup>	[ <b>1</b> ]/ mol L <sup>-1</sup>	[ <b>1</b> ]/[ <b>6e</b> ]	$k_{\text{obs}} / \text{s}^{-1}$
$1.39 \times 10^{-4}$	$1.95 \times 10^{-3}$	14.0	$4.95 \times 10^1$
	$2.60 \times 10^{-3}$	18.7	$5.78 \times 10^1$
	$3.25 \times 10^{-3}$	23.4	$6.56 \times 10^1$
	$3.90 \times 10^{-3}$	28.1	$7.44 \times 10^1$

  
 $k_2 = 1.27 \times 10^4 \text{ L mol}^{-1} \text{ s}^{-1}$ 
  

**Table S21.** Reactivity of NFSI (**1**) towards carbanions **6** in MeCN.

Nucleophile	$N$ (DMSO)	$s_N$ (DMSO)	$k_2 / \text{L mol}^{-1} \text{ s}^{-1}$	$\log k_2$	$\log k_2/s_N$
<b>6a</b>	14.49	0.86	$1.29 \times 10^2$	2.11	2.45
<b>6b</b>	14.96	0.96	$7.71 \times 10^2$	2.89	3.01
<b>6c</b>	16.26	0.83	$1.02 \times 10^3$	3.01	3.62
<b>6d</b>	17.33	0.74	$6.28 \times 10^2$	2.80	3.78
<b>6e</b>	19.61	0.60	$1.27 \times 10^4$	4.10	6.84

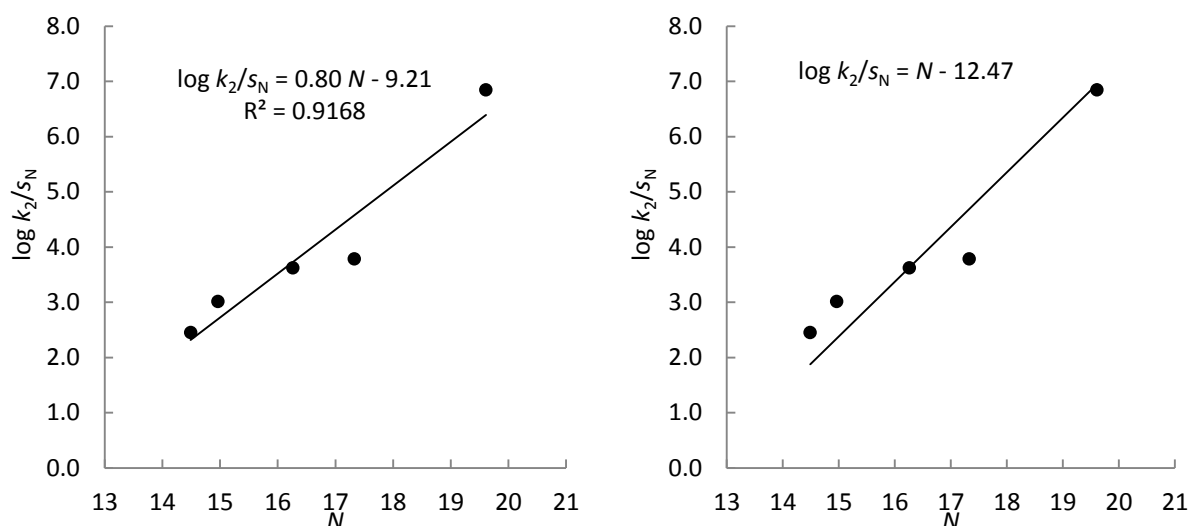


**Figure S2.** Correlations of  $(\log k_2)/s_N$  versus the nucleophilicity of carbanions **6a–e** (determined in DMSO) for their reactions with NFSI (**1**) in MeCN at 20 °C: as obtained (left) and with slope enforced to 1.0, as required by eq (3) (right).

### 3.4.5.3. Kinetic Investigations of the Reactions of *N*-Fluoro-2,4,6-trimethylpyridinium Tetrafluoroborate (**2a**-BF<sub>4</sub>) with Enamines **5**

**Table S22.** Kinetics of the reaction of **2a**-BF<sub>4</sub> with **5a** in MeCN (20 °C, stopped-flow,  $\lambda = 317$  nm)

[ <b>5a</b> ]/ mol L <sup>-1</sup>	[ <b>2a</b> -BF <sub>4</sub> ]/ mol L <sup>-1</sup>	[ <b>2a</b> -BF <sub>4</sub> ]/ [ <b>5a</b> ]	$k_{\text{obs}} / \text{s}^{-1}$
$8.85 \times 10^{-5}$	$1.19 \times 10^{-3}$	13.4	$1.40 \times 10^{-2}$
	$2.39 \times 10^{-3}$	27.0	$2.37 \times 10^{-2}$
	$3.58 \times 10^{-3}$	40.5	$3.98 \times 10^{-2}$
	$4.78 \times 10^{-3}$	54.0	$5.17 \times 10^{-2}$
	$5.97 \times 10^{-3}$	67.5	$6.56 \times 10^{-2}$
	$7.16 \times 10^{-3}$	80.9	$7.71 \times 10^{-2}$

$$k_2 = 1.08 \times 10^1 \text{ L mol}^{-1} \text{ s}^{-1}$$

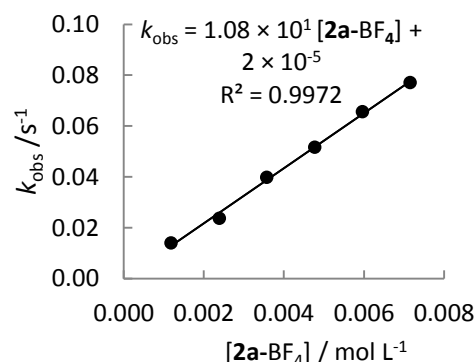


**Table S23.** Kinetics of the reaction of **2a**-BF<sub>4</sub> with **5c** in MeCN (20 °C, diode array UV-Vis spectrometer,  $\lambda = 375$  nm)

[ <b>5c</b> ]/ mol L <sup>-1</sup>	[ <b>2a</b> -BF <sub>4</sub> ]/ mol L <sup>-1</sup>	[ <b>2a</b> -BF <sub>4</sub> ]/ [ <b>5b</b> ]	$k_{\text{obs}} / \text{s}^{-1}$
$8.89 \times 10^{-5}$	$8.48 \times 10^{-4}$	9.5	$2.09 \times 10^{-3}$
$9.10 \times 10^{-5}$	$1.62 \times 10^{-3}$	17.8	$3.39 \times 10^{-3}$
$8.62 \times 10^{-5}$	$2.47 \times 10^{-3}$	28.7	$4.85 \times 10^{-3}$
$8.50 \times 10^{-5}$	$3.24 \times 10^{-3}$	38.1	$6.08 \times 10^{-3}$
$8.16 \times 10^{-5}$	$3.62 \times 10^{-3}$	44.4	$6.77 \times 10^{-3}$

$$k_2 = 1.68 \text{ L mol}^{-1} \text{ s}^{-1}$$

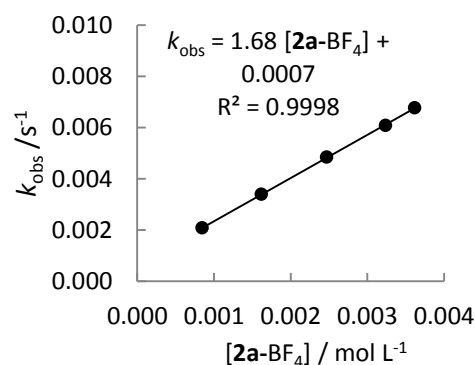


**Table S24.** Kinetics of the reaction of **2a**-BF<sub>4</sub> with **5e** in MeCN (20 °C, diode array UV-Vis spectrometer,  $\lambda = 316$  nm)

[ <b>5e</b> ]/ mol L <sup>-1</sup>	[ <b>2a</b> -BF <sub>4</sub> ]/ mol L <sup>-1</sup>	[ <b>2a</b> -BF <sub>4</sub> ]/ [ <b>5e</b> ]	$k_{\text{obs}} / \text{s}^{-1}$
$1.34 \times 10^{-4}$	$1.55 \times 10^{-3}$	11.6	$5.47 \times 10^{-4}$
$2.69 \times 10^{-4}$	$2.04 \times 10^{-3}$	7.6	$6.93 \times 10^{-4}$
$1.36 \times 10^{-4}$	$2.62 \times 10^{-3}$	19.3	$8.01 \times 10^{-4}$
$2.63 \times 10^{-4}$	$3.31 \times 10^{-3}$	12.6	$1.04 \times 10^{-3}$
$1.35 \times 10^{-4}$	$3.66 \times 10^{-3}$	27.1	$1.09 \times 10^{-3}$

$$k_2 = 2.62 \times 10^{-1} \text{ L mol}^{-1} \text{ s}^{-1}$$

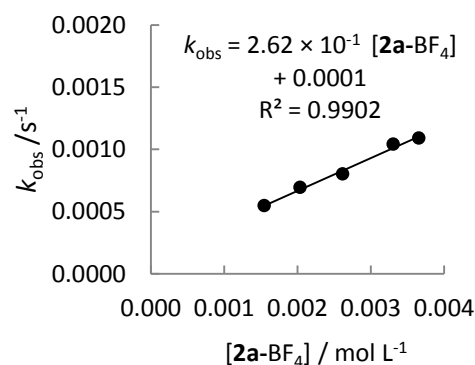


**Table S25.** Kinetics of the reaction of **2a**-BF<sub>4</sub> with **5g** in MeCN (20 °C, stopped-flow,  $\lambda = 310$  nm)

[ <b>5g</b> ]/ mol L <sup>-1</sup>	[ <b>2a</b> -BF <sub>4</sub> ]/ mol L <sup>-1</sup>	[ <b>2a</b> -BF <sub>4</sub> ]/ [ <b>5g</b> ]	$k_{\text{obs}}/\text{s}^{-1}$
$4.50 \times 10^{-5}$	$1.19 \times 10^{-3}$	26.4	$2.05 \times 10^{-2}$
	$2.39 \times 10^{-3}$	53.1	$3.39 \times 10^{-2}$
	$3.58 \times 10^{-3}$	79.6	$4.62 \times 10^{-2}$
	$4.78 \times 10^{-3}$	106.2	$5.79 \times 10^{-2}$
	$5.97 \times 10^{-3}$	132.7	$6.82 \times 10^{-2}$

$$k_2 = 9.99 \text{ L mol}^{-1} \text{ s}^{-1}$$

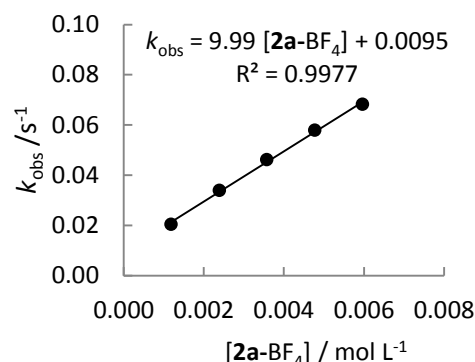


**Table S26.** Determination of the reactivity parameter  $E$  of  $N$ -fluoro-2,4,6-trimethylpyridinium tetrafluoroborate (**2a**-BF<sub>4</sub>) towards enamines in MeCN

Nucleophile	$N$ (MeCN)	$s_N$ (MeCN)	$k_2/\text{L mol}^{-1} \text{ s}^{-1}$	$\log k_2$	$\log k_2/s_N$
<b>5a</b>	11.66	0.82	$1.08 \times 10^1$	1.03	1.26
<b>5c</b>	10.63	0.84	1.68	0.23	0.27
<b>5e</b>	9.94	0.86	$2.62 \times 10^{-1}$	-0.58	-0.68
<b>5g</b> <sup>a</sup>	13.87	0.76	9.99	1.00	1.32

<sup>a</sup> Aminostyrene **5g** was not used in the correlation for determination of electrophilicity parameter  $E$ .

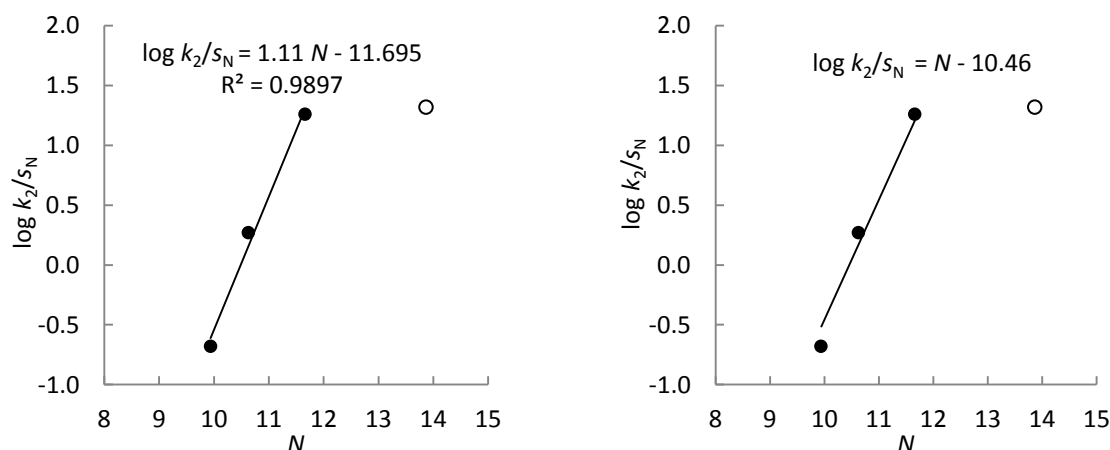


**Figure S3.** Correlations of  $(\log k_2)/s_N$  versus the nucleophilicity of enamines **5** (determined in MeCN) for their reactions with  $N$ -fluoro-2,4,6-trimethylpyridinium tetrafluoroborate (**2a**-BF<sub>4</sub>) in MeCN at 20 °C: as obtained (left) and with slope enforced to 1.0, as required by eq (3) (right). Open circles:  $\beta$ -aminostyrene **5g**, which was not used for the determination of  $E$  parameter.

### 3.4.5.4. Kinetic Investigations of the Reactions of *N*-Fluoro-2,4,6-trimethylpyridinium Tetrafluoroborate (**2a**-BF<sub>4</sub>) with Carbanions **6**

**Table S27.** Kinetics of the reaction of **2a**-BF<sub>4</sub> with **6a** in MeCN (20 °C, stopped-flow,  $\lambda = 476$  nm)

[ <b>6a</b> ]/ mol L <sup>-1</sup>	[ <b>2a</b> -BF <sub>4</sub> ]/ mol L <sup>-1</sup>	[ <b>2a</b> -BF <sub>4</sub> ]/ [ <b>6a</b> ]	$k_{\text{obs}}^a$ / s <sup>-1</sup>
$1.15 \times 10^{-4}$	$1.14 \times 10^{-3}$	9.9	1.45
	$2.27 \times 10^{-3}$	19.7	2.31
	$3.41 \times 10^{-3}$	29.7	3.12
	$4.55 \times 10^{-3}$	39.6	3.92
	$5.68 \times 10^{-3}$	49.4	4.81
	$6.82 \times 10^{-3}$	59.3	5.70

$$k_2 = 7.43 \times 10^2 \text{ L mol}^{-1} \text{ s}^{-1}$$

<sup>a</sup> The decays of absorbances were not strictly monoexponential

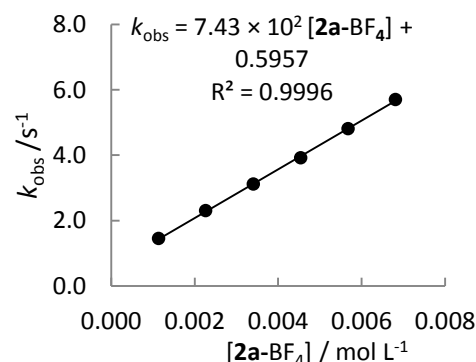


**Table S28.** Kinetics of the reaction of **2a**-BF<sub>4</sub> with **6b** in MeCN (20 °C, stopped-flow,  $\lambda = 530$  nm)

[ <b>6b</b> ]/ mol L <sup>-1</sup>	[ <b>2a</b> -BF <sub>4</sub> ]/ mol L <sup>-1</sup>	[ <b>2a</b> -BF <sub>4</sub> ]/ [ <b>6b</b> ]	$k_{\text{obs}}$ / s <sup>-1</sup>
$7.25 \times 10^{-5}$	$7.71 \times 10^{-4}$	10.6	2.64
	$1.54 \times 10^{-3}$	21.2	3.77
	$2.31 \times 10^{-3}$	31.9	4.69
	$3.08 \times 10^{-3}$	42.5	5.65
	$3.85 \times 10^{-3}$	53.1	6.68
	$4.63 \times 10^{-3}$	63.9	7.84
	$5.40 \times 10^{-3}$	74.5	8.95

$$k_2 = 1.34 \times 10^3 \text{ L mol}^{-1} \text{ s}^{-1}$$

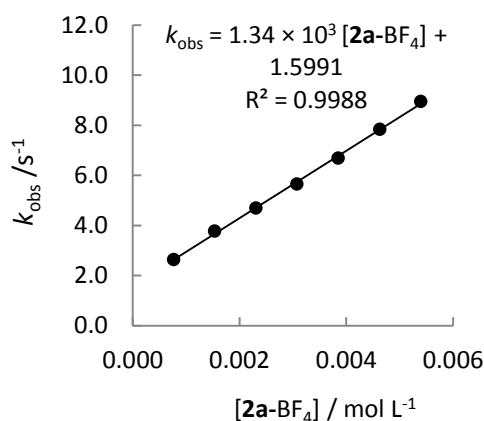


**Table S29.** Kinetics of the reaction of **2a**-BF<sub>4</sub> with **6c** in MeCN (20 °C, stopped-flow,  $\lambda = 450$  nm)

[ <b>6c</b> ]/ mol L <sup>-1</sup>	[ <b>2a</b> -BF <sub>4</sub> ]/ mol L <sup>-1</sup>	[ <b>2a</b> -BF <sub>4</sub> ]/ [ <b>6c</b> ]	$k_{\text{obs}}$ / s <sup>-1</sup>
$1.39 \times 10^{-4}$	$1.81 \times 10^{-3}$	13.0	$1.01 \times 10^1$
	$3.62 \times 10^{-3}$	26.0	$1.76 \times 10^1$
	$5.43 \times 10^{-3}$	39.1	$2.52 \times 10^1$
	$7.24 \times 10^{-3}$	52.1	$3.31 \times 10^1$
	$9.05 \times 10^{-3}$	65.1	$3.99 \times 10^1$

$$k_2 = 4.15 \times 10^3 \text{ L mol}^{-1} \text{ s}^{-1}$$

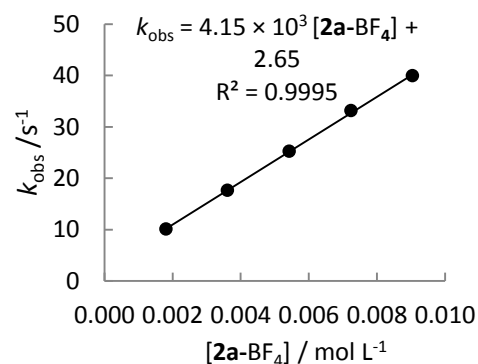


**Table S30.** Kinetics of the reaction of **2a**-BF<sub>4</sub> with **6d** in MeCN (20 °C, stopped-flow,  $\lambda = 305$  nm)

[ <b>6d</b> ]/ mol L <sup>-1</sup>	[ <b>2a</b> -BF <sub>4</sub> ]/ mol L <sup>-1</sup>	[ <b>2a</b> -BF <sub>4</sub> ]/ [ <b>6d</b> ]	$k_{\text{obs}} / \text{s}^{-1}$
$1.03 \times 10^{-4}$	$1.06 \times 10^{-3}$	10.3	$1.86 \times 10^1$
	$1.60 \times 10^{-3}$	15.5	$2.85 \times 10^1$
	$2.13 \times 10^{-3}$	20.7	$3.95 \times 10^1$
	$2.66 \times 10^{-3}$	25.8	$5.01 \times 10^1$
	$3.19 \times 10^{-3}$	31.0	$6.11 \times 10^1$

$$k_2 = 2.00 \times 10^4 \text{ L mol}^{-1} \text{ s}^{-1}$$

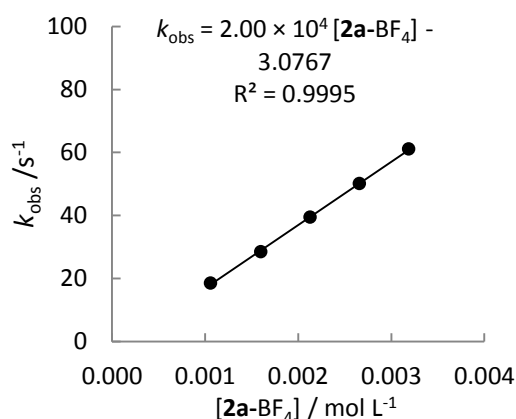


**Table S31.** Kinetics of the reaction of **2a**-BF<sub>4</sub> with **6f** in MeCN (20 °C, stopped-flow,  $\lambda = 550$  nm)

[ <b>6f</b> ]/ mol L <sup>-1</sup>	[ <b>2a</b> -BF <sub>4</sub> ]/ mol L <sup>-1</sup>	[ <b>2a</b> -BF <sub>4</sub> ]/ [ <b>6f</b> ]	$k_{\text{obs}} / \text{s}^{-1}$
$1.12 \times 10^{-4}$	$7.72 \times 10^{-4}$	6.9	$7.27 \times 10^1$
	$9.65 \times 10^{-4}$	8.6	$8.80 \times 10^1$
	$1.16 \times 10^{-3}$	10.4	$1.05 \times 10^2$
	$1.35 \times 10^{-3}$	12.1	$1.19 \times 10^2$
	$1.74 \times 10^{-3}$	15.5	$1.52 \times 10^2$

$$k_2 = 8.18 \times 10^4 \text{ L mol}^{-1} \text{ s}^{-1}$$

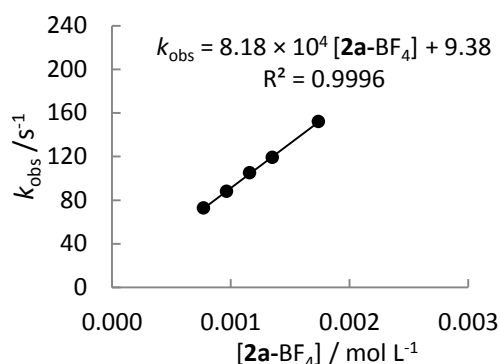


**Table S32.** Reactivity of the *N*-fluoro-2,4,6-trimethylpyridinium tetrafluoroborate (**2a**-BF<sub>4</sub>) towards carbanions **6** in MeCN.

Nucleophile	<i>N</i> (DMSO)	<i>s<sub>N</sub></i> (DMSO)	$k_2 / \text{L mol}^{-1} \text{ s}^{-1}$	$\log k_2$	$\log k_2/s_N$
<b>6a</b>	14.49	0.86	$7.43 \times 10^2$	2.87	3.34
<b>6b</b>	14.96	0.96	$1.34 \times 10^3$	3.13	3.26
<b>6c</b>	16.26	0.83	$4.15 \times 10^3$	3.62	4.21
<b>6d</b>	17.33	0.74	$2.00 \times 10^4$	4.30	5.81
<b>6f</b>	20.00	0.71	$8.18 \times 10^4$	4.91	6.92

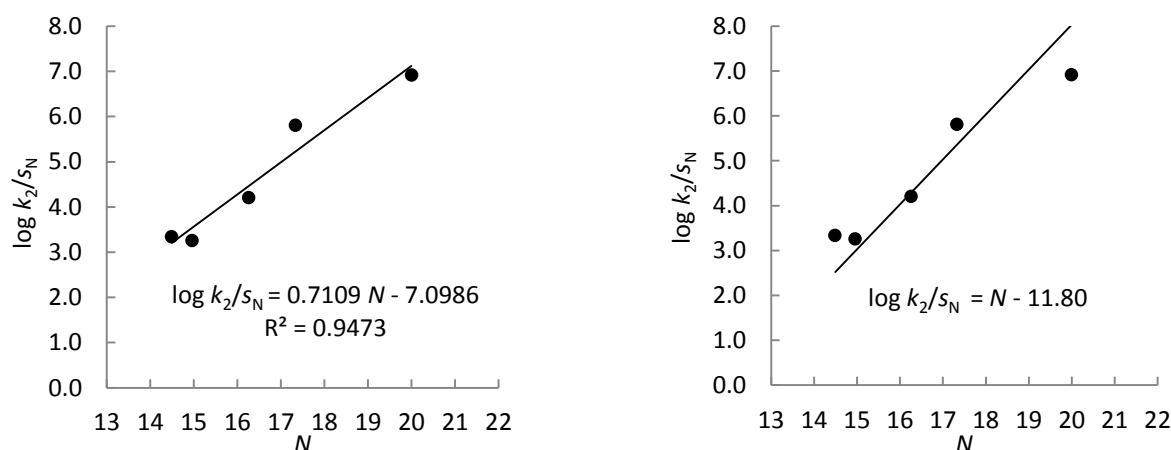


**Figure S4.** Correlations of  $(\log k_2)/s_N$  versus the nucleophilicity of carbanions **6** (determined in DMSO) for their reactions with *N*-fluoro-2,4,6-trimethylpyridinium tetrafluoroborate (**2a-BF<sub>4</sub>**) in MeCN at 20 °C: as obtained (left) and with slope enforced to 1.0, as required by eq (3) (right).

### 3.4.5.5. Kinetic Investigations of the Reactions of *N*-Fluoro-2,4,6-trimethylpyridinium Triflate (**2a-OTf**) with Enamines **5** and Carbanions **6**

**Table S33.** Kinetics of the reaction of **2a-OTf** with **5a** in MeCN (20 °C, stopped-flow,  $\lambda = 317$  nm)

[ <b>5a</b> ]/ mol L <sup>-1</sup>	[ <b>2a-OTf</b> ]/ mol L <sup>-1</sup>	[ <b>2a-OTf</b> ]/ [ <b>5a</b> ]	$k_{\text{obs}} / \text{s}^{-1}$
$9.38 \times 10^{-5}$	$1.02 \times 10^{-3}$	11.5	$9.94 \times 10^{-3}$
	$2.03 \times 10^{-3}$	22.9	$1.84 \times 10^{-2}$
	$3.05 \times 10^{-3}$	34.5	$2.76 \times 10^{-2}$
	$4.07 \times 10^{-3}$	46.0	$3.67 \times 10^{-2}$
	$5.08 \times 10^{-3}$	57.4	$4.45 \times 10^{-2}$

$$k_2 = 8.60 \text{ L mol}^{-1} \text{ s}^{-1}$$

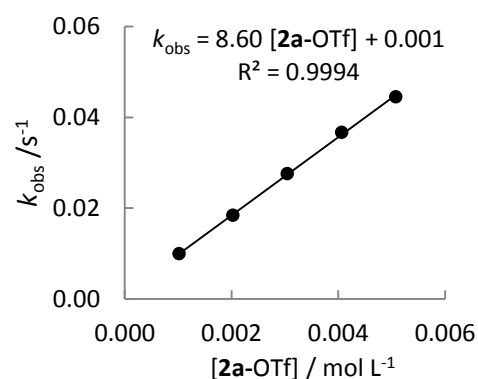


**Table S34.** Kinetics of the reaction of **2a-OTf** with **6b** in MeCN (20 °C, stopped-flow,  $\lambda = 530$  nm)

[ <b>6b</b> ]/ mol L <sup>-1</sup>	[ <b>2a-OTf</b> ]/ mol L <sup>-1</sup>	[ <b>2a-OTf</b> ]/ [ <b>6b</b> ]	$k_{\text{obs}} / \text{s}^{-1}$
$8.45 \times 10^{-5}$	$8.87 \times 10^{-4}$	10.5	6.40
	$1.77 \times 10^{-3}$	20.9	9.37
	$2.66 \times 10^{-3}$	31.5	$1.16 \times 10^1$
	$3.55 \times 10^{-3}$	42.0	$1.43 \times 10^1$
	$4.43 \times 10^{-3}$	52.4	$1.69 \times 10^1$

$$k_2 = 2.92 \times 10^3 \text{ L mol}^{-1} \text{ s}^{-1}$$

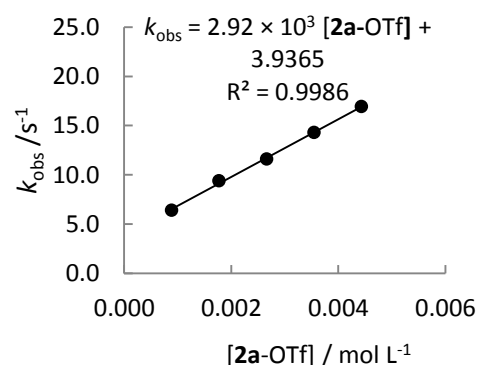
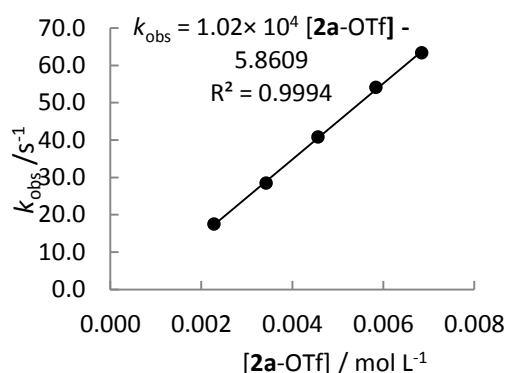


**Table S35.** Kinetics of the reaction of **2a**-OTf with **6c** in MeCN (20 °C, stopped-flow,  $\lambda = 450$  nm)

[ <b>6c</b> ]/ mol L <sup>-1</sup>	[ <b>2a</b> -OTf]/ mol L <sup>-1</sup>	[ <b>2a</b> -OTf]/ [ <b>6c</b> ]	$k_{\text{obs}} / \text{s}^{-1}$
$2.24 \times 10^{-4}$	$2.28 \times 10^{-3}$	10.2	$1.75 \times 10^1$
	$3.43 \times 10^{-3}$	15.3	$2.85 \times 10^1$
	$4.57 \times 10^{-3}$	20.4	$4.08 \times 10^1$
	$5.84 \times 10^{-3}$	26.1	$5.41 \times 10^1$
	$6.85 \times 10^{-3}$	30.6	$6.34 \times 10^1$

$$k_2 = 1.02 \times 10^4 \text{ L mol}^{-1} \text{ s}^{-1}$$

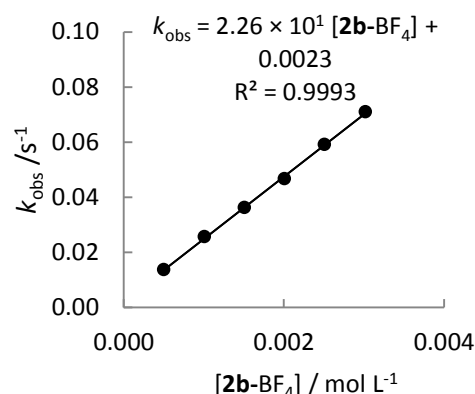


### 3.4.5.6. Kinetic Investigations of the Reactions of *N*-Fluoropyridinium Tetrafluoroborate (**2b**-BF<sub>4</sub>) with Enamines **5**

**Table S36.** Kinetics of the reaction of **2b**-BF<sub>4</sub> with **5a** in MeCN (20 °C, stopped-flow,  $\lambda = 317$  nm)

[ <b>5a</b> ]/ mol L <sup>-1</sup>	[ <b>2b</b> -BF <sub>4</sub> ]/ mol L <sup>-1</sup>	[ <b>2b</b> -BF <sub>4</sub> ]/ [ <b>5a</b> ]	$k_{\text{obs}}^a / \text{s}^{-1}$
$8.30 \times 10^{-5}$	$5.03 \times 10^{-4}$	6.1	$1.37 \times 10^{-2}$
	$1.01 \times 10^{-3}$	12.2	$2.57 \times 10^{-2}$
	$1.51 \times 10^{-3}$	18.2	$3.62 \times 10^{-2}$
	$2.01 \times 10^{-3}$	24.2	$4.67 \times 10^{-2}$
	$2.51 \times 10^{-3}$	30.2	$5.91 \times 10^{-2}$
	$3.02 \times 10^{-3}$	36.4	$7.10 \times 10^{-2}$

$$k_2 = 2.26 \times 10^1 \text{ L mol}^{-1} \text{ s}^{-1}$$

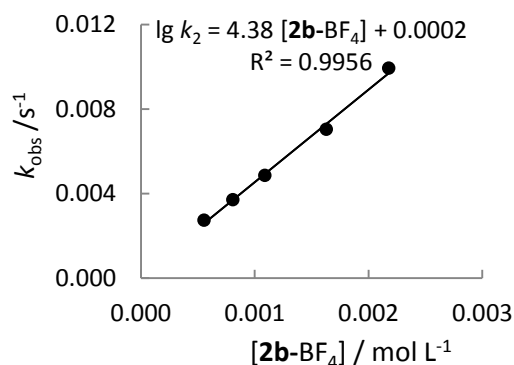


<sup>a</sup> The decays of absorbances were not strictly monoexponential

**Table S37.** Kinetics of the reaction of **2b**-BF<sub>4</sub> with **5c** in MeCN (20 °C, diode array UV-Vis spectrometer,  $\lambda = 375$  nm)

[ <b>5c</b> ]/ mol L <sup>-1</sup>	[ <b>2b</b> -BF <sub>4</sub> ]/ mol L <sup>-1</sup>	[ <b>2b</b> -BF <sub>4</sub> ]/ [ <b>5c</b> ]	$k_{\text{obs}}^a / \text{s}^{-1}$
$5.96 \times 10^{-5}$	$5.55 \times 10^{-4}$	9.3	$2.74 \times 10^{-3}$
$5.77 \times 10^{-5}$	$8.08 \times 10^{-4}$	14.0	$3.70 \times 10^{-3}$
$5.86 \times 10^{-5}$	$1.09 \times 10^{-3}$	18.6	$4.86 \times 10^{-3}$
$5.83 \times 10^{-5}$	$1.63 \times 10^{-3}$	28.0	$7.03 \times 10^{-3}$
$5.84 \times 10^{-5}$	$2.18 \times 10^{-3}$	37.3	$9.92 \times 10^{-3}$

$$k_2 = 4.38 \text{ L mol}^{-1} \text{ s}^{-1}$$



<sup>a</sup> The decays of absorbances were not strictly monoexponential.



**Table S38.** Kinetics of the reaction of **2b**-BF<sub>4</sub> with **5d** in MeCN (20 °C, diode array UV-Vis spectrometer,  $\lambda = 465$  nm)

[ <b>5d</b> ]/ mol L <sup>-1</sup>	[ <b>2b</b> -BF <sub>4</sub> ]/ mol L <sup>-1</sup>	[ <b>2b</b> -BF <sub>4</sub> ]/ [ <b>5d</b> ]	$k_{\text{obs}}^{\text{a}}/\text{s}^{-1}$
$7.57 \times 10^{-5}$	$8.64 \times 10^{-4}$	11.4	$2.90 \times 10^{-3}$
$8.03 \times 10^{-5}$	$1.32 \times 10^{-3}$	16.4	$4.26 \times 10^{-3}$
$7.42 \times 10^{-5}$	$1.69 \times 10^{-3}$	22.8	$5.90 \times 10^{-3}$
$1.48 \times 10^{-4}$	$2.45 \times 10^{-3}$	16.6	$8.54 \times 10^{-3}$

$$k_2 = 3.61 \text{ L mol}^{-1} \text{ s}^{-1}$$

<sup>a</sup> The decays of absorbances were not strictly monoexponential.

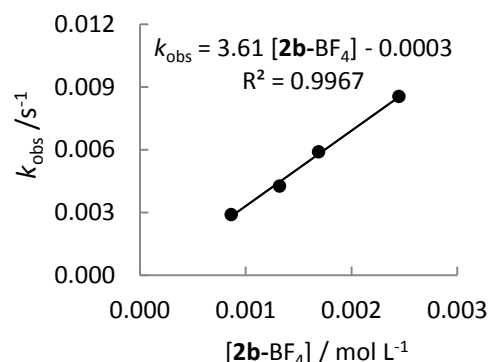


**Table S39.** Kinetics of the reaction of **2b**-BF<sub>4</sub> with **5e** in MeCN (20 °C, diode array UV-Vis spectrometer,  $\lambda = 316$  nm)

[ <b>5e</b> ]/ mol L <sup>-1</sup>	[ <b>2b</b> -BF <sub>4</sub> ]/ mol L <sup>-1</sup>	[ <b>2b</b> -BF <sub>4</sub> ]/ [ <b>5e</b> ]	$k_{\text{obs}}^{\text{a}}/\text{s}^{-1}$
$1.35 \times 10^{-4}$	$1.12 \times 10^{-3}$	8.3	$1.38 \times 10^{-3}$
$1.52 \times 10^{-4}$	$1.69 \times 10^{-3}$	11.1	$2.05 \times 10^{-3}$
$1.73 \times 10^{-4}$	$1.91 \times 10^{-3}$	11.0	$2.29 \times 10^{-3}$
$1.74 \times 10^{-4}$	$2.33 \times 10^{-3}$	13.4	$2.70 \times 10^{-3}$
$1.75 \times 10^{-4}$	$2.71 \times 10^{-3}$	15.5	$3.01 \times 10^{-3}$

$$k_2 = 1.03 \text{ L mol}^{-1} \text{ s}^{-1}$$

<sup>a</sup> The decays of absorbances were not strictly monoexponential.

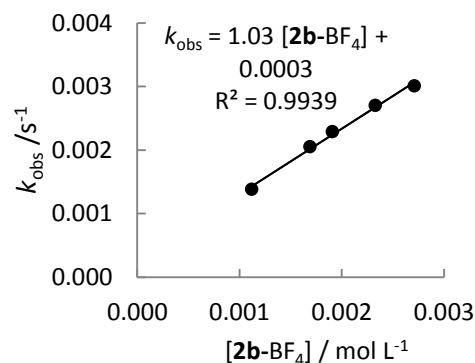


**Table S40.** Kinetics of the reaction of **2b**-BF<sub>4</sub> with **5g** in MeCN (20 °C, stopped-flow,  $\lambda = 310$  nm)

[ <b>5g</b> ]/ mol L <sup>-1</sup>	[ <b>2b</b> -BF <sub>4</sub> ]/ mol L <sup>-1</sup>	[ <b>2b</b> -BF <sub>4</sub> ]/ [ <b>5g</b> ]	$k_{\text{obs}}^{\text{a}}/\text{s}^{-1}$
$1.13 \times 10^{-4}$	$1.10 \times 10^{-3}$	9.7	$4.82 \times 10^{-2}$
	$1.65 \times 10^{-3}$	14.6	$7.48 \times 10^{-2}$
	$2.21 \times 10^{-3}$	19.6	$9.76 \times 10^{-2}$
	$2.76 \times 10^{-3}$	24.4	$1.24 \times 10^{-1}$
	$3.31 \times 10^{-3}$	29.3	$1.49 \times 10^{-1}$

$$k_2 = 4.53 \times 10^1 \text{ L mol}^{-1} \text{ s}^{-1}$$

<sup>a</sup> The decays of absorbances were not strictly monoexponential.

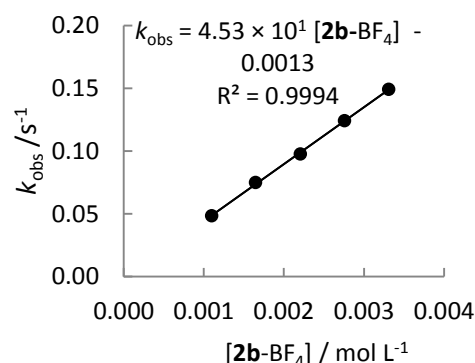


**Table S41.** Determination of the reactivity parameter  $E$  of  $N$ -fluoropyridinium tetrafluoroborate (**2b**-BF<sub>4</sub>) towards enamines in MeCN

Nucleophile	$N$ (MeCN)	$s_N$ (MeCN)	$k_2 / \text{L mol}^{-1} \text{s}^{-1}$	$\log k_2$	$\log k_2/s_N$
<b>5a</b>	11.66	0.82	$2.26 \times 10^1$	1.35	1.65
<b>5c</b>	10.63	0.84	4.38	0.63	0.76
<b>5d</b>	10.42	0.82	3.61	0.56	0.68
<b>5e</b>	9.94	0.86	1.03	0.01	0.01
<b>5g</b> <sup>a</sup>	13.87	0.76	$4.53 \times 10^1$	1.66	2.18

<sup>a</sup> Aminostyrene **5g** was not used in the correlation for determination of electrophilicity parameter  $E$ .

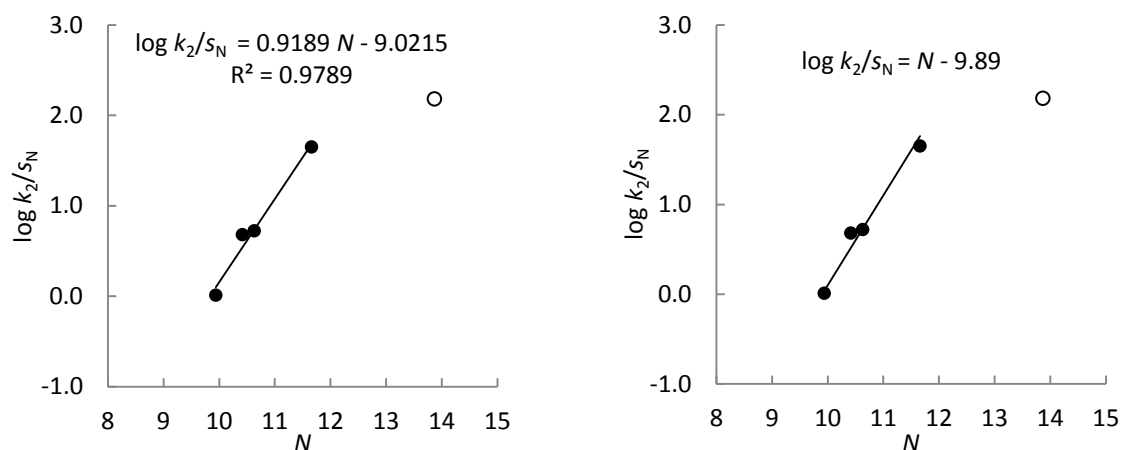


**Figure S5.** Correlations of  $(\log k_2)/s_N$  versus the nucleophilicity of enamines **5** (determined in MeCN) for their reactions with  $N$ -fluoropyridinium tetrafluoroborate (**2b**-BF<sub>4</sub>) in MeCN at 20 °C: as obtained (left) and with slope enforced to 1.0, as required by eq (3) (right). Open circles:  $\beta$ -aminostyrene **5g**, which was not used for the determination of  $E$  parameter.

### 3.4.5.7. Kinetic Investigations of the Reactions of *N*-Fluoro-2,6-dichloropyridinium Tetrafluoroborate (**2c-BF<sub>4</sub>**) with Enamines **5**

**Table S42.** Kinetics of the reaction of **2c-BF<sub>4</sub>** with **5a** in MeCN (20 °C, stopped-flow,  $\lambda = 310$  nm)

[ <b>5a</b> ]/ mol L <sup>-1</sup>	[ <b>2c-BF<sub>4</sub></b> ]/ mol L <sup>-1</sup>	[ <b>2c-BF<sub>4</sub></b> ]/ [ <b>5a</b> ]	$k_{\text{obs}}/\text{s}^{-1}$
$9.22 \times 10^{-5}$	$6.60 \times 10^{-4}$	7.2	$8.41 \times 10^1$
	$7.70 \times 10^{-4}$	8.4	$1.01 \times 10^2$
	$8.79 \times 10^{-4}$	9.5	$1.14 \times 10^2$
	$9.89 \times 10^{-4}$	10.7	$1.28 \times 10^2$
	$1.10 \times 10^{-3}$	11.9	$1.42 \times 10^2$

$$k_2 = 1.30 \times 10^5 \text{ L mol}^{-1} \text{ s}^{-1}$$

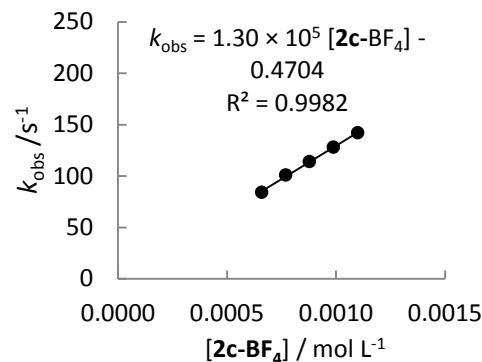


**Table S43.** Kinetics of the reaction of **2c-BF<sub>4</sub>** with **5c** in MeCN (20 °C, stopped-flow,  $\lambda = 375$  nm)

[ <b>5c</b> ]/ mol L <sup>-1</sup>	[ <b>2c-BF<sub>4</sub></b> ]/ mol L <sup>-1</sup>	[ <b>2c-BF<sub>4</sub></b> ]/ [ <b>5c</b> ]	$k_{\text{obs}}/\text{s}^{-1}$
$3.38 \times 10^{-5}$	$7.21 \times 10^{-4}$	21.3	$2.32 \times 10^1$
	$9.61 \times 10^{-4}$	28.4	$3.20 \times 10^1$
	$1.20 \times 10^{-3}$	35.5	$4.10 \times 10^1$
	$1.44 \times 10^{-3}$	42.6	$5.50 \times 10^1$
	$1.68 \times 10^{-3}$	49.7	$6.81 \times 10^1$

$$k_2 = 4.71 \times 10^4 \text{ L mol}^{-1} \text{ s}^{-1}$$

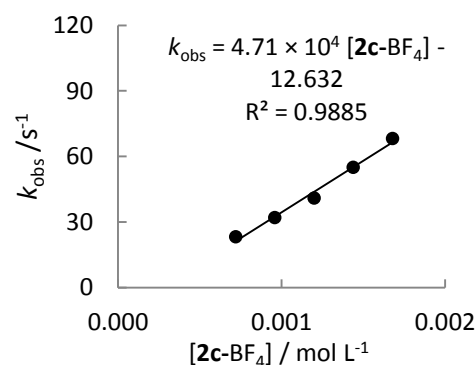


**Table S44.** Kinetics of the reaction of **2c-BF<sub>4</sub>** with **5d** in MeCN (20 °C, stopped-flow,  $\lambda = 465$  nm)

[ <b>5d</b> ]/ mol L <sup>-1</sup>	[ <b>2c-BF<sub>4</sub></b> ]/ mol L <sup>-1</sup>	[ <b>2c-BF<sub>4</sub></b> ]/ [ <b>5d</b> ]	$k_{\text{obs}}/\text{s}^{-1}$
$4.66 \times 10^{-5}$	$4.82 \times 10^{-4}$	10.3	9.10
	$9.65 \times 10^{-4}$	28.6	$2.08 \times 10^1$
	$1.45 \times 10^{-3}$	42.9	$3.48 \times 10^1$
	$1.93 \times 10^{-3}$	57.1	$5.13 \times 10^1$

$$k_2 = 2.91 \times 10^4 \text{ L mol}^{-1} \text{ s}^{-1}$$

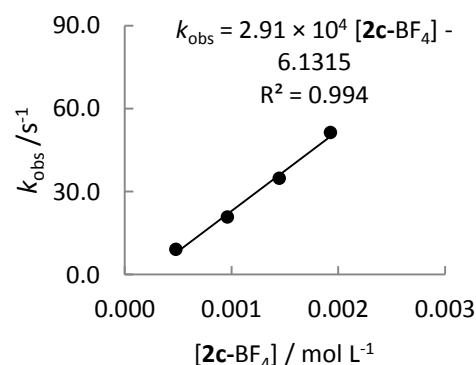


**Table S45.** Kinetics of the reaction of **2c-BF<sub>4</sub>** with **5e** in MeCN (20 °C, stopped-flow,  $\lambda = 316$  nm)

[ <b>5e</b> ]/ mol L <sup>-1</sup>	[ <b>2c-BF<sub>4</sub></b> ]/ mol L <sup>-1</sup>	[ <b>2c-BF<sub>4</sub></b> ]/ [ <b>5e</b> ]	$k_{\text{obs}}/\text{s}^{-1}$
$5.19 \times 10^{-5}$	$5.47 \times 10^{-4}$	10.5	2.55
	$8.20 \times 10^{-4}$	24.3	3.60
	$1.09 \times 10^{-3}$	32.2	4.85
	$1.37 \times 10^{-3}$	40.5	6.32
	$1.64 \times 10^{-3}$	48.5	7.50

$$k_2 = 4.61 \times 10^3 \text{ L mol}^{-1} \text{ s}^{-1}$$

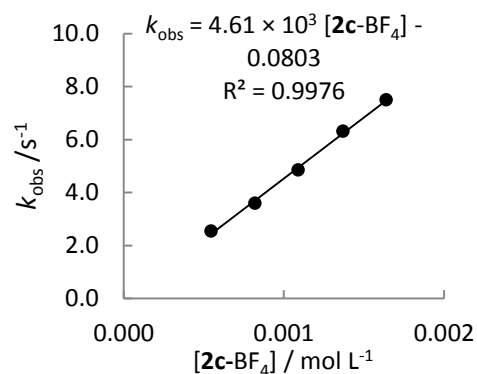


**Table S46.** Kinetics of the reaction of **2c-BF<sub>4</sub>** with **5g** in MeCN (20 °C, stopped-flow,  $\lambda = 310$  nm)

[ <b>5g</b> ]/ mol L <sup>-1</sup>	[ <b>2c-BF<sub>4</sub></b> ]/ mol L <sup>-1</sup>	[ <b>2c-BF<sub>4</sub></b> ]/ [ <b>5g</b> ]	$k_{\text{obs}}/\text{s}^{-1}$
$3.46 \times 10^{-5}$	$1.35 \times 10^{-4}$	3.9	$3.27 \times 10^1$
	$2.03 \times 10^{-4}$	5.9	$4.83 \times 10^1$
	$2.70 \times 10^{-4}$	7.8	$6.46 \times 10^1$
	$3.38 \times 10^{-4}$	9.8	$8.13 \times 10^1$

$$k_2 = 2.40 \times 10^5 \text{ L mol}^{-1} \text{ s}^{-1}$$

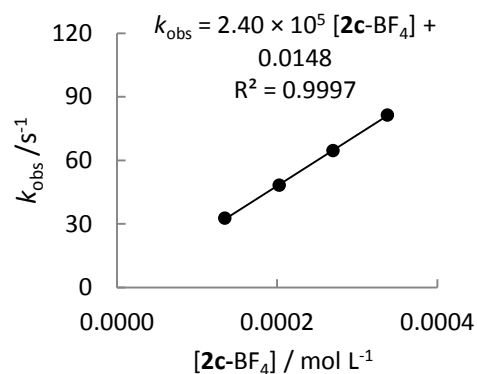


**Table S47.** Kinetics of the reaction of **2c-BF<sub>4</sub>** with **5h** in MeCN (20 °C, stopped-flow,  $\lambda = 300$  nm)

[ <b>5h</b> ]/ mol L <sup>-1</sup>	[ <b>2c-BF<sub>4</sub></b> ]/ mol L <sup>-1</sup>	[ <b>2c-BF<sub>4</sub></b> ]/ [ <b>5h</b> ]	$k_{\text{obs}}/\text{s}^{-1}$
$2.00 \times 10^{-5}$	$2.70 \times 10^{-4}$	13.5	2.80
	$3.38 \times 10^{-4}$	16.9	3.61
	$4.05 \times 10^{-4}$	20.3	4.13
	$4.73 \times 10^{-4}$	23.7	4.99
	$6.76 \times 10^{-4}$	33.8	6.87

$$k_2 = 9.97 \times 10^3 \text{ L mol}^{-1} \text{ s}^{-1}$$

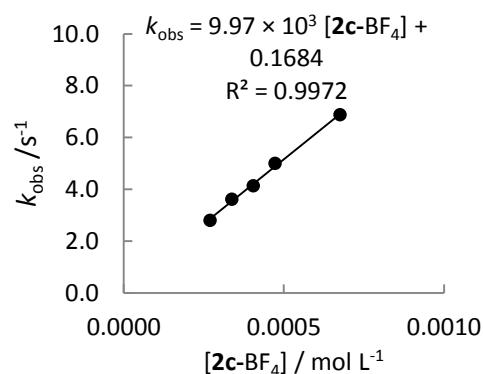


**Table S48.** Determination of the reactivity parameter  $E$  of  $N$ -fluoro-2,6-dichloropyridinium tetrafluoroborate (**2c**-BF<sub>4</sub>) towards enamines in MeCN

Nucleophile	$N$ (MeCN)	$s_N$ (MeCN)	$k_2 / \text{L mol}^{-1} \text{s}^{-1}$	$\log k_2$	$\log k_2/s_N$
<b>5a</b>	11.66	0.82	$1.30 \times 10^5$	5.11	6.24
<b>5c</b>	10.63	0.84	$4.71 \times 10^4$	4.67	5.56
<b>5d</b>	10.42	0.82	$2.91 \times 10^4$	4.46	5.44
<b>5e</b>	9.94	0.86	$4.61 \times 10^3$	3.66	4.26
<b>5g</b> <sup>a</sup>	13.87	0.76	$2.40 \times 10^5$	5.38	7.08
<b>5h</b> <sup>a</sup>	11.66	0.83	$9.97 \times 10^3$	4.00	4.76

<sup>a</sup> aminostyrenes **5g** and **5h** were not used in the correlation for determination of electrophilicity parameter  $E$ .

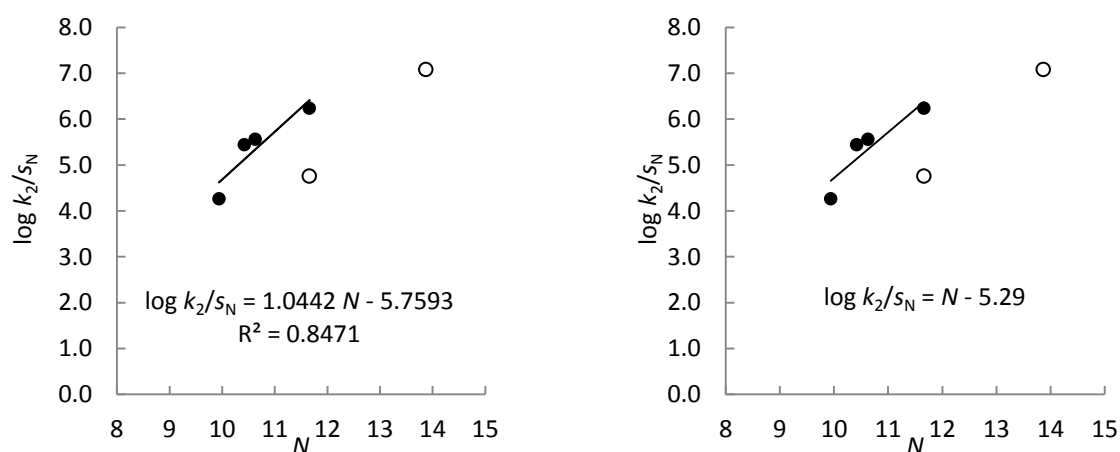


**Figure S6.** Correlations of  $(\log k_2)/s_N$  versus the nucleophilicity of enamines **5** (determined in MeCN) for their reactions with  $N$ -fluoro-2,6-dichloropyridinium tetrafluoroborate (**2c**-BF<sub>4</sub>) in MeCN at 20 °C: as obtained (left) and with slope enforced to 1.0, as required by eq (3) (right). Open circles:  $\beta$ -aminostyrenes **5g,h**, which were not used for the determination of  $E$  parameter.

### 3.4.5.8. Kinetic Investigations of the Reactions of Selectfluor (**3**) with Enamines **5**

**Table S49.** Kinetics of the reaction of **3** with **5a** in MeCN (20 °C, stopped-flow,  $\lambda = 315$  nm)

$[\mathbf{5a}] / \text{mol L}^{-1}$	$[\mathbf{3}] / \text{mol L}^{-1}$	$[\mathbf{3}] / [\mathbf{5a}]$	$k_{\text{obs}} / \text{s}^{-1}$
$1.06 \times 10^{-4}$	$6.66 \times 10^{-4}$	6.3	$8.68 \times 10^1$
	$9.99 \times 10^{-4}$	9.4	$1.20 \times 10^2$
	$1.33 \times 10^{-3}$	12.5	$1.54 \times 10^2$
	$1.67 \times 10^{-3}$	15.8	$1.96 \times 10^2$

$k_2 = 1.08 \times 10^5 \text{ L mol}^{-1} \text{s}^{-1}$

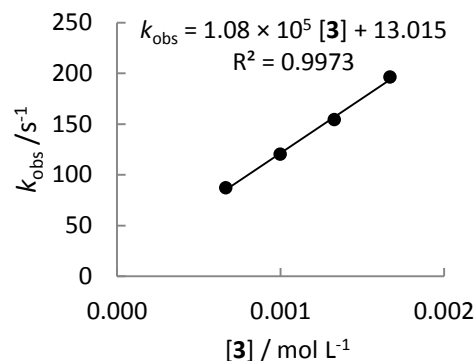


**Table S50.** Kinetics of the reaction of **3** with **5b** in MeCN (20 °C, stopped-flow,  $\lambda = 300$  nm)

[ <b>5b</b> ]/ mol L <sup>-1</sup>	[ <b>3</b> ]/ mol L <sup>-1</sup>	[ <b>3</b> ]/ [ <b>5b</b> ]	$k_{\text{obs}}/\text{s}^{-1}$
$3.06 \times 10^{-5}$	$1.76 \times 10^{-4}$	5.8	$3.47 \times 10^1$
	$3.53 \times 10^{-4}$	11.6	$6.62 \times 10^1$
	$5.29 \times 10^{-4}$	17.3	$1.01 \times 10^2$
	$7.06 \times 10^{-4}$	23.1	$1.33 \times 10^2$

$$k_2 = 1.87 \times 10^5 \text{ L mol}^{-1} \text{ s}^{-1}$$

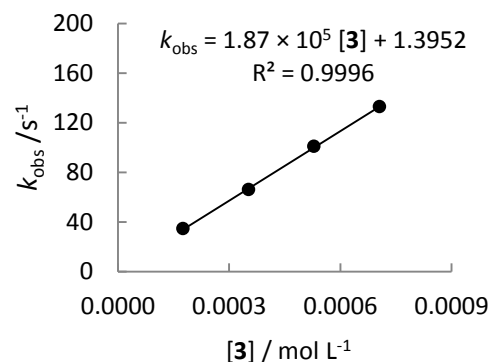


**Table S51.** Kinetics of the reaction of **3** with **5c** in MeCN (20 °C, stopped-flow,  $\lambda = 375$  nm)

[ <b>5c</b> ]/ mol L <sup>-1</sup>	[ <b>3</b> ]/ mol L <sup>-1</sup>	[ <b>3</b> ]/ [ <b>5c</b> ]	$k_{\text{obs}}/\text{s}^{-1}$
$3.64 \times 10^{-5}$	$4.05 \times 10^{-4}$	11.1	$2.11 \times 10^1$
	$6.08 \times 10^{-4}$	16.7	$3.19 \times 10^1$
	$8.11 \times 10^{-4}$	22.3	$4.17 \times 10^1$
	$1.01 \times 10^{-3}$	27.7	$5.24 \times 10^1$
	$1.22 \times 10^{-3}$	33.5	$6.26 \times 10^1$

$$k_2 = 5.09 \times 10^4 \text{ L mol}^{-1} \text{ s}^{-1}$$

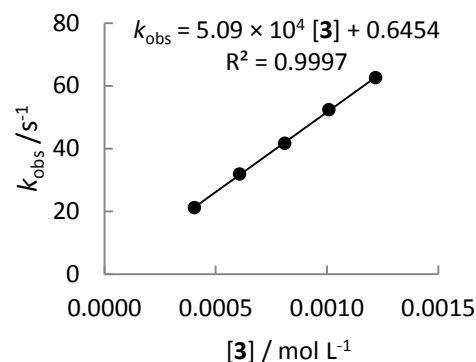


**Table S52.** Kinetics of the reaction of **3** with **5d** in MeCN (20 °C, stopped-flow,  $\lambda = 465$  nm)

[ <b>5d</b> ]/ mol L <sup>-1</sup>	[ <b>3</b> ]/ mol L <sup>-1</sup>	[ <b>3</b> ]/ [ <b>5d</b> ]	$k_{\text{obs}}/\text{s}^{-1}$
$3.74 \times 10^{-5}$	$4.29 \times 10^{-4}$	11.5	$1.63 \times 10^1$
	$6.44 \times 10^{-4}$	17.2	$2.41 \times 10^1$
	$8.58 \times 10^{-4}$	22.9	$3.16 \times 10^1$
	$1.07 \times 10^{-3}$	28.6	$3.91 \times 10^1$
	$1.29 \times 10^{-3}$	34.5	$4.67 \times 10^1$

$$k_2 = 3.53 \times 10^4 \text{ L mol}^{-1} \text{ s}^{-1}$$

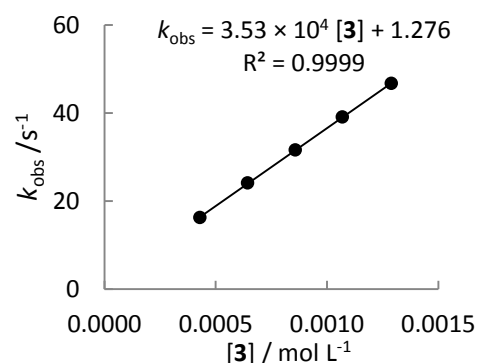


**Table S53.** Kinetics of the reaction of **3** with **5e** in MeCN (20 °C, stopped-flow,  $\lambda = 316$  nm)

[ <b>5e</b> ]/ mol L <sup>-1</sup>	[ <b>3</b> ]/ mol L <sup>-1</sup>	[ <b>3</b> ]/ [ <b>5e</b> ]	$k_{\text{obs}}/\text{s}^{-1}$
$7.97 \times 10^{-5}$	$9.96 \times 10^{-4}$	12.5	$1.04 \times 10^1$
	$1.59 \times 10^{-3}$	19.9	$1.65 \times 10^1$
	$2.19 \times 10^{-3}$	27.5	$2.24 \times 10^1$
	$2.99 \times 10^{-3}$	37.5	$2.96 \times 10^1$
	$3.99 \times 10^{-3}$	50.1	$4.01 \times 10^1$

$$k_2 = 9.82 \times 10^3 \text{ L mol}^{-1} \text{ s}^{-1}$$

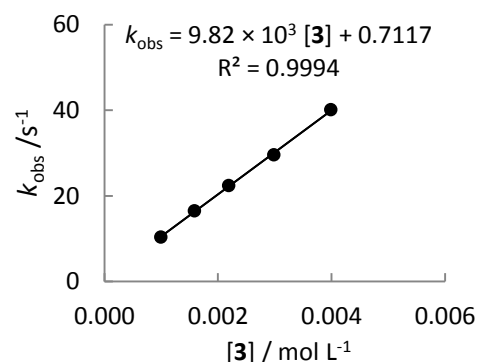


**Table S54.** Kinetics of the reaction of **3** with **5f** in MeCN (20 °C, stopped-flow,  $\lambda = 306$  nm)

[ <b>5f</b> ]/ mol L <sup>-1</sup>	[ <b>3</b> ]/ mol L <sup>-1</sup>	[ <b>3</b> ]/ [ <b>5f</b> ]	$k_{\text{obs}}/\text{s}^{-1}$
$1.03 \times 10^{-4}$	$1.22 \times 10^{-3}$	11.8	2.82
	$1.83 \times 10^{-3}$	17.8	4.30
	$2.44 \times 10^{-3}$	23.7	5.63
	$3.05 \times 10^{-3}$	29.6	7.10
	$3.66 \times 10^{-3}$	35.5	8.45

$$k_2 = 2.30 \times 10^3 \text{ L mol}^{-1} \text{ s}^{-1}$$

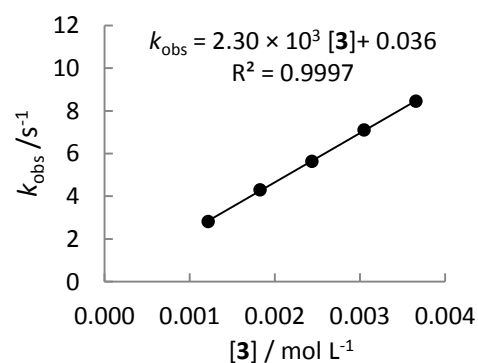


**Table S55.** Kinetics of the reaction of **3** with **5g** in MeCN (20 °C, stopped-flow,  $\lambda = 310$  nm)

[ <b>5g</b> ]/ mol L <sup>-1</sup>	[ <b>3</b> ]/ mol L <sup>-1</sup>	[ <b>3</b> ]/ [ <b>5g</b> ]	$k_{\text{obs}}/\text{s}^{-1}$
$1.01 \times 10^{-4}$	$1.09 \times 10^{-3}$	10.8	$8.67 \times 10^1$
	$1.63 \times 10^{-3}$	16.1	$1.32 \times 10^2$
	$2.17 \times 10^{-3}$	21.5	$1.82 \times 10^2$
	$2.72 \times 10^{-3}$	26.9	$2.25 \times 10^2$
	$3.26 \times 10^{-3}$	32.3	$2.75 \times 10^2$

$$k_2 = 8.14 \times 10^4 \text{ L mol}^{-1} \text{ s}^{-1}$$

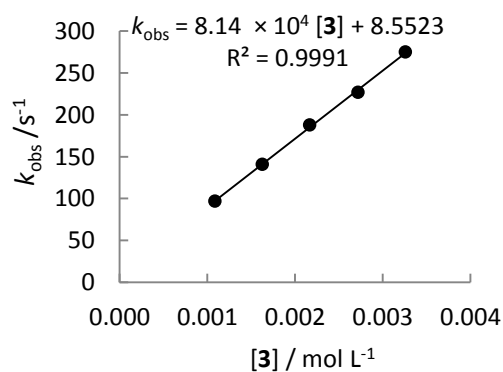


**Table S56.** Kinetics of the reaction of **3** with **5h** in MeCN (20 °C, stopped-flow,  $\lambda = 300$  nm)

[ <b>5h</b> ]/ mol L <sup>-1</sup>	[ <b>3</b> ]/ mol L <sup>-1</sup>	[ <b>3</b> ]/ [ <b>5h</b> ]	$k_{\text{obs}}/\text{s}^{-1}$
$8.88 \times 10^{-5}$	$9.15 \times 10^{-4}$	10.3	$1.01 \times 10^1$
	$1.37 \times 10^{-3}$	15.4	$1.46 \times 10^1$
	$1.83 \times 10^{-3}$	20.6	$1.79 \times 10^1$
	$2.29 \times 10^{-3}$	25.8	$2.12 \times 10^1$
	$2.74 \times 10^{-3}$	30.9	$2.45 \times 10^1$

$$k_2 = 7.75 \times 10^3 \text{ L mol}^{-1} \text{ s}^{-1}$$

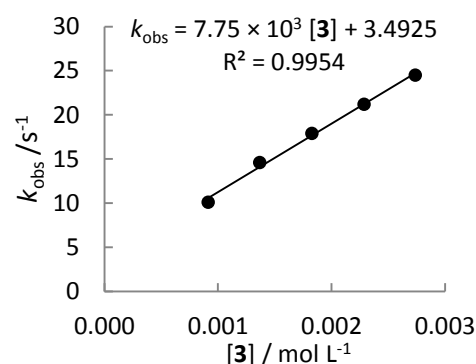


**Table S57.** Determination of the Reactivity Parameter  $E$  of Selectfluor (**3**) towards Enamines in MeCN

Nucleophile	$N$ (MeCN)	$s_N$ (MeCN)	$k_2/\text{L mol}^{-1} \text{ s}^{-1}$	$\log k_2$	$\log k_2/s_N$
<b>5a</b>	11.66	0.82	$1.08 \times 10^5$	5.03	6.14
<b>5b</b>	11.99	0.84	$1.87 \times 10^5$	5.27	6.28
<b>5c</b>	10.63	0.84	$5.09 \times 10^4$	4.71	5.60
<b>5d</b>	10.42	0.82	$3.53 \times 10^4$	4.55	5.55
<b>5e</b>	9.94	0.86	$9.82 \times 10^3$	3.99	4.64
<b>5f</b>	8.78	0.83	$2.30 \times 10^3$	3.36	4.05
<b>5g</b> <sup>a</sup>	13.87	0.76	$8.14 \times 10^4$	4.91	6.46
<b>5h</b> <sup>a</sup>	11.66	0.83	$7.75 \times 10^3$	3.89	4.69

<sup>a</sup> Aminostyrenes **5g** and **5h** were not used in the correlation for determination of electrophilicity parameter  $E$ .

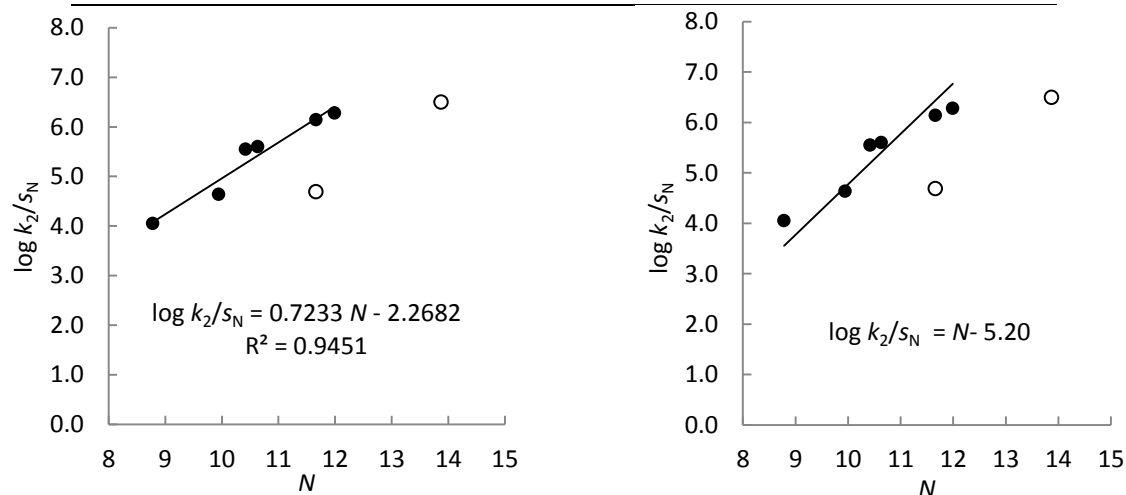


**Figure S7.** Correlations of  $(\log k_2)/s_N$  versus the nucleophilicity of enamines **5** (determined in MeCN) for their reactions with Selectfluor (**3**) in MeCN at 20 °C: as obtained (left) and with slope enforced to 1.0, as required by eq (3) (right). Open circles:  $\beta$ -aminostyrenes **5g,h**, which were not used for the determination of  $E$  parameter.



### 3.4.5.9. Kinetic Investigations of the Reactions of Cinchona Alkaloid Derived *N*-Fluoroammonium salt **4**

**Table S58.** Kinetics of the reaction of **4** with **5d** in MeCN (20 °C, stopped-flow,  $\lambda = 465$  nm)

[ <b>5d</b> ]/ mol L <sup>-1</sup>	[ <b>4</b> ]/ mol L <sup>-1</sup>	[ <b>4</b> ]/ [ <b>5d</b> ]	$k_{\text{obs}}/\text{s}^{-1}$
$6.66 \times 10^{-5}$	$6.75 \times 10^{-4}$	10.1	$3.35 \times 10^{-1}$
	$1.41 \times 10^{-3}$	21.1	$4.97 \times 10^{-1}$
	$1.97 \times 10^{-3}$	29.6	$6.22 \times 10^{-1}$
	$2.25 \times 10^{-3}$	33.8	$6.96 \times 10^{-1}$

$$k_2 = 2.27 \times 10^2 \text{ L mol}^{-1} \text{ s}^{-1}$$

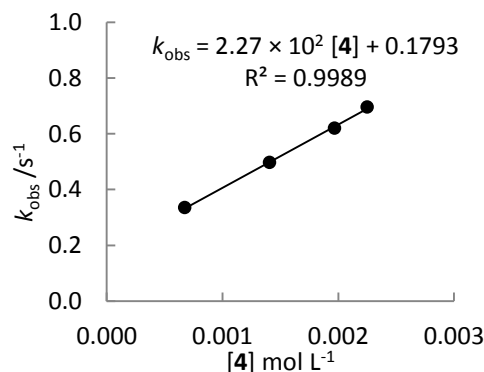
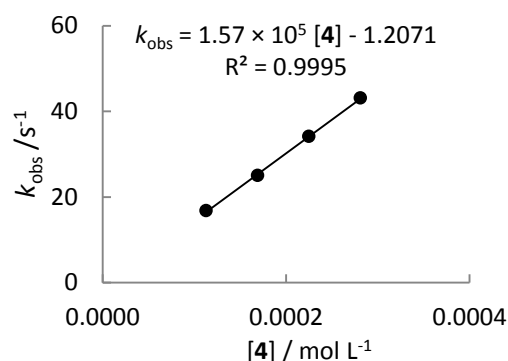


**Table S59.** Kinetics of the reaction of **4** with **6b** in MeCN (20 °C, stopped-flow,  $\lambda = 530$  nm)

[ <b>6b</b> ]/ mol L <sup>-1</sup>	[ <b>4</b> ]/ mol L <sup>-1</sup>	[ <b>4</b> ]/ [ <b>6b</b> ]	$k_{\text{obs}}/\text{s}^{-1}$
$2.00 \times 10^{-5}$	$1.13 \times 10^{-4}$	5.7	$1.68 \times 10^1$
	$1.69 \times 10^{-4}$	8.5	$2.50 \times 10^1$
	$2.25 \times 10^{-4}$	11.3	$3.41 \times 10^1$
	$2.81 \times 10^{-4}$	14.1	$4.31 \times 10^1$

$$k_2 = 1.57 \times 10^5 \text{ L mol}^{-1} \text{ s}^{-1}$$

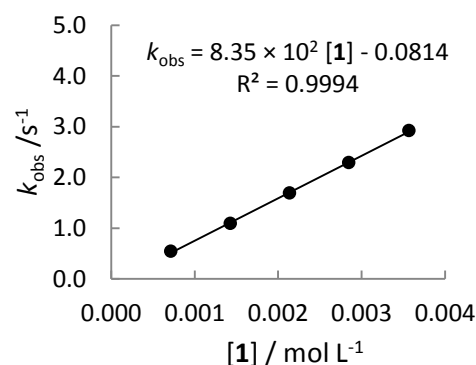


### 3.4.6. Determination of the Rate Constants for Reactions of Carbanion **6b** with NFSI (**1**) and *N*-Fluoro-2,4,6-trimethylpyridinium Salts **2a-BF<sub>4</sub>** and **2a-OTf** in the Presence of **18-Crown-6** Ether

**Table S60.** Kinetics of the reaction of **1** with **6b** in MeCN (20 °C, stopped-flow,  $\lambda = 530$  nm)

[ <b>6b</b> ] <sup>a</sup> / mol L <sup>-1</sup>	[ <b>1</b> ]/ mol L <sup>-1</sup>	[ <b>1</b> ]/ [ <b>6b</b> ]	$k_{\text{obs}}/\text{s}^{-1}$
$3.33 \times 10^{-5}$	$7.14 \times 10^{-4}$	21.4	$5.42 \times 10^{-1}$
	$1.43 \times 10^{-3}$	42.9	1.09
	$2.14 \times 10^{-3}$	64.3	1.69
	$2.85 \times 10^{-3}$	85.6	2.29
	$3.57 \times 10^{-3}$	107	2.92

$$k_2 = 8.35 \times 10^2 \text{ L mol}^{-1} \text{ s}^{-1}$$

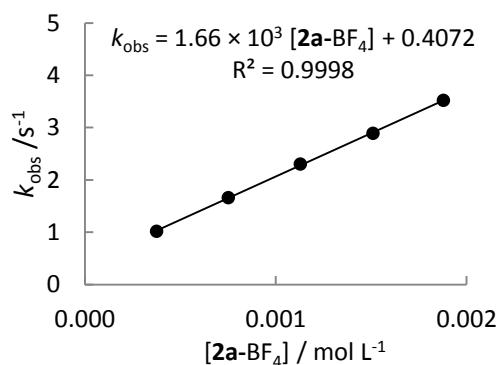


<sup>a</sup> In the presence of 1.05 equiv of 18-crown-6 with respect to **6b-K**

**Table S61.** Kinetics of the reaction of **2a**-BF<sub>4</sub> with **6b** in MeCN (20 °C, stopped-flow,  $\lambda = 530$  nm)

[ <b>6b</b> ] <sup>a</sup> / mol L <sup>-1</sup>	[ <b>2a</b> -BF <sub>4</sub> ]/ mol L <sup>-1</sup>	[ <b>2a</b> -BF <sub>4</sub> ]/ [ <b>6b</b> ]	$k_{\text{obs}}/\text{s}^{-1}$
$3.33 \times 10^{-5}$	$3.77 \times 10^{-4}$	11.3	1.02
	$7.53 \times 10^{-4}$	22.6	1.66
	$1.13 \times 10^{-3}$	33.9	2.30
	$1.51 \times 10^{-3}$	45.3	2.89
	$1.88 \times 10^{-3}$	56.5	3.52

$$k_2 = 1.66 \times 10^3 \text{ L mol}^{-1} \text{ s}^{-1}$$

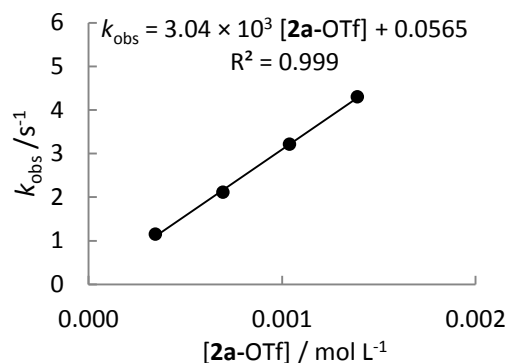


<sup>a</sup> In the presence of 1.05 equiv of 18-crown-6 with respect to **6b**-K

**Table S62.** Kinetics of the reaction of **2a**-OTf with **6b** in MeCN (20 °C, stopped-flow,  $\lambda = 530$  nm)

[ <b>6b</b> ] <sup>a</sup> / mol L <sup>-1</sup>	[ <b>2a</b> -OTf]/ mol L <sup>-1</sup>	[ <b>2a</b> -OTf]/ [ <b>6b</b> ]	$k_{\text{obs}}/\text{s}^{-1}$
$3.33 \times 10^{-5}$	$3.47 \times 10^{-4}$	10.4	1.15
	$6.95 \times 10^{-4}$	20.9	2.11
	$1.04 \times 10^{-3}$	31.2	3.21
	$1.39 \times 10^{-3}$	41.7	4.30

$$k_2 = 3.04 \times 10^3 \text{ L mol}^{-1} \text{ s}^{-1}$$



<sup>a</sup> In the presence of 1.05 equiv of 18-crown-6 with respect to **6b**-K

### 3.4.7. Determination of the Rate Constants for Reactions of Carbanions **6a** and **6f** with the Benzhydrylium ions **11a,b** and the Quinone Methides **11c-g** in MeCN

**Table S63.** Kinetics of the reaction of **11a** with **6a** in MeCN (20 °C, stopped-flow,  $\lambda = 635$  nm)

[ <b>11a</b> ]/ mol L <sup>-1</sup>	[ <b>6a</b> ]/ mol L <sup>-1</sup>	[18-crown-6]/ mol L <sup>-1</sup>	[ <b>6a</b> ]/[ <b>11a</b> ]	$k_{\text{obs}}/\text{s}^{-1}$
$9.38 \times 10^{-6}$	$5.67 \times 10^{-5}$		6.0	$1.56 \times 10^1$
	$1.13 \times 10^{-4}$	$1.19 \times 10^{-4}$	12.0	$3.49 \times 10^1$
	$1.70 \times 10^{-4}$		18.1	$5.39 \times 10^1$
	$2.27 \times 10^{-4}$	$2.38 \times 10^{-4}$	24.2	$7.34 \times 10^1$
	$2.83 \times 10^{-4}$		30.2	$9.38 \times 10^1$

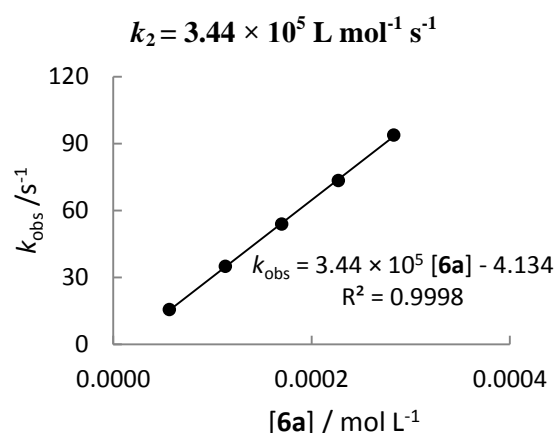


**Table S64.** Kinetics of the reaction of **11b** with **6a** in MeCN (20 °C, stopped-flow,  $\lambda = 631$  nm)

[ <b>11b</b> ]/ mol L <sup>-1</sup>	[ <b>6a</b> ]/ mol L <sup>-1</sup>	[18-crown-6]/ mol L <sup>-1</sup>	[ <b>6a</b> ]/[ <b>11b</b> ]	$k_{\text{obs}}/\text{s}^{-1}$
$1.00 \times 10^{-5}$	$3.67 \times 10^{-4}$		36.7	$3.15 \times 10^1$
	$7.34 \times 10^{-4}$	$7.71 \times 10^{-4}$	73.4	$6.18 \times 10^1$
	$1.10 \times 10^{-3}$		110	$9.32 \times 10^1$
	$1.47 \times 10^{-3}$		147	$1.22 \times 10^2$

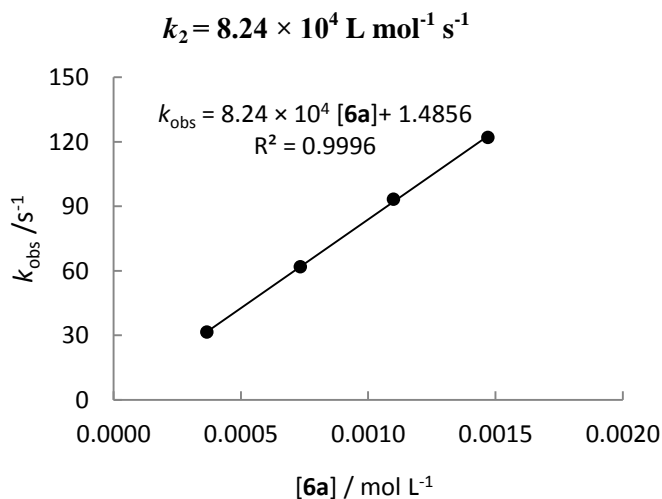


**Table S65.** Kinetics of the reaction of **11c** with **6f** in MeCN (20 °C, stopped-flow,  $\lambda = 422$  nm)

[ <b>11c</b> ]/ mol L <sup>-1</sup>	[ <b>6f</b> ]/ mol L <sup>-1</sup>	[ <b>6f</b> ]/ [ <b>11c</b> ]	$k_{\text{obs}}/\text{s}^{-1}$
$1.13 \times 10^{-5}$	$7.25 \times 10^{-5}$	6.4	$4.16 \times 10^1$
	$1.45 \times 10^{-4}$	12.8	$1.05 \times 10^2$
	$2.18 \times 10^{-4}$	19.3	$1.59 \times 10^2$
	$2.90 \times 10^{-4}$	25.7	$2.37 \times 10^2$
	$3.63 \times 10^{-4}$	32.1	$3.06 \times 10^2$

$$k_2 = 9.10 \times 10^5 \text{ L mol}^{-1} \text{ s}^{-1}$$

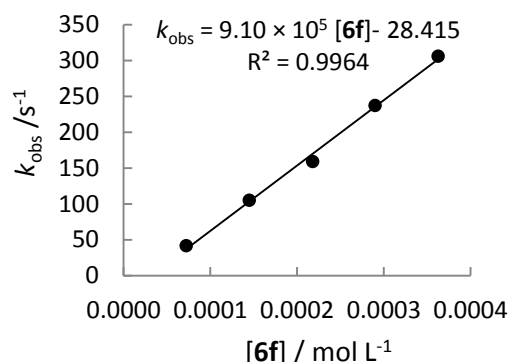


**Table S66.** Kinetics of the reaction of **11d** with **6f** in MeCN (20 °C, stopped-flow,  $\lambda = 374$  nm)

[ <b>11d</b> ]/ mol L <sup>-1</sup>	[ <b>6f</b> ]/ mol L <sup>-1</sup>	[18-crown-6]/ mol L <sup>-1</sup>	[ <b>6f</b> ]/[ <b>11d</b> ]	$k_{\text{obs}}/\text{s}^{-1}$
$2.59 \times 10^{-5}$	$1.65 \times 10^{-4}$		6.4	9.11
	$3.30 \times 10^{-4}$	$3.47 \times 10^{-4}$	12.7	$1.77 \times 10^1$
	$4.95 \times 10^{-4}$		19.1	$2.58 \times 10^1$
	$6.60 \times 10^{-4}$		25.5	$3.48 \times 10^1$
	$9.89 \times 10^{-4}$		38.2	$5.34 \times 10^1$

$$k_2 = 5.37 \times 10^4 \text{ L mol}^{-1} \text{ s}^{-1}$$

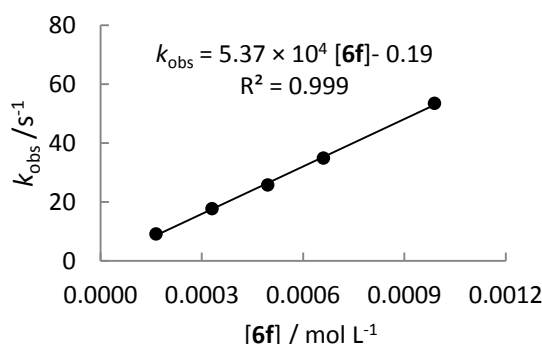


**Table S67.** Kinetics of the reaction of **11e** with **6f** in MeCN (20 °C, stopped-flow,  $\lambda = 354$  nm)

[ <b>11e</b> ]/ mol L <sup>-1</sup>	[ <b>6f</b> ]/ mol L <sup>-1</sup>	[ <b>6f</b> ]/ [ <b>11e</b> ]	$k_{\text{obs}}/\text{s}^{-1}$
$5.28 \times 10^{-5}$	$2.92 \times 10^{-4}$	5.5	1.03
	$3.64 \times 10^{-4}$	14.1	1.52
	$4.37 \times 10^{-4}$	16.8	1.91
	$5.10 \times 10^{-4}$	19.7	2.43

$$k_2 = 6.31 \times 10^3 \text{ L mol}^{-1} \text{ s}^{-1}$$

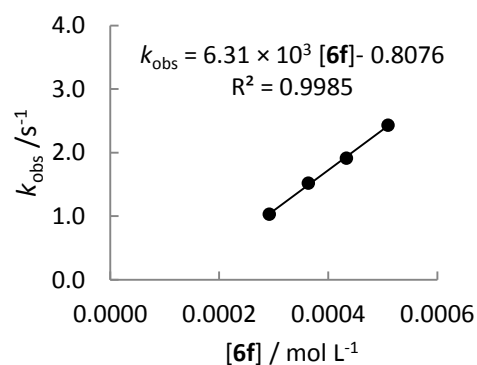


**Table S68.** Kinetics of the reaction of **11f** with **6f** in MeCN (20 °C, stopped-flow,  $\lambda = 371$  nm)

[ <b>11f</b> ]/ mol L <sup>-1</sup>	[ <b>6f</b> ]/ mol L <sup>-1</sup>	[ <b>6f</b> ]/ [ <b>11f</b> ]	$k_{\text{obs}}/\text{s}^{-1}$
$7.47 \times 10^{-5}$	$7.31 \times 10^{-4}$	9.8	1.44
	$1.10 \times 10^{-3}$	14.7	2.18
	$1.46 \times 10^{-3}$	19.5	2.92
	$1.83 \times 10^{-3}$	24.5	3.65
	$2.19 \times 10^{-3}$	29.3	4.35

$k_2 = 1.99 \times 10^3 \text{ L mol}^{-1} \text{ s}^{-1}$

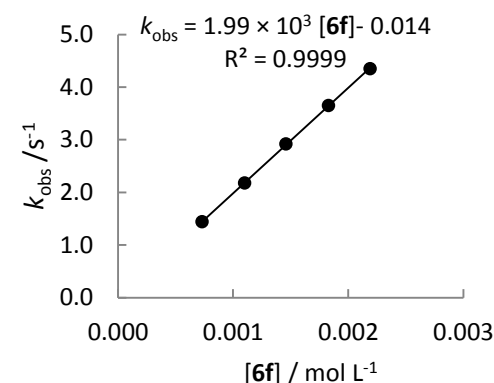


**Table S69.** Kinetics of the reaction of **11g** with **6f** in MeCN (20 °C, stopped-flow,  $\lambda = 393$  nm)

[ <b>11g</b> ]/ mol L <sup>-1</sup>	[ <b>6f</b> ]/ mol L <sup>-1</sup>	[18-crown-6]/ mol L <sup>-1</sup>	[ <b>6f</b> ]/[ <b>11g</b> ]	$k_{\text{obs}}/\text{s}^{-1}$
$4.15 \times 10^{-5}$	$2.90 \times 10^{-4}$		7.0	$3.70 \times 10^{-1}$
	$5.80 \times 10^{-4}$		14.0	$7.05 \times 10^{-1}$
	$8.70 \times 10^{-4}$	$9.14 \times 10^{-4}$	21.0	1.23
	$1.16 \times 10^{-3}$		28.0	1.64
	$1.45 \times 10^{-3}$	$1.52 \times 10^{-3}$	34.9	2.09

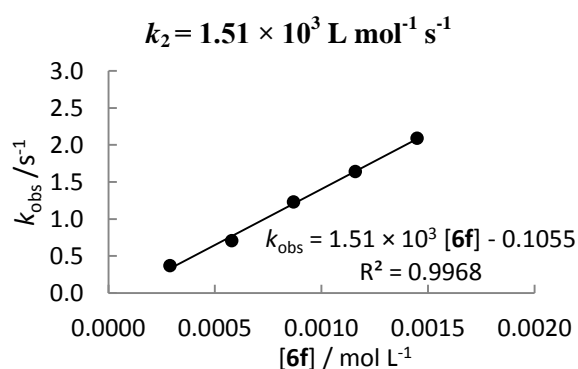
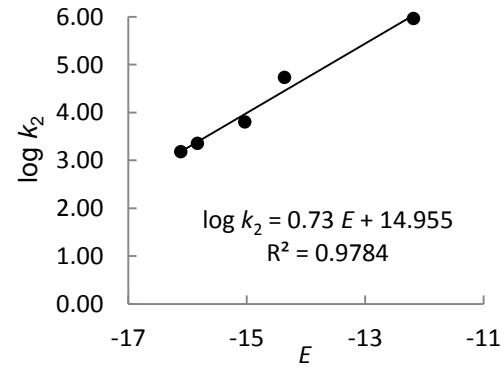


**Table S70.** Determination of the Reactivity Parameters  $N$  and  $s_N$  of the Carbanion **6f** in MeCN

Electrophile	$E$	$k_2$ , L mol <sup>-1</sup> s <sup>-1</sup>	$\log k_2$
<b>11c</b>	-12.18	$9.10 \times 10^5$	5.96
<b>11d</b>	-14.36	$5.37 \times 10^4$	4.73
<b>11e</b>	-15.03	$6.31 \times 10^3$	3.80
<b>11f</b>	-15.83	$1.99 \times 10^3$	3.35
<b>11g</b>	-16.11	$1.51 \times 10^3$	3.18

$N = 20.43, s_N = 0.73$



### 3.4.8. Determination of the Gibbs Energy of Electron Transfer ( $\Delta G^{\circ}_{\text{ET}}$ ) and the Gibbs Energy of Activation for the Polar Fluorine Transfer ( $\Delta G^{\ddagger}_{\text{P}}$ )

The second-order rate constants  $k_2$ (eq 3) for the fluorination of enamines **12a-f** were calculated from the linear free energy relationship  $\log k_2 = s_N (N + E)$ , using corresponding electrophilicities  $E$  of the N-F reagent determined from the reactions towards deoxybenzoin-derived enamines and the nucleophilicity parameters  $N$  and  $s_N$  of the enamines **12a-f**.<sup>38a</sup> The Gibbs energies of activation ( $\Delta G^{\ddagger}_{\text{P}}$ ) for polar fluorine transfer were estimated from  $k_2$ (eq 3) by using the Eyring equation (5).

$$k_2 = (k_b T/h) \exp(-\Delta G^{\ddagger}/RT) \quad (5)$$

**Table S71.** The second-order rate constants  $k_2$ (eq 3) and the corresponding Gibbs energies of activation ( $\Delta G^{\ddagger}_{\text{P}}$ ) for the polar fluorine transfer from N-F reagents **1-3** to the enamines **12a-f**

Nu	NFSI ( <b>1</b> )		<b>2a</b>		<b>2b</b>		Selectfluor ( <b>3</b> )	
	$E = -8.44$		$E = -10.46$		$E = -9.89$		$E = -5.20$	
	$k_2(\text{eq 3}) /$ $\text{L mol}^{-1} \text{s}^{-1}$	$\Delta G^{\ddagger}_{\text{P}} /$ $\text{kJ mol}^{-1}$	$k_2(\text{eq 3}) /$ $\text{L mol}^{-1} \text{s}^{-1}$	$\Delta G^{\ddagger}_{\text{P}} /$ $\text{kJ mol}^{-1}$	$k_2(\text{eq 3}) /$ $\text{L mol}^{-1} \text{s}^{-1}$	$\Delta G^{\ddagger}_{\text{P}} /$ $\text{kJ mol}^{-1}$	$k_2(\text{eq 3}) /$ $\text{L mol}^{-1} \text{s}^{-1}$	$\Delta G^{\ddagger}_{\text{P}} /$ $\text{kJ mol}^{-1}$
<b>12a</b>	$2.66 \times 10^6$	36	$4.86 \times 10^4$	45	$1.50 \times 10^5$	43	$1.62 \times 10^9$	20
<b>12b</b>	$2.68 \times 10^5$	41	$5.92 \times 10^3$	51	$1.74 \times 10^4$	48	$1.22 \times 10^8$	26
<b>12c</b>	$1.19 \times 10^4$	49	$2.62 \times 10^2$	58	$7.70 \times 10^2$	56	$5.40 \times 10^6$	34
<b>12d</b>	$3.67 \times 10^5$	41	$6.71 \times 10^3$	50	$2.08 \times 10^4$	48	$2.24 \times 10^8$	25
<b>12e</b>	$9.66 \times 10^3$	49	$2.23 \times 10^2$	59	$6.47 \times 10^2$	56	$4.07 \times 10^6$	35
<b>12f</b>	$2.86 \times 10^2$	58	6.03	67	$1.79 \times 10^1$	65	$1.40 \times 10^5$	43

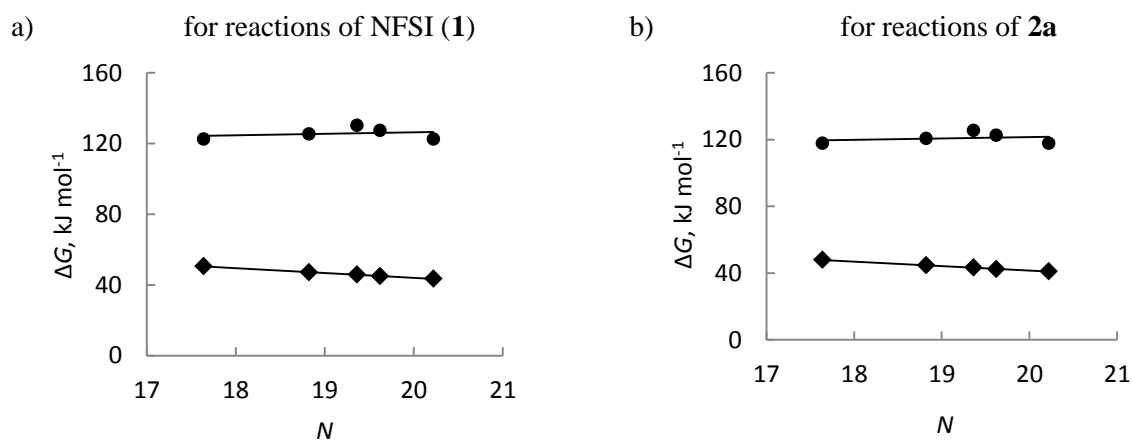
By applying the same method, we have used the oxidation potentials ( $E^{\text{ox}}$ ) reported for representative carbanions **13a-e**,<sup>61</sup> to calculate the Gibbs energy of electron transfer ( $\Delta G^{\circ}_{\text{ET}}$ ) of their reactions with NFSI (**1**) and fluorocollidinium salt **2a** (Table S72). The Gibbs energies of activation ( $\Delta G^{\ddagger}_{\text{P}}$ ) for polar fluorine transfer from N-F reagents to carbanions **13** were estimated from the second-order rate constants  $k_2$ (eq 3) calculated by using the linear free energy relationship  $\log k_2 = s_N(N + E)$  and corresponding nucleophilicity parameters of the carbanions **13** and electrophilicity parameters for N-F reagents determined from the reactions with carbanions **6**. Figure S8 shows that for both N-F reagents  $\Delta G^{\circ}_{\text{ET}}$  are approx. 70-80  $\text{kJ mol}^{-1}$  higher than  $\Delta G^{\ddagger}_{\text{P}}$ .

**Table S72.** The calculated Gibbs energies of electron transfer ( $\Delta G^\circ_{\text{ET}}$ ) from carbanions **13** to N-F reagents **1** and **2a**, the second-order rate constants  $k_2$ (eq 3) and the corresponding Gibbs energies of activation ( $\Delta G^\ddagger_{\text{P}}$ ) for the polar fluorine transfer from N-F reagents **1** and **2a** to the carbanions **13a-e**.

Nucleophile	$N$ ( $s_N$ ) <sup>a</sup>	$E^{\text{ox}, b}$ V vs SCE	NFSI ( <b>1</b> ) $E = -12.47^c$			<b>2a</b> $E = -11.80^c$		
			$\Delta G^\circ_{\text{ET}} /$ kJ mol <sup>-1</sup>	$k_2(\text{eq 3}) /$ L mol <sup>-1</sup> s <sup>-1</sup>	$\Delta G^\ddagger_{\text{P}} /$ kJ mol <sup>-1</sup>	$\Delta G^\circ_{\text{ET}} /$ kJ mol <sup>-1</sup>	$k_2(\text{eq 3}) /$ L mol <sup>-1</sup> s <sup>-1</sup>	$\Delta G^\ddagger_{\text{P}} /$ kJ mol <sup>-1</sup>
$\text{EtO}_2\text{C}-\text{C}^--\text{CO}_2\text{Et}$ <b>13a</b>	20.22 (0.65)	0.49	123	$1.09 \times 10^5$	44	118	$2.97 \times 10^5$	41
$\text{NC}-\text{C}^--\text{CO}_2\text{Et}$ <b>13b</b>	19.62 (0.67)	0.54	127	$6.17 \times 10^4$	45	123	$1.74 \times 10^5$	42
$\text{NC}-\text{C}^--\text{CN}$ <b>13c</b>	19.36 (0.67)	0.57	130	$4.13 \times 10^4$	46	125	$1.16 \times 10^5$	43
$\text{Me}-\text{C}(=\text{O})-\text{C}^--\text{C}(=\text{O})-\text{Me}$ <b>13d</b>	18.82 (0.69)	0.52	125	$2.41 \times 10^4$	47	121	$6.98 \times 10^4$	45
$\text{Me}-\text{C}(=\text{O})-\text{C}^--\text{CO}_2\text{Et}$ <b>13e</b>	17.64 (0.73)	0.49	123	$5.94 \times 10^3$	51	118	$1.83 \times 10^4$	48

<sup>a</sup> In DMSO, from ref 33c <sup>b</sup>  $E^{\text{ox}}$  (in DMSO) was used without solvent correction, from ref 61 <sup>c</sup> Determined from the correlation with carbanions **6** (see Table 21 and 32)

**Figure S8.** Comparison of calculated Gibbs energies of electron transfer ( $\Delta G^\circ_{\text{ET}}$ ) from carbanions **13** to N-F reagents **1** and **2a** and the corresponding Gibbs energies of activation ( $\Delta G^\ddagger_{\text{P}}$ ) for the polar fluorine transfer from N-F reagents **1** and **2a** to the carbanions **13a-e**.



### 3.6. References

- (1) (a) Cartwright, D. Recent Developments in Fluorine-Containing Agrochemicals. In *Organofluorine Chemistry. Principles and Commercial Applications*; Banks, R. E., Smart, B. E., Tatlow, J. C., Eds.; Plenum Press: New York, 1994; pp 237–262. (b) Lang, R. W. Fluorinated Agrochemicals. In *Chemistry of Organic Fluorine Compounds II*; Hudlicky, M. Pavlath, A. E., Eds; ACS Monograph 187; American Chemical Society: Washington, DC, 1995; p 1143. (c) Jeschke, P. *ChemBioChem* **2004**, *5*, 570–589. (d) Maienfisch, P.; Hall, R. G. *Chimia* **2004**, *58*, 93–99. (e) Fujiwara, T.; O'Hagan, D. *J. Fluorine Chem.* **2014**, *167*, 16–29.
- (2) (a) Elliot, A. J. Fluorinated Pharmaceuticals. In *Chemistry of Organic Fluorine Compounds II*; Hudlicky, M.; Pavlath, A. E., Eds. ACS Monograph 187; American Chemical Society, Washington, DC, 1995; pp 1119–1125. (b) Böhm, H. J.; Banner, D.; Bendels, S.; Kansy, M.; Kuhn, B.; Müller, K.; Obst-Sander, U.; Stahl, M. *ChemBioChem* **2004**, *5*, 637–643. (c) Müller, K.; Faeh, C.; Diederich, F. *Science* **2007**, *317*, 1881–1886. (d) Bégué, J. P.; Bonnet-Delpon D. *Bioorganic and Medicinal Chemistry of Fluorine*, Wiley: New York, 2008. (e) Tressaud, A.; G. Haufe, *Fluorine and Health – Molecular Imaging, Biomedical Materials and Pharmaceuticals*; Elsevier: Amsterdam, 2008. (f) Kirk, K. L. *Org. Process Res. Dev.* **2008**, *12*, 305–321. (g) Purser, S.; Moore, P. R.; Swallow, S., Gouverneur V. *Chem. Soc. Rev.* **2008**, *37*, 320–330. (h) Yerien, D. E.; Bonesi, S.; Postigo, A. *Org. Biomol. Chem.* **2016**, *14*, 8398–8427.
- (3) (a) Hung M. H.; Farnham, W. B.; Feiring, A. E.; Rozen, S. Functional fluoromonomers and fluoropolymers. In: *Fluoropolymers*. Hougham G., Cassidy P. E., Johns K., Davidson T. (Eds), Plenum Publishing Co, New York, 1999. (b) Wei, H. C.; Lagow, R. J. *Chem Commun.* **2000**, *21*, 2139–2141. (c) Hird, M. *Chem. Soc. Rev.* **2007**, *36*, 2070–2095. (d) Kirsch, P.; Binder, W.; Hahn, A.; Jährling, K.; Lenges, M.; Lietzau, L.; Maillard, D.; Meyer, V.; Poetsch, E.; Ruhl, A.; Unger G.; Fröhlich, R. *Eur. J. Org. Chem.* **2008**, 3479–3487.
- (4) (a) Olah, G. A.; Shih, J. G.; Prakash, G. K. S. Fluorine-Containing Reagents in Organic Synthesis. In *Fluorine the First Hundred Years (1886-1989)*; Banks, R. E., Sharp, D. W. A., Tatlow, J. C., Eds; Elsevier Sequoia: Lausanne and New York, 1986. (b) *Organofluorine Chemistry. Principles and Commercial Applications*, Banks, R. E., Smart, B. E., and Tatlow, J. C., Eds., New York: Plenum Press, 1994. (c) Hiyama, T. *Organofluorine Compounds: Chemistry and Applications*; Yamamoto, H. Ed.; Springer: Berlin, 2000. (d) Chambers, R. D. *Fluorine in Organic Chemistry*; Blackwell: Oxford, UK, 2004. (e) O'Hagan, D. *Chem. Soc. Rev.* **2008**, *37*, 308–319. (f) Kirsch, P. *Modern Fluoroorganic Chemistry* 2nd ed.; Wiley-



VCH: Weinheim, 2013. (g) Liang, T.; Neumann, C. N.; Ritter, T. *Angew. Chem. Int. Ed.* **2013**, *52*, 8214–8264. (h) Furuya, T.; C. A. Kuttruff, C. A.; Ritter, T. *Curr. Opin. Drug Discovery Dev.* **2008**, *11*, 803–819.

(5) (a) Purrington, S. T.; Kagen, B. S.; Patrick, T. B. *Chem. Rev.* **1986**, *86*, 997–1018. (b) Hutchinson J.; Sandford G. Elemental Fluorine in Organic Chemistry. In *Organofluorine Chemistry (Topics in Current Chemistry Vol. 193)*; Chambers, R. D., Ed.; Springer: Berlin, Heidelberg, 1997; pp 1–43. (c) Sandford, G. *J. Fluorine Chem.* **2007**, *128*, 90–104. (d) Rozen, S. Electrophilic Fluorination Reactions with F<sub>2</sub> and some Reagents Directly Derived From It. In *Synthetic Fluorine Chemistry*; Olah, G. A.; Chambers, R. D.; Prakash, G. K. S. Eds., Wiley, New York, 1992, pp 143–161. (e) Lagow, R. J. High-yield reactions of elemental fluorine. In *Fluorine The First Hundred Years (1886–1986)*; Banks, R. E., Sharp, D. W. A., Tatlow, J. C., Eds.; Elsevier Sequoia: Lausanne and New York, 1986; pp 321–325. (f) Adcock, J. L.; Cherry, M. L. *Ind. Eng. Chem. Res.* **1987**, *26*, 208–215.

(6) Hiller, A.; Fischer, C.; Jorbanova, A.; Pett, J. T.; Steinbach, J. *Appl. Radiat. Isot.* **2008**, *66*, 152–157.

(7) (a) Tius, M. A. *Tetrahedron*, **1995**, *51*, 6605–6634. (b) Filler, R. *Isr. J. Chem.* **1978**, *17*, 71–79.

(8) (a) Hesse, R. H. *Isr. J. Chem.* **1978**, *17*, 60–70. (b) Middleton, W. J.; Bingham, E. M. *J. Am. Chem. Soc.* **1980**, *102*, 4845–4846. (c) Barton, D. H. R.; Ganguly, A. K.; Hesse, R. H.; Loo, S. N.; Pechet, M. M. *Chem. Commun.* **1968**, 806–808. (d) For a review about reagents containing the O–F group, see: Rozen, S. *Chem. Rev.* **1996**, *96*, 1717–1736.

(9) (a) Lerman, O.; Tor, Y.; Hebel, D.; Rozen, S. *J. Org. Chem.* **1984**, *49*, 806–813. (b) Rozen, S.; Lerman, O.; Kol, M.; Hebel, D. *J. Org. Chem.* **1985**, *50*, 4753–4758.

(10) Rozen, S.; Menahem, Y. *J. Fluorine Chem.* **1980**, *16*, 19–31.

(11) Reviews: (a) Lal, G. S.; Pez, G. P.; Syvret, R. G. *Chem. Rev.* **1996**, *96*, 1737–1756. (b) Taylor, S. D.; Kotoris, C. C.; Hum, G. *Tetrahedron* **1999**, *55*, 12431–12477. (c) Umemoto, T. *J. Fluorine Chem.* **2014**, *167*, 3–15. (d) Baudoux, J.; Cahard, D. Electrophilic Fluorination With N–F Reagents. In *Organic Reactions*; Denmark, S. E., Ed.; Wiley: Hoboken, 2007; Chapter 2, pp 347–672. (e) Champagne, P. A.; Desroches, J.; Hamel, J.-D.; Vandamme, M.; Paquin, J.-F. *Chem. Rev.* **2015**, *115*, 9073–9174.

(12) Differding, E.; Ofner, H. *Synlett* **1991**, 187–189.

- (13) (a) Barnette W. E., *J. Am. Chem. Soc.* **1984**, *106*, 452–454. (b) Davis, F. A.; Han, W. *Tetrahedron Lett.* **1991**, *32*, 1631–1634. (c) Resnati, G.; Desmarteau, D. D. *J. Org. Chem.* **1991**, *56*, 4925–4929. (d) Davis, F. A.; Han, W.; Murphy, C. K. *J. Org. Chem.* **1995**, *60*, 4730–4737. (e) Yasui, H.; Yamamoto, T.; Ishimaru, T.; Fukuzumi, T.; Tokunaga, E.; Akikazu, K.; Shiro, M.; Shibata, N. *J. Fluorine Chem.* **2011**, *132*, 222–225.
- (14) (a) Umemoto, T.; Tomita, K. *Tetrahedron Lett.* **1986**, *27*, 3271–3274. (b) Umemoto, T.; Kawada, K.; Tomita, K. *Tetrahedron Lett.* **1986**, *27*, 4465–4468. (c) Umemoto, T.; Tomizawa, G. *Tetrahedron Lett.* **1987**, *28*, 2705–2708. (d) Umemoto, T.; Tomizawa, G. *J. Org. Chem.* **1989**, *54*, 1726–1731. (e) Umemoto, T.; Fukami, S.; Tomizawa, G.; Harasawa, K.; Kawada, K.; Tomia, K. *J. Am. Chem. Soc.* **1990**, *112*, 8563–8575. (f) Umemoto, T.; Tomizawa, G. *J. Org. Chem.* **1995**, *60*, 6563–6570. (g) Umemoto, T.; Nagayoshi, M.; Adachi, K.; Tomizawa, G. *J. Org. Chem.* **1998**, *63*, 3379–3385. (h) Kiselyov, A. S. *Chem. Soc. Rev.* **2005**, *34*, 1031–1037.
- (15) (a) Banks, R. E.; Du Boisson, R. A.; Tsiliopoulos, E. *J. Fluorine Chem.* **1986**, *32*, 461–466. (b) Banks, R. E.; Sharif I. *J. Fluorine Chem.* **1991**, *55*, 207–214.
- (16) (a) Banks, R. E.; Mohialdin-Khaffaf, S. N.; Lal, G. S.; Sharif, I.; Syvret, R. G. *J. Chem. Soc. Chem. Commun.* **1992**, 595–596. (b) Lal, G. S. *J. Org. Chem.* **1993**, *58*, 2791–2796. (c) Banks, R. E.; Besheesh, M. K.; Mohialdin-Khaffaf, S. N.; Sharif, I. *J. Chem. Soc., Perkin Trans. 1* **1996**, 2069–2076. (d) Banks, R. E. *J. Fluorine Chem.* **1998**, *87*, 1–17. (e) Nyffeler, P. T.; Durón, S. G.; Burkart, M. D.; Vincent, S. P.; Wong, C. H. *Angew. Chem., Int. Ed.* **2004**, *44*, 192–212. (f) Singh, R. P.; Shreeve, J. M. *Acc. Chem. Res.* **2004**, *37*, 31–44. (g) Stavber, S. *Molecules* **2011**, *16*, 6432–6464.
- (17) Reviews: (a) Muñiz, K. *Angew. Chem., Int. Ed.* **2001**, *40*, 1653–1656. (b) Ma, J.-A.; Cahard, D. *Chem. Rev.* **2008**, *108*, PR1–PR43. (c) Brunet, V.A.; O'Hagan, D. *Angew. Chem., Int. Ed.* **2008**, *47*, 1179–1182. (d) Cao, L. L.; Gao, B. L.; Ma, S. T.; Liu, Z. P. *Curr. Org. Chem.* **2010**, *14*, 808–916. (e) Furuya, T.; Kamlet, A. S.; Ritter, T. *Nature* **2011**, *473*, 470–477. (f) Lin, J. H.; Xiao, J. C. *Tetrahedron Lett.* **2014**, *55*, 6147–6155.
- (18) (a) Cahard, D.; Audouard, C.; Plaquevent, J. C.; Roques, N. *Org. Lett.* **2000**, *2*, 3699–3701. (b) Shibata, N.; Suzuki, E.; Asahi, T.; Shiro, M. *J. Am. Chem. Soc.* **2001**, *123*, 7001–7009. (c) Baudequin, C.; Loubassou, J. F.; Plaquevent, J. C.; Cahard, D. *J. Fluorine Chem.* **2003**, *122*, 189–193.

- (19) (a) Differding, E.; Lang, R.W. *Tetrahedron Lett.* **1988**, 29, 6087–6090. (b) Differding, E.; Lang, R. W. *Helv. Chim. Acta* **1989**, 72, 1248–1252. (c) Davis, F. A.; Rüegg, G. M.; Murphy, C. K. *Tetrahedron Lett.* **1991**, 32, 1779–1782. (d) Davis, F. A, Zhou, P.; Murphy, C. K. *Tetrahedron Lett.* **1993**, 34, 3971–3974.
- (20) (a) Pereira, R.; Wolstenhulme, J.; Sandford, G.; Claridge, T. D. W.; Gouverneur, V.; Cvengroš, J. *Chem. Commun.* **2016**, 52, 1606–1609. (b) Wolstenhulme, J. R.; Rosenqvist, J.; Lozano, J.; Ilupeju, J.; Wurz, N.; Engle, K. M.; Pidgeon, G. W.; Moore P.R.; Sandford, G.; Gouverneur, V. *Angew. Chem., Int. Ed.* **2013**, 52, 9796–9800.
- (21) Gilicinski, A. G.; Pez, G. P.; Syvret, R. G.; Lal, G. S. *J. Fluorine Chem.* **1992**, 59, 157–162.
- (22) Sudlow, K.; Woolf, A. A. *J. Fluorine Chem.* **1994**, 66, 9–11.
- (23) Oliver, E. W.; Evans, D. H. *J. Electroanal. Chem.* **1999**, 474, 1–8.
- (24) Umemoto, T.; Harasawa, K.; Tomizawa, G.; Kawata, K.; Tomita, K. *J. Fluorine Chem.* **1991**, 53, 369–377.
- (25) Toullec, P. Y.; Devillers, I.; Frantz, R.; Togni, A. *Helv. Chim. Acta* **2004**, 87, 2706–2711.
- (26) (a) Xue, X.-S.; Wang, Y.; Li, M. Cheng, J.-P. *J. Org. Chem.* **2016**, 81, 4280–4289. (b) Li, M.; Zheng, H.; Xue, X.-S.; Cheng, J.-P. *Tetrahedron Lett.* **2018**, 59, 1278–1285.
- (27) (a) For enamines **5a–h** see: Timofeeva, D. S.; Mayer, R. J.; Mayer, P.; Ofial, A. R.; Mayr, H. *Chem. Eur. J.* **2018**, 24, 5901–5910. (b) For carbanions **6a,d** see: Berger, S. T. A.; Ofial, A. R.; Mayr, H. *J. Am. Chem. Soc.* **2007**, 129, 9753–9761. (c) For carbanion **6b** see: Puente, Á.; He, S.; Corral-Bautista, F.; Ofial, A. R.; Mayr, H. *Eur. J. Org. Chem.* **2016**, 1841–1848. (d) For the determination of the nucleophilicity of carbanion **6c** see Supporting Information of this paper. (e) For carbanion **6e** see: Kaumanns, O.; Appel, R.; Lemek, T.; Seeliger, F.; Mayr, H. *J. Org. Chem.* **2009**, 74, 75–81. (f) For carbanion **6f** see: Corral-Bautista, F.; Mayr, H. *Eur. J. Org. Chem.* **2013**, 4255–4261. (g) For a comprehensive database of nucleophilicity parameters  $N$  and  $s_N$  as well as electrophilicity parameters  $E$ , see: <http://www.cup.lmu.de/oc/mayr/DBintro.html>.
- (28) (a) Peng, W.; Shreeve, J. M. *J. Org. Chem.* **2005**, 70, 5760–5763. (b) Purrington, S. T.; Jones, W. A. *J. Fluorine Chem.* **1984**, 26, 43–46. (c) Dinér, P.; Kjærsgaard, A.; Lie, M. A.;

Jørgensen, K. A. *Chem. Eur. J.* **2008**, *14*, 122–127. (d) Nakanishi, S. *Steroids* **1963**, *2*, 765–770.

(29) Dilman D. A.; Belyakov, P. A.; Struchkova M. I.; Arkhipov, D. E.; Korlyukov, A. A.; Tartakovsky, V. A. *J. Org. Chem.* **2010**, *75*, 5367–5370.

(30) (a) Terrier, F. *Modern Nucleophilic Aromatic Substitution*; Wiley-VCH: Weinheim, 2013. (b) Makosza, M. Nucleophilic substitution of hydrogen in electron-deficient arenes. In *Arene Chemistry: Reaction Mechanisms and Methods for Aromatic Compound*; Mortier, J. Ed.; Wiley, Hoboken NJ, 2016; pp 269–298. (c) Makosza, M. *Synthesis* **2017**, *49*, 3247–3254. (d) Seeliger, F.; Błazej, S.; Bernhardt, S.; Makosza, M.; Mayr, H. *Chem. Eur. J.* **2008**, *14*, 6108–6118. (e) Guo, X.; Mayr, H. *J. Am. Chem. Soc.* **2014**, *136*, 11499–11512.

(31) Gakh, A.; Kiselyov, A. S.; Semenov, V. V. *Tetrahedron Lett.* **1990**, *31*, 7379–7382.

(32) Kiselyov A. S.; Strekowski, L. *J. Heterocycl. Chem.* **1993**, *30*, 1361–1364.

(33) (a) Mayr, H.; Patz, M. *Angew. Chem., Int. Ed. Engl.* **1994**, *33*, 938–957. (b) Mayr, H.; Bug, T.; Gotta, M. F.; Hering, N.; Irrgang, B.; Janker, B.; Kempf, B.; Loos, R.; Ofial, A. R.; Remennikov, G.; Schimmel, H. *J. Am. Chem. Soc.* **2001**, *123*, 9500–9512. (c) Lucius, R.; Loos, R.; Mayr, H. *Angew. Chem., Int. Ed.* **2002**, *41*, 91–95. (d) Mayr, H.; Kempf, B.; Ofial, A. R. *Acc. Chem. Res.* **2003**, *36*, 66–77. (e) Mayr, H.; Ofial, A. R. *Pure Appl. Chem.* **2005**, *77*, 1807–1821. (f) Mayr, H.; Ofial, A. R. *SAR QSAR Environ. Res.* **2015**, *26*, 619–646. (g) D. Richter, N. Hampel, T. Singer, A. R. Ofial, H. Mayr, *Eur. J. Org. Chem.* **2009**, 3203–3211.

(34) Phan, T. B.; Breugst, M.; Mayr, H. *Angew. Chem., Int. Ed.* **2006**, *45*, 3869–3874.

(35) C. Hansch, C.; Leo, A.; Taft, R. W. *Chem. Rev.* **1991**, *91*, 165–195.

(36) (a) Differding, E.; Rüegg, G. M. *Tetrahedron Lett.* **1991**, *32*, 3815–3818. (b) Differding, E.; Wehrli, M. *Tetrahedron Lett.* **1991**, *32*, 3819–3822. (c) Differding, E.; Bersier, P. M. *Tetrahedron* **1992**, *48*, 1595–1604. (d) Andrieux, C. P.; Differding, E.; Robert, M.; Savéant, J.-M. *J. Am. Chem. Soc.* **1993**, *115*, 6592–6599. (e) Vincent, S. P.; Burkart, M. D.; Tsai, C.-Y.; Zhang, Z.; Wong, C.-H. *J. Org. Chem.* **1999**, *64*, 5264–5279.

(37) Schoeller, W. W.; Niemann, J.; Rademacher, P. *J. Chem. Soc., Perkin Trans. 2* **1988**, 369–373.

(38) (a) Kempf, B.; Hampel, N.; Ofial, A. R.; Mayr, H. *Chem. Eur. J.* **2003**, *9*, 2209–2218. (b) Ammer, J.; Nolte, C.; Mayr, H. *J. Am. Chem. Soc.* **2012**, *134*, 13902–13911.

- (39) (a) Intermediate data of these calculations are given in Table S71 (Experimental Section). (b) An analogous comparison of  $\Delta G^\ddagger_P$  with  $\Delta G^\circ_{ET}$  for the fluorinations of five carbanions by N-F reagents **1** and **2a** (see Table S72 and Figure S8 of the Experimental Section) reveals the polar mechanism to be preferred by 72–82 kJ mol<sup>-1</sup>. (c) Instead of comparing the Gibbs activation energy for the polar fluorination ( $\Delta G^\ddagger_P$ ) with  $\Delta G^\circ_{ET}$  one might also use the Marcus or Rehm-Weller relationships to calculate Gibbs energies of activation for electron transfer  $\Delta G^\ddagger_{ET}$ . Given that both approaches would require to estimate the intrinsic barriers for electron transfer, we consider the comparison of  $\Delta G^\ddagger_P$  with  $\Delta G^\circ_{ET}$  (Table 6, Figure 9 and Experimental Section) more convincing in cases where  $\Delta G^\circ_{ET}$  is significantly larger than  $\Delta G^\ddagger_P$ .
- (40) (a) Baidya, M.; Kobayashi, S.; Brotzel, F.; Schmidhammer, U.; Riedle, E.; Mayr, H. *Angew. Chem., Int. Ed.* **2007**, *46*, 6176–6179. (b) Mayr, H.; Ofial, A. R. *Acc. Chem. Res.* **2016**, *49*, 952–965.
- (41) (a) Linnell, R. H. *J. Org. Chem.* **1960**, *25*, 290. (b) Hall, N. F.; Sprinkle, M. R. *J. Am. Chem. Soc.* **1932**, *54*, 3469–3485. (c) Johnson, C. D.; Katritzky, A. R. Ridgewell, B. J.; Shakir, N.; White, A. M. *Tetrahedron* **1965**, *21*, 1055–1059. (d) Exner, O.; Janák, P. *Collect. Czech. Chem. Commun.* **1975**, *40*, 2510–2523. (e) Meloun, M.; Syrový, T.; Vrána, A. *Anal. Chim. Acta* **2005**, *533*, 97–110.
- (42) Christe, K. O.; Dixon, D. A. *J. Am. Chem. Soc.* **1992**, *114*, 2978–2985.
- (43) (a) Marcus, R. A. *J. Chem. Phys.* **1956**, *24*, 966–978. (b) Marcus, R. A. *J. Phys. Chem.* **1968**, *72*, 891–899.
- (44) Zupan, M.; Iskra, J.; Stavber, S. *Tetrahedron* **1996**, *52*, 11341–11348.
- (45) Shamma, T.; Buchholz, H.; Prakash, G. K. S.; Olah, G. A. *Isr. J. Chem.* **1999**, *39*, 207–210.
- (46) Stavber, G.; Zupan, M.; Stavber, S. *Tetrahedron Lett.* **2007**, *48*, 2671–2673.
- (47) Zupan, M.; Iskra, J.; Stavber, S. *J. Org. Chem.* **1995**, *60*, 259–260.
- (48) Wang, W.; Xu, B.; Hammond, G. B. *Synthesis* **2011**, 2383–2386.
- (49) (a) Thibaudeau, S.; Gouverneur, V. *Org. Lett.* **2003**, *5*, 4891–4893. (b) Tredwell, M.; Gouverneur, V. *Org. Biomol. Chem.* **2006**, *4*, 26–32. (c) Sawicki, M.; Kwok, A.; Tredwell, M.; Gouverneur, V. *Beilstein J. Org. Chem.* **2007**, *3*, No. 34 (doi: 10.1186/1860-5397-3-34).

- (d) S. C. Wilkinson, S. C.; O. Lozano, O.; M. Schuler, M.; M. Pacheco, M.; R. Salmon, R.; V. Gouverneur, V. *Angew. Chem., Int. Ed.* **2009**, *48*, 7083–7086.
- (50) (a) Ueno, T.; Toda, H.; Yasunami, M.; Yoshifuji, M. *Bull. Chem. Soc. Jpn.* **1996**, *69*, 1645–1656. (b) Muthyala, R. S.; Liu, R. S. H. *J. Fluorine Chem.* **1998**, *89*, 173–175.
- (51) Sandford, C.; Rasappan, R.; Aggarwal, V. K. *J. Am. Chem. Soc.* **2015**, *137*, 10100–10103.
- (52) Fuglseth, E.; Thvedt, T. H. K.; Møll, M. F.; Hoff, B. H. *Tetrahedron* **2008**, *64*, 7318–7323.
- (53) Bélanger, G.; Doré, M.; Ménard, F.; Darsigny, V. *J. Org. Chem.* **2006**, *71*, 7481–7484.
- (54) Hendrickson, J. B.; Giga, A.; Wareing, J. *J. Am. Chem. Soc.* **1974**, *96*, 2275–2276.
- (55) Puente, Á.; Ofial, A. R.; Mayr, H. *Eur. J. Org. Chem.* **2017**, 1196–1202.
- (56) Bailey, W. F.; Jiang, X.-L.; McLeod, C. E. *J. Org. Chem.* **1995**, *60*, 7791–7795.
- (57) Gottlieb, H. E.; Kotlyar, V.; Nudelman, A. *J. Org. Chem.* **1997**, *62*, 7512–7515.
- (58) (a) Wu, S.-W.; Liu, F. *Org. Lett.* **2016**, *18*, 3642–3645. (b) Kitamura, T.; Muta, K.; Muta, K. *J. Org. Chem.* **2014**, *79*, 5842–5846.
- (59) Toru, S.; Shoji, H. *J. Fluorine Chem.* **2014**, *168*, 55–60.
- (60) (a) Xiaomin, H.; Lu, Q.; Mali, X.; Xia, C. *J. Organomet. Chem.* **2017**, *853*, 168–177. (b) Wang, X.; Wu, Y.; Liu, Q.; Li, Z.; Yan, H.; Ji, C.; Duana, J.; Liu, Z. *Chem. Commun.* **2015**, *51*, 784–787.
- (61) Corral Bautista, F.; Appel, R.; Frickel, J. S.; Mayr, H. *Chem. Eur. J.* **2015**, *21*, 875–884.
- (62) (a) Bordwell, F. G.; Harrelson, J. A.; Satish, A. V. *J. Org. Chem.* **1989**, *54*, 3101–3105. (b) Zhang, X.-M.; Bordwell, F. G. *J. Phys. Org. Chem.* **1994**, *7*, 751–756.

## Chapter 4

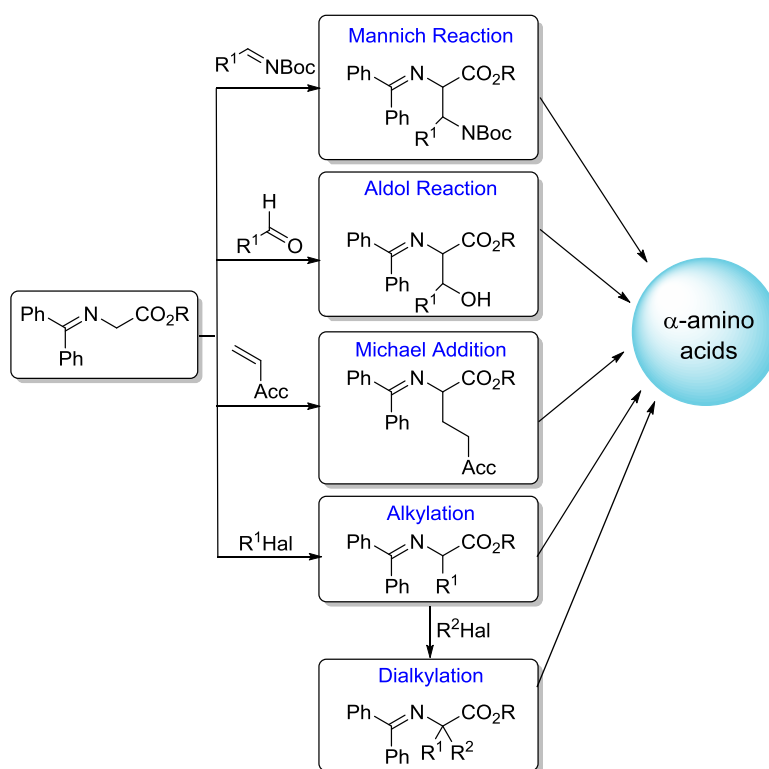
Nucleophilic Reactivities  
of Schiff Base Derivatives of Amino Acids

Daria S. Timofeeva, Armin R. Ofial, Herbert Mayr

*Tetrahedron* **2018**, submitted

## 4.1. Introduction

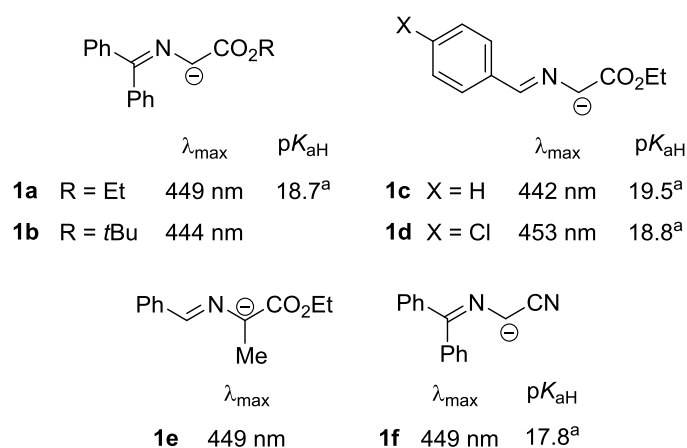
$\alpha$ -Imino esters have become frequently used building blocks for synthesizing racemic and optically active  $\alpha$ -amino acids and derivatives, which are of great importance in pharmaceutical, biological and synthetic chemistry.<sup>1</sup> The benzophenone-derived imines of glycine alkyl esters were introduced by O'Donnell in 1978,<sup>2</sup> and in the last 30 years these substrates have been used for the synthesis of  $\alpha$ -amino acids via a wide variety of synthetic routes, including phase transfer catalyzed alkylations<sup>3-5</sup>, Michael,<sup>6-11</sup> aldol,<sup>12,13</sup> and Mannich<sup>14-17</sup> reactions (Scheme 1).

**Scheme 1.** Amino acids from benzophenone imines of glycine esters.

During the last decades our research group has developed comprehensive nucleophilicity and electrophilicity scales, which afford a direct comparison of the reactivities of different classes of compounds.<sup>18</sup> We have shown that the rates of the reactions of  $\pi$ -, n- and  $\sigma$ -nucleophiles with  $C_{sp^2}$ -centered electrophiles can be described by the linear Gibbs energy relationship (1), where  $k_2$  (20 °C) [ $L\ mol^{-1}\ s^{-1}$ ] is a second-order rate constant,  $N$  and  $s_N$  are solvent-dependent nucleophile-specific parameters and  $E$  is an electrophile-specific parameter.<sup>19</sup>

$$\lg k_2(20^\circ C) = s_N(N + E) \quad (1)$$

This method has already been employed to determine the reactivity of various carbanions,<sup>20</sup> including nitronate anions,<sup>20b</sup> alkoxycarbonyl-,<sup>20f</sup> cyano-,<sup>19b,20d</sup> phosphoryl-,<sup>20e</sup> and sulfonyl-stabilized<sup>20g</sup> carbanions and revealed that  $pK_a$  values of the conjugate acids do not serve as reliable measure of relative reactivities.<sup>20b,c,d,f</sup>

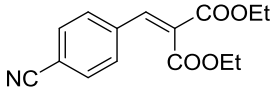
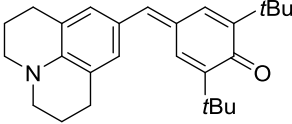
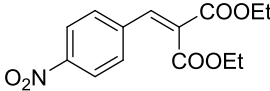
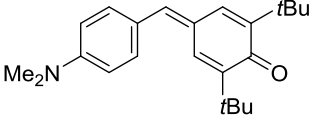
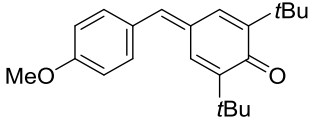


**Scheme 2.** UV-Vis absorption maxima and  $pK_{aH}$  values in DMSO of Schiff base derivatives of amino acids investigated in this work. Counterion  $K^+$ . <sup>a</sup> From Ref. 21.

We now report on the kinetics of the reactions of the potassium salts of different glycine- and alanine-derived imino esters **1a-e** and imino acetonitrile **1f** (Scheme 2) with the Michael acceptors **2a-e** (reference electrophiles, Table 1) in DMSO solution. The resulting second-order rate constants will then be used to determine the nucleophilicities of the title compounds according to Eq. (1).



**Table 1.** Quinone methides and benzylidene malonates as reference electrophiles employed in this work.

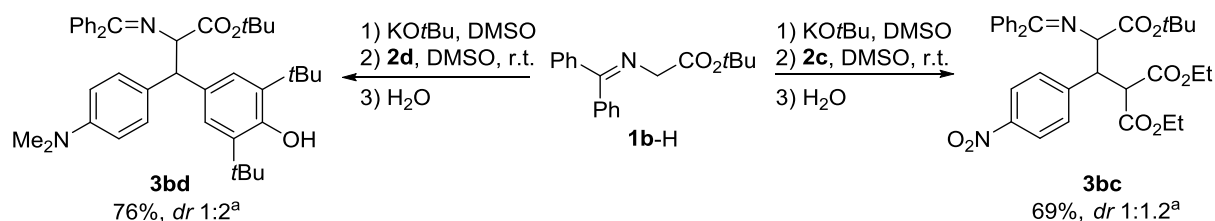
Electrophile	$E^a$	$\lambda_{\max}^b$
	<b>2a</b> -18.06	283
	<b>2b</b> -17.90	521
	<b>2c</b> -17.67	302
	<b>2d</b> -17.29	486
	<b>2e</b> -16.11	393

<sup>a</sup> From Refs. 19b, 22. <sup>b</sup> In DMSO solution, given in nm.

## 4.2. Results and Discussions

### 4.2.1. Products of the Reactions of the Carbanions **1** with Reference Electrophiles **2**

In order to examine the course of the reactions studied kinetically, we have characterized the products of representative combinations of the carbanions **1** with benzylidene malonate **2c** or quinone methide **2d**.

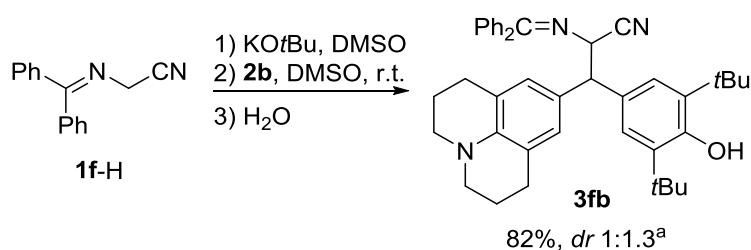


**Scheme 3.** Reactions of *tert*-butyl imino ester **1b-H** with the reference electrophiles **2c** and **2d** in DMSO at 20 °C. <sup>a</sup> Determined from <sup>1</sup>H NMR spectra of the crude product.

The benzophenone-derived *tert*-butyl glycine imino ester anion **1b** (1.1 equiv.), which was generated from **1b-H** by treatment with KOtBu in DMSO, reacted with the reference electrophiles **2c** and **2d** to afford the adducts **3bc** and **3bd**, respectively, as a mixture of two

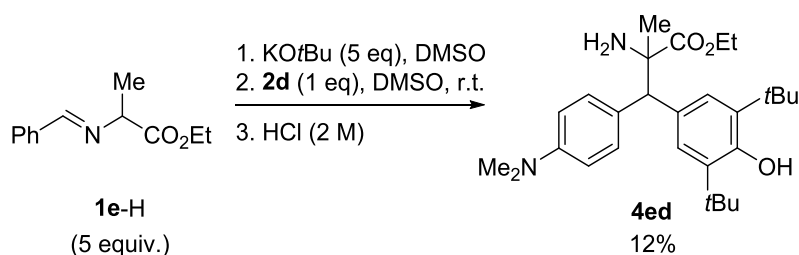
diastereomers after aqueous work up (Scheme 3). The products were isolated in moderate yields after purification by column chromatography and characterized by mass spectrometry and  $^1\text{H}$  and  $^{13}\text{C}$  NMR spectroscopy. Analogous products have recently been reported by Deng and coworkers via enantioselective copper-catalyzed additions of glycine Schiff bases to *para*-quinone methides.<sup>11</sup> The conjugate additions of glycine imino esters to arylidene malonates catalyzed by AgOAc/ThioClick Ferrosphos complexes have been reported to give the corresponding adducts in good yields with high enantioselectivities.<sup>10</sup>

As shown in Scheme 4, the imino acetonitrile anion **1f** was obtained by deprotonation of the corresponding CH acid with 1.05 equivalents of KO $t$ Bu. Addition to the quinone methide **2b**, followed by aqueous workup, gave the product **3fb** in 82% yield as mixture of two diastereoisomers.



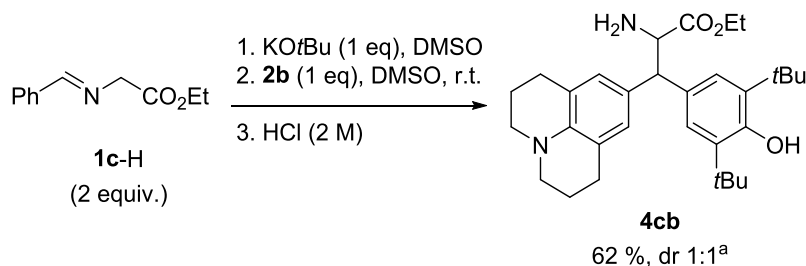
**Scheme 4.** Reaction of imino acetonitrile **1f-H** with the quinone methide **2b** in DMSO at 20 °C. <sup>a</sup> Determined from the  $^1\text{H}$  NMR spectrum of the crude product.

When 1.1 equivalents of the potassium salt of **1e-H**, derived from alanine ester and benzaldehyde, was combined with quinone methide **2d**, only a small degree of conversion was observed, probably due to the reversibility of these reactions. When this reaction was carried out with 5 equivalents of **1e**, a higher degree of conversion of **2d** was observed. However, as the corresponding adduct **3ed** could not be separated from the crude reaction mixture, it was hydrolyzed to provide 12 % of the amino ester **4ed** (*dr* 2:3) after column chromatography (Scheme 5).



**Scheme 5.** Reaction of **1e-H** with the quinone methide **2d** in DMSO at 20 °C.

Fair yield of **4cb** was obtained when **2b** was combined with 2 equivalents of **1c-H** and 1 equivalent of KOtBu and the resulting imino ester **3cb** was hydrolyzed with 2 M HCl (Scheme 6).



**Scheme 6.** Reaction of **1c-H** with the quinone methide **2b** in DMSO at 20 °C.

#### 4.2.2. Kinetic Investigations

The reactions of the 2-aza-allyl anions **1a-f** with the quinone methides **2b,d,e** and the benzylidene malonates **2a** and **2c** were performed in DMSO solution at 20 °C and monitored by UV-vis spectroscopy at or close to the absorption maxima of the electrophiles **2** (Table 1) using stopped-flow techniques. The potassium salts (**1a-f**)-K were not isolated because of their low stability but were generated in solution by deprotonation of the corresponding CH acids (**1a-f**)-H with KOtBu (typically 1.05 equivalents) in DMSO directly before the kinetic experiments. In order to simplify the evaluation of the kinetic experiments, the nucleophiles **1a-f** were employed in large excess ( $\geq 10$  equiv.) over the electrophiles **2**. Therefore, the concentrations of **1** can be considered almost constant throughout the reactions, resulting in pseudo-first-order kinetics in all runs (Eq. 2).

$$-d[2]/dt = k_2[1][2];$$

$$\text{for } [1] \gg [2] \Rightarrow -d[2]/dt = k_{\text{obs}}[2] \text{ with } k_{\text{obs}} = k_2[1] \quad (2)$$

As a consequence, monoexponential decays of the concentrations of the UV/Vis-active electrophiles were observed. The first-order rate constants  $k_{\text{obs}}$  [ $\text{s}^{-1}$ ] were derived by least-squares fitting of the exponential function  $A_t = A_0 \exp(-k_{\text{obs}}t) + C$  to the time-dependent absorbances  $A_t$  of the electrophiles (Figure 1). Plots of  $k_{\text{obs}}$  against the concentrations of the nucleophiles **1** were linear as illustrated in Figure 1 (insert); the small negative intercepts may be due to partial decomposition of the carbanions **1**. Second-order rate constants  $k_2$  [ $\text{L mol}^{-1} \text{s}^{-1}$ ] (Table 2) for the reactions of carbanions **1a-f** with the reference electrophiles **2a-e** were derived from the slopes of these plots.

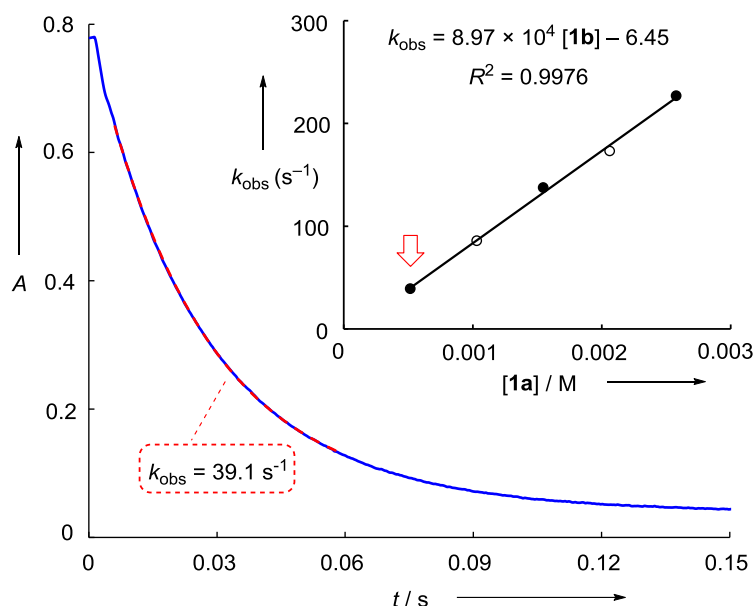


**Figure. 1.** Exponential decay of the absorbance of **1a** ( $[\mathbf{1a}]_0 = 4.52 \times 10^{-5} \text{ mol L}^{-1}$ ) at 425 nm during its reaction with **2d** ( $[\mathbf{2d}]_0 = 5.15 \times 10^{-4} \text{ mol L}^{-1}$ ) at 20 °C in DMSO solution. Inset: Correlation of the rate constants  $k_{\text{obs}}$  with  $[\mathbf{1a}]$  in DMSO at 20 °C. The tagged data point refers to the depicted absorption-time trace. Open circles: In the presence of 18-crown-6 ether (1.1 equiv. with respect to **1a-K**). Filled circles: Without 18-crown-6 ether.

We also investigated the effect of ion-pairing on the measured rate constants by using 18-crown-6 ether as an additive. As depicted by the open symbols in Figure 1, the pseudo-first-order rate constants  $k_{\text{obs}}$ , measured in the presence and in the absence of 18-crown-6 ether (1.1 equiv. with respect to **1a**), were on the same plots of  $k_{\text{obs}}$  versus concentration  $[\mathbf{1}]$ , indicating that interaction of the carbanion with  $\text{K}^+$  does not play a significant role, and the rate constants listed in Table 2 refer to the reactivities of the free carbanions **1a-f**.

As the 2-aza-allyl anions **1** are colored, we have also conducted kinetic experiments, where diethyl benzylidene malonates **2a** and **2c** were employed in excess ( $\geq 10$  equiv.) over the nucleophile **1a** and monitored the exponential decays of the UV/Vis-absorbances of **1a**. In these cases second-order rate constants  $k_2$  were obtained from the slopes of the plots of  $k_{\text{obs}}$  against the concentrations of **2a** and **2c**. The resulting second-order rate constants differed by a factor of 1.2 from those determined with an excess of carbanion, indicating the error limits of the measured rate constants.

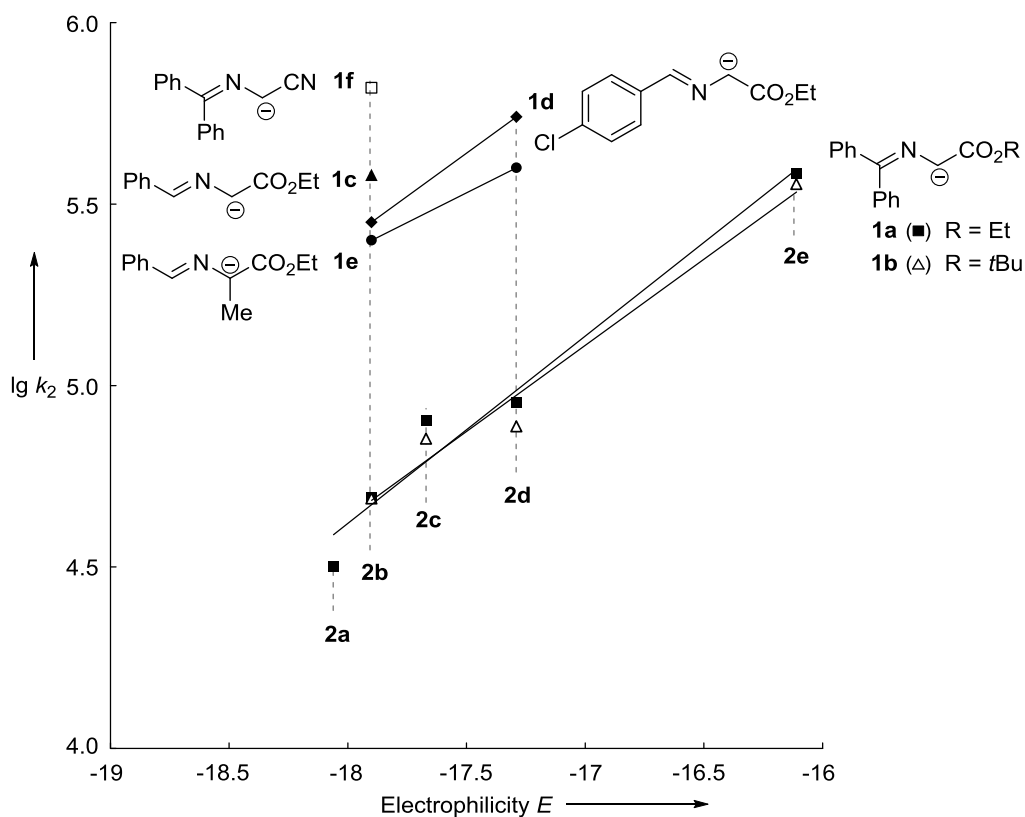
**Table 2.** Second-order rate constants  $k_2$  for the reactions of the carbanions **1a-f** with the reference electrophiles **2a-e** in DMSO at 20 °C.

Carbanion <sup>a</sup>	$N$ ( $s_N$ ) <sup>b</sup>	Electrophile <sup>c</sup>	$k_2 /$ $\text{L mol}^{-1} \text{s}^{-1}$
<b>1a</b>	26.95 (0.52)	<b>2a</b>	$3.16 \times 10^4$
			$2.69 \times 10^4$ <sup>d</sup>
		<b>2b</b>	$4.92 \times 10^4$
		<b>2c</b>	$8.01 \times 10^4$
			$6.78 \times 10^4$ <sup>d</sup>
		<b>2d</b>	$8.97 \times 10^4$ <sup>e</sup>
		<b>2e</b>	$3.84 \times 10^5$ <sup>e</sup>
<b>1b</b>	27.77 (0.47)	<b>2b</b>	$4.88 \times 10^4$
		<b>2c</b>	$7.13 \times 10^4$
		<b>2d</b>	$7.71 \times 10^4$
		<b>2e</b>	$3.59 \times 10^5$ <sup>e</sup>
<b>1c</b>	$\approx 29.1$ <sup>f</sup>	<b>2b</b>	$3.82 \times 10^5$
<b>1d</b>	29.02 (0.49)	<b>2b</b>	$2.79 \times 10^5$
		<b>2d</b>	$5.55 \times 10^5$
<b>1e</b>	30.82 (0.41)	<b>2b</b>	$2.22 \times 10^5$
		<b>2d</b>	$3.97 \times 10^5$
<b>1f</b>	$\approx 29.5$ <sup>f</sup>	<b>2b</b>	$6.65 \times 10^5$

<sup>a</sup> Counterion  $\text{K}^+$ . <sup>b</sup> The nucleophilicity parameters  $N$  and  $s_N$  were determined by correlation analysis using Eq. (1). <sup>c</sup> Minor component in the pseudo-first order kinetics. <sup>d</sup> Pseudo-first order kinetics measured with **1a** as a minor component. <sup>e</sup> The decays of absorbances were not strictly monoexponential; therefore, only the initial 50% of the decays were used for evaluation of the pseudo-first-order rate constants  $k_{\text{obs}}$ . <sup>f</sup> For an estimated  $s_N = 0.50$ .

#### 4.2.3. Correlation analysis

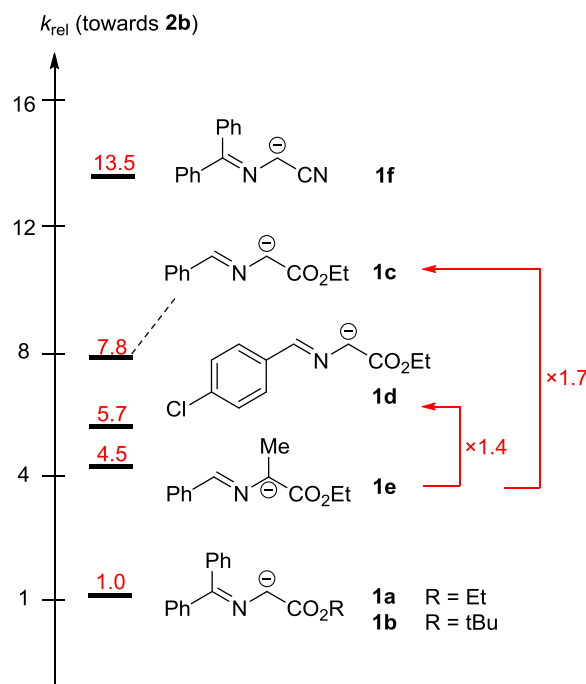
As shown in Figure 2, plots of  $\lg k_2$  for the reactions of the anions **1a** and **1b** with the reference electrophiles **2** versus the electrophilicity parameters  $E$  of **2** are linear. The slopes of these correlations equal the nucleophile-specific parameters  $s_N$ , and the negative intercepts on the abscissa ( $\lg k_2 = 0$ ) correspond to the nucleophilicity parameters  $N$ , which are listed in Table 2.



**Figure. 2.** Correlations of  $\lg k_2$  for the reactions of the carbanions **1** with reference electrophiles **2a-e** at 20 °C in DMSO with their electrophilicity parameters  $E$ .

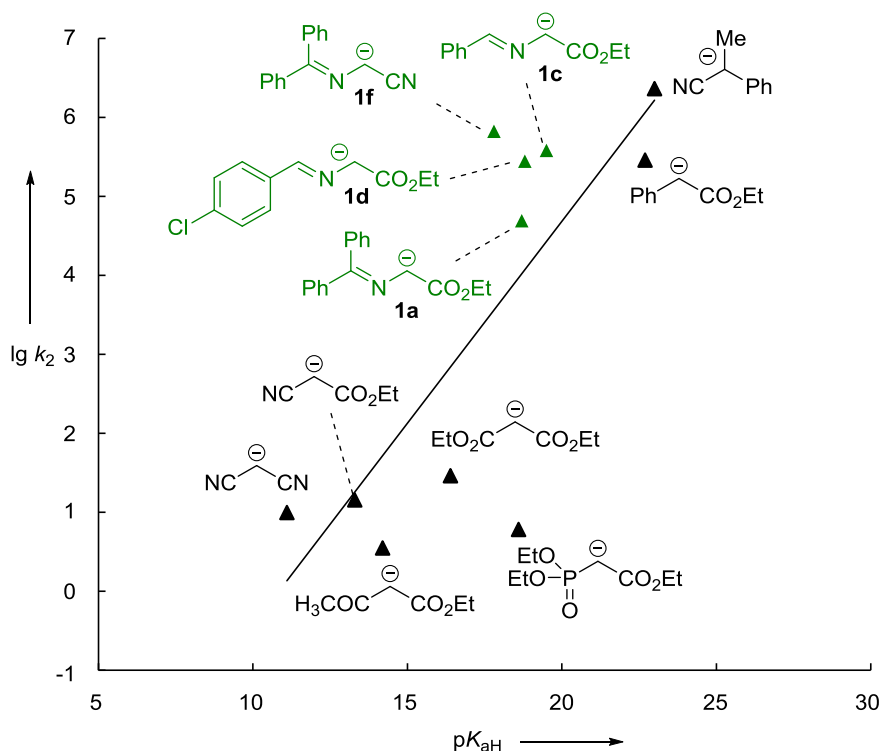
Since similar slopes  $s_N$  have also been found for the 2-point correlations for **1e** and **1d** (0.42 and 0.52, Table 2), one can conclude that the relative reactivities of these carbanions depend only slightly on the electrophilicity of the reaction partners. The relative rate constants towards electrophile **2b**, which are depicted in Figure 3, can, therefore, be considered to be representative for the relative reactivities.

Figure 3 shows that the nature of the ester group (*tert*-butyl or ethyl) has no effect on the reactivity of the benzophenone derived Schiff bases **1a,b**. Removal of one phenyl group to give the benzaldehyde derivative **1c** increases nucleophilicity by a factor of 7.8, and the *p*-Cl substitution in **1d** reduces reactivity by a factor of 1.4. In analogy to previously reported relative reactivities of secondary and tertiary carbanions,<sup>20a</sup> the comparison of **1c** and **1e** shows that an extra methyl group at the carbanionic center has only a slight effect on nucleophilic reactivity. The cyano-substituted carbanion **1f** is 13.5 times more reactive than the corresponding ester derivative **1a**.



**Figure 3.** Relative reactivities of the nucleophiles **1a-f** towards the quinone methide **2b** (DMSO, 20 °C).

In previous work<sup>20a</sup> we have shown that the nucleophilic reactivities of carbanions in water as well as in DMSO correlate only poorly with the corresponding  $pK_{\text{aH}}$  values in these solvents. O'Donnell and co-workers have systematically studied the  $pK_{\text{aH}}$  values of the Schiff base derivatives of amino acids and related compounds that were of interest for the synthesis of the amino acids by phase-transfer alkylations.<sup>21</sup> The Brønsted correlation in Figure 4, which plots the second-order rate constants for the reactions of various carbanions with quinone methide **2b** against the corresponding  $pK_{\text{aH}}$  values,<sup>21,23</sup> is of low quality and again demonstrates the limitation of  $pK_{\text{a}}$  values for predicting nucleophilic reactivities. It is obvious, however, that the 2-aza-allyl anions **1** are more reactive than expected from the  $pK_{\text{a}}$  values of the conjugate CH-acids **1-H**. We have not examined whether the positive deviations of anions **1** from the Brønsted plots are due to lower intrinsic barriers for these reactions or due to the fact that the rate constants refer to reactions with a carbon center whereas the  $pK_{\text{aH}}$  values correspond to associations with the proton.<sup>24</sup>



**Figure 4.** Brønsted correlation for the reactions of the quinone methide **2b** with carbanions derived from amino acid derivatives **1** and related carbanions in DMSO at 20 °C.  $pK_{aH}$  from ref 21 (for anions **1**) and ref 23 (for other carbanions).

### 4.3. Conclusion

The second-order rate constants of the reactions of the  $\alpha$ -iminoesters **1a** and **1b**, derived from benzophenone and glycine esters, with quinone methides and arylidene malonates **2a-e** (reference electrophiles) correlate linearly with the electrophilicity parameters  $E$  of **2**, which allowed us to calculate the susceptibilities  $s_N$  (slopes in Figure 2) and the nucleophilicities  $N$  (negative intercepts on the abscissa in Figure 2) of **1a,b**. Since the corresponding two-point correlations for **1d** and **1e** yield similar susceptibilities  $s_N$ , we concluded that the relative reactivities of the carbanions **1a-f** are almost independent of the electrophilicity of their reaction partners. The structure-reactivity relationships derived from the reactivities toward the quinone methide **2b** were, therefore, considered to be representative for the reactivities of these carbanions. Comparison of **1a** and **1c** shows that the benzophenone-derived iminoester is 8 times less reactive than the benzaldehyde-derived iminoester and that the cyano derivative **1f** is 13 times more reactive than the ester derivative **1a**.

Since kinetics of the reactions of the quinone methide **2b** with other carbanions have previously been reported, we can also compare the nucleophilicities of the iminoesters **1** with those of other types of carbanions. Figure 5, which compares the influence of various  $\alpha$ -



substituents on ethyl acetate anions, shows that the imino substituted carbanions have a similar nucleophilicity as the anion derived from ethyl phenylacetate. Even though the relative reactivities of the carbanions in Figure 5 will somewhat vary with the nature of the electrophile because of the different magnitude of  $s_N$ , one can see that replacement of the imino group in **1a,c** by cyano, alkoxycarbonyl, acyl, phosphoryl, and sulfonyl groups leads to a significant reduction of nucleophilicity. One, therefore, can expect that all electrophiles known to react with these types of carbanions will also react with the corresponding imino-substituted carbanions. More precise predictions of potential electrophilic reaction partners can be obtained by using Eq. (1), which combines the  $N$  and  $s_N$  parameters determined in this work with the electrophilicity parameters accessible through ref. 19g.

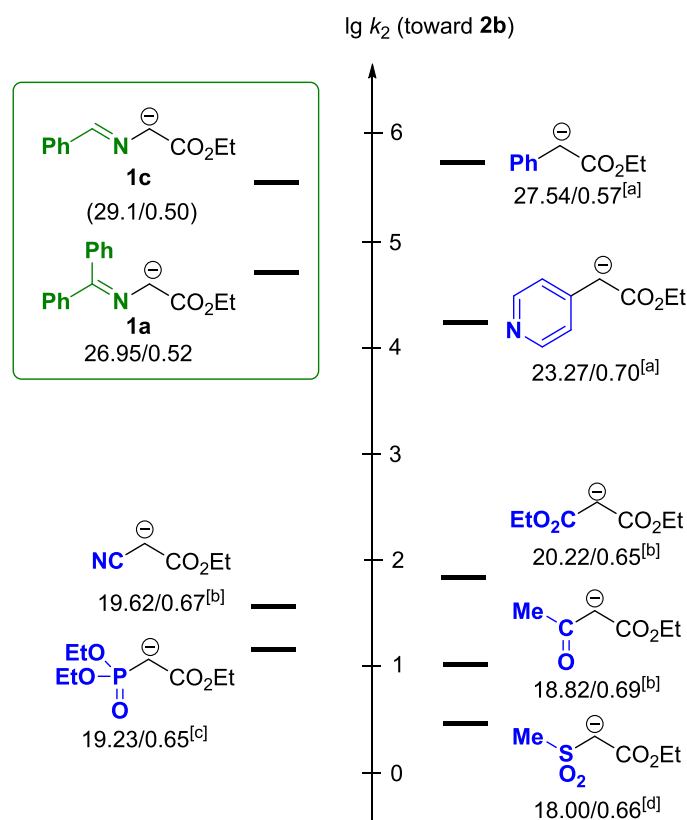


**Figure 5.** Comparison of second-order rate constants ( $\lg k_2$ ) for the reactions of the quinone methide **2b** with the carbanions derived from  $\alpha$ -imino esters **1** and related carbanions.  $N$  and  $s_N$  are given below each nucleophile (reactivities refer to DMSO as solvent). <sup>a</sup> From ref 20f. <sup>b</sup> From ref 19b. <sup>c</sup> From ref 20e. <sup>d</sup> From ref 20g.

## 4.4. Experimental Section

### 4.4.1. General

#### Materials

All solvents were of p.a. quality and were dried by standard procedures prior to use. Commercially available DMSO ( $\text{H}_2\text{O}$  content < 50 ppm) was used without further purification. Unless otherwise specified, materials were obtained from commercial sources and used without further purification. The reference electrophiles used in this work were synthesized according to literature procedures.<sup>19b, e, 22</sup> The imino esters **1c-H**, **1d-H** and **1e-H** were synthesized as described in Section 2. The imino esters **1a-H** and **1b-H** were purchased from ABCR (Germany). The imino acetonitrile **1f-H** was purchased from Sigma-Aldrich (Germany). All reactions were performed in carefully dried Schlenk glassware under  $\text{N}_2$  atmosphere. Purification of reaction products was carried out by flash column chromatography using silica gel 60 (0.040–0.063 mm) as the stationary phase and EtOAc and freshly distilled n-Pentane as eluents. Visualization of thin layer chromatography was accomplished with an ultraviolet lamp at 254 nm.

#### Analytics

$^1\text{H}$ -NMR (599 or 400 MHz) and  $^{13}\text{C}$ -NMR (151 or 101 MHz) were recorded on Varian or Bruker NMR spectrometers. The chemical shifts are given in ppm and refer to the solvent ( $\text{CDCl}_3$ ) residual signal as internal standards ( $\delta_{\text{H}} = 7.26$ ,  $\delta_{\text{C}} = 77.0$ ).<sup>25</sup> The following abbreviations were used for signal multiplicities: s = singlet, d = doublet, t = triplet, q = quartet, bs = broad signal. Signal assignments are based on additional 2D-NMR experiments (COSY, HSQC, and HMBC). Chemical shifts marked with (\*) refer to the major isomer when the product was obtained as a mixture of two diastereomers. High-resolution mass spectra (HRMS) were obtained by using a Thermo Finnigan LTQ FT (ESI).

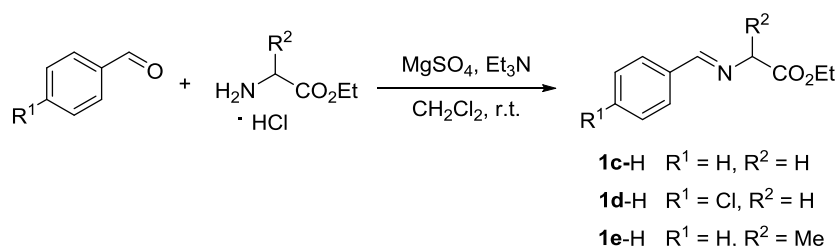
#### Kinetics

The rates of all investigated reactions were determined photometrically. UV-vis spectra were recorded by using a J&M TIDAS diode array spectrometer controlled by TIDASDAQ3 (v3) software and connected to a Helma 661.502-QX quartz suprasil immersion probe (light path  $d = 5$  mm) via fiber optic cables and standard SMA connectors. As all reactions were fast ( $\tau_{1/2} < 10$  s), the kinetics were monitored using stopped-flow techniques (Hi-Tech SF-61DX2 instrument or Applied Photophysics SX.20MV-R). All kinetic measurements were carried out in DMSO (Acros Organics,  $\text{H}_2\text{O}$  content < 50 ppm) under exclusion of moisture ( $\text{N}_2$

atmosphere). The temperature of all solutions was kept constant at  $20.0 \pm 0.1$  °C by using a circulating bath thermostat. In all runs the concentration of the nucleophiles **1a-f** was at least 10 times higher than the concentration of the Michael acceptors **2**, resulting in pseudo-first-order kinetics with an exponential decay of the concentration of the reference electrophile. First-order rate constants  $k_{\text{obs}}$  [ $\text{s}^{-1}$ ] were obtained by least-squares fitting of the absorbances to a single-exponential  $A_t = A_0 \exp(-k_{\text{obs}}t) + C$  (average from 10 kinetic runs for each nucleophile concentration). The second-order rate constants  $k_2$  were obtained from the slopes of the linear plots of  $k_{\text{obs}}$  against the concentration of the excess components (typically 3 to 5 different concentrations were used for this evaluation). Nucleophile-specific parameter  $s_N$  and nucleophilicity parameter  $N$  were determined applying the linear free energy relationship  $\lg k_2(20\text{ °C}) = s_N(E + N)$ .

#### 4.4.2. Synthesis of $\alpha$ -Imino Esters

General procedure (GP 1) for the synthesis of **1-H**<sup>7</sup>



To a suspension of the corresponding amino acid ester hydrochloride (1.20 equiv) and  $\text{MgSO}_4$  (1.25 equiv) in dry  $\text{CH}_2\text{Cl}_2$  (25 mL) was added  $\text{Et}_3\text{N}$  (1.20 equiv). The mixture was stirred at room temperature for 1 h and then the corresponding aldehyde (1.00 equiv) was added. The reaction was stirred at room temperature overnight. The resulting precipitate was removed by filtration. The filtrate was washed with water (15 mL), the aqueous phase was extracted with  $\text{CH}_2\text{Cl}_2$  ( $3 \times 30$  mL), and the combined organic phases were washed with brine ( $3 \times 30$  mL), dried over  $\text{MgSO}_4$  and concentrated. The resulting imino esters were obtained of sufficient purity to be used for kinetic measurements and product studies without further purification.

**Ethyl *N*-benzylideneglycinate (**1c-H**)** was synthesized according to GP 1 from benzaldehyde (2.0 mL, 20 mmol), ethyl glycinate hydrochloride (3.33 g, 2 mmol),  $\text{MgSO}_4$  (3.0 g, 25 mmol), and  $\text{Et}_3\text{N}$  (3.3 mL, 24 mmol): **1c-H** (3.60 g, 94%) was obtained as clear yellow oil.  $^1\text{H-NMR}$  spectroscopic data were in agreement with the literature.<sup>21</sup>

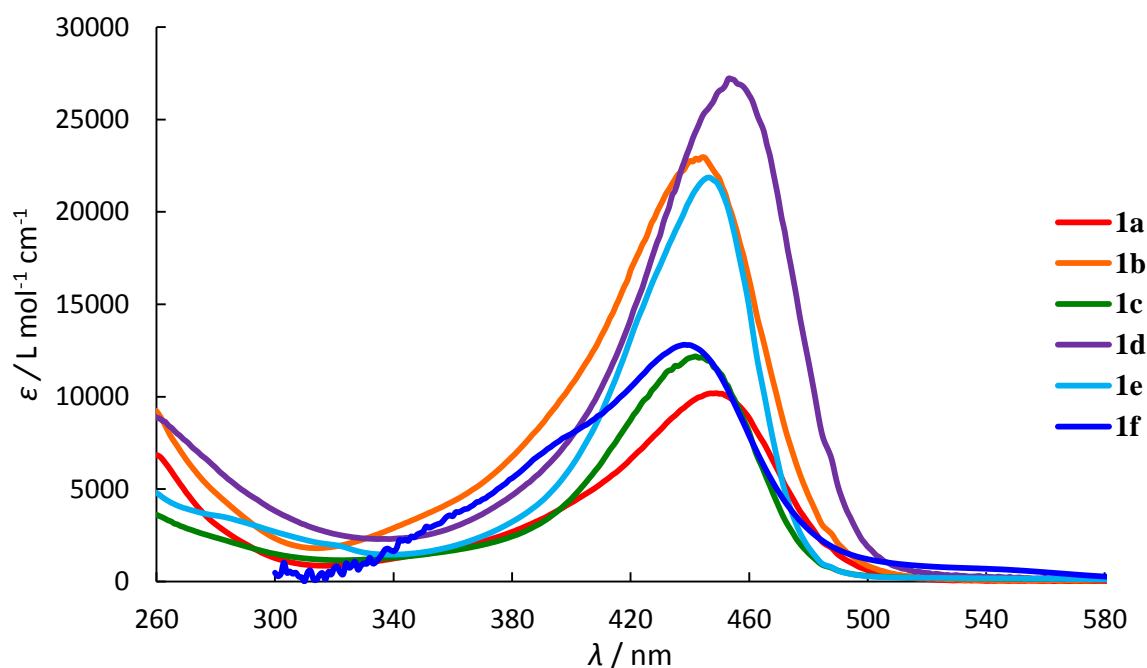
**Ethyl *N*-[(4-chlorophenyl)methylene]glycinate (**1d-H**)** was synthesized according to GP 1 from 4-chlorobenzaldehyde (4.70 g, 33.4 mmol), ethyl glycinate hydrochloride (5.00 g, 35.8

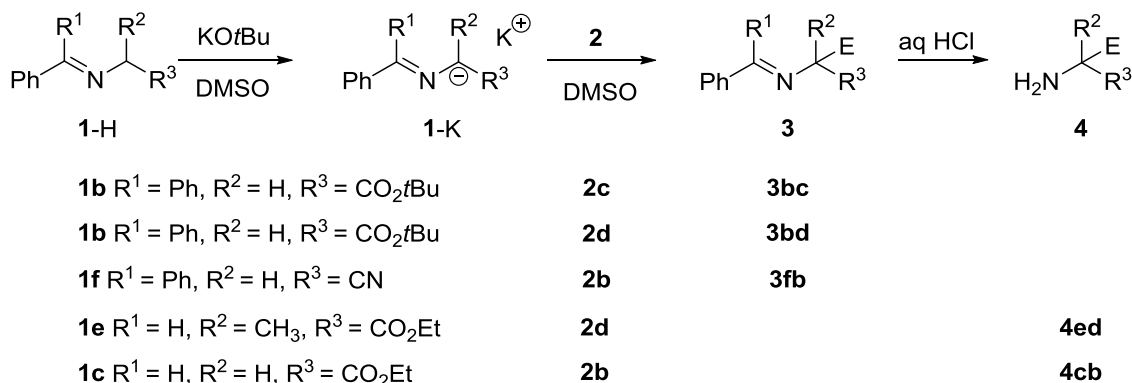
mmol),  $\text{MgSO}_4$  (5.0 g, 42 mmol), and  $\text{Et}_3\text{N}$  (5.8 mL, 36 mmol): **1d-H** (7.20 g, 95%) was obtained as clear yellow oil.  $^1\text{H-NMR}$  spectroscopic data were in agreement with the literature.<sup>21</sup>

**Ethyl *N*-benzylidenealaninate (1e-H)** was synthesized according to GP 1 from benzaldehyde (1.4 mL, 14 mmol), ethyl alaninate hydrochloride (2.50 g, 16.2 mmol),  $\text{MgSO}_4$  (2.0 g, 17 mmol) and  $\text{Et}_3\text{N}$  (2.30 mL 16.5 mmol): **1e-H** (2.67 g, 93%) was obtained as clear yellow oil.  $^1\text{H-NMR}$  spectroscopic data were in agreement with the literature.<sup>26</sup>

#### 4.4.3. UV-Vis Spectra of Potassium Salts (1a-f)-K

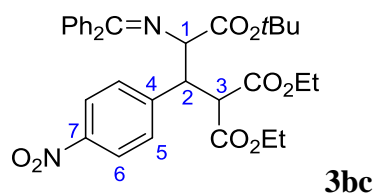
The UV-Vis Spectra of the potassium salts **1a-f** derived from corresponding conjugate CH acids (**1a-f**)-H, were recorded by using diode array UV-vis spectrometers. The temperature during all experiments was kept constant by using a circulating bath ( $20.0 \pm 0.1$  °C). A solution of KO $t$ Bu in dry DMSO was added to solutions of the CH acids (**1a-f**)-H in dry DMSO, respectively. In all cases a full deprotonation of the CH acid with 1.05 equivalents of KO $t$ Bu was monitored, as the absorption did not increase with further addition of the base.



4.4.4. Products of the Reactions of the Carbanions **1** with Reference Electrophiles **2***General procedure (GP 2) for reactions of **1** with **2***

Potassium salts **1-K** were generated by addition of the amino acid derivatives **1-H** to a solution of KOtBu in dry DMSO (5 mL). Subsequently, a solution of the quinone methides **2b,d** or benzylidene malonate **2c** in DMSO (5 mL) was added. The mixture was stirred for 30 minutes before water (10 mL) was added. The mixture was extracted with ethyl acetate (3 × 20 mL), and the combined organic phases were washed with brine (3 × 20 mL), dried over MgSO<sub>4</sub> and the solvent was evaporated under reduced pressure. The crude reaction products were purified by column chromatography (silica gel, pentane/ethyl acetate = 10/1) to give a mixture of two diastereomers, which was subsequently characterized by NMR spectroscopy and mass spectrometry.

**3-(tert-Butyl) 1,1-diethyl 3-((diphenylmethylene)amino)-2-(4-nitrophenyl)propane-1,1,3-tricarboxylate (**3bc**)** was prepared according to GP 2 from **1b-H** (115 mg, 0.389 mmol), KOtBu (46.7 mg, 0.425 mmol), and **2c** (104 mg, 0.354 mmol): **3bc** (143 mg, 69%, *dr* ≈ 1:1.2) was obtained as a yellow oil.

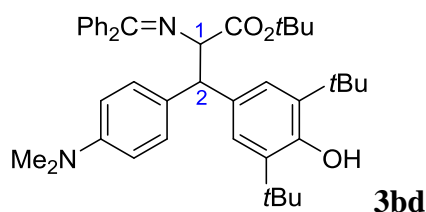


**<sup>1</sup>H NMR** (CDCl<sub>3</sub>, 599 MHz): δ = 8.18 (d, *J* = 8.0 Hz, 2 H, 6-H\*), 8.09 (d, *J* = 8.2 Hz, 2 H, H-6), 7.88 (d, *J* = 8.2 Hz, 2 H, 5-H\*), 7.68 (t, *J* = 8.4 Hz, 2 H + 2 H\*, Ph), 7.47–7.34 (m, 2 H of 5-H and 6 H\* + 6 H of Ph), 7.07 (d, *J* = 7.2 Hz, 2 H + 2 H\*, Ph), 4.49 (d, *J* = 3.9 Hz, 1 H, 1-H\*), 4.39–4.36 (m, 1 H, 2-H), 4.31 (d, *J* = 6.6 Hz, 1 H, 1-H), 4.23 (d, *J* = 9.4 Hz, 1 H, 3-H), 4.17–4.04 (m, 2 H\* + 4 H, 2-H\*, 3-H\* and 2 × OCH<sub>2</sub>), 3.92–3.84 (m, 4 H, 2 × OCH<sub>2</sub>\*), 1.23 (s, 9 H, C(CH<sub>3</sub>)<sub>3</sub>), 1.18–1.13 (m, 9 H\* + 6 H, C(CH<sub>3</sub>)<sub>3</sub>\* and 2 × OCH<sub>2</sub>CH<sub>3</sub>), 0.98–0.93 (m, 6 H, 2 × OCH<sub>2</sub>CH<sub>3</sub>\*).

**$^{13}\text{C}$  NMR** ( $\text{CDCl}_3$ , 101 MHz):  $\delta$  = 173.30 (s,  $\text{Ph}_2\text{C}=\text{N}^*$ ), 172.11 (s,  $\text{Ph}_2\text{C}=\text{N}$ ), 168.92 (s,  $\text{CO}_2t\text{Bu}$ ), 168.81 (s,  $\text{CO}_2t\text{Bu}^*$ ), 167.84 (s,  $\text{CO}_2\text{Et}$ ), 167.68 (s,  $\text{CO}_2\text{Et}$ ), 167.65 (s,  $\text{CO}_2\text{Et}^*$ ), 167.19 (s,  $\text{CO}_2\text{Et}^*$ ), 147.39 (s, C-4\*), 147.15 (s, C-4 or C-7), 147.13 (s, C-7 or C-4), 146.04 (s, C-7\*), 139.33 (s, Ph), 139.11 (s, Ph), 136.09 (s, Ph), 136.03 (s, Ph), 131.60 (d, C-5\*), 130.95 (d, Ph), 130.57 (d, C-5), 130.21 (d, Ph), 129.16 (d, Ph), 128.99 (d, Ph), 128.60 (d, Ph), 128.50 (d, Ph), 128.42 (d, Ph), 128.34 (d, Ph), 128.23 (d, Ph), 127.73 (d, Ph), 127.60 (d, Ph), 123.18 (d, C-6), 122.94 (d, C-6\*), 82.00 (s,  $\text{OC}(\text{CH}_3)_3$ ), 81.97 (s,  $\text{OC}(\text{CH}_3)_3^*$ ), 68.64 (d, C-1), 65.80 (d, C-1\*), 61.94 (t,  $\text{OCH}_2^*$ ), 61.87 (t,  $\text{OCH}_2$ ), 61.71 (t,  $\text{OCH}_2^*$ ), 61.58 (t,  $\text{OCH}_2$ ), 54.91 (d, C-3\*), 54.29 (d, C-3), 48.63 (d, C-2), 47.42 (d, C-2\*), 27.89 (q,  $\text{OC}(\text{CH}_3)_3$  of both isomers), 14.04 (q,  $\text{OCH}_2\text{CH}_3$ ), 13.89 (q,  $\text{OCH}_2\text{CH}_3^*$ ). Resonances in the aromatic region could not be assigned unambiguously to a certain diastereomer.

**HRMS** (ESI):  $m/z$  calcd for  $\text{C}_{33}\text{H}_{36}\text{N}_2\text{O}_8^+$   $[\text{M}+\text{H}]^+$ : 589.2544; found: 589.2543.

**tert-Butyl 3-(3,5-di-tert-butyl-4-hydroxyphenyl)-3-(4-(dimethylamino)phenyl)-2-((diphenylmethylene)amino)propanoate (3bd)** was prepared according GP 2 from **1b-H** (94.5 mg, 0.320 mmol),  $\text{KO}t\text{Bu}$  (39.6 mg, 0.353 mmol), and **2d** (99.2 mg, 0.294 mmol): **3bd** (141 mg, 76%,  $dr \approx 1:2$ ) was obtained as a yellow-orange solid.



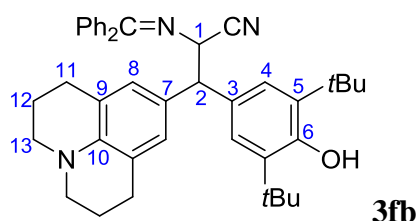
**$^1\text{H}$  NMR** ( $\text{CDCl}_3$ , 599 MHz):  $\delta$  = 7.81 (d,  $J$  = 7.5 Hz, 2 H, Ar), 7.61–7.54 (m, 2 H + 2 H\*, Ar), 7.49 (t,  $J$  = 7.6 Hz, 2 H, Ar), 7.37–7.25 (m, 4 H + 10 H\*, Ar), 7.09 (s, 2 H, Ar), 7.09 (s, 2 H, Ar), 7.08 (s, 2 H, Ar\*), 6.95 (s, 2 H, Ar), 6.63 (d,  $J$  = 8.1 Hz, 2 H, Ar\*), 6.57 (bs, 2 H, Ar), 4.94–4.93 (bs, 2 H, OH, both isomers), 4.56 (d,  $J$  = 9.2 Hz, 1 H, 2-H\*), 4.50 (s, 2 H, 1-H and 2-H), 4.46 (d,  $J$  = 9.3 Hz, 1 H, 1-H\*), 2.87 (s, 6 H,  $\text{NMe}_2$ ), 2.86 (s, 6 H,  $\text{NMe}_2^*$ ), 1.31 (s, 18 H,  $\text{C}(\text{CH}_3)_3$ ), 1.30 (s, 18 H,  $\text{C}(\text{CH}_3)_3^*$ ), 1.18 (s, 9 H,  $\text{OC}(\text{CH}_3)_3^*$ ), 1.15 (s, 9 H,  $\text{OC}(\text{CH}_3)_3$ ).

**$^{13}\text{C}$  NMR** ( $\text{CDCl}_3$ , 101 MHz):  $\delta$  = 170.45 (s,  $\text{CO}_2$  of both isomers), 169.81 (s,  $\text{Ph}_2\text{C}=\text{N}$  of both isomers), 152.17 (s,  $\text{C}_q\text{-OH}$  of both isomers), 149.46 (s,  $\text{C}_q\text{-NMe}_2$  of both isomers), 139.97 (s, Ar), 136.51 (s, Ar), 136.45 (s, Ar), 135.27 (s, Ar), 135.05 (s, Ar), 132.60 (s, Ar), 130.05 (d, Ar), 129.68 (d, Ar), 129.04 (d, Ar), 128.29 (d, Ar), 128.05 (d, Ar), 127.97 (s, Ar), 127.92 (s, Ar), 127.84 (d, Ar), 126.12 (d, Ar), 125.67 (d, Ar), 113.00 (d, Ar), 80.70 (q,  $\text{OC}(\text{CH}_3)_3$ ), 72.41 (d, C-1 both isomers), 54.65 (d, C-2), 54.39 (d, C-2\*), 41.13 (q,  $\text{NMe}_2$  of

both isomers), 34.37 (s,  $\underline{\text{C}}(\text{CH}_3)_3^*$ ), 34.32 (s,  $\underline{\text{C}}(\text{CH}_3)_3$ ), 30.42 (q,  $\text{C}(\underline{\text{CH}}_3)_3^*$ ), 30.36 (q,  $\text{C}(\underline{\text{CH}}_3)_3$ ), 27.82 (q,  $\text{OC}(\underline{\text{CH}}_3)_3^*$ ), 27.79 (q,  $\text{OC}(\underline{\text{CH}}_3)_3$ ). Resonances in the aromatic region could not be assigned unambiguously to a certain diastereomer.

**HRMS** (ESI):  $m/z$  calcd for  $\text{C}_{42}\text{H}_{52}\text{N}_2\text{O}_3^+ [\text{M}+\text{H}]^+$ : 633.4051; found: 633.4051.

**3-(3,5-Di-*tert*-butyl-4-hydroxyphenyl)-2-((diphenylmethylene)amino)-3-(julolidin-9-yl)propanenitrile (3fb)** was prepared according to GP 2 starting from **1f-H** (55 mg, 0.25 mmol),  $\text{KO}^t\text{Bu}$  (31 mg, 0.28 mmol), and **2b** (88.2 mg, 0.23 mmol): **3fb** (115 mg, 82%,  $dr \approx 1:1.3$ ) was obtained as a red oil.

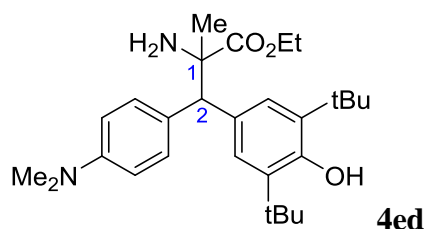


**$^1\text{H}$  NMR** ( $\text{CDCl}_3$ , 400 MHz):  $\delta$  = 7.82–7.80 (m, 2 H, Ph), 7.62–7.58 (m, 2 H, Ph), 7.52–7.28 (m, 18 H, Ph), 7.03 (s, 2 H, 4-H), 6.96 (s, 2 H, 4-H\*), 6.85 (bs, 2 H, Ph), 6.73 (bs, 2 H, Ph), 6.65 (s, 2 H, 8-H\*), 6.63 (s, 2 H, 8-H), 5.06 (bs, 2 H, OH), 5.01 (bs, 2 H, OH\*), 4.68 (d,  $J$  = 8.2 Hz, 1 H, H-1), 4.62 (d,  $J$  = 9.9 Hz, 1 H, 1-H\*), 4.40 (d,  $J$  = 9.9 Hz, 1 H, 2-H\*), 4.28 (d,  $J$  = 8.2 Hz, 1 H, 2-H), 3.09–3.04 (m,  $2 \times 4$  H, 13-H and 13-H\*), 2.70–2.63 (m,  $2 \times 4$  H, 11-H and 11-H\*), 1.95–1.90 (m,  $2 \times 4$  H, 12-H and 12-H\*), 1.38 (s, 18 H,  $\text{C}(\underline{\text{CH}}_3)_3$ ), 1.33 (s, 18 H,  $\text{C}(\underline{\text{CH}}_3)_3^*$ ).

**$^{13}\text{C}$  NMR** ( $\text{CDCl}_3$ , 151 MHz):  $\delta$  = 172.66 (s,  $\text{Ph}_2\text{C}=\text{N}$ ), 172.59 (s,  $\text{Ph}_2\text{C}=\text{N}^*$ ), 152.78 (s, C-6), 152.60 (s, C-6\*), 142.19 (s, C-10\*), 141.86 (s, C-10), 139.01 (s, Ph), 138.94 (s, Ph), 137.66 (s, Ph), 135.50 (s, C-5), 135.40 (s, C-5\*), 135.38 (s, Ph), 135.33 (s, Ph), 132.49 (d, Ph), 131.1 (s, C-3\* or C-7\*), 130.89 (d, Ph\*), 130.88 (d, Ph), 130.68 (s, C-3 or C-7), 130.11 (d, Ph), 129.23 (s, Ph), 129.19 (s, Ph), 129.12 (d, Ph), 120.07 (d, Ph), 128.69 (d, Ph), 128.35 (d, Ph), 128.07 (d, Ph), 128.04 (d, Ph\*), 127.80 (d, Ph), 127.77 (d, Ph\*), 127.58 (d, C-8), 127.01 (d, C-8\*), 125.55 (d, C-4\*), 125.42 (d, C-4), 121.60 (s, C-9\*), 121.23 (s, C-9), 119.43 (s, CN\*), 119.42 (s, CN), 59.09 (d, C-1), 58.98 (d, C-1\*), 55.48 (d, C-2\*), 55.30 (d, C-2), 50.07 (t, C-13), 50.05 (t, C-13\*), 34.38 (s,  $\underline{\text{C}}(\text{CH}_3)_3$ ), 34.33 (s,  $\underline{\text{C}}(\text{CH}_3)_3^*$ ), 30.31 (q,  $\text{C}(\underline{\text{CH}}_3)_3$ ), 30.26 (q,  $\text{C}(\underline{\text{CH}}_3)_3^*$ ), 27.76 (t, C-11\*), 27.75 (t, C-11), 22.25 (t, C-12), 25.20 (t, C-12\*). Resonances in the aromatic region could not be assigned unambiguously to a certain diastereomer.

**HRMS** (ESI):  $m/z$  calcd for  $\text{C}_{42}\text{H}_{48}\text{N}_3\text{O}^+ [\text{M}+\text{H}]^+$ : 610.3792; found: 610.3786.

**Ethyl 2-amino-3-(3,5-di-*tert*-butyl-4-hydroxyphenyl)-3-(4-(dimethylamino)phenyl)-2-methylpropano-ate (4ed)** was prepared according to GP 2 **1e**-H (294 mg, 1.43 mmol), KO<sup>t</sup>Bu (168 mg, 1.50 mmol), and **2d** (96.6 mg, 0.286 mmol) to furnish the crude product, which was dissolved in THF. Aqueous HCl (1 M) was added at 0 °C. After stirring for 1–2 h at 0 °C, the reaction mixture was quenched with saturated aq NaHCO<sub>3</sub> (pH > 8) and extracted with ethyl acetate (3 × 20 mL). The combined organic phases were washed with brine (3 × 20 mL), dried over MgSO<sub>4</sub>, and the solvent was evaporated under reduced pressure. The resulting mixture was purified by column chromatography (pentane/ethyl acetate = 4/1) to yield **4ed** (16 mg, 12%, *dr* ≈ 2:3) as an orange oil.



**<sup>1</sup>H NMR** (CDCl<sub>3</sub>, 400 MHz): δ = 7.50 (d, *J* = 8.8 Hz, 2 H, Ar), 7.38 (s, 2 H, Ar\*), 7.30 (d, *J* = 8.8 Hz, 2 H, Ar\*), 7.21 (s, 2 H, Ar), 6.70 (d, *J* = 8.9 Hz, 2 H, Ar), 6.64 (d, *J* = 8.9 Hz, 2 H, Ar\*), 5.03 (bs, 1 H, OH\*), 4.99 (bs, 1 H, OH), 4.21 (s, 1 H, 2-H), 4.18 (s, 1H, 2-H\*), 4.06–3.99 (m, 4 H, OCH<sub>2</sub> of both isomers), 2.92 (s, 6 H, NMe<sub>2</sub>), 2.88 (s, 6 H, NMe<sub>2</sub>\*), 1.42 (s, 18 H, C(CH<sub>3</sub>)<sub>3</sub>\*), 1.38 (s, 18 H, C(CH<sub>3</sub>)<sub>3</sub>), 1.31 (s, 3 H, CH<sub>3</sub>\*), 1.28 (s, 3 H, CH<sub>3</sub>), 1.13 (t, 3 H, *J* = 7.4 Hz, OCH<sub>2</sub>CH<sub>3</sub>\*), 1.09 (t, 3 H, *J* = 7.4 Hz, OCH<sub>2</sub>CH<sub>3</sub>).

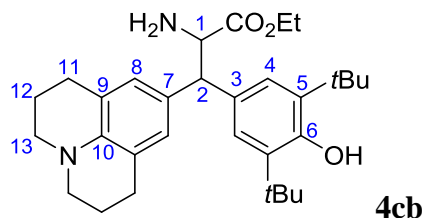
**<sup>13</sup>C NMR** (CDCl<sub>3</sub>, 101 MHz): δ = 177.7 (s, CO<sub>2</sub> of both diastereomers), 152.48 (s, Ar\*), 152.35 (s, Ar), 149.45 (s, Ar), 149.38 (s, Ar\*), 135.26 (s, Ar), 135.18 (s, Ar\*), 132.25 (s, Ar), 131.28 (s, Ar\*), 131.06 (d, Ar), 130.07 (d, Ar\*), 129.72 (s, Ar\*), 129.07 (s, Ar), 126.80 (d, Ar\*), 125.75 (d, Ar), 112.67 (d, Ar\*), 112.57 (d, Ar), 62.16 (s, C-1\*), 62.12 (s, C-1), 61.09 (t, OCH<sub>2</sub>\*), 61.04 (t, OCH<sub>2</sub>), 58.30 (d, C-2\*), 57.82 (d, C-2), 40.87 (q, NMe<sub>2</sub> of both diastereomers), 34.48 (s, C(CH<sub>3</sub>)<sub>3</sub>\*), 34.45 (s, C(CH<sub>3</sub>)<sub>3</sub>), 30.58 (q, C(CH<sub>3</sub>)<sub>3</sub>\*), 30.50 (q, C(CH<sub>3</sub>)<sub>3</sub>), 27.34 (q, CH<sub>3</sub>), 27.07 (q, CH<sub>3</sub>\*), 14.22 (q, OCH<sub>2</sub>CH<sub>3</sub>\*), 14.15 (q, OCH<sub>2</sub>CH<sub>3</sub>).

**HRMS** (ESI): *m/z* calcd for C<sub>28</sub>H<sub>42</sub>N<sub>2</sub>O<sub>3</sub> [M+H]<sup>+</sup>: 455.3268; found: 455.3269.

**Ethyl 2-amino-3-(3,5-di-*tert*-butyl-4-hydroxyphenyl)-3-(julolidin-9-yl)propanoate (4cb)** was prepared according to GP 2 from **1c**-H (105 mg, 0.55 mmol), KO<sup>t</sup>Bu (30 mg, 0.27 mmol), and **2b** (100 mg, 0.26 mmol). NMR analysis of the crude product showed the formation of the adduct as a 1:1 mixture of two diastereoisomers. The crude material was dissolved in THF and aq HCl (1 M) was added at 0 °C. After stirring for 1–2 h at 0 °C, the reaction mixture was quenched with saturated aq NaHCO<sub>3</sub> (pH > 8) and extracted with ethyl



acetate ( $3 \times 20$  mL). The combined organic phases were washed with brine ( $3 \times 20$  mL), dried over  $\text{MgSO}_4$ , and the solvent was evaporated under reduced pressure. The crude reaction product was purified by column chromatography (silica gel, pentane/ethyl acetate = 4/1): **4cb** (80 mg, 62%) as red oil.



Owing to their slightly different retention factors, diastereomerically enriched samples of both diastereomers **4cb-A** and **4cb-B** were obtained after column chromatography, which were used for the assignment of resonances in the NMR spectra. We have not attempted to clarify the relative configurations of the stereocenters in both isomers.

#### **4cb-A:**

**$^1\text{H}$  NMR** ( $\text{CDCl}_3$ , 599 MHz):  $\delta$  = 7.09 (s, 2 H, 4-H), 6.71 (s, 2 H, 8-H), 5.04 (bs, 1 H, OH), 4.03 (d,  $J$  = 9.2 Hz, 1 H, 1-H), 4.00–3.95 (m, 2 H,  $\text{OCH}_2$ ), 3.84 (d,  $J$  = 9.2 Hz, 1 H, 2-H), 3.06–3.04 (m, 4 H, 13-H), 2.71–2.68 (m, 4 H, 11-H), 1.95–1.90 (m, 4 H, 12-H), 1.61 (bs, 2 H,  $\text{NH}_2$ ), 1.41 (s, 18 H,  $\text{C}(\text{CH}_3)_3$ ), 1.03 (t,  $J$  = 7.1 Hz, 3 H,  $\text{OCH}_2\text{CH}_3$ ).

**$^{13}\text{C}$  NMR** ( $\text{CDCl}_3$ , 151 MHz):  $\delta$  = 174.9 (s,  $\text{C}=\text{O}$ ), 152.6 (s, C-6), 141.7 (s, C-10), 135.9 (s, C-5), 131.8 (s, C-3), 129.2 (s, C-7), 126.8 (d, C-8), 125.1 (d, C-4), 121.5 (s, C-9), 60.6 (t,  $\text{OCH}_2$ ), 60.1 (d, C-1), 56.9 (d, C-2), 50.2 (t, C-13), 34.5 (s,  $\text{C}(\text{CH}_3)_3$ ), 30.5 (q,  $\text{C}(\text{CH}_3)_3$ ), 27.8 (t, C-11), 22.4 (t, C-12), 14.0 (q,  $\text{OCH}_2\text{CH}_3$ ).

#### **4cb-B:**

**$^1\text{H}$  NMR** ( $\text{CDCl}_3$ , 599 MHz):  $\delta$  = 7.07 (s, 2 H, 4-H), 6.75 (s, 2 H, 8-H), 4.99 (bs, 1 H, OH), 4.00 (d,  $J$  = 10.0 Hz, 1 H, 1-H), 3.88–3.84 (m, 2 H,  $\text{OCH}_2$ ), 3.72 (d,  $J$  = 10.0 Hz, 1 H, 2-H), 3.09–3.07 (m, 4 H, 13-H), 2.74–2.72 (m, 4 H, 11-H), 1.97–1.93 (m, 4 H, 12-H), 1.61 (bs, 2 H,  $\text{NH}_2$ ), 1.39 (s, 18 H,  $\text{C}(\text{CH}_3)_3$ ), 0.87 (t,  $J$  = 7.1 Hz, 3 H,  $\text{OCH}_2\text{CH}_3$ ).

**$^{13}\text{C}$  NMR** ( $\text{CDCl}_3$ , 151 MHz):  $\delta$  = 175.1 (s,  $\text{C}=\text{O}$ ), 152.4 (s, C-6), 142.0 (s, C-10), 135.4 (s, C-5), 132.8 (s, C-3), 128.4 (s, C-7), 127.0 (d, C-8), 124.7 (d, C-4), 121.9 (s, C-9), 60.4 (t,  $\text{OCH}_2$ ), 60.1 (d, C-1), 57.8 (d, C-2), 50.1 (t, C-13), 34.4 (s,  $\text{C}(\text{CH}_3)_3$ ), 30.4 (q,  $\text{C}(\text{CH}_3)_3$ ), 27.9 (t, C-11), 22.3 (t, C-12), 13.9 (q,  $\text{OCH}_2\text{CH}_3$ ).

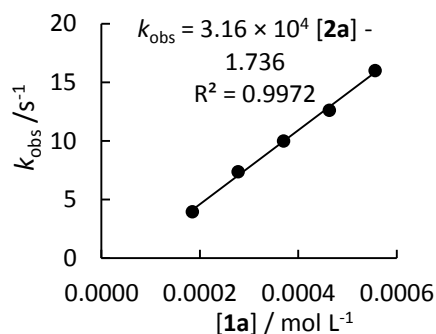
**HRMS** (ESI):  $m/z$  calcd for  $\text{C}_{31}\text{H}_{45}\text{N}_2\text{O}_3^+$   $[\text{M}+\text{H}]^+$ : 493.3425, found: 493.3425.

## 4.4.5. Determination of Rate Constants

4.4.5.1. Reactions of the Potassium Salt of Ethyl *N*-(Diphenylmethylene)glycinate **1a****Table S1.** Kinetics of the reaction of **1a** (generated from **1a**-H by addition of 1.05 equivalents of KO<sup>*t*</sup>Bu) with **2a** in DMSO (20 °C, stopped-flow, followed at 300 nm)

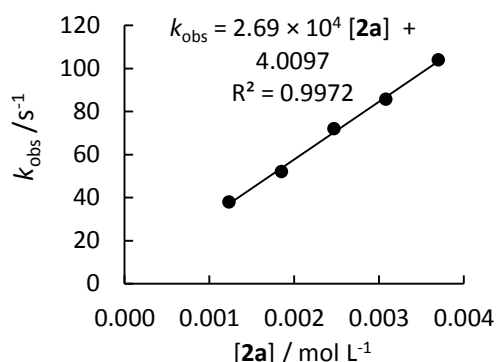
[ <b>2a</b> ] / mol L <sup>-1</sup>	[ <b>1a</b> ] / mol L <sup>-1</sup>	[18-crown-6] / mol L <sup>-1</sup>	[ <b>1a</b> ]/ [ <b>2a</b> ]	<i>k</i> <sub>obs</sub> / s <sup>-1</sup>
1.76 × 10 <sup>-5</sup>	1.85 × 10 <sup>-4</sup>	—	10.5	3.95
	2.78 × 10 <sup>-4</sup>	2.96 × 10 <sup>-4</sup>	15.8	7.37
	3.70 × 10 <sup>-4</sup>	—	21.1	1.00 × 10 <sup>1</sup>
	4.63 × 10 <sup>-4</sup>	4.94 × 10 <sup>-4</sup>	26.4	1.26 × 10 <sup>1</sup>
	5.56 × 10 <sup>-4</sup>	—	31.6	1.60 × 10 <sup>1</sup>

$$k_2 = 3.16 \times 10^4 \text{ L mol}^{-1} \text{ s}^{-1}$$

**Table S2.** Kinetics of the reaction of **1a** (generated from **1a**-H by addition of 1.05 equivalents of KO<sup>*t*</sup>Bu) with **2a** in DMSO (20 °C, stopped-flow, followed at 450 nm)

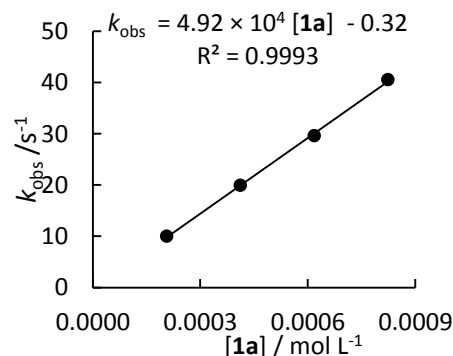
[ <b>1a</b> ]/ mol L <sup>-1</sup>	[ <b>2a</b> ]/ mol L <sup>-1</sup>	[ <b>2a</b> ]/[ <b>1a</b> ]	<i>k</i> <sub>obs</sub> / s <sup>-1</sup>
1.25 × 10 <sup>-4</sup>	1.23 × 10 <sup>-3</sup>	9.8	3.79 × 10 <sup>1</sup>
	1.85 × 10 <sup>-3</sup>	14.8	5.20 × 10 <sup>1</sup>
	2.47 × 10 <sup>-3</sup>	19.8	7.19 × 10 <sup>1</sup>
	3.08 × 10 <sup>-3</sup>	24.3	8.56 × 10 <sup>1</sup>
	3.70 × 10 <sup>-3</sup>	29.6	1.04 × 10 <sup>2</sup>

$$k_2 = 2.69 \times 10^4 \text{ L mol}^{-1} \text{ s}^{-1}$$

**Table S3.** Kinetics of the reaction of **1a** (generated from **1a**-H by addition of 1.05 equivalents of KO<sup>*t*</sup>Bu) with **2b** in DMSO (20 °C, stopped-flow, followed at 521 nm)

[ <b>2b</b> ] / mol L <sup>-1</sup>	[ <b>1a</b> ] / mol L <sup>-1</sup>	[18-crown-6] / mol L <sup>-1</sup>	[ <b>1a</b> ]/ [ <b>2b</b> ]	<i>k</i> <sub>obs</sub> / s <sup>-1</sup>
1.70 × 10 <sup>-5</sup>	2.06 × 10 <sup>-4</sup>	—	12.1	9.98
	4.12 × 10 <sup>-4</sup>	4.40 × 10 <sup>-4</sup>	24.2	1.99 × 10 <sup>1</sup>
	6.18 × 10 <sup>-4</sup>	—	36.6	2.96 × 10 <sup>1</sup>
	8.24 × 10 <sup>-4</sup>	8.80 × 10 <sup>-4</sup>	48.4	4.05 × 10 <sup>1</sup>

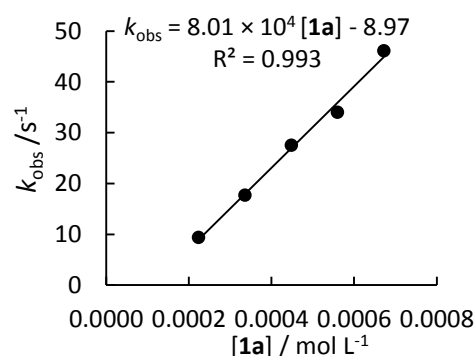
$$k_2 = 4.92 \times 10^4 \text{ L mol}^{-1} \text{ s}^{-1}$$



**Table S4.** Kinetics of the reaction of **1a** (generated from **1a-H** by addition of 1.05 equivalents of KO<sup>t</sup>Bu) with **2c** in DMSO (20 °C, stopped-flow, followed at 302 nm)

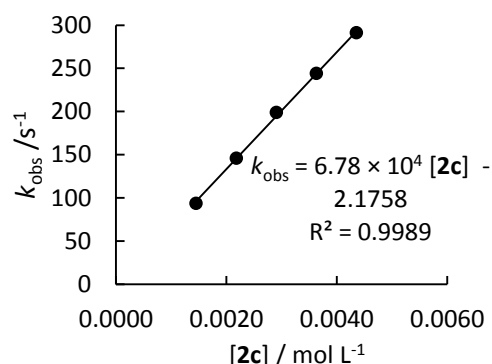
[ <b>2c</b> ] / mol L <sup>-1</sup>	[ <b>1a</b> ] / mol L <sup>-1</sup>	[18-crown-6] / mol L <sup>-1</sup>	[ <b>1a</b> ]/ [ <b>2c</b> ]	$k_{\text{obs}} / \text{s}^{-1}$
$1.94 \times 10^{-5}$	$2.24 \times 10^{-4}$	—	11.6	9.37
	$3.36 \times 10^{-4}$	$3.55 \times 10^{-4}$	17.4	$1.77 \times 10^1$
	$4.48 \times 10^{-4}$	—	23.1	$2.75 \times 10^1$
	$5.60 \times 10^{-4}$	$6.01 \times 10^{-4}$	28.9	$3.40 \times 10^1$
	$6.72 \times 10^{-4}$	—	34.6	$4.61 \times 10^1$

$$k_2 = 8.01 \times 10^4 \text{ L mol}^{-1} \text{ s}^{-1}$$

**Table S5.** Kinetics of the reaction of **1a** (generated from **1a-H** by addition of 1.05 equivalents of KO<sup>t</sup>Bu) with **2c** in DMSO (20 °C, stopped-flow, followed at 450 nm)

[ <b>1a</b> ]/ mol L <sup>-1</sup>	[ <b>2c</b> ]/ mol L <sup>-1</sup>	[ <b>2c</b> ]/[ <b>1a</b> ]	$k_{\text{obs}} / \text{s}^{-1}$
$1.35 \times 10^{-4}$	$1.45 \times 10^{-3}$	10.7	$9.37 \times 10^1$
	$2.18 \times 10^{-3}$	16.1	$1.46 \times 10^2$
	$2.91 \times 10^{-3}$	21.6	$1.99 \times 10^2$
	$3.63 \times 10^{-3}$	26.9	$2.44 \times 10^2$
	$4.36 \times 10^{-3}$	32.3	$2.91 \times 10^2$

$$k_2 = 6.78 \times 10^4 \text{ L mol}^{-1} \text{ s}^{-1}$$

**Table S6.** Kinetics of the reaction of **1a** (generated from **1a-H** by addition of 1.05 equivalents of KO<sup>t</sup>Bu) with **2d** in DMSO (20 °C, stopped-flow, followed at 521 nm)

[ <b>2d</b> ] / mol L <sup>-1</sup>	[ <b>1a</b> ] / mol L <sup>-1</sup>	[18-crown-6] / mol L <sup>-1</sup>	[ <b>1a</b> ]/ [ <b>2d</b> ]	$k_{\text{obs}} / \text{s}^{-1}$
$4.52 \times 10^{-5}$	$5.15 \times 10^{-4}$	—	11.4	$3.91 \times 10^1$
	$1.03 \times 10^{-3}$	$1.08 \times 10^{-3}$	22.8	$8.58 \times 10^1$
	$1.55 \times 10^{-3}$	—	34.3	$1.37 \times 10^2$
	$2.06 \times 10^{-3}$	$2.17 \times 10^{-3}$	45.6	$1.73 \times 10^2$
	$2.58 \times 10^{-3}$	—	57.1	$2.27 \times 10^2$

$$k_2 = 8.97 \times 10^4 \text{ L mol}^{-1} \text{ s}^{-1}$$

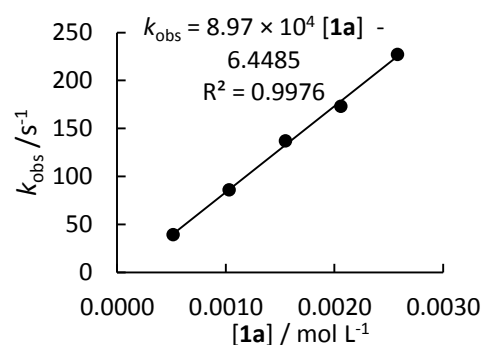
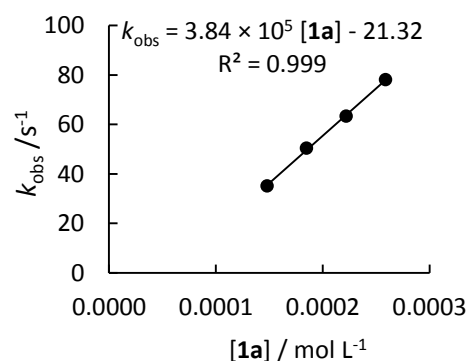


**Table S7.** Kinetics of the reaction of **1a** (generated from **1a**-H by addition of 1.05 equivalents of KO<sup>*t*</sup>Bu) with **2e** in DMSO (20 °C, stopped-flow, followed at 371 nm)

[ <b>2e</b> ] / mol L <sup>-1</sup>	[ <b>1a</b> ] / mol L <sup>-1</sup>	[18-crown-6] / mol L <sup>-1</sup>	[ <b>1a</b> ]/ [ <b>2e</b> ]	<i>k</i> <sub>obs</sub> / s <sup>-1</sup>
1.58 × 10 <sup>-5</sup>	1.48 × 10 <sup>-4</sup>	1.54 × 10 <sup>-4</sup>	9.4	3.51 × 10 <sup>1</sup>
	1.85 × 10 <sup>-4</sup>	—	11.7	5.04 × 10 <sup>1</sup>
	2.22 × 10 <sup>-4</sup>	—	14.1	3.63 × 10 <sup>1</sup>
	2.59 × 10 <sup>-4</sup>	2.69 × 10 <sup>-4</sup>	16.4	7.81 × 10 <sup>2</sup>

$$k_2 = 3.84 \times 10^5 \text{ L mol}^{-1} \text{ s}^{-1}$$

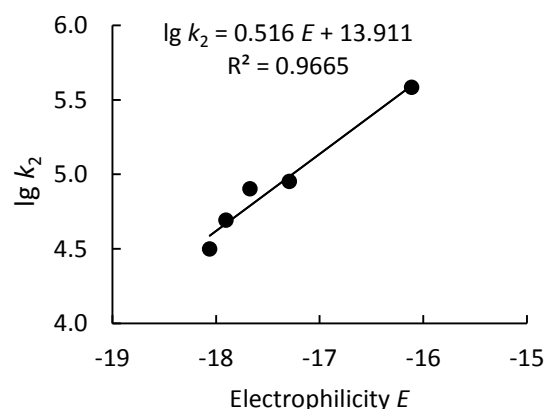


Determination of the Reactivity Parameters *N* and *s<sub>N</sub>* of the Potassium Salt of Glycine Imino Ester **1a** in DMSO.

**Table S8.** Rate Constants of the reactions of **1a** with reference electrophiles **2** (DMSO, 20 °C).

Electrophile	<i>E</i>	<i>k</i> <sub>2</sub> / L mol <sup>-1</sup> s <sup>-1</sup>	lg <i>k</i> <sub>2</sub>
<b>2a</b>	-18.06	3.16 × 10 <sup>4</sup>	4.50
<b>2b</b>	-17.90	4.92 × 10 <sup>4</sup>	4.69
<b>2c</b>	-17.67	8.01 × 10 <sup>4</sup>	4.90
<b>2d</b>	-17.29	8.97 × 10 <sup>4</sup>	4.95
<b>2e</b>	-16.11	3.84 × 10 <sup>5</sup>	5.58

$$N = 26.95, s_N = 0.52$$

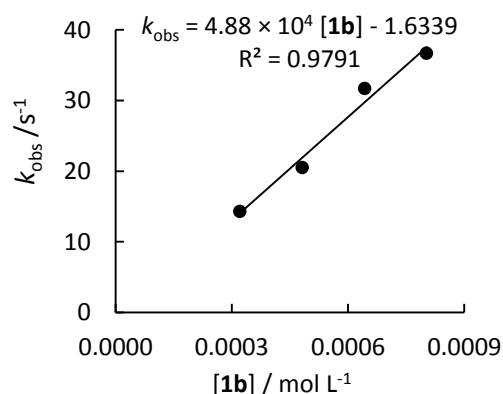


#### 4.4.5.2. Reactions of the Potassium Salt of *tert*-Butyl *N*-(Diphenylmethylene)glycinate **1b**

**Table S10.** Kinetics of the reaction of **1b** (generated from **1b**-H by addition of 1.05 equivalents of KO<sup>*t*</sup>Bu) with **2b** in DMSO (20 °C, stopped-flow, followed at 521 nm)

[ <b>2b</b> ] / mol L <sup>-1</sup>	[ <b>1b</b> ] / mol L <sup>-1</sup>	[ <b>1b</b> ]/ [ <b>2b</b> ]	<i>k</i> <sub>obs</sub> / s <sup>-1</sup>
1.66 × 10 <sup>-5</sup>	3.21 × 10 <sup>-4</sup>	19.3	1.43 × 10 <sup>1</sup>
	4.82 × 10 <sup>-4</sup>	29.0	2.05 × 10 <sup>1</sup>
	6.43 × 10 <sup>-4</sup>	38.7	3.17 × 10 <sup>1</sup>
	8.03 × 10 <sup>-4</sup>	48.4	4.44 × 10 <sup>1</sup>

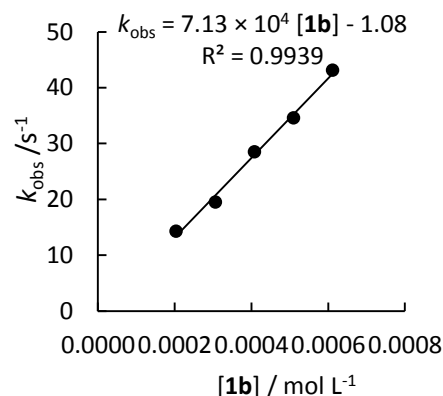
$$k_2 = 4.88 \times 10^4 \text{ L mol}^{-1} \text{ s}^{-1}$$



**Table S11.** Kinetics of the reaction of **1b** (generated from **1b-H** by addition of 1.05 equivalents of KO<sup>t</sup>Bu) with **2c** in DMSO (20 °C, stopped-flow, followed at 302 nm)

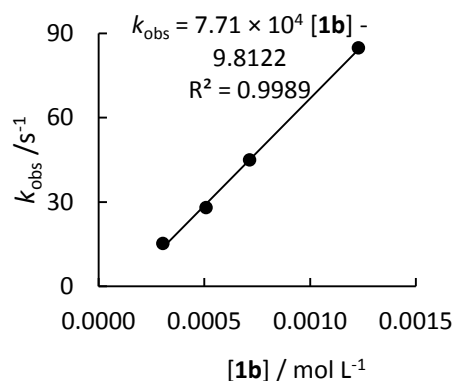
[ <b>2c</b> ] / mol L <sup>-1</sup>	[ <b>1b</b> ] / mol L <sup>-1</sup>	[18-crown-6] / mol L <sup>-1</sup>	[ <b>1b</b> ]/ [ <b>2c</b> ]	$k_{\text{obs}} / \text{s}^{-1}$
$1.53 \times 10^{-5}$	$2.04 \times 10^{-4}$	$3.41 \times 10^{-4}$	13.3	$1.43 \times 10^1$
	$3.06 \times 10^{-4}$		20.0	$1.95 \times 10^1$
	$4.08 \times 10^{-4}$		26.7	$2.85 \times 10^1$
	$5.10 \times 10^{-4}$	$5.71 \times 10^{-4}$	33.3	$3.46 \times 10^1$
	$6.12 \times 10^{-4}$		39.9	$4.31 \times 10^1$

$$k_2 = 7.13 \times 10^4 \text{ L mol}^{-1} \text{ s}^{-1}$$

**Table S12.** Kinetics of the reaction of **1b** (generated from **1b-H** by addition of 1.05 equivalents of KO<sup>t</sup>Bu) with **2d** in DMSO (20 °C, stopped-flow, followed at 521 nm)

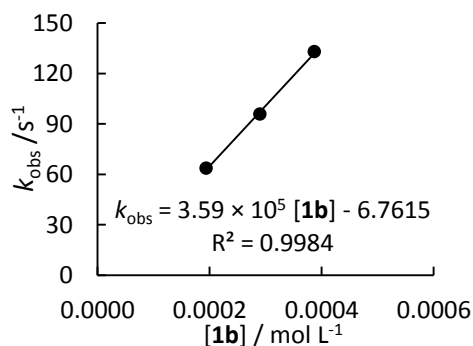
[ <b>2d</b> ] / mol L <sup>-1</sup>	[ <b>1b</b> ] / mol L <sup>-1</sup>	[18-crown-6] / mol L <sup>-1</sup>	[ <b>1b</b> ]/ [ <b>2d</b> ]	$k_{\text{obs}} / \text{s}^{-1}$
$2.19 \times 10^{-5}$	$3.06 \times 10^{-4}$	—	14.0	$1.60 \times 10^1$
	$5.10 \times 10^{-4}$	$5.55 \times 10^{-4}$	23.3	$2.80 \times 10^1$
	$7.15 \times 10^{-4}$	—	32.6	$4.30 \times 10^1$
	$1.22 \times 10^{-3}$	$1.35 \times 10^{-3}$	55.9	$9.11 \times 10^1$

$$k_2 = 7.71 \times 10^4 \text{ L mol}^{-1} \text{ s}^{-1}$$

**Table S13.** Kinetics of the reaction of **1b** (generated from **1b-H** by addition of 1.05 equivalents of KO<sup>t</sup>Bu) with **2e** in DMSO (20 °C, stopped-flow, followed at 371 nm)

[ <b>2e</b> ] / mol L <sup>-1</sup>	[ <b>1b</b> ] / mol L <sup>-1</sup>	[18-crown-6] / mol L <sup>-1</sup>	[ <b>1b</b> ]/ [ <b>2e</b> ]	$k_{\text{obs}} / \text{s}^{-1}$
$2.27 \times 10^{-5}$	$1.94 \times 10^{-4}$	$2.16 \times 10^{-4}$	8.5	$6.37 \times 10^1$
	$2.90 \times 10^{-4}$	—	12.8	$9.58 \times 10^1$
	$3.87 \times 10^{-4}$	$3.95 \times 10^{-4}$	17.0	$1.33 \times 10^2$

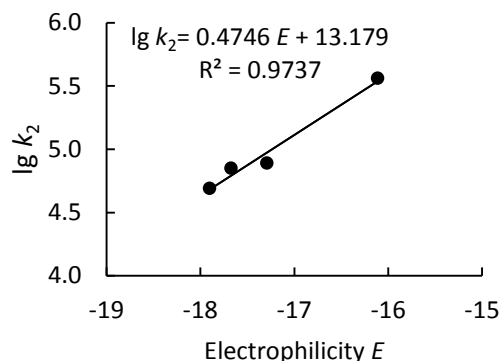
$$k_2 = 3.59 \times 10^5 \text{ L mol}^{-1} \text{ s}^{-1}$$



Determination of the Reactivity Parameters  $N$  and  $s_N$  of the Potassium Salt of Glycine Imino Ester **1b** in DMSO.**Table S14.** Rate Constants of the reactions of **1b** with reference electrophiles **2** (DMSO, 20 °C).

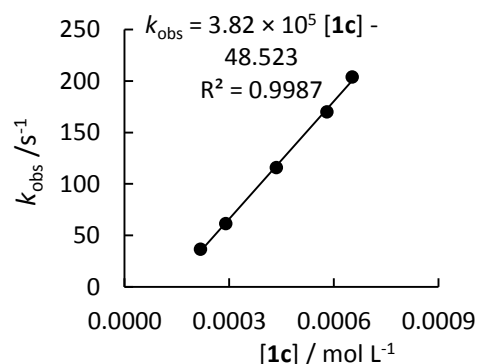
Electrophile	$E$	$k_2 / \text{L mol}^{-1} \text{s}^{-1}$	$\lg k_2$
<b>2b</b>	-17.90	$4.88 \times 10^4$	4.69
<b>2c</b>	-17.67	$7.13 \times 10^4$	4.85
<b>2d</b>	-17.29	$7.71 \times 10^4$	4.89
<b>2e</b>	-16.11	$3.59 \times 10^5$	5.56

$$N = 27.77, s_N = 0.47$$

**4.4.5.3. Reactions of the Potassium Salt of Ethyl *N*-Benzylideneglycinate **1c******Table S15.** Kinetics of the reaction of **1c** (generated from **1c-H** by addition of 1.05 equivalents of KO<sup>*t*</sup>Bu) with **2b** in DMSO (20 °C, stopped-flow, followed at 521 nm)

[ <b>2b</b> ] / mol·L <sup>-1</sup>	[ <b>1c</b> ] / mol·L <sup>-1</sup>	[18-crown-6] / mol·L <sup>-1</sup>	[ <b>1c</b> ]/ [ <b>2b</b> ]	$k_{\text{obs}} / \text{s}^{-1}$
$1.38 \times 10^{-5}$	$2.18 \times 10^{-4}$	—	15.8	$3.64 \times 10^1$
	$2.90 \times 10^{-4}$	$3.21 \times 10^{-4}$	21.0	$6.15 \times 10^1$
	$4.35 \times 10^{-4}$	—	31.5	$1.16 \times 10^2$
	$5.80 \times 10^{-4}$	$6.42 \times 10^{-4}$	42.2	$1.70 \times 10^2$
	$6.53 \times 10^{-4}$	—	47.3	$2.04 \times 10^2$

$$k_2 = 3.82 \times 10^5 \text{ L mol}^{-1} \text{s}^{-1}$$

**4.4.5.4. Reactions of the Potassium Salt of Ethyl *N*-(*p*-chlorobenzylidene)glycinate **1d******Table S16.** Kinetics of the reaction of **1d** (generated from **1d-H** by addition of 1.05 equivalents of KO<sup>*t*</sup>Bu) with **2b** in DMSO (20 °C, stopped-flow, followed at 521 nm)

[ <b>2b</b> ] / mol L <sup>-1</sup>	[ <b>1d</b> ] / mol L <sup>-1</sup>	[18-crown-6] / mol L <sup>-1</sup>	[ <b>1d</b> ]/ [ <b>2b</b> ]	$k_{\text{obs}} / \text{s}^{-1}$
$1.66 \times 10^{-5}$	$2.32 \times 10^{-4}$	—	14.0	$4.36 \times 10^1$
	$3.09 \times 10^{-4}$	$3.51 \times 10^{-4}$	18.6	$6.69 \times 10^1$
	$4.64 \times 10^{-4}$	—	28.0	$1.14 \times 10^2$
	$6.19 \times 10^{-4}$	$7.02 \times 10^{-4}$	37.3	$1.51 \times 10^2$

$$k_2 = 2.79 \times 10^5 \text{ L mol}^{-1} \text{s}^{-1}$$

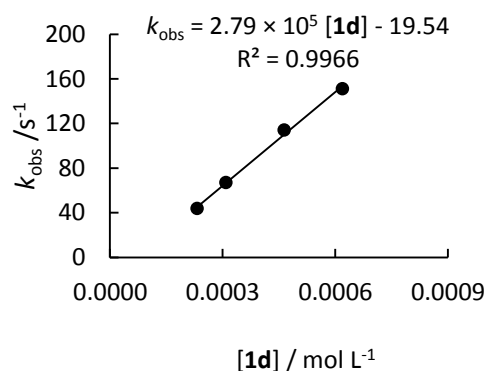
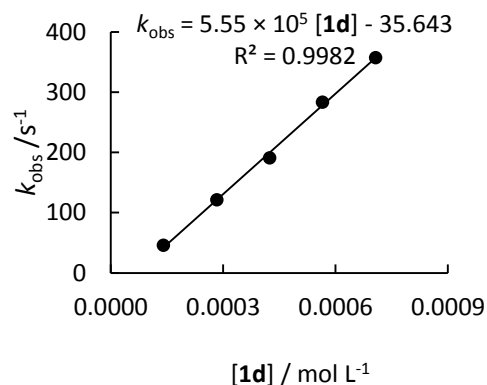


**Table S17.** Kinetics of the reaction of **1d**-K (generated from **1d** by addition of 1.05 equivalents of KO<sup>t</sup>Bu) with **2d** in DMSO (20 °C, stopped-flow, followed at 500 nm)

[ <b>2d</b> ] / mol L <sup>-1</sup>	[ <b>1d</b> ] / mol L <sup>-1</sup>	[18-crown-6] / mol L <sup>-1</sup>	[ <b>1d</b> ]/ [ <b>2d</b> ]	$k_{\text{obs}} / \text{s}^{-1}$
1.99 × 10 <sup>-5</sup>	1.41 × 10 <sup>-4</sup>	—	7.1	4.58 × 10 <sup>1</sup>
	2.83 × 10 <sup>-4</sup>	3.12 × 10 <sup>-4</sup>	14.2	1.21 × 10 <sup>2</sup>
	4.24 × 10 <sup>-4</sup>	—	21.3	1.91 × 10 <sup>2</sup>
	5.65 × 10 <sup>-4</sup>	6.24 × 10 <sup>-4</sup>	28.4	2.83 × 10 <sup>2</sup>
	7.07 × 10 <sup>-4</sup>	—	35.5	3.57 × 10 <sup>2</sup>

$$k_2 = 5.55 \times 10^5 \text{ L mol}^{-1} \text{ s}^{-1}$$

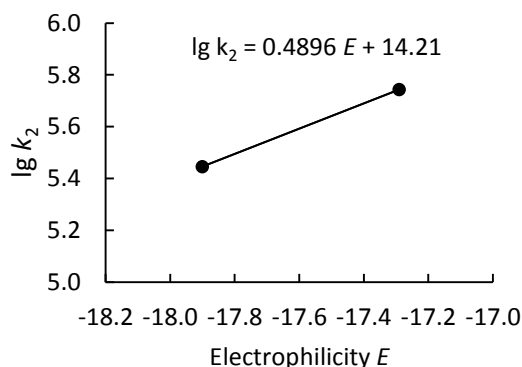


Determination of the Reactivity Parameters  $N$  and  $s_N$  of the Potassium Salt of Glycine Imino Ester **1d** in DMSO.

**Table S18.** Rate Constants of the reactions of **1d** with reference electrophiles **2** (DMSO, 20 °C).

Electrophile	$E$	$k_2 / \text{L mol}^{-1} \text{ s}^{-1}$	$\lg k_2$
<b>2b</b>	-17.90	$2.79 \times 10^5$	5.45
<b>2d</b>	-17.29	$5.55 \times 10^5$	5.74

$$N = 29.02, s_N = 0.49$$



#### 4.4.5.5. Reactions of the Potassium Salt of Ethyl *N*-Benzylidenealaninate **1e**

**Table S19.** Kinetics of the reaction of **1e** (generated from **1e**-H by addition of 1.05 equivalents of KO<sup>t</sup>Bu) with **2b** in DMSO (20 °C, stopped-flow, followed at 521 nm)

[ <b>2b</b> ] / mol L <sup>-1</sup>	[ <b>1e</b> ] / mol L <sup>-1</sup>	[18-crown-6] / mol L <sup>-1</sup>	[ <b>1e</b> ]/ [ <b>2b</b> ]	$k_{\text{obs}} / \text{s}^{-1}$
2.17 × 10 <sup>-5</sup>	2.68 × 10 <sup>-4</sup>	—	12.4	3.78 × 10 <sup>1</sup>
	3.58 × 10 <sup>-4</sup>	4.09 × 10 <sup>-4</sup>	16.5	5.47 × 10 <sup>1</sup>
	4.47 × 10 <sup>-4</sup>	—	20.6	6.95 × 10 <sup>1</sup>
	5.36 × 10 <sup>-4</sup>	6.13 × 10 <sup>-4</sup>	24.7	9.44 × 10 <sup>1</sup>
	6.26 × 10 <sup>-4</sup>	—	28.8	1.17 × 10 <sup>2</sup>

$$k_2 = 2.22 \times 10^5 \text{ L mol}^{-1} \text{ s}^{-1}$$

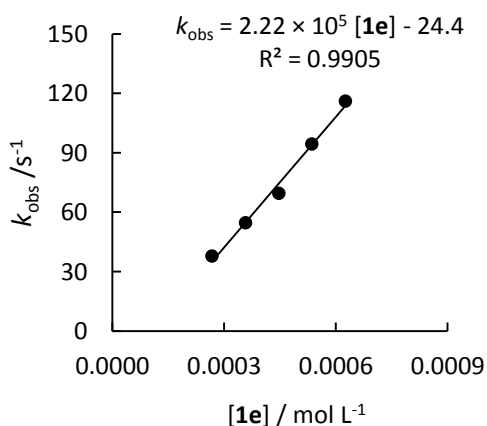
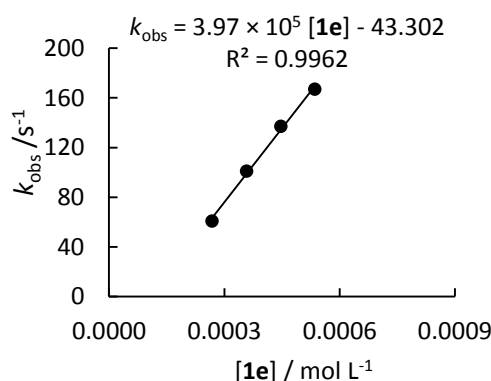


**Table S20.** Kinetics of the reaction of **1e** (generated from **1e-H** by addition of 1.05 equivalents of KO<sup>t</sup>Bu) with **2d** in DMSO (20 °C, stopped-flow, followed at 521 nm)

[ <b>2d</b> ] / mol L <sup>-1</sup>	[ <b>1e</b> ] / mol L <sup>-1</sup>	[18-crown-6] / mol L <sup>-1</sup>	[ <b>1e</b> ]/ [ <b>2d</b> ]	$k_{\text{obs}} / \text{s}^{-1}$
$2.42 \times 10^{-5}$	$2.68 \times 10^{-4}$	—	11.1	$6.08 \times 10^1$
	$3.58 \times 10^{-4}$	$4.09 \times 10^{-4}$	14.8	$1.01 \times 10^2$
	$4.47 \times 10^{-4}$		18.5	$1.37 \times 10^2$
	$5.36 \times 10^{-4}$	$6.30 \times 10^{-4}$	22.1	$1.67 \times 10^2$

$$k_2 = 3.97 \times 10^5 \text{ L mol}^{-1} \text{ s}^{-1}$$

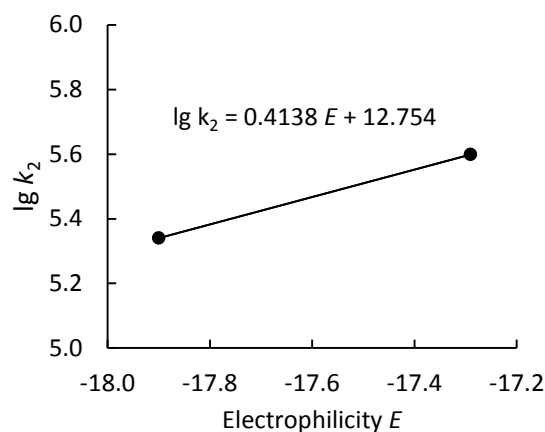


Determination of Reactivity Parameters  $N$  and  $s_N$  for the Anion of Alanine Imino Ester **1e** in DMSO.

**Table S21.** Rate Constants for the reactions of **1e** with reference electrophiles **2** (DMSO, 20 °C).

Elektrophile	$E$	$k_2 / \text{L} \cdot \text{mol}^{-1} \cdot \text{s}^{-1}$	$\log k_2$
<b>2b</b>	-17.90	$2.22 \times 10^5$	5.40
<b>2d</b>	-17.29	$3.97 \times 10^5$	5.80

$$N = 30.82, s_N = 0.41$$

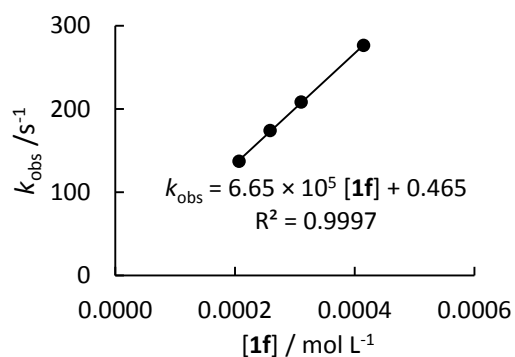


#### 4.5.5.6. Reactions of the Potassium Salt of 2-((Diphenylmethylene)amino)acetonitrile **1f**

**Table S22.** Kinetics of the reaction of **1f** (generated from **1f-H** by addition of 1.05 equivalents of KO<sup>t</sup>Bu) with **2b** in DMSO (20 °C, stopped-flow, followed at 521 nm)

[ <b>2b</b> ] / mol L <sup>-1</sup>	[ <b>1f</b> ] / mol L <sup>-1</sup>	[ <b>1f</b> ]/ [ <b>2b</b> ]	$k_{\text{obs}} / \text{s}^{-1}$
$2.20 \times 10^{-5}$	$2.07 \times 10^{-4}$	9.4	$1.37 \times 10^2$
	$2.59 \times 10^{-4}$	11.8	$1.74 \times 10^2$
	$3.11 \times 10^{-4}$	14.2	$2.08 \times 10^2$
	$4.15 \times 10^{-4}$	18.9	$2.76 \times 10^2$

$$k_2 = 6.65 \times 10^5 \text{ L mol}^{-1} \text{ s}^{-1}$$





## 4.5. References

1. For reviews on the preparation of  $\alpha$ -amino acids, see: (a) Williams, R. M. *Synthesis of Optically Active  $\alpha$ -Amino Acids*; Pergamon Press: Oxford, 1989. (b) O'Donnell, M. J. *Acc. Chem. Res.* **2004**, *37*, 506–517. (c) Hashimoto, T.; Maruoka, K. *Chem. Rev.* **2007**, *107*, 5656–5682. (d) Shirakawa, S.; Maruoka, K. *Angew. Chem. Int. Ed.* **2013**, *52*, 4312–4348; (e) Nájera, C.; Sansano, J. M. *Chem. Rev.* **2007**, *107*, 4584–4671. (f) Maruoka, K.; Ooi, T. *Chem. Rev.* **2003**, *103*, 3013–3028.
2. O'Donnell, M. J.; Eckrich, T. M. *Tetrahedron Lett.* **1978**, *47*, 4625–4628.
3. He, W.; Wang, Q.; Wang, Q.; Zhang, B.; Sun, X.; Zhang, S. *Synlett* **2009**, 1311–1314.
4. Waser, M.; Gratzer, K.; Herchl, R.; Müller, N. *Org. Biomol. Chem.* **2012**, *10*, 251–254.
5. Schettini, R.; De Riccardis, F.; Della Sala, G.; Izzo, I. *J. Org. Chem.* **2016**, *81*, 2494–2505.
6. Arai, S.; Takahashi, F.; Tsuji, R.; Nishida, A. *Heterocycles* **2006**, *67*, 495–501.
7. Cabrera, S.; Arrayás, R. G.; Martín-Matute, B.; Cossío, F. P.; Carretero, J. C. *Tetrahedron* **2007**, *63*, 6587–6602.
8. Ma, T.; Fu, X.; Kee, C. W.; Zong, L.; Pan, Y.; Huang, K.-W.; Tan, C.-H. *J. Am. Chem. Soc.* **2011**, *133*, 2828–2831.
9. Nie, J.; Hua, M.-Q.; Xiong, H.-Y.; Zheng, Y.; Ma, J.-A. *J. Org. Chem.* **2012**, *77*, 4209–4216.
10. Konno, T.; Watanabe, S.; Takahashi, T.; Tokoro, Y.; Fukuzawa, S. *Org. Lett.* **2013**, *15*, 4418–4421.
11. He, F.-S.; Jin, J.-H.; Yang, Z.-T.; Yu, X.; Fossey J. S.; Deng, W.-P. *ACS Catal.* **2016**, *6*, 652–656.
12. Ooi, T.; Kameda, M.; Taniguchi, M.; Maruoka, K. *J. Am. Chem. Soc.* **2004**, *126*, 9685–9694.
13. Mettath, S.; Srikanth, G. S. C.; Dangerfield, B. S.; Castle, S. L. *J. Org. Chem.* **2004**, *69*, 6489–6492.
14. (a) Arrayás, R. G.; Carretero, J. C. *Chem. Soc. Rev.* **2009**, *38*, 1940–1948. (b) Hernando, E.; Arrayás, R. G.; Carretero, J. C. *Chem. Commun.* **2012**, *48*, 9622–9624;
15. Yamashita, Y.; Yoshimoto, S.; Masuda, K.; Kobayashi, S. *Asian J. Org. Chem.* **2012**, *1*, 327–330.
16. Bandar, J. S.; Lambert, T. H. *J. Am. Chem. Soc.* **2013**, *135*, 11799–11802.
17. Kano, T.; Kobayashi, R.; Maruoka, K. *Angew. Chem. Int. Ed.* **2015**, *54*, 8471–8474.

18. Mayr, H.; Patz, M. *Angew. Chem.* **1994**, *106*, 990–1010; *Angew. Chem. Int. Ed. Engl.* **1994**, *33*, 938–957.
19. (a) Mayr, H.; Bug, T.; Gotta, M. F.; Hering, N.; Irrgang, B.; Janker, B.; Kempf, B.; Loos, R.; Ofial, A. R.; Remennikov, G.; Schimmel, H. *J. Am. Chem. Soc.* **2001**, *123*, 9500–9512. (b) Lucius, R.; Loos, R.; Mayr, H. *Angew. Chem.* **2002**, *114*, 97–102; *Angew. Chem., Int. Ed.* **2002**, *41*, 91–95. (c) Mayr, H.; Kempf, B.; Ofial, A. R. *Acc. Chem. Res.* **2003**, *36*, 66–77. (d) Mayr, H.; Ofial, A. R. *Pure Appl. Chem.* **2005**, *77*, 1807–1821. (e) D. Richter, N. Hampel, T. Singer, A. R. Ofial, H. Mayr, *Eur. J. Org. Chem.* **2009**, 3203–3211. (f) H. Mayr, *Tetrahedron* **2015**, *71*, 5095–5111. (g) For a comprehensive listing of nucleophilicity parameters  $N$ ,  $s_N$  and electrophilicity parameters  $E$ , see: <http://www.cup.uni-muenchen.de/oc/mayr/DBintro.html>.
20. (a) Bug, T.; Mayr, H. *J. Am. Chem. Soc.* **2003**, *125*, 12980–12986. (b) Bug, T.; Lemek, T.; Mayr, H. *J. Org. Chem.* **2004**, *69*, 7565–7576. (c) Berger, S. T. A.; Ofial, A. R.; Mayr, H. *J. Am. Chem. Soc.* **2007**, *129*, 9753–9761. (d) Kaumanns, O.; Appel, R.; Lemek, T.; Seeliger, F.; Mayr, H. *J. Org. Chem.* **2009**, *74*, 75–81. (e) Appel, R.; Loos, R.; Mayr, H. *J. Am. Chem. Soc.* **2009**, *131*, 704–714. (f) Corral Bautista, F.; Mayr, H. *Eur. J. Org. Chem.* **2013**, 4255–4261. (g) Appel, R.; Mayr, H. *Chem. Eur. J.* **2010**, *16*, 8610–8614.
21. (a) O'Donnell, M. J.; Bennett, W. D.; Bruder, W. A.; Jacobsen, W. N.; Knuth, K.; LeClef, B.; Polt, R. L.; Bordwell, F. G.; Mrozack, S. R.; Cripe, T. A. *J. Am. Chem. Soc.* **1988**, *110*, 8520–8525. b)  $pK_a$  values for **1a** and **1e** have not been reported.
22. Kaumanns, O.; Lucius, R.; Mayr, H. *Chem. Eur. J.* **2008**, *14*, 9675–9682.
23. From <http://www.chem.wisc.edu/areas/reich/pkatable/>
24. Mayr, H.; Ofial, A. R. *Acc. Chem. Res.* **2016**, *49*, 952–965.
25. Fulmer, G. F.; Miller, A. J. M.; Sherden, N. H.; Gottlieb, H. E.; Nudelman, A.; Stoltz, B. M.; Bercaw, J. E.; Goldberg, K. I. *Organometallics* **2010**, *29*, 2176–2179.
26. De Wachter, R.; Brans, L.; Ballet, S.; Van den Eynde, I.; Feytens, D.; Keresztes, A.; Toth, G.; Urbanczyk-Lipkowska, Z.; Tourwé, D. *Tetrahedron* **2009**, *65*, 2266–2278.